

SIMULATION OF BIPED LOCOMOTION OF HUMANOID ROBOTS IN  
3D SPACE

A THESIS SUBMITTED TO  
THE GRADUATE SCHOOL OF NATURAL AND APPLIED SCIENCES  
OF  
MIDDLE EAST TECHNICAL UNIVERSITY

BY

GÖKCAN AKALIN

IN PARTIAL FULFILLMENT OF THE REQUIREMENTS  
FOR  
THE DEGREE OF MASTER OF SCIENCE  
IN  
MECHANICAL ENGINEERING

SEPTEMBER 2010

Approval of the thesis:

**SIMULATION OF BIPED LOCOMOTION OF HUMANOID  
ROBOTS IN 3D SPACE**

submitted by **GÖKCAN AKALIN** in partial fulfillment of the requirements for  
the degree of **Master of Science in Mechanical Engineering Department,**  
**Middle East Technical University** by,

Prof. Dr. Canan Özgen  
Dean, Graduate School of **Natural and Applied Sciences** \_\_\_\_\_

Prof. Dr. Süha Oral  
Head of Department, **Mechanical Engineering** \_\_\_\_\_

Prof. Dr. M. Kemal Özgören  
Supervisor, **Mechanical Engineering Dept., METU** \_\_\_\_\_

**Examining Committee Members:**

Prof. Dr. Eres Söylemez  
Mechanical Engineering Dept., METU \_\_\_\_\_

Prof. Dr. M. Kemal Özgören  
Mechanical Engineering Dept., METU \_\_\_\_\_

Prof. Dr. S. Kemal İder  
Mechanical Engineering Dept., METU \_\_\_\_\_

Prof. Dr. Reşit Soylu  
Mechanical Engineering Dept., METU \_\_\_\_\_

Prof. Dr. Kemal Leblebicioğlu  
Electrical and Electronics Dept., METU \_\_\_\_\_

Date: 14.09.2010

**I hereby declare that all information in this document has been obtained and presented in accordance with academic rules and ethical conduct. I also declare that, as required by these rules and conduct, I have fully cited and referenced all material and results that are not original to this work.**

Name, Last name : Gökcan AKALIN

Signature :

## **ABSTRACT**

# **SIMULATION OF BIPED LOCOMOTION OF HUMANOID ROBOTS IN 3D SPACE**

Akalın, Gökcan

M.S., Department of Mechanical Engineering

Supervisor: Prof. Dr. M. Kemal Özgören

September 2010, 281 pages

The main goal of this thesis is to simulate the response of a humanoid robot using a specified control algorithm which can achieve a sustainable biped locomotion with 4 basic locomotion phases. Basic parts for the body of the humanoid robot model are shaped according to the specified basic physical parameters and assumed kinematic model.

The kinematic model, which does not change according to locomotion phases and consists of 27 segments including 14 virtual segments, provides a humanoid robot model with 26 degrees of freedom (DOF). Corresponding kinematic relations for the robot model are obtained by recursive formulations. Derivation of dynamic equations is carried out by the Newton-Euler formulation. A trajectory definition algorithm which defines positions, orientations, translational and angular velocities for the hip and its mass center, toe part of the foot and its toe point is created. A

control strategy based on predictive optimum command acceleration calculations and computed torque control method is implemented.

The simulation is executed in Simulink and the visualization of the simulation is established in a virtual environment by Virtual Reality Toolbox of MATLAB. The simulation results and the user defined reference input are displayed simultaneously in the virtual environment.

In this study, a simulation environment for the biped locomotion of humanoid robots is created. By the help of this thesis, the user can test various control strategies by modifying the modular structure of the simulation and acquire necessary information for the preliminary design study of a humanoid robot construction.

Keywords: Bipedal Locomotion, Humanoid Robots, Simulation, Computed Torque Control

## ÖZ

# İNSANSI ROBOTLARIN 3 BOYUTLU UZAYDA 2 AYAKLI HAREKETİNİN BENZETİMİ

Akalın, Gökcan

Yüksek Lisans, Makina Mühendisliği Bölümü

Tez Yöneticisi: Prof. Dr. M. Kemal Özgören

Eylül 2010, 281 sayfa

Bu tezin ana amacı, 4 temel hareket evresini kapsayan sürdürülebilir bir 2 ayaklı yürüyüşü gerçekleştirebilmesi amacıyla belirlenmiş olan bir kontrol algoritması kullanılarak, bir insansı robotun tepkisinin simüle edilmesidir. İnsansı robot modelini oluşturan temel vücut parçaları, belirlenmiş olan temel fiziksel parametreler ve varsayılmış olan kinematik modeller doğrultusunda şekillendirilmiştir.

Çeşitli hareket evrelerinde değişmeyen ve 14 ü sanal olmak üzere toplam 27 parçadan oluşan kinematik model, 26 serbestlik derecesi olan bir insansı robot modelini oluşturmaktadır. Robot modeli için sözkonusu olan kinematik ilişkiler yenilemeli formülasyonlar ile elde edilmiştir. Dinamik denklemlerin türetilmesi Newton-Euler formülasyonu ile gerçekleştirilmiştir. Kalça ve kalça kütle merkezi,

ayak ucu ve ayak ucu noktası için konumları, açısız konumları, doğrusal ve açısız hızlarını tanımlayan bir yörünge tanımlama algoritması oluşturulmuştur. Öngörülü en iyi komut ivmesi hesaplanması ve hesaplanan tork kontrol yöntemi tabanlı bir kontrol stratejisi uygulanmıştır. Simülasyon MATLAB Simulink'te yürütölmekte ve simülasyonun görüntülenmesi MATLAB Simulink Virtual Reality Toolbox ile sanal bir ortam içinde gerçekleştirilmektedir. Simülasyon sonuçları ve kullanıcı tarafından tanımlanmış olan referans girdisi sanal ortamda aynı anda gösterilmektedir.

Bu çalışmada insansı robotların iki ayaklı hareketi için bir simülasyon ortamı kurulmuştur. Bu tezin yardımıyla kullanıcı, simülasyonun modöler yapısını deęiştirerek çeşitli kontrol stratejilerini test edebilir ve insansı bir robotun yapılmasının öntasarım çalışması için gerekli olan bilgiyi elde edebilir.

Anahtar Kelimeler: İki Ayaklı Yürüyüş, İnsansı Robotlar, Simülasyon, Hesaplanan Tork Kontrol Yöntemi

**To My Parents**

## **ACKNOWLEDGEMENTS**

First of all, I would like to express my sincere gratitude to my supervisor Prof. Dr. M. Kemal Özgören for his invaluable guidance and support throughout the thesis study.

I am always indebted to my friends Ferhat Sağlam, Serter Yılmaz, Yusuf Duran, Mert Aydın, Ahmet Ketenci, Hamdullah Yücel, Mehmet Kılıç and Çağrı Batıhan for their colorful and brilliant personalities, which makes graduate life much fun than it actually is.

Additionally, I am grateful to TÜBİTAK for its significant support to my graduate study by the scholarship.

Most importantly, I would like to thank my family and precious relatives for their special appreciation and endless patience in every part of my life.

## TABLE OF CONTENTS

ABSTRACT .....	iv
ÖZ.....	vi
ACKNOWLEDGEMENTS .....	ix
TABLE OF CONTENTS .....	x
LIST OF FIGURES.....	xviii
LIST OF TABLES .....	xxvi
LIST OF SYMBOLS .....	xxvii
LIST OF ABBREVIATIONS .....	xxviii
CHAPTERS	
1.INTRODUCTION.....	1
1.1.Motivation .....	1
1.2. Phases of Gait Cycle .....	4
1.3. Review of Literature on Simulation Studies .....	6
1.4. Review of Literature on Control Strategies.....	11
1.5. Review of Literature on Humanoid Robots .....	19
1.6. Scope of Thesis .....	23

2.PHYSICAL MODELLING .....	25
3.REFERENCE TRAJECTORY GENERATION.....	43
3.1. Locomotion Definition.....	43
3.1.1. $P_{hip}$ .....	43
3.1.2. $V_{hip}$ .....	45
3.1.3. $R$ .....	45
3.1.4. $t_{SSP}$ and PTR .....	46
3.1.5. SW .....	46
3.1.6. SH and $k_{SH}$ .....	46
3.1.7. $k_{Adj}$ .....	47
3.1.8. $\Delta\theta_{PLN}$ and $\Delta\theta_{ADJ}$ .....	47
3.1.9. $T_{dir}$ .....	47
3.2. Trajectory Definition.....	48
3.2.1. Finding Arc Centers .....	49
3.2.2. Definition of Local Coordinate Systems.....	51
3.2.2.1. For Turning Leftward Direction.....	52
3.2.2.2. For Turning Rightward Direction .....	54
3.2.3. Trajectory Definition during SSP and DSP Pairs .....	55
3.2.3.1. The Definition of $\theta_h(t)$ .....	58
3.2.3.2. Trajectory Definitions for CoM of Body 17 and Body 17.....	59

3.2.3.2.1. Translational Position and Velocity Definitions for CoM of Body 17 .....	59
3.2.3.2.1.1. For Turning Left.....	60
3.2.3.2.1.2. For Turning Right.....	60
3.2.3.2.2. Angular Position and Angular Velocity Definitions for Body 17.....	61
3.2.3.2.2.1. For SSPs .....	61
3.2.3.2.2.1. For DSPs .....	61
3.2.3.2.2.1.1. For Turning Left.....	61
3.2.3.2.2.1.1. For Turning Right.....	62
3.2.3.3. Trajectory Definitions for Toe Points, Body 1 and Body 2 .....	63
3.2.3.3.1. Translational Position and Velocity Definitions for Toe Points on Body 1 and Body 2.....	63
3.2.3.3.2. Angular Position and Angular Velocity Definitions for Body 1 and Body 2 .....	72
4.MATHEMATICAL MODELING .....	75
4.1. The Derivation of Kinematic Equations.....	75
4.1.1. Transformation Matrices .....	77
4.1.1.1. For RFFSSP .....	80
4.1.1.2. For LFFSSP.....	81
4.1.1.3. For RFFDSP and LFFDSP .....	82
4.1.2. Position Relations.....	83

4.1.2.1. For RFFSSP .....	83
4.1.2.2. For LFFSSP.....	84
4.1.2.3. For RFFDSP and LFFDSP .....	85
4.1.3. Angular Velocity Relations.....	85
4.1.3.1. For RFFSSP .....	86
4.1.3.2. For LFFSSP.....	87
4.1.3.2. For RFFDSP and LFFDSP.....	88
4.1.4. Translational Velocity Relations.....	89
4.1.4.1. For RFFSSP .....	90
4.1.4.2. For LFFSSP.....	90
4.1.4.3. For RFFDSP and LFFDSP.....	91
4.1.5. Angular Acceleration Relations .....	92
4.1.5.1. For RFFSSP .....	93
4.1.5.2. For LFFSSP.....	94
4.1.5.2. For RFFDSP and LFFDSP.....	95
4.1.6. Translational Acceleration Relations .....	96
4.1.6.1. For RFFSSP .....	96
4.1.6.2. For LFFSSP.....	97
4.1.6.3. For RFFDSP and LFFDSP.....	98
4.2. Calculation of Jacobian Matrices and Their Time Derivatives.....	99
4.2.1. Definition of Jacobian Matrices .....	100

4.2.1.1 For RFFSSP .....	100
4.2.1.2 For LFFSSP .....	101
4.2.1.3 For RFFDSP .....	102
4.2.1.4 For LFFDSP .....	103
4.2.2. Calculation Procedure of Jacobian Matrices .....	104
4.2.3. Calculation Procedure of Time Derivatives of Jacobian Matrices.....	105
4.3. Derivation of Dynamic Equations.....	105
4.4. Direct Dynamic Solution.....	109
4.4.1. For RFFSSP .....	113
4.4.2. For LFFSSP .....	116
4.4.3. For RFFDSP .....	118
4.4.4. For LFFDSP .....	121
4.5. Transition from Single Support to Double Support Phases .....	124
4.5.1. From RFFSSP to LFFDSP .....	125
4.5.2. From LFFSSP to RFFDSP .....	126
5.CONTROL STRATEGY .....	128
5.1. Calculation of Optimum Command Accelerations .....	128
5.1.1. Calculation of Optimum Command Accelerations for Lower Bodies	129
5.1.1.1. For RFFSSP .....	129
5.1.1.1.1. For Body 17 and the mass center of Body 17 .....	130
5.1.1.1.1.1. Definition of Variables.....	130

5.1.1.1.1.2. Calculation Procedure .....	132
5.1.1.1.2. For Body 2 and the toe point of Body 2.....	134
5.1.1.1.2.1. Definition of Variables.....	134
5.1.1.1.2.2. Calculation Procedure .....	137
5.1.1.2. For LFFSSP.....	138
5.1.1.2.1. For Body 17 and the mass center of Body 17 .....	139
5.1.1.2.1.1. Definition of Variables.....	139
5.1.1.2.1.2. Calculation Procedure .....	140
5.1.1.2.2. For Body 1 and the toe point of Body 1.....	142
5.1.1.2.2.1. Definition of Variables.....	142
5.1.1.2.2.2. Calculation Procedure .....	144
5.1.1.3. For RFFDSP .....	146
5.1.1.3.1. Definition of Variables.....	146
5.1.1.3.2. Calculation Procedure .....	150
5.1.1.4. For LFFDSP .....	153
5.1.1.4.1. Definition of Variables.....	153
5.1.1.4.2. Calculation Procedure .....	156
5.1.2. For UpperBodies .....	159
5.2. Calculation of Actuator Torques .....	160
5.2.1. For RFFSSP .....	161
5.2.2. For LFFSSP.....	161

5.2.3. For RFFDSP .....	162
5.2.4. For LFFDSP .....	163
6.SIMULATION ENVIRONMENT AND RESULTS.....	165
6.1. Simulation Model.....	167
6.1.1. Phase Selector .....	174
6.1.1.1. Phase Shifting Decision for Single Support Phases .....	175
6.1.1.2. Phase Shifting Decision for Double Support Phases .....	182
6.1.2. Trajectory Definition.....	185
6.1.3. Models Related with Locomotion Phases (RFFSSP, LFFSSP, RFFDSP, LFFDSP) .....	190
6.1.4. Results of Dynamic Solutions .....	201
6.1.5. Integration .....	203
6.1.6. Visualization.....	206
6.1.7. Definition of Physical Parameters.....	215
6.1.8. Reading and Arrangement of Several Variables .....	218
6.2. Simulation Results.....	219
6.2.1. Simulation Number 1 .....	219
6.2.1.1. Reference Input .....	219
6.2.1.2. Joint Space Positions .....	221
6.2.1.3. Task Space Positions .....	225
6.2.1.4. Actuator Torques.....	226

6.2.1.5. Ground Reaction Forces and Moments.....	230
6.2.2. Simulation Number 2 .....	233
6.2.2.1. Reference Input .....	233
6.2.2.2. Task Space Positions.....	235
6.2.3. Simulation Number 3 .....	238
6.2.3.1. Reference Input .....	238
6.2.3.2. Task Space Positions.....	239
7.DISCUSSION AND CONCLUSION.....	242
REFERENCES.....	247
APPENDICES	
A.EQUIVALANCE TABLE FOR DATA STORE BLOCK AND USER DEFINED MATLAB FUNCTION LABELS IN THE SIMULATION MODEL .....	254
B.SIMULATION PARAMATERS .....	261
B.1. Simulation Number 1.....	261
B.2. Simulation Number 2.....	268
B.3. Simulation Number 3.....	275

## LIST OF FIGURES

### FIGURES

Figure 1.1 Unimate While Transporting Products [50].....	1
Figure 1.2 Viking 1 Lander Model [51].....	2
Figure 1.4 Snapshots of Bipedal Gait Simulation [5] .....	7
Figure 1.5 Foot Model by Gilchrist and Winter.....	8
Figure 1.6 Superimposed Simulation Results of a Stable Walking [7].....	8
Figure 1.7 Walking on Uneven Terrain in Yobotics [8] .....	9
Figure 1.8 Side and Front View of The Skeleton Model [14].....	9
Figure 1.9 Perturbation of a biped system into unviable and viable conditions [19] .....	13
Figure 1.10 Generated paths for CoM and head for varying step lengths [21].....	14
Figure 1.11 Posture Control Principle of Honda Robot P2 [37] .....	16
Figure 1.12 Different Walking Principles with Foot Toe and Sole [11].....	18
Figure 1.13 Hondo biped robots up to the present [53] .....	19
Figure 1.14 HRP-4C and HRP-2 [54] .....	20
Figure 1.15 Humanoid REEM-B [55].....	21
Figure 1.16 H7 climbing up stairs [56] .....	21

Figure 1.17 Humanoid robot HUBO2 [57] .....	22
Figure 1.18 WABIAN-2 knee-stretch walking [58].....	23
Figure 2.1: Overall Kinematic Structure of the Robot .....	26
Figure 2.2: Isometric View of Modeled Bodies .....	29
Fig. 2.3: Body Coordinate Systems for the Initial Posture.....	32
Figure 2.4: The Definition of Joint Space Variable $\theta_3$ .....	34
Figure 2.5: Dimensions of Body 1, Body 3, Body 5 and Body 7 .....	35
Figure 2.6: Dimensions of Body 2, Body 4, Body 6 and Body 8 .....	35
Figure 2.7: Dimensions of Body 9, Body 10, Body 11, Body 12, Body 13, Body 14, Body 15 and Body 16.....	36
Figure 2.8: Dimensions of Body 17, Body 18 and Body 19 .....	37
Figure 2.9 Dimensions of Body 20, Body 21, Body 22, Body 25 and Body 26....	38
Figure 2.10: Dimensions of Body 27 .....	38
Figure 2.11: Dimensions of Body 23 .....	39
Figure 2.12: Dimensions of Body 24 .....	39
Fig 2.13: Actuator Torques .....	42
Figure 3.1: Transition of Phases for a Biped Locomotion .....	44
Figure 3.2: The Definition of Desired CoM of Body 17.....	44
Figure 3.3: Labeling of Radius of Curvatures.....	45
Figure 3.4: Turning Direction Convention.....	48
Figure 3.5: The Definition of Finding Arc Centers Problem.....	48

Figure 3.6: Local Coordinate System $CS_{k+1}$ for Turning Leftward Direction .	52
Figure 3.7: Local Coordinate System $CS_{k+1}$ for Turning Rightward Direction	54
Figure 3.8: $\theta_{h,SSP_k}$ , $\Delta\theta_{PLN_k}$ and $\Delta\theta_{ADJ_k}$ for Turning Left During a LFFSSP and RFFDSP pair .....	56
Figure 3.9: $\theta_{h,SSP_k}$ , $\Delta\theta_{PLN_k}$ and $\Delta\theta_{ADJ_k}$ for Turning Right During a LFFSSP and RFFDSP pair .....	56
Figure 3.10: $\theta_{h,SSP_k}$ , $\Delta\theta_{PLN_k}$ and $\Delta\theta_{ADJ_k}$ for Turning Left During a RFFSSP and LFFDSP pair .....	57
Figure 3.11: $\theta_{h,SSP_k}$ , $\Delta\theta_{PLN_k}$ and $\Delta\theta_{ADJ_k}$ for Turning Right During a RFFSSP and LFFDSP pair .....	57
Figure 3.12: The definition of $\theta_{ri,k}$ and $\theta_{Rrot,k}$ during LFFSSP for Turning Left ...	64
Fig 3.13: The definition of $\theta_{li,k}$ and $\theta_{Lrot,k}$ during RFFSSP for Turning Left .....	64
Fig 3.14: The definition of $\theta_{ri,k}$ and $\theta_{Rrot,k}$ during LFFSSP for Turning Right.....	65
Fig 3.15: The definition of $\theta_{li,k}$ and $\theta_{Lrot,k}$ during RFFSSP for Turning Right .....	65
Figure 3.16: $R_{gen,k}(t)$ function.....	68
Figure 6.1: Overview of Top Level System.....	169
Figure 6.2: Part A of Top Level System .....	170
Figure 6.3: Part B of Top Level System.....	171
Figure 6.4: Part C of Top Level System.....	172
Figure 6.5: Part D of Top Level System .....	173
Figure 6.6: Phase Selector .....	174
Figure 6.7: LFFSSP Phase Shifting Decision .....	176

Figure 6.8: Expected Resultant Hip and Toe Point Locations for the Current Phase .....	177
Figure 6.9: Changing Phase Number in LFFSSP.....	178
Figure 6.10: Contacting Bodies Before Phase Change .....	179
Figure 6.11: Contacting Bodies After Phase Change.....	179
Figure 6.12: TD2 Function Output Definition for DES.....	180
Figure 6.13: Subsystem1 .....	181
Figure 6.14: Changing of Reset Values for the Initialization of $\bar{q}_{lower}$ at the Beginning of RFFDSP .....	182
Figure 6.15: RFFDSP Phase Shifting Decision .....	184
Figure 6.16: Overall View of Trajectory Definition .....	185
Figure 6.17: Main Subsystem of Trajectory Definition.....	186
Figure 6.18: Trajectory Definition DES or DES2.....	188
Figure 6.19: TD2 Function Output Definition for DES.....	189
Figure 6.20: Overall View of LFSSP.....	190
Figure 6.21: Part A of LFSSP .....	191
Figure 6.21: Part B of LFSSP .....	192
Figure 6.22: Overall View of LFSSP Kinematic Equations .....	193
Figure 6.23: Part A of LFSSP Kinematic Equations.....	194
Figure 6.23: Part B of LFSSP Kinematic Equations.....	195
Figure 6.24: Overall View of Optimum Command Accelerations Calculation LFFSSP .....	196

Figure 6.25: Part A of Optimum Command Accelerations Calculation LFFSSP	197
Figure 6.26: Part B of Optimum Command Accelerations Calculation LFFSSP	198
Figure 6.27: Part B of Optimum Command Accelerations Calculation LFFSSP	199
Figure 6.28: Computed Torque Control LFFSSP .....	200
Figure 6.29: Direct Dynamic Solution LFFSSP.....	201
Figure 6.30: Results of Dynamic Solutions .....	202
Figure 6.31: Overall View of Integration Subsystem .....	203
Figure 6.32: Part A of Integration Subsystem.....	204
Figure 6.33: Part B of Integration Subsystem.....	205
Figure 6.34: V-Realm Builder.....	206
Figure 6.35: Overall View of Visualization Subsystem.....	208
Figure 6.36: LFFSSP Calculation of Task Space Variables .....	209
Figure 6.37: LFFSSP Body Orientations .....	210
Figure 6.38: Positions.....	211
Figure 6.39: Translational Velocities .....	211
Figure 6.40: Angular Velocities .....	211
Figure 6.41: Translational Accelerations .....	212
Figure 6.42: Angular Accelerations .....	212
Figure 6.43: Virtual Reality Interface .....	213
Figure 6.44: Subsystem2 in Virtual Reality Interface.....	214
Figure 6.45: Subsystem in Virtual Reality Interface.....	215

Figure 6.46: Definition of Physical Parameters .....	215
Figure 6.47: Dimensions Definitions .....	216
Figure 6.48: Body Mass Definitions .....	217
Figure 6.49: Body Inertia Tensor Definitions .....	218
Figure 6.50: Reading and Arrangement of Several Values.....	219
Figure 6.51: Isometric View of Reference Trajectories for Parameter Set 1 .....	220
Figure 6.52: Reference Trajectories on X-Y Plane for Parameter Set 1 .....	220
Figure 6.53: Reference Trajectories on X-Z Plane for Parameter Set 1 .....	221
Figure 6.54: Joint Space Positions from $\theta_3$ to $\theta_6$ .....	221
Figure 6.55: Joint Space Positions from $\theta_7$ to $\theta_{10}$ .....	222
Figure 6.56: Joint Space Positions from $\theta_{11}$ to $\theta_{14}$ .....	222
Figure 6.57: Joint Space Positions from $\theta_{15}$ to $\theta_{171}$ .....	223
Figure 6.58: Joint Space Positions from $\theta_{18}$ to $\theta_{20}$ .....	223
Figure 6.59: Joint Space Positions from $\theta_{21}$ to $\theta_{24}$ .....	224
Figure 6.60: Joint Space Positions from $\theta_{25}$ to $\theta_{27}$ .....	224
Figure 6.61: Position of Mass Center of Body 17 with Its Reference Input .....	225
Figure 6.62: Position of Toe Point on Right Foot (Body 1) with Its Reference Input .....	225
Figure 6.63: Position of Toe Point on Left Foot (Body 2) with Its Reference Input .....	226
Figure 6.64: Actuator Torques from $T_1$ to $T_7$ in the Right Leg.....	226
Figure 6.65: Actuator Torques $T_9$ to $T_{15}$ in the Right Leg .....	227

Figure 6.66: Actuator Torques from $T_2$ to $T_8$ in the Left Leg.....	227
Figure 6.67: Actuator Torques from $T_{10}$ to $T_{16}$ in the Left Leg .....	228
Figure 6.68: Actuator Torques from $T_{17}$ to $T_{19}$ .....	228
Figure 6.69: Actuator Torques from $T_{20}$ to $T_{23}$ .....	229
Figure 6.70: Actuator Torques from $T_{24}$ to $T_{26}$ .....	229
Figure 6.71: Ground Reaction Forces for Body 1 and Body 3 .....	230
Figure 6.72: Ground Reaction Forces for Body 2 and Body 4 .....	230
Figure 6.73: Ground Reaction Moments.....	231
Figure 6.74: Ground Reaction Moments.....	231
Figure 6.75: Simulation Output for Simulation Number 1 in Virtual Reality Environment .....	232
Figure 6.76: Isometric View of Reference Trajectories for Parameter Set 2.....	233
Figure 6.77: Reference Trajectories on X-Y Plane for Parameter Set 2 .....	234
Figure 6.78: Reference Trajectories on X-Z Plane for Parameter Set 2 .....	234
Figure 6.79: Position of Mass Center of Body 17 with Its Reference Input.....	235
Figure 6.80: Position of Toe Point on Right Foot (Body 1) with Its Reference Input .....	235
Figure 6.81 Position of Toe Point on Left Foot (Body 2) with Its Reference Input .....	236
Figure 6.82: Simulation Output for Simulation Number 2 in Virtual Reality Environment .....	237
Figure 6.83: Isometric View of Reference Trajectories for Parameter Set 3.....	238

Figure 6.84: Reference Trajectories on X-Y Plane for Parameter Set 3 .....	239
Figure 6.85: Position of Mass Center of Body 17 with Its Reference Input .....	239
Figure 6.86: Position of Toe Point on Right Foot (Body 1) with Its Reference Input .....	240
Figure 6.87 Position of Toe Point on Left Foot (Body 2) with Its Reference Input .....	240
Figure 6.88: Simulation Output for Simulation Number 3 in Virtual Reality Environment .....	241

## LIST OF TABLES

### TABLES

Table 2.1: Body Numbering for Lower Bodies.....	27
Table 2.2: Body Numbering for Upper Bodies .....	27
Table 2.3: Basic Length Proportions.....	27
Table 2.4: Basic Mass Proportions.....	28
Table 2.5: Inertia Tensor Components of Bodies .....	30
Table 2.6: Explanation of Joint Space Variables .....	33
Table A.1: Equivalence Table.....	254

## LIST OF SYMBOLS

$(\vec{\quad})$ : Vector

$(\bar{\quad})$ : Column matrix

$(\hat{\quad})$ : Matrix

$(\dot{\quad})$ : Time derivative

$(\sim)$ : Skew symmetric matrix operator of a column vector  $(\bar{\quad})$

$(\quad)^T$ : Transpose of a matrix

$(\quad)^{-1}$ : Inverse of a matrix

$(\hat{\quad})_{m \times n}$ : Matrix with m rows and n columns

$\bar{0}_{m \times 1}$ : m by 1 column matrix which includes zero elements only

$\hat{0}_{m \times n}$ : m by n matrix which includes zero elements only

$\hat{C}^{(a,b)}$ : Component transformation matrix from Frame b to Frame a

$\vec{u}_i^{(k)}$ :  $i^{\text{th}}$  basis vector of reference frame K

$\bar{u}_i$ : Column matrix representation of  $i^{\text{th}}$  basis vector

$\bar{k}^{(a)}$ : Column matrix representation of vector  $\vec{k}$ , resolved in Frame a

$m_k$ : Mass of Body K

## **LIST OF ABBREVIATIONS**

ZMP: Zero Moment Point

CoM: Center of Mass

DOF: Degrees of Freedom

CoP: Center of Pressure

FZMP: Fictitious Zero Moment Point

CPG: Central Pattern Generators

LFFSSP: Left Foot Flat Single Support Phase

RFFSSP: Right Foot Flat Single Support Phase

LFFDSP: Left Foot Flat Double Support Phase

RFFDDSP: Right Foot Flat Double Support Phase

SSP: Single Support Phase

DSP: Double Support Phase

# CHAPTER 1

## INTRODUCTION

### 1.1.Motivation

“Robot” is a term introduced to lives of many people by the propagation of industrialization throughout the world. Although there does not exist a consensus about the exact definition of the term “robot”, there are various definitions made by The International Organization for Standardization, The Robotics Institute of America and many other robot societies. A machine which has the ability to accomplish complex tasks by sensing change in the working environment or following programmed instructions and reacting accordingly can be called as a robot.

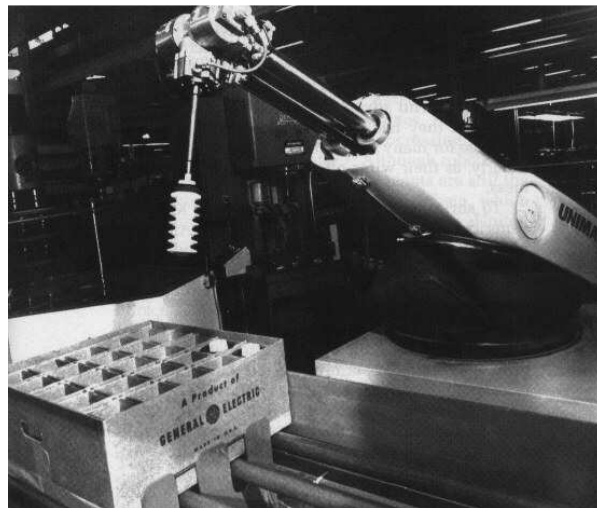


**Figure 1.1 Unimate While Transporting Products [50]**

Robots can be said to be the product of industrialization since they are mainly developed to carry out tasks which endanger human life, increase the production

rates of repetitive tasks and achieve a production quality that can only be reached by a staff with a long years of experience and intensive trainings. The first known robot ever built is “Unimate” by General Motors Company. The purpose of Unimate was to pick and carry hot die-castings from machines and to perform welding on automobile bodies [1].

Since the introduction of robot technology to the industry, the field of robotics leaped into the daily lives of humanity and became a constituent and a modifying factor to the human society. According to Xie, it is past time to consider robots as “merely mechanisms attached to controls” and suggests that robots have already become capable enough to carry out many critical works nowadays and are going to become much and much significant component in human societies like tutoring children, working as tour guides and private drivers, doing the shopping [2].

Nowadays robots have a very wide range of use, beyond the prediction of common people. In the space exploration program of Mars, lander or rover robots like Viking 1, Viking 2, Mars Pathfinder, etc. are sent to make several experiments and measurements instead of humans due to unpredictable, risky nature of the exploration procedure and many other reasons. Robots are used in situations endangering human lives like bomb diffuser robots, rescue-exploration and medical operations where physical and sensor aspects of humans become an obstacle or a limitation. There are immense amount of robot applications bringing a lot of benefits which makes the robot technology an integral part of the technological aspects of present day’s human society.



**Figure 1.2 Viking 1 Lander Model [51]**

With recent developments in robotics and increasingly wide applications of robots, new opportunities arise for daily lives of people where humanoid robot concept is one of these. Humanoid robots are expected to have overall resemblance to human body, autonomous operation, imitation of mental and physical capabilities of humans.

Almost everything artificially designed in Earth is compatible with humans. Humanoid robots with similar bodies and physical abilities will be able to use and benefit from all devices, which is a very efficient way to integrate capabilities of humanoid robots into the current human society with the least possible changes. Employment of humanoid robots into repetitive, arduous and dangerous jobs instead of humans will provide better life conditions and more spare time for humans to pursue their own interests. Furthermore, humanoid robots can carry out missions where shortcomings of biological structures prohibit human participation such as space exploration and colonization on planets. Moreover, interaction of humanoid robots with humans will be easier due to humans' tendency to set up interactions with physical forms fundamentally similar to humans.

With all expected benefits of robots being humanoid; a motivation exists to develop necessary methods, strategies and perform scientific researches to build an information base in order to deal with complications originated from the complexity of constructing humanoid robots with advanced abilities similar to humans. Biped locomotion of humanoid robots is one of those advanced abilities. Other than mental and sensor capabilities of humans, biped locomotion is possibly the most important ability to be imitated for the movement of humanoid robots.

Biped locomotion's most significant advantage over other kind of locomotion techniques is mobility. However, the level of mobility that can be achieved with biped locomotion is directly related with the ability to control this complex procedure. As Sano and Forusho admit; although biped locomotion is periodic with overall stability, it mainly employs unstable motions which result to control difficulties from the viewpoint of stability [3].

In order to minimize the fieldwork, trial-error procedure and cost during the construction of a biped robot; simulation studies are widely used. In other words, simulation studies are essential for the preliminary design process of biped robots. Observing possible outcomes for different design parameters and related design improvements, testing the efficiency and the performance of different control strategies, understanding the system behavior or gaining an engineering instinct for the corresponding complex dynamic system are some of potential benefits of simulation studies for the locomotion of biped robots.

## 1.2. Phases of Gait Cycle

Since “biological solutions” are key points for understanding and inspiration to the problem of designing humanoid robots capable of achieving biped locomotion, inspection of the gait cycle becomes essential [4].

The gait cycle begins with the initial contact of the foot and contact of the same foot to the ground again ends the gait cycle. The gait cycle is categorized in 2 main phases with a total of 8 subphases as shown in figure 1.3.

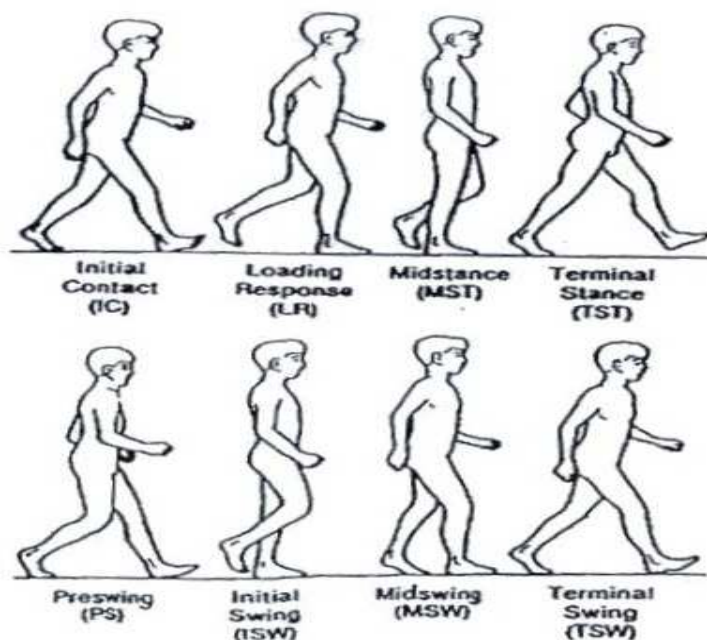


Figure 1.3 Gait Cycle [52]

Stance phases constitute phases between heel-strike and toe-off for the specified foot. Initial contact, loading response, mid-stance, terminal stance and preswing phases are grouped as stance phases in which most of the gait cycle (approximately 60 percent) takes place.

In initial contact phase, the knee extends and the heel of the right foot contacts the ground while ankle is considered to be approximately in neutral position. At the same time, the left leg is at the end of its terminal stance phase.

In loading response phase, the first double support condition of the gait cycle begins and ends with the contralateral toe leaving the ground. In this phase, absorption of impact forces due to the foot striking to the ground and weight transfer of the body from limb to limb occurs. In the mean time, preswing phase of the left leg ends.

Midstance phase begins when contralateral toe is off the ground and ends when the center of gravity of the body is over the contact area of supporting foot, which is right foot for figure 1.3. Toward the end of midstance phase, the knee and the ankle of the right leg return to their neutral positions. Meanwhile, the left leg moves forward in its midswing phase.

As the midstance phase ends, the terminal stance phase begins. During this phase, the heel of the supporting foot rises and loses its contact with the ground. The terminal stance phase ends when the left foot contacts the ground. During the terminal stance phase, the left leg proceeds in the terminal swing phase.

In the beginning of preswing phase, the initial contact of left foot with the ground occurs. This phase is the second double support condition during the gait cycle. The body weight is transferred from right leg to left leg. During the preswing phase, the knee flexes and the ankle plantarflexes significantly. Also, the toes of right foot begin to dorsiflex to deviate from the neutral position. The phase ends as the toe of right foot leaves the ground.

After the preswing phase, swing phases begin. Initial swing, midswing and terminal swing phases are grouped as swing phases. The swing phases account for approximately 40 percent of the gait cycle.

Initial swing phase begins when the toe of right foot is off the ground and continues until the right foot goes past the support foot in the forward direction. The right leg moves forward by increased hip and knee flexions. Meanwhile, the left foot is in its midstance phase.

After the initial swing phase, the midswing phase continues until the tibia of right foot becomes vertical. In this phase, the advancement of the right leg is achieved by additional hip flexion and the ankle begins to return its neutral position. During this phase, the left leg is at the end of its midstance phase.

The terminal swing phase is the last phase of the gait cycle. The terminal swing phase begins when the tibia is vertical and ends with the initial contact of right foot. The movement of the right leg is achieved by total knee extension and the ankle returns to its neutral position.

### **1.3. Review of Literature on Simulation Studies**

Different simulation studies throughout the world for the biped locomotion will be examined under this heading. Motivation of simulation studies for biped locomotion differs significantly depending on the application area like biomechanics studies, testing the performance of control strategy proposed, validating the efficiency or the applicability of trajectory generation methods and etc.

In a simulation study for the development of walking controllers, movements of some joints are restricted according physiological limitations of human body and foot is modeled as an ellipsoid providing a single point of contact with the floor as demonstrated in Figure 1.4. Also, spring damper systems regarding the penetration of foot into the floor and nonlinear spring damper systems modeling the total resistance to joint movement due to contact and deformation of tissues are used. Actuation in muscular structure is applied. Head, arms, upper and middle trunk are

reduced to a single body. Hence, it is a direct dynamic simulation with no prior information about walking kinematics [5].

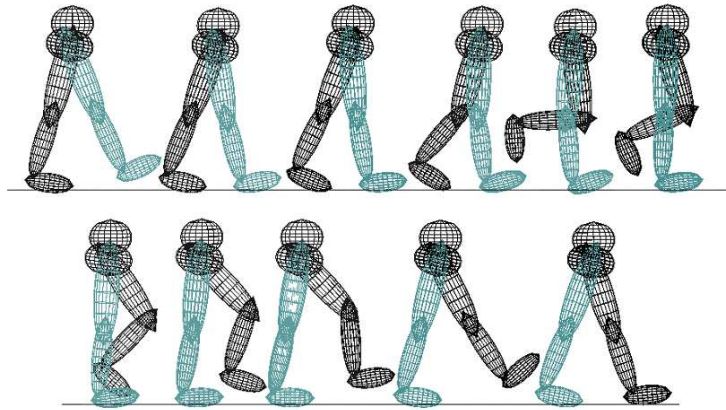


**Figure 1.4 Snapshots of Bipedal Gait Simulation [5]**

A simulation model for a normal human walking with a 9 segment 3D model which has 20 degrees of freedom is developed by Gilchrist and Winter. The purpose of this study is to build a realistic model for human gait capable enough to achieve predicted gait characteristics by using the system description, initial conditions and driving torques determined according to an inverse dynamic analysis of a normal walking trial. In this study, the foot is modeled in 2 segments with nonlinear springs and dampers, the midline of foot base is considered for modeling ground contact. Similarly, spring and damper elements are applied to knee and ankle to avoid nonphysiological motions. For the rest of joints, dampers are used to provide a smooth and realistic motion. However, the model succeeded to reflect the original measured kinematics in acceptable boundaries only for a slightly more than one step [6].

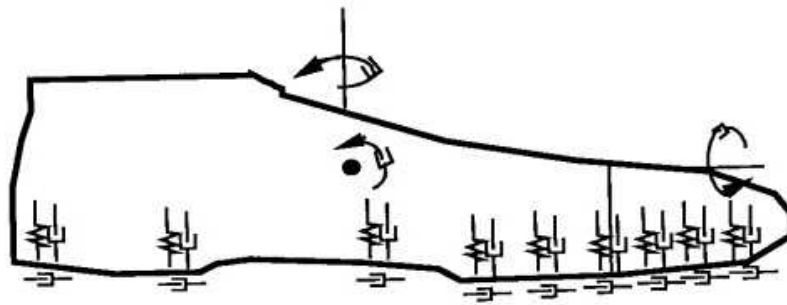


**Figure 1.5 Foot Model by Gilchrist and Winter**

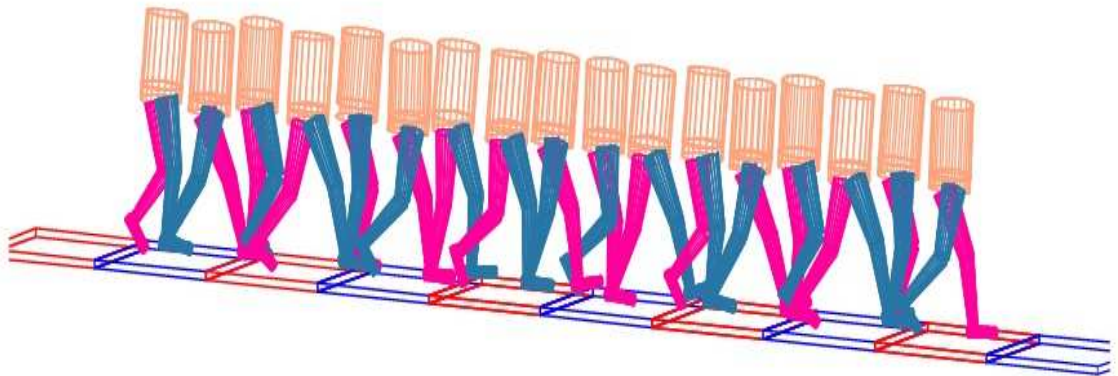


**Figure 1.6 Superimposed Simulation Results of a Stable Walking [7]**

In a different simulation study, a direct dynamics approach is employed to the analysis of human gait. The simulation model is prepared and executed in MSC.ADAMS environment. The presented model has 21 degrees of freedom with 16 segments where head and arm properties are distributed into trunk. In a similar fashion to some studies, ground reaction forces are based on spring and damper systems. Moreover, displacements of human body segments are measured to be used for the pattern of relative joint motions. Hence, actuator torques are found from torque equation formulations ensuring the realization of measured patterns. Because of considerably significant errors resulting from measurement

inaccuracies and post processing operations, resulting trunk motion for the gait pattern is to be controlled to prevent instability [7].

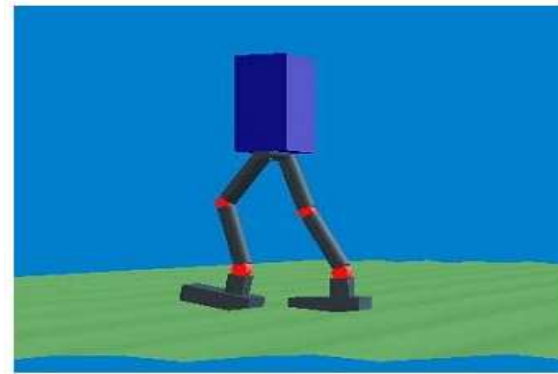


**Figure 1.7 Walking on Uneven Terrain in Yobotics [8]**

Another simulation study to investigate the performance of an anthropomorphic biped robot controller based on a dynamical walking algorithm is carried out on Yobotics Simulation Construction Set. A nonlinear model based on ground contact point and ground height is used for the generation of ground reaction forces. In this study, the gait cycle is divided into 6 phases such that a forward falling phase is devised as an additional phase to single support phases [8].

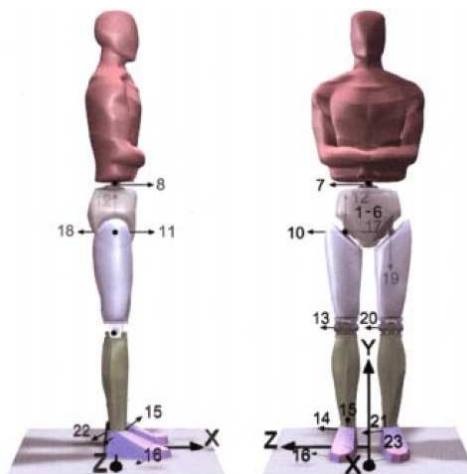


**Figure 1.8 Side and Front View of The Skeleton Model [14]**

For the dynamic optimization problem of consumed metabolic energy per unit distance traveled, a simulation study with a 10 segment, 23 degrees of freedom biped model is performed. Actuation of the biped model is achieved by a total of 54 modeled muscles. Head, arms and torso are lumped into a single rigid body. Also, each foot is modeled in 2 segments and foot ground interaction is modeled by spring and damper components scattered to corners of the hindfoot and distal end of the toe part. The solution of optimization problem is produced after a computation effort equivalent to approximately 10000 hours [14].

To present the effectiveness of proposed locomotion controller, a simulation model for a planar 5 link biped robot is built. The dynamic equations of the biped robot are obtained by SD/FAST software. A linear spring damper system is used to model ground reaction forces [17].

A simulation model for the inspection of planar humanoid gait is built by Özyurt. The kinematic configuration allows 5 DOF for each leg, where the simulation model has 10 DOF in total. Head, arms and torso are lumped into a single body. Also, there exists 2 types of foot model where flat foot is lumped into a single body and swinging foot consists of 2 segments. The interaction between foot and ground is modeled by kinematic constraints [68].

Modeling of the biped locomotion has a significant importance on determining the practical balance between computational efficiency and complexity of mathematical models defining physical phenomenon involved in the simulation. Because of this reason, there exist various approaches or assumptions involved in the simulation depending on the application area, computer resources and feasibility.

Although the division of biped locomotion into various phases and the extent of assumptions for defined phases vary, biped locomotion can be categorized in 2 basic phases. All phases including the contact of a single and both foot with ground can be grouped into respectively single support and double support phases. However, physical details of humanoid biped locomotion like heel contact, foot rolling on heel and toe are implemented or not into the simulation by considering

area of usage, control strategy, hardware capabilities, task space requirements and planned walking speeds. Regarding physical details involved and their role or significance in humanoid biped locomotion, simulation studies focusing on specific phases are performed [9, 10, 11, 12, 15]. For instance, the performance of the control strategy on level ground for slide mode control during double support phases by considering double impact occurring at the heel strike is investigated in a simulation study presented by Mu and Wu [9]. Similarly, energy efficiency of the phenomenon that is heel rising of the stance foot and following the rotation of stance foot about toes for fast walking is investigated by consecutive simulation studies [12].

The foot and its contact with ground is an additional modeling problem. Especially for simulation studies analyzing the human walking by building realistic models as much as possible, a significant care is given to modeling of the foot; since simulation studies for biomechanics involve inverse dynamics problem for finding resulting actuation torques of muscles, simulation models to understand muscle actuation patterns [14], finding metabolically efficient gaits [13,14], forward dynamics simulations to assist orthotic-prosthetic designs and rehabilitation consultations [16]. Various approaches are adapted for modeling ground contact and kinematic structure of the foot like models depending on spring and dampers, special contact modeling formulations, fixed contact models and segmented foot models.

Various comprehensive software packages like MATLAB, MSC.Adams, DynaFlexPro, SD/FAST are utilized for their mathematical libraries, mathematical modeling and simulation tools.

#### **1.4. Review of Literature on Control Strategies**

Developing control strategies for biped locomotion of humanoid robots to maintain a sustainable and rhythmic locomotion robust to unpredictable and unmodeled internal and external system dynamics, ensuring energy efficiency and computational feasibility, sufficiently generalized to handle all kinds of occasions and purposes, realistic enough to utilize current level of engineering

instrumentations, keeping construction costs in reasonable boundaries is a challenging and popular engineering problem investigated by many researchers throughout the world.

Since a humanoid robot during the biped locomotion is not fixed to the ground; variety of possible biped locomotion motions are restricted according to ground conditions, the design of supporting foot, actuator and controller capabilities, assumed stability criterion. Because of this reason, the generation of proper reference trajectories for task space or joint space variables is considered to be the first essential step for controlling biped locomotion. In other words, unrealistic or inconvenient reference trajectories can possibly lead to toppling over, sliding and collisions.

Studies about generating reference trajectories can be divided into 2 categories according to the type of use. Online reference trajectory generation methods are expected to respond to changing conditions in the working environment by ensuring the stability criterion imposed and compensating side effects sourced from tracking errors of the controller or disturbances against endangered postural stability.

In a study on walking planning for biped robots, a gait trajectory is generated by an artificial vector field based on an electric field according to predictive simulations performed online for 400 milliseconds ahead. The stability criterion is based on ZMP (Zero Moment Point) and the stability is ensured according to present and predicted states, then the improvement of gait parameters are done by updating the artificial vector field [18].

In a study presented by Wieber and Chevallereau, the problem of adapting reference trajectories to maintain stability under small disturbances is investigated. The viability condition, a condition for a system to realize a movement without getting inside a set of positions considered as fallen, for states is defined. With the adaptation of parameters used in the trajectory definition, the magnitude of the external disturbance force that can be compensated without falling is increased [19].

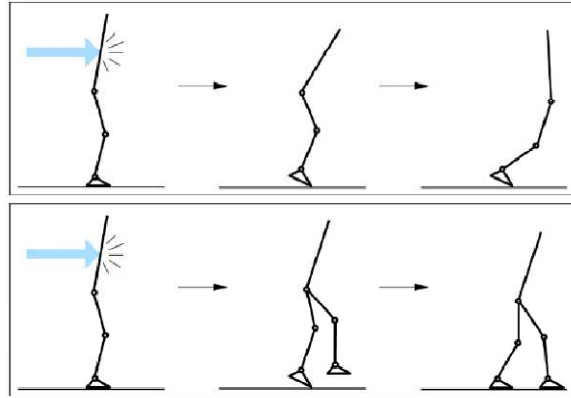


**Figure 1.9 Perturbation of a biped system into unviable and viable conditions**  
[19]

Most of trajectory generation methods for controlling biped motion can be considered as offline methods. These methods involve careful consideration of various stability criteria and margin selections, actuator and joint limitations, energy efficiency, ground conditions, division of biped locomotion into phases and modeling of biped locomotion phases, locomotion specifications or requirements, presence of adequate mathematical tools.

As an example, a method which is able to produce hip trajectory by iterative computation for planning walking patterns for biped robots is presented. Ground conditions, ZMP based stability, the correlation between actuator specifications and walking is considered for the generation of reference trajectories in this work. The determination of correlation between actuator requirements and the trajectory enables the selection of trajectories with small actuator torques and joint velocities [20].

A trajectory generation method is developed to build a reference trajectory database for biped locomotion in a practical time. The suggested method optimizes necessary control torques based on an energy based cost function, ensures the postural stability by evaluating ZMP and friction conditions of the support foot and additionally keeps joint angles and control torques in given boundaries. The

generated trajectories are intended to be linked together to support the adaptation of step lengths to changing conditions [21].

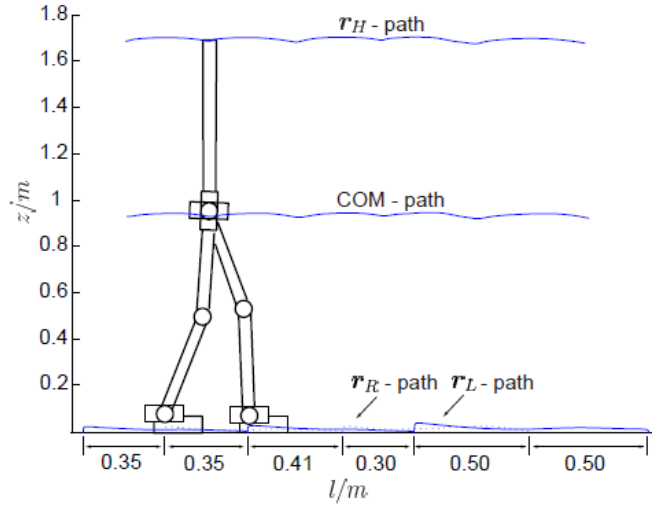


**Figure 1.10 Generated paths for CoM and head for varying step lengths [21]**

In a different study, gait generation is investigated as an optimization problem with multiple objectives. The optimization problem is based on ZMP displacement, required actuator torques, joint angle and actuator boundaries, stability and state feasibility. Trajectory selection among various trajectories satisfying optimization criteria are carried out according to the least ZMP displacement and actuator torque requirement conditions. To handle the complex optimization problem, EDA (Estimation of Distribution Algorithms) using spline-based probability function with Q learning based updating rule is applied [22].

The stability approach is a distinguishing element for a reference trajectory generation method. The static stability (or balance) criterion which requires the projection of center of mass of the system on the ground to stay in the convex hull shaped from support area or areas is practiced in various studies [26, 32]. Since the static stability criterion is a very conservative approach, attainable walking speeds with this approach is greatly limited. Because of this deficiency, generating humanlike gaits by using static stability criterion is a slight possibility. Therefore, dynamic stability criteria are widely used in order to evaluate the feasibility of

generated trajectories. Zero Moment Point criterion and related stability margin are frequently used to prevent the rotation of support foot under unpredictable disturbance forces [18, 20, 21, 22]. Although there exists a misconception about the definition of ZMP and its difference from CoP (Center of Pressure); ZMP, CoP and FZMP (Fictitious ZMP) or FRI (Foot Rotation Indicator) concepts are investigated in various explanatory studies [23, 24, 25]. Moreover, ZMP based methods mainly depend on the accuracy of the dynamic model. The deficiency of most ZMP based trajectory definition methods is sourced from the fundamental requirement that either rolling of the support foot is not tolerated or ZMP criteria to the foot rotation is not applicable due to the movement of contact boundary which restricts the level of resemblance to humanlike gaits and walking speeds. Furthermore, generating high accelerations for massive hips in order to keep ZMP in a reasonable boundary during phase transitions may result to energy inefficient gaits. Another approach to generate dynamically stable reference trajectories is to model the biped robot as an inverted pendulum [28, 29, 30, 33]. The advantage of this approach is enabling to generate reference trajectories using limited information of the robot dynamics. On the other hand, the tracking of this kind of reference trajectory relies on robust feedback control due to approximated robot dynamics. Additionally, the inverted pendulum approach is not suitable for tasks requiring precise foot placement; to cope with this limitation a method involving the combination of ZMP and inverted pendulum approach is devised [31].

Since a great majority of humanoid robots have 6 degrees of freedom for foot with respect to the hip, joint trajectories of lower bodies for given reference trajectories of the foot and the hip in task space can be derived uniquely. Therefore, a common and simple method to control a biped robot is to design a control system to track these derived joint trajectories [39].

In some studies, central pattern generators (CPGs) which are thought to be the fundamental structure responsible for all rhythmic motions of animals are utilized [17, 34, 35, 36]. In this method, different rhythmic motions are generated by tuning parameters of the neural oscillator network constituting the central pattern generator. However, tuning of parameters for a realizable biped locomotion and different environmental conditions is a computational burden which complicates

the implementation for real time applications. Various methods are applied in order to tune CPG parameters like Genetic Algorithms (GAs) [36], Reinforcement Learning (RL) [34], Policy Gradient Methods [35]. Ability to produce stable periodic gait patterns, modify the locomotion characteristics like locomotion speed or direction by adjusting various parameters are some advantages of CPGs. However, designing CPG controllers and adjusting CPG parameters to adapt changing conditions while ensuring a stable robot system is difficult to implement for autonomous biped robots.

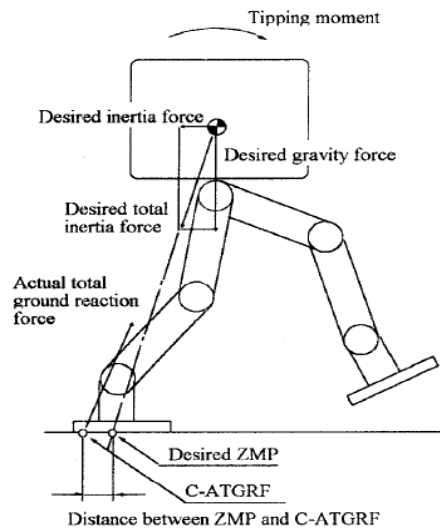


**Figure 1.11 Posture Control Principle of Honda Robot P2 [37]**

As a practical example, the biped locomotion control for Honda Humanoid Robot P2 can be given. The control algorithms implemented on Honda P2 are grouped in 3 segments as Ground Reaction Force Control, Model ZMP Control and Foot Landing Position Control. Ground Reaction Force Control tries to control the location of the point on ground where all measured reaction forces induce zero moment (called C-ATGRF in this study) by adjusting support foot's rotation in single support phases and lowering or lifting front or rear foot in double support phases to generate a recovering moment preventing tipping over. Model ZMP Control changes the position of desired ZMP to a much suitable position by inducing strong acceleration on the upper body to change the direction of total

inertial forces, thus generating a recovering moment. Foot Landing Position Control compensates the long term effect of modified upper body position sourced from increased accelerations of Model ZMP Control by adjusting stride length or moving foot landing position to a much ideal location for bringing back the humanoid robot to its desired walking pattern [37].

A control strategy adaptive to various terrains is introduced, which produces actuator commands equivalent to alpha excitation signals in an organic muscle. A set of intermediate states are supplied to the controller instead of reference trajectories where the arrival time information of given intermediate states is not provided. The speed of the system is indirectly adjusted by the velocity given states. Hence, adapting to a different motion is performed by changing intermediate states being supplied to the controller. The system is actuated by 16 muscular actuators including the related muscular actuation model. The transition from the present state to the next state is achieved by making the next state an equilibrium point while present state is continuously attached [38].

In a different study, offline generated optimal trajectories are controlled by local PD joint controllers. Moreover, required modifications in task space trajectories are calculated in order to decrease the difference between desired and real stability condition. Then, necessary deviations in joint space trajectories are determined by an online compensation algorithm depending on the modified task space and a predefined hip trajectory deviation pattern is applied by a heuristic compensation algorithm [39].

In order to investigate different control strategies employed in the biped locomotion, a comprehensive theoretical study is carried out. In this study, different control strategies which are grouped as high level and low level controllers for various scenarios are tested. Advantages and insufficiencies of various control strategies are stated, their comparisons are done [69].

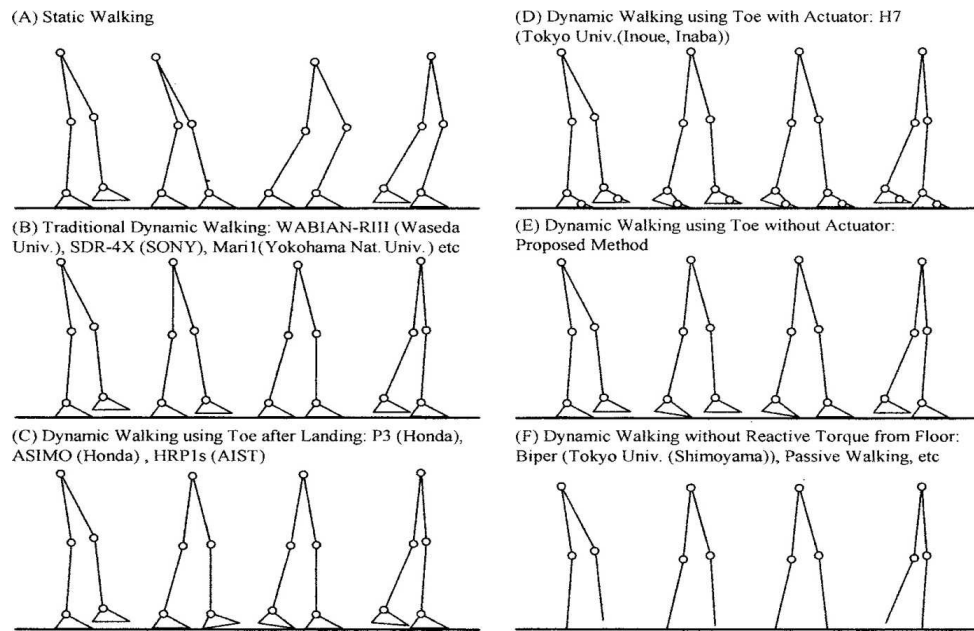


**Figure 1.12 Different Walking Principles with Foot Toe and Sole [11]**

In order to avoid the speed limitation imposed by full foot contact assumption, a control strategy utilizing computed torque control method which considers the point contact of support foot during locomotion phases is introduced. The proposed method is able to track the desired circular path given for CoM and the heel of swing leg, while the support foot is rotating on toe point and the system is underactuated [11].

In a different study, computed torque control method with an optimization algorithm to supply command accelerations based on a quadratic cost function including predicted errors is used [68].

There exist several studies concentrating on specific locomotion phases [9, 10, 40, 41]. For instance Liu, Li and Xu investigated the control problem of biped locomotion for the double support phase considering external disturbances and parametric uncertainties. Fuzzy neural network controller with quadratic stabilization and  $H_\infty$  approach to ensure the robustness is implemented. Fuzzy neural network controller consists of nonlinear dynamic system learning,  $H_\infty$

control for close loop stability and variable structure control components to deal with uncertainties [10].

### 1.5. Review of Literature on Humanoid Robots

By the realization of prospective future of humanoid robots in human society, studies on building mechanical systems able to move like humans are intensified. It is possible to say that finding satisfactory solutions to the engineering problem of designing systems capable of performing human movement is considered to be the first and critical step in building humanoid robots. Throughout the world, experimental biped robots are built to test the efficiency or feasibility of biped locomotion control methods.



**Figure 1.13 Honda biped robots up to the present [53]**

Honda Motor Company invested in research and development studies for building a humanoid robot more than 20 years. Up to the present time, a total of 11 biped robots are constructed. After building 7 experimental robots on biped locomotion, production of robots which can interact with the environment and relatively more humanoid has started. By continuous development efforts, the maximum movement speed of Honda biped robots reached to 6 km/h from 0.25 km/h. Moreover, significant amount of both size and weight reduction in humanoid robots is achieved as such from 175 to 54 kg weight and from 195 to 130 cms

height. The most advanced humanoid robot Honda presented is called as ASIMO which is the acronym of **A**dvanced **S**tep in **I**nnovative **M**obility. The goal of operating ASIMO for a great variety of applications leads to 34 degrees of freedom. Several abilities of ASIMO can be listed as creating walking patterns in real time, changing foot placement and turning angle at will, moving smoothly without transitional pauses, walking while each arm carrying 2kg weights. Placements of joints, joint movement ranges, center of gravity of bodies are determined regarding measurements on humans. Joint angle sensors at each joint, 6-axis force sensor at each foot, a speed sensor and a gyroscope are employed. [42]



**Figure 1.14 HRP-4C and HRP-2 [54]**

In the context of Humanoid Robots Project, several humanoid robots (HRP series) are produced. The most advanced humanoid robot of these HRP series is HRP-4C at the present. HRP-4C is implemented with walking algorithms experimented on HRP-2 and benefits from the patented technology of Honda Motor Company. Its significant features are being purposefully designed to have human appearance and mimics, weight lightness, utilizing measured human walking patterns. [43]



**Figure 1.15 Humanoid REEM-B [55]**

A different humanoid robot named as REEM-B designed by Pal Technology Robotics is able to maintain maximum walking speed of 1.5 km/h, carry up to 12 kg weights while walking, walk upstairs or downstairs, follow a predefined trajectory. [44]



**Figure 1.16 H7 climbing up stairs [56]**

H7 with 30 degrees of freedom and 57 kgs weight is designed by University of Tokyo to be used as an experimental humanoid robot for biped locomotion,

autonomous operation and human interaction research areas. The operating system of control computer in H7 is Linux based which enables to implement various qualified development tools and libraries. [45]



**Figure 1.17 Humanoid robot HUBO2 [57]**

The Korea Advanced Institute of Science and Technology developed several biped robots for researching biped locomotion and implementing various methods . The last designed and more advanced HUBO2 can move at maximum speed of 3 km/h and weighs 45 kgs. [46, 47]



**Figure 1.18 WABIAN-2 knee-stretch walking [58]**

A different humanoid robot development study is being carried out by Waseda University. WABIAN-2R which is the last robot in series has 7 degrees of freedom for each leg different than popular humanoid robots, in order to provide more independence on knee extension and flexibility to produce smoother gaits. Furthermore, the significance of pelvis motion for the human gait is taken into consideration; therefore a waist mechanism with 2 degrees of freedom is introduced. By avoiding the common bent-knee gait with the introduction of specified developments, more energy efficient walking is achieved. [48, 49]

### **1.6. Scope of Thesis**

The main objective of this study is to create a simulation environment for the investigation of biped locomotion of humanoid robots in 3D space with the control strategy proposed.

Basic physical properties and kinematic configuration of the humanoid robot is introduced in chapter 2. The procedure to determine the physical parameters is

explained. Also the definition of joint space variables, body coordinate systems, basic physical dimensions, actuator torques and conventions used throughout the thesis are presented.

In chapter 3, variables defining the characteristics of reference motion for the humanoid robot are introduced. In addition to this, the calculation of reference trajectories is explained.

In chapter 4, derivation of kinematic equations and dynamic equations are shown. The assumptions used for the mathematical model of locomotion phases are specified. Also the direct dynamic solution and additional operations for the transition from single to double support phases are explained.

Chapter 5 includes the explanation of the control strategy used for the simulation of biped locomotion. The calculation procedure of optimum command accelerations and the application of computed torque control method for all locomotion phases are expressed.

In chapter 6, the construction of a simulation environment by the commercial mathematical tool MATLAB and MATLAB.Simulink is explained. After describing the basic logic behind the simulation, simulation results for different sample reference inputs are demonstrated.

In chapter 7, the thesis is discussed and evaluated. Insufficiencies of the simulation model and suggestions for the future work are indicated.

## CHAPTER 2

### PHYSICAL MODELLING

The physical model, which all simulations of the thesis study are based on, is explained in this chapter. Since the mechanical design of a biped robot is not in the scope of this thesis, basic parameters defining physical properties are identified by considering popular humanoid robots, geometrical and weight proportions of human body. Basic properties of the physical model used in the thesis can be listed as:

- All joints of the physical model are revolute and accompanied with actuators. Namely, all joints present on the model are controlled actively by torque actuators.
- Possible physical properties of actuators are not distributed to or included in adjacent bodies
- All joints are assumed to be able to perform full rotation. In other words, any mechanical systems to impose limitations on joint positions are not existent.
- All joints are assumed to be frictionless and not to have any damper elements.
- The trunk is divided into 2 segments as uppertrunk and lowertrunk bodies. Forearm and arm is lumped into a single arm body.
- The model consists of 13 bodies in total where there are 4 bodies for each leg, 2 bodies for the chest, one body for each arm and one body for the head.
- A revolute joint for the toe part of the foot, a spherical joint for the ankle, a revolute joint for the knee, a spherical joint between the thigh and lowertrunk body, a spherical joint between lowertrunk and uppertrunk

body, a universal joint for the shoulder and a spherical joint for the neck are used, which leads to a total of 26 degrees of freedom system as shown in Figure 2.1.

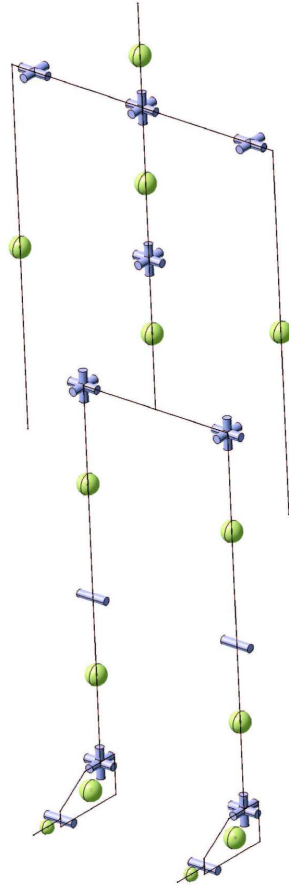


**Figure 2.1: Overall Kinematic Structure of the Robot**

Bodies are numbered in an orderly fashion such that numbering of bodies starts from the ground. Odd numbers for bodies of the right leg and even numbers for bodies of the left leg are used, in order to avoid any confusion. After this point, bodies are referred with their body numbers in the thesis. Excluded body numbers in Table 2.1 and Table 2.2 are virtual bodies which are massless, dimensionless and used for modeling kinematic relations between bodies having universal or spherical joints.

**Table 2.1: Body Numbering for Lower Bodies**

	Right Leg	Left Leg
Foot-Toe Body	1	2
Foot-Main Body	3	4
Shank	9	10
Thigh	11	12

**Table 2.2: Body Numbering for Upper Bodies**

	Body Number
Lowertrunk (Hip)	17
Uppertrunk	20
Left Arm	24
Right Arm	23
Head	27

Total body mass and the height is chosen as 55 kg and 1.6 m by considering popular and most advanced humanoid robots in the world [42, 43, 44, 45, 46, 47, 48, 49]. After the selection of these basic parameters, body masses and several basic body dimensions are determined by utilizing body weight and measurement proportions obtained in a medical study [59].

Mass ratio of uppertrunk body (Body 20) to lowertrunk body (Body 17) is taken to be 1 for simplicity. Mass proportions of the thigh (Body 11, Body 12) and the shank (Body 9, Body 10) with respect to the total lowerlimb mass are assumed to be the same as their length proportions to the total lowerlimb length with an additional assumption of 15 percent bias for the thigh.

**Table 2.3: Basic Length Proportions**

	Ratio to Body Height	Length (mm)
Upperlimb ( $l_{23z}$ , $l_{24z}$ )	0.4426	708
Lowerlimb	0.5001	800
Trunk	0.3670	587
Head ( $l_{27}$ )	0.1500	240 ( <i>201 is used</i> )
Lowertrunk	$0.3670 \times 0.50$	294
Uppertrunk	$0.3670 \times 0.50$	294
	Ratio to Lowerlimb	Length (mm)
Thigh ( $l_{11}$ , $l_{12}$ )	0.5147	412
Shank ( $l_9$ , $l_{10}$ )	0.4023	322
Foot Length	0.2830	226
Foot Height	0.0970	78

**Table 2.4: Basic Mass Proportions**

	Ratio to Total Mass	Mass (kg)
Body 23 ,Body 24 (Upperlimb or Arm)	0.0482	2.651
Lowerlimb (Leg)	0.1426	7.843
Body 27 (Head)	0.0856	4.708
Trunk	0.5336	29.348
Body 11, Body 12 (Thigh)	$(0.5147+0.15)\times 0.1426(=0.0948)$	5.213
Body 9, Body 10 (Shank)	$(0.4023-0.15)\times 0.1426(=0.0360)$	1.979
Body 1, Body 2 (Foot-Toe)	$(1-0.5147-0.4023)\times 0.1426\times 0.20(=0.0024)$	0.130
Body 3, Body 4 (Foot-Main)	$(1-0.5147-0.4023)\times 0.1426\times 0.80(=0.0096)$	0.521

After the determination of basic parameters, solid modeling of bodies is done to find realistic enough inertia tensor matrices as shown in table 2.5. Then, CoM of bodies and inertia tensor matrices with respect to the body reference frames at CoMs are found by a commercial CAD (computer aided drawing) program CATIA V5.R16. Bodies of upperlimb, lowerlimb and head are assumed to be in shape of truncated cones or cylinders. An isometric view of modeled bodies is shown in Figure 2.2.

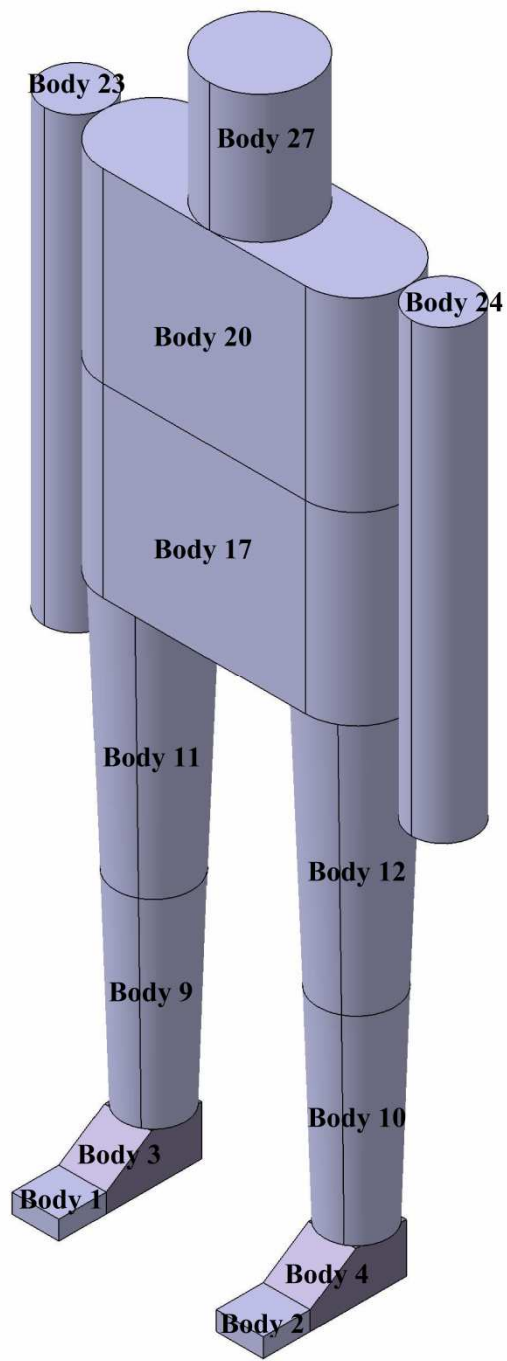


**Figure 2.2: Isometric View of Modeled Bodies**

**Table 2.5: Inertia Tensor Components of Bodies**

	Inertia Tensor Components ( $J_{xx}, J_{yy}, J_{zz}, J_{xy}, J_{xz}, J_{yz}$ ) ( $\text{kg}\cdot\text{m}^2$ )
Body 1, Body 2	0.00007 0.00007 0.00012 0.00000 0.00000 0.00000
Body 3, Body 4	0.00048 0.00100 0.00100 0.00000 0.00012 0.00000
Body 9, Body 10	0.01800 0.01800 0.00300 0.00000 0.00000 0.00000
Body 11, Body 12	0.07900 0.07900 0.01200 0.00000 0.00000 0.00000
Body 17, Body 20	0.35300 0.13500 0.27700 0.00000 0.00000 0.00000
Body 23, Body 24	0.11200 0.11200 0.00300 0.00000 0.00000 0.00000
Body 27	0.02300 0.02300 0.01500 0.00000 0.00000 0.00000

All body coordinate systems are orthogonal right handed coordinate systems and located on the proximal end of bodies. The initial robot posture where all joints are

at zero positions is shown in Figure 2.3. Body coordinates are arranged in such a way that all body coordinates have the same orientation at the initial posture with respect to inertial frame fixed to the ground. Hence, Denavit- Hartenberg convention for describing kinematic relations is not employed [60]. The position of the inertial frame (or Frame 0) and its orientation are shown in Figure 2.3.

Özgören's notation for describing vectors, matrices and exponential rotation matrices is applied throughout the thesis [67]. Therefore, conventions used for describing basic physical features are explained as shown below:

$O_k$ : Point of origin of the body coordinate system or the reference frame for Body K

$\vec{c}_k$ : Mass center vector of Body K with initial point as  $O_k$  and terminal point as CoM of Body K

$\vec{l}_{k,z}$ : Distance vector between body coordinate systems of Body K and Body Z with initial point as  $O_k$  and terminal point as  $O_z$

$\vec{u}_i^{(k)}$ :  $i^{\text{th}}$  basis vector of reference frame K

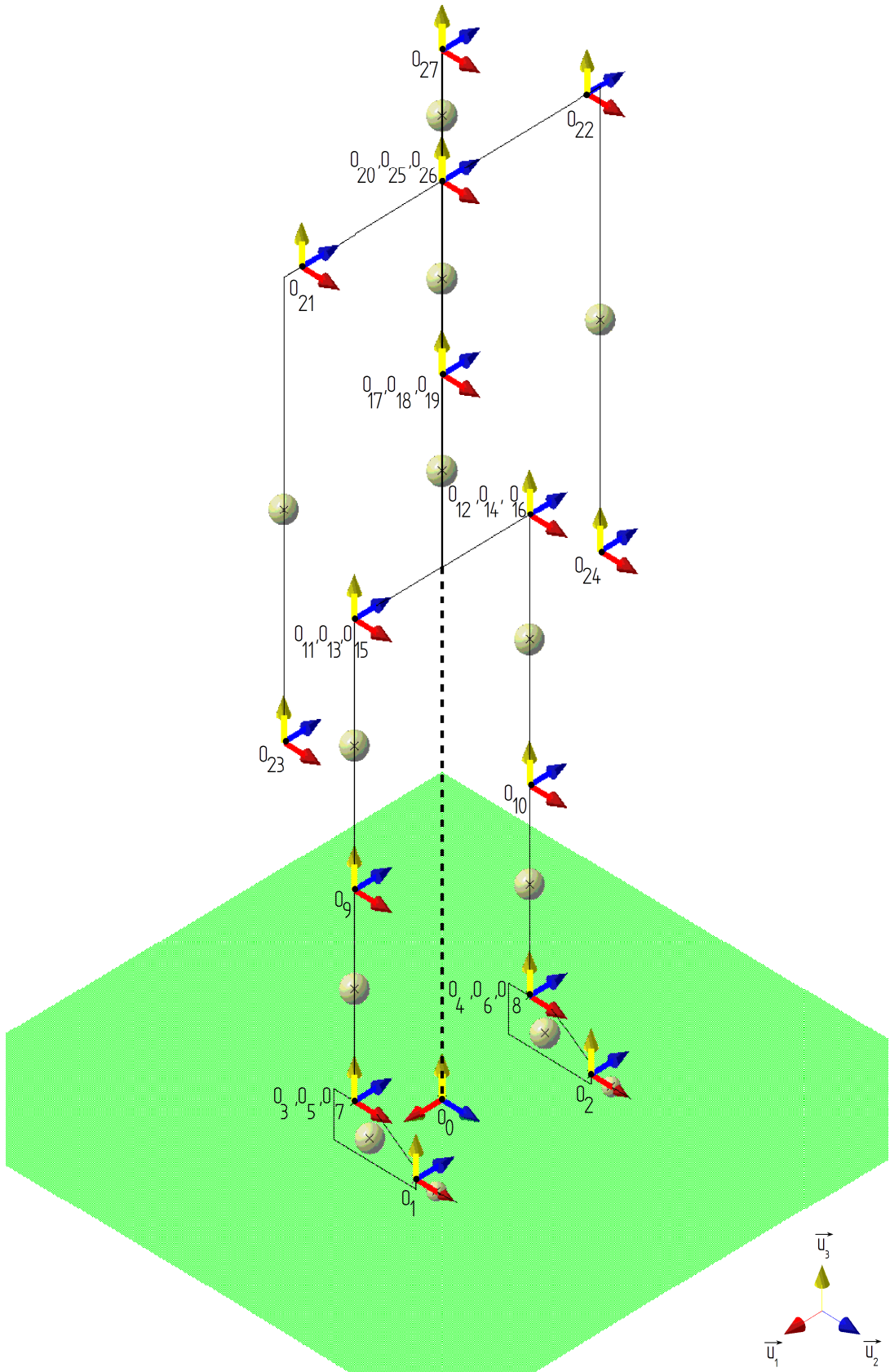


**Fig. 2.3: Body Coordinate Systems for the Initial Posture**

Variables indicating joint space positions are explained in Table 2.6.

**Table 2.6: Explanation of Joint Space Variables**

$\theta_3:$	Rotation of Reference Frame	3	with respect to Reference Frame	1	about	$\vec{u}_2^{(1)}$
$\theta_4:$		4		2		$\vec{u}_2^{(2)}$
$\theta_5:$		5		3		$\vec{u}_2^{(3)}$
$\theta_6:$		6		4		$\vec{u}_2^{(4)}$
$\theta_7:$		7		5		$\vec{u}_3^{(5)}$
$\theta_8:$		8		6		$\vec{u}_3^{(6)}$
$\theta_9:$		9		7		$\vec{u}_1^{(7)}$
$\theta_{10}:$		10		8		$\vec{u}_1^{(8)}$
$\theta_{11}:$		11		9		$\vec{u}_2^{(9)}$
$\theta_{12}:$		12		10		$\vec{u}_2^{(10)}$
$\theta_{13}:$		13		11		$\vec{u}_2^{(11)}$
$\theta_{14}:$		14		12		$\vec{u}_2^{(12)}$
$\theta_{15}:$		15		13		$\vec{u}_1^{(13)}$
$\theta_{16}:$		16		14		$\vec{u}_1^{(14)}$
$\theta_{17,r}:$		17		15		$\vec{u}_3^{(15)}$
$\theta_{17,l}:$		17		16		$\vec{u}_3^{(16)}$
$\theta_{18}:$		18		17		$\vec{u}_2^{(17)}$
$\theta_{19}:$		19		18		$\vec{u}_3^{(18)}$
$\theta_{20}:$		20		19		$\vec{u}_1^{(19)}$
$\theta_{21}:$		21		20		$\vec{u}_1^{(20)}$
$\theta_{22}:$		22		20		$\vec{u}_1^{(20)}$
$\theta_{23}:$		23		21		$\vec{u}_2^{(21)}$
$\theta_{24}:$		24		22		$\vec{u}_2^{(22)}$
$\theta_{25}:$		25		20		$\vec{u}_3^{(20)}$
$\theta_{26}:$		26		25		$\vec{u}_2^{(25)}$
$\theta_{27}:$		27		26		$\vec{u}_1^{(26)}$

As an example, the definition and the positive sign convention of joint space variable  $\theta_3$  are shown in Figure 2.4. The positive sign conventions for other joint space variables are similar to the shown example.

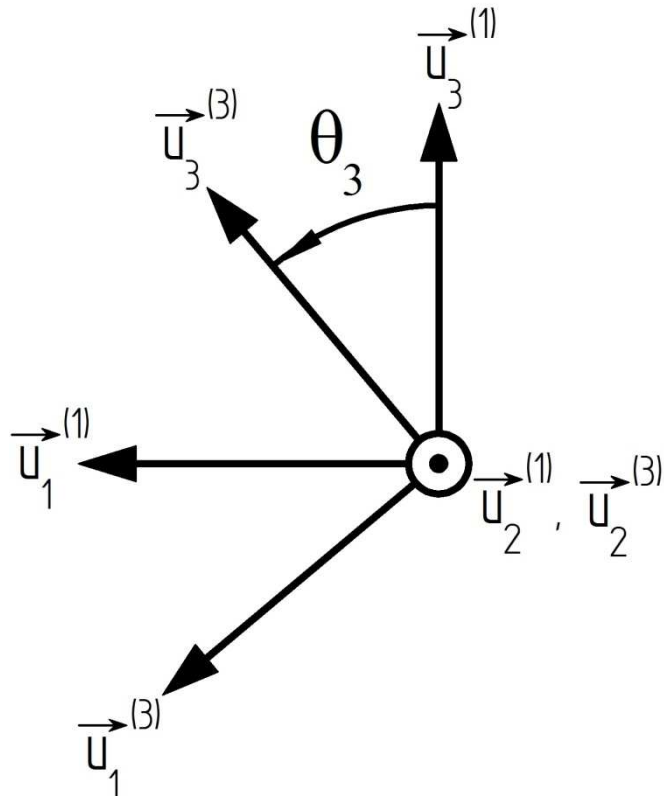


**Figure 2.4: The Definition of Joint Space Variable  $\theta_3$**

The definition of scalar parameters for describing basic physical features of bodies are shown in

- Figure 2.5 for Body 1, Body 3 , Body 5 and Body 7
- Figure 2.6 for Body 2, Body 4 , Body 6 and Body 8
- Figure 2.7 for Body 9, Body 10, Body 11, Body 12, Body 13, Body 14, Body 15 and Body 16
- Figure 2.8 for Body 17, Body 18 and Body 19
- Figure 2.9 for Body 20, Body 21, Body 22, Body 25 and Body 26
- Figure 2.10 for Body 27
- Figure 2.11 for Body 23
- Figure 2.12 for Body 24

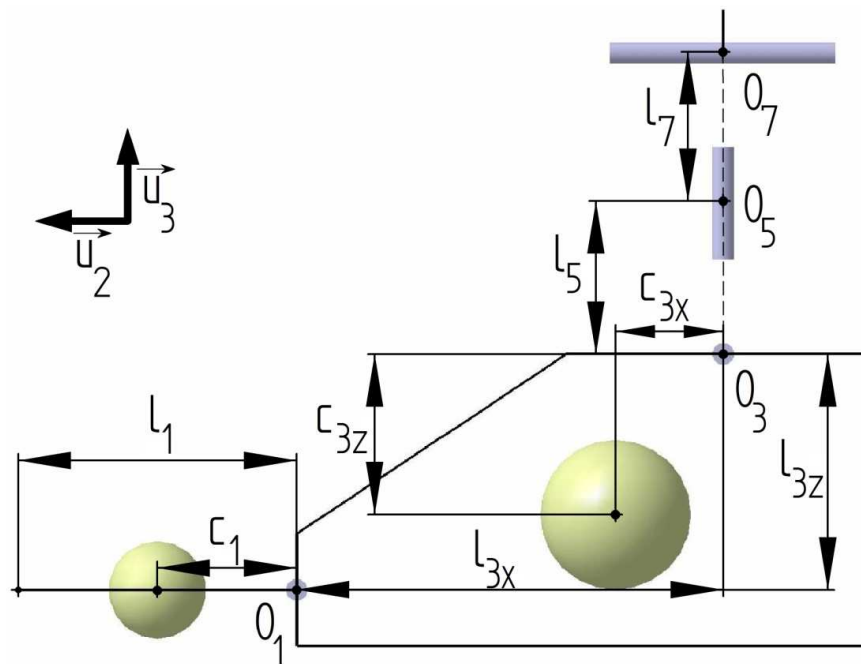


**Figure 2.5: Dimensions of Body 1, Body 3, Body 5 and Body 7**

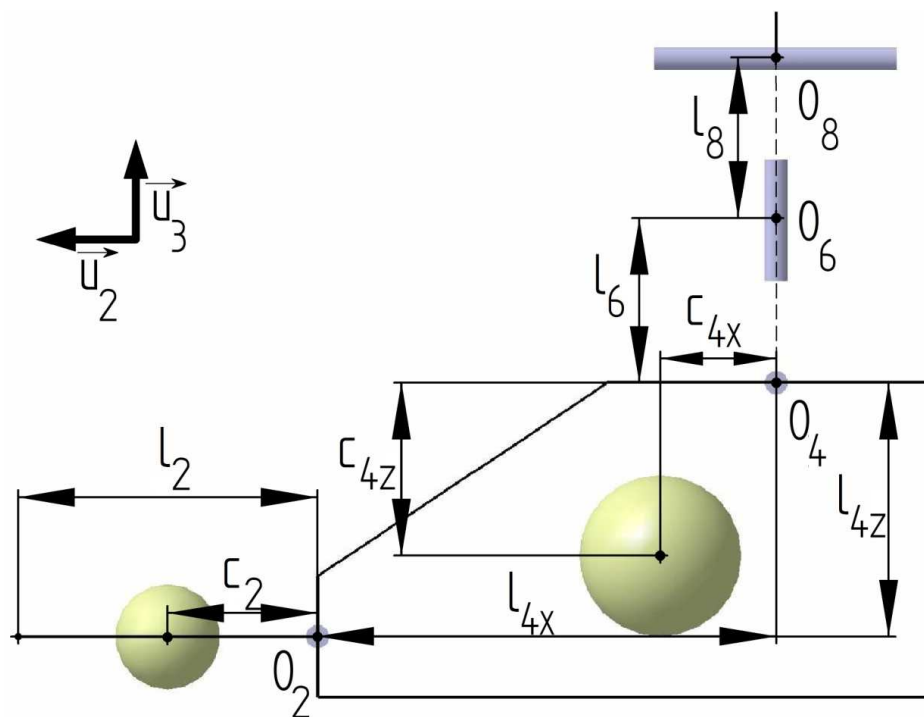


**Figure 2.6: Dimensions of Body 2, Body 4, Body 6 and Body 8**

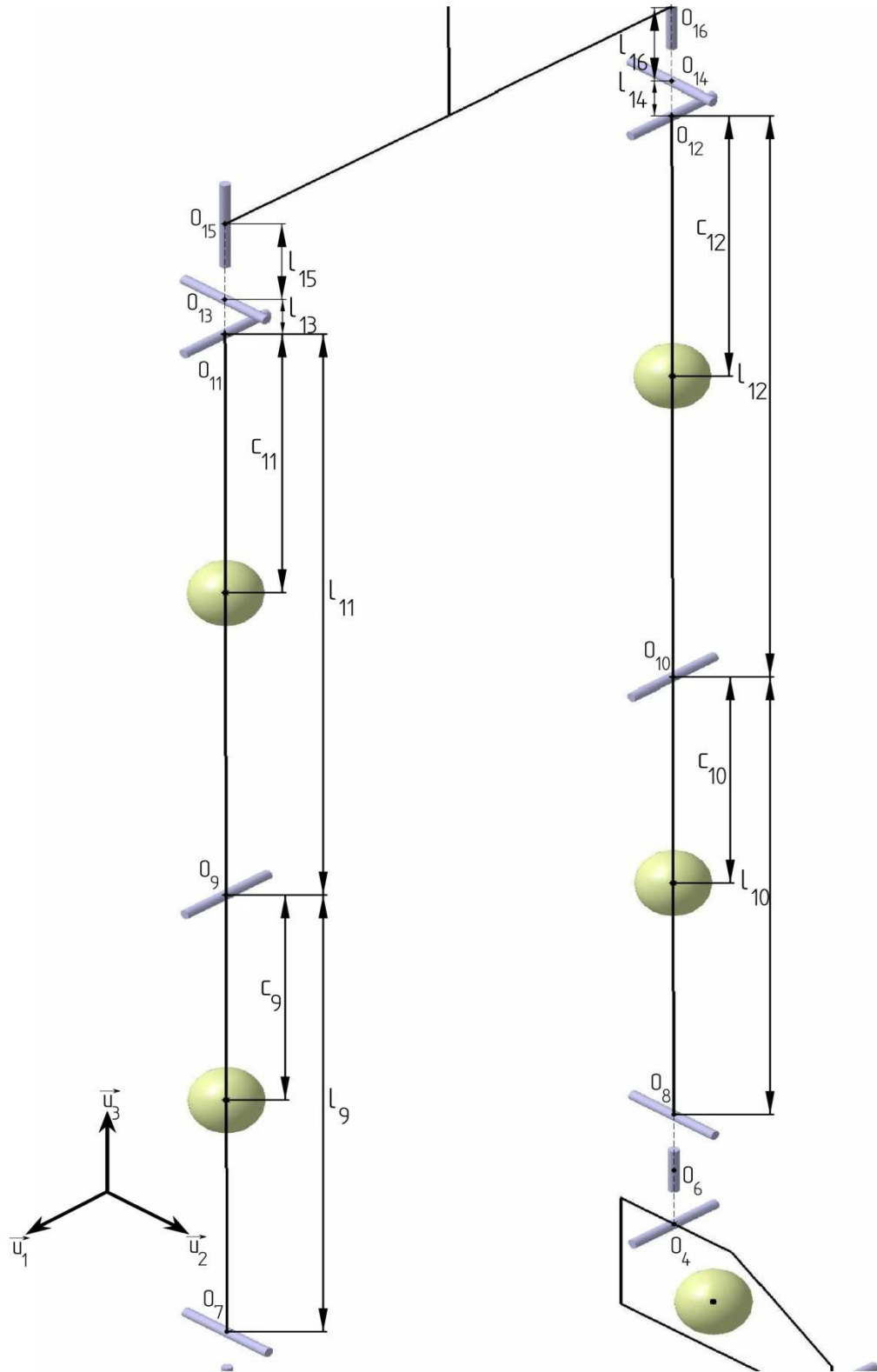


**Figure 2.7: Dimensions of Body 9, Body 10, Body 11, Body 12, Body 13, Body 14, Body 15 and Body 16**

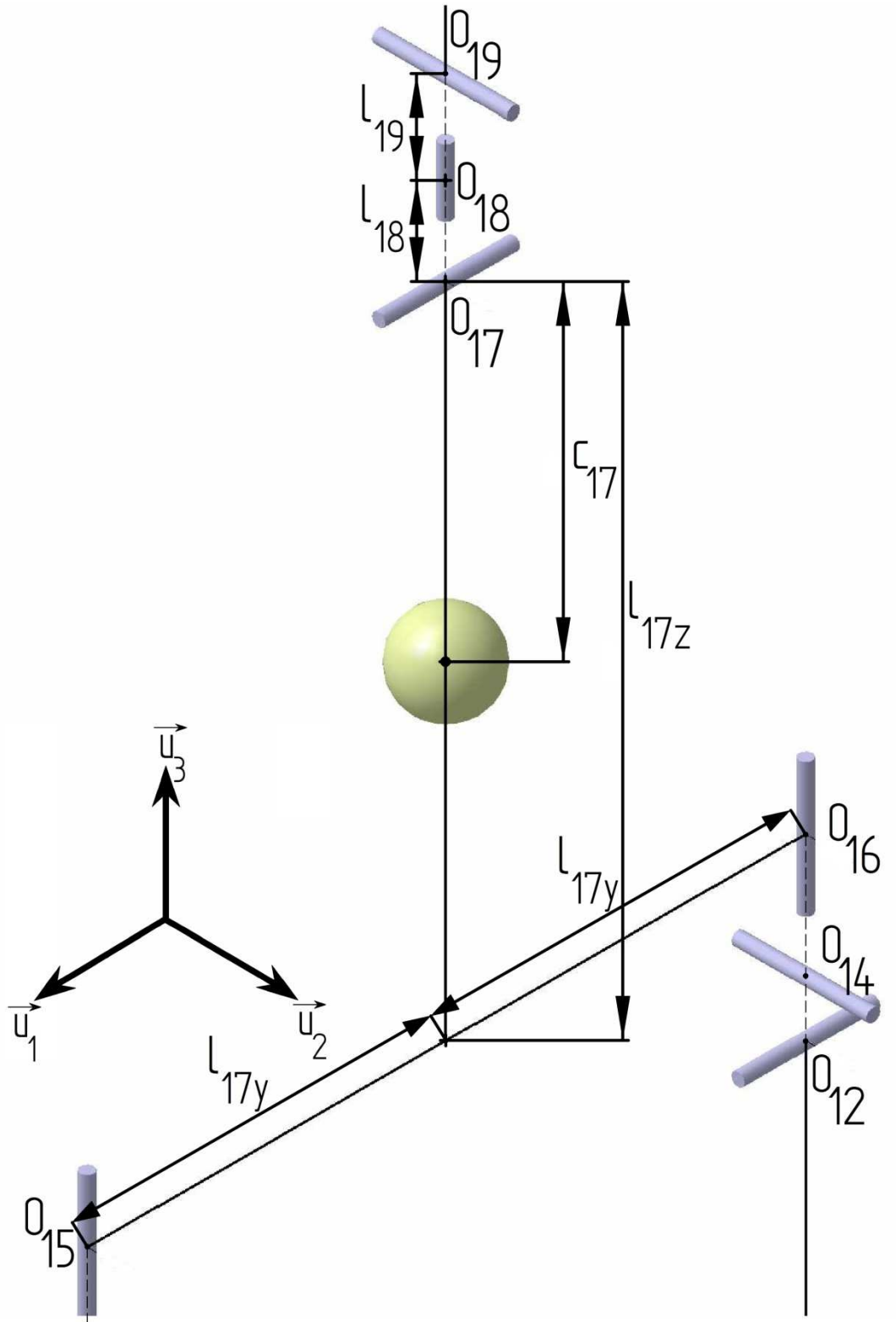


**Figure 2.8: Dimensions of Body 17, Body 18 and Body 19**

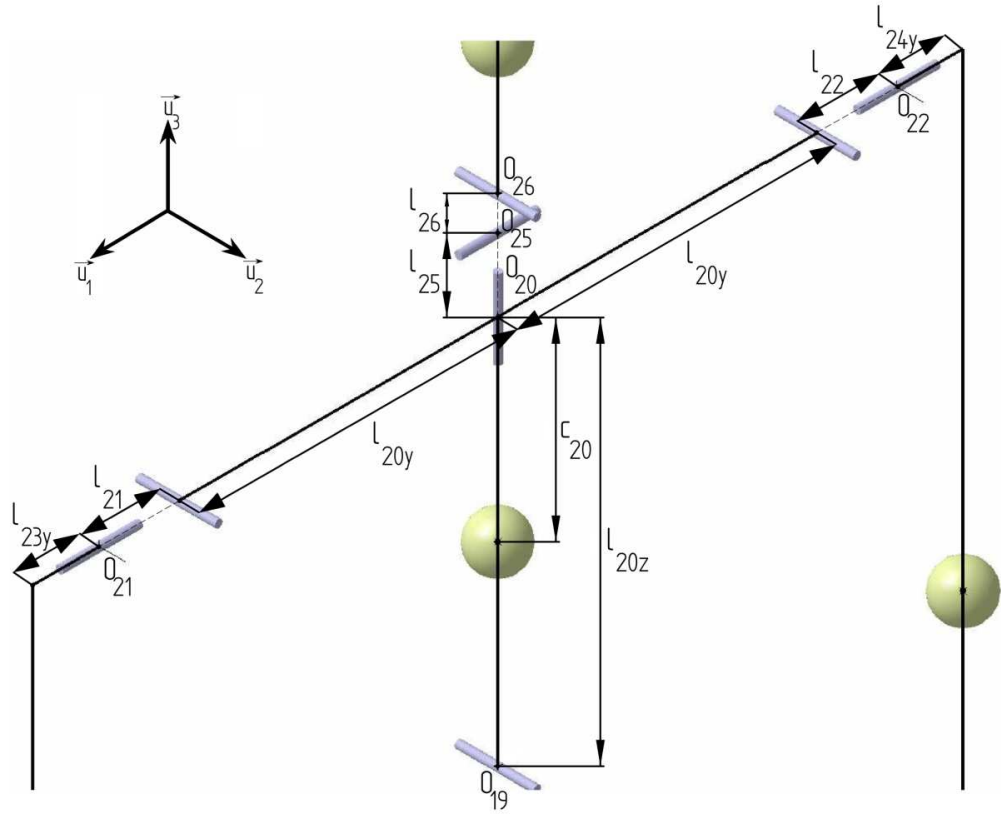


**Figure 2.9 Dimensions of Body 20, Body 21, Body 22, Body 25 and Body 26**

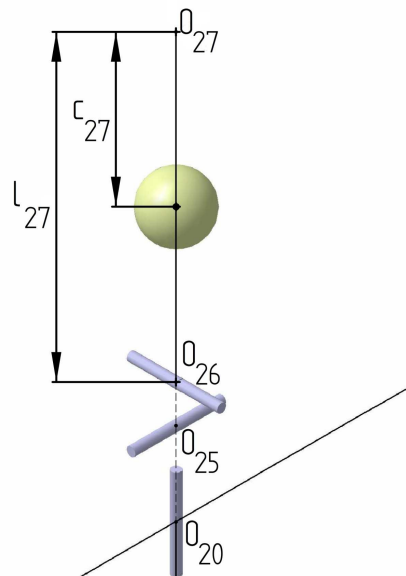


**Figure 2.10: Dimensions of Body 27**

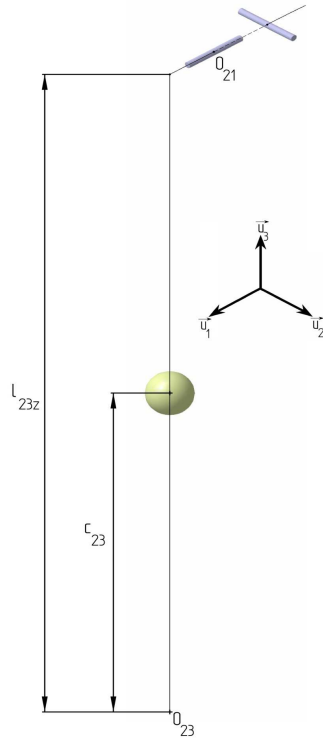


**Figure 2.11: Dimensions of Body 23**

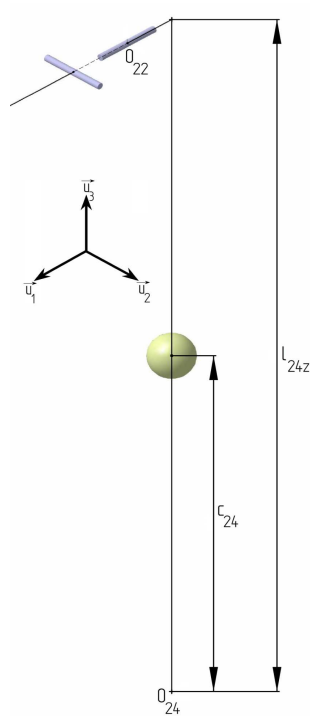


**Figure 2.12: Dimensions of Body 24**

According to given parameters, basic dimensions of bodies can be expressed as shown below:

$$\vec{c}_1 = c_1 \vec{u}_1^{(1)}$$

$$\vec{l}_{1,tp1} = l_1 \vec{u}_1^{(1)}$$

$$\vec{c}_2 = c_2 \vec{u}_1^{(2)}$$

$$\vec{l}_{2,tp2} = l_2 \vec{u}_1^{(2)}$$

$$\vec{c}_3 = c_{3x} \vec{u}_1^{(3)} - c_{3z} \vec{u}_3^{(3)}$$

$$\vec{l}_{3,1} = l_{3x} \vec{u}_1^{(3)} - l_{3z} \vec{u}_3^{(3)}$$

$$\vec{c}_4 = c_{4x} \vec{u}_1^{(4)} - c_{4z} \vec{u}_3^{(4)}$$

$$\vec{l}_{4,2} = l_{4x} \vec{u}_1^{(4)} - l_{4z} \vec{u}_3^{(4)}$$

$$\vec{c}_9 = -c_9 \vec{u}_3^{(9)}$$

$$\vec{l}_{9,3} = -l_9 \vec{u}_3^{(9)} - l_7 \vec{u}_3^{(7)} - l_5 \vec{u}_3^{(5)}$$

$$\vec{c}_{10} = -c_{10} \vec{u}_3^{(10)}$$

$$\vec{l}_{10,4} = -l_{10} \vec{u}_3^{(10)} - l_8 \vec{u}_3^{(8)} - l_6 \vec{u}_3^{(6)}$$

$$\vec{c}_{11} = -c_{11} \vec{u}_3^{(11)}$$

$$\vec{l}_{11,9} = -l_{11} \vec{u}_3^{(11)}$$

$$\vec{c}_{12} = -c_{12} \vec{u}_3^{(12)}$$

$$\vec{l}_{12,10} = -l_{12} \vec{u}_3^{(12)}$$

$$\vec{c}_{17} = -c_{17} \vec{u}_3^{(17)}$$

$$\vec{l}_{17,11} = -l_{17z}\vec{u}_3^{(17)} - l_{17y}\vec{u}_2^{(17)} - l_{15}\vec{u}_3^{(15)} - l_{13}\vec{u}_3^{(13)}$$

$$\vec{l}_{17,12} = -l_{17z}\vec{u}_3^{(17)} + l_{17y}\vec{u}_2^{(17)} - l_{16}\vec{u}_3^{(16)} - l_{14}\vec{u}_3^{(14)}$$

$$\vec{c}_{20} = -c_{20}\vec{u}_3^{(20)}$$

$$\vec{l}_{20,17} = -l_{20z}\vec{u}_3^{(20)} - l_{19}\vec{u}_3^{(19)} - l_{18}\vec{u}_3^{(18)}$$

$$\vec{l}_{20,21} = -l_{20y}\vec{u}_2^{(20)} - l_{21}\vec{u}_2^{(21)}$$

$$\vec{l}_{20,22} = +l_{20y}\vec{u}_2^{(20)} + l_{22}\vec{u}_2^{(22)}$$

$$\vec{c}_{23} = c_{23}\vec{u}_3^{(23)}$$

$$\vec{l}_{23,21} = +l_{23z}\vec{u}_3^{(23)} + l_{23y}\vec{u}_2^{(23)}$$

$$\vec{c}_{24} = c_{24}\vec{u}_3^{(24)}$$

$$\vec{l}_{24,22} = +l_{24z}\vec{u}_3^{(24)} - l_{24y}\vec{u}_2^{(24)}$$

$$\vec{c}_{27} = -c_{27}\vec{u}_3^{(27)}$$

$$\vec{l}_{27,20} = -l_{27}\vec{u}_3^{(27)} - l_{26}\vec{u}_3^{(26)} - l_{25}\vec{u}_3^{(25)}$$

The location of toe points “P<sub>tpR</sub>” and “P<sub>tpL</sub>” relatively on Body 1 and Body 2 is defined by  $\vec{l}_{1,tp1}$  and  $\vec{l}_{2,tp2}$ .

Since Body 5, Body 6, Body 7, Body 8, Body 13, Body 14, Body 15, Body 16, Body 18, Body 19, Body 21, Body 22, Body 25 and Body 26 are virtual;  $l_5, l_6, l_7, l_8, l_{13}, l_{14}, l_{15}, l_{16}, l_{18}, l_{19}, l_{21}, l_{22}, l_{25}$  and  $l_{26}$  are taken as zero. Therefore,

- $O_3, O_5$  and  $O_7$
- $O_4, O_6$  and  $O_8$
- $O_{11}, O_{13}$  and  $O_{15}$
- $O_{12}, O_{14}$  and  $O_{16}$
- $O_{17}, O_{18}$  and  $O_{19}$

- $O_{20}$ ,  $O_{25}$  and  $O_{26}$

are coincident points.

Actuator torques for a specific joint are applied in terms of the body reference frame which has the highest index number of adjacent non-virtual bodies. Numbering of actuator torques is shown in Figure 2.13. A detailed explanation of actuator torques is to be done in mathematical modeling chapter.

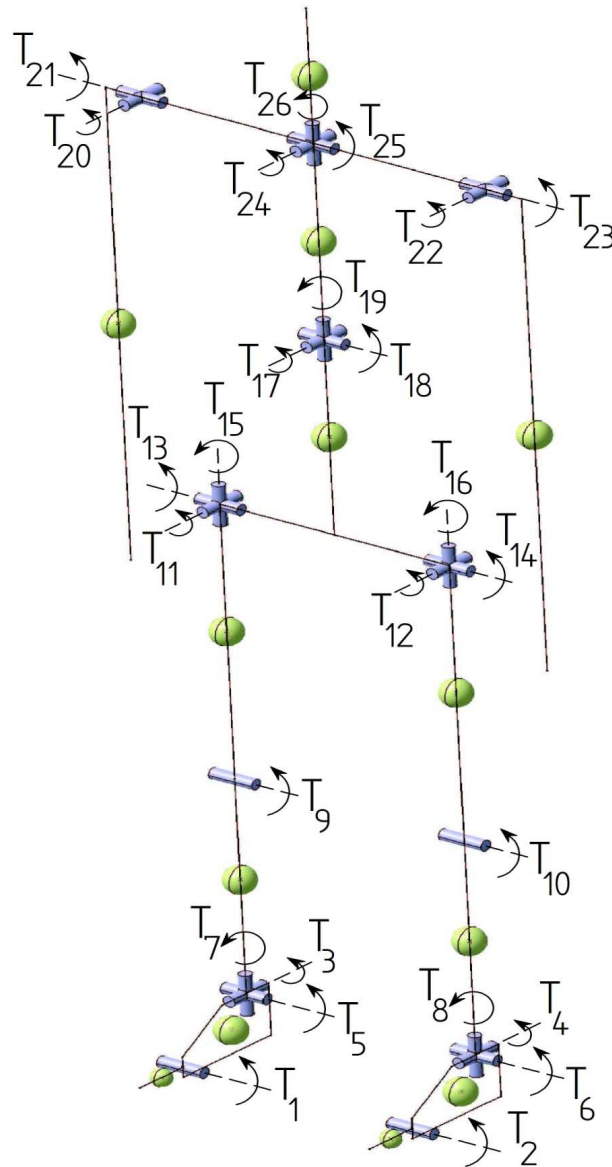


**Fig 2.13: Actuator Torques**

## CHAPTER 3

### REFERENCE TRAJECTORY GENERATION

The importance of generating feasible reference trajectories for task space or joint space variables is explained in chapter 1. However, devising a reference trajectory generation algorithm to supply convenient reference trajectories by considering various factors for controlling a biped robot is a major subject which must be examined in depth as a separate study and is not in the scope of the thesis. On the other hand, generating reference trajectories rapidly according to given parameters defining the locomotion is strongly required. Therefore, it is possible to choose a reference trajectory which can be controlled, does not require impossible actuator torques and does not result to nonphysical situations like colliding or intersecting bodies by doing several trials based on locomotion parameters. Consequently, a simple reference trajectory generation algorithm is created to define trajectories for toe points  $P_{tpR}$  and  $P_{tpL}$ , Body 1 and Body 2, CoM of Body 17 and Body 17. For translational definitions, trajectories are constructed in 2 components; in other words, components in the plane formed by  $\vec{u}_1^{(0)}$ ,  $\vec{u}_2^{(0)}$  and in  $\vec{u}_3^{(0)}$  direction are defined separately.

#### 3.1. Locomotion Definition

Locomotion parameters to be supplied into the reference trajectory generation algorithm are shown and explained under this heading.

##### 3.1.1. $P_{hip}$

In the thesis, the biped locomotion is modeled by 4 basic phases which are LFFSSP, RFFSSP, LFFDSP and RFFDSP. According to these basic phases, a biped locomotion is a continuous cyclic transition between single support and double support phases as shown in Figure 3.1.

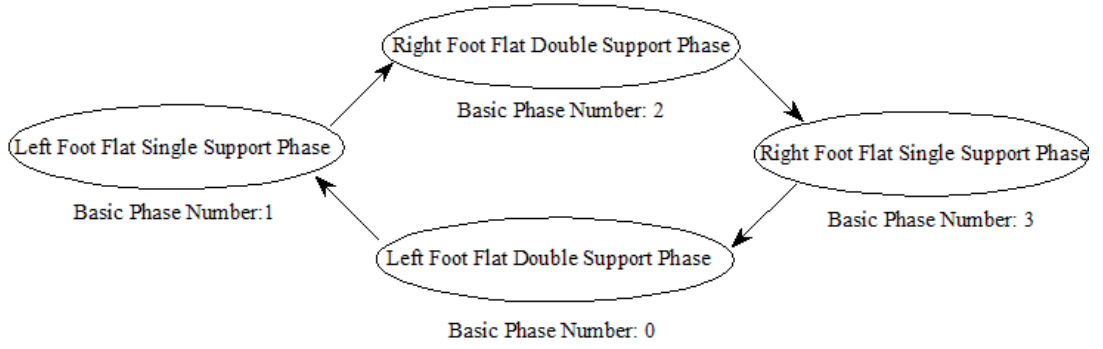


**Figure 3.1: Transition of Phases for a Biped Locomotion**

General form of  $P_{hip}$  can be described as:

$$P_{hip} = \begin{bmatrix} \bar{P}_1^T \\ \bar{P}_2^T \\ \vdots \\ \bar{P}_n^T \end{bmatrix} \text{ where } \bar{P}_k \text{ is the matrix representation of position vector } \vec{P}_k \text{ resolved}$$

in the inertial frame for  $P_k$  (Point K).

Desired positions of CoM of Body 17 are expressed by points  $P_1, P_2, \dots, P_n$ . These points indicate the desired position of CoM of Body 17 for the beginning or ending of a SSP and DSP pair as shown in Figure 3.2.

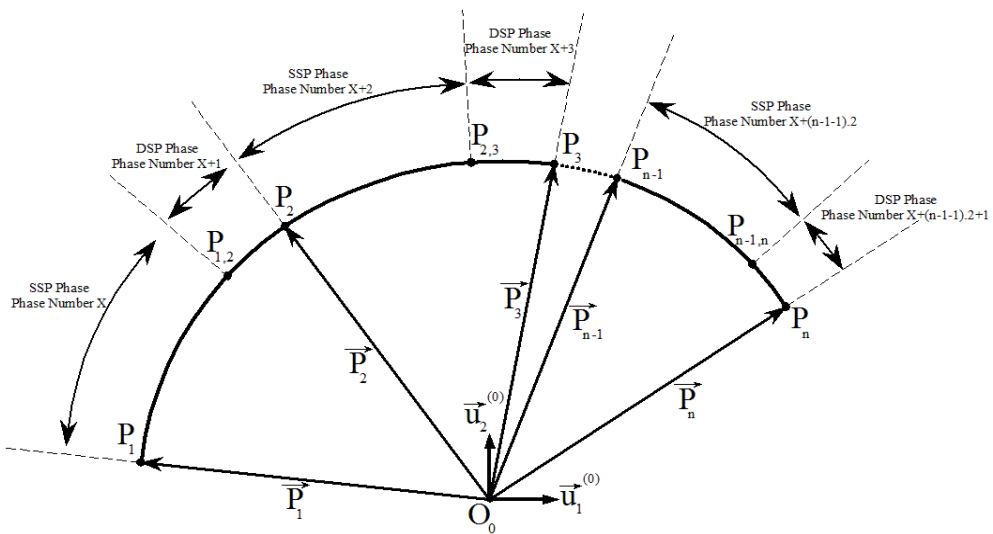


**Figure 3.2: The Definition of Desired CoM of Body 17**

### 3.1.2. $V_{hip}$

General form of  $V_{hip}$  can be described as:

$$V_{hip} = \begin{bmatrix} V_1 \\ V_{1,2} \\ V_2 \\ \vdots \\ V_{n-1} \\ V_{n-1,n} \\ V_n \end{bmatrix} \text{ where } V_k \text{ and } V_{k,k+1} \text{ are the magnitude of desired velocities (both}$$

differentiated and resolved in the inertial frame) of CoM of Body 17 at points  $P_k$  and  $P_{k,k+1}$  shown in Figure 3.2.

### 3.1.3. $R$

General form of  $R$  can be described as:

$$R = \begin{bmatrix} R_1 \\ R_2 \\ \vdots \\ R_{n-1} \end{bmatrix} \text{ where } R_k \text{ is the radius of curvature of the projected CoM path of Body}$$

17 to the plane formed by  $\vec{u}_1^{(0)}$  and  $\vec{u}_2^{(0)}$  between points  $P_k$  and  $P_{k+1}$  as shown in Figure 3.3.

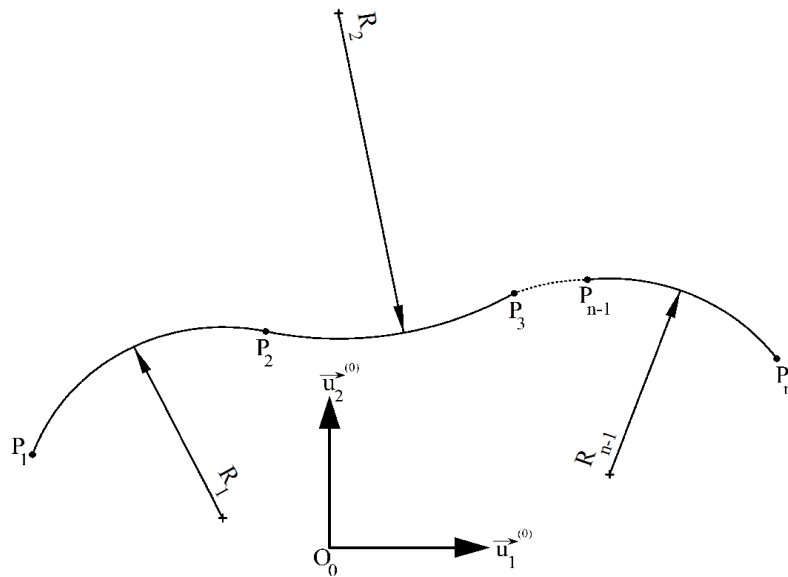


**Figure 3.3: Labeling of Radius of Curvatures**

### 3.1.4. $t_{SSP}$ and PTR

General form of  $t_{SSP}$  can be described as:

$$t_{SSP} = \begin{bmatrix} t_{SSP,1} \\ t_{SSP,2} \\ \vdots \\ t_{SSP,n-1} \end{bmatrix} \text{ where } t_{SSP,k} \text{ is the duration time of SSP that occurs during the}$$

motion of CoM of Body 17 between points  $P_k$  and  $P_{k,k+1}$

General form of PTR can be describes as:

$$PTR = \begin{bmatrix} PTR_1 \\ PTR_2 \\ \vdots \\ PTR_{n-1} \end{bmatrix} \text{ where } PTR_k \text{ is the ratio of the duration time of SSP to the}$$

duration time of DSP that occurs during the motion of CoM of Body 17 between points  $P_k$  and  $P_{k+1}$ .

### 3.1.5. SW

General form of SW can be described as:

$$SW = \begin{bmatrix} SW_1 \\ SW_2 \\ \vdots \\ SW_{n-1} \end{bmatrix} \text{ where } SW_k \text{ is the step width for the swing leg in SSP during the}$$

motion of CoM of Body 17 between points  $P_k$  and  $P_{k,k+1}$ .

### 3.1.6. SH and $k_{SH}$

General form of SH can be described as:

$$SH = \begin{bmatrix} SH_1 \\ SH_2 \\ \vdots \\ SH_{n-1} \end{bmatrix} \text{ where } SH_k \text{ is the specified step height of the swing leg in SSP for}$$

the specified time during the motion of CoM of Body 17 between points  $P_k$  and  $P_{k,k+1}$ .

General form of  $k_{SH}$  can be described as:

$$k_{SH} = \begin{bmatrix} k_{SH,1} \\ k_{SH,2} \\ \vdots \\ k_{SH,n-1} \end{bmatrix} \text{ where } k_{SH,k} \text{ is the ratio of specified step height time to the duration time of SSP } (t_{SSP,k}) \text{ during the motion of CoM of Body 17 between points } P_k \text{ and } P_{k,k+1}.$$

### 3.1.7. $k_{Adj}$

General form of  $k_{Adj}$  can be described as:

$$k_{Adj} = \begin{bmatrix} k_{Adj,1} \\ k_{Adj,2} \\ \vdots \\ k_{Adj,n-1} \end{bmatrix} \text{ where } k_{Adj,k} \text{ is the desired adjustment time ratio during the motion of CoM of Body 17 between points } P_k \text{ and } P_{k,k+1}.$$

### 3.1.8. $\Delta\theta_{PLN}$ and $\Delta\theta_{ADJ}$

General form of  $\Delta\theta_{PLN}$  and  $\Delta\theta_{ADJ}$  can be described as:

$$\Delta\theta_{PLN} = \begin{bmatrix} \Delta\theta_{PLN,1} \\ \Delta\theta_{PLN,2} \\ \vdots \\ \Delta\theta_{PLN,n-1} \end{bmatrix}, \Delta\theta_{ADJ} = \begin{bmatrix} \Delta\theta_{ADJ,1} \\ \Delta\theta_{ADJ,2} \\ \vdots \\ \Delta\theta_{ADJ,n-1} \end{bmatrix} \text{ where } \Delta\theta_{PLN,k} \text{ for SSP and } \Delta\theta_{ADJ,k} \text{ for DSP are desired angular differences during the motion of CoM of Body 17 between points } P_k \text{ and } P_{k+1}.$$

### 3.1.9. $T_{dir}$

General form of  $T_{dir}$  can be described as:

$$T_{dir} = \begin{bmatrix} T_{dir,1} \\ T_{dir,2} \\ \vdots \\ T_{dir,n-1} \end{bmatrix} \text{ where } T_{dir,k} \text{ is turning direction indicator for the motion of CoM of Body 17 between points } P_k \text{ and } P_{k+1}.$$

$T_{dir,k}$  can take +1 or -1 values only. +1 and -1 values mean turning leftward and rightward direction as shown in Figure 3.4

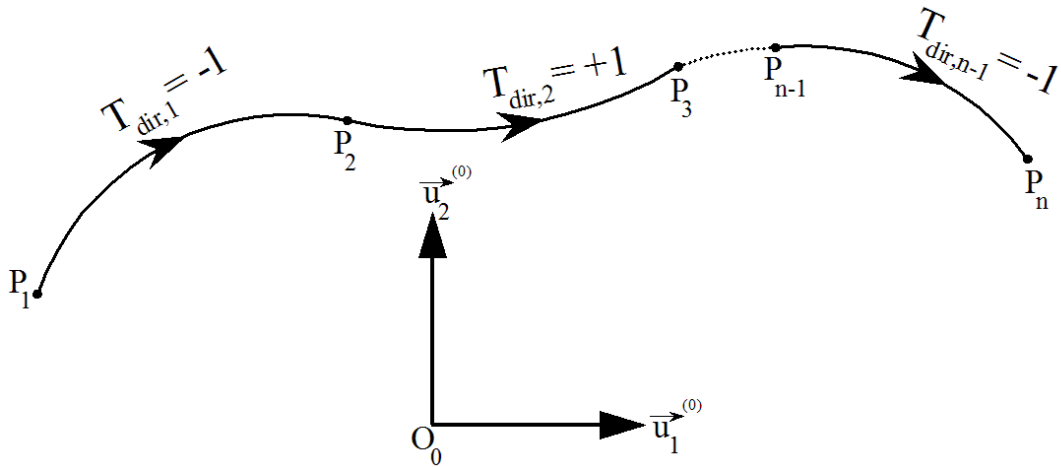


**Figure 3.4: Turning Direction Convention**

### 3.2. Trajectory Definition

The path of CoM position of Body 17 lying in the plane formed by  $\vec{u}_1^{(0)}$  and  $\vec{u}_2^{(0)}$  is made of arcs. Cartesian coordinate systems are placed to the arc centers to be used during trajectory definitions. According to  $P_{hip}$ ,  $R$  and  $T_{dir}$  definitions, the location of arc centers is calculated.

For given CoM positions of Body 17 as  $P_k$  and  $P_{k+1}$ , the problem of finding arc centers is illustrated in Figure 3.5.

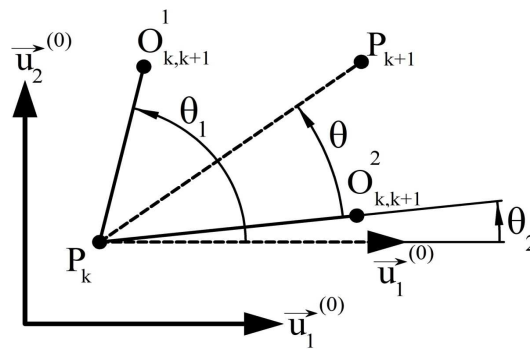


**Figure 3.5: The Definition of Finding Arc Centers Problem**

### 3.2.1. Finding Arc Centers

For  $\bar{P}_k = \begin{bmatrix} P_{kx} \\ P_{ky} \\ P_{kz} \end{bmatrix}$ ,  $\bar{P}_{k+1} = \begin{bmatrix} P_{k+1x} \\ P_{k+1y} \\ P_{k+1z} \end{bmatrix}$ ,  $O_{k,k+1x}$  and  $O_{k,k+1y}$  are  $\vec{u}_1^{(0)}$  and  $\vec{u}_2^{(0)}$  components

of point  $O_{k,k+1}$ ; the solution to the problem of finding the center of an arc with radius  $R_k$  passing through  $P_k$  and  $P_{k+1}$  can be obtained from equations shown below:

$$(P_{kx} - O_{k,k+1x})^2 + (P_{ky} - O_{k,k+1y})^2 = (P_{k+1x} - O_{k,k+1x})^2 + (P_{k+1y} - O_{k,k+1y})^2 \quad (3.1)$$

$$(P_{kx} - O_{k,k+1x})^2 + (P_{ky} - O_{k,k+1y})^2 = R_k^2 \quad (3.2)$$

Since there exist 2 sets of solution to equation (3.1) and (3.2) such as  $(O_{k,k+1x}^1, O_{k,k+1y}^1)$  and  $(O_{k,k+1x}^2, O_{k,k+1y}^2)$ , an algorithm is devised to choose the correct center of arc for a given  $T_{dir,k}$  value.

Using atan2 function, described as  $\theta = atan2(\sin \theta, \cos \theta)$  for  $-\pi \leq \theta \leq \pi$  [61]:

$$\theta_1 = atan2(O_{k,k+1y}^1 - P_{ky}, O_{k,k+1x}^1 - P_{kx})$$

$$\theta_2 = atan2(O_{k,k+1y}^2 - P_{ky}, O_{k,k+1x}^2 - P_{kx})$$

$$\theta = atan2(P_{k+1y} - P_{ky}, P_{k+1x} - P_{kx})$$

Pseudo code of the algorithm is shown below.

Version 1:

IF  $\left(\frac{-\pi}{2} \leq \theta_1 - \theta \leq \frac{\pi}{2}\right)$  {

$A = \theta_1 - \theta$  }

ELSE {

IF  $\left(\theta_1 - \theta < -\frac{\pi}{2}\right)$  {

$$A = \theta_1 - \theta + 2\pi \}$$

ELSE {

$$A = \theta_1 - \theta - 2\pi \}$$

}

IF ( $T_{dir,k} = +1$ ) {

IF ( $A > 0$ ) {

$$\text{Arc Center} \rightarrow (O_{k,k+1}^1 x^1, O_{k,k+1}^1 y^1) \}$$

ELSE {

$$\text{Arc Center} \rightarrow (O_{k,k+1}^2 x^2, O_{k,k+1}^2 y^2) \}$$

}

ELSE {

IF ( $A < 0$ ) {

$$\text{Arc Center} \rightarrow (O_{k,k+1}^1 x^1, O_{k,k+1}^1 y^1) \}$$

ELSE {

$$\text{Arc Center} \rightarrow (O_{k,k+1}^2 x^2, O_{k,k+1}^2 y^2) \}$$

}

Version 2:

IF ( $-\frac{\pi}{2} \leq \theta_2 - \theta \leq \frac{\pi}{2}$ ) {

$$B = \theta_2 - \theta \}$$

ELSE {

```

IF  $(\theta_2 - \theta < -\frac{\pi}{2})$  {

   $B = \theta_2 - \theta + 2\pi$  }

ELSE {

   $B = \theta_2 - \theta - 2\pi$  }

}

IF  $(T_{dir,k} = +1)$  {

  IF  $(B > 0)$  {

    Arc Center  $\rightarrow (O_{k,k+1}^2 x^2, O_{k,k+1}^2 y^2)$  }

  ELSE {

    Arc Center  $\rightarrow (O_{k,k+1}^1 x^1, O_{k,k+1}^1 y^1)$  }

  }

  ELSE {

    IF  $(B < 0)$  {

      Arc Center  $\rightarrow (O_{k,k+1}^2 x^2, O_{k,k+1}^2 y^2)$  }

      ELSE {

        Arc Center  $\rightarrow (O_{k,k+1}^1 x^1, O_{k,k+1}^1 y^1)$  }

      }

    }

```

### 3.2.2. Definition of Local Coordinate Systems

Since local coordinate system definitions and parameter conventions change according to the turning direction, this heading will be examined in 2 subsections.

### 3.2.2.1. For Turning Leftward Direction

Local coordinate system  $CS_{k,k+1}$  is positioned at the arc center for the path between  $P_k$  and  $P_{k+1}$  with an orientation with respect the inertial frame as shown in Figure 3.6.

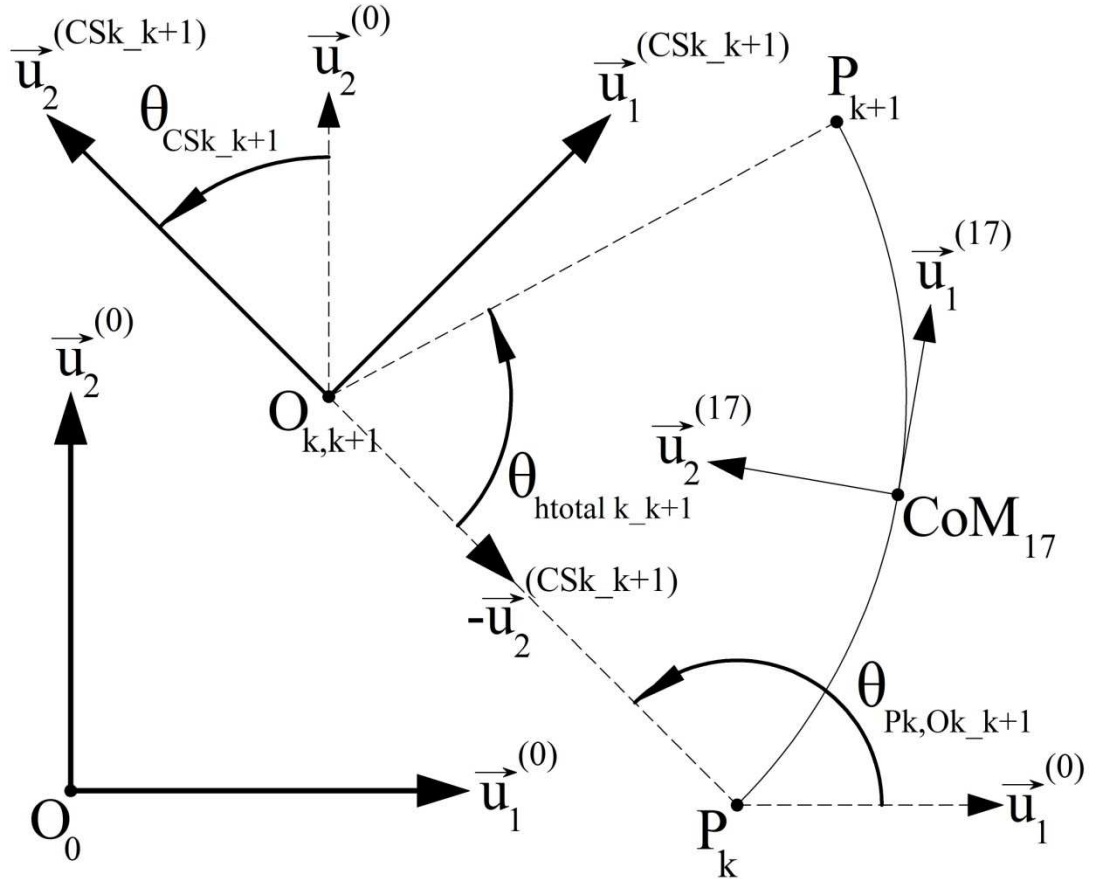


**Figure 3.6: Local Coordinate System  $CS_{k,k+1}$  for Turning Leftward Direction**

The definition of several parameters shown in Figure 3.6 is explained below.

$$\theta_{Pk,Ok_{k+1}} = atan2(O_{k,k+1y} - P_{ky}, O_{k,k+1x} - P_{kx})$$

$$\theta_{CS_{k,k+1}} = \theta_{Pk,Ok_{k+1}} - \frac{\pi}{2}$$

$\hat{C}^{(a,b)}$  is the component transformation matrix from frame b to frame a. Using the exponential representation of rotation matrices by Rodrigues Formula [62], the transformation matrix from local coordinate system CSk\_k+1 to the inertial frame can be expressed as:

$$\hat{C}^{(0,CSk_{k+1})} = e^{\tilde{u}_3 \theta_{CSk_{k+1}}}$$

$$\hat{C}^{(CSk_{k+1},0)} = e^{\tilde{u}_3(-\theta_{CSk_{k+1}})}, \text{ since } \hat{C}^{(0,CSk_{k+1})} \cdot \hat{C}^{(CSk_{k+1},0)} = \hat{I}$$

Then, the position vector of point P<sub>k+1</sub> in local coordinate system CSk\_k+1 can be defined as:

$$\begin{aligned} \bar{P}_{k+1}^{(CSk_{k+1})} &= \\ (P_{k+1x} - O_{k,k+1x}) \hat{C}^{(CSk_{k+1},0)} \bar{u}_1 &+ (P_{k+1y} - O_{k,k+1y}) \hat{C}^{(CSk_{k+1},0)} \bar{u}_2 \end{aligned}$$

$$\bar{P}_{k+1}^{(CSk_{k+1})} = K_x \bar{u}_1 + K_y \bar{u}_2 \text{ for}$$

$$K_x = [(P_{k+1x} - O_{k,k+1x}) \cdot \cos(\theta_{CSk_{k+1}}) + (P_{k+1y} - O_{k,k+1y}) \cdot \sin(\theta_{CSk_{k+1}})]$$

$$K_y = [(P_{k+1y} - O_{k,k+1y}) \cdot \cos(\theta_{CSk_{k+1}}) - (P_{k+1x} - O_{k,k+1x}) \cdot \sin(\theta_{CSk_{k+1}})]$$

$$\text{As a result, } \theta_{htotal\ k_{k+1}} = atan2(K_x, -K_y)$$

### 3.2.2.2. For Turning Rightward Direction

Local coordinate system  $CS_{k,k+1}$  is positioned at the arc center for the path between  $P_k$  and  $P_{k+1}$  with an orientation with respect the inertial frame as shown in Figure 3.7.

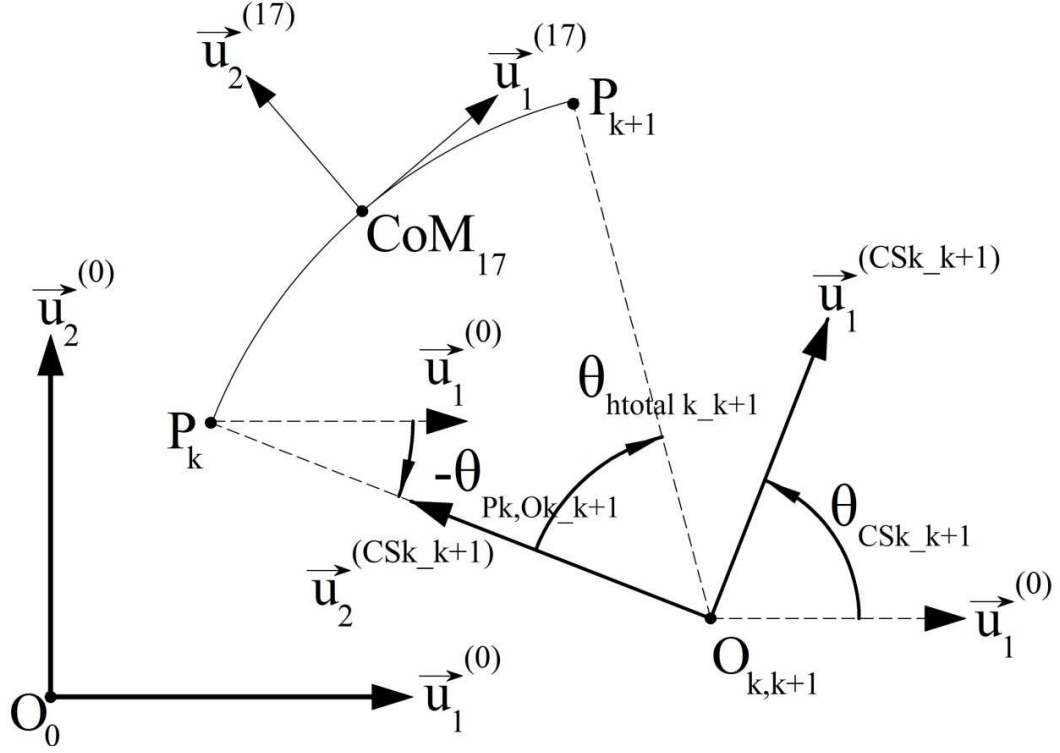


**Figure 3.7: Local Coordinate System  $CS_{k,k+1}$  for Turning Rightward Direction**

The definition of several parameters shown in Figure 3.7 is explained below.

$$\theta_{Pk,Ok,k+1} = \text{atan2}(O_{k,k+1y} - P_{ky}, O_{k,k+1x} - P_{kx})$$

$$\theta_{CS_{k,k+1}} = \theta_{Pk,Ok,k+1} + \frac{\pi}{2}$$

The transformation matrix from local coordinate system  $CS_{k,k+1}$  to the inertial frame can be expressed as:

$$\hat{C}^{(0,CS_{k,k+1})} = e^{\tilde{u}_3 \theta_{CS_{k,k+1}}}, \text{ then } \hat{C}^{(CS_{k,k+1},0)} = e^{\tilde{u}_3 (-\theta_{CS_{k,k+1}})}$$

The position vector of point  $P_{k+1}$  in local coordinate system  $CSk_{k+1}$  can be defined as:

$$\begin{aligned} \bar{P}_{k+1}^{(CSk_{k+1})} = & (P_{k+1x} - O_{k,k+1x})\hat{C}^{(CSk_{k+1},0)}\bar{u}_1 + (P_{k+1y} - O_{k,k+1y})\hat{C}^{(CSk_{k+1},0)}\bar{u}_2 \\ K_x = & [(P_{k+1x} - O_{k,k+1x}) \cdot \cos(\theta_{CSk_{k+1}}) + (P_{k+1y} - O_{k,k+1y}) \cdot \sin(\theta_{CSk_{k+1}})] \end{aligned} \quad (3.3)$$

$$K_y = [(P_{k+1y} - O_{k,k+1y}) \cdot \cos(\theta_{CSk_{k+1}}) - (P_{k+1x} - O_{k,k+1x}) \cdot \sin(\theta_{CSk_{k+1}})] \quad (3.4)$$

For equations (3.3) and (3.4),  $\bar{P}_{k+1}^{(CSk_{k+1})} = K_x\bar{u}_1 + K_y\bar{u}_2$

As a result,  $\theta_{htotal\ k_{k+1}} = atan2(K_x, K_y)$

### 3.2.3. Trajectory Definition during SSP and DSP Pairs

Since  $P_k$  and  $P_{k+1}$  points indicate the desired position of CoM of Body 17 respectively for the beginning and ending of a SSP and DSP pair,  $P_{k,k+1}$  is the point where SSP ends and DSP begins.

The definition of several parameters for a LFFSSP and RFFDSP pair is shown in Figure 3.8 for turning left and Figure 3.9 for turning right.  $P_{tpR}$  shown in Figure 3.8 and 3.9 is the position of toe point on Body 1 at the end of LFFSSP.

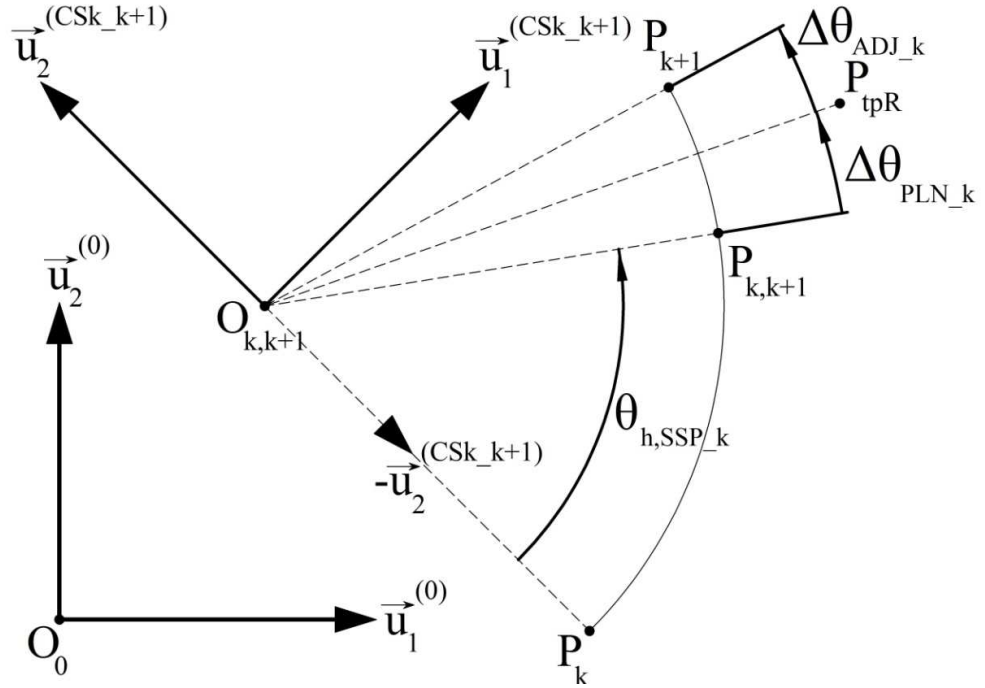


**Figure 3.8:  $\theta_{h,SSP_k}$ ,  $\Delta\theta_{PLN_k}$  and  $\Delta\theta_{ADJ_k}$  for Turning Left During a LFFSSP and RFFDSP pair**

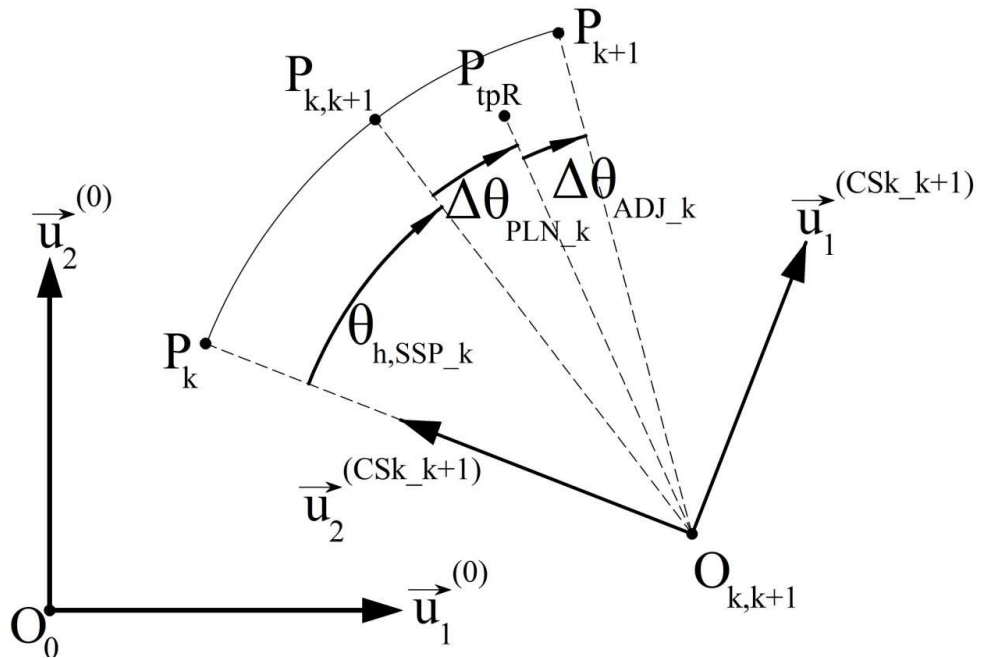


**Figure 3.9:  $\theta_{h,SSP_k}$ ,  $\Delta\theta_{PLN_k}$  and  $\Delta\theta_{ADJ_k}$  for Turning Right During a LFFSSP and RFFDSP pair**

Similarly, the definition of several parameters for a RFFSSP and LFFDSP pair is shown in Figure 3.10 for turning left and Figure 3.11 for turning right.  $P_{tpL}$  shown in Figure 3.10 and 3.11 is the position of toe point on Body 2 at the end of RFFSSP.

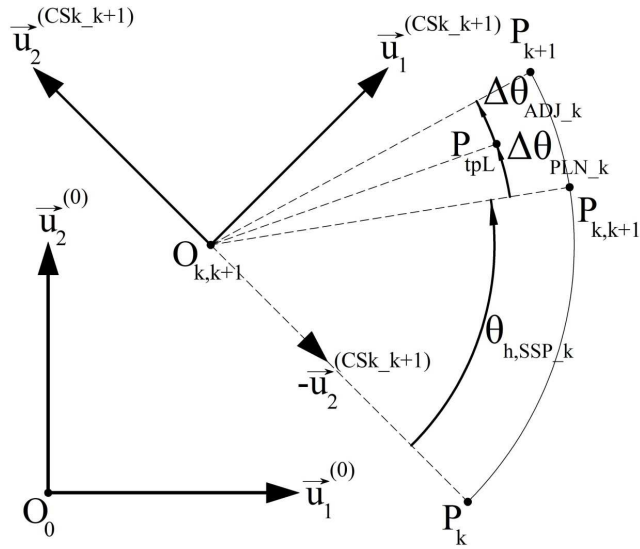


**Figure 3.10:  $\theta_{h,SSP_k}$ ,  $\Delta\theta_{PLN_k}$  and  $\Delta\theta_{ADJ_k}$  for Turning Left During a RFFSSP and LFFDSP pair**

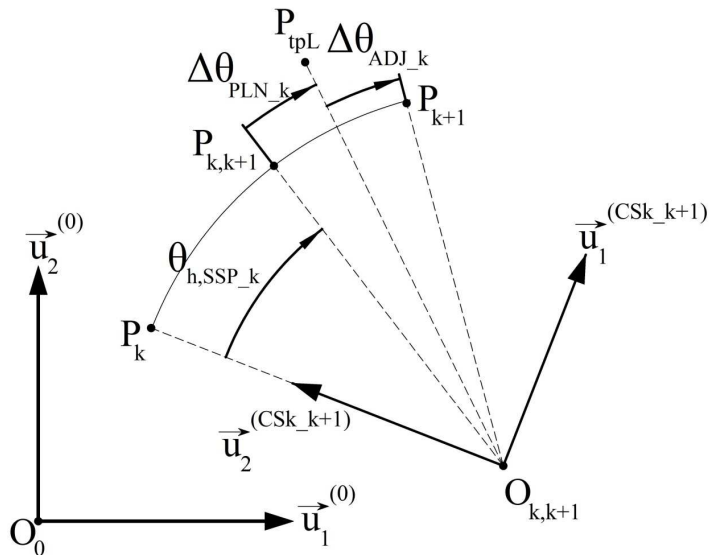


**Figure 3.11:  $\theta_{h,SSP_k}$ ,  $\Delta\theta_{PLN_k}$  and  $\Delta\theta_{ADJ_k}$  for Turning Right During a RFFSSP and LFFDSP pair**

Then,  $\theta_{h,SSP\_k}$  between points  $P_k$  and  $P_{k+1}$  can be calculated as:

$$\theta_{h,SSP\_k} = \theta_{htotal\ k\_k+1} - (\Delta\theta_{PLN\_k} + \Delta\theta_{ADJ\_k})$$

$t_{DSP,k}$ , the duration time of DSP between points  $P_{k,k+1}$  and  $P_{k+1}$ , is calculated as

$$t_{DSP,k} = \frac{t_{SSP,k}}{PTR_k}$$

### 3.2.3.1. The Definition of $\theta_h(t)$

All times are local phase times, not global times; which means that “t” is assumed to be zero at the beginning of each phase. Also  $\theta_h(t)$  definitions are independent of specified turning directions.

$\theta_{h,k}(t) = c_3^k t^3 + c_2^k t^2 + c_1^k t + c_0^k$  between points  $P_k$  and  $P_{k,k+1}$  for  $0 \leq t \leq t_{SSP,k}$  with conditions to be satisfied such as:

- $\theta_{h,k}(0) = 0$
- $\theta_{h,k}(t_{SSP,k}) = \theta_{h,SSP\_k}$
- $\frac{d\theta_{h,k}}{dt} \Big|_{t=0} = \frac{V_k}{R_k}$
- $\frac{d\theta_{h,k}}{dt} \Big|_{t=t_{SSP,k}} = \frac{V_{k,k+1}}{R_k}$

Then, the problem of finding proper polynomial coefficients can be described as:

$$\begin{bmatrix} 0 & 0 & 0 & 1 \\ t_{SSP,k}^3 & t_{SSP,k}^2 & t_{SSP,k} & 1 \\ 0 & 0 & 1 & 0 \\ 3 \cdot t_{SSP,k}^2 & 2 \cdot t_{SSP,k} & 1 & 0 \end{bmatrix} \begin{bmatrix} c_3^k \\ c_2^k \\ c_1^k \\ c_0^k \end{bmatrix} = \begin{bmatrix} 0 \\ \theta_{h,SSP\_k} \\ \frac{V_k}{R_k} \\ \frac{V_{k,k+1}}{R_k} \end{bmatrix}$$

Similarly,  $\theta_{h,k}(t) = d_3^k t^3 + d_2^k t^2 + d_1^k t + d_0^k$  between points  $P_{k,k+1}$  and  $P_{k+1}$  for  $0 \leq t \leq t_{DSP,k}$  with conditions to be satisfied such as:

- $\theta_{h,k}(0) = \theta_{h,SSP\_k}$
- $\theta_{h,k}(t_{DSP,k}) = \theta_{htotal\ k\_k+1}$
- $\frac{d\theta_{h,k}}{dt} \Big|_{t=0} = \frac{V_{k,k+1}}{R_k}$

- $\frac{d\theta_{h,k}}{dt} \Big|_{t=t_{DSP,k}} = \frac{V_{k+1}}{R_k} 1$

$$\begin{bmatrix} 0 & 0 & 0 & 1 \\ t_{DSP,k}^3 & t_{DSP,k}^2 & t_{DSP,k} & 1 \\ 0 & 0 & 1 & 0 \\ 3 \cdot t_{DSP,k}^2 & 2 \cdot t_{DSP,k} & 1 & 0 \end{bmatrix} \begin{bmatrix} d_3^k \\ d_2^k \\ d_1^k \\ d_0^k \end{bmatrix} = \begin{bmatrix} \theta_{h,SPP_k} \\ \theta_{htotal\ k,k+1} \\ \frac{V_{k,k+1}}{R_k} \\ \frac{V_{k+1}}{R_k} \end{bmatrix}$$

Since the velocity component of CoM of Body 17 in  $\vec{u}_3^{(0)}$  is always assumed to be zero (which will be shown in the trajectory definition for  $\vec{u}_3^{(0)}$  direction),  $\frac{d\theta_{h,k}}{dt}$  can be expressed directly as  $\frac{Velocity}{Arc\ Radius}$ .

### 3.2.3.2. Trajectory Definitions for CoM of Body 17 and Body 17

Definitions for translational and angular features of the trajectory will be explained in separate headings.

#### 3.2.3.2.1. Translational Position and Velocity Definitions for CoM of Body 17

$\vec{P}_{ref\_c,17}$ , and  $\vec{V}_{ref\_c,17}$ , the reference position and velocity vector of CoM of Body 17 differentiated with respect to and resolved in the inertial frame, in matrix forms between points  $P_k$  and  $P_{k+1}$  can be described as:

$$\vec{P}_{ref\_c,17}^k = P_{ref\_c,17x}^k \bar{u}_1 + P_{ref\_c,17y}^k \bar{u}_2 + P_{ref\_c,17z}^k \bar{u}_3 \quad (3.5)$$

$$\vec{V}_{ref\_c,17}^k = V_{ref\_c,17x}^k \bar{u}_1 + V_{ref\_c,17y}^k \bar{u}_2 + V_{ref\_c,17z}^k \bar{u}_3 \quad (3.6)$$

Although  $P_{kz}$  and  $P_{k+1z}$  are given by the input,  $P_{ref\_c,17z}^k$  in equation (3.5) is taken to be constant and the same during all phases. Therefore,

$$P_{ref\_c,17z}^k = P_{kz} = P_{k+1z} \text{ and } V_{ref\_c,17z}^k = 0$$

According to the definition of  $\theta_{h,k}(t)$  and local coordinate systems;  $P_{ref\_c,17x}^k$ ,  $P_{ref\_c,17y}^k$ ,  $V_{ref\_c,17x}^k$  and  $V_{ref\_c,17y}^k$  is calculated.

### 3.2.3.2.1.1. For Turning Left

$$\begin{aligned} \bar{P}_{ref\_c,17}^k = & \\ & O_{k,k+1x}\bar{u}_1 + O_{k,k+1y}\bar{u}_2 + P_{ref\_c,17z}^k\bar{u}_3 + R_k \cdot \sin(\theta_{h,k}(t)) \hat{C}^{(0,CSk_{k+1})}\bar{u}_1 - \\ & R_k \cdot \cos(\theta_{h,k}(t)) \hat{C}^{(0,CSk_{k+1})}\bar{u}_2 \end{aligned} \quad (3.7)$$

From equation (3.7), equation (3.8) and equation (3.9) can be derived such as:

$$P_{ref\_c,17x}^k = O_{k,k+1x} + R_k \cdot \sin(\theta_{h,k}(t) + \theta_{CSk_{k+1}}) \quad (3.8)$$

$$P_{ref\_c,17y}^k = O_{k,k+1y} - R_k \cdot \cos(\theta_{h,k}(t) + \theta_{CSk_{k+1}}) \quad (3.9)$$

Using equation (3.8) and (3.9):

$$V_{ref\_c,17x}^k = R_k \cdot \dot{\theta}_{h,k}(t) \cdot \cos(\theta_{h,k}(t) + \theta_{CSk_{k+1}}) \quad (3.10)$$

$$V_{ref\_c,17y}^k = R_k \cdot \dot{\theta}_{h,k}(t) \cdot \sin(\theta_{h,k}(t) + \theta_{CSk_{k+1}}) \quad (3.11)$$

### 3.2.3.2.1.2. For Turning Right

$$\begin{aligned} \bar{P}_{ref\_c,17}^k = & \\ & O_{k,k+1x}\bar{u}_1 + O_{k,k+1y}\bar{u}_2 + P_{ref\_c,17z}^k\bar{u}_3 + R_k \cdot \sin(\theta_{h,k}(t)) \hat{C}^{(0,CSk_{k+1})}\bar{u}_1 + \\ & R_k \cdot \cos(\theta_{h,k}(t)) \hat{C}^{(0,CSk_{k+1})}\bar{u}_2 \end{aligned} \quad (3.12)$$

From equation (3.12), equation (3.13) and equation (3.14) can be derived such as:

$$P_{ref\_c,17x}^k = O_{k,k+1x} + R_k \cdot \sin(\theta_{h,k}(t) - \theta_{CSk_{k+1}}) \quad (3.13)$$

$$P_{ref\_c,17y}^k = O_{k,k+1y} + R_k \cdot \cos(\theta_{h,k}(t) - \theta_{CSk_{k+1}}) \quad (3.14)$$

Using equation (3.13) and (3.14):

$$V_{ref\_c,17x}^k = R_k \cdot \dot{\theta}_{h,k}(t) \cdot \cos(\theta_{h,k}(t) - \theta_{CSk_{k+1}}) \quad (3.15)$$

$$V_{ref\_c,17y}^k = -R_k \cdot \dot{\theta}_{h,k}(t) \cdot \sin(\theta_{h,k}(t) - \theta_{CSk_{k+1}}) \quad (3.16)$$

### 3.2.3.2.2. Angular Position and Angular Velocity Definitions for Body 17

Angular position of Body 17 is given in terms of component transformation matrices and defined such that Body 17 is always parallel to the plane formed by  $\vec{u}_1^{(0)}$  and  $\vec{u}_2^{(0)}$ .

Angular velocity of Body 17, differentiated with respect to and resolved in the inertial frame, is to be found by the definition:

$$\tilde{W}_{17\_ref} = \frac{d\hat{C}_{ref}^{(0,17)}}{dt} \cdot \hat{C}_{ref}^{(0,17)T} \quad (3.17)$$

$$\text{Using equation (3.17), } \bar{w}_{17\_ref} = \begin{bmatrix} \bar{u}_3^T \tilde{W}_{17\_ref} \bar{u}_2 \\ \bar{u}_1^T \tilde{W}_{17\_ref} \bar{u}_3 \\ \bar{u}_2^T \tilde{W}_{17\_ref} \bar{u}_1 \end{bmatrix} \quad (3.18)$$

#### 3.2.3.2.2.1. For SSPs

The angular position definition between  $P_k$  and  $P_{k,k+1}$  using  $\theta_{h,k}(t)$  definition for turning left:

$$\begin{aligned} \hat{C}_{ref}^{(0,17)} &= \hat{C}^{(0,CSk\_k+1)} \cdot \hat{C}^{(CSk\_k+1,17)} \\ &= e^{\tilde{u}_3 \theta_{CSk\_k+1}} \cdot e^{\tilde{u}_3 \theta_{h,k}(t)} = e^{\tilde{u}_3 (\theta_{CSk\_k+1} + \theta_{h,k}(t))} \end{aligned}$$

Similarly for turning right:

$$= e^{\tilde{u}_3 \theta_{CSk\_k+1}} \cdot e^{\tilde{u}_3 (-\theta_{h,k}(t))} = e^{\tilde{u}_3 (\theta_{CSk\_k+1} - \theta_{h,k}(t))}$$

#### 3.2.3.2.2.1. For DSPs

##### 3.2.3.2.2.1.1. For Turning Left

The angular position definition between  $P_{k,k+1}$  and  $P_{k+1}$  for turning left is described below. At the beginning of DSP or for  $t=0$ :

$$\hat{C}_{ref}^{(0,17)} = \hat{C}^{(0,CSk\_k+1)} \cdot e^{\tilde{u}_3 \theta_{h,SSP\_k}} = e^{\tilde{u}_3 (\theta_{CSk\_k+1} + \theta_{h,SSP\_k})}$$

At the end of DSP or for  $t = t_{DSP,k}$ :

$$\hat{C}_{ref}^{(0,17)} = \hat{C}^{(0,CSk+1,k+2)} = e^{\tilde{u}_3 \theta_{CSk+1,k+2}}$$

In a more general form,  $\hat{C}_{ref}^{(0,17)} = e^{\tilde{u}_3 \theta_{h_{or},k}(t)}$

For  $\theta_{h_{or},k}(t) = e_3^k t^3 + e_2^k t^2 + e_1^k t + e_0^k$  with conditions to be satisfied such as:

- $\theta_{h_{or},k}(0) = \theta_{CSk_{k+1}} + \theta_{h,SSP_k}$
- $\theta_{h_{or},k}(t_{DSP,k}) = \theta_{CSk+1_{k+2}}$
- $\frac{d\theta_{h_{or},k}(t)}{dt} \Big|_{t=0} = \frac{V_{k,k+1}}{R_k}$
- If the turning direction for the next phase is leftwards  $\frac{d\theta_{h_{or},k}(t)}{dt} \Big|_{t=t_{DSP,k}} = \frac{V_{k+1}}{R_{k+1}}$
- If the turning direction for the next phase is rightwards  $\frac{d\theta_{h_{or},k}(t)}{dt} \Big|_{t=t_{DSP,k}} = -\frac{V_{k+1}}{R_{k+1}}$

Then, the problem of finding proper polynomial coefficients can be described as:

$$\begin{bmatrix} 0 & 0 & 0 & 1 \\ t_{DSP,k}^3 & t_{DSP,k}^2 & t_{DSP,k} & 1 \\ 0 & 0 & 1 & 0 \\ 3 \cdot t_{DSP,k}^2 & 2 \cdot t_{DSP,k} & 1 & 0 \end{bmatrix} \begin{bmatrix} e_3^k \\ e_2^k \\ e_1^k \\ e_0^k \end{bmatrix} = \begin{bmatrix} \theta_{CSk_{k+1}} + \theta_{h,SSP_k} \\ \theta_{CSk+1_{k+2}} \\ \frac{V_{k,k+1}}{R_k} \\ \frac{V_{k+1}}{R_{k+1}} \text{ or } -\frac{V_{k+1}}{R_{k+1}} \end{bmatrix}$$

### 3.2.3.2.2.1.1. For Turning Right

Similarly at the beginning of DSP or for  $t=0$ :

$$\hat{C}_{ref}^{(0,17)} = \hat{C}^{(0,CSk_{k+1})} \cdot e^{\tilde{u}_3(-\theta_{h,SSP_k})} = e^{\tilde{u}_3(\theta_{CSk_{k+1}} - \theta_{h,SSP_k})}$$

At the end of DSP or for  $t = t_{DSP,k}$ :

$$\hat{C}_{ref}^{(0,17)} = \hat{C}^{(0,CSk+1,k+2)} = e^{\tilde{u}_3 \theta_{CSk+1,k+2}}$$

In a more general form,  $\hat{C}_{ref}^{(0,17)} = e^{\tilde{u}_3 \theta_{h_{or,k}}(t)}$

For  $\theta_{h_{or,k}}(t) = e_3^k t^3 + e_2^k t^2 + e_1^k t + e_0^k$  with conditions to be satisfied such as:

- $\theta_{h_{or,k}}(0) = \theta_{CSk_{k+1}} - \theta_{h,SSP_k}$
- $\theta_{h_{or,k}}(t_{DSP,k}) = \theta_{CSk+1_{k+2}}$
- $\left. \frac{d\theta_{h_{or,k}}(t)}{dt} \right|_{t=0} = -\frac{V_{k,k+1}}{R_k}$
- If the turning direction for the next phase is leftwards  $\left. \frac{d\theta_{h_{or,k}}(t)}{dt} \right|_{t=t_{DSP,k}} = \frac{V_{k+1}}{R_{k+1}}$
- If the turning direction for the next phase is rightwards  $\left. \frac{d\theta_{h_{or,k}}(t)}{dt} \right|_{t=t_{DSP,k}} = -\frac{V_{k+1}}{R_{k+1}}$

Then, the problem of finding proper polynomial coefficients can be described as:

$$\begin{bmatrix} 0 & 0 & 0 & 1 \\ t_{DSP,k}^3 & t_{DSP,k}^2 & t_{DSP,k} & 1 \\ 0 & 0 & 1 & 0 \\ 3 \cdot t_{DSP,k}^2 & 2 \cdot t_{DSP,k} & 1 & 0 \end{bmatrix} \begin{bmatrix} e_3^k \\ e_2^k \\ e_1^k \\ e_0^k \end{bmatrix} = \begin{bmatrix} \theta_{CSk_{k+1}} - \theta_{h,SSP_k} \\ \theta_{CSk+1_{k+2}} \\ -\frac{V_{k,k+1}}{R_k} \\ \frac{V_{k+1}}{R_{k+1}} \text{ or } -\frac{V_{k+1}}{R_{k+1}} \end{bmatrix}$$

### 3.2.3.3. Trajectory Definitions for Toe Points, Body 1 and Body 2

#### 3.2.3.3.1. Translational Position and Velocity Definitions for Toe Points on Body 1 and Body 2

$P_{tpR,i}^k$  and  $P_{tpL,i}^k$ ,  $P_{tpR,f}^k$  and  $P_{tpL,f}^k$  are points showing the initial and final positions of toe points  $P_{tpR}$  and  $P_{tpL}$  on Body 1 and Body 2 at the beginning and end of LFFSSP and RFFSSP during the motion of CoM of Body 17 between points  $P_k$  and  $P_{k,k+1}$

$\theta_{Rrot,k}$  for LFFSSP and  $\theta_{Lrot,k}$  for RFFSSP are calculated by using the definitions shown in Figure 3.12, Figure 3.13, Figure 3.14, Figure 3.15.

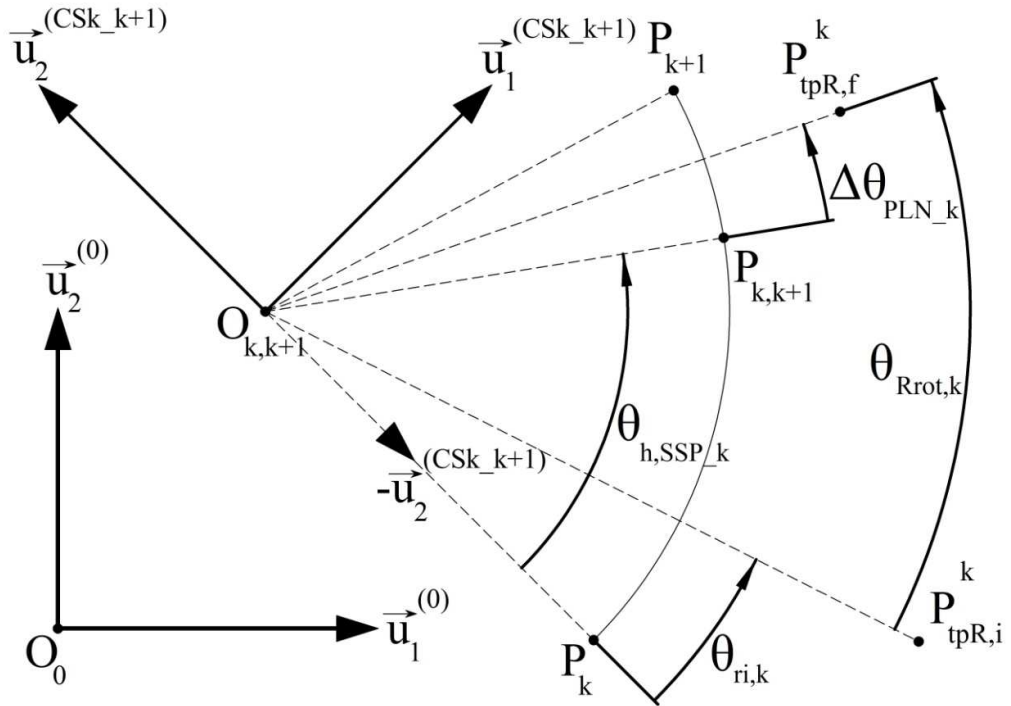


Figure 3.12: The definition of  $\theta_{ri,k}$  and  $\theta_{Rrot,k}$  during LFFSSP for Turning Left

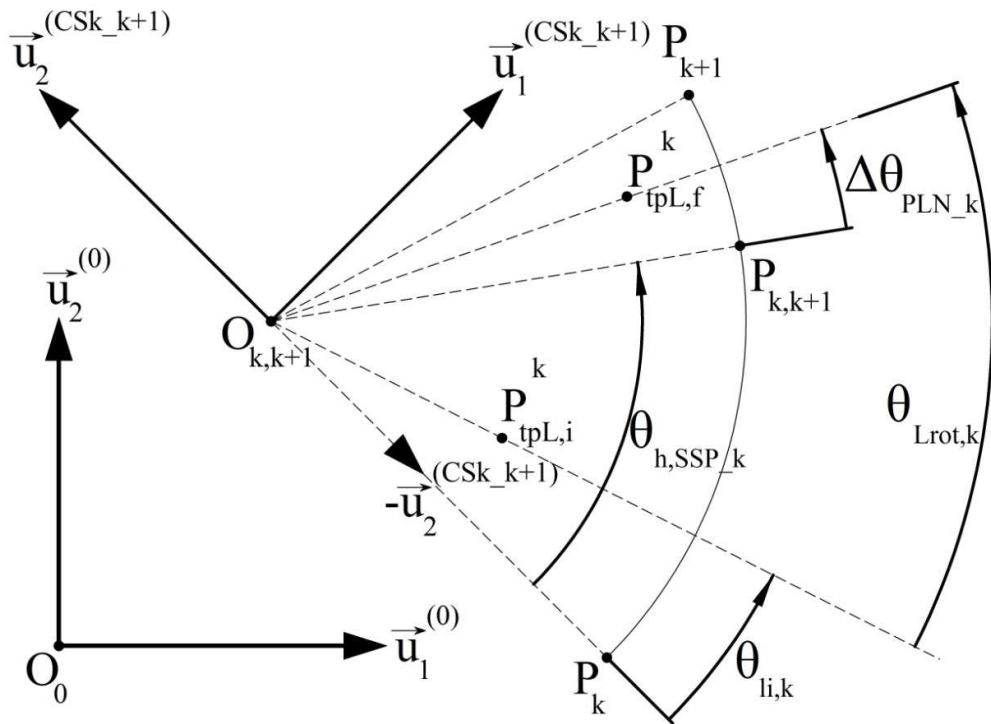


Fig 3.13: The definition of  $\theta_{li,k}$  and  $\theta_{Lrot,k}$  during RFFSSP for Turning Left

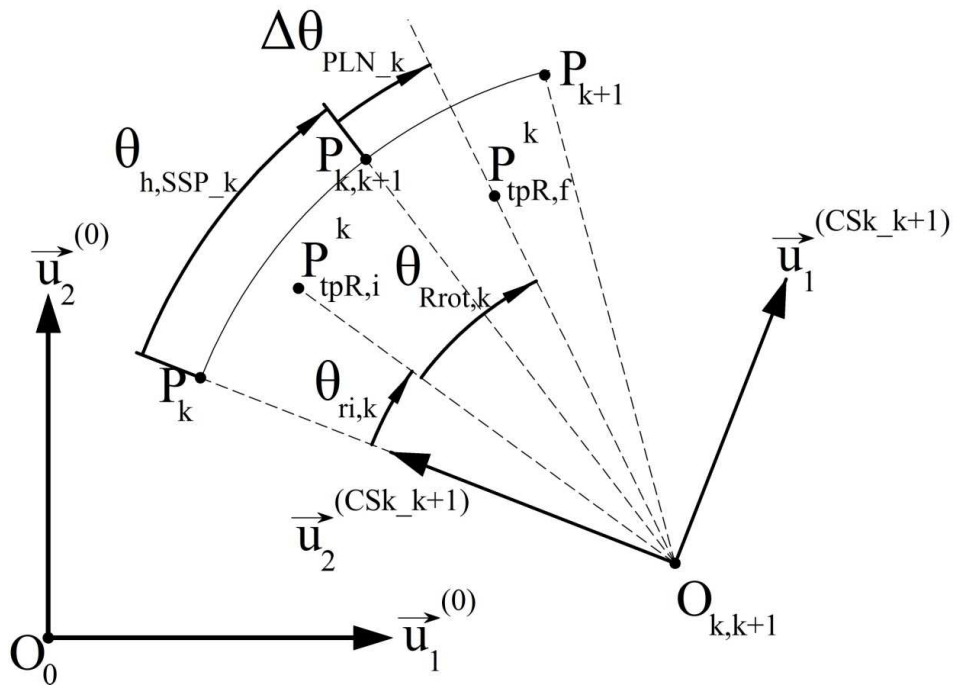


Fig 3.14: The definition of  $\theta_{ri,k}$  and  $\theta_{Rrot,k}$  during LFFSSP for Turning Right

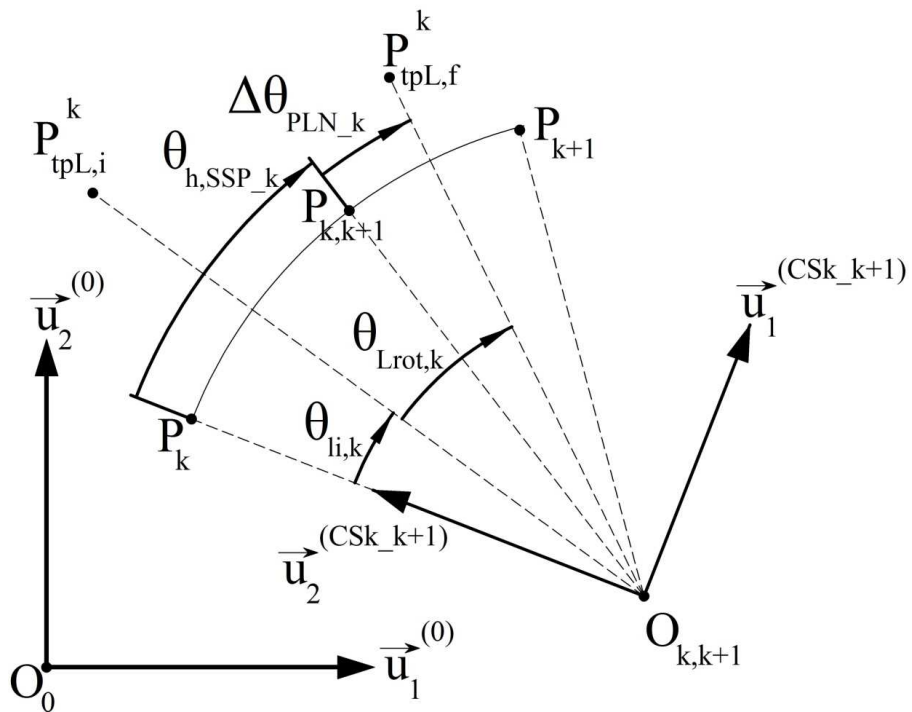


Fig 3.15: The definition of  $\theta_{li,k}$  and  $\theta_{Lrot,k}$  during RFFSSP for Turning Right

Then,  $\theta_{Rrot,k} = \theta_{h,SSP_k} + \Delta\theta_{PLN_k} - \theta_{ri,k}$  and similarly  $\theta_{Lrot,k} = \theta_{h,SSP_k} + \Delta\theta_{PLN_k} - \theta_{li,k}$

$\theta_{ri,k}$  is calculated as shown below:

Since the projection of  $P_{tpR,i}^k$  onto the plane formed by  $\vec{u}_1^{(0)}$  and  $\vec{u}_2^{(0)}$  is considered, its component in  $\vec{u}_3^{(0)}$  direction is disregarded. Then:

$$\bar{P}_{tpR,i}^{k(0)} = P_{tpRx,i}^k \bar{u}_1 + P_{tpRy,i}^k \bar{u}_2 \quad (3.19)$$

For equation (3.19):

$$\begin{aligned} \bar{P}_{tpR,i}^{k(CSk_{k+1})} &= \\ &(P_{tpRx,i}^k - O_{k,k+1x}) \hat{C}^{(CSk_{k+1,0})} \bar{u}_1 + (P_{tpRy,i}^k - O_{k,k+1y}) \hat{C}^{(CSk_{k+1,0})} \bar{u}_2 \\ K_{Rx} &= \\ &[(P_{tpRx,i}^k - O_{k,k+1x}) \cdot \cos(\theta_{CSk_{k+1}}) + (P_{tpRy,i}^k - O_{k,k+1y}) \cdot \sin(\theta_{CSk_{k+1}})] \end{aligned} \quad (3.20)$$

$$\begin{aligned} K_{Ry} &= \\ &[(P_{tpRy,i}^k - O_{k,k+1y}) \cdot \cos(\theta_{CSk_{k+1}}) - (P_{tpRx,i}^k - O_{k,k+1x}) \cdot \sin(\theta_{CSk_{k+1}})] \end{aligned} \quad (3.21)$$

Using equation (3.20) and (3.21):

$$\bar{P}_{tpR,i}^{k(CSk_{k+1})} = K_{Rx} \bar{u}_1 + K_{Ry} \bar{u}_2 \quad (3.22)$$

Then,  $\theta_{ri,k}$  can be obtained by equation (3.23) for turning left and equation (3.24) for turning right.

$$\theta_{ri,k} = \text{atan2}(K_{Rx}, -K_{Ry}) \quad (3.23)$$

$$\theta_{ri,k} = \text{atan2}(K_{Rx}, K_{Ry}) \quad (3.24)$$

The same procedure is employed for calculating  $\theta_{li,k}$ .

$$K_{Lx} = [(P_{tpLx,i}^k - O_{k,k+1x}) \cdot \cos(\theta_{CSk_{k+1}}) + (P_{tpLy,i}^k - O_{k,k+1y}) \cdot \sin(\theta_{CSk_{k+1}})] \quad (3.25)$$

$$K_{Ly} = [(P_{tpLy,i}^k - O_{k,k+1y}) \cdot \cos(\theta_{CSk_{k+1}}) - (P_{tpLx,i}^k - O_{k,k+1x}) \cdot \sin(\theta_{CSk_{k+1}})] \quad (3.26)$$

By equation (3.25) and (3.26):

$$\bar{P}_{tpL,i}^{k(CSk_{k+1})} = K_{Lx}\bar{u}_1 + K_{Ly}\bar{u}_2 \quad (3.27)$$

Then,  $\theta_{li,k}$  can be obtained by equation (3.28) for turning left and equation (3.29) for turning right.

$$\theta_{li,k} = \text{atan2}(K_{Lx}, -K_{Ly}) \quad (3.28)$$

$$\theta_{li,k} = \text{atan2}(K_{Lx}, K_{Ly}) \quad (3.29)$$

For  $\theta_{rot,k}(t) = f_3^k t^3 + f_2^k t^2 + f_1^k t + f_0^k$  with conditions to be satisfied such as:

- $\theta_{rot,k}(0) = 0$
- $\theta_{rot,k}(t_{SSP,k}) = \theta_{Rrot,k}$  for LFFSSP,  $\theta_{rot,k}(t_{SSP,k}) = \theta_{Lrot,k}$  for RFFSSP
- $\frac{d\theta_{rot,k}(t)}{dt} \Big|_{t=0} = 0$
- $\frac{d\theta_{rot,k}(t)}{dt} \Big|_{t=t_{SSP,k}} = 0$

Then, the problem of finding proper polynomial coefficients can be described as:

$$\begin{bmatrix} 0 & 0 & 0 & 1 \\ t_{SSP,k}^3 & t_{SSP,k}^2 & t_{SSP,k} & 1 \\ 0 & 0 & 1 & 0 \\ 3 \cdot t_{SSP,k}^2 & 2 \cdot t_{SSP,k} & 1 & 0 \end{bmatrix} \begin{bmatrix} f_3^k \\ f_2^k \\ f_1^k \\ f_0^k \end{bmatrix} = \begin{bmatrix} 0 \\ \theta_{Rrot,k} \text{ or } \theta_{Lrot,k} \\ 0 \\ 0 \end{bmatrix}$$

A function named as  $R_{gen,k}(t)$  is defined to ensure the adjustment of step width to the desired value during the motion of CoM of Body 17 between points  $P_k$  and  $P_{k,k+1}$  as shown in Figure 3.16.

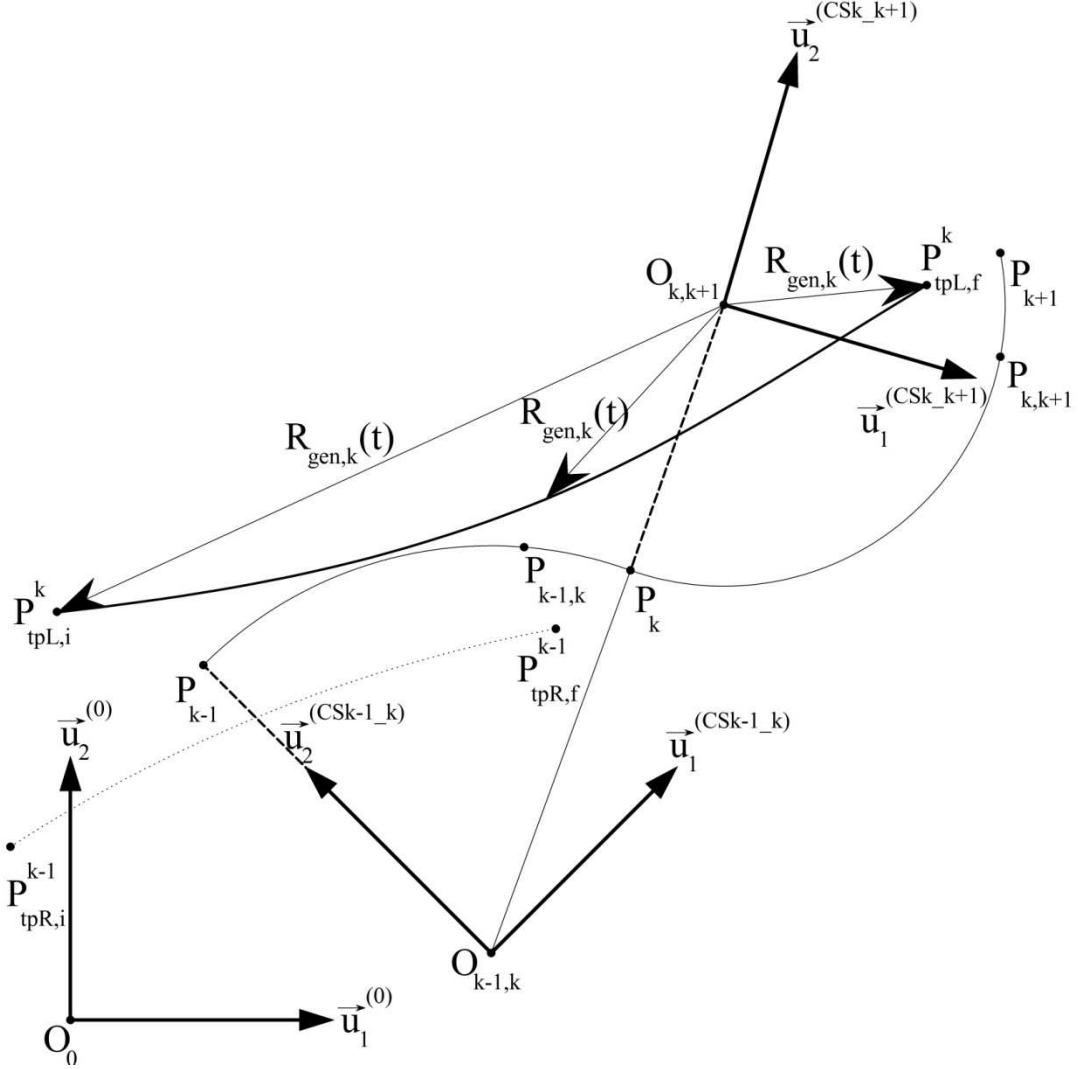


**Figure 3.16:  $R_{gen,k}(t)$  function**

$$R_{gen,k}(t) = \begin{cases} R_{c,k}(t), & t \leq t_{z,k} \\ R_{f,k}, & t_{SSP,k} \geq t > t_{z,k} \end{cases}, t_{z,k} = \frac{t_{SSP,k}}{k_{Adj,k}}$$

$$\text{For RFFSSP, } R_{o,k} = \sqrt{(O_{k,k+1x} - P_{tpLx,i}^k)^2 + (O_{k,k+1y} - P_{tpLy,i}^k)^2} \quad (3.30)$$

$$\text{For LFFSSP, } R_{o,k} = \sqrt{(O_{k,k+1x} - P_{tpRx,i}^k)^2 + (O_{k,k+1y} - P_{tpRy,i}^k)^2} \quad (3.31)$$

During RFFSSP for turning left and LFFSSP for turning right:

$$R_{f,k} = R_k - \frac{SW_k}{2} \quad (3.32)$$

During RFFSSP for turning right and LFFSSP for turning left:

$$R_{f,k} = R_k + \frac{SW_k}{2} \quad (3.33)$$

Then a function  $R_{c,k}(t) = g_3^k t^3 + g_2^k t^2 + g_1^k t + g_0^k$  is defined with conditions shown below:

- $R_{c,k}(0) = R_{o,k}$ , where  $R_{o,k}$  is defined by equation (3.30) or (3.31)
- $R_{c,k}(t_{z,k}) = R_{f,k}$ , where  $R_{f,k}$  is defined by equation (3.32) or (3.33)
- $\frac{dR_{c,k}(t)}{dt} \Big|_{t=0} = 0$
- $\frac{dR_{c,k}(t)}{dt} \Big|_{t=t_{z,k}} = 0$

Then, the problem of finding proper polynomial coefficients can be described as:

$$\begin{bmatrix} 0 & 0 & 0 & 1 \\ t_{z,k}^3 & t_{z,k}^2 & t_{z,k} & 1 \\ 0 & 0 & 1 & 0 \\ 3 \cdot t_{z,k}^2 & 2 \cdot t_{z,k} & 1 & 0 \end{bmatrix} \begin{bmatrix} g_3^k \\ g_2^k \\ g_1^k \\ g_0^k \end{bmatrix} = \begin{bmatrix} R_{o,k} \\ R_{f,k} \\ 0 \\ 0 \end{bmatrix}$$

A polynomial function is introduced to express the position of toe point in  $\vec{u}_3^{(0)}$  direction.

$P_{z,k}(t) = h_4^k t^4 + h_3^k t^3 + h_2^k t^2 + h_1^k t + h_0^k$  with conditions to satisfy:

- $P_{z,k}(0) = 0.015$  m (Height of the toe point with respect to the plane of  $\vec{u}_1^{(0)}$  and  $\vec{u}_2^{(0)}$  while the toe part of the foot for the corresponding toe point is flatly fixed to the ground)
- $P_{z,k}(t_{SSP,k}) = 0.015$  m

- $P_{z,k}(k_{SH,k} \cdot t_{SSP,k}) = SH_k$
- $\frac{dP_{z,k}(t)}{dt} \Big|_{t=0} = 0$
- $\frac{dP_{z,k}(t)}{dt} \Big|_{t=t_{SSP,k}} = 0$

Then, the problem of finding proper polynomial coefficients becomes:

$$\begin{bmatrix} 0 & 0 & 0 & 0 & 1 \\ t_{SSP,k}^4 & t_{SSP,k}^3 & t_{SSP,k}^2 & t_{SSP,k} & 1 \\ (k_{SH,k} \cdot t_{SSP,k})^4 & (k_{SH,k} \cdot t_{SSP,k})^3 & (k_{SH,k} \cdot t_{SSP,k})^2 & (k_{SH,k} \cdot t_{SSP,k}) & 1 \\ 0 & 0 & 0 & 1 & 0 \\ 4 \cdot t_{SSP,k}^3 & 3 \cdot t_{SSP,k}^2 & 2 \cdot t_{SSP,k} & 1 & 0 \end{bmatrix} \begin{bmatrix} h_4^k \\ h_3^k \\ h_2^k \\ h_1^k \\ h_0^k \end{bmatrix} = \begin{bmatrix} 0.015 \\ 0.015 \\ SH_k \\ 0 \\ 0 \end{bmatrix}$$

Having all this information, the reference position and velocity vectors of toe points differentiated with respect to and resolved in the inertial frame, can be expressed in matrix forms during the motion of CoM of Body 17 between points  $P_k$  and  $P_{k,k+1}$  as shown below.

For turning left:

$$\begin{aligned} \bar{P}_{tpR_{ref}}^k(t)^{(CSk_{k+1})} &= R_{gen,k} \cdot \sin(\theta_{ri,k} + \theta_{rot,k}) \bar{u}_1 \\ &- R_{gen,k} \cdot \cos(\theta_{ri,k} + \theta_{rot,k}) \bar{u}_2 + P_{z,k} \bar{u}_3 \\ \bar{P}_{tpR_{ref}}^k(t)^{(0)} &= [R_{gen,k} \cdot \sin(\theta_{ri,k} + \theta_{rot,k} + \theta_{CSk_{k+1}}) + O_{k,k+1x}] \bar{u}_1 + \\ &[-R_{gen,k} \cdot \cos(\theta_{ri,k} + \theta_{rot,k} + \theta_{CSk_{k+1}}) + O_{k,k+1y}] \bar{u}_2 + P_{z,k} \bar{u}_3 \end{aligned} \quad (3.34)$$

$$\begin{aligned}
\bar{V}_{tpR_{ref}}^k(t)^{(0)} = & \\
& [\dot{R}_{gen,k} \cdot \sin(\theta_{ri,k} + \theta_{rot,k} + \theta_{CSk_{k+1}}) + \\
& R_{gen,k} \cdot (\dot{\theta}_{ri,k} + \dot{\theta}_{rot,k} + \dot{\theta}_{CSk_{k+1}}) \cdot \cos(\theta_{ri,k} + \theta_{rot,k} + \theta_{CSk_{k+1}})] \bar{u}_1 + \\
& [-\dot{R}_{gen,k} \cdot \cos(\theta_{ri,k} + \theta_{rot,k} + \theta_{CSk_{k+1}}) + \\
& R_{gen,k} \cdot (\dot{\theta}_{ri,k} + \dot{\theta}_{rot,k} + \dot{\theta}_{CSk_{k+1}}) \cdot \sin(\theta_{ri,k} + \theta_{rot,k} + \theta_{CSk_{k+1}})] \bar{u}_2 + \dot{P}_{z,k} \bar{u}_3
\end{aligned} \tag{3.35}$$

$$\begin{aligned}
\bar{P}_{tpL_{ref}}^k(t)^{(CSk_{k+1})} = & R_{gen,k} \cdot \sin(\theta_{li,k} + \theta_{rot,k}) \bar{u}_1 \\
& - R_{gen,k} \cdot \cos(\theta_{li,k} + \theta_{rot,k}) \bar{u}_2 + P_{z,k} \bar{u}_3 \\
\bar{P}_{tpL_{ref}}^k(t)^{(0)} = & [R_{gen,k} \cdot \sin(\theta_{li,k} + \theta_{rot,k} + \theta_{CSk_{k+1}}) + O_{k,k+1x}] \bar{u}_1 + \\
& [-R_{gen,k} \cdot \cos(\theta_{li,k} + \theta_{rot,k} + \theta_{CSk_{k+1}}) + O_{k,k+1y}] \bar{u}_2 + P_{z,k} \bar{u}_3
\end{aligned} \tag{3.36}$$

$$\begin{aligned}
\bar{V}_{tpL_{ref}}^k(t)^{(0)} = & \\
& [\dot{R}_{gen,k} \cdot \sin(\theta_{li,k} + \theta_{rot,k} + \theta_{CSk_{k+1}}) + \\
& R_{gen,k} \cdot (\dot{\theta}_{li,k} + \dot{\theta}_{rot,k} + \dot{\theta}_{CSk_{k+1}}) \cdot \cos(\theta_{li,k} + \theta_{rot,k} + \theta_{CSk_{k+1}})] \bar{u}_1 + \\
& [-\dot{R}_{gen,k} \cdot \cos(\theta_{li,k} + \theta_{rot,k} + \theta_{CSk_{k+1}}) + \\
& R_{gen,k} \cdot (\dot{\theta}_{li,k} + \dot{\theta}_{rot,k} + \dot{\theta}_{CSk_{k+1}}) \cdot \sin(\theta_{li,k} + \theta_{rot,k} + \theta_{CSk_{k+1}})] \bar{u}_2 + \dot{P}_{z,k} \bar{u}_3
\end{aligned} \tag{3.37}$$

For turning right:

$$\begin{aligned}
\bar{P}_{tpR_{ref}}^k(t)^{(CSk_{k+1})} = & R_{gen,k} \cdot \sin(\theta_{ri,k} + \theta_{rot,k}) \bar{u}_1 \\
& + R_{gen,k} \cdot \cos(\theta_{ri,k} + \theta_{rot,k}) \bar{u}_2 + P_{z,k} \bar{u}_3 \\
\bar{P}_{tpR_{ref}}^k(t)^{(0)} = & [R_{gen,k} \cdot \sin(\theta_{ri,k} + \theta_{rot,k} - \theta_{CSk_{k+1}}) + O_{k,k+1x}] \bar{u}_1 + \\
& [R_{gen,k} \cdot \cos(\theta_{ri,k} + \theta_{rot,k} - \theta_{CSk_{k+1}}) + O_{k,k+1y}] \bar{u}_2 + P_{z,k} \bar{u}_3
\end{aligned} \tag{3.38}$$

$$\begin{aligned}
\bar{V}_{tpR_{ref}}^k(t)^{(0)} = & \\
& [\dot{R}_{gen,k} \cdot \sin(\theta_{ri,k} + \theta_{rot,k} - \theta_{CSk_{k+1}}) + \\
& R_{gen,k} \cdot (\dot{\theta}_{ri,k} + \dot{\theta}_{rot,k} - \dot{\theta}_{CSk_{k+1}}) \cdot \cos(\theta_{ri,k} + \theta_{rot,k} - \theta_{CSk_{k+1}})] \bar{u}_1 + \\
& [\dot{R}_{gen,k} \cdot \cos(\theta_{ri,k} + \theta_{rot,k} - \theta_{CSk_{k+1}}) - \\
& R_{gen,k} \cdot (\dot{\theta}_{ri,k} + \dot{\theta}_{rot,k} - \dot{\theta}_{CSk_{k+1}}) \cdot \sin(\theta_{ri,k} + \theta_{rot,k} - \theta_{CSk_{k+1}})] \bar{u}_2 + \dot{P}_{z,k} \bar{u}_3
\end{aligned} \tag{3.39}$$

$$\begin{aligned}
\bar{P}_{tpL_{ref}}^k(t)^{(CSk_{k+1})} = & R_{gen,k} \cdot \sin(\theta_{li,k} + \theta_{rot,k}) \bar{u}_1 \\
& + R_{gen,k} \cdot \cos(\theta_{li,k} + \theta_{rot,k}) \bar{u}_2 + P_{z,k} \bar{u}_3 \\
\bar{P}_{tpL_{ref}}^k(t)^{(0)} = & [R_{gen,k} \cdot \sin(\theta_{li,k} + \theta_{rot,k} - \theta_{CSk_{k+1}}) + O_{k,k+1x}] \bar{u}_1 + \\
& [R_{gen,k} \cdot \cos(\theta_{li,k} + \theta_{rot,k} - \theta_{CSk_{k+1}}) + O_{k,k+1y}] \bar{u}_2 + P_{z,k} \bar{u}_3
\end{aligned} \tag{3.40}$$

$$\begin{aligned}
\bar{V}_{tpL_{ref}}^k(t)^{(0)} = & \\
& [\dot{R}_{gen,k} \cdot \sin(\theta_{li,k} + \theta_{rot,k} - \theta_{CSk_{k+1}}) + \\
& R_{gen,k} \cdot (\dot{\theta}_{li,k} + \dot{\theta}_{rot,k} - \dot{\theta}_{CSk_{k+1}}) \cdot \cos(\theta_{li,k} + \theta_{rot,k} - \theta_{CSk_{k+1}})] \bar{u}_1 + \\
& [\dot{R}_{gen,k} \cdot \cos(\theta_{li,k} + \theta_{rot,k} - \theta_{CSk_{k+1}}) - \\
& R_{gen,k} \cdot (\dot{\theta}_{li,k} + \dot{\theta}_{rot,k} - \dot{\theta}_{CSk_{k+1}}) \cdot \sin(\theta_{li,k} + \theta_{rot,k} - \theta_{CSk_{k+1}})] \bar{u}_2 + \dot{P}_{z,k} \bar{u}_3
\end{aligned} \tag{3.41}$$

### 3.2.3.3.2. Angular Position and Angular Velocity Definitions for Body 1 and Body 2

Angular positions of Body 1 and Body 2 are given in terms of component transformation matrices and defined such that Body 1 and Body 2 are always parallel to the plane formed by  $\bar{u}_1^{(0)}$  and  $\bar{u}_2^{(0)}$ .

Angular velocities of Body 1 and Body 2, differentiated with respect to and resolved in the inertial frame, is to be found by definitions:

$$\tilde{W}_{1_{ref}} = \frac{d\hat{C}_{ref}^{(0,1)}}{dt} \cdot \hat{C}_{ref}^{(0,1)T} \tag{3.42}$$

$$\tilde{W}_{2\_ref} = \frac{d\hat{C}_{ref}^{(0,2)}}{dt} \cdot \hat{C}_{ref}^{(0,2)T} \quad (3.43)$$

Using equation (3.42) and (3.43), equation (3.44) and (3.45) can be found such that:

$$\bar{W}_{1\_ref} = \begin{bmatrix} \bar{u}_3^T \tilde{W}_{1\_ref} \bar{u}_2 \\ \bar{u}_1^T \tilde{W}_{1\_ref} \bar{u}_3 \\ \bar{u}_2^T \tilde{W}_{1\_ref} \bar{u}_1 \end{bmatrix} \quad (3.44)$$

$$\bar{W}_{2\_ref} = \begin{bmatrix} \bar{u}_3^T \tilde{W}_{2\_ref} \bar{u}_2 \\ \bar{u}_1^T \tilde{W}_{2\_ref} \bar{u}_3 \\ \bar{u}_2^T \tilde{W}_{2\_ref} \bar{u}_1 \end{bmatrix} \quad (3.45)$$

During the motion of CoM of Body 17 between points  $P_k$  and  $P_{k,k+1}$ , the initial orientation (for  $t = 0$ ) of Body 1 or Body 2 is defined as:

If  $T_{dir,k-1} = +1$ ,

$$\hat{C}_{ref}^{(0,1)} \text{ or } \hat{C}_{ref}^{(0,2)} = e^{\tilde{u}_3 \left( \theta_{CSk-1,k} + (\theta_{h,SSP_{k-1}} + \Delta\theta_{PLN_{k-1}}) \right)} = e^{\tilde{u}_3 \theta_{Fori,k}} \quad (3.46)$$

If  $T_{dir,k-1} = -1$ ,

$$\hat{C}_{ref}^{(0,1)} \text{ or } \hat{C}_{ref}^{(0,2)} = e^{\tilde{u}_3 \left( \theta_{CSk-1,k} - (\theta_{h,SSP_{k-1}} + \Delta\theta_{PLN_{k-1}}) \right)} = e^{\tilde{u}_3 \theta_{Fori,k}} \quad (3.47)$$

The final orientation ( $t = t_{SSP,k}$ ) of Body 1 or Body 2 is defined as:

For  $T_{dir,k} = +1$ ,

$$\hat{C}_{ref}^{(0,1)} \text{ or } \hat{C}_{ref}^{(0,2)} = e^{\tilde{u}_3 \left( \theta_{CSk,k+1} + (\theta_{h,SSP_k} + \Delta\theta_{PLN_k}) \right)} = e^{\tilde{u}_3 \theta_{Forf,k}} \quad (3.48)$$

For  $T_{dir,k} = -1$ ,

$$\hat{C}_{ref}^{(0,1)} \text{ or } \hat{C}_{ref}^{(0,2)} = e^{\tilde{u}_3 \left( \theta_{CSk,k+1} - (\theta_{h,SSP_k} + \Delta\theta_{PLN_k}) \right)} = e^{\tilde{u}_3 \theta_{Forf,k}} \quad (3.49)$$

Then,  $\hat{C}_{ref}^{(0,1)}$  or  $\hat{C}_{ref}^{(0,2)}$  can be defined by function  $\theta_{For,k}(t)$  as  $e^{\tilde{u}_3 \theta_{For,k}}$ .

$\theta_{Fori,k}$  and  $\theta_{Forf,k}$  values are added or subtracted with  $2\pi$  if necessary, in order to reduce  $\theta_{Fori,k}$  and  $\theta_{Forf,k}$  values to  $-\pi$  and  $+\pi$  interval. Additionally after the reduction,  $(\theta_{Forf,k} - \theta_{Fori,k})$  is reduced to  $-\pi$  and  $+\pi$  interval if necessary by subtraction or addition of  $2\pi$  to  $\theta_{Fori,k}$ .

For  $\theta_{For,k}(t) = j_3^k t^3 + j_2^k t^2 + j_1^k t + j_0^k$  with conditions to be satisfied:

- $\theta_{For,k}(0) = \theta_{Fori,k}$ , where  $\theta_{Fori,k}$  is defined by (3.46) or (3.47)
- $\theta_{For,k}(t_{SSP,k}) = \theta_{Forf,k}$ , where  $\theta_{Forf,k}$  is defined by (3.48) or (3.49)
- $\frac{d\theta_{For,k}(t)}{dt} \Big|_{t=0} = 0$
- $\frac{d\theta_{For,k}(t)}{dt} \Big|_{t=t_{SSP,k}} = 0$ s

Then, the problem of finding proper coefficients can be described as:

$$\begin{bmatrix} 0 & 0 & 0 & 1 \\ t_{SSP,k}^3 & t_{SSP,k}^2 & t_{SSP,k} & 1 \\ 0 & 0 & 1 & 0 \\ 3 \cdot t_{SSP,k}^2 & 2 \cdot t_{SSP,k} & 1 & 0 \end{bmatrix} \begin{bmatrix} j_3 \\ j_2 \\ j_1 \\ j_0 \end{bmatrix} = \begin{bmatrix} \theta_{Fori,k} \\ \theta_{Forf,k} \\ 0 \\ 0 \end{bmatrix}$$

## CHAPTER 4

### MATHEMATICAL MODELING

In this chapter, mathematical model behind the simulation is introduced. Mathematical modeling is achieved in three steps. Kinematic equations are derived in order to find kinematic characteristics of bodies. Derivation of dynamic equations is achieved by Newton-Euler equations in a general form for all phases. During the direct dynamic solution procedure, generalized dynamic equations are arranged into the form which enables the calculation of joint space accelerations by implementing assumptions related with biped locomotion and its phases.

#### 4.1. The Derivation of Kinematic Equations

In order to keep equations as general as possible, simplifications in kinematic equations resulting from kinematic assumptions regarding the locomotion phase are avoided. Hence, the application of these assumptions is done during the dynamic solution process. However, kinematic information for at least one body with respect to the inertial frame is supplied to initialize the recursive calculations. Kinematic assumptions depending on the locomotion phase are explained below.

Several bodies are assumed to be rigidly fixed to the ground as if welded to the ground:

- Body 1 and Body 3 for RFFSSP
- Body 2 and Body 4 for LFFSSP
- Body 1, Body 3 and Body 2 for RFFDSP
- Body 2, Body 4 and Body 1 for LFFDSP

Assumptions for Body 1 and Body 2 are implemented by supplying proper kinematic values to kinematic equations; but kinematic constraint equations

embedded in the direct dynamic solution procedure and some joint variables being taken as zero during the transition procedure from single to double support phases are used to ensure this assumption on Body 3 and Body 4. All values supplied to kinematic equations remain constant within its relevant phase.

Kinematic equations are shown according to the order of recursive calculations. In double support phases, calculations begin from both Body 1 and Body 2 until kinematic characteristics of Body 17 are found from left (beginning from Body 2) and right (beginning from Body 1). Compatibility of kinematic characteristics of Body 17 from left and right in double support phases is provided by constraint equations during direct dynamic solution procedure and several operations done during phase transitions from single to double support phases. Jacobian matrices and their approximate time derivatives are calculated by kinematic equations related with them, mostly to be used in the following chapter. Several expressions of joint space variables used in the thesis are shown below:

$$\bar{q} = \begin{bmatrix} \theta_3 \\ \theta_4 \\ \theta_5 \\ \theta_6 \\ \theta_7 \\ \theta_8 \\ \theta_9 \\ \theta_{10} \\ \theta_{11} \\ \theta_{12} \\ \theta_{13} \\ \theta_{14} \\ \theta_{15} \\ \theta_{16} \\ \theta_{17,r} \\ \theta_{17,l} \\ \theta_{18} \\ \theta_{19} \\ \theta_{20} \\ \theta_{21} \\ \theta_{22} \\ \theta_{23} \\ \theta_{24} \\ \theta_{25} \\ \theta_{26} \\ \theta_{27} \end{bmatrix} \quad (4.1)$$

$$\bar{q}_{R,H} = [\theta_3 \quad \theta_5 \quad \theta_7 \quad \theta_9 \quad \theta_{11} \quad \theta_{13} \quad \theta_{15} \quad \theta_{17,r}]^T \quad (4.2)$$

$$\bar{q}_{L,H} = [\theta_4 \quad \theta_6 \quad \theta_8 \quad \theta_{10} \quad \theta_{12} \quad \theta_{14} \quad \theta_{16} \quad \theta_{17,l}]^T \quad (4.3)$$

$$\bar{q}_{lower} = [\theta_3 \quad \theta_4 \quad \theta_5 \quad \theta_6 \quad \theta_7 \quad \theta_8 \quad \theta_9 \quad \theta_{10} \quad \theta_{11} \quad \theta_{12} \quad \theta_{13} \quad \theta_{14} \quad \theta_{15} \quad \theta_{16} \quad \theta_{17,r} \quad \theta_{17,l}]^T \quad (4.4)$$

$$\bar{q}_{upper} = [\theta_{18} \quad \theta_{19} \quad \theta_{20} \quad \theta_{21} \quad \theta_{22} \quad \theta_{23} \quad \theta_{24} \quad \theta_{25} \quad \theta_{26} \quad \theta_{27}]^T \quad (4.5)$$

#### 4.1.1. Transformation Matrices

In order to express position, velocity and acceleration features in different frames; transformation matrices are frequently used. Since the exponential representation of transformation matrices are frequently used in the thesis, some frequently used basic properties related with them are shown below:

$$(e^{\tilde{n}\theta})^{-1} = (e^{\tilde{n}\theta})^T = e^{(-\tilde{n})\theta} = e^{\tilde{n}(-\theta)} = e^{-\tilde{n}\theta}$$

$$e^{\tilde{n}\theta_i} e^{\tilde{n}\theta_j} = e^{\tilde{n}\theta_j} e^{\tilde{n}\theta_i} = e^{\tilde{n}(\theta_i + \theta_j)}$$

$$e^{\tilde{n}\theta} \bar{n} = \bar{n}, \bar{n}^T e^{\tilde{n}\theta} = \bar{n}^T$$

$$\frac{d(e^{\tilde{n}\theta})}{d\theta} = \tilde{n} e^{\tilde{n}\theta} = e^{\tilde{n}\theta} \tilde{n}$$

$$(e^{\tilde{n}\theta} \bar{k}) = e^{\tilde{n}\theta} \tilde{k} e^{-\tilde{n}\theta}$$

$$e^{\tilde{u}_i \theta} \bar{u}_j = \bar{u}_j \cos \theta + (\tilde{u}_i \bar{u}_j) \sin \theta, \bar{u}_j^T e^{\tilde{u}_i \theta} = \bar{u}_j^T \cos \theta + (\tilde{u}_j \bar{u}_i)^T \sin \theta,$$

where  $\bar{u}_i$  and  $\bar{u}_j$  are basis vectors in matrix form. Also, the tilde symbol is used as a skew symmetric matrix operator such that:

$$\tilde{k} = \begin{bmatrix} 0 & -k_3 & k_2 \\ k_3 & 0 & -k_1 \\ -k_2 & k_1 & 0 \end{bmatrix} \text{ for } \bar{k} = \begin{bmatrix} k_1 \\ k_2 \\ k_3 \end{bmatrix}$$

Using joint space variable definitions in Table 2.6 and the sign convention explained in Figure 2.4, transformation matrices for adjacent frames can be expressed as shown below:

$$\hat{C}^{(1,3)} = e^{\tilde{u}_2\theta_3}$$

$$\hat{C}^{(2,4)} = e^{\tilde{u}_2\theta_4}$$

$$\hat{C}^{(3,5)} = e^{\tilde{u}_2\theta_5}$$

$$\hat{C}^{(4,6)} = e^{\tilde{u}_2\theta_6}$$

$$\hat{C}^{(5,7)} = e^{\tilde{u}_3\theta_7}$$

$$\hat{C}^{(6,8)} = e^{\tilde{u}_3\theta_8}$$

$$\hat{C}^{(7,9)} = e^{\tilde{u}_1\theta_9}$$

$$\hat{C}^{(8,10)} = e^{\tilde{u}_1\theta_{10}}$$

$$\hat{C}^{(9,11)} = e^{\tilde{u}_2\theta_{11}}$$

$$\hat{C}^{(10,12)} = e^{\tilde{u}_2\theta_{12}}$$

$$\hat{C}^{(11,13)} = e^{\tilde{u}_2\theta_{13}}$$

$$\hat{C}^{(12,14)} = e^{\tilde{u}_2\theta_{14}}$$

$$\hat{C}^{(13,15)} = e^{\tilde{u}_1\theta_{15}}$$

$$\hat{C}^{(14,16)} = e^{\tilde{u}_1\theta_{16}}$$

$$\hat{C}^{(15,17)} = e^{\tilde{u}_3\theta_{17,r}}$$

$$\hat{C}^{(16,17)} = e^{\tilde{u}_3\theta_{17,l}}$$

$$\hat{C}^{(17,18)} = e^{\tilde{u}_2\theta_{18}}$$

$$\hat{C}^{(18,19)} = e^{\tilde{u}_3\theta_{19}}$$

$$\hat{C}^{(19,20)} = e^{\tilde{u}_1 \theta_{20}}$$

$$\hat{C}^{(20,21)} = e^{\tilde{u}_1 \theta_{21}}$$

$$\hat{C}^{(20,22)} = e^{\tilde{u}_1 \theta_{22}}$$

$$\hat{C}^{(21,23)} = e^{\tilde{u}_2 \theta_{23}}$$

$$\hat{C}^{(22,24)} = e^{\tilde{u}_2 \theta_{24}}$$

$$\hat{C}^{(20,25)} = e^{\tilde{u}_3 \theta_{25}}$$

$$\hat{C}^{(25,26)} = e^{\tilde{u}_2 \theta_{26}}$$

$$\hat{C}^{(26,27)} = e^{\tilde{u}_1 \theta_{27}}$$

Calculation of transformation matrices for lowerbody frames depends on the locomotion phase. However, calculation of transformation matrices for upperbody frames are the same for all phases, noting that  $\hat{C}^{(0,17-fR)}$  in RFFDSP and  $\hat{C}^{(0,17-fL)}$  in LFFDSP are used as  $\hat{C}^{(0,17)}$ .

$$\hat{C}^{(0,18)} = \hat{C}^{(0,17)} \hat{C}^{(17,18)}$$

$$\hat{C}^{(0,19)} = \hat{C}^{(0,18)} \hat{C}^{(18,19)}$$

$$\hat{C}^{(0,20)} = \hat{C}^{(0,19)} \hat{C}^{(19,20)}$$

$$\hat{C}^{(0,21)} = \hat{C}^{(0,20)} \hat{C}^{(20,21)}$$

$$\hat{C}^{(0,23)} = \hat{C}^{(0,21)} \hat{C}^{(21,23)}$$

$$\hat{C}^{(0,22)} = \hat{C}^{(0,20)} \hat{C}^{(20,22)}$$

$$\hat{C}^{(0,24)} = \hat{C}^{(0,22)} \hat{C}^{(22,24)}$$

$$\hat{C}^{(0,25)} = \hat{C}^{(0,20)} \hat{C}^{(20,25)}$$

$$\hat{C}^{(0,26)} = \hat{C}^{(0,25)} \hat{C}^{(25,26)}$$

$$\hat{C}^{(0,27)} = \hat{C}^{(0,26)} \hat{C}^{(26,27)}$$

#### 4.1.1.1. For RFFSSP

Considering that Body 1 is assumed to be rigidly fixed to the ground and contents of  $\hat{C}^{(0,1)}$  at the end of previous locomotion phase are supplied to RFFSSP, calculation of transformation matrices begins from body coordinate system of Body 1. The procedure is shown below:

$$\hat{C}^{(0,3)} = \hat{C}^{(0,1)} \hat{C}^{(1,3)},$$

$$\hat{C}^{(0,5)} = \hat{C}^{(0,3)} \hat{C}^{(3,5)}$$

$$\hat{C}^{(0,7)} = \hat{C}^{(0,5)} \hat{C}^{(5,7)}$$

$$\hat{C}^{(0,9)} = \hat{C}^{(0,7)} \hat{C}^{(7,9)}$$

$$\hat{C}^{(0,11)} = \hat{C}^{(0,9)} \hat{C}^{(9,11)}$$

$$\hat{C}^{(0,13)} = \hat{C}^{(0,11)} \hat{C}^{(11,13)}$$

$$\hat{C}^{(0,15)} = \hat{C}^{(0,13)} \hat{C}^{(13,15)}$$

$$\hat{C}^{(0,17)} = \hat{C}^{(0,15)} \hat{C}^{(15,17)}$$

$$\hat{C}^{(0,16)} = \hat{C}^{(0,17)} \hat{C}^{(16,17)}^T$$

$$\hat{C}^{(0,14)} = \hat{C}^{(0,16)} \hat{C}^{(14,16)}^T$$

$$\hat{C}^{(0,12)} = \hat{C}^{(0,14)} \hat{C}^{(12,14)}^T$$

$$\hat{C}^{(0,10)} = \hat{C}^{(0,12)} \hat{C}^{(10,12)}^T$$

$$\hat{C}^{(0,8)} = \hat{C}^{(0,10)} \hat{C}^{(8,10)}^T$$

$$\hat{C}^{(0,6)} = \hat{C}^{(0,8)} \hat{C}^{(6,8)}^T$$

$$\hat{C}^{(0,4)} = \hat{C}^{(0,6)} \hat{C}^{(4,6)}^T$$

$$\hat{C}^{(0,2)} = \hat{C}^{(0,4)} \hat{C}^{(2,4)T}$$

#### 4.1.1.2. For LFFSSP

Similarly, Calculation of transformation matrices begins from body coordinate system of Body 2, where  $\hat{C}^{(0,2)}$  is supplied to LFFSSP. The procedure is shown below:

$$\hat{C}^{(0,4)} = \hat{C}^{(0,2)} \hat{C}^{(2,4)},$$

$$\hat{C}^{(0,6)} = \hat{C}^{(0,4)} \hat{C}^{(4,6)}$$

$$\hat{C}^{(0,8)} = \hat{C}^{(0,6)} \hat{C}^{(6,8)}$$

$$\hat{C}^{(0,10)} = \hat{C}^{(0,8)} \hat{C}^{(8,10)}$$

$$\hat{C}^{(0,12)} = \hat{C}^{(0,10)} \hat{C}^{(10,12)}$$

$$\hat{C}^{(0,14)} = \hat{C}^{(0,12)} \hat{C}^{(12,14)}$$

$$\hat{C}^{(0,16)} = \hat{C}^{(0,14)} \hat{C}^{(14,16)}$$

$$\hat{C}^{(0,17)} = \hat{C}^{(0,16)} \hat{C}^{(16,17)}$$

$$\hat{C}^{(0,15)} = \hat{C}^{(0,17)} \hat{C}^{(15,17)T}$$

$$\hat{C}^{(0,13)} = \hat{C}^{(0,15)} \hat{C}^{(13,15)T}$$

$$\hat{C}^{(0,11)} = \hat{C}^{(0,13)} \hat{C}^{(11,13)T}$$

$$\hat{C}^{(0,9)} = \hat{C}^{(0,11)} \hat{C}^{(9,11)T}$$

$$\hat{C}^{(0,7)} = \hat{C}^{(0,9)} \hat{C}^{(7,9)T}$$

$$\hat{C}^{(0,5)} = \hat{C}^{(0,7)} \hat{C}^{(5,7)T}$$

$$\hat{C}^{(0,3)} = \hat{C}^{(0,5)} \hat{C}^{(3,5)T}$$

$$\hat{C}^{(0,1)} = \hat{C}^{(0,3)} \hat{C}^{(1,3)T}$$

#### 4.1.1.3. For RFFDSP and LFFDSP

Calculation of transformation matrices, where  $\hat{C}^{(0,1)}$  and  $\hat{C}^{(0,2)}$  are supplied, is shown below:

$$\hat{C}^{(0,3)} = \hat{C}^{(0,1)} \hat{C}^{(1,3)},$$

$$\hat{C}^{(0,5)} = \hat{C}^{(0,3)} \hat{C}^{(3,5)}$$

$$\hat{C}^{(0,7)} = \hat{C}^{(0,5)} \hat{C}^{(5,7)}$$

$$\hat{C}^{(0,9)} = \hat{C}^{(0,7)} \hat{C}^{(7,9)}$$

$$\hat{C}^{(0,11)} = \hat{C}^{(0,9)} \hat{C}^{(9,11)}$$

$$\hat{C}^{(0,13)} = \hat{C}^{(0,11)} \hat{C}^{(11,13)}$$

$$\hat{C}^{(0,15)} = \hat{C}^{(0,13)} \hat{C}^{(13,15)}$$

$$\hat{C}^{(0,17_{fR})} = \hat{C}^{(0,15)} \hat{C}^{(15,17)}$$

$$\hat{C}^{(0,4)} = \hat{C}^{(0,2)} \hat{C}^{(2,4)},$$

$$\hat{C}^{(0,6)} = \hat{C}^{(0,4)} \hat{C}^{(4,6)}$$

$$\hat{C}^{(0,8)} = \hat{C}^{(0,6)} \hat{C}^{(6,8)}$$

$$\hat{C}^{(0,10)} = \hat{C}^{(0,8)} \hat{C}^{(8,10)}$$

$$\hat{C}^{(0,12)} = \hat{C}^{(0,10)} \hat{C}^{(10,12)}$$

$$\hat{C}^{(0,14)} = \hat{C}^{(0,12)} \hat{C}^{(12,14)}$$

$$\hat{C}^{(0,16)} = \hat{C}^{(0,14)} \hat{C}^{(14,16)}$$

$$\hat{C}^{(0,17_{fL})} = \hat{C}^{(0,16)} \hat{C}^{(16,17)}$$

#### 4.1.2. Position Relations

$\bar{P}_{c,k}$  is a vector describing the position of mass center of Body K in matrix form of  $\bar{P}_{c,k}$ , resolved in the inertial frame (Frame 0).  $\bar{P}_{tpR}$  and  $\bar{P}_{tpL}$  are matrix forms of  $\vec{P}_{tpR}$  and  $\vec{P}_{tpL}$ , resolved in the inertial frame. Expression of position relations differs according to the locomotion phase for lowerbodies. On the other hand, expression of position relations for upperbodies is common for all phases, noting that  $\hat{C}^{(0,17-fR)}$ ,  $\bar{P}_{c,17-fR}$  in RFFDSP and  $\hat{C}^{(0,17-fL)}$ ,  $\bar{P}_{c,17-fL}$  in LFFDSP are used as  $\hat{C}^{(0,17)}$  and  $\bar{P}_{c,17}$  in these expressions.

$$\bar{P}_{c,20} = \bar{P}_{c,17} - \vec{c}_{17} - \vec{l}_{20,17} + \vec{c}_{20}$$

$$\bar{P}_{c,20} = \bar{P}_{c,17} + c_{17}\bar{u}_3^{(17)} + (l_{20z} - c_{20})\bar{u}_3^{(20)}$$

$$\bar{P}_{c,20} = \bar{P}_{c,17} + c_{17}\hat{C}^{(0,17)}\bar{u}_3 + (l_{20z} - c_{20})\hat{C}^{(0,20)}\bar{u}_3$$

Applying the similar procedure for other position relations:

$$\bar{P}_{c,23} = \bar{P}_{c,20} + c_{20}\hat{C}^{(0,20)}\bar{u}_3 - l_{20y}\hat{C}^{(0,20)}\bar{u}_2 + \hat{C}^{(0,23)}[(c_{23} - l_{23z})\bar{u}_3 - l_{23y}\bar{u}_2]$$

$$\bar{P}_{c,24} = \bar{P}_{c,20} + c_{20}\hat{C}^{(0,20)}\bar{u}_3 + l_{20y}\hat{C}^{(0,20)}\bar{u}_2 + \hat{C}^{(0,24)}[(c_{24} - l_{24z})\bar{u}_3 + l_{24y}\bar{u}_2]$$

$$\bar{P}_{c,27} = \bar{P}_{c,20} + c_{20}\hat{C}^{(0,20)}\bar{u}_3 + (l_{27} - c_{27})\hat{C}^{(0,27)}\bar{u}_3$$

##### 4.1.2.1. For RFFSSP

Calculation of position relations for RFFSSP is shown below, where  $\bar{P}_{tpR}$  and  $\hat{C}^{(0,1)}$  are supplied.

$$\bar{P}_{c,1} = \bar{P}_{tpR} + (c_1 - l_1)\hat{C}^{(0,1)}\bar{u}_1$$

$$\bar{P}_{c,3} = \bar{P}_{c,1} - c_1\hat{C}^{(0,1)}\bar{u}_1 + \hat{C}^{(0,3)}[(c_{3x} - l_{3x})\bar{u}_1 + (l_{3z} - c_{3z})\bar{u}_3]$$

$$\bar{P}_{c,9} = \bar{P}_{c,3} - \hat{C}^{(0,3)}(c_{3x}\bar{u}_1 - c_{3z}\bar{u}_3) + \hat{C}^{(0,9)}(l_9 - c_9)\bar{u}_3$$

$$\bar{P}_{c,11} = \bar{P}_{c,9} + c_9\hat{C}^{(0,9)}\bar{u}_3 + \hat{C}^{(0,11)}(l_{11} - c_{11})\bar{u}_3$$

$$\bar{P}_{c,17} = \bar{P}_{c,11} + c_{11}\hat{C}^{(0,11)}\bar{u}_3 + \hat{C}^{(0,17)}[(l_{17z} - c_{17})\bar{u}_3 + l_{17y}\bar{u}_2]$$

$$\bar{P}_{c,12} = \bar{P}_{c,17} + \hat{C}^{(0,17)}[(c_{17} - l_{17z})\bar{u}_3 + l_{17y}\bar{u}_2] - c_{12}\hat{C}^{(0,12)}\bar{u}_3$$

$$\bar{P}_{c,10} = \bar{P}_{c,12} + (c_{12} - l_{12})\hat{C}^{(0,12)}\bar{u}_3 - c_{10}\hat{C}^{(0,10)}\bar{u}_3$$

$$\bar{P}_{c,4} = \bar{P}_{c,10} + \hat{C}^{(0,10)}(c_{10} - l_{10})\bar{u}_3 + \hat{C}^{(0,4)}(c_{4x}\bar{u}_1 - c_{4z}\bar{u}_3)$$

$$\bar{P}_{c,2} = \bar{P}_{c,4} + \hat{C}^{(0,4)}[(l_{4x} - c_{4x})\bar{u}_1 + (c_{4z} - l_{4z})\bar{u}_3] + c_2\hat{C}^{(0,2)}\bar{u}_1$$

$$\bar{P}_{tpL} = \bar{P}_{c,4} + \hat{C}^{(0,4)}[(l_{4x} - c_{4x})\bar{u}_1 + (c_{4z} - l_{4z})\bar{u}_3] + l_2\hat{C}^{(0,2)}\bar{u}_1$$

#### 4.1.2.2. For LFFSSP

Calculation of position relations for LFFSSP is shown below, where  $\bar{P}_{tpL}$  and  $\hat{C}^{(0,2)}$  are supplied.

$$\bar{P}_{c,2} = \bar{P}_{tpL} + (c_2 - l_2)\hat{C}^{(0,2)}\bar{u}_1$$

$$\bar{P}_{c,4} = \bar{P}_{c,2} - c_2\hat{C}^{(0,2)}\bar{u}_1 + \hat{C}^{(0,4)}[(c_{4x} - l_{4x})\bar{u}_1 + (l_{4z} - c_{4z})\bar{u}_3]$$

$$\bar{P}_{c,10} = \bar{P}_{c,4} - \hat{C}^{(0,4)}(c_{4x}\bar{u}_1 - c_{4z}\bar{u}_3) + \hat{C}^{(0,10)}(l_{10} - c_{10})\bar{u}_3$$

$$\bar{P}_{c,12} = \bar{P}_{c,10} + c_{10}\hat{C}^{(0,10)}\bar{u}_3 + \hat{C}^{(0,12)}(l_{12} - c_{12})\bar{u}_3$$

$$\bar{P}_{c,17} = \bar{P}_{c,12} + c_{12}\hat{C}^{(0,12)}\bar{u}_3 + \hat{C}^{(0,17)}[(l_{17z} - c_{17})\bar{u}_3 - l_{17y}\bar{u}_2]$$

$$\bar{P}_{c,11} = \bar{P}_{c,17} + \hat{C}^{(0,17)}[(c_{17} - l_{17z})\bar{u}_3 - l_{17y}\bar{u}_2] - c_{11}\hat{C}^{(0,11)}\bar{u}_3$$

$$\bar{P}_{c,9} = \bar{P}_{c,11} + \hat{C}^{(0,11)}(c_{11} - l_{11})\bar{u}_3 - c_9\hat{C}^{(0,9)}\bar{u}_3$$

$$\bar{P}_{c,3} = \bar{P}_{c,9} + \hat{C}^{(0,9)}(c_9 - l_9)\bar{u}_3 + \hat{C}^{(0,3)}(c_{3x}\bar{u}_1 - c_{3z}\bar{u}_3)$$

$$\bar{P}_{c,1} = \bar{P}_{c,3} + \hat{C}^{(0,3)}[(l_{3x} - c_{3x})\bar{u}_1 + (c_{3z} - l_{3z})\bar{u}_3] + c_1\hat{C}^{(0,1)}\bar{u}_1$$

$$\bar{P}_{tpR} = \bar{P}_{c,3} + \hat{C}^{(0,3)}[(l_{3x} - c_{3x})\bar{u}_1 + (c_{3z} - l_{3z})\bar{u}_3] + l_1\hat{C}^{(0,1)}\bar{u}_1$$

#### 4.1.2.3. For RFFDSP and LFFDSP

Calculation of position relations for RFFDSP and LFFDSP is shown below; also  $\bar{P}_{tpR}$ ,  $\bar{P}_{tpL}$ ,  $\hat{C}^{(0,1)}$  and  $\hat{C}^{(0,2)}$  are supplied.

$$\bar{P}_{c,1} = \bar{P}_{tpR} + (c_1 - l_1)\hat{C}^{(0,1)}\bar{u}_1$$

$$\bar{P}_{c,3} = \bar{P}_{c,1} - c_1\hat{C}^{(0,1)}\bar{u}_1 + \hat{C}^{(0,3)}[(c_{3x} - l_{3x})\bar{u}_1 + (l_{3z} - c_{3z})\bar{u}_3]$$

$$\bar{P}_{c,9} = \bar{P}_{c,3} - \hat{C}^{(0,3)}(c_{3x}\bar{u}_1 - c_{3z}\bar{u}_3) + \hat{C}^{(0,9)}(l_9 - c_9)\bar{u}_3$$

$$\bar{P}_{c,11} = \bar{P}_{c,9} + c_9\hat{C}^{(0,9)}\bar{u}_3 + \hat{C}^{(0,11)}(l_{11} - c_{11})\bar{u}_3$$

$$\bar{P}_{c,17_{fR}} = \bar{P}_{c,11} + c_{11}\hat{C}^{(0,11)}\bar{u}_3 + \hat{C}^{(0,17_{fR})}[(l_{17z} - c_{17})\bar{u}_3 + l_{17y}\bar{u}_2]$$

$$\bar{P}_{c,2} = \bar{P}_{tpL} + (c_2 - l_2)\hat{C}^{(0,2)}\bar{u}_1$$

$$\bar{P}_{c,4} = \bar{P}_{c,2} - c_2\hat{C}^{(0,2)}\bar{u}_1 + \hat{C}^{(0,4)}[(c_{4x} - l_{4x})\bar{u}_1 + (l_{4z} - c_{4z})\bar{u}_3]$$

$$\bar{P}_{c,10} = \bar{P}_{c,4} - \hat{C}^{(0,4)}(c_{4x}\bar{u}_1 - c_{4z}\bar{u}_3) + \hat{C}^{(0,10)}(l_{10} - c_{10})\bar{u}_3$$

$$\bar{P}_{c,12} = \bar{P}_{c,10} + c_{10}\hat{C}^{(0,10)}\bar{u}_3 + \hat{C}^{(0,12)}(l_{12} - c_{12})\bar{u}_3$$

$$\bar{P}_{c,17_{fL}} = \bar{P}_{c,12} + c_{12}\hat{C}^{(0,12)}\bar{u}_3 + \hat{C}^{(0,17_{fL})}[(l_{17z} - c_{17})\bar{u}_3 - l_{17y}\bar{u}_2]$$

#### 4.1.3. Angular Velocity Relations

$\bar{w}_k$  is a vector describing the angular velocity of frame K with respect to the inertial frame in matrix form of  $\vec{w}_k$ , resolved in the inertial frame. Expression of angular velocity relations differs according to the locomotion phase for lowerbodies. On the other hand, expression of angular velocity relations for upperbodies is common for all phases, noting that  $\hat{C}^{(0,17_{fR})}$ ,  $\bar{w}_{17_{fR}}$  in RFFDSP and  $\hat{C}^{(0,17_{fL})}$ ,  $\bar{w}_{17_{fL}}$  in LFFDSP are used as  $\hat{C}^{(0,17)}$  and  $\bar{w}_{17}$  in expressions shown below.

$$\vec{w}_{18} = \vec{w}_{17} + \dot{\theta}_{18}\vec{u}_2^{(17)}$$

$$\bar{w}_{18} = \bar{w}_{17} + \dot{\theta}_{18} \hat{C}^{(0,17)} \bar{u}_2$$

Applying the similar procedure for other angular velocity relations:

$$\bar{w}_{19} = \bar{w}_{18} + \dot{\theta}_{19} \hat{C}^{(0,18)} \bar{u}_3$$

$$\bar{w}_{20} = \bar{w}_{19} + \dot{\theta}_{20} \hat{C}^{(0,19)} \bar{u}_1$$

$$\bar{w}_{21} = \bar{w}_{20} + \dot{\theta}_{21} \hat{C}^{(0,20)} \bar{u}_1$$

$$\bar{w}_{22} = \bar{w}_{20} + \dot{\theta}_{22} \hat{C}^{(0,20)} \bar{u}_1$$

$$\bar{w}_{23} = \bar{w}_{21} + \dot{\theta}_{23} \hat{C}^{(0,21)} \bar{u}_2$$

$$\bar{w}_{24} = \bar{w}_{22} + \dot{\theta}_{24} \hat{C}^{(0,22)} \bar{u}_2$$

$$\bar{w}_{25} = \bar{w}_{20} + \dot{\theta}_{25} \hat{C}^{(0,20)} \bar{u}_3$$

$$\bar{w}_{26} = \bar{w}_{25} + \dot{\theta}_{26} \hat{C}^{(0,25)} \bar{u}_2$$

$$\bar{w}_{27} = \bar{w}_{26} + \dot{\theta}_{27} \hat{C}^{(0,26)} \bar{u}_1$$

#### 4.1.3.1. For RFFSSP

Calculation of angular velocities for RFFSSP is shown below, where  $\bar{w}_1$ ,  $\hat{C}^{(0,1)}$  are supplied to RFFSSP.  $\bar{w}_1$  is supplied as  $\bar{0}_{3 \times 1}$  in the simulation since Body 1 is assumed to be rigidly fixed to the ground during RFFSSP.

$$\bar{w}_3 = \bar{w}_1 + \dot{\theta}_3 \hat{C}^{(0,1)} \bar{u}_2$$

$$\bar{w}_5 = \bar{w}_3 + \dot{\theta}_5 \hat{C}^{(0,3)} \bar{u}_2$$

$$\bar{w}_7 = \bar{w}_5 + \dot{\theta}_7 \hat{C}^{(0,5)} \bar{u}_3$$

$$\bar{w}_9 = \bar{w}_7 + \dot{\theta}_9 \hat{C}^{(0,7)} \bar{u}_1$$

$$\bar{w}_{11} = \bar{w}_9 + \dot{\theta}_{11} \hat{C}^{(0,9)} \bar{u}_2$$

$$\bar{w}_{13} = \bar{w}_{11} + \dot{\theta}_{13} \hat{C}^{(0,11)} \bar{u}_2$$

$$\bar{w}_{15} = \bar{w}_{13} + \dot{\theta}_{15} \hat{C}^{(0,13)} \bar{u}_1$$

$$\bar{w}_{17} = \bar{w}_{15} + \dot{\theta}_{17,r} \hat{C}^{(0,15)} \bar{u}_3$$

$$\bar{w}_{16} = \bar{w}_{17} - \dot{\theta}_{17,l} \hat{C}^{(0,17)} \bar{u}_3$$

$$\bar{w}_{14} = \bar{w}_{16} - \dot{\theta}_{16} \hat{C}^{(0,16)} \bar{u}_1$$

$$\bar{w}_{12} = \bar{w}_{14} - \dot{\theta}_{14} \hat{C}^{(0,14)} \bar{u}_2$$

$$\bar{w}_{10} = \bar{w}_{12} - \dot{\theta}_{12} \hat{C}^{(0,12)} \bar{u}_2$$

$$\bar{w}_8 = \bar{w}_{10} - \dot{\theta}_{10} \hat{C}^{(0,10)} \bar{u}_1$$

$$\bar{w}_6 = \bar{w}_8 - \dot{\theta}_8 \hat{C}^{(0,8)} \bar{u}_3$$

$$\bar{w}_4 = \bar{w}_6 - \dot{\theta}_6 \hat{C}^{(0,6)} \bar{u}_2$$

$$\bar{w}_2 = \bar{w}_4 - \dot{\theta}_4 \hat{C}^{(0,4)} \bar{u}_2$$

#### 4.1.3.2. For LFFSSP

Calculation of angular velocities for LFFSSP is shown below, where  $\bar{w}_2$ ,  $\hat{C}^{(0,2)}$  are supplied to LFFSSP.  $\bar{w}_2$  is supplied as  $\bar{0}_{3 \times 1}$  in the simulation since Body 2 is assumed to be rigidly fixed to the ground during LFFSSP.

$$\bar{w}_4 = \bar{w}_2 + \dot{\theta}_4 \hat{C}^{(0,2)} \bar{u}_2$$

$$\bar{w}_6 = \bar{w}_4 + \dot{\theta}_6 \hat{C}^{(0,4)} \bar{u}_2$$

$$\bar{w}_8 = \bar{w}_6 + \dot{\theta}_8 \hat{C}^{(0,6)} \bar{u}_3$$

$$\bar{w}_{10} = \bar{w}_8 + \dot{\theta}_{10} \hat{C}^{(0,8)} \bar{u}_1$$

$$\bar{w}_{12} = \bar{w}_{10} + \dot{\theta}_{12} \hat{C}^{(0,10)} \bar{u}_2$$

$$\bar{w}_{14} = \bar{w}_{12} + \dot{\theta}_{14} \hat{C}^{(0,12)} \bar{u}_2$$

$$\bar{w}_{16} = \bar{w}_{14} + \dot{\theta}_{16} \hat{C}^{(0,14)} \bar{u}_1$$

$$\bar{w}_{17} = \bar{w}_{16} + \dot{\theta}_{17,l} \hat{C}^{(0,16)} \bar{u}_3$$

$$\bar{w}_{15} = \bar{w}_{17} - \dot{\theta}_{17,r} \hat{C}^{(0,17)} \bar{u}_3$$

$$\bar{w}_{13} = \bar{w}_{15} - \dot{\theta}_{15} \hat{C}^{(0,15)} \bar{u}_1$$

$$\bar{w}_{11} = \bar{w}_{13} - \dot{\theta}_{13} \hat{C}^{(0,13)} \bar{u}_2$$

$$\bar{w}_9 = \bar{w}_{11} - \dot{\theta}_{11} \hat{C}^{(0,11)} \bar{u}_2$$

$$\bar{w}_7 = \bar{w}_9 - \dot{\theta}_9 \hat{C}^{(0,9)} \bar{u}_1$$

$$\bar{w}_5 = \bar{w}_7 - \dot{\theta}_7 \hat{C}^{(0,7)} \bar{u}_3$$

$$\bar{w}_3 = \bar{w}_5 - \dot{\theta}_5 \hat{C}^{(0,5)} \bar{u}_2$$

$$\bar{w}_1 = \bar{w}_3 - \dot{\theta}_3 \hat{C}^{(0,3)} \bar{u}_2$$

#### 4.1.3.2. For RFFDSP and LFFDSP

The procedure of calculating angular velocities for RFFDSP and LFFDSP is shown below; where  $\bar{w}_1$ ,  $\bar{w}_2$ ,  $\hat{C}^{(0,1)}$ ,  $\hat{C}^{(0,2)}$  are supplied.  $\bar{w}_1$  and  $\bar{w}_2$  are supplied as  $\bar{0}_{3 \times 1}$  in the simulation since Body 1 and Body 2 are assumed to be rigidly fixed to the ground during RFFDSP and LFFDSP.

$$\bar{w}_3 = \bar{w}_1 + \dot{\theta}_3 \hat{C}^{(0,1)} \bar{u}_2$$

$$\bar{w}_5 = \bar{w}_3 + \dot{\theta}_5 \hat{C}^{(0,3)} \bar{u}_2$$

$$\bar{w}_7 = \bar{w}_5 + \dot{\theta}_7 \hat{C}^{(0,5)} \bar{u}_3$$

$$\bar{w}_9 = \bar{w}_7 + \dot{\theta}_9 \hat{C}^{(0,7)} \bar{u}_1$$

$$\bar{w}_{11} = \bar{w}_9 + \dot{\theta}_{11} \hat{C}^{(0,9)} \bar{u}_2$$

$$\bar{w}_{13} = \bar{w}_{11} + \dot{\theta}_{13} \hat{C}^{(0,11)} \bar{u}_2$$

$$\bar{w}_{15} = \bar{w}_{13} + \dot{\theta}_{15} \hat{C}^{(0,13)} \bar{u}_1$$

$$\bar{w}_{17_{fR}} = \bar{w}_{15} + \dot{\theta}_{17,r} \hat{C}^{(0,15)} \bar{u}_3$$

$$\bar{w}_4 = \bar{w}_2 + \dot{\theta}_4 \hat{C}^{(0,2)} \bar{u}_2$$

$$\bar{w}_6 = \bar{w}_4 + \dot{\theta}_6 \hat{C}^{(0,4)} \bar{u}_2$$

$$\bar{w}_8 = \bar{w}_6 + \dot{\theta}_8 \hat{C}^{(0,6)} \bar{u}_3$$

$$\bar{w}_{10} = \bar{w}_8 + \dot{\theta}_{10} \hat{C}^{(0,8)} \bar{u}_1$$

$$\bar{w}_{12} = \bar{w}_{10} + \dot{\theta}_{12} \hat{C}^{(0,10)} \bar{u}_2$$

$$\bar{w}_{14} = \bar{w}_{12} + \dot{\theta}_{14} \hat{C}^{(0,12)} \bar{u}_2$$

$$\bar{w}_{16} = \bar{w}_{14} + \dot{\theta}_{16} \hat{C}^{(0,14)} \bar{u}_1$$

$$\bar{w}_{17_{fL}} = \bar{w}_{16} + \dot{\theta}_{17,l} \hat{C}^{(0,16)} \bar{u}_3$$

#### 4.1.4. Translational Velocity Relations

$\bar{V}_{c,k}$  is a vector describing the translational velocity of the mass center of Body K in matrix form of  $\vec{V}_{c,k}$ , differentiated with respect to and resolved in the inertial frame. Expression of translational velocity relations differs according to the locomotion phase for lowerbodies. On the other hand, expression of translational velocity relations for upperbodies is common for all phases, noting that  $\hat{C}^{(0,17_{fR})}$ ,  $\bar{w}_{17_{fR}}$  in RFFDSP and  $\hat{C}^{(0,17_{fL})}$ ,  $\bar{w}_{17_{fL}}$  in LFFDSP are used as  $\hat{C}^{(0,17)}$  and  $\bar{w}_{17}$  in expressions shown below.

$$\vec{V}_{c,20} = \vec{V}_{c,17} + c_{17} \vec{w}_{17} \times \vec{u}_3^{(17)} + (l_{20z} - c_{20}) \vec{w}_{20} \times \vec{u}_3^{(20)}$$

$$\bar{V}_{c,20} = \bar{V}_{c,17} + c_{17} \tilde{w}_{17} \hat{C}^{(0,17)} \bar{u}_3 + (l_{20z} - c_{20}) \tilde{w}_{20} \hat{C}^{(0,20)} \bar{u}_3$$

Applying the similar procedure for other translational velocity relations:

$$\bar{V}_{c,23} = \bar{V}_{c,20} + c_{20} \tilde{w}_{20} \hat{C}^{(0,20)} \bar{u}_3 - l_{20y} \tilde{w}_{20} \hat{C}^{(0,20)} \bar{u}_2 + (c_{23} - l_{23z}) \tilde{w}_{23} \hat{C}^{(0,23)} \bar{u}_3 - l_{23y} \tilde{w}_{23} \hat{C}^{(0,23)} \bar{u}_2$$

$$\bar{V}_{c,24} = \bar{V}_{c,20} + c_{20}\tilde{w}_{20}\hat{C}^{(0,20)}\bar{u}_3 + l_{20y}\tilde{w}_{20}\hat{C}^{(0,20)}\bar{u}_2 + (c_{24} - l_{24z})\tilde{w}_{24}\hat{C}^{(0,24)}\bar{u}_3 + l_{24y}\tilde{w}_{24}\hat{C}^{(0,24)}\bar{u}_2$$

$$\bar{V}_{c,27} = \bar{V}_{c,20} + c_{20}\tilde{w}_{20}\hat{C}^{(0,20)}\bar{u}_3 + (l_{27} - c_{27})\tilde{w}_{27}\hat{C}^{(0,27)}\bar{u}_3$$

#### 4.1.4.1. For RFFSSP

The procedure of calculating translational velocities for RFFSSP is shown below; where  $\bar{w}_1$ ,  $\bar{V}_{tpR}$ ,  $\hat{C}^{(0,1)}$  are supplied.  $\bar{w}_1$  and  $\bar{V}_{tpR}$  are supplied as  $\bar{0}_{3 \times 1}$  in the simulation since Body 1 is assumed to be rigidly fixed to the ground during RFFSSP.

$$\bar{V}_{c,1} = \bar{V}_{tpR} + (c_1 - l_1)\tilde{w}_1\hat{C}^{(0,1)}\bar{u}_1$$

$$\bar{V}_{c,3} = \bar{V}_{c,1} - c_1\tilde{w}_1\hat{C}^{(0,1)}\bar{u}_1 + (c_{3x} - l_{3x})\tilde{w}_3\hat{C}^{(0,3)}\bar{u}_1 + (l_{3z} - c_{3z})\tilde{w}_3\hat{C}^{(0,3)}\bar{u}_3$$

$$\bar{V}_{c,9} = \bar{V}_{c,3} - c_{3x}\tilde{w}_3\hat{C}^{(0,3)}\bar{u}_1 + c_{3z}\tilde{w}_3\hat{C}^{(0,3)}\bar{u}_3 + (l_9 - c_9)\tilde{w}_9\hat{C}^{(0,9)}\bar{u}_3$$

$$\bar{V}_{c,11} = \bar{V}_{c,9} + c_9\tilde{w}_9\hat{C}^{(0,9)}\bar{u}_3 + (l_{11} - c_{11})\tilde{w}_{11}\hat{C}^{(0,11)}\bar{u}_3$$

$$\bar{V}_{c,17} = \bar{V}_{c,11} + c_{11}\tilde{w}_{11}\hat{C}^{(0,11)}\bar{u}_3 + l_{17y}\tilde{w}_{17}\hat{C}^{(0,17)}\bar{u}_2 + (l_{17z} - c_{17})\tilde{w}_{17}\hat{C}^{(0,17)}\bar{u}_3$$

$$\bar{V}_{c,12} = \bar{V}_{c,17} + l_{17y}\tilde{w}_{17}\hat{C}^{(0,17)}\bar{u}_2 + (c_{17} - l_{17z})\tilde{w}_{17}\hat{C}^{(0,17)}\bar{u}_3 - c_{12}\tilde{w}_{12}\hat{C}^{(0,12)}\bar{u}_3$$

$$\bar{V}_{c,10} = \bar{V}_{c,12} + (c_{12} - l_{12})\tilde{w}_{12}\hat{C}^{(0,12)}\bar{u}_3 - c_{10}\tilde{w}_{10}\hat{C}^{(0,10)}\bar{u}_3$$

$$\bar{V}_{c,4} = \bar{V}_{c,10} + (c_{10} - l_{10})\tilde{w}_{10}\hat{C}^{(0,10)}\bar{u}_3 + c_{4x}\tilde{w}_4\hat{C}^{(0,4)}\bar{u}_1 - c_{4z}\tilde{w}_4\hat{C}^{(0,4)}\bar{u}_3$$

$$\bar{V}_{c,2} = \bar{V}_{c,4} + (l_{4x} - c_{4x})\tilde{w}_4\hat{C}^{(0,4)}\bar{u}_1 + (c_{4z} - l_{4z})\tilde{w}_4\hat{C}^{(0,4)}\bar{u}_3 + c_2\tilde{w}_2\hat{C}^{(0,2)}\bar{u}_1$$

$$\bar{V}_{tpL} = \bar{V}_{c,4} + (l_{4x} - c_{4x})\tilde{w}_4\hat{C}^{(0,4)}\bar{u}_1 + (c_{4z} - l_{4z})\tilde{w}_4\hat{C}^{(0,4)}\bar{u}_3 + l_2\tilde{w}_2\hat{C}^{(0,2)}\bar{u}_1$$

#### 4.1.4.2. For LFFSSP

The procedure of calculating translational velocities for LFFSSP is shown below; where  $\bar{w}_2$ ,  $\bar{V}_{tpL}$ ,  $\hat{C}^{(0,2)}$  are supplied.  $\bar{w}_2$  and  $\bar{V}_{tpL}$  are supplied as  $\bar{0}_{3 \times 1}$  in the

simulation since Body 2 is assumed to be rigidly fixed to the ground during LFFSSP.

$$\bar{V}_{c,2} = \bar{V}_{tpL} + (c_2 - l_2)\tilde{w}_2\hat{C}^{(0,2)}\bar{u}_1$$

$$\bar{V}_{c,4} = \bar{V}_{c,2} - c_2\tilde{w}_2\hat{C}^{(0,2)}\bar{u}_1 + (c_{4x} - l_{4x})\tilde{w}_4\hat{C}^{(0,4)}\bar{u}_1 + (l_{4z} - c_{4z})\tilde{w}_4\hat{C}^{(0,4)}\bar{u}_3$$

$$\bar{V}_{c,10} = \bar{V}_{c,4} - c_{4x}\tilde{w}_4\hat{C}^{(0,4)}\bar{u}_1 + c_{4z}\tilde{w}_4\hat{C}^{(0,4)}\bar{u}_3 + (l_{10} - c_{10})\tilde{w}_{10}\hat{C}^{(0,10)}\bar{u}_3$$

$$\bar{V}_{c,12} = \bar{V}_{c,10} + c_{10}\tilde{w}_{10}\hat{C}^{(0,10)}\bar{u}_3 + (l_{12} - c_{12})\tilde{w}_{12}\hat{C}^{(0,12)}\bar{u}_3$$

$$\bar{V}_{c,17} = \bar{V}_{c,12} + c_{12}\tilde{w}_{12}\hat{C}^{(0,12)}\bar{u}_3 - l_{17y}\tilde{w}_{17}\hat{C}^{(0,17)}\bar{u}_2 + (l_{17z} - c_{17})\tilde{w}_{17}\hat{C}^{(0,17)}\bar{u}_3$$

$$\bar{V}_{c,11} = \bar{V}_{c,17} - l_{17y}\tilde{w}_{17}\hat{C}^{(0,17)}\bar{u}_2 + (c_{17} - l_{17z})\tilde{w}_{17}\hat{C}^{(0,17)}\bar{u}_3 - c_{11}\tilde{w}_{11}\hat{C}^{(0,11)}\bar{u}_3$$

$$\bar{V}_{c,9} = \bar{V}_{c,11} + (c_{11} - l_{11})\tilde{w}_{11}\hat{C}^{(0,11)}\bar{u}_3 - c_9\tilde{w}_9\hat{C}^{(0,9)}\bar{u}_3$$

$$\bar{V}_{c,3} = \bar{V}_{c,9} + (c_9 - l_9)\tilde{w}_9\hat{C}^{(0,9)}\bar{u}_3 + c_{3x}\tilde{w}_3\hat{C}^{(0,3)}\bar{u}_1 - c_{3z}\tilde{w}_3\hat{C}^{(0,3)}\bar{u}_3$$

$$\bar{V}_{c,1} = \bar{V}_{c,3} + (l_{3x} - c_{3x})\tilde{w}_3\hat{C}^{(0,3)}\bar{u}_1 + (c_{3z} - l_{3z})\tilde{w}_3\hat{C}^{(0,3)}\bar{u}_3 + c_1\tilde{w}_1\hat{C}^{(0,1)}\bar{u}_1$$

$$\bar{V}_{tpR} = \bar{V}_{c,1} + (l_{3x} - c_{3x})\tilde{w}_3\hat{C}^{(0,3)}\bar{u}_1 + (c_{3z} - l_{3z})\tilde{w}_3\hat{C}^{(0,3)}\bar{u}_3 + l_1\tilde{w}_1\hat{C}^{(0,1)}\bar{u}_1$$

#### 4.1.4.3. For RFFDSP and LFFDSP

The procedure of calculating translational velocities for LFFDSP and RFFDSP is shown below; where  $\bar{w}_1$ ,  $\bar{w}_2$ ,  $\bar{V}_{tpR}$ ,  $\bar{V}_{tpL}$ ,  $\hat{C}^{(0,1)}$  and  $\hat{C}^{(0,2)}$  are supplied.  $\bar{w}_1$ ,  $\bar{w}_2$ ,  $\bar{V}_{tpR}$  and  $\bar{V}_{tpL}$  are supplied as  $\bar{0}_{3 \times 1}$  in the simulation since Body1 and Body 2 are assumed to be rigidly fixed to the ground during RFFDSP and LFFDSP.

$$\bar{V}_{c,1} = \bar{V}_{tpR} + (c_1 - l_1)\tilde{w}_1\hat{C}^{(0,1)}\bar{u}_1$$

$$\bar{V}_{c,3} = \bar{V}_{c,1} - c_1\tilde{w}_1\hat{C}^{(0,1)}\bar{u}_1 + (c_{3x} - l_{3x})\tilde{w}_3\hat{C}^{(0,3)}\bar{u}_1 + (l_{3z} - c_{3z})\tilde{w}_3\hat{C}^{(0,3)}\bar{u}_3$$

$$\bar{V}_{c,9} = \bar{V}_{c,3} - c_{3x}\tilde{w}_3\hat{C}^{(0,3)}\bar{u}_1 + c_{3z}\tilde{w}_3\hat{C}^{(0,3)}\bar{u}_3 + (l_9 - c_9)\tilde{w}_9\hat{C}^{(0,9)}\bar{u}_3$$

$$\bar{V}_{c,11} = \bar{V}_{c,9} + c_9\tilde{w}_9\hat{C}^{(0,9)}\bar{u}_3 + (l_{11} - c_{11})\tilde{w}_{11}\hat{C}^{(0,11)}\bar{u}_3$$

$$\begin{aligned}
\bar{V}_{c,17_{fR}} &= \\
\bar{V}_{c,11} + c_{11}\tilde{w}_{11}\hat{C}^{(0,11)}\bar{u}_3 + l_{17y}\tilde{w}_{17}\hat{C}^{(0,17_{fR})}\bar{u}_2 + (l_{17z} - c_{17})\tilde{w}_{17}\hat{C}^{(0,17_{fR})}\bar{u}_3 \\
\bar{V}_{c,2} &= \bar{V}_{tpL} + (c_2 - l_2)\tilde{w}_2\hat{C}^{(0,2)}\bar{u}_1 \\
\bar{V}_{c,4} &= \bar{V}_{c,2} - c_2\tilde{w}_2\hat{C}^{(0,2)}\bar{u}_1 + (c_{4x} - l_{4x})\tilde{w}_4\hat{C}^{(0,4)}\bar{u}_1 + (l_{4z} - c_{4z})\tilde{w}_4\hat{C}^{(0,4)}\bar{u}_3 \\
\bar{V}_{c,10} &= \bar{V}_{c,4} - c_{4x}\tilde{w}_4\hat{C}^{(0,4)}\bar{u}_1 + c_{4z}\tilde{w}_4\hat{C}^{(0,4)}\bar{u}_3 + (l_{10} - c_{10})\tilde{w}_{10}\hat{C}^{(0,10)}\bar{u}_3 \\
\bar{V}_{c,12} &= \bar{V}_{c,10} + c_{10}\tilde{w}_{10}\hat{C}^{(0,10)}\bar{u}_3 + (l_{12} - c_{12})\tilde{w}_{12}\hat{C}^{(0,12)}\bar{u}_3 \\
\bar{V}_{c,17_{fL}} &= \\
\bar{V}_{c,12} + c_{12}\tilde{w}_{12}\hat{C}^{(0,12)}\bar{u}_3 - l_{17y}\tilde{w}_{17}\hat{C}^{(0,17_{fL})}\bar{u}_2 + (l_{17z} - c_{17})\tilde{w}_{17}\hat{C}^{(0,17_{fL})}\bar{u}_3
\end{aligned}$$

#### 4.1.5. Angular Acceleration Relations

$\bar{\alpha}_k$  is a vector describing the angular acceleration of frame K with respect to the inertial frame in matrix form of  $\vec{\alpha}_k$ , differentiated with respect to and resolved in the inertial frame. Expression of angular acceleration relations differs according to the locomotion phase for lowerbodies. On the other hand, expression of angular acceleration relations for upperbodies is common for all phases, noting that  $\hat{C}^{(0,17_{fR})}$ ,  $\bar{w}_{17_{fR}}$ ,  $\bar{\alpha}_{17_{fR}}$  in RFFDSP and  $\hat{C}^{(0,17_{fL})}$ ,  $\bar{w}_{17_{fL}}$ ,  $\bar{\alpha}_{17_{fL}}$  in LFFDSP are used as  $\hat{C}^{(0,17)}$ ,  $\bar{w}_{17}$  and  $\bar{\alpha}_{17}$  in expressions shown below.

$$\vec{\alpha}_{18} = \vec{\alpha}_{17} + \ddot{\theta}_{18}\bar{u}_2^{(17)} + \dot{\theta}_{18}\bar{w}_{17} \times \bar{u}_2^{(17)}$$

$$\bar{\alpha}_{18} = \bar{\alpha}_{17} + \ddot{\theta}_{18}\hat{C}^{(0,17)}\bar{u}_2 + \dot{\theta}_{18}\tilde{w}_{17}\hat{C}^{(0,17)}\bar{u}_2$$

Applying the similar procedure for other angular acceleration relations:

$$\bar{\alpha}_{19} = \bar{\alpha}_{18} + \ddot{\theta}_{19}\hat{C}^{(0,18)}\bar{u}_3 + \dot{\theta}_{19}\tilde{w}_{18}\hat{C}^{(0,18)}\bar{u}_3$$

$$\bar{\alpha}_{20} = \bar{\alpha}_{19} + \ddot{\theta}_{20}\hat{C}^{(0,19)}\bar{u}_1 + \dot{\theta}_{20}\tilde{w}_{19}\hat{C}^{(0,19)}\bar{u}_1$$

$$\bar{\alpha}_{21} = \bar{\alpha}_{20} + \ddot{\theta}_{21}\hat{C}^{(0,20)}\bar{u}_1 + \dot{\theta}_{21}\tilde{w}_{20}\hat{C}^{(0,20)}\bar{u}_1$$

$$\bar{\alpha}_{22} = \bar{\alpha}_{20} + \ddot{\theta}_{22}\hat{C}^{(0,20)}\bar{u}_1 + \dot{\theta}_{22}\tilde{w}_{20}\hat{C}^{(0,20)}\bar{u}_1$$

$$\bar{\alpha}_{23} = \bar{\alpha}_{21} + \ddot{\theta}_{23}\hat{C}^{(0,21)}\bar{u}_2 + \dot{\theta}_{23}\tilde{w}_{21}\hat{C}^{(0,21)}\bar{u}_2$$

$$\bar{\alpha}_{24} = \bar{\alpha}_{22} + \ddot{\theta}_{24}\hat{C}^{(0,22)}\bar{u}_2 + \dot{\theta}_{24}\tilde{w}_{22}\hat{C}^{(0,22)}\bar{u}_2$$

$$\bar{\alpha}_{25} = \bar{\alpha}_{20} + \ddot{\theta}_{25}\hat{C}^{(0,20)}\bar{u}_3 + \dot{\theta}_{25}\tilde{w}_{20}\hat{C}^{(0,20)}\bar{u}_3$$

$$\bar{\alpha}_{26} = \bar{\alpha}_{25} + \ddot{\theta}_{26}\hat{C}^{(0,25)}\bar{u}_2 + \dot{\theta}_{26}\tilde{w}_{25}\hat{C}^{(0,25)}\bar{u}_2$$

$$\bar{\alpha}_{27} = \bar{\alpha}_{26} + \ddot{\theta}_{27}\hat{C}^{(0,26)}\bar{u}_1 + \dot{\theta}_{27}\tilde{w}_{26}\hat{C}^{(0,26)}\bar{u}_1$$

#### 4.1.5.1. For RFFSSP

Calculation of angular accelerations for RFFSSP is shown below; where  $\bar{\alpha}_1$ ,  $\bar{w}_1$ ,  $\hat{C}^{(0,1)}$  are supplied.  $\bar{\alpha}_1$  and  $\bar{w}_1$  are supplied as  $\bar{0}_{3 \times 1}$  in the simulation since Body 1 is assumed to be rigidly fixed to the ground during RFFSSP.

$$\bar{\alpha}_3 = \bar{\alpha}_1 + \ddot{\theta}_3\hat{C}^{(0,1)}\bar{u}_2 + \dot{\theta}_3\tilde{w}_1\hat{C}^{(0,1)}\bar{u}_2$$

$$\bar{\alpha}_5 = \bar{\alpha}_3 + \ddot{\theta}_5\hat{C}^{(0,3)}\bar{u}_2 + \dot{\theta}_5\tilde{w}_3\hat{C}^{(0,3)}\bar{u}_2$$

$$\bar{\alpha}_7 = \bar{\alpha}_5 + \ddot{\theta}_7\hat{C}^{(0,5)}\bar{u}_3 + \dot{\theta}_7\tilde{w}_5\hat{C}^{(0,5)}\bar{u}_3$$

$$\bar{\alpha}_9 = \bar{\alpha}_7 + \ddot{\theta}_9\hat{C}^{(0,7)}\bar{u}_1 + \dot{\theta}_9\tilde{w}_7\hat{C}^{(0,7)}\bar{u}_1$$

$$\bar{\alpha}_{11} = \bar{\alpha}_9 + \ddot{\theta}_{11}\hat{C}^{(0,9)}\bar{u}_2 + \dot{\theta}_{11}\tilde{w}_9\hat{C}^{(0,9)}\bar{u}_2$$

$$\bar{\alpha}_{13} = \bar{\alpha}_{11} + \ddot{\theta}_{13}\hat{C}^{(0,11)}\bar{u}_2 + \dot{\theta}_{13}\tilde{w}_{11}\hat{C}^{(0,11)}\bar{u}_2$$

$$\bar{\alpha}_{15} = \bar{\alpha}_{13} + \ddot{\theta}_{15}\hat{C}^{(0,13)}\bar{u}_1 + \dot{\theta}_{15}\tilde{w}_{13}\hat{C}^{(0,13)}\bar{u}_1$$

$$\bar{\alpha}_{17} = \bar{\alpha}_{15} + \ddot{\theta}_{17,r}\hat{C}^{(0,15)}\bar{u}_3 + \dot{\theta}_{17,r}\tilde{w}_{15}\hat{C}^{(0,15)}\bar{u}_3$$

$$\bar{\alpha}_{16} = \bar{\alpha}_{17} - \ddot{\theta}_{17,l}\hat{C}^{(0,17)}\bar{u}_3 - \dot{\theta}_{17,l}\tilde{w}_{17}\hat{C}^{(0,17)}\bar{u}_3$$

$$\bar{\alpha}_{14} = \bar{\alpha}_{16} - \ddot{\theta}_{16}\hat{C}^{(0,16)}\bar{u}_1 - \dot{\theta}_{16}\tilde{w}_{16}\hat{C}^{(0,16)}\bar{u}_1$$

$$\bar{\alpha}_{12} = \bar{\alpha}_{14} - \ddot{\theta}_{14}\hat{C}^{(0,14)}\bar{u}_2 - \dot{\theta}_{14}\tilde{w}_{14}\hat{C}^{(0,14)}\bar{u}_2$$

$$\bar{\alpha}_{10} = \bar{\alpha}_{12} - \ddot{\theta}_{12}\hat{C}^{(0,12)}\bar{u}_2 - \dot{\theta}_{12}\tilde{w}_{12}\hat{C}^{(0,12)}\bar{u}_2$$

$$\bar{\alpha}_8 = \bar{\alpha}_{10} - \ddot{\theta}_{10}\hat{C}^{(0,10)}\bar{u}_1 - \dot{\theta}_{10}\tilde{w}_{10}\hat{C}^{(0,10)}\bar{u}_1$$

$$\bar{\alpha}_6 = \bar{\alpha}_8 - \ddot{\theta}_8\hat{C}^{(0,8)}\bar{u}_3 - \dot{\theta}_8\tilde{w}_8\hat{C}^{(0,8)}\bar{u}_3$$

$$\bar{\alpha}_4 = \bar{\alpha}_6 - \ddot{\theta}_6\hat{C}^{(0,6)}\bar{u}_2 - \dot{\theta}_6\tilde{w}_6\hat{C}^{(0,6)}\bar{u}_2$$

$$\bar{\alpha}_2 = \bar{\alpha}_4 - \ddot{\theta}_4\hat{C}^{(0,4)}\bar{u}_2 - \dot{\theta}_4\tilde{w}_4\hat{C}^{(0,4)}\bar{u}_2$$

#### 4.1.5.2. For LFFSSP

Calculation of angular accelerations for LFFSSP is shown below; where  $\bar{\alpha}_2$ ,  $\bar{w}_2$ ,  $\hat{C}^{(0,2)}$  are supplied.  $\bar{\alpha}_2$  and  $\bar{w}_2$  are supplied as  $\bar{0}_{3 \times 1}$  in the simulation since Body 2 is assumed to be rigidly fixed to the ground during LFFSSP.

$$\bar{\alpha}_4 = \bar{\alpha}_2 + \ddot{\theta}_4\hat{C}^{(0,2)}\bar{u}_2 + \dot{\theta}_4\tilde{w}_2\hat{C}^{(0,2)}\bar{u}_2$$

$$\bar{\alpha}_6 = \bar{\alpha}_4 + \ddot{\theta}_6\hat{C}^{(0,4)}\bar{u}_2 + \dot{\theta}_6\tilde{w}_4\hat{C}^{(0,4)}\bar{u}_2$$

$$\bar{\alpha}_8 = \bar{\alpha}_6 + \ddot{\theta}_8\hat{C}^{(0,6)}\bar{u}_3 + \dot{\theta}_8\tilde{w}_6\hat{C}^{(0,6)}\bar{u}_3$$

$$\bar{\alpha}_{10} = \bar{\alpha}_8 + \ddot{\theta}_{10}\hat{C}^{(0,8)}\bar{u}_1 + \dot{\theta}_{10}\tilde{w}_8\hat{C}^{(0,8)}\bar{u}_1$$

$$\bar{\alpha}_{12} = \bar{\alpha}_{10} + \ddot{\theta}_{12}\hat{C}^{(0,10)}\bar{u}_2 + \dot{\theta}_{12}\tilde{w}_{10}\hat{C}^{(0,10)}\bar{u}_2$$

$$\bar{\alpha}_{14} = \bar{\alpha}_{12} + \ddot{\theta}_{14}\hat{C}^{(0,12)}\bar{u}_2 + \dot{\theta}_{14}\tilde{w}_{12}\hat{C}^{(0,12)}\bar{u}_2$$

$$\bar{\alpha}_{16} = \bar{\alpha}_{14} + \ddot{\theta}_{16}\hat{C}^{(0,14)}\bar{u}_1 + \dot{\theta}_{16}\tilde{w}_{14}\hat{C}^{(0,14)}\bar{u}_1$$

$$\bar{\alpha}_{17} = \bar{\alpha}_{16} + \ddot{\theta}_{17,l}\hat{C}^{(0,16)}\bar{u}_3 + \dot{\theta}_{17,l}\tilde{w}_{16}\hat{C}^{(0,16)}\bar{u}_3$$

$$\bar{\alpha}_{15} = \bar{\alpha}_{17} - \ddot{\theta}_{17,r}\hat{C}^{(0,17)}\bar{u}_3 - \dot{\theta}_{17,r}\tilde{w}_{17}\hat{C}^{(0,17)}\bar{u}_3$$

$$\bar{\alpha}_{13} = \bar{\alpha}_{15} - \ddot{\theta}_{15}\hat{C}^{(0,15)}\bar{u}_1 - \dot{\theta}_{15}\tilde{w}_{15}\hat{C}^{(0,15)}\bar{u}_1$$

$$\bar{\alpha}_{11} = \bar{\alpha}_{13} - \ddot{\theta}_{13}\hat{C}^{(0,13)}\bar{u}_2 - \dot{\theta}_{13}\tilde{w}_{13}\hat{C}^{(0,13)}\bar{u}_2$$

$$\bar{\alpha}_9 = \bar{\alpha}_{11} - \ddot{\theta}_{11}\hat{C}^{(0,11)}\bar{u}_2 - \dot{\theta}_{11}\tilde{w}_{11}\hat{C}^{(0,11)}\bar{u}_2$$

$$\bar{\alpha}_7 = \bar{\alpha}_9 - \ddot{\theta}_9\hat{C}^{(0,9)}\bar{u}_1 - \dot{\theta}_9\tilde{w}_9\hat{C}^{(0,9)}\bar{u}_1$$

$$\bar{\alpha}_5 = \bar{\alpha}_7 - \ddot{\theta}_7 \hat{C}^{(0,7)} \bar{u}_3 - \dot{\theta}_7 \tilde{w}_7 \hat{C}^{(0,7)} \bar{u}_3$$

$$\bar{\alpha}_3 = \bar{\alpha}_5 - \ddot{\theta}_5 \hat{C}^{(0,5)} \bar{u}_2 - \dot{\theta}_5 \tilde{w}_5 \hat{C}^{(0,5)} \bar{u}_2$$

$$\bar{\alpha}_1 = \bar{\alpha}_3 - \ddot{\theta}_3 \hat{C}^{(0,3)} \bar{u}_2 - \dot{\theta}_3 \tilde{w}_3 \hat{C}^{(0,3)} \bar{u}_2$$

#### 4.1.5.2. For RFFDSP and LFFDSP

The procedure of calculating angular accelerations for RFFDSP and LFFDSP is shown below; where  $\bar{\alpha}_1$ ,  $\bar{\alpha}_2$ ,  $\bar{w}_1$ ,  $\bar{w}_2$ ,  $\hat{C}^{(0,1)}$  and  $\hat{C}^{(0,2)}$  are supplied.  $\bar{\alpha}_1$ ,  $\bar{\alpha}_2$ ,  $\bar{w}_1$  and  $\bar{w}_2$  are supplied as  $\bar{0}_{3 \times 1}$  in the simulation since Body 1 and Body 2 are assumed to be rigidly fixed to the ground during RFFDSP and LFFDSP.

$$\bar{\alpha}_3 = \bar{\alpha}_1 + \ddot{\theta}_3 \hat{C}^{(0,1)} \bar{u}_2 + \dot{\theta}_3 \tilde{w}_1 \hat{C}^{(0,1)} \bar{u}_2$$

$$\bar{\alpha}_5 = \bar{\alpha}_3 + \ddot{\theta}_5 \hat{C}^{(0,3)} \bar{u}_2 + \dot{\theta}_5 \tilde{w}_3 \hat{C}^{(0,3)} \bar{u}_2$$

$$\bar{\alpha}_7 = \bar{\alpha}_5 + \ddot{\theta}_7 \hat{C}^{(0,5)} \bar{u}_3 + \dot{\theta}_7 \tilde{w}_5 \hat{C}^{(0,5)} \bar{u}_3$$

$$\bar{\alpha}_9 = \bar{\alpha}_7 + \ddot{\theta}_9 \hat{C}^{(0,7)} \bar{u}_1 + \dot{\theta}_9 \tilde{w}_7 \hat{C}^{(0,7)} \bar{u}_1$$

$$\bar{\alpha}_{11} = \bar{\alpha}_9 + \ddot{\theta}_{11} \hat{C}^{(0,9)} \bar{u}_2 + \dot{\theta}_{11} \tilde{w}_9 \hat{C}^{(0,9)} \bar{u}_2$$

$$\bar{\alpha}_{13} = \bar{\alpha}_{11} + \ddot{\theta}_{13} \hat{C}^{(0,11)} \bar{u}_2 + \dot{\theta}_{13} \tilde{w}_{11} \hat{C}^{(0,11)} \bar{u}_2$$

$$\bar{\alpha}_{15} = \bar{\alpha}_{13} + \ddot{\theta}_{15} \hat{C}^{(0,13)} \bar{u}_1 + \dot{\theta}_{15} \tilde{w}_{13} \hat{C}^{(0,13)} \bar{u}_1$$

$$\bar{\alpha}_{17_{fR}} = \bar{\alpha}_{15} + \ddot{\theta}_{17,r} \hat{C}^{(0,15)} \bar{u}_3 + \dot{\theta}_{17,r} \tilde{w}_{15} \hat{C}^{(0,15)} \bar{u}_3$$

$$\bar{\alpha}_4 = \bar{\alpha}_2 + \ddot{\theta}_4 \hat{C}^{(0,2)} \bar{u}_2 + \dot{\theta}_4 \tilde{w}_2 \hat{C}^{(0,2)} \bar{u}_2$$

$$\bar{\alpha}_6 = \bar{\alpha}_4 + \ddot{\theta}_6 \hat{C}^{(0,4)} \bar{u}_2 + \dot{\theta}_6 \tilde{w}_4 \hat{C}^{(0,4)} \bar{u}_2$$

$$\bar{\alpha}_8 = \bar{\alpha}_6 + \ddot{\theta}_8 \hat{C}^{(0,6)} \bar{u}_3 + \dot{\theta}_8 \tilde{w}_6 \hat{C}^{(0,6)} \bar{u}_3$$

$$\bar{\alpha}_{10} = \bar{\alpha}_8 + \ddot{\theta}_{10} \hat{C}^{(0,8)} \bar{u}_1 + \dot{\theta}_{10} \tilde{w}_8 \hat{C}^{(0,8)} \bar{u}_1$$

$$\bar{\alpha}_{12} = \bar{\alpha}_{10} + \ddot{\theta}_{12} \hat{C}^{(0,10)} \bar{u}_2 + \dot{\theta}_{12} \tilde{w}_{10} \hat{C}^{(0,10)} \bar{u}_2$$

$$\bar{a}_{14} = \bar{a}_{12} + \ddot{\theta}_{14} \hat{C}^{(0,12)} \bar{u}_2 + \dot{\theta}_{14} \tilde{w}_{12} \hat{C}^{(0,12)} \bar{u}_2$$

$$\bar{a}_{16} = \bar{a}_{14} + \ddot{\theta}_{16} \hat{C}^{(0,14)} \bar{u}_1 + \dot{\theta}_{16} \tilde{w}_{14} \hat{C}^{(0,14)} \bar{u}_1$$

$$\bar{a}_{17\_fL} = \bar{a}_{16} + \ddot{\theta}_{17,l} \hat{C}^{(0,16)} \bar{u}_3 + \dot{\theta}_{17,l} \tilde{w}_{16} \hat{C}^{(0,16)} \bar{u}_3$$

#### 4.1.6. Translational Acceleration Relations

$\bar{a}_{c,k}$  is a vector describing the translational acceleration of the mass center of Body K in matrix form of  $\vec{a}_{c,k}$ , differentiated with respect to and resolved in the inertial frame. Expression of translational acceleration relations differs according to the locomotion phase for lowerbodies. On the other hand, expression of translational acceleration relations for upperbodies is common for all phases, noting that  $\hat{C}^{(0,17\_fR)}$ ,  $\bar{w}_{17\_fR}$ ,  $\bar{a}_{c,17\_fR}$  in RFFDSP and  $\hat{C}^{(0,17\_fL)}$ ,  $\bar{w}_{17\_fL}$ ,  $\bar{a}_{c,17\_fL}$  in LFFDSP are used as  $\hat{C}^{(0,17)}$ ,  $\bar{w}_{17}$  and  $\bar{a}_{c,17}$  in expressions shown below.

$$\begin{aligned} \vec{a}_{c,20} = & \vec{a}_{c,17} + c_{17} \left[ \vec{\alpha}_{17} \times \vec{u}_3^{(17)} + \vec{w}_{17} \times \left( \vec{w}_{17} \times \vec{u}_3^{(17)} \right) \right] \\ & + (l_{20z} - c_{20}) \left[ \vec{\alpha}_{20} \times \vec{u}_3^{(20)} + \vec{w}_{20} \times \left( \vec{w}_{20} \times \vec{u}_3^{(20)} \right) \right] \end{aligned}$$

$$\bar{a}_{c,20} = \bar{a}_{c,17} + c_{17} [\tilde{\alpha}_{17} + \tilde{w}_{17}^2] \hat{C}^{(0,17)} \bar{u}_3 + (l_{20z} - c_{20}) [\tilde{\alpha}_{20} + \tilde{w}_{20}^2] \hat{C}^{(0,20)} \bar{u}_3$$

Applying the similar procedure for other translational acceleration relations:

$$\begin{aligned} \bar{a}_{c,23} = & \bar{a}_{c,20} - l_{20y} [\tilde{\alpha}_{20} + \tilde{w}_{20}^2] \hat{C}^{(0,20)} \bar{u}_2 + (c_{23} - l_{23z}) [\tilde{\alpha}_{23} + \tilde{w}_{23}^2] \hat{C}^{(0,23)} \bar{u}_3 - \\ & l_{23y} [\tilde{\alpha}_{23} + \tilde{w}_{23}^2] \hat{C}^{(0,23)} \bar{u}_2 + c_{20} [\tilde{\alpha}_{20} + \tilde{w}_{20}^2] \hat{C}^{(0,20)} \bar{u}_3 \end{aligned}$$

$$\begin{aligned} \bar{a}_{c,24} = & \bar{a}_{c,20} + l_{20y} [\tilde{\alpha}_{20} + \tilde{w}_{20}^2] \hat{C}^{(0,20)} \bar{u}_2 + (c_{24} - l_{24z}) [\tilde{\alpha}_{24} + \tilde{w}_{24}^2] \hat{C}^{(0,24)} \bar{u}_3 + \\ & l_{24y} [\tilde{\alpha}_{24} + \tilde{w}_{24}^2] \hat{C}^{(0,24)} \bar{u}_2 + c_{20} [\tilde{\alpha}_{20} + \tilde{w}_{20}^2] \hat{C}^{(0,20)} \bar{u}_3 \end{aligned}$$

$$\bar{a}_{c,27} = \bar{a}_{c,20} + c_{20} [\tilde{\alpha}_{20} + \tilde{w}_{20}^2] \hat{C}^{(0,20)} \bar{u}_3 + (l_{27} - c_{27}) [\tilde{\alpha}_{27} + \tilde{w}_{27}^2] \hat{C}^{(0,27)} \bar{u}_3$$

##### 4.1.6.1. For RFFSSP

Calculation of translational accelerations for RFFSSP is shown below; where  $\bar{a}_{tpR}$ ,  $\bar{a}_1$ ,  $\bar{w}_1$  and  $\hat{C}^{(0,1)}$  are supplied.  $\bar{a}_{tpR}$ ,  $\bar{a}_1$  and  $\bar{w}_1$  are supplied as  $\bar{0}_{3 \times 1}$  in the

simulation since Body 1 is assumed to be rigidly fixed to the ground during RFFSSP.

$$\bar{a}_{c,1} = \bar{a}_{tpR} + (c_1 - l_1)[\tilde{\alpha}_1 + \tilde{w}_1^2]\hat{C}^{(0,1)}\bar{u}_1$$

$$\begin{aligned}\bar{a}_{c,3} &= \bar{a}_{c,1} - c_1[\tilde{\alpha}_1 + \tilde{w}_1^2]\hat{C}^{(0,1)}\bar{u}_1 + (c_{3x} - l_{3x})[\tilde{\alpha}_3 + \tilde{w}_3^2]\hat{C}^{(0,3)}\bar{u}_1 + \\ &(l_{3z} - c_{3z})[\tilde{\alpha}_3 + \tilde{w}_3^2]\hat{C}^{(0,3)}\bar{u}_3\end{aligned}$$

$$\begin{aligned}\bar{a}_{c,9} &= \bar{a}_{c,3} - c_{3x}[\tilde{\alpha}_3 + \tilde{w}_3^2]\hat{C}^{(0,3)}\bar{u}_1 + c_{3z}[\tilde{\alpha}_3 + \tilde{w}_3^2]\hat{C}^{(0,3)}\bar{u}_3 \\ &+(l_9 - c_9)[\tilde{\alpha}_9 + \tilde{w}_9^2]\hat{C}^{(0,9)}\bar{u}_3\end{aligned}$$

$$\bar{a}_{c,11} = \bar{a}_{c,9} + c_9[\tilde{\alpha}_9 + \tilde{w}_9^2]\hat{C}^{(0,9)}\bar{u}_3 + (l_{11} - c_{11})[\tilde{\alpha}_{11} + \tilde{w}_{11}^2]\hat{C}^{(0,11)}\bar{u}_3$$

$$\begin{aligned}\bar{a}_{c,17} &= \bar{a}_{c,11} + c_{11}[\tilde{\alpha}_{11} + \tilde{w}_{11}^2]\hat{C}^{(0,11)}\bar{u}_3 + l_{17y}[\tilde{\alpha}_{17} + \tilde{w}_{17}^2]\hat{C}^{(0,17)}\bar{u}_2 + \\ &(l_{17z} - c_{17})[\tilde{\alpha}_{17} + \tilde{w}_{17}^2]\hat{C}^{(0,17)}\bar{u}_3\end{aligned}$$

$$\begin{aligned}\bar{a}_{c,12} &= \bar{a}_{c,17} + l_{17y}[\tilde{\alpha}_{17} + \tilde{w}_{17}^2]\hat{C}^{(0,17)}\bar{u}_2 + (c_{17} - l_{17z})[\tilde{\alpha}_{17} + \tilde{w}_{17}^2]\hat{C}^{(0,17)}\bar{u}_3 - \\ &c_{12}[\tilde{\alpha}_{12} + \tilde{w}_{12}^2]\hat{C}^{(0,12)}\bar{u}_3\end{aligned}$$

$$\bar{a}_{c,10} = \bar{a}_{c,12} + (c_{12} - l_{12})[\tilde{\alpha}_{12} + \tilde{w}_{12}^2]\hat{C}^{(0,12)}\bar{u}_3 - c_{10}[\tilde{\alpha}_{10} + \tilde{w}_{10}^2]\hat{C}^{(0,10)}\bar{u}_3$$

$$\begin{aligned}\bar{a}_{c,4} &= \bar{a}_{c,10} + (c_{10} - l_{10})[\tilde{\alpha}_{10} + \tilde{w}_{10}^2]\hat{C}^{(0,10)}\bar{u}_3 + c_{4x}[\tilde{\alpha}_4 + \tilde{w}_4^2]\hat{C}^{(0,4)}\bar{u}_1 - \\ &c_{4z}[\tilde{\alpha}_4 + \tilde{w}_4^2]\hat{C}^{(0,4)}\bar{u}_3\end{aligned}$$

$$\begin{aligned}\bar{a}_{c,2} &= \bar{a}_{c,4} + (l_{4x} - c_{4x})[\tilde{\alpha}_4 + \tilde{w}_4^2]\hat{C}^{(0,4)}\bar{u}_1 + (c_{4z} - l_{4z})[\tilde{\alpha}_4 + \tilde{w}_4^2]\hat{C}^{(0,4)}\bar{u}_3 + \\ &c_2[\tilde{\alpha}_2 + \tilde{w}_2^2]\hat{C}^{(0,2)}\bar{u}_1\end{aligned}$$

#### 4.1.6.2. For LFFSSP

Calculation of translational accelerations for LFFSSP is shown below; where  $\bar{a}_{tpL}$ ,  $\bar{\alpha}_2$ ,  $\bar{w}_2$  and  $\hat{C}^{(0,2)}$  are supplied.  $\bar{a}_{tpL}$ ,  $\bar{\alpha}_2$  and  $\bar{w}_2$  are supplied as  $\bar{0}_{3 \times 1}$  in the simulation since Body 2 is assumed to be rigidly fixed to the ground during LFFSSP.

$$\bar{a}_{c,2} = \bar{a}_{tpL} + (c_2 - l_2)[\tilde{\alpha}_2 + \tilde{w}_2^2]\hat{C}^{(0,2)}\bar{u}_1$$

$$\bar{a}_{c,4} = \bar{a}_{c,2} - c_2[\tilde{\alpha}_2 + \tilde{w}_2^2]\hat{C}^{(0,2)}\bar{u}_1 + (c_{4x} - l_{4x})[\tilde{\alpha}_4 + \tilde{w}_4^2]\hat{C}^{(0,4)}\bar{u}_1 + (l_{4z} - c_{4z})[\tilde{\alpha}_4 + \tilde{w}_4^2]\hat{C}^{(0,4)}\bar{u}_3$$

$$\bar{a}_{c,10} = \bar{a}_{c,4} - c_{4x}[\tilde{\alpha}_4 + \tilde{w}_4^2]\hat{C}^{(0,4)}\bar{u}_1 + c_{4z}[\tilde{\alpha}_4 + \tilde{w}_4^2]\hat{C}^{(0,4)}\bar{u}_3 + (l_{10} - c_{10})[\tilde{\alpha}_{10} + \tilde{w}_{10}^2]\hat{C}^{(0,10)}\bar{u}_3$$

$$\bar{a}_{c,12} = \bar{a}_{c,10} + c_{10}[\tilde{\alpha}_{10} + \tilde{w}_{10}^2]\hat{C}^{(0,10)}\bar{u}_3 + (l_{12} - c_{12})[\tilde{\alpha}_{12} + \tilde{w}_{12}^2]\hat{C}^{(0,12)}\bar{u}_3$$

$$\bar{a}_{c,17} = \bar{a}_{c,12} + c_{12}[\tilde{\alpha}_{12} + \tilde{w}_{12}^2]\hat{C}^{(0,12)}\bar{u}_3 - l_{17y}[\tilde{\alpha}_{17} + \tilde{w}_{17}^2]\hat{C}^{(0,17)}\bar{u}_2 + (l_{17z} - c_{17})[\tilde{\alpha}_{17} + \tilde{w}_{17}^2]\hat{C}^{(0,17)}\bar{u}_3$$

$$\bar{a}_{c,11} = \bar{a}_{c,17} - l_{17y}[\tilde{\alpha}_{17} + \tilde{w}_{17}^2]\hat{C}^{(0,17)}\bar{u}_2 + (c_{17} - l_{17z})[\tilde{\alpha}_{17} + \tilde{w}_{17}^2]\hat{C}^{(0,17)}\bar{u}_3 - c_{11}[\tilde{\alpha}_{11} + \tilde{w}_{11}^2]\hat{C}^{(0,11)}\bar{u}_3$$

$$\bar{a}_{c,9} = \bar{a}_{c,11} + (c_{11} - l_{11})[\tilde{\alpha}_{11} + \tilde{w}_{11}^2]\hat{C}^{(0,11)}\bar{u}_3 - c_9[\tilde{\alpha}_9 + \tilde{w}_9^2]\hat{C}^{(0,9)}\bar{u}_3$$

$$\bar{a}_{c,3} = \bar{a}_{c,9} + (c_9 - l_9)[\tilde{\alpha}_9 + \tilde{w}_9^2]\hat{C}^{(0,9)}\bar{u}_3 + c_{3x}[\tilde{\alpha}_3 + \tilde{w}_3^2]\hat{C}^{(0,3)}\bar{u}_1 - c_{3z}[\tilde{\alpha}_3 + \tilde{w}_3^2]\hat{C}^{(0,3)}\bar{u}_3$$

$$\bar{a}_{c,1} = \bar{a}_{c,3} + (l_{3x} - c_{3x})[\tilde{\alpha}_3 + \tilde{w}_3^2]\hat{C}^{(0,3)}\bar{u}_1 + (c_{3z} - l_{3z})[\tilde{\alpha}_3 + \tilde{w}_3^2]\hat{C}^{(0,3)}\bar{u}_3 + c_1[\tilde{\alpha}_1 + \tilde{w}_1^2]\hat{C}^{(0,1)}\bar{u}_1$$

#### 4.1.6.3. For RFFDSP and LFFDSP

Calculation of translational accelerations for RFFDSP and LFFDSP is shown below; where  $\bar{a}_{tpR}$ ,  $\bar{a}_{tpL}$ ,  $\bar{\alpha}_1$ ,  $\bar{\alpha}_2$ ,  $\bar{w}_1$ ,  $\bar{w}_2$ ,  $\hat{C}^{(0,1)}$  and  $\hat{C}^{(0,2)}$  are supplied.  $\bar{a}_{tpR}$ ,  $\bar{a}_{tpL}$ ,  $\bar{\alpha}_1$ ,  $\bar{\alpha}_2$ ,  $\bar{w}_1$  and  $\bar{w}_2$  are supplied as  $\bar{0}_{3 \times 1}$  in the simulation since Body 1 and Body 2 are assumed to be rigidly fixed to the ground during RFFDSP and LFFDSP.

$$\bar{a}_{c,1} = \bar{a}_{tpR} + (c_1 - l_1)[\tilde{\alpha}_1 + \tilde{w}_1^2]\hat{C}^{(0,1)}\bar{u}_1$$

$$\bar{a}_{c,3} = \bar{a}_{c,1} - c_1[\tilde{\alpha}_1 + \tilde{w}_1^2]\hat{C}^{(0,1)}\bar{u}_1 + (c_{3x} - l_{3x})[\tilde{\alpha}_3 + \tilde{w}_3^2]\hat{C}^{(0,3)}\bar{u}_1 + (l_{3z} - c_{3z})[\tilde{\alpha}_3 + \tilde{w}_3^2]\hat{C}^{(0,3)}\bar{u}_3$$

$$\begin{aligned}
\bar{a}_{c,9} &= \bar{a}_{c,3} - c_{3x}[\tilde{\alpha}_3 + \tilde{w}_3^2]\hat{C}^{(0,3)}\bar{u}_1 + c_{3z}[\tilde{\alpha}_3 + \tilde{w}_3^2]\hat{C}^{(0,3)}\bar{u}_3 \\
&+ (l_9 - c_9)[\tilde{\alpha}_9 + \tilde{w}_9^2]\hat{C}^{(0,9)}\bar{u}_3 \\
\bar{a}_{c,11} &= \bar{a}_{c,9} + c_9[\tilde{\alpha}_9 + \tilde{w}_9^2]\hat{C}^{(0,9)}\bar{u}_3 + (l_{11} - c_{11})[\tilde{\alpha}_{11} + \tilde{w}_{11}^2]\hat{C}^{(0,11)}\bar{u}_3 \\
\bar{a}_{c,17_{fR}} &= \bar{a}_{c,11} + c_{11}[\tilde{\alpha}_{11} + \tilde{w}_{11}^2]\hat{C}^{(0,11)}\bar{u}_3 + l_{17y}[\tilde{\alpha}_{17} + \tilde{w}_{17}^2]\hat{C}^{(0,17_{fR})}\bar{u}_2 + \\
&(l_{17z} - c_{17})[\tilde{\alpha}_{17} + \tilde{w}_{17}^2]\hat{C}^{(0,17_{fR})}\bar{u}_3 \\
\bar{a}_{c,2} &= \bar{a}_{tpL} + (c_2 - l_2)[\tilde{\alpha}_2 + \tilde{w}_2^2]\hat{C}^{(0,2)}\bar{u}_1 \\
\bar{a}_{c,4} &= \bar{a}_{c,2} - c_2[\tilde{\alpha}_2 + \tilde{w}_2^2]\hat{C}^{(0,2)}\bar{u}_1 + (c_{4x} - l_{4x})[\tilde{\alpha}_4 + \tilde{w}_4^2]\hat{C}^{(0,4)}\bar{u}_1 + \\
&(l_{4z} - c_{4z})[\tilde{\alpha}_4 + \tilde{w}_4^2]\hat{C}^{(0,4)}\bar{u}_3 \\
\bar{a}_{c,10} &= \bar{a}_{c,4} - c_{4x}[\tilde{\alpha}_4 + \tilde{w}_4^2]\hat{C}^{(0,4)}\bar{u}_1 + c_{4z}[\tilde{\alpha}_4 + \tilde{w}_4^2]\hat{C}^{(0,4)}\bar{u}_3 \\
&+ (l_{10} - c_{10})[\tilde{\alpha}_{10} + \tilde{w}_{10}^2]\hat{C}^{(0,10)}\bar{u}_3 \\
\bar{a}_{c,12} &= \bar{a}_{c,10} + c_{10}[\tilde{\alpha}_{10} + \tilde{w}_{10}^2]\hat{C}^{(0,10)}\bar{u}_3 + (l_{12} - c_{12})[\tilde{\alpha}_{12} + \tilde{w}_{12}^2]\hat{C}^{(0,12)}\bar{u}_3 \\
\bar{a}_{c,17_{fL}} &= \bar{a}_{c,12} + c_{12}[\tilde{\alpha}_{12} + \tilde{w}_{12}^2]\hat{C}^{(0,12)}\bar{u}_3 - l_{17y}[\tilde{\alpha}_{17} + \tilde{w}_{17}^2]\hat{C}^{(0,17_{fL})}\bar{u}_2 + \\
&(l_{17z} - c_{17})[\tilde{\alpha}_{17} + \tilde{w}_{17}^2]\hat{C}^{(0,17_{fL})}\bar{u}_3
\end{aligned}$$

## 4.2. Calculation of Jacobian Matrices and Their Time Derivatives

The analytical expression of jacobian matrices are lengthy, requires careful and laborious work due to the complexity of system. Therefore, required jacobian matrices are calculated numerically during each simulation step. For this reason, time derivatives of jacobian matrices are calculated approximately and numerically.

Some joint space variables are taken as zero which is ensured by constraint equations and phase changing operations.

## 4.2.1. Definition of Jacobian Matrices

### 4.2.1.1 For RFFSSP

Since  $\dot{\theta}_3$  is taken to be zero during jacobian matrix calculations,  $\ddot{\bar{q}}_{R_H}$  can be reduced to  $\ddot{\bar{q}}_{R_Hr}$  as shown below:

$$\ddot{\bar{q}}_{R_Hr} = \begin{bmatrix} \dot{\theta}_5 \\ \dot{\theta}_7 \\ \dot{\theta}_9 \\ \dot{\theta}_{11} \\ \dot{\theta}_{13} \\ \dot{\theta}_{15} \\ \dot{\theta}_{17,r} \end{bmatrix}. \quad (4.6)$$

By using equation (4.3) and (4.6) , it can be expressed that:

$$\text{For } \ddot{\bar{q}}_{R_L} = \begin{bmatrix} \ddot{\bar{q}}_{R_Hr} \\ \ddot{\bar{q}}_{L_H} \end{bmatrix},$$

$$\begin{bmatrix} \bar{V}_{c,17} \\ \bar{W}_{17} \end{bmatrix} = \hat{J}_{v,17\_fR} \ddot{\bar{q}}_{R_Hr} \quad (4.7)$$

$$\begin{bmatrix} \bar{V}_{tpL} \\ \bar{W}_2 \end{bmatrix} = \hat{J}_{v,tpL} \ddot{\bar{q}}_{R_L} \quad (4.8)$$

$$\dot{\bar{C}}_{diag}^{(0,k)} = \text{diag} \left( \dot{\hat{C}}^{(0,k)} \right) = \text{diag}(\tilde{w}_k \hat{C}^{(0,k)}) = \text{diag} \left( \left[ \hat{J}_{v,k_w} \widetilde{\dot{\bar{q}}} \right] \hat{C}^{(0,k)} \right) \quad (4.9)$$

$$\bar{W}_{17} = \hat{J}_{v,17\_fR_w} \ddot{\bar{q}}_{R_Hr} \quad (4.10)$$

$$\bar{W}_2 = \hat{J}_{v,tpL_w} \ddot{\bar{q}}_{R_L}. \quad (4.11)$$

Using equation (4.9), (4.10) and (4.11):

$$\dot{\bar{C}}_{diag}^{(0,17)} = \hat{J}_{v,cdiag0\_17\_fR} \ddot{\bar{q}}_{R_Hr} \quad (4.12)$$

$$\dot{\bar{C}}_{diag}^{(0,2)} = \hat{J}_{v,cdiag0\_2} \ddot{\bar{q}}_{R_L} \quad (4.13)$$

$\hat{J}_{v,17\_fR_w}$  and  $\hat{J}_{v,tpL_w}$  matrices can be extracted from equation (4.14) and (4.15):

$$\hat{J}_{v,17\_fR} = \begin{bmatrix} \hat{J}_{v,17\_fR_V} \\ \hat{J}_{v,17\_fR_w} \end{bmatrix} \quad (4.14)$$

$$\hat{J}_{v,tpL} = \begin{bmatrix} \hat{J}_{v,tpL_V} \\ \hat{J}_{v,tpL_w} \end{bmatrix}. \quad (4.15)$$

In summary:  $\hat{J}_{v,17\_fR}$ ,  $\hat{J}_{v,tpL}$ ,  $\hat{J}_{v,Cdiag0\_17\_fR}$  and  $\hat{J}_{v,Cdiag0\_2}$  are jacobian matrices that are needed to be calculated during RFFSSP.

#### 4.2.1.2 For LFFSSP

Since  $\dot{\theta}_4$  is taken to be zero during jacobian matrix calculations,  $\dot{\bar{q}}_{L_H}$  can be reduced to  $\dot{\bar{q}}_{L_Hr}$  as shown below:

$$\dot{\bar{q}}_{L_Hr} = \begin{bmatrix} \dot{\theta}_6 \\ \dot{\theta}_8 \\ \dot{\theta}_{10} \\ \dot{\theta}_{12} \\ \dot{\theta}_{14} \\ \dot{\theta}_{16} \\ \dot{\theta}_{17,1} \end{bmatrix}. \quad (4.16)$$

By using equation (4.2) and (4.16) , it can be expressed that:

$$\text{For } \dot{\bar{q}}_{L_R} = \begin{bmatrix} \dot{\bar{q}}_{L_Hr} \\ \dot{\bar{q}}_{R_H} \end{bmatrix},$$

$$\begin{bmatrix} \bar{V}_{c,17} \\ \bar{W}_{17} \end{bmatrix} = \hat{J}_{v,17\_fL} \dot{\bar{q}}_{L_Hr} \quad (4.17)$$

$$\begin{bmatrix} \bar{V}_{tpR} \\ \bar{W}_1 \end{bmatrix} = \hat{J}_{v,tpR} \dot{\bar{q}}_{L_R}. \quad (4.18)$$

$$\bar{W}_{17} = \hat{J}_{v,17\_fL_w} \dot{\bar{q}}_{L_Hr} \quad (4.19)$$

$$\bar{W}_1 = \hat{J}_{v,tpR_w} \dot{\bar{q}}_{L_R} \quad (4.20)$$

Using equation (4.9), (4.19) and (4.20):

$$\dot{\hat{C}}_{diag}^{(0,17)} = \hat{J}_{v,Cdiag0_{17}_{fL}} \dot{\hat{q}}_{L_Hr} \quad (4.21)$$

$$\dot{\hat{C}}_{diag}^{(0,1)} = \hat{J}_{v,Cdiag0_{1}} \dot{\hat{q}}_{L_R}, \text{ where} \quad (4.22)$$

$\hat{J}_{v,17_{fL}_w}$  and  $\hat{J}_{v,tpR}_w$  matrices can be extracted from equation (4.23) and (4.24):

$$\hat{J}_{v,17_{fL}} = \begin{bmatrix} \hat{J}_{v,17_{fL}_V} \\ \hat{J}_{v,17_{fL}_w} \end{bmatrix} \quad (4.23)$$

$$\hat{J}_{v,tpR} = \begin{bmatrix} \hat{J}_{v,tpR}_V \\ \hat{J}_{v,tpR}_w \end{bmatrix}. \quad (4.24)$$

In summary:  $\hat{J}_{v,17_{fL}}$ ,  $\hat{J}_{v,tpR}$ ,  $\hat{J}_{v,Cdiag0_{17}_{fL}}$  and  $\hat{J}_{v,Cdiag0_{1}}$  are jacobian matrices that are needed to be calculated during RFFSSP.

#### 4.2.1.3 For RFFDSP

In addition to  $\hat{J}_{v,17_{fR}}$  and  $\hat{J}_{v,Cdiag0_{17}_{fR}}$  as defined in RFFSSP;  $\hat{J}_{v,17_{fL}_{all}}$  and  $\hat{J}_{v,Cdiag0_{17}_{fL}_{all}}$  are required in RFFDSP with definitions shown in equation (4.25) and (4.27).

$$\begin{bmatrix} \bar{V}_{c,17_{fL}} \\ \bar{W}_{17_{fL}} \end{bmatrix} = \hat{J}_{v,17_{fL}_{all}} \dot{\hat{q}}_{L_H} \quad (4.25)$$

$$\bar{W}_{17_{fL}} = \hat{J}_{v,17_{fL}_{all}_w} \dot{\hat{q}}_{L_H} \quad (4.26)$$

Using equation (4.9) and (4.26):

$$\dot{\hat{C}}_{diag}^{(0,17_{fL})} = \hat{J}_{v,Cdiag0_{17}_{fL}_{all}} \dot{\hat{q}}_{L_H} \quad (4.27)$$

$\bar{V}_{c,17_{fR}}$ ,  $\bar{W}_{17_{fR}}$  and  $\dot{\hat{C}}_{diag}^{(0,17_{fR})}$  are used instead of  $\bar{V}_{c,17}$ ,  $\bar{W}_{17}$  and  $\dot{\hat{C}}_{diag}^{(0,17)}$  for the definition of  $\hat{J}_{v,17_{fR}}$  and  $\hat{J}_{v,Cdiag0_{17}_{fR}}$ .

$\hat{J}_{v,17_{fL\_all\_w}}$  can be extracted from equation (4.28):

$$\hat{J}_{v,17_{fL\_all}} = \begin{bmatrix} \hat{J}_{v,17_{fL\_all\_v}} \\ \hat{J}_{v,17_{fL\_all\_w}} \end{bmatrix} \quad (4.28)$$

In summary:  $\hat{J}_{v,17_{fR}}$ ,  $\hat{J}_{v,Cdiag0_{17_{fR}}}$ ,  $\hat{J}_{v,17_{fL\_all}}$  and  $\hat{J}_{v,Cdiag0_{17_{fL\_all}}}$  are jacobian matrices that are needed to be calculated during RFFDSP.

#### 4.2.1.4 For LFFDSP

In addition to  $\hat{J}_{v,17_{fL}}$  and  $\hat{J}_{v,Cdiag0_{17_{fL}}}$  as defined in LFFSSP;  $\hat{J}_{v,17_{fR\_all}}$  and  $\hat{J}_{v,Cdiag0_{17_{fR\_all}}}$  are required in LFFDSP with definitions shown in equation (4.29) and (4.31)

$$\begin{bmatrix} \bar{V}_{c,17_{fR}} \\ \bar{W}_{17_{fR}} \end{bmatrix} = \hat{J}_{v,17_{fR\_all}} \dot{\bar{q}}_{R,H} \quad (4.29)$$

$$\bar{W}_{17_{fR}} = \hat{J}_{v,17_{fR\_all\_w}} \dot{\bar{q}}_{R,H} \quad (4.30)$$

Using equation (4.9) and (4.30):

$$\dot{\bar{C}}_{diag}^{(0,17_{fR})} = \hat{J}_{v,Cdiag0_{17_{fR\_all}}} \dot{\bar{q}}_{R,H} \quad (4.31)$$

$\bar{V}_{c,17_{fL}}$ ,  $\bar{W}_{17_{fL}}$  and  $\dot{\bar{C}}_{diag}^{(0,17_{fL})}$  are used instead of  $\bar{V}_{c,17}$ ,  $\bar{W}_{17}$  and  $\dot{\bar{C}}_{diag}^{(0,17)}$  for the definition of  $\hat{J}_{v,17_{fL}}$  and  $\hat{J}_{v,Cdiag0_{17_{fL}}}$ .

$\hat{J}_{v,17_{fR\_all\_w}}$  can be extracted from equation (4.32):

$$\hat{J}_{v,17_{fR\_all}} = \begin{bmatrix} \hat{J}_{v,17_{fR\_all\_v}} \\ \hat{J}_{v,17_{fR\_all\_w}} \end{bmatrix} \quad (4.32)$$

In summary:  $\hat{J}_{v,17_{fL}}$ ,  $\hat{J}_{v,Cdiag0_{17_{fL}}}$ ,  $\hat{J}_{v,17_{fR\_all}}$  and  $\hat{J}_{v,Cdiag0_{17_{fR\_all}}}$  are jacobian matrices that are needed to be calculated during LFFDSP.

#### 4.2.2. Calculation Procedure of Jacobian Matrices

Calculation procedure of jacobian matrices numerically is explained by an example. Exemplary calculation procedure of  $\hat{J}_{v,17_{fR}}$  and  $\hat{J}_{v,Cdiag0_{17_{fR}}}$  is shown below:

At any instant of the simulation,  $\begin{bmatrix} \bar{V}_{c,17} \\ \bar{W}_{17} \end{bmatrix}$  can be calculated for a given  $\dot{q}_{R_{Hr}}$  since

all transformation matrices are known. So for  $\dot{q}_{R_{Hr}} = \dot{q}_{R_{Hr1}} = \begin{bmatrix} 1 \\ 0 \\ 0 \\ 0 \\ 0 \\ 0 \\ 0 \end{bmatrix}$ ,  $\begin{bmatrix} \bar{V}_{c,17} \\ \bar{W}_{17} \end{bmatrix}$  can be

calculated from kinematic equations of RFFSSP, which is also the 1<sup>st</sup> column of  $\hat{J}_{v,17_{fR}}$ .

$$\hat{J}_{v,17_{fR}} = \begin{bmatrix} \bar{J}_{v,17_{fR}}^1 & \bar{J}_{v,17_{fR}}^2 & \bar{J}_{v,17_{fR}}^3 & \bar{J}_{v,17_{fR}}^4 & \bar{J}_{v,17_{fR}}^5 & \bar{J}_{v,17_{fR}}^6 & \bar{J}_{v,17_{fR}}^7 \end{bmatrix} \quad (4.33)$$

If  $\hat{J}_{v,17_{fR}}$  is described as shown in equation (4.33):

$$\hat{J}_{v,17_{fR}} \begin{bmatrix} 1 \\ 0 \\ 0 \\ 0 \\ 0 \\ 0 \\ 0 \end{bmatrix} = \bar{J}_{v,17_{fR}}^1.$$

Using this information, other columns of  $\hat{J}_{v,17_{fR}}$  can be obtained similarly by

$$\text{calculating } \begin{bmatrix} \bar{V}_{c,17} \\ \bar{W}_{17} \end{bmatrix} \text{ for each } \dot{q}_{R_{Hr}} \text{ given as } \dot{q}_{R_{Hr}}^2 = \begin{bmatrix} 0 \\ 1 \\ 0 \\ 0 \\ 0 \\ 0 \\ 0 \end{bmatrix}, \dot{q}_{R_{Hr}}^3 = \begin{bmatrix} 0 \\ 0 \\ 1 \\ 0 \\ 0 \\ 0 \\ 0 \end{bmatrix} \text{ and vice}$$

versa.

The similar procedure is followed for the calculation of  $\hat{J}_{v,cdiag0_{17}_fR}$  with a slight difference that  $\dot{\hat{C}}_{diag}^{(0,17)}$  is calculated for each  $\dot{\hat{q}}_{R_Hr}$  using the equation shown below:

$$\dot{\hat{C}}_{diag}^{(0,17)} = \text{diag} \left( \left[ \hat{J}_{v,17_fR_w} \widetilde{\hat{q}}_{R_Hr} \right] \hat{C}^{(0,17)} \right)$$

#### 4.2.3. Calculation Procedure of Time Derivatives of Jacobian Matrices

Using forward finite divided difference formula derived from truncated Taylor Expansion of  $\hat{J}_v$ . The time derivative of jacobian matrix  $\hat{J}_v$  is calculated as shown below:

$$\dot{\hat{J}}_v(t_0) \cong \frac{\hat{J}_v(t_0 + \Delta t) - \hat{J}_v(t_0)}{\Delta t}. \quad (4.34)$$

Where  $\hat{J}_v(t_0)$  is defined as:

$$\begin{bmatrix} \bar{V}(t_0) \\ \bar{w}(t_0) \end{bmatrix} = \hat{J}_v(t_0) \cdot \dot{\hat{q}}(t_0). \quad (4.35)$$

$$\bar{q}(t_0 + \Delta t) \cong \bar{q}(t_0) + \dot{\bar{q}}(t_0) \cdot \Delta t \quad (4.36)$$

After recalculating all transformation matrices for  $\bar{q}(t + \Delta t)$  by using equation (4.36),  $\hat{J}_v(t + \Delta t)$  is obtained in the same manner explained in previous heading. Therefore, all time derivatives of jacobian matrices are calculated by this logic.

#### 4.3. Derivation of Dynamic Equations

Newton-Euler formulation is used for deriving dynamic equations which are written in a general manner. Therefore, these equations can be used for all phases. However, additional equations are inserted into the direct dynamic solution procedure to remove inexistent forces and moments related with the current locomotion phase.

For Body K, Newton Euler equations with respect to the mass center of Body K become:

$$m_k \cdot \vec{a}_{c,k} = \sum \vec{F} \quad (4.37)$$

$$\check{J}_{c,k} \cdot \vec{a}_k + \vec{w}_k \times \check{J}_{c,k} \cdot \vec{w}_k = \sum \vec{M}_c \quad (4.38)$$

In matrix form, equations (4.37) and (4.38) are resolved in the body coordinate system of Body K:

$$m_k \hat{C}^{(0,k)T} \vec{a}_{c,k} = \bar{F}_{(k-1),k}^{(k)} - \hat{C}^{(k,k+1)} \bar{F}_{k,(k+1)}^{(k+1)} - m_k g \hat{C}^{(0,k)T} \vec{u}_3 \quad (4.39)$$

$$\begin{aligned} \hat{J}_{c,k}^{(k)} \hat{C}^{(0,k)T} \vec{a}_k + \hat{C}^{(0,k)T} \tilde{w}_k \hat{C}^{(0,k)} \hat{J}_{c,k}^{(k)} \hat{C}^{(0,k)T} \vec{w}_k = \\ \bar{M}_{(k-1),k}^{(k)} - \hat{C}^{(k,k+1)} \bar{M}_{k,(k+1)}^{(k+1)} + \tilde{r}_{1,k} \bar{F}_{(k-1),k}^{(k)} - \tilde{r}_{2,k} \hat{C}^{(k,k+1)} \bar{F}_{k,(k+1)}^{(k+1)} \end{aligned} \quad (4.40)$$

All forces and moments are expressed with respect to the same convention by using Newton's action-reaction law as shown in equation (4.41):

$$\bar{F}_{(k+1),k}^{(k)} = -\bar{F}_{k,(k+1)}^{(k+1)} = -\hat{C}^{(k,k+1)} \bar{F}_{k,(k+1)}^{(k+1)} \quad (4.41)$$

Where,  $\bar{F}_{k,(k+1)}^{(k+1)}$  and  $\bar{M}_{k,(k+1)}^{(k+1)}$  are the resultant force and moment acting onto Body K+1 from Body K, resolved in body coordinate system of Body K+1.  $\tilde{r}_{1,k}$  and  $\tilde{r}_{2,k}$  are corresponding moment arms for  $\bar{F}_{(k-1),k}^{(k)}$  and  $\bar{F}_{k,(k+1)}^{(k+1)}$ . Also,  $\hat{J}_{c,k}^{(k)}$  is the inertia tensor matrix of Body K with respect to the mass center of Body K and resolved in body coordinate system of Body K.

Generalized dynamic equations for the humanoid robot are shown below.

For Body 1:

$$m_1 \hat{C}^{(0,1)T} \vec{a}_{c,1} = \bar{F}_{0,1}^{(1)} - \hat{C}^{(1,3)} \bar{F}_{1,3}^{(3)} - m_1 g \hat{C}^{(0,1)T} \vec{u}_3 \quad (4.42)$$

$$\begin{aligned} \hat{J}_{c,1}^{(1)} \hat{C}^{(0,1)T} \vec{a}_1 + \hat{C}^{(0,1)T} \tilde{w}_1 \hat{C}^{(0,1)} \hat{J}_{c,1}^{(1)} \hat{C}^{(0,1)T} \vec{w}_1 = \bar{M}_{0,1}^{(1)} - \hat{C}^{(1,3)} \bar{M}_{1,3}^{(3)} + \\ \tilde{c}_1 \hat{C}^{(1,3)} \bar{F}_{1,3}^{(3)} \end{aligned} \quad (4.43)$$

For Body 3:

$$m_3 \hat{C}^{(0,3)T} \bar{a}_{c,3} = \bar{F}_{0,3}^{(3)} + \bar{F}_{1,3}^{(3)} - \hat{C}^{(3,9)} \bar{F}_{3,9}^{(9)} - m_3 g \hat{C}^{(0,3)T} \bar{u}_3 \quad (4.44)$$

$$\begin{aligned} \hat{J}_{c,3}^{(3)} \hat{C}^{(0,3)T} \bar{\alpha}_3 + \hat{C}^{(0,3)T} \tilde{w}_3 \hat{C}^{(0,3)} \hat{J}_{c,3}^{(3)} \hat{C}^{(0,3)T} \bar{w}_3 &= \bar{M}_{0,3}^{(3)} + \bar{M}_{1,3}^{(3)} - \\ \hat{C}^{(3,9)} \bar{M}_{3,9}^{(9)} + (\tilde{l}_{3,1} - \tilde{c}_3) \bar{F}_{1,3}^{(3)} + \tilde{c}_3 \hat{C}^{(3,9)} \bar{F}_{3,9}^{(9)} \end{aligned} \quad (4.45)$$

For Body 9:

$$m_9 \hat{C}^{(0,9)T} \bar{a}_{c,9} = \bar{F}_{3,9}^{(9)} - \hat{C}^{(9,11)} \bar{F}_{9,11}^{(11)} - m_9 g \hat{C}^{(0,9)T} \bar{u}_3 \quad (4.46)$$

$$\begin{aligned} \hat{J}_{c,9}^{(9)} \hat{C}^{(0,9)T} \bar{\alpha}_9 + \hat{C}^{(0,9)T} \tilde{w}_9 \hat{C}^{(0,9)} \hat{J}_{c,9}^{(9)} \hat{C}^{(0,9)T} \bar{w}_9 &= \bar{M}_{3,9}^{(9)} - \hat{C}^{(9,11)} \bar{M}_{9,11}^{(11)} + \\ (\tilde{l}_{9,3} - \tilde{c}_9) \bar{F}_{3,9}^{(9)} + \tilde{c}_9 \hat{C}^{(9,11)} \bar{F}_{9,11}^{(11)} \end{aligned} \quad (4.47)$$

For Body 11:

$$m_{11} \hat{C}^{(0,11)T} \bar{a}_{c,11} = \bar{F}_{9,11}^{(11)} - \hat{C}^{(11,17)} \bar{F}_{11,17}^{(17)} - m_{11} g \hat{C}^{(0,11)T} \bar{u}_3 \quad (4.48)$$

$$\begin{aligned} \hat{J}_{c,11}^{(11)} \hat{C}^{(0,11)T} \bar{\alpha}_{11} + \hat{C}^{(0,11)T} \tilde{w}_{11} \hat{C}^{(0,11)} \hat{J}_{c,11}^{(11)} \hat{C}^{(0,11)T} \bar{w}_{11} &= \bar{M}_{9,11}^{(11)} - \\ \hat{C}^{(11,17)} \bar{M}_{11,17}^{(17)} + (\tilde{l}_{11,9} - \tilde{c}_{11}) \bar{F}_{9,11}^{(11)} + \tilde{c}_{11} \hat{C}^{(11,17)} \bar{F}_{11,17}^{(17)} \end{aligned} \quad (4.49)$$

For Body 2:

$$m_2 \hat{C}^{(0,2)T} \bar{a}_{c,2} = \bar{F}_{0,2}^{(2)} - \hat{C}^{(2,4)} \bar{F}_{2,4}^{(4)} - m_2 g \hat{C}^{(0,2)T} \bar{u}_3 \quad (4.50)$$

$$\begin{aligned} \hat{J}_{c,2}^{(2)} \hat{C}^{(0,2)T} \bar{\alpha}_2 + \hat{C}^{(0,2)T} \tilde{w}_2 \hat{C}^{(0,2)} \hat{J}_{c,2}^{(2)} \hat{C}^{(0,2)T} \bar{w}_2 &= \bar{M}_{0,2}^{(2)} - \hat{C}^{(2,4)} \bar{M}_{2,4}^{(4)} + \\ \tilde{c}_2 \hat{C}^{(2,4)} \bar{F}_{2,4}^{(4)} \end{aligned} \quad (4.51)$$

For Body 4:

$$m_4 \hat{C}^{(0,4)T} \bar{a}_{c,4} = \bar{F}_{0,4}^{(4)} + \bar{F}_{2,4}^{(4)} - \hat{C}^{(4,10)} \bar{F}_{4,10}^{(10)} - m_4 g \hat{C}^{(0,4)T} \bar{u}_3 \quad (4.52)$$

$$\begin{aligned} \hat{J}_{c,4}^{(4)} \hat{C}^{(0,4)T} \bar{\alpha}_4 + \hat{C}^{(0,4)T} \tilde{w}_4 \hat{C}^{(0,4)} \hat{J}_{c,4}^{(4)} \hat{C}^{(0,4)T} \bar{w}_4 &= \bar{M}_{0,4}^{(4)} + \bar{M}_{2,4}^{(4)} - \\ \hat{C}^{(4,10)} \bar{M}_{4,10}^{(10)} + (\tilde{l}_{4,2} - \tilde{c}_4) \bar{F}_{2,4}^{(4)} + \tilde{c}_4 \hat{C}^{(4,10)} \bar{F}_{4,10}^{(10)} \end{aligned} \quad (4.53)$$

For Body 10:

$$m_{10}\hat{C}^{(0,10)T}\bar{a}_{c,10} = \bar{F}_{4,10}^{(10)} - \hat{C}^{(10,12)}\bar{F}_{10,12}^{(12)} - m_{10}g\hat{C}^{(0,10)T}\bar{u}_3 \quad (4.54)$$

$$\begin{aligned} \hat{J}_{c,10}^{(10)}\hat{C}^{(0,10)T}\bar{\alpha}_{10} + \hat{C}^{(0,10)T}\tilde{w}_{10}\hat{C}^{(0,10)}\hat{J}_{c,10}^{(10)}\hat{C}^{(0,10)T}\bar{w}_{10} = \bar{M}_{4,10}^{(10)} - \\ \hat{C}^{(10,12)}\bar{M}_{10,12}^{(12)} + (\tilde{l}_{10,4} - \tilde{c}_{10})\bar{F}_{4,10}^{(10)} + \tilde{c}_{10}\hat{C}^{(10,12)}\bar{F}_{10,12}^{(12)} \end{aligned} \quad (4.55)$$

For Body 12:

$$m_{12}\hat{C}^{(0,12)T}\bar{a}_{c,12} = \bar{F}_{10,12}^{(12)} - \hat{C}^{(12,17)}\bar{F}_{12,17}^{(17)} - m_{12}g\hat{C}^{(0,12)T}\bar{u}_3 \quad (4.56)$$

$$\begin{aligned} \hat{J}_{c,12}^{(12)}\hat{C}^{(0,12)T}\bar{\alpha}_{12} + \hat{C}^{(0,12)T}\tilde{w}_{12}\hat{C}^{(0,12)}\hat{J}_{c,12}^{(12)}\hat{C}^{(0,12)T}\bar{w}_{12} = \bar{M}_{10,12}^{(12)} - \\ \hat{C}^{(12,17)}\bar{M}_{12,17}^{(17)} + (\tilde{l}_{12,10} - \tilde{c}_{12})\bar{F}_{10,12}^{(12)} + \tilde{c}_{12}\hat{C}^{(12,17)}\bar{F}_{12,17}^{(17)} \end{aligned} \quad (4.57)$$

For Body 17:

$$m_{17}\hat{C}^{(0,17)T}\bar{a}_{c,17} = \bar{F}_{11,17}^{(17)} + \bar{F}_{12,17}^{(17)} - \hat{C}^{(17,20)}\bar{F}_{17,20}^{(20)} - m_{17}g\hat{C}^{(0,17)T}\bar{u}_3 \quad (4.58)$$

$$\begin{aligned} \hat{J}_{c,17}^{(17)}\hat{C}^{(0,17)T}\bar{\alpha}_{17} + \hat{C}^{(0,17)T}\tilde{w}_{17}\hat{C}^{(0,17)}\hat{J}_{c,17}^{(17)}\hat{C}^{(0,17)T}\bar{w}_{17} = \bar{M}_{11,17}^{(17)} + \\ \bar{M}_{12,17}^{(17)} - \hat{C}^{(17,20)}\bar{M}_{17,20}^{(20)} + (\tilde{l}_{17,11} - \tilde{c}_{17})\bar{F}_{11,17}^{(17)} + \\ (\tilde{l}_{17,12} - \tilde{c}_{17})\bar{F}_{12,17}^{(17)} + \tilde{c}_{17}\hat{C}^{(17,20)}\bar{F}_{17,20}^{(20)} \end{aligned} \quad (4.59)$$

For Body 20:

$$m_{20}\hat{C}^{(0,20)T}\bar{a}_{c,20} = \bar{F}_{17,20}^{(20)} - \hat{C}^{(20,23)}\bar{F}_{20,23}^{(23)} - \hat{C}^{(20,24)}\bar{F}_{20,24}^{(24)} - \hat{C}^{(20,27)}\bar{F}_{20,27}^{(27)} - m_{20}g\hat{C}^{(0,20)T}\bar{u}_3 \quad (4.60)$$

$$\begin{aligned} \hat{J}_{c,20}^{(20)}\hat{C}^{(0,20)T}\bar{\alpha}_{20} + \hat{C}^{(0,20)T}\tilde{w}_{20}\hat{C}^{(0,20)}\hat{J}_{c,20}^{(20)}\hat{C}^{(0,20)T}\bar{w}_{20} = \\ \bar{M}_{17,20}^{(20)} - \hat{C}^{(20,23)}\bar{M}_{20,23}^{(23)} - \hat{C}^{(20,24)}\bar{M}_{20,24}^{(24)} - \hat{C}^{(20,27)}\bar{M}_{20,27}^{(27)} + \\ (\tilde{l}_{20,17} - \tilde{c}_{20})\bar{F}_{17,20}^{(20)} - (\tilde{l}_{20,21} - \tilde{c}_{20})\hat{C}^{(20,23)}\bar{F}_{20,23}^{(23)} \\ - (\tilde{l}_{20,22} - \tilde{c}_{20})\hat{C}^{(20,24)}\bar{F}_{20,24}^{(24)} + \tilde{c}_{20}\hat{C}^{(20,27)}\bar{F}_{20,27}^{(27)} \end{aligned} \quad (4.61)$$

For Body 23:

$$m_{23}\hat{C}^{(0,23)T}\bar{a}_{c,23} = \bar{F}_{20,23}^{(23)} - m_{23}g\hat{C}^{(0,23)T}\bar{u}_3 \quad (4.62)$$

$$\begin{aligned} \hat{J}_{c,23}^{(23)}\hat{C}^{(0,23)T}\bar{\alpha}_{23} + \hat{C}^{(0,23)T}\tilde{w}_{23}\hat{C}^{(0,23)}\hat{J}_{c,23}^{(23)}\hat{C}^{(0,23)T}\bar{w}_{23} = \bar{M}_{20,23}^{(23)} + \\ (\tilde{l}_{23,21} - \tilde{c}_{23})\bar{F}_{20,23}^{(23)} \end{aligned} \quad (4.63)$$

For Body 24:

$$m_{24}\hat{C}^{(0,24)T}\bar{a}_{c,24} = \bar{F}_{20,24}^{(24)} - m_{24}g\hat{C}^{(0,24)T}\bar{u}_3 \quad (4.64)$$

$$\begin{aligned} \hat{J}_{c,24}^{(24)}\hat{C}^{(0,24)T}\bar{\alpha}_{24} + \hat{C}^{(0,24)T}\tilde{w}_{24}\hat{C}^{(0,24)}\hat{J}_{c,24}^{(24)}\hat{C}^{(0,24)T}\bar{w}_{24} = \bar{M}_{20,24}^{(24)} + \\ (\tilde{l}_{24,22} - \tilde{c}_{24})\bar{F}_{20,24}^{(24)} \end{aligned} \quad (4.65)$$

For Body 27:

$$m_{27}\hat{C}^{(0,27)T}\bar{a}_{c,27} = \bar{F}_{20,27}^{(27)} - m_{27}g\hat{C}^{(0,27)T}\bar{u}_3 \quad (4.66)$$

$$\begin{aligned} \hat{J}_{c,27}^{(27)}\hat{C}^{(0,27)T}\bar{\alpha}_{27} + \hat{C}^{(0,27)T}\tilde{w}_{27}\hat{C}^{(0,27)}\hat{J}_{c,27}^{(27)}\hat{C}^{(0,27)T}\bar{w}_{27} = \bar{M}_{20,27}^{(27)} + \\ (\tilde{l}_{27,20} - \tilde{c}_{27})\bar{F}_{20,27}^{(27)} \end{aligned} \quad (4.67)$$

#### 4.4. Direct Dynamic Solution

A generalized vector of forces and moments is defined including reaction forces, reaction moments and actuator torques present in dynamic equations by equation (4.68).

$$\bar{F} = \begin{bmatrix} \bar{F}_{0,1}^{(1)} \\ \bar{F}_{1,3}^{(3)} \\ \bar{M}_{0,1}^{(1)} \\ \bar{M}_{1,3}^{(3)} \\ \bar{F}_{0,3}^{(3)} \\ \bar{F}_{3,9}^{(9)} \\ \bar{M}_{0,3}^{(3)} \\ \bar{M}_{3,9}^{(9)} \\ \bar{F}_{9,11}^{(11)} \\ \bar{M}_{9,11}^{(11)} \\ \bar{F}_{11,17}^{(17)} \\ \bar{M}_{11,17}^{(17)} \\ \bar{F}_{12,17}^{(17)} \\ \bar{F}_{17,20}^{(20)} \\ \bar{M}_{12,17}^{(17)} \\ \bar{M}_{17,20}^{(20)} \\ \bar{F}_{10,12}^{(12)} \\ \bar{M}_{10,12}^{(12)} \\ \bar{F}_{4,10}^{(10)} \\ \bar{M}_{4,10}^{(10)} \\ \bar{F}_{0,4}^{(4)} \\ \bar{F}_{2,4}^{(4)} \\ \bar{M}_{0,4}^{(4)} \\ \bar{M}_{2,4}^{(4)} \\ \bar{F}_{0,2}^{(2)} \\ \bar{M}_{0,2}^{(2)} \\ \bar{F}_{20,23}^{(23)} \\ \bar{F}_{20,24}^{(24)} \\ \bar{F}_{20,27}^{(27)} \\ \bar{M}_{20,23}^{(23)} \\ \bar{M}_{20,24}^{(24)} \\ \bar{M}_{20,27}^{(27)} \end{bmatrix} \quad (4.68)$$

$$\text{For } \bar{F}_{k,(k+1)}^{(k+1)} = \begin{bmatrix} F_{k,(k+1)x}^{(k+1)} \\ F_{k,(k+1)y}^{(k+1)} \\ F_{k,(k+1)z}^{(k+1)} \end{bmatrix} \quad \text{and} \quad \bar{M}_{k,(k+1)}^{(k+1)} = \begin{bmatrix} M_{k,(k+1)x}^{(k+1)} \\ M_{k,(k+1)y}^{(k+1)} \\ M_{k,(k+1)z}^{(k+1)} \end{bmatrix},$$

actuating torques can be defined by using a matrix named as  $\hat{\phi}$  for extraction as shown in equation (4.69).

$$\bar{T} = \begin{bmatrix} T_1 \\ T_3 \\ T_5 \\ T_7 \\ T_9 \\ T_{11} \\ T_{13} \\ T_{15} \\ T_2 \\ T_4 \\ T_6 \\ T_8 \\ T_{10} \\ T_{12} \\ T_{14} \\ T_{16} \\ T_{17} \\ T_{18} \\ T_{19} \\ T_{20} \\ T_{21} \\ T_{22} \\ T_{23} \\ T_{24} \\ T_{25} \\ T_{26} \end{bmatrix} = \begin{bmatrix} M_{1,3y}^{(3)} \\ M_{3,9x}^{(9)} \\ M_{3,9y}^{(9)} \\ M_{3,9z}^{(9)} \\ M_{9,11y}^{(9)} \\ M_{11,17x}^{(17)} \\ M_{11,17y}^{(17)} \\ M_{11,17z}^{(17)} \\ M_{2,4y}^{(4)} \\ M_{4,10x}^{(10)} \\ M_{4,10y}^{(10)} \\ M_{4,10z}^{(10)} \\ M_{10,12y}^{(12)} \\ M_{12,17x}^{(17)} \\ M_{12,17y}^{(17)} \\ M_{12,17z}^{(17)} \\ M_{17,20x}^{(20)} \\ M_{17,20y}^{(20)} \\ M_{17,20z}^{(20)} \\ M_{20,23x}^{(23)} \\ M_{20,23y}^{(23)} \\ M_{20,24x}^{(24)} \\ M_{20,24y}^{(24)} \\ M_{20,27x}^{(27)} \\ M_{20,27y}^{(27)} \\ M_{20,27z}^{(27)} \end{bmatrix} = \hat{\phi} \bar{F} \quad (4.69)$$

Dynamic equations for Body K can be arranged into the form as shown below:

$$\bar{Z}_k(\bar{q}, \dot{\bar{q}}, \ddot{\bar{q}}) = \hat{K}_k(\bar{q}) \bar{F}$$

Then, dynamic equations describing the humanoid robot which are from equation (4.42) to (4.67) can be expressed by equation (4.72), with components described by equation (4.70) and (4.71).

$$\bar{Z} = \begin{bmatrix} \bar{Z}_1 \\ \bar{Z}_3 \\ \bar{Z}_9 \\ \bar{Z}_{11} \\ \bar{Z}_2 \\ \bar{Z}_4 \\ \bar{Z}_{10} \\ \bar{Z}_{12} \\ \bar{Z}_{17} \\ \bar{Z}_{20} \\ \bar{Z}_{23} \\ \bar{Z}_{24} \\ \bar{Z}_{27} \end{bmatrix}, \hat{K} = \begin{bmatrix} \hat{K}_1 \\ \hat{K}_3 \\ \hat{K}_9 \\ \hat{K}_{11} \\ \hat{K}_2 \\ \hat{K}_4 \\ \hat{K}_{10} \\ \hat{K}_{12} \\ \hat{K}_{17} \\ \hat{K}_{20} \\ \hat{K}_{23} \\ \hat{K}_{24} \\ \hat{K}_{27} \end{bmatrix} \quad (4.70), (4.71)$$

$$\bar{Z}(\bar{q}, \dot{\bar{q}}, \ddot{\bar{q}}) = \hat{K}(\bar{q})\bar{F} \quad (4.72)$$

Further arrangement is required to perform direct dynamic solution as such:

$$\bar{Z}(\bar{q}, \dot{\bar{q}}, \ddot{\bar{q}}) = \hat{M}(\bar{q})\ddot{\bar{q}} + \bar{B}(\bar{q}, \dot{\bar{q}}) = \hat{K}(\bar{q})\bar{F}$$

Although all dynamic and kinematic equations are obtained, it is a time consuming and complicated process to obtain analytical expressions of  $\hat{M}$  and  $\bar{B}$ . Furthermore, it is unlikely to document and implement their analytical expressions in open form due to the complexity of system. So, numerical values of  $\hat{M}$  and  $\bar{B}$  are calculated at each solution step.

During the simulation,  $\bar{q}$  and  $\dot{\bar{q}}$  are known at any instant.

By implementing the vector  $\ddot{\bar{q}} = \ddot{\bar{q}}_0 = \begin{bmatrix} 0 \\ \vdots \\ 0 \end{bmatrix}$  which contains zero values only, the numerical value of  $\bar{B}$  can be found since  $\bar{Z}$  can be calculated for a known set of  $\bar{q}$ ,  $\dot{\bar{q}}$  and  $\ddot{\bar{q}}$ .

$$\bar{Z}_0 = \hat{M}(\bar{q})\ddot{\bar{q}}_0 + \bar{B}(\bar{q}, \dot{\bar{q}}) = \bar{B}(\bar{q}, \dot{\bar{q}})$$

It can be showed that  $\hat{M}(\bar{q}) = [\bar{M}_1 \quad \bar{M}_2 \quad \dots \quad \bar{M}_{26}]$

For a vector  $\ddot{\bar{q}}_k$  which contains 1 for the  $k^{\text{th}}$  row and zero for remaining rows,  $\bar{Z}$  can be calculated where  $\bar{B}(\bar{q}, \dot{\bar{q}})$  is already calculated as  $\bar{Z}_0$ :

$$\bar{Z}_k = \hat{M}(\bar{q})\ddot{\bar{q}}_k + \bar{B}(\bar{q}, \dot{\bar{q}}) = \bar{M}_k + \bar{Z}_0$$

$$\text{Then, } \bar{M}_k = \bar{Z}_k - \bar{Z}_0$$

$\hat{M}(\bar{q})$  matrix can be constructed at any instant by applying the procedure shown above for all  $k$  values from 1 to 26; since the dimension of  $\ddot{\bar{q}}$  is 26 as specified before.

All unknowns to be solved during the direct dynamic solution procedure are  $\ddot{\bar{q}}$  and  $\bar{F}$ .

$$\text{Then, Total Number of Unknowns} = 26 [\ddot{\bar{q}}] + 32 \times 3[\bar{F}] = 122$$

Newton-Euler equations for 13 bodies :

$$\hat{M}(\bar{q})\ddot{\bar{q}} - \hat{K}(\bar{q})\bar{F} = -\bar{B}(\bar{q}, \dot{\bar{q}}) \quad (13 \times 2 \times 3 = 78 \text{ equations}) \quad (4.73)$$

Equations for assigning actuator torques :

$$\hat{\phi}\bar{F} = \bar{T} \quad (26 \text{ equations}) \quad (4.74)$$

Remaining equations depend on the locomotion phase.

#### 4.4.1. For RFFSSP

Since it is assumed that Body 2 and Body 4 do not interact with the ground during RFFSSP, several ground reaction forces and moments are expected to be zero given as shown:

$$\bar{F}_{0,2}^{(2)} = \bar{M}_{0,2}^{(2)} = \bar{F}_{0,4}^{(4)} = \bar{M}_{0,4}^{(4)} = \begin{bmatrix} 0 \\ 0 \\ 0 \end{bmatrix}$$

This condition can be described as:

$$\hat{\Phi}_{ZGR, RFFSSP} \bar{F} = \begin{bmatrix} \bar{F}_{0,4}^{(4)} \\ \bar{M}_{0,4}^{(4)} \\ \bar{F}_{0,2}^{(2)} \\ \bar{M}_{0,2}^{(2)} \end{bmatrix} = \begin{bmatrix} 0 \\ \vdots \\ 0 \end{bmatrix} \quad (4 \times 3 = 12 \text{ equations}) \quad (4.75)$$

$\hat{\Phi}_{ZGR, RFFSSP}$  is a matrix for the extraction of related ground reaction forces and moments.

During RFFSSP, Body 1 and Body 3 are assumed to be rigidly fixed to the ground. This assumption is ensured for Body 1 by supplying proper  $\hat{C}^{(0,1)}$ ,  $\bar{P}_{tpR}$ ,  $\bar{w}_1$ ,  $\bar{V}_{tpR}$ ,  $\bar{\alpha}_1$ ,  $\bar{a}_{tpR}$  to kinematic equations of RFFSSP. For Body 3, kinematic constraints are implemented in order to satisfy the assumption:

$$\bar{a}_{c,3} = \bar{\alpha}_3 = \begin{bmatrix} 0 \\ 0 \\ 0 \end{bmatrix}$$

$\bar{a}_{c,3}$  can be expressed as  $\bar{a}_{c,3} = \hat{A}_3(\bar{q})\ddot{\bar{q}} + \bar{B}_3(\bar{q}, \dot{\bar{q}})$ .

Similarly,  $\bar{\alpha}_3$  can be expressed as  $\bar{\alpha}_3 = \hat{A}_{\alpha 3}(\bar{q})\ddot{\bar{q}} + \bar{B}_{\alpha 3}(\bar{q}, \dot{\bar{q}})$

Then, kinematic conditions can be described as:

$$\hat{A}_3 \ddot{\bar{q}} = -\bar{B}_3 \text{ and } \hat{A}_{\alpha 3} \ddot{\bar{q}} = -\bar{B}_{\alpha 3}$$

However, rank of matrix  $\begin{bmatrix} \hat{A}_3 \\ \hat{A}_{\alpha 3} \end{bmatrix}$  is always found as 1 due to the kinematic structure for system of linear equations  $\begin{bmatrix} \hat{A}_3 \\ \hat{A}_{\alpha 3} \end{bmatrix} \ddot{\bar{q}} = \begin{bmatrix} -\bar{B}_3 \\ -\bar{B}_{\alpha 3} \end{bmatrix}$ . If unnecessary equations are eliminated, kinematic conditions are reduced to  $\ddot{\bar{\theta}}_3 = 0$  which can be described as:

$$\bar{\Phi}_{qddZ, RFFSSP} \ddot{\bar{q}} = 0 \quad (1 \text{ equation}). \quad (4.76)$$

$\bar{\Phi}_{qddZ, RFFSSP}$  is a row vector for the extraction of  $\ddot{\bar{\theta}}_3$  from  $\ddot{\bar{q}}$ .

According to the assumption of Body 1 and Body 3 being rigidly fixed to the ground, reaction forces and moments between these bodies such as  $\bar{F}_{1,3}^{(3)}$ ,  $M_{1,3x}^{(3)}$ ,  $M_{1,3z}^{(3)}$  can not be determined unless additional equations for modeling the interaction between Body 1 and Body 3 (like assuming bodies are deformable so that equations related with solid mechanic principles are involved) are introduced. Therefore, it is assumed that,

$$\bar{F}_{1,3}^{(3)} = \bar{0}_{3 \times 1} \text{ and } M_{1,3x}^{(3)} = M_{1,3z}^{(3)} = 0$$

without examining this modeling problem. Then, this assumption can be described as:

$$\hat{\phi}_{ZR, RFFSSP} \bar{F} = \begin{bmatrix} \bar{F}_{1,3}^{(3)} \\ M_{1,3x}^{(3)} \\ M_{1,3z}^{(3)} \end{bmatrix} = \begin{bmatrix} 0 \\ \vdots \\ 0 \end{bmatrix} \text{ (5 equations)} \quad (4.77)$$

$\hat{\phi}_{ZR, RFFSSP}$  is a matrix for the extraction of  $\bar{F}_{1,3}^{(3)}$ ,  $M_{1,3x}^{(3)}$  and  $M_{1,3z}^{(3)}$ .

Then, *Total Number of Equations* = 78 + 26 + 12 + 1 + 5 = 122

The final form of system equations of RFFSSP for direct dynamic solution procedure is as shown below by using equation (4.73), (4.74), (4.75), (4.76) and (4.77):

$$\begin{bmatrix} \hat{M}_{78 \times 26} & -\hat{K}_{78 \times 96} \\ \hat{O}_{26 \times 26} & \hat{\phi}_{26 \times 96} \\ \hat{O}_{12 \times 26} & \hat{\phi}_{ZGR, RFFSSP}_{12 \times 96} \\ \hat{O}_{5 \times 26} & \hat{\phi}_{ZR, RFFSSP}_{5 \times 96} \\ \hat{\phi}_{qddZ, RFFSSP}_{1 \times 26} & \hat{O}_{1 \times 96} \end{bmatrix}_{122 \times 122} \begin{bmatrix} \ddot{q}_{26 \times 1} \\ \bar{F}_{96 \times 1} \end{bmatrix}_{122 \times 1} = \begin{bmatrix} -\bar{B}_{78 \times 1} \\ \bar{T}_{26 \times 1} \\ \bar{O}_{12 \times 1} \\ \bar{O}_{5 \times 1} \\ 0 \end{bmatrix}_{122 \times 1} \quad (4.78)$$

$\hat{O}$  and  $\bar{O}$  are matrices and vectors with zero components only. Also, matrices and vectors are given with their dimensions for clarity.

#### 4.4.2. For LFFSSP

A procedure similar to RFFSSP is followed.

Since it is assumed that Body 1 and Body 3 do not interact with the ground during LFFSSP, several ground reaction forces and moments are expected to be zero given as shown:

$$\bar{F}_{0,1}^{(1)} = \bar{M}_{0,1}^{(1)} = \bar{F}_{0,3}^{(3)} = \bar{M}_{0,3}^{(3)} = \begin{bmatrix} 0 \\ 0 \\ 0 \end{bmatrix}$$

This condition can be described as:

$$\hat{\Phi}_{ZGR,LFFSSP} \bar{F} = \begin{bmatrix} \bar{F}_{0,3}^{(3)} \\ \bar{M}_{0,3}^{(3)} \\ \bar{F}_{0,1}^{(1)} \\ \bar{M}_{0,1}^{(1)} \end{bmatrix} = \begin{bmatrix} 0 \\ \vdots \\ 0 \end{bmatrix} \quad (4 \times 3 = 12 \text{ equations}) \quad (4.79)$$

$\hat{\Phi}_{ZGR,LFFSSP}$  is a matrix for the extraction of related ground reaction forces and moments.

During LFFSSP, Body 2 and Body 4 are assumed to be rigidly fixed to the ground. This assumption is ensured for Body 2 by supplying proper  $\hat{C}^{(0,2)}$ ,  $\bar{P}_{tpL}$ ,  $\bar{w}_2$ ,  $\bar{V}_{tpL}$ ,  $\bar{\alpha}_2$ ,  $\bar{a}_{tpL}$  to kinematic equations of LFFSSP. For Body 4, kinematic constraints are implemented in order to satisfy the assumption:

$$\bar{a}_{c,4} = \bar{\alpha}_4 = \begin{bmatrix} 0 \\ 0 \\ 0 \end{bmatrix}$$

$\bar{a}_{c,4}$  can be expressed as  $\bar{a}_{c,4} = \hat{A}_4(\bar{q})\ddot{\bar{q}} + \bar{B}_4(\bar{q}, \dot{\bar{q}})$ .

Similarly,  $\bar{\alpha}_4$  can be expressed as  $\bar{\alpha}_4 = \hat{A}_{\alpha 4}(\bar{q})\ddot{\bar{q}} + \bar{B}_{\alpha 4}(\bar{q}, \dot{\bar{q}})$

Then, kinematic conditions can be described as:

$$\hat{A}_4 \ddot{\bar{q}} = -\bar{B}_4 \text{ and } \hat{A}_{\alpha 4} \ddot{\bar{q}} = -\bar{B}_{\alpha 4}$$

However, rank of matrix  $\begin{bmatrix} \hat{A}_4 \\ \hat{A}_{\alpha 4} \end{bmatrix}$  is always found as 1 due to the kinematic structure for system of linear equations  $\begin{bmatrix} \hat{A}_4 \\ \hat{A}_{\alpha 4} \end{bmatrix} \ddot{\vec{q}} = \begin{bmatrix} -\bar{B}_4 \\ -\bar{B}_{\alpha 4} \end{bmatrix}$ . If unnecessary equations are eliminated, kinematic conditions are reduced to  $\ddot{\theta}_4 = 0$  which can be described as:

$$\bar{\Phi}_{qddZ, LFFSSP} \ddot{\vec{q}} = 0 \text{ (1 equation)}. \quad (4.80)$$

$\bar{\Phi}_{qddZ, LFFSSP}$  is a row vector for the extraction of  $\ddot{\theta}_4$  from  $\ddot{\vec{q}}$ .

According to the assumption of Body 2 and Body 4 being rigidly fixed to the ground, reaction forces and moments between these bodies such as  $\bar{F}_{2,4}^{(4)}$ ,  $M_{2,4x}^{(4)}$ ,  $M_{2,4z}^{(4)}$  can not be determined unless additional equations for modeling the interaction between Body 2 and Body 4 are introduced. Therefore, it is assumed that  $\bar{F}_{2,4}^{(4)} = \bar{0}_{3 \times 1}$  and  $M_{2,4x}^{(4)} = M_{2,4z}^{(4)} = 0$  without examining this modeling problem. Then, this assumption can be described as:

$$\hat{\Phi}_{ZR, LFFSSP} \bar{F} = \begin{bmatrix} \bar{F}_{2,4}^{(4)} \\ M_{2,4x}^{(4)} \\ M_{2,4z}^{(4)} \end{bmatrix} = \begin{bmatrix} 0 \\ \vdots \\ 0 \end{bmatrix} \text{ (5 equations)} \quad (4.81)$$

$\hat{\Phi}_{ZR, LFFSSP}$  is a matrix for the extraction of  $\bar{F}_{2,4}^{(4)}$ ,  $M_{2,4x}^{(4)}$  and  $M_{2,4z}^{(4)}$ . Then, *Total Number of Equations* = 78 + 26 + 12 + 1 + 5 = 122

Likewise, the final form of system equations of LFFSSP for direct dynamic solution procedure is such that by using equation (4.73), (4.74), (4.79), (4.80) and (4.81):

$$\begin{bmatrix} \hat{M}_{78 \times 26} & -\hat{K}_{78 \times 96} \\ \hat{O}_{26 \times 26} & \hat{\Phi}_{26 \times 96} \\ \hat{O}_{12 \times 26} & \hat{\Phi}_{ZR, LFFSSP} 12 \times 96 \\ \hat{O}_{5 \times 26} & \hat{\Phi}_{ZR, LFFSSP} 5 \times 96 \\ \bar{\Phi}_{qddZ, LFFSSP} 1 \times 26 & \hat{O}_{1 \times 96} \end{bmatrix}_{122 \times 122} \begin{bmatrix} \ddot{\vec{q}}_{26 \times 1} \\ \bar{F}_{96 \times 1} \end{bmatrix}_{122 \times 1} = \begin{bmatrix} -\bar{B}_{78 \times 1} \\ \bar{T}_{26 \times 1} \\ \bar{O}_{12 \times 1} \\ \bar{O}_{5 \times 1} \\ 0 \end{bmatrix}_{122 \times 1} \quad (4.82)$$

#### 4.4.3. For RFFDSP

Since it is assumed that Body 4 does not interact with the ground during RFFDSP, several ground reaction forces and moments are expected to be zero given as shown:

$$\bar{F}_{0,4}^{(4)} = \bar{M}_{0,4}^{(4)} = \begin{bmatrix} 0 \\ 0 \\ 0 \end{bmatrix}$$

This condition can be described as:

$$\hat{\phi}_{ZGR,RFFDSP} \bar{F} = \begin{bmatrix} \bar{F}_{0,4}^{(4)} \\ \bar{M}_{0,4}^{(4)} \end{bmatrix} = \begin{bmatrix} 0 \\ \vdots \\ 0 \end{bmatrix} \quad (2 \times 3 = 6 \text{ equations}) \quad (4.83)$$

$\hat{\phi}_{ZGR,RFFDSP}$  is a matrix for the extraction of related ground reaction forces and moments.

During RFFDSP Body 1, Body 2 and Body 3 are assumed to be rigidly fixed to the ground. This assumption is ensured for Body 1 and Body 2 by supplying proper  $\hat{C}^{(0,1)}$ ,  $\hat{C}^{(0,2)}$ ,  $\bar{P}_{tpR}$ ,  $\bar{P}_{tpL}$ ,  $\bar{w}_1$ ,  $\bar{w}_2$ ,  $\bar{V}_{tpR}$ ,  $\bar{V}_{tpL}$ ,  $\bar{\alpha}_1$ ,  $\bar{\alpha}_2$ ,  $\bar{a}_{tpR}$ ,  $\bar{a}_{tpL}$  to kinematic equations of RFFDSP. For Body 3, kinematic constraints are implemented in order to satisfy the assumption:

$$\bar{a}_{c,3} = \bar{\alpha}_3 = \begin{bmatrix} 0 \\ 0 \\ 0 \end{bmatrix}$$

$\bar{a}_{c,3}$  can be expressed as  $\bar{a}_{c,3} = \hat{A}_3(\bar{q})\ddot{\bar{q}} + \bar{B}_3(\bar{q}, \dot{\bar{q}})$ .

Similarly,  $\bar{\alpha}_3$  can be expressed as  $\bar{\alpha}_3 = \hat{A}_{\alpha 3}(\bar{q})\ddot{\bar{q}} + \bar{B}_{\alpha 3}(\bar{q}, \dot{\bar{q}})$

Then, kinematic conditions can be described as:

$$\hat{A}_3\ddot{\bar{q}} = -\bar{B}_3 \text{ and } \hat{A}_{\alpha 3}\ddot{\bar{q}} = -\bar{B}_{\alpha 3}$$

However, rank of matrix  $\begin{bmatrix} \hat{A}_3 \\ \hat{A}_{\alpha 3} \end{bmatrix}$  is always found as 1 due to the kinematic structure for system of linear equations  $\begin{bmatrix} \hat{A}_3 \\ \hat{A}_{\alpha 3} \end{bmatrix} \ddot{\bar{q}} = \begin{bmatrix} -\bar{B}_3 \\ -\bar{B}_{\alpha 3} \end{bmatrix}$ . If unnecessary equations are eliminated, kinematic conditions are reduced to  $\ddot{\theta}_3 = 0$  which can be described as:

$$\bar{\Phi}_{qddZ,RFFDSP} \ddot{\bar{q}} = 0 \text{ (1 equation).} \quad (4.84)$$

$\bar{\Phi}_{qddZ,RFFDSP}$  is a row vector for the extraction of  $\ddot{\theta}_3$  from  $\ddot{\bar{q}}$ .

Additional kinematic constraints are introduced in order to ensure the compatibility necessary for the closed kinematic chain formed during RFFDSP. (3×2=6 equations)

$\bar{a}_{c,17_fR} = \bar{a}_{c,17_fL}$  and  $\bar{\alpha}_{17_fR} = \bar{\alpha}_{17_fL}$ , where

$$\bar{a}_{c,17_fR} = \hat{A}_{17R}(\bar{q})\ddot{\bar{q}} + \bar{B}_{17R}(\bar{q}, \dot{\bar{q}}) \text{ and } \bar{a}_{c,17_fL} = \hat{A}_{17L}(\bar{q})\ddot{\bar{q}} + \bar{B}_{17L}(\bar{q}, \dot{\bar{q}}),$$

$$\bar{\alpha}_{17_fR} = \hat{A}_{\alpha 17R}(\bar{q})\ddot{\bar{q}} + \bar{B}_{\alpha 17R}(\bar{q}, \dot{\bar{q}}) \text{ and } \bar{\alpha}_{17_fL} = \hat{A}_{\alpha 17L}(\bar{q})\ddot{\bar{q}} + \bar{B}_{\alpha 17L}(\bar{q}, \dot{\bar{q}}).$$

Following that, kinematic constraints can be expressed as:

$$(\hat{A}_{17R} - \hat{A}_{17L})\ddot{\bar{q}} = \bar{B}_{17L} - \bar{B}_{17R} \quad (4.85)$$

$$(\hat{A}_{\alpha 17R} - \hat{A}_{\alpha 17L})\ddot{\bar{q}} = \bar{B}_{\alpha 17L} - \bar{B}_{\alpha 17R} \quad (4.86)$$

$\hat{A}_{17R}$ ,  $\hat{A}_{17L}$ ,  $\hat{A}_{\alpha 17R}$ ,  $\hat{A}_{\alpha 17L}$ ,  $\bar{B}_{17R}$ ,  $\bar{B}_{17L}$ ,  $\bar{B}_{\alpha 17R}$  and  $\bar{B}_{\alpha 17L}$  are found numerically despite the possibility of expressing them analytically, by taking into account that analytical derivation becomes unpractical due to the complexity of equations. Calculation of these matrices and vectors is explained by an example:

At any instant,  $\bar{q}$  and  $\dot{\bar{q}}$  are known. By using  $\bar{q}$ ,  $\dot{\bar{q}}$  and applying  $\ddot{\bar{q}}$  as  $\ddot{\bar{q}} = \ddot{\bar{q}}_0 = \begin{bmatrix} 0 \\ \vdots \\ 0 \end{bmatrix}$  which contains zero values only,  $\bar{B}_{17R}$  can be calculated; since  $\bar{a}_{c,17_fR}$  is obtained from kinematic equations of RFFDSP for known  $\bar{q}$ ,  $\dot{\bar{q}}$  and given  $\ddot{\bar{q}}_0$ :

$$\bar{a}_{c,17_{fR_0}} = \hat{A}_{17R} \ddot{q}_0 + \bar{B}_{17R} = \bar{B}_{17R}$$

For  $\hat{A}_{17R} = [\bar{A}_{17R,1} \quad \dots \quad \bar{A}_{17R,26}]$  and a vector  $\ddot{q}_k$  which contains 1 for the  $k^{\text{th}}$  row and zero for remaining rows,  $\bar{a}_{c,17_{fR_k}} = \hat{A}_{17R} \ddot{q}_k + \bar{B}_{17R} = \bar{A}_{17R,k} + \bar{a}_{c,17_{fR_0}}$ .

Then,  $\hat{A}_{17R}$  matrix can be constructed at any instant by applying  $\bar{A}_{17R,k} = \bar{a}_{c,17_{fR_k}} - \bar{a}_{c,17_{fR_0}}$  for all  $k$  values from 1 to 26; since  $\bar{a}_{c,17_{fR_k}}$  is calculated for known  $\bar{q}$ ,  $\dot{q}$  and given  $\ddot{q}_k$  from kinematic equations of RFFDSP. Thus,  $\hat{A}_{17R}$ ,  $\bar{B}_{17R}$  and similarly others can be calculated numerically by this procedure.

According to the assumption of Body 1, Body 2 and Body 3 being rigidly fixed to the ground, reaction forces and moments between Body 1 and Body 3 such as  $\bar{F}_{1,3}^{(3)}$ ,  $M_{1,3x}^{(3)}$ ,  $M_{1,3z}^{(3)}$  can not be determined unless additional equations for modeling the interaction between Body 1 and Body 3 are introduced. Therefore, it is assumed that  $\bar{F}_{1,3}^{(3)} = \bar{0}_{3 \times 1}$  and  $M_{1,3x}^{(3)} = M_{1,3z}^{(3)} = 0$  without examining this modeling problem. Then, this assumption can be described as:

$$\hat{\phi}_{ZR,RFFDSP} \bar{F} = \begin{bmatrix} \bar{F}_{1,3}^{(3)} \\ M_{1,3x}^{(3)} \\ M_{1,3z}^{(3)} \end{bmatrix} = \begin{bmatrix} 0 \\ \vdots \\ 0 \end{bmatrix} \text{ (5 equations)} \quad (4.87)$$

$\hat{\phi}_{ZR,RFFDSP}$  is a matrix for the extraction of  $\bar{F}_{1,3}^{(3)}$ ,  $M_{1,3x}^{(3)}$  and  $M_{1,3z}^{(3)}$ . Then, *Total Number of Equations* = 78 + 26 + 6 + 1 + 6 + 5 = 122

The final form of system equations of RFFDSP for direct dynamic solution procedure is as shown in equation (4.88) by using equation (4.73), (4.74), (4.83), (4.84), (4.85), (4.86) and (4.87).

$$\begin{bmatrix}
\hat{M}_{78 \times 26} & -\hat{K}_{78 \times 96} \\
\hat{O}_{26 \times 26} & \hat{\Phi}_{26 \times 96} \\
\hat{O}_{6 \times 26} & \hat{\Phi}_{ZGR, RFFDSP}_{6 \times 96} \\
\hat{O}_{5 \times 26} & \hat{\Phi}_{ZR, RFFDSP}_{5 \times 96} \\
\bar{\Phi}_{qddZ, RFFDSP}_{1 \times 26} & \hat{O}_{1 \times 96} \\
(\hat{A}_{17R} - \hat{A}_{17L})_{3 \times 26} & \hat{O}_{3 \times 96} \\
(\hat{A}_{\alpha 17R} - \hat{A}_{\alpha 17L})_{3 \times 26} & \hat{O}_{3 \times 96}
\end{bmatrix}_{122 \times 122} \begin{bmatrix} \ddot{\bar{q}}_{26 \times 1} \\ \bar{F}_{96 \times 1} \end{bmatrix}_{122 \times 1} = \begin{bmatrix} -\bar{B}_{78 \times 1} \\ \bar{T}_{26 \times 1} \\ \bar{O}_{6 \times 1} \\ \bar{O}_{5 \times 1} \\ 0 \\ (\bar{B}_{17L} - \bar{B}_{17R})_{3 \times 1} \\ (\bar{B}_{\alpha 17L} - \bar{B}_{\alpha 17R})_{3 \times 1} \end{bmatrix}_{122 \times 1} \quad (4.88)$$

#### 4.4.4. For LFFDSP

A procedure similar to RFFDSP is followed.

Since it is assumed that Body 3 does not interact with the ground during LFFDSP, several ground reaction forces and moments are expected to be zero given as shown:

$$\bar{F}_{0,3}^{(3)} = \bar{M}_{0,3}^{(3)} = \begin{bmatrix} 0 \\ 0 \\ 0 \end{bmatrix}$$

This condition can be described as:

$$\hat{\Phi}_{ZGR, LFFDSP} \bar{F} = \begin{bmatrix} \bar{F}_{0,3}^{(3)} \\ \bar{M}_{0,3}^{(3)} \end{bmatrix} = \begin{bmatrix} 0 \\ \vdots \\ 0 \end{bmatrix} \quad (2 \times 3 = 6 \text{ equations}) \quad (4.89)$$

$\hat{\Phi}_{ZGR, LFFDSP}$  is a matrix for the extraction of related ground reaction forces and moments.

During LFFDSP Body 1, Body 2 and Body 4 are assumed to be rigidly fixed to the ground. This assumption is ensured for Body 1 and Body 2 by supplying proper  $\hat{C}^{(0,1)}$ ,  $\hat{C}^{(0,2)}$ ,  $\bar{P}_{tpR}$ ,  $\bar{P}_{tpL}$ ,  $\bar{w}_1$ ,  $\bar{w}_2$ ,  $\bar{V}_{tpR}$ ,  $\bar{V}_{tpL}$ ,  $\bar{\alpha}_1$ ,  $\bar{\alpha}_2$ ,  $\bar{a}_{tpR}$ ,  $\bar{a}_{tpL}$  to kinematic

equations of LFFDSP. For Body 4, kinematic constraints are implemented in order to satisfy the assumption:

$$\bar{a}_{c,4} = \bar{\alpha}_4 = \begin{bmatrix} 0 \\ 0 \\ 0 \end{bmatrix}$$

$\bar{a}_{c,4}$  can be expressed as  $\bar{a}_{c,4} = \hat{A}_4(\bar{q})\ddot{\bar{q}} + \bar{B}_4(\bar{q}, \dot{\bar{q}})$ .

Similarly,  $\bar{\alpha}_4$  can be expressed as  $\bar{\alpha}_4 = \hat{A}_{\alpha 4}(\bar{q})\ddot{\bar{q}} + \bar{B}_{\alpha 4}(\bar{q}, \dot{\bar{q}})$

Then, kinematic conditions can be described as:

$$\hat{A}_4\ddot{\bar{q}} = -\bar{B}_4 \text{ and } \hat{A}_{\alpha 4}\ddot{\bar{q}} = -\bar{B}_{\alpha 4}$$

However, rank of matrix  $\begin{bmatrix} \hat{A}_4 \\ \hat{A}_{\alpha 4} \end{bmatrix}$  is always found as 1 due to the kinematic structure

for system of linear equations  $\begin{bmatrix} \hat{A}_4 \\ \hat{A}_{\alpha 4} \end{bmatrix} \ddot{\bar{q}} = \begin{bmatrix} -\bar{B}_4 \\ -\bar{B}_{\alpha 4} \end{bmatrix}$ . If unnecessary equations are eliminated, kinematic conditions are reduced to  $\ddot{\theta}_4 = 0$  which can be described as:

$$\bar{\Phi}_{qddZ,LFFDSP}\ddot{\bar{q}} = 0 \text{ (1 equation)}. \quad (4.90)$$

$\bar{\Phi}_{qddZ,LFFDSP}$  is a row vector for the extraction of  $\ddot{\theta}_4$  from  $\ddot{\bar{q}}$ .

Additional kinematic constraints are introduced in order to ensure the compatibility necessary for the closed kinematic chain formed during LFFDSP. (3×2=6 equations)

$\bar{a}_{c,17_{fR}} = \bar{a}_{c,17_{fL}}$  and  $\bar{\alpha}_{17_{fR}} = \bar{\alpha}_{17_{fL}}$ , where

$$\bar{a}_{c,17_{fR}} = \hat{A}_{17R}(\bar{q})\ddot{\bar{q}} + \bar{B}_{17R}(\bar{q}, \dot{\bar{q}}) \text{ and } \bar{a}_{c,17_{fL}} = \hat{A}_{17L}(\bar{q})\ddot{\bar{q}} + \bar{B}_{17L}(\bar{q}, \dot{\bar{q}}),$$

$$\bar{\alpha}_{17_{fR}} = \hat{A}_{\alpha 17R}(\bar{q})\ddot{\bar{q}} + \bar{B}_{\alpha 17R}(\bar{q}, \dot{\bar{q}}) \text{ and } \bar{\alpha}_{17_{fL}} = \hat{A}_{\alpha 17L}(\bar{q})\ddot{\bar{q}} + \bar{B}_{\alpha 17L}(\bar{q}, \dot{\bar{q}}).$$

Following that, kinematic constraints can be expressed as:

$$(\hat{A}_{17R} - \hat{A}_{17L})\ddot{\bar{q}} = \bar{B}_{17L} - \bar{B}_{17R} \quad (4.91)$$

$$(\hat{A}_{\alpha 17R} - \hat{A}_{\alpha 17L})\ddot{\bar{q}} = \bar{B}_{\alpha 17L} - \bar{B}_{\alpha 17R} \quad (4.92)$$

For LFFDSP,  $\hat{A}_{17R}$ ,  $\hat{A}_{17L}$ ,  $\hat{A}_{\alpha 17R}$ ,  $\hat{A}_{\alpha 17L}$ ,  $\bar{B}_{17R}$ ,  $\bar{B}_{17L}$ ,  $\bar{B}_{\alpha 17R}$  and  $\bar{B}_{\alpha 17L}$  are found numerically too for the same reasons and by the same procedure mentioned before.

According to the assumption of Body 1, Body 2 and Body 4 being rigidly fixed to the ground, reaction forces and moments between Body 2 and Body 4 such as  $\bar{F}_{2,4}^{(4)}$ ,  $M_{2,4x}^{(4)}$ ,  $M_{2,4z}^{(4)}$  can not be determined unless additional equations for modeling the interaction between Body 2 and Body 4 are introduced. Therefore, it is assumed that  $\bar{F}_{2,4}^{(4)} = \bar{0}_{3 \times 1}$  and  $M_{2,4x}^{(4)} = M_{2,4z}^{(4)} = 0$  without examining this modeling problem. Then, this assumption can be described as:

$$\hat{\Phi}_{ZR,LFFDSP} \bar{F} = \begin{bmatrix} \bar{F}_{2,4}^{(4)} \\ M_{2,4x}^{(4)} \\ M_{2,4z}^{(4)} \end{bmatrix} = \begin{bmatrix} 0 \\ \vdots \\ 0 \end{bmatrix} \text{ (5 equations)} \quad (4.93)$$

$\hat{\Phi}_{ZR,LFFDSP}$  is a matrix for the extraction of  $\bar{F}_{2,4}^{(4)}$ ,  $M_{2,4x}^{(4)}$  and  $M_{2,4z}^{(4)}$ .

Then, *Total Number of Equations* = 78 + 26 + 6 + 1 + 6 + 5 = 122

Similar to RFFDSP, the final form of system equations of LFFDSP for direct dynamic solution procedure is shown in equation (4.94) by using equation (4.73), (4.74), (4.89), (4.90), (4.91), (4.92) and (4.93).

$$\begin{bmatrix}
\hat{M}_{78 \times 26} & -\hat{K}_{78 \times 96} \\
\hat{O}_{26 \times 26} & \hat{\Phi}_{26 \times 96} \\
\hat{O}_{6 \times 26} & \hat{\Phi}_{ZGR, LFFDSP}_{6 \times 96} \\
\hat{O}_{5 \times 26} & \hat{\Phi}_{ZR, LFFDSP}_{5 \times 96} \\
\bar{\Phi}_{qddZ, LFFDSP}_{1 \times 26} & \hat{O}_{1 \times 96} \\
(\hat{A}_{17R} - \hat{A}_{17L})_{3 \times 26} & \hat{O}_{3 \times 96} \\
(\hat{A}_{\alpha 17R} - \hat{A}_{\alpha 17L})_{3 \times 26} & \hat{O}_{3 \times 96}
\end{bmatrix}_{122 \times 122} \begin{bmatrix} \ddot{\bar{q}}_{26 \times 1} \\ \bar{F}_{96 \times 1} \end{bmatrix}_{122 \times 1} = \begin{bmatrix} -\bar{B}_{78 \times 1} \\ \bar{T}_{26 \times 1} \\ \bar{O}_{6 \times 1} \\ \bar{O}_{5 \times 1} \\ 0 \\ (\bar{B}_{17L} - \bar{B}_{17R})_{3 \times 1} \\ (\bar{B}_{\alpha 17L} - \bar{B}_{\alpha 17R})_{3 \times 1} \end{bmatrix}_{122 \times 1} \quad (4.94)$$

#### 4.5. Transition from Single Support to Double Support Phases

Reference trajectories are given in such a way that the velocity of contacting body relative to the ground is planned to become zero at the instant of contact. However, there always exists a tracking error caused by the control effort. As a consequence, desired collision free contact of foot with the ground is never accomplished. This situation occurs at the instant of phase transitions from single to double support phases. Since bodies and the ground are assumed to be rigid, the impact happens in an infinitely small amount of time interval. In other words, joint space velocities are changed instantly to satisfy the contact conditions which enforce zero angular and translational velocity relative to the ground for the contacting body after the impact. It is assumed that joint space velocities of only lowerbodies are affected by the impact. Modification of joint space velocities are carried out manually by an optimization based algorithm, where weighting coefficients determine the sensitivity of variation in joint space velocities to the impact.

#### 4.5.1. From RFFSSP to LFFDSP

For  $\dot{\bar{q}}_{R\_L} = \begin{bmatrix} \dot{\bar{q}}_{R\_Hr} \\ \dot{\bar{q}}_{L\_H} \end{bmatrix}$ , defined by using equation (4.3) and (4.6):

$\dot{\bar{q}}_{R\_L\_end}$  and  $\dot{\bar{q}}_{R\_L\_ini}$  are  $\dot{\bar{q}}_{R\_L}$  at the end of RFFSSP and the beginning of LFFDSP. In the same manner,  $\bar{V}_{tpL\_end}$ ,  $\bar{V}_{tpL\_ini}$ ,  $\bar{w}_{2\_end}$ ,  $\bar{w}_{2\_ini}$  are  $\bar{V}_{tpL}$  and  $\bar{w}_2$  at the end of RFFSSP and the beginning of LFFDSP.

It is impossible to provide a perfect landing condition for the left foot at the end of RFFSSP. For this reason:

$$\begin{bmatrix} \bar{V}_{tpL\_end} \\ \bar{w}_{2\_end} \end{bmatrix} \neq \begin{bmatrix} 0 \\ \vdots \\ 0 \end{bmatrix}$$

At the instant when LFFDSP begins, the following conditions must be satisfied:

$$\hat{J}_{v,tpL} \dot{\bar{q}}_{R\_L\_ini} = \begin{bmatrix} \bar{V}_{tpL\_ini} \\ \bar{w}_{2\_ini} \end{bmatrix} = \begin{bmatrix} 0 \\ \vdots \\ 0 \end{bmatrix}, \dot{\theta}_4 = 0 \quad (4.95)$$

After dropping  $\dot{\theta}_4$  and the related column from  $\dot{\bar{q}}_{R\_L\_ini}$  and  $\hat{J}_{v,tpL}$ , the equation (4.95) becomes:

$$\hat{J}_{v,tpL_r} \dot{\bar{q}}_{R\_L\_ini_r} = \begin{bmatrix} \bar{V}_{tpL\_ini} \\ \bar{w}_{2\_ini} \end{bmatrix} = \begin{bmatrix} 0 \\ \vdots \\ 0 \end{bmatrix} \quad (4.96)$$

Then, a cost function is employed to minimize the total variation in joint space velocities sourced from instant changes. The cost function is taken into the consideration while  $\dot{\bar{q}}_{R\_L\_end}$  is manipulated to be  $\dot{\bar{q}}_{R\_L\_ini}$  with the condition shown by equation (4.96) to be satisfied. Therefore an optimization problem arises such that:

$$\text{Minimize } C = \frac{1}{2} \Delta \dot{\bar{q}}_{R\_L_r}^T \hat{W}_{adj,RFFSSP\_LFFDSP} \Delta \dot{\bar{q}}_{R\_L_r}, \text{ subject to } \hat{J}_{v,tpL_r} \dot{\bar{q}}_{R\_L\_ini_r} = \begin{bmatrix} \bar{V}_{tpL\_ini} \\ \bar{w}_{2\_ini} \end{bmatrix}; \text{ where } \begin{bmatrix} \bar{V}_{tpL\_ini} \\ \bar{w}_{2\_ini} \end{bmatrix} \text{ is supplied as } \begin{bmatrix} \bar{V}_{tpL\_ini} \\ \bar{w}_{2\_ini} \end{bmatrix} = \begin{bmatrix} 0 \\ \vdots \\ 0 \end{bmatrix}.$$

$\Delta \dot{\bar{q}}_{R\_L\_r} = \dot{\bar{q}}_{R\_L\_end\_r} - \dot{\bar{q}}_{R\_L\_ini\_r}$ , where  $\dot{\bar{q}}_{R\_L\_end\_r}$  is the reduced form after dropping  $\dot{\theta}_4$  from  $\dot{\bar{q}}_{R\_L\_end}$ .

$\widehat{W}_{adj,RFFSSP\_LFFDSP}$  is a diagonal matrix including weighting coefficients such as

$$\widehat{W}_{adj,RFFSSP\_LFFDSP} = \begin{bmatrix} W_1 & \dots & 0 \\ \vdots & \ddots & \vdots \\ 0 & \dots & W_{14} \end{bmatrix}.$$

By applying the method of Lagrange Multipliers [63]:

$$\begin{aligned} & \dot{\bar{q}}_{R\_L\_ini\_r} \\ &= \dot{\bar{q}}_{R\_L\_end\_r} + \widehat{W}_{adj,RFFSSP\_LFFDSP}^{-1} \hat{J}_{v,tpL_r}^T \left( \hat{J}_{v,tpL_r} \widehat{W}_{adj,RFFSSP\_LFFDSP}^{-1} \hat{J}_{v,tpL_r}^T \right)^{-1} \\ & \cdot \left( \begin{bmatrix} \bar{V}_{tpL\_ini} \\ \bar{W}_{2\_ini} \end{bmatrix} - \hat{J}_{v,tpL_r} \dot{\bar{q}}_{R\_L\_end\_r} \right) \end{aligned} \quad (4.97)$$

At the beginning of LFFDSP, joint space variables in  $\dot{\bar{q}}_{R\_L}$  are switched with  $\dot{\bar{q}}_{R\_L\_ini}$  (where  $\dot{\theta}_4$  in  $\dot{\bar{q}}_{R\_L\_ini}$  is taken as zero).

#### 4.5.2. From LFFSSP to RFFDSP

A similar procedure is carried out.

For  $\dot{\bar{q}}_{L\_R} = \begin{bmatrix} \dot{\bar{q}}_{L\_Hr} \\ \dot{\bar{q}}_{R\_H} \end{bmatrix}$ , defined by using equation (4.2) and (4.16):

$\dot{\bar{q}}_{L\_R\_end}$  and  $\dot{\bar{q}}_{L\_R\_ini}$  are  $\dot{\bar{q}}_{L\_R}$  at the end of LFFSSP and the beginning of RFFDSP. In the same manner  $\bar{V}_{tpR\_end}$ ,  $\bar{V}_{tpR\_ini}$ ,  $\bar{w}_{1\_end}$ ,  $\bar{w}_{1\_ini}$  are  $\bar{V}_{tpR}$  and  $\bar{w}_1$  at the end of LFFSSP and the beginning of RFFDSP.

It is impossible to provide a perfect landing condition for the left foot at the end of RFFSSP. For this reason:

$$\begin{bmatrix} \bar{V}_{tpR\_end} \\ \bar{w}_{1\_end} \end{bmatrix} \neq \begin{bmatrix} 0 \\ \vdots \\ 0 \end{bmatrix}$$

At the instant when RFFDSP begins, the following conditions must be satisfied:

$$\hat{J}_{v,tpR} \dot{\bar{q}}_{L_R ini} = \begin{bmatrix} \bar{V}_{tpR ini} \\ \bar{w}_{1 ini} \end{bmatrix} = \begin{bmatrix} 0 \\ \vdots \\ 0 \end{bmatrix}, \dot{\theta}_3 = 0 \quad (4.98)$$

After dropping  $\dot{\theta}_3$  and the related column from  $\dot{\bar{q}}_{L_R ini}$  and  $\hat{J}_{v,tpR}$ , the equation (4.98) becomes:

$$\hat{J}_{v,tpR_r} \dot{\bar{q}}_{L_R ini_r} = \begin{bmatrix} \bar{V}_{tpR ini} \\ \bar{w}_{1 ini} \end{bmatrix} = \begin{bmatrix} 0 \\ \vdots \\ 0 \end{bmatrix} \quad (4.99)$$

Then, a cost function is employed to minimize the total variation in joint space velocities sourced from instant changes. The cost function is taken into the consideration while  $\dot{\bar{q}}_{L_R end}$  is manipulated to be  $\dot{\bar{q}}_{L_R ini}$  with the condition shown by equation (4.99) to be satisfied. Therefore an optimization problem arises such that:

$$\text{Minimize } C = \frac{1}{2} \Delta \dot{\bar{q}}_{L_R_r}^T \widehat{W}_{adj,LFFSSP\_RFFDSP} \Delta \dot{\bar{q}}_{L_R_r}, \text{ subject to } \hat{J}_{v,tpR_r} \dot{\bar{q}}_{L_R ini_r} = \begin{bmatrix} \bar{V}_{tpR ini} \\ \bar{w}_{1 ini} \end{bmatrix}; \text{ where } \begin{bmatrix} \bar{V}_{tpR ini} \\ \bar{w}_{1 ini} \end{bmatrix} \text{ is supplied as } \begin{bmatrix} \bar{V}_{tpR ini} \\ \bar{w}_{1 ini} \end{bmatrix} = \begin{bmatrix} 0 \\ \vdots \\ 0 \end{bmatrix}.$$

$\Delta \dot{\bar{q}}_{L_R_r} = \dot{\bar{q}}_{L_R end_r} - \dot{\bar{q}}_{L_R ini_r}$ , where  $\dot{\bar{q}}_{L_R end_r}$  is the reduced form after dropping  $\dot{\theta}_3$  from  $\dot{\bar{q}}_{L_R end}$ .

$\widehat{W}_{adj,LFFSSP\_RFFDSP}$  is a diagonal matrix including weighting coefficients.

By applying the method of Lagrange Multipliers:

$$\begin{aligned} & \dot{\bar{q}}_{L_R ini_r} \\ &= \dot{\bar{q}}_{L_R end_r} + \widehat{W}_{adj,LFFSSP\_RFFDSP}^{-1} \hat{J}_{v,tpR_r}^T \left( \hat{J}_{v,tpR_r} \widehat{W}_{adj,LFFSSP\_RFFDSP}^{-1} \hat{J}_{v,tpR_r}^T \right)^{-1} \\ & \left( \begin{bmatrix} \bar{V}_{tpR ini} \\ \bar{w}_{1 ini} \end{bmatrix} - \hat{J}_{v,tpR_r} \dot{\bar{q}}_{L_R end_r} \right) \end{aligned} \quad (4.100)$$

At the beginning of RFFDSP, joint space variables in  $\dot{\bar{q}}_{L_R}$  are switched with  $\dot{\bar{q}}_{L_R ini}$  (where  $\dot{\theta}_3$  in  $\dot{\bar{q}}_{L_R ini}$  is taken as zero).

## CHAPTER 5

### CONTROL STRATEGY

Tracking of reference trajectories which define characteristics of a biped locomotion is achieved by a 2 step control strategy which are computed torque control and optimum command accelerations calculation.

#### 5.1. Calculation of Optimum Command Accelerations

As explained in chapter 3, reference trajectories are supplied for Body 1, Body 2, Body 17, toe points and the mass center of Body 17. In order to apply computed torque control method for finding actuator torques, desired joint space accelerations which will be called as command accelerations  $\ddot{q}_c$  in the thesis must be supplied. Due to the redundant kinematic structure of the biped robot, it is not able to find unique joint space accelerations which satisfy reference trajectories given for bodies and points specified in chapter 3. In order to cope with this problem, simple optimization algorithms based on quadratic cost functions, which are formed according to the requirements of locomotion phases, are created [68].

Future tracking errors are estimated in the light of present values of joint space variables; for instance  $\overline{\Delta P}_{RFFSSP\_c,17\_f}$ ,  $\overline{\Delta v}_{RFFSSP\_17\_f}$  and  $\overline{\Delta OR}_{RFFSSP\_17\_f}$  in RFFSSP. These estimated tracking errors form the basis of cost functions. Along with these estimated tracking errors, joint space accelerations are added to cost functions; so that joint space accelerations with greater values are penalized such as by the expression  $\frac{1}{2} \ddot{q}_{R\_Hr}(t)^T \cdot \widehat{W}_{RFFSSP\_qR\_Hrdd} \cdot \ddot{q}_{R\_Hr}(t)$  in RFFSSP, since higher joint space accelerations result higher values of actuator torques which is an unfavorable situation for instrumentation and power consumption aspects. As mentioned in previous chapters, full rotation of all joints is available. Regarding this, full rotation of specific joints is occasionally observed during the simulation;

because it is calculated to be feasible according to the control method within the prediction time range. However, the control of biped robot becomes more difficult and the tracking performance reduces in the long run; because online adjustment of weighting coefficients to compensate significantly changing conditions of this nonlinear system, for instance the full rotation of some joints, is not available in the thesis. Considering this, deviation of some specific joint space variables from their initial positions is penalized by an additional component in cost functions in order to avoid excessive rotation in several joints such as  $\frac{1}{2}\overline{\Delta q}_{RFFSSP\_R\_Hr\_f}^T \cdot \widehat{W}_{RFFSSP\_qR\_Hr} \cdot \overline{\Delta q}_{RFFSSP\_R\_Hr\_f}$  for RFFSSP. Joint space variables  $\theta_3$  and  $\dot{\theta}_3$ ,  $\theta_4$  and  $\dot{\theta}_4$  being different from zero is penalized during single support phases by a cost function such as  $\frac{1}{2}\Delta\theta_4 \cdot W_{P,\theta_4} \cdot \Delta\theta_4$  and  $\frac{1}{2}\Delta\dot{\theta}_4 \cdot W_{V,\theta_4} \cdot \Delta\dot{\theta}_4$  for RFFSSP; because Body 1 and Body 3 at the end of LFFSSP, Body 2 and Body 4 at the end of RFFSSP are expected to have the same orientation, where reference orientations are supplied for Body 1 and Body 2.

Optimum command accelerations  $\ddot{q}_c$  are calculated in two separate headings. Calculation procedure of optimum command accelerations of joint space variables regarding upper bodies  $\ddot{q}_{upper\_c}$  is the same for all phases. On the other hand, the procedure for optimum command accelerations of joint space variables regarding lower bodies  $\ddot{q}_{lower\_c}$  depends on the locomotion phase.

### **5.1.1. Calculation of Optimum Command Accelerations for Lower Bodies**

#### **5.1.1.1. For RFFSSP**

Calculation of optimum command accelerations during RFFSSP is accomplished in 2 steps. In the first step, optimum command accelerations for joint space variables from Body 3 to Body 17 are calculated according to given reference inputs for Body 17 and its mass center. In the second step, optimum command accelerations for joint space variables from Body 17 to Body 2 are calculated according to determined command accelerations in the first step and given reference inputs for Body 2 and its toe point. So the calculation of optimum command accelerations for RFFSSP can be divided into 2 parts.

Optimum command accelerations for dropped joint space variables are taken as zero due to locomotion phase assumptions. Since Body 3 is assumed to be rigidly fixed to the ground, command acceleration  $\ddot{\theta}_{3c}$  is taken as zero.

#### 5.1.1.1.1. For Body 17 and the mass center of Body 17

##### 5.1.1.1.1.1. Definition of Variables

Variables that are used in the cost function are expressed.

$t$  is the present phase time which is elapsed time from the beginning of current phase and  $\Delta t_{1\_RFFSSP}$  is the prediction time range used in the first step of optimum command acceleration calculations in RFFSSP.

$$\overline{\Delta P}_{RFFSSP\_c,17\_f} = \bar{P}_{c,17_r}(t + \Delta t_{1\_RFFSSP}) - \bar{P}_{c,17_a}(t + \Delta t_{1\_RFFSSP})$$

$\bar{P}_{c,17_r}(t + \Delta t_{1\_RFFSSP})$  is the reference value of  $\bar{P}_{c,17}$  at phase time  $t + \Delta t_{1\_RFFSSP}$ .

$\bar{P}_{c,17_a}(t + \Delta t_{1\_RFFSSP})$  is the predicted actual value of  $\bar{P}_{c,17}$  at phase time  $t + \Delta t_{1\_RFFSSP}$ .

Using the truncated Taylor Expansion of  $\bar{P}_{c,17_a}(t + \Delta t_{1\_RFFSSP})$  and the definition of  $\bar{q}_{R\_Hr}$  by equation (4.6):

$$\begin{aligned} \bar{P}_{c,17_a}(t + \Delta t_{1\_RFFSSP}) & \cong \bar{P}_{c,17_a}(t) + \bar{V}_{c,17_a}(t) \cdot \Delta t_{1\_RFFSSP} + \bar{a}_{c,17_a}(t) \cdot \frac{\Delta t_{1\_RFFSSP}^2}{2} \\ & = \bar{P}_{c,17_a}(t) + \hat{J}_{v,17\_fR_V}(t) \cdot \dot{\bar{q}}_{R\_Hr}(t) \cdot \Delta t_{1\_RFFSSP} \\ & \quad + \hat{J}_{v,17\_fR_V}(t) \cdot \dot{\bar{q}}_{R\_Hr}(t) \cdot \frac{\Delta t_{1\_RFFSSP}^2}{2} \\ & \quad + \hat{J}_{v,17\_fR_V}(t) \cdot \ddot{\bar{q}}_{R\_Hr}(t) \cdot \frac{\Delta t_{1\_RFFSSP}^2}{2} \end{aligned}$$

Then,

$$\begin{aligned} \overline{\Delta P}_{RFFSSP\_c,17\_f} = & \\ \bar{P}_{c,17_r}(t + \Delta t_{1\_RFFSSP}) - \bar{P}_{c,17_a}(t) - \hat{J}_{v,17\_fR_V}(t) \cdot \dot{\bar{q}}_{R\_Hr}(t) \cdot \Delta t_{1\_RFFSSP} - & \\ \hat{J}_{v,17\_fR_V}(t) \cdot \ddot{\bar{q}}_{R\_Hr}(t) \cdot \frac{\Delta t_{1\_RFFSSP}^2}{2} - \hat{J}_{v,17\_fR_V}(t) \cdot \ddot{\bar{q}}_{R\_Hr}(t) \cdot \frac{\Delta t_{1\_RFFSSP}^2}{2} & \end{aligned} \quad (5.1)$$

The same convention and procedure are used for other definitions.

$\overline{\Delta v}_{RFFSSP\_17\_f} = \bar{v}_{17_r}(t + \Delta t_{1\_RFFSSP}) - \bar{v}_{17_a}(t + \Delta t_{1\_RFFSSP})$ , for

$$\bar{v}_{17}(t + \Delta t_{1\_RFFSSP}) = \begin{bmatrix} \bar{V}_{c,17}(t + \Delta t_{1\_RFFSSP}) \\ \bar{w}_{17}(t + \Delta t_{1\_RFFSSP}) \end{bmatrix}$$

Then,

$$\begin{aligned} \overline{\Delta v}_{RFFSSP\_17\_f} = & \\ \bar{v}_{17_r}(t + \Delta t_{1\_RFFSSP}) - \hat{J}_{v,17\_fR}(t) \cdot \dot{\bar{q}}_{R\_Hr}(t) - \hat{J}_{v,17\_fR}(t) \cdot \dot{\bar{q}}_{R\_Hr}(t) \cdot \Delta t_{1\_RFFSSP} - & \\ \hat{J}_{v,17\_fR}(t) \cdot \ddot{\bar{q}}_{R\_Hr}(t) \cdot \Delta t_{1\_RFFSSP} & \end{aligned} \quad (5.2)$$

For

$$\overline{\Delta OR}_{RFFSSP\_17\_f} = \bar{C}_{diag_r}^{(0,17)}(t + \Delta t_{1\_RFFSSP}) - \bar{C}_{diag_a}^{(0,17)}(t + \Delta t_{1\_RFFSSP}),$$

it can be expressed that:

$$\begin{aligned} \overline{\Delta OR}_{RFFSSP\_17\_f} = & \\ \bar{C}_{diag_r}^{(0,17)}(t + \Delta t_{1\_RFFSSP}) - \bar{C}_{diag_a}^{(0,17)}(t) - & \\ \hat{J}_{v,Cdiag0\_17\_fR}(t) \cdot \dot{\bar{q}}_{R\_Hr}(t) \cdot \Delta t_{1\_RFFSSP} - \hat{J}_{v,Cdiag0\_17\_fR}(t) \cdot \dot{\bar{q}}_{R\_Hr}(t) \cdot \frac{\Delta t_{1\_RFFSSP}^2}{2} - & \\ \hat{J}_{v,Cdiag0\_17\_fR}(t) \cdot \ddot{\bar{q}}_{R\_Hr}(t) \cdot \frac{\Delta t_{1\_RFFSSP}^2}{2} & \end{aligned} \quad (5.3)$$

$\overline{\Delta q}_{RFFSSP\_R\_Hr\_f} = \bar{q}_{R\_Hr_a}(t + \Delta t_{1\_RFFSSP}) - \bar{q}_{R\_Hr_0}$ , where  $\bar{q}_{R\_Hr_0}$  is the vector of basic joint space positions for  $\bar{q}_{R\_Hr}$ . Joint space position deviations, which are penalized in the cost function, are calculated with respect to  $\bar{q}_{R\_Hr_0}$ . Initial values of  $\bar{q}_{R\_Hr}$  are used as  $\bar{q}_{R\_Hr_0}$ . So,  $\bar{q}_{R\_Hr_0}$  is taken as a vector with zero components only in the simulation.

Then,

$$\overline{\Delta q}_{RFFSSP\_R\_Hr\_f} = \bar{q}_{R\_Hr}(t) + \dot{\bar{q}}_{R\_Hr}(t) \cdot \Delta t_{1\_RFFSSP} + \ddot{\bar{q}}_{R\_Hr}(t) \cdot \frac{\Delta t_{1\_RFFSSP}^2}{2} - \bar{q}_{R\_Hr_0} \quad (5.4)$$

The cost function for the first step of optimum command accelerations calculation in RFFSSP is defined as shown below:

$$\begin{aligned} C_{RFFSSP,1} = & \\ & \frac{1}{2} \overline{\Delta P}_{RFFSSP\_c,17\_f}^T \cdot \widehat{W}_{RFFSSP\_P,17} \cdot \overline{\Delta P}_{RFFSSP\_c,17\_f} + \\ & \frac{1}{2} \overline{\Delta OR}_{RFFSSP\_17\_f}^T \cdot \widehat{W}_{RFFSSP\_OR,17} \cdot \overline{\Delta OR}_{RFFSSP\_17\_f} + \\ & \frac{1}{2} \overline{\Delta v}_{RFFSSP\_17\_f}^T \cdot \widehat{W}_{RFFSSP\_v,17} \cdot \overline{\Delta v}_{RFFSSP\_17\_f} + \\ & \frac{1}{2} \overline{\Delta q}_{RFFSSP\_R\_Hr\_f}^T \cdot \widehat{W}_{RFFSSP\_qR\_Hr} \cdot \overline{\Delta q}_{RFFSSP\_R\_Hr\_f} + \\ & \frac{1}{2} \ddot{\bar{q}}_{R\_Hr}(t)^T \cdot \widehat{W}_{RFFSSP\_qR\_Hrdd} \cdot \ddot{\bar{q}}_{R\_Hr}(t) \end{aligned} \quad (5.5)$$

#### 5.1.1.1.2. Calculation Procedure

$$\text{For optimum cost value } \frac{\partial C_{RFFSSP,1}}{\partial \ddot{\bar{q}}_{R\_Hr}} = 0, \quad (5.6)$$

optimum command accelerations can be calculated. The equation (5.6) can be converted into the form  $\ddot{\bar{q}}_{R\_Hr}^T \hat{Z}_{RFFSSP,1} = \bar{G}_{RFFSSP,1}$  by using row vector convention for the differentiation of a dimensionless variable by a vector  $\bar{x} = \begin{bmatrix} x_1 \\ x_2 \end{bmatrix}$  as shown below:

- $\frac{\partial y}{\partial \bar{x}} = \begin{bmatrix} \frac{\partial y}{\partial x_1} & \frac{\partial y}{\partial x_2} \end{bmatrix}$
- $\frac{\partial (\bar{x}^T \hat{A} \bar{x})}{\partial \bar{x}} = 2 \bar{x}^T \hat{A}$ , where  $\hat{A}$  is a symmetric matrix
- $\frac{\partial \hat{A} \bar{x}}{\partial \bar{x}} = \hat{A}$

Therefore,

$$\begin{aligned}
\frac{\partial C_{RFFSSP,1}}{\partial \ddot{q}_{R_{Hr}}} &= \overline{\Delta P}_{RFFSSP\_c,17\_f}^T \cdot \widehat{W}_{RFFSSP\_p,17} \cdot \left[ -\hat{J}_{v,17\_fR_v}(t) \cdot \frac{\Delta t_{1\_RFFSSP}^2}{2} \right] + \\
\overline{\Delta OR}_{RFFSSP\_17\_f}^T \cdot \widehat{W}_{RFFSSP\_or,17} \cdot \left[ -\hat{J}_{v,Cdiag0\_17\_fR}(t) \cdot \frac{\Delta t_{1\_RFFSSP}^2}{2} \right] + \\
\overline{\Delta v}_{RFFSSP\_17\_f}^T \cdot \widehat{W}_{RFFSSP\_v,17} \cdot \left[ -\hat{J}_{v,17\_fR}(t) \cdot \ddot{q}_{R_{Hr}}(t) \cdot \Delta t_{1\_RFFSSP} \right] + \\
\overline{\Delta q}_{RFFSSP\_R_{Hr}\_f}^T \cdot \widehat{W}_{RFFSSP\_qR_{Hr}} \cdot \frac{\Delta t_{1\_RFFSSP}^2}{2} + \ddot{q}_{R_{Hr}}(t)^T \cdot \widehat{W}_{RFFSSP\_qR_{Hr}dd} \quad (5.7)
\end{aligned}$$

After inserting derived expressions of  $\overline{\Delta P}_{RFFSSP\_c,17\_f}$ ,  $\overline{\Delta OR}_{RFFSSP\_17\_f}$ ,  $\overline{\Delta v}_{RFFSSP\_17\_f}$  and  $\overline{\Delta q}_{RFFSSP\_R_{Hr}\_f}$  which are equation (5.1), (5.2), (5.3) and (5.4) into equation (5.7), the equation can be expressed as:

$$\ddot{q}_{R_{Hr}}^T \hat{Z}_{RFFSSP,1} = \bar{G}_{RFFSSP,1} \quad (5.8)$$

Then, components of equation (5.8) can be expressed as:

$$\begin{aligned}
\bar{G}_{RFFSSP,1} &= \\
&\left[ \begin{array}{c} \bar{P}_{c,17_r}(t + \Delta t_{1\_RFFSSP}) - \bar{P}_{c,17_a}(t) - \hat{J}_{v,17\_fR_v}(t) \cdot \dot{q}_{R_{Hr}}(t) \cdot \Delta t_{1\_RFFSSP} \\ -\hat{J}_{v,17\_fR_v}(t) \cdot \dot{q}_{R_{Hr}}(t) \cdot \frac{\Delta t_{1\_RFFSSP}^2}{2} \end{array} \right]^T \\
&\cdot \widehat{W}_{RFFSSP\_p,17} \cdot \hat{J}_{v,17\_fR_v}(t) \cdot \frac{\Delta t_{1\_RFFSSP}^2}{2} \\
&+ \left[ \begin{array}{c} \bar{v}_{17_r}(t + \Delta t_{1\_RFFSSP}) - \hat{J}_{v,17\_fR}(t) \cdot \dot{q}_{R_{Hr}}(t) \\ -\hat{J}_{v,17\_fR}(t) \cdot \dot{q}_{R_{Hr}}(t) \cdot \Delta t_{1\_RFFSSP} \end{array} \right]^T \cdot \widehat{W}_{RFFSSP\_v,17} \cdot \hat{J}_{v,17\_fR}(t) \cdot \Delta t_{1\_RFFSSP} \\
&+ \left[ \begin{array}{c} \bar{C}_{diag_r}^{(0,17)}(t + \Delta t_{1\_RFFSSP}) - \bar{C}_{diag_a}^{(0,17)}(t) \\ -\hat{J}_{v,Cdiag0\_17\_fR}(t) \cdot \dot{q}_{R_{Hr}}(t) \cdot \Delta t_{1\_RFFSSP} - \hat{J}_{v,Cdiag0\_17\_fR}(t) \cdot \dot{q}_{R_{Hr}}(t) \cdot \frac{\Delta t_{1\_RFFSSP}^2}{2} \end{array} \right]^T \\
&\cdot \widehat{W}_{RFFSSP\_or,17} \cdot \hat{J}_{v,Cdiag0\_17\_fR}(t) \cdot \frac{\Delta t_{1\_RFFSSP}^2}{2} - \\
&\left[ \bar{q}_{R_{Hr}}(t) - \bar{q}_{R_{Hr}0} \right]^T \cdot \widehat{W}_{RFFSSP\_qR_{Hr}} \cdot \frac{\Delta t_{1\_RFFSSP}^2}{2} - \\
&\dot{q}_{R_{Hr}}(t)^T \cdot \widehat{W}_{RFFSSP\_qR_{Hr}} \cdot \frac{\Delta t_{1\_RFFSSP}^3}{2} \quad (5.9)
\end{aligned}$$

$$\begin{aligned}
\hat{Z}_{RFFSSP,1} = & \\
& \hat{W}_{RFFSSP\_qR\_Hrdd} + \hat{W}_{RFFSSP\_qR\_Hr} \cdot \frac{\Delta t_{1\_RFFSSP}^4}{4} + \\
& \hat{J}_{v,17\_fR_V}(t)^T \cdot \hat{W}_{RFFSSP\_P,17} \cdot \hat{J}_{v,17\_fR_V}(t) \cdot \frac{\Delta t_{1\_RFFSSP}^4}{4} + \\
& \hat{J}_{v,Cdiag0\_17\_fR}(t)^T \cdot \hat{W}_{RFFSSP\_OR,17} \cdot \hat{J}_{v,Cdiag0\_17\_fR}(t) \cdot \frac{\Delta t_{1\_RFFSSP}^4}{4} + \\
& \hat{J}_{v,17\_fR}(t)^T \cdot \hat{W}_{RFFSSP\_v,17} \cdot \hat{J}_{v,17\_fR}(t) \cdot \Delta t_{1\_RFFSSP}^2
\end{aligned} \tag{5.10}$$

$\hat{W}_{RFFSSP\_P,17}$ ,  $\hat{W}_{RFFSSP\_OR,17}$ ,  $\hat{W}_{RFFSSP\_v,17}$ ,  $\hat{W}_{RFFSSP\_qR\_Hr}$  and  $\hat{W}_{RFFSSP\_qR\_Hrdd}$  are diagonal matrices with weighting coefficients.

With derived expression, optimum command accelerations for joint space variables from Body 3 to Body 17 during RFFSSP can be calculated by equation (5.11):

$$\ddot{q}_{R\_Hr_c}(t) = \left[ \bar{G}_{RFFSSP,1} \cdot \hat{Z}_{RFFSSP,1}^{-1} \right]^T \tag{5.11}$$

#### 5.1.1.1.2. For Body 2 and the toe point of Body 2

##### 5.1.1.1.2.1. Definition of Variables

The same conventions and derivation procedures of the first step are implemented. However, several jacobian matrices are segmented using the definition of  $\bar{q}_{R\_L}$  in chapter 4 as shown below:

$$\begin{aligned}
\begin{bmatrix} \bar{V}_{tpL} \\ \bar{W}_2 \end{bmatrix} &= \begin{bmatrix} \hat{J}_{v,tpL\_R\_Hr_V} & \hat{J}_{v,tpL\_L\_H_V} \\ \hat{J}_{v,tpL\_R\_Hr_W} & \hat{J}_{v,tpL\_L\_H_W} \end{bmatrix} \begin{bmatrix} \dot{\bar{q}}_{R\_Hr} \\ \dot{\bar{q}}_{L\_H} \end{bmatrix} \\
\dot{\bar{C}}_{diag}^{(0,2)} &= \begin{bmatrix} \hat{J}_{v,Cdiag0\_2\_R\_Hr} & \hat{J}_{v,Cdiag0\_2\_L\_H} \end{bmatrix} \begin{bmatrix} \dot{\bar{q}}_{R\_Hr} \\ \dot{\bar{q}}_{L\_H} \end{bmatrix}
\end{aligned}$$

$t$  is the present phase time and  $\Delta t_{2\_RFFSSP}$  is the prediction time range used in the second step of optimum command accelerations calculation in RFFSSP.

$$\overline{\Delta P}_{RFFSSP\_tpL\_f} = \bar{P}_{tpL_r}(t + \Delta t_{2\_RFFSSP}) - \bar{P}_{tpL_a}(t + \Delta t_{2\_RFFSSP})$$

Using the truncated Taylor Expansion of  $\bar{P}_{tpL_a}(t + \Delta t_{2\_RFFSSP})$  and segmented jacobian matrices mentioned above,  $\overline{\Delta P}_{RFFSSP\_tpL\_f}$  can be expressed as shown below where optimum command accelerations ( $\ddot{q}_{R\_Hr_c}$ ) that are calculated in the first step and unknown joint space accelerations ( $\ddot{q}_{L\_H}$ ) are expressed in separate terms.

$$\begin{aligned} \overline{\Delta P}_{RFFSSP\_tpL\_f} = & \\ & \left[ \begin{array}{c} \bar{P}_{tpL_r}(t + \Delta t_{2\_RFFSSP}) - \bar{P}_{tpL_a}(t) - \hat{J}_{v,tpL_V}(t) \cdot \dot{\bar{q}}_{R\_L}(t) \cdot \Delta t_{2\_RFFSSP} \\ - \hat{J}_{v,tpL_V}(t) \cdot \dot{\bar{q}}_{R\_L}(t) \cdot \frac{\Delta t_{2\_RFFSSP}^2}{2} \end{array} \right] - \\ & \left[ \hat{J}_{v,tpL\_R\_Hr_V}(t) \cdot \ddot{q}_{R\_Hr_c}(t) + \hat{J}_{v,tpL\_L\_H_V}(t) \cdot \ddot{q}_{L\_H}(t) \right] \frac{\Delta t_{2\_RFFSSP}^2}{2} \end{aligned} \quad (5.12)$$

The similar procedure is applied for other definitions.

$$\overline{\Delta v}_{RFFSSP\_2\_f} = \bar{v}_{2_r}(t + \Delta t_{2\_RFFSSP}) - \bar{v}_{2_a}(t + \Delta t_{2\_RFFSSP}), \text{ for}$$

$$\bar{v}_2(t + \Delta t_{2\_RFFSSP}) = \begin{bmatrix} \bar{V}_{tpL}(t + \Delta t_{2\_RFFSSP}) \\ \bar{w}_2(t + \Delta t_{2\_RFFSSP}) \end{bmatrix}$$

Then,

$$\begin{aligned} \overline{\Delta v}_{RFFSSP\_2\_f} = & \\ & \left[ \bar{v}_{2_r}(t + \Delta t_{2\_RFFSSP}) - \hat{J}_{v,tpL}(t) \cdot \dot{\bar{q}}_{R\_L}(t) - \hat{J}_{v,tpL}(t) \cdot \dot{\bar{q}}_{R\_L}(t) \cdot \Delta t_{2\_RFFSSP} \right] - \\ & \left[ \hat{J}_{v,tpL\_R\_Hr}(t) \cdot \ddot{q}_{R\_Hr_c}(t) + \hat{J}_{v,tpL\_L\_H}(t) \cdot \ddot{q}_{L\_H}(t) \right] \Delta t_{2\_RFFSSP} \end{aligned} \quad (5.13)$$

$$\text{For } \overline{\Delta OR}_{RFFSSP\_2\_f} = \bar{C}_{diag_r}^{(0,2)}(t + \Delta t_{2\_RFFSSP}) - \bar{C}_{diag_a}^{(0,2)}(t + \Delta t_{2\_RFFSSP}),$$

$$\begin{aligned} \overline{\Delta OR}_{RFFSSP\_2\_f} = & \\ & \left[ \begin{array}{c} \bar{C}_{diag_r}^{(0,2)}(t + \Delta t_{2\_RFFSSP}) - \bar{C}_{diag_a}^{(0,2)}(t) - \hat{J}_{v,Cdiag0\_2}(t) \cdot \dot{\bar{q}}_{R\_L}(t) \cdot \Delta t_{2\_RFFSSP} \\ - \hat{J}_{v,Cdiag0\_2}(t) \cdot \dot{\bar{q}}_{R\_L}(t) \cdot \frac{\Delta t_{2\_RFFSSP}^2}{2} \end{array} \right] \\ & - \left[ \hat{J}_{v,Cdiag0\_2\_R\_Hr}(t) \cdot \ddot{q}_{R\_Hr_c}(t) + \hat{J}_{v,Cdiag0\_2\_L\_H}(t) \cdot \ddot{q}_{L\_H}(t) \right] \frac{\Delta t_{2\_RFFSSP}^2}{2} \end{aligned} \quad (5.14)$$

$\overline{\Delta q}_{RFFSSP\_L\_H\_f} = \bar{q}_{L\_H\_a}(t + \Delta t_{2\_RFFSSP}) - \bar{q}_{L\_H_0}$ , where  $\bar{q}_{L\_H_0}$  is the vector of basic joint space positions for  $\bar{q}_{L\_H}$ . Initial values of  $\bar{q}_{L\_H}$  are used as  $\bar{q}_{L\_H_0}$ . So,  $\bar{q}_{L\_H_0}$  is taken as a vector with zero components only in the simulation.

Then,

$$\overline{\Delta q}_{RFFSSP\_L\_H\_f} = \bar{q}_{L\_H}(t) + \dot{\bar{q}}_{L\_H}(t) \cdot \Delta t_{2\_RFFSSP} + \ddot{\bar{q}}_{L\_H}(t) \cdot \frac{\Delta t_{2\_RFFSSP}^2}{2} - \bar{q}_{L\_H_0} \quad (5.15)$$

$\theta_4$  and  $\dot{\theta}_4$  being different from zero is penalized by using expressions shown below in the cost function.

$$\Delta \theta_4 = \theta_4(t) = \bar{\varphi}_{\theta_4} \cdot \bar{q}_{L\_H}(t) + \bar{\varphi}_{\theta_4} \cdot \dot{\bar{q}}_{L\_H}(t) \cdot \Delta t_{3\_RFFSSP} + \bar{\varphi}_{\theta_4} \cdot \ddot{\bar{q}}_{L\_H}(t) \cdot \frac{\Delta t_{3\_RFFSSP}^2}{2} \quad (5.16)$$

$$\Delta \dot{\theta}_4 = \dot{\theta}_4(t) = \bar{\varphi}_{\theta_4} \cdot \dot{\bar{q}}_{L\_H}(t) + \bar{\varphi}_{\theta_4} \cdot \ddot{\bar{q}}_{L\_H}(t) \cdot \Delta t_{3\_RFFSSP} \quad (5.17)$$

The cost function for the second step of optimum command accelerations calculation in RFFSSP is defined as shown below:

$$\begin{aligned} C_{RFFSSP,2} = & \\ & \frac{1}{2} \overline{\Delta P}_{RFFSSP\_tpL\_f}^T \cdot \widehat{W}_{RFFSSP\_P,tpL} \cdot \overline{\Delta P}_{RFFSSP\_tpL\_f} + \\ & \frac{1}{2} \overline{\Delta OR}_{RFFSSP\_2\_f}^T \cdot \widehat{W}_{RFFSSP\_OR,2} \cdot \overline{\Delta OR}_{RFFSSP\_2\_f} + \\ & \frac{1}{2} \overline{\Delta v}_{RFFSSP\_2\_f}^T \cdot \widehat{W}_{RFFSSP\_v,2} \cdot \overline{\Delta v}_{RFFSSP\_2\_f} + \\ & \frac{1}{2} \overline{\Delta q}_{RFFSSP\_L\_H\_f}^T \cdot \widehat{W}_{RFFSSP\_qL\_H} \cdot \overline{\Delta q}_{RFFSSP\_L\_H\_f} + \frac{1}{2} \Delta \theta_4 \cdot W_{P,\theta_4} \cdot \Delta \theta_4 + \\ & \frac{1}{2} \Delta \dot{\theta}_4 \cdot W_{V,\theta_4} \cdot \Delta \dot{\theta}_4 + \frac{1}{2} \ddot{\bar{q}}_{L\_H}(t)^T \cdot \widehat{W}_{RFFSSP\_qL\_Hdd} \cdot \ddot{\bar{q}}_{L\_H}(t) \end{aligned} \quad (5.18)$$

### 5.1.1.1.2.2. Calculation Procedure

$$\text{For optimum cost value, } \frac{\partial C_{RFFSSP,2}}{\partial \ddot{q}_{L,H}} = 0, \quad (5.19)$$

optimum command accelerations can be calculated. The equation (5.19) can be converted into the form:

$$\ddot{q}_{L,H}^T \hat{Z}_{RFFSSP,2} = \bar{G}_{RFFSSP,2} \quad (5.20)$$

Components of the equation (5.20) are as shown below:

$$\begin{aligned} \bar{G}_{RFFSSP,2} = & \left[ \begin{array}{c} \bar{P}_{tpL_r}(t + \Delta t_{2\_RFFSSP}) - \bar{P}_{tpL_a}(t) - \hat{J}_{v,tpL_v}(t) \cdot \dot{\bar{q}}_{R,L}(t) \cdot \Delta t_{2\_RFFSSP} \\ - \hat{J}_{v,tpL_v}(t) \cdot \dot{\bar{q}}_{R,L}(t) \cdot \frac{\Delta t_{2\_RFFSSP}^2}{2} \end{array} \right]^T \\ & \cdot \hat{W}_{RFFSSP\_P,tpL} \cdot \hat{J}_{v,tpL\_L,H_v}(t) \cdot \frac{\Delta t_{2\_RFFSSP}^2}{2} \\ & - \ddot{q}_{R\_Hr_c}(t)^T \cdot \hat{J}_{v,tpL\_R\_Hr_v}(t)^T \cdot \hat{W}_{RFFSSP\_P,tpL} \cdot \hat{J}_{v,tpL\_L,H_v}(t) \cdot \frac{\Delta t_{2\_RFFSSP}^4}{4} \\ & + \left[ \begin{array}{c} \bar{v}_{2_r}(t + \Delta t_{2\_RFFSSP}) - \hat{J}_{v,tpL}(t) \cdot \dot{\bar{q}}_{R,L}(t) \\ - \hat{J}_{v,tpL}(t) \cdot \dot{\bar{q}}_{R,L}(t) \cdot \Delta t_{2\_RFFSSP} \end{array} \right]^T \cdot \hat{W}_{RFFSSP\_v,2} \cdot \hat{J}_{v,tpL\_L,H}(t) \cdot \Delta t_{2\_RFFSSP} \\ & - \ddot{q}_{R\_Hr_c}(t)^T \cdot \hat{J}_{v,tpL\_R\_Hr}(t)^T \cdot \hat{W}_{RFFSSP\_v,2} \cdot \hat{J}_{v,tpL\_L,H}(t) \cdot \Delta t_{2\_RFFSSP}^2 \\ & + \left[ \begin{array}{c} \bar{C}_{diag_r}^{(0,2)}(t + \Delta t_{2\_RFFSSP}) - \bar{C}_{diag_a}^{(0,2)}(t) \\ - \hat{J}_{v,cdiag0\_2}(t) \cdot \dot{\bar{q}}_{R,L}(t) \cdot \Delta t_{2\_RFFSSP} - \hat{J}_{v,cdiag0\_2}(t) \cdot \dot{\bar{q}}_{R,L}(t) \cdot \frac{\Delta t_{2\_RFFSSP}^2}{2} \end{array} \right]^T \\ & \cdot \hat{W}_{RFFSSP\_OR,2} \cdot \hat{J}_{v,cdiag0\_2\_L,H}(t) \cdot \frac{\Delta t_{2\_RFFSSP}^2}{2} \\ & - \ddot{q}_{R\_Hr_c}(t)^T \cdot \hat{J}_{v,cdiag0\_2\_R\_Hr}(t)^T \cdot \hat{W}_{RFFSSP\_OR,2} \cdot \hat{J}_{v,cdiag0\_2\_L,H}(t) \cdot \frac{\Delta t_{2\_RFFSSP}^4}{4} \\ & - [\bar{q}_{L,H}(t) - \bar{q}_{L,H_0}]^T \cdot \hat{W}_{RFFSSP\_qL,H} \cdot \frac{\Delta t_{2\_RFFSSP}^2}{2} \\ & - \dot{\bar{q}}_{L,H}(t)^T \cdot \hat{W}_{RFFSSP\_qL,H} \cdot \frac{\Delta t_{2\_RFFSSP}^3}{2} - \bar{q}_{L,H}(t)^T \cdot \bar{\Phi}_{\theta_4}^T \cdot W_{P,\theta_4} \cdot \bar{\Phi}_{\theta_4} \cdot \frac{\Delta t_{3\_RFFSSP}^2}{2} \\ & - \dot{\bar{q}}_{L,H}(t)^T \cdot \bar{\Phi}_{\theta_4}^T \cdot W_{P,\theta_4} \cdot \bar{\Phi}_{\theta_4} \cdot \frac{\Delta t_{3\_RFFSSP}^3}{2} - \dot{\bar{q}}_{L,H}(t)^T \cdot \bar{\Phi}_{\theta_4}^T \cdot W_{V,\theta_4} \cdot \bar{\Phi}_{\theta_4} \cdot \Delta t_{3\_RFFSSP} \end{aligned} \quad (5.21)$$

$$\begin{aligned}
\hat{Z}_{RFFSSP,2} = & \\
& \hat{W}_{RFFSSP\_qL\_Hdd} + \hat{W}_{RFFSSP\_qL\_H} \cdot \frac{\Delta t_{2\_RFFSSP}^4}{4} + \\
& \hat{J}_{v,tpL\_L\_H_V}(t)^T \cdot \hat{W}_{RFFSSP\_P,tpL} \cdot \hat{J}_{v,tpL\_L\_H_V}(t) \cdot \frac{\Delta t_{2\_RFFSSP}^4}{4} + \\
& \hat{J}_{v,Cdiag0\_2\_L\_H}(t)^T \cdot \hat{W}_{RFFSSP\_OR,2} \cdot \hat{J}_{v,Cdiag0\_2\_L\_H}(t) \cdot \frac{\Delta t_{2\_RFFSSP}^4}{4} + \\
& \hat{J}_{v,tpL\_L\_H}(t)^T \cdot \hat{W}_{RFFSSP\_v,2} \cdot \hat{J}_{v,tpL\_L\_H}(t) \cdot \Delta t_{2\_RFFSSP}^2 + \\
& \bar{\Phi}_{\theta_4}^T \cdot W_{P,\theta_4} \cdot \bar{\Phi}_{\theta_4} \cdot \frac{\Delta t_{3\_RFFSSP}^4}{4} + \bar{\Phi}_{\theta_4}^T \cdot W_{V,\theta_4} \cdot \bar{\Phi}_{\theta_4} \cdot \Delta t_{3\_RFFSSP}^2 \tag{5.22}
\end{aligned}$$

$\hat{W}_{RFFSSP\_P,tpL}$ ,  $\hat{W}_{RFFSSP\_OR,2}$ ,  $\hat{W}_{RFFSSP\_v,2}$ ,  $\hat{W}_{RFFSSP\_qL\_H}$ ,  $W_{P,\theta_4}$ ,  $W_{V,\theta_4}$  and  $\hat{W}_{RFFSSP\_qL\_Hdd}$  are weighting coefficients or diagonal matrices with weighting coefficients.

With derived expression, optimum command accelerations from Body 17 to Body 2 for RFFSSP can be calculated by equation (5.23):

$$\ddot{q}_{L_Hc}(t) = \left[ \bar{G}_{RFFSSP,2} \cdot \hat{Z}_{RFFSSP,2}^{-1} \right]^T \tag{5.23}$$

### 5.1.1.2. For LFFSSP

Similar to RFFSSP, calculation of optimum command accelerations during LFFSSP is accomplished in 2 steps. In the first step, optimum command accelerations for joint space variables from Body 4 to Body 17 are calculated according to given reference inputs for Body 17 and its mass center. In the second step, optimum command accelerations for joint space variables from Body 17 to Body 1 are calculated according to determined joint space accelerations in the first step and given reference inputs for Body 1 and its toe point. Command acceleration  $\ddot{\theta}_{4c}$  is taken as zero by considering the assumption that Body 4 is rigidly fixed to the ground. Since the calculation procedure and the convention is the same as RFFSSP's, only the final form of equations are included.

### 5.1.1.2.1. For Body 17 and the mass center of Body 17

#### 5.1.1.2.1.1. Definition of Variables

$t$  is the present phase time and  $\Delta t_{1\_LFFSSP}$  is the prediction time range used in the first step of optimum command acceleration calculations in LFFSSP.

$$\overline{\Delta P}_{LFFSSP\_c,17\_f} = \bar{P}_{c,17_r}(t + \Delta t_{1\_LFFSSP}) - \bar{P}_{c,17_a}(t + \Delta t_{1\_LFFSSP})$$

Using the truncated Taylor Expansion of  $\bar{P}_{c,17_a}(t + \Delta t_{1\_LFFSSP})$  and the definition of  $\bar{q}_{L\_Hr}$  by equation (4.16):

$$\begin{aligned} \overline{\Delta P}_{LFFSSP\_c,17\_f} = & \\ & \bar{P}_{c,17_r}(t + \Delta t_{1\_LFFSSP}) - \bar{P}_{c,17_a}(t) - \hat{J}_{v,17\_fL_V}(t) \cdot \dot{\bar{q}}_{L\_Hr}(t) \cdot \Delta t_{1\_LFFSSP} - \\ & \hat{J}_{v,17\_fL_V}(t) \cdot \dot{\bar{q}}_{L\_Hr}(t) \cdot \frac{\Delta t_{1\_LFFSSP}^2}{2} - \hat{J}_{v,17\_fL_V}(t) \cdot \ddot{\bar{q}}_{L\_Hr}(t) \cdot \frac{\Delta t_{1\_LFFSSP}^2}{2} \end{aligned} \quad (5.24)$$

The same convention and procedure are used for other definitions.

$$\overline{\Delta v}_{LFFSSP\_17\_f} = \bar{v}_{17_r}(t + \Delta t_{1\_LFFSSP}) - \bar{v}_{17_a}(t + \Delta t_{1\_LFFSSP}), \text{ for}$$

$$\bar{v}_{17}(t + \Delta t_{1\_LFFSSP}) = \begin{bmatrix} \bar{V}_{c,17}(t + \Delta t_{1\_LFFSSP}) \\ \bar{W}_{17}(t + \Delta t_{1\_LFFSSP}) \end{bmatrix}$$

Then,

$$\begin{aligned} \overline{\Delta v}_{LFFSSP\_17\_f} = & \\ & \bar{v}_{17_r}(t + \Delta t_{1\_LFFSSP}) - \hat{J}_{v,17\_fL}(t) \cdot \dot{\bar{q}}_{L\_Hr}(t) - \hat{J}_{v,17\_fL}(t) \cdot \dot{\bar{q}}_{L\_Hr}(t) \cdot \Delta t_{1\_LFFSSP} - \\ & \hat{J}_{v,17\_fL}(t) \cdot \ddot{\bar{q}}_{L\_Hr}(t) \cdot \Delta t_{1\_LFFSSP} \end{aligned} \quad (5.25)$$

For

$$\overline{\Delta OR}_{LFFSSP\_17\_f} = \bar{C}_{diag_r}^{(0,17)}(t + \Delta t_{1\_LFFSSP}) - \bar{C}_{diag_a}^{(0,17)}(t + \Delta t_{1\_LFFSSP}),$$

$$\begin{aligned}
\overline{\Delta OR}_{LFFSSP\_17\_f} = & \\
\bar{C}_{diag_r}^{(0,17)}(t + \Delta t_{1\_LFFSSP}) - \bar{C}_{diag_a}^{(0,17)}(t) - & \\
\hat{J}_{v,Cdiag0\_17\_fL}(t) \cdot \dot{\bar{q}}_{L\_Hr}(t) \cdot \Delta t_{1\_LFFSSP} - \hat{J}_{v,Cdiag0\_17\_fL}(t) \cdot \dot{\bar{q}}_{L\_Hr}(t) \cdot \frac{\Delta t_{1\_LFFSSP}^2}{2} - & \\
\hat{J}_{v,Cdiag0\_17\_fL}(t) \cdot \ddot{\bar{q}}_{L\_Hr}(t) \cdot \frac{\Delta t_{1\_LFFSSP}^2}{2} & \quad (5.26)
\end{aligned}$$

$\overline{\Delta q}_{LFFSSP\_R\_Hr\_f} = \bar{q}_{L\_Hr}(t + \Delta t_{1\_LFFSSP}) - \bar{q}_{L\_Hr0}$ , where  $\bar{q}_{L\_Hr0}$  is taken as a vector with zero components only.

Then,

$$\overline{\Delta q}_{LFFSSP\_L\_Hr\_f} = \bar{q}_{L\_Hr}(t) + \dot{\bar{q}}_{L\_Hr}(t) \cdot \Delta t_{1\_LFFSSP} + \ddot{\bar{q}}_{L\_Hr}(t) \cdot \frac{\Delta t_{1\_LFFSSP}^2}{2} - \bar{q}_{L\_Hr0} \quad (5.27)$$

The cost function for the first step of optimum command accelerations calculation in LFFSSP is defined as shown below:

$$\begin{aligned}
C_{LFFSSP,1} = & \\
\frac{1}{2} \overline{\Delta P}_{LFFSSP\_c,17\_f}^T \cdot \widehat{W}_{LFFSSP\_P,17} \cdot \overline{\Delta P}_{LFFSSP\_c,17\_f} + & \\
\frac{1}{2} \overline{\Delta OR}_{LFFSSP\_17\_f}^T \cdot \widehat{W}_{LFFSSP\_OR,17} \cdot \overline{\Delta OR}_{LFFSSP\_17\_f} + & \\
\frac{1}{2} \overline{\Delta v}_{LFFSSP\_17\_f}^T \cdot \widehat{W}_{LFFSSP\_v,17} \cdot \overline{\Delta v}_{LFFSSP\_17\_f} + & \\
\frac{1}{2} \overline{\Delta q}_{LFFSSP\_L\_Hr\_f}^T \cdot \widehat{W}_{LFFSSP\_qL\_Hr} \cdot \overline{\Delta q}_{LFFSSP\_L\_Hr\_f} + & \\
\frac{1}{2} \ddot{\bar{q}}_{L\_Hr}(t)^T \cdot \widehat{W}_{LFFSSP\_qL\_Hrdd} \cdot \ddot{\bar{q}}_{L\_Hr}(t) & \quad (5.28)
\end{aligned}$$

### 5.1.1.2.1.2. Calculation Procedure

$$\text{For optimum cost value } \frac{\partial C_{LFFSSP,1}}{\partial \ddot{\bar{q}}_{L\_Hr}} = 0, \quad (5.29)$$

optimum command accelerations can be calculated. The equation (5.29) can be converted into the form  $\ddot{\bar{q}}_{L\_Hr}^T \hat{Z}_{LFFSSP,1} = \bar{G}_{LFFSSP,1}$ .

Therefore,

$$\begin{aligned}
\frac{\partial C_{LFFSSP,1}}{\partial \ddot{q}_{L, Hr}} &= \overline{\Delta P}_{LFFSSP\_c,17\_f}^T \cdot \widehat{W}_{LFFSSP\_P,17} \cdot \left[ -\hat{J}_{v,17\_fL_V}(t) \cdot \frac{\Delta t_{1\_LFFSSP}^2}{2} \right] + \\
\overline{\Delta OR}_{LFFSSP\_17\_f}^T \cdot \widehat{W}_{LFFSSP\_OR,17} \cdot \left[ -\hat{J}_{v,Cdiag0\_17\_fL}(t) \cdot \frac{\Delta t_{1\_LFFSSP}^2}{2} \right] + \\
\overline{\Delta v}_{LFFSSP\_17\_f}^T \cdot \widehat{W}_{LFFSSP\_v,17} \cdot \left[ -\hat{J}_{v,17\_fL}(t) \cdot \ddot{q}_{L, Hr}(t) \cdot \Delta t_{1\_LFFSSP} \right] + \\
\overline{\Delta q}_{LFFSSP\_L, Hr\_f}^T \cdot \widehat{W}_{LFFSSP\_qL, Hr} \cdot \frac{\Delta t_{1\_LFFSSP}^2}{2} + \ddot{q}_{L, Hr}(t)^T \cdot \widehat{W}_{LFFSSP\_qL, Hrdd} \quad (5.30)
\end{aligned}$$

After inserting derived expressions of  $\overline{\Delta P}_{LFFSSP\_c,17\_f}$ ,  $\overline{\Delta OR}_{LFFSSP\_17\_f}$ ,  $\overline{\Delta v}_{LFFSSP\_17\_f}$  and  $\overline{\Delta q}_{LFFSSP\_L, Hr\_f}$  which are equation (5.24), (5.25), (5.26) and (5.27) into equation (5.31), the equation can be expressed as:

$$\ddot{q}_{L, Hr}^T \hat{Z}_{LFFSSP,1} = \bar{G}_{LFFSSP,1} \quad (5.31)$$

Components of the equation (5.31) are determined such as:

$$\begin{aligned}
&\bar{G}_{LFFSSP,1} \\
&= \left[ \begin{array}{c} \bar{P}_{c,17_r}(t + \Delta t_{1\_LFFSSP}) - \bar{P}_{c,17_a}(t) - \hat{J}_{v,17\_fL_V}(t) \cdot \ddot{q}_{L, Hr}(t) \cdot \Delta t_{1\_LFFSSP} \\ -\hat{J}_{v,17\_fL_V}(t) \cdot \ddot{q}_{L, Hr}(t) \cdot \frac{\Delta t_{1\_LFFSSP}^2}{2} \end{array} \right]^T \\
&\cdot \widehat{W}_{LFFSSP\_P,17} \cdot \hat{J}_{v,17\_fL_V}(t) \cdot \frac{\Delta t_{1\_LFFSSP}^2}{2} \\
&+ \left[ \begin{array}{c} \bar{v}_{17_r}(t + \Delta t_{1\_LFFSSP}) - \hat{J}_{v,17\_fL}(t) \cdot \ddot{q}_{L, Hr}(t) \\ -\hat{J}_{v,17\_fL}(t) \cdot \ddot{q}_{L, Hr}(t) \cdot \Delta t_{1\_LFFSSP} \end{array} \right]^T \cdot \widehat{W}_{LFFSSP\_v,17} \cdot \hat{J}_{v,17\_fL}(t) \cdot \Delta t_{1\_LFFSSP} \\
&+ \left[ \begin{array}{c} \bar{C}_{diag_r}^{(0,17)}(t + \Delta t_{1\_LFFSSP}) - \bar{C}_{diag_a}^{(0,17)}(t) \\ -\hat{J}_{v,Cdiag0\_17\_fL}(t) \cdot \ddot{q}_{L, Hr}(t) \cdot \Delta t_{1\_LFFSSP} - \hat{J}_{v,Cdiag0\_17\_fL}(t) \cdot \ddot{q}_{L, Hr}(t) \cdot \frac{\Delta t_{1\_LFFSSP}^2}{2} \end{array} \right]^T \\
&\cdot \widehat{W}_{LFFSSP\_OR,17} \cdot \hat{J}_{v,Cdiag0\_17\_fL}(t) \cdot \frac{\Delta t_{1\_LFFSSP}^2}{2} - \\
&[\bar{q}_{L, Hr}(t) - \bar{q}_{L, Hr_0}]^T \cdot \widehat{W}_{LFFSSP\_qL, Hr} \cdot \frac{\Delta t_{1\_LFFSSP}^2}{2} - \\
&\ddot{q}_{L, Hr}(t)^T \cdot \widehat{W}_{LFFSSP\_qL, Hr} \cdot \frac{\Delta t_{1\_LFFSSP}^3}{2} \quad (5.32)
\end{aligned}$$

$$\begin{aligned}
\hat{Z}_{LFFSSP,1} = & \\
& \hat{W}_{LFFSSP\_qL\_Hrdd} + \hat{W}_{LFFSSP\_qL\_Hr} \cdot \frac{\Delta t_{1\_LFFSSP}^4}{4} + \\
& \hat{J}_{v,17\_fL_V}(t)^T \cdot \hat{W}_{LFFSSP\_P,17} \cdot \hat{J}_{v,17\_fL_V}(t) \cdot \frac{\Delta t_{1\_LFFSSP}^4}{4} + \\
& \hat{J}_{v,Cdiag0\_17\_fL}(t)^T \cdot \hat{W}_{LFFSSP\_OR,17} \cdot \hat{J}_{v,Cdiag0\_17\_fL}(t) \cdot \frac{\Delta t_{1\_LFFSSP}^4}{4} + \\
& \hat{J}_{v,17\_fL}(t)^T \cdot \hat{W}_{LFFSSP\_v,17} \cdot \hat{J}_{v,17\_fL}(t) \cdot \Delta t_{1\_LFFSSP}^2
\end{aligned} \tag{5.33}$$

$\hat{W}_{LFFSSP\_P,17}$ ,  $\hat{W}_{LFFSSP\_OR,17}$ ,  $\hat{W}_{LFFSSP\_v,17}$ ,  $\hat{W}_{LFFSSP\_qL\_Hr}$  and  $\hat{W}_{LFFSSP\_qL\_Hrdd}$  are diagonal matrices with weighting coefficients.

With derived expression, optimum command accelerations from Body 4 to Body 17 for LFFSSP can be calculated by equation (5.34):

$$\ddot{\bar{q}}_{L\_Hr_c}(t) = \left[ \bar{G}_{LFFSSP,1} \cdot \hat{Z}_{LFFSSP,1}^{-1} \right]^T \tag{5.34}$$

### 5.1.1.2.2. For Body 1 and the toe point of Body 1

#### 5.1.1.2.2.1. Definition of Variables

The same conventions and derivation procedures of the first step are implemented. However, several jacobian matrices are segmented using the definition of  $\bar{q}_{L\_R}$  in chapter 4 as shown below:

$$\begin{aligned}
\begin{bmatrix} \bar{V}_{tpR} \\ \bar{W}_1 \end{bmatrix} &= \begin{bmatrix} \hat{J}_{v,tpL\_L\_Hr_V} & \hat{J}_{v,tpL\_R\_H_V} \\ \hat{J}_{v,tpL\_L\_Hr_w} & \hat{J}_{v,tpL\_R\_H_w} \end{bmatrix} \begin{bmatrix} \dot{\bar{q}}_{L\_Hr} \\ \dot{\bar{q}}_{R\_H} \end{bmatrix} \\
\dot{\bar{C}}_{diag}^{(0,1)} &= \begin{bmatrix} \hat{J}_{v,Cdiag0\_1\_L\_Hr} & \hat{J}_{v,Cdiag0\_1\_R\_H} \end{bmatrix} \begin{bmatrix} \dot{\bar{q}}_{L\_Hr} \\ \dot{\bar{q}}_{R\_H} \end{bmatrix}
\end{aligned}$$

$t$  is the present phase time and  $\Delta t_{2\_LFFSSP}$  is the prediction time range used in the second step of optimum command acceleration calculation in LFFSSP.

$$\overline{\Delta P}_{LFFSSP\_tpR\_f} = \bar{P}_{tpR_r}(t + \Delta t_{2\_LFFSSP}) - \bar{P}_{tpR_a}(t + \Delta t_{2\_LFFSSP})$$

Using the truncated Taylor Expansion of  $\bar{P}_{tpR_a}(t + \Delta t_{2\_LFFSSP})$  and segmented jacobian matrices mentioned above,  $\overline{\Delta P}_{LFFSSP\_tpR\_f}$  can be expressed as shown below where optimum command accelerations ( $\ddot{q}_{L\_Hr_c}$ ) that are calculated in the first step and unknown joint space accelerations ( $\ddot{q}_{R\_H}$ ) are expressed in separate terms.

$$\begin{aligned} \overline{\Delta P}_{LFFSSP\_tpR\_f} = & \\ & \left[ \begin{array}{l} \bar{P}_{tpR_r}(t + \Delta t_{2\_LFFSSP}) - \bar{P}_{tpR_a}(t) - \hat{J}_{v,tpR_V}(t) \cdot \dot{\bar{q}}_{L\_R}(t) \cdot \Delta t_{2\_LFFSSP} \\ - \hat{J}_{v,tpR_V}(t) \cdot \dot{\bar{q}}_{L\_R}(t) \cdot \frac{\Delta t_{2\_LFFSSP}^2}{2} \end{array} \right] - \\ & \left[ \hat{J}_{v,tpR\_L\_Hr_V}(t) \cdot \ddot{q}_{L\_Hr_c}(t) + \hat{J}_{v,tpR\_R\_H_V}(t) \cdot \ddot{q}_{R\_H}(t) \right] \frac{\Delta t_{2\_LFFSSP}^2}{2} \end{aligned} \quad (5.35)$$

Applying the similar procedure for other definitions:

$$\overline{\Delta v}_{LFFSSP\_1\_f} = \bar{v}_{1_r}(t + \Delta t_{2\_LFFSSP}) - \bar{v}_{1_a}(t + \Delta t_{2\_LFFSSP}), \text{ for}$$

$$\bar{v}_1(t + \Delta t_{2\_LFFSSP}) = \begin{bmatrix} \bar{V}_{tpR}(t + \Delta t_{2\_LFFSSP}) \\ \bar{w}_1(t + \Delta t_{2\_LFFSSP}) \end{bmatrix}$$

$$\begin{aligned} \overline{\Delta v}_{LFFSSP\_1\_f} = & \\ & \left[ \begin{array}{l} \bar{v}_{1_r}(t + \Delta t_{2\_LFFSSP}) - \hat{J}_{v,tpR}(t) \cdot \dot{\bar{q}}_{L\_R}(t) - \hat{J}_{v,tpR}(t) \cdot \dot{\bar{q}}_{L\_R}(t) \cdot \Delta t_{2\_LFFSSP} \\ \left[ \hat{J}_{v,tpR\_L\_Hr}(t) \cdot \ddot{q}_{L\_Hr_c}(t) + \hat{J}_{v,tpR\_R\_H}(t) \cdot \ddot{q}_{R\_H}(t) \right] \Delta t_{2\_LFFSSP} \end{array} \right] \end{aligned} \quad (5.36)$$

$$\text{For } \overline{\Delta OR}_{LFFSSP\_1\_f} = \bar{C}_{diag_r}^{(0,1)}(t + \Delta t_{2\_LFFSSP}) - \bar{C}_{diag_a}^{(0,1)}(t + \Delta t_{2\_LFFSSP}),$$

$$\begin{aligned} \overline{\Delta OR}_{LFFSSP\_1\_f} = & \\ & \left[ \begin{array}{l} \bar{C}_{diag_r}^{(0,1)}(t + \Delta t_{2\_LFFSSP}) - \bar{C}_{diag_a}^{(0,1)}(t) \\ - \hat{J}_{v,Cdiag0\_1}(t) \cdot \dot{\bar{q}}_{L\_R}(t) \cdot \Delta t_{2\_LFFSSP} - \hat{J}_{v,Cdiag0\_1}(t) \cdot \dot{\bar{q}}_{L\_R}(t) \cdot \frac{\Delta t_{2\_LFFSSP}^2}{2} \end{array} \right] - \\ & \left[ \hat{J}_{v,Cdiag0\_1\_L\_Hr}(t) \cdot \ddot{q}_{L\_Hr_c}(t) + \hat{J}_{v,Cdiag0\_1\_R\_H}(t) \cdot \ddot{q}_{R\_H}(t) \right] \frac{\Delta t_{2\_LFFSSP}^2}{2} \end{aligned} \quad (5.37)$$

$\overline{\Delta q}_{LFFSSP\_R\_H\_f} = \bar{q}_{R\_H_a}(t + \Delta t_{2\_LFFSSP}) - \bar{q}_{R\_H_0}$ , where  $\bar{q}_{R\_H_0}$  is taken as a vector with zero components only.

$$\overline{\Delta q}_{LFFSSP\_R\_H\_f} = \bar{q}_{R\_H}(t) + \dot{\bar{q}}_{R\_H}(t) \cdot \Delta t_{2\_LFFSSP} + \ddot{\bar{q}}_{R\_H}(t) \cdot \frac{\Delta t_{2\_LFFSSP}^2}{2} - \bar{q}_{R\_H0} \quad (5.38)$$

$\theta_3$  and  $\dot{\theta}_3$  being different from zero is penalized by using expressions shown below in the cost function.

$$\Delta \theta_3 = \theta_3(t) = \bar{\theta}_{\theta_3} \cdot \bar{q}_{R\_H}(t) + \bar{\theta}_{\theta_3} \cdot \dot{\bar{q}}_{R\_H}(t) \cdot \Delta t_{3\_LFFSSP} + \bar{\theta}_{\theta_3} \cdot \ddot{\bar{q}}_{R\_H}(t) \cdot \frac{\Delta t_{3\_LFFSSP}^2}{2} \quad (5.39)$$

$$\Delta \dot{\theta}_3 = \dot{\theta}_3(t) = \bar{\theta}_{\theta_3} \cdot \dot{\bar{q}}_{R\_H}(t) + \bar{\theta}_{\theta_3} \cdot \ddot{\bar{q}}_{R\_H}(t) \cdot \Delta t_{3\_LFFSSP} \quad (5.40)$$

The cost function for the second step of optimum command accelerations calculation in LFFSSP is defined as shown below:

$$\begin{aligned} C_{LFFSSP,2} = & \\ & \frac{1}{2} \overline{\Delta P}_{LFFSSP\_tpR\_f}^T \cdot \widehat{W}_{LFFSSP\_P,tpR} \cdot \overline{\Delta P}_{LFFSSP\_tpR\_f} + \\ & \frac{1}{2} \overline{\Delta OR}_{LFFSSP\_1\_f}^T \cdot \widehat{W}_{LFFSSP\_OR,1} \cdot \overline{\Delta OR}_{LFFSSP\_1\_f} + \\ & \frac{1}{2} \overline{\Delta v}_{LFFSSP\_1\_f}^T \cdot \widehat{W}_{LFFSSP\_v,1} \cdot \overline{\Delta v}_{LFFSSP\_1\_f} + \\ & \frac{1}{2} \overline{\Delta q}_{LFFSSP\_R\_H\_f}^T \cdot \widehat{W}_{LFFSSP\_qR\_H} \cdot \overline{\Delta q}_{LFFSSP\_R\_H\_f} + \frac{1}{2} \Delta \theta_3 \cdot W_{P,\theta_3} \cdot \Delta \theta_3 + \\ & \frac{1}{2} \Delta \dot{\theta}_3 \cdot W_{V,\theta_3} \cdot \Delta \dot{\theta}_3 + \frac{1}{2} \ddot{\bar{q}}_{R\_H}(t)^T \cdot \widehat{W}_{LFFSSP\_qR\_Hdd} \cdot \ddot{\bar{q}}_{R\_H}(t) \end{aligned} \quad (5.41)$$

#### 5.1.1.2.2.2. Calculation Procedure

$$\text{For optimum cost value, } \frac{\partial C_{LFFSSP,2}}{\partial \ddot{\bar{q}}_{R\_H}} = 0, \quad (5.42)$$

optimum command accelerations can be calculated. The equation (5.42) can be converted into the form:

$$\ddot{\bar{q}}_{R\_H}^T \hat{Z}_{LFFSSP,2} = \bar{G}_{LFFSSP,2} \quad (5.43)$$

Components of the equation (5.43) are shown by equation (5.44) and (5.45).

$$\begin{aligned}
\hat{Z}_{LFFSSP,2} = & \\
& \widehat{W}_{LFFSSP\_qR\_Hdd} + \widehat{W}_{LFFSSP\_qR\_H} \cdot \frac{\Delta t_{2\_LFFSSP}^4}{4} + \\
& \hat{J}_{v,tpR\_R\_H_V}(t)^T \cdot \widehat{W}_{LFFSSP\_P,tpR} \cdot \hat{J}_{v,tpR\_R\_H_V}(t) \cdot \frac{\Delta t_{2\_LFFSSP}^4}{4} + \\
& \hat{J}_{v,Cdiag0\_1\_R\_H}(t)^T \cdot \widehat{W}_{LFFSSP\_OR,1} \cdot \hat{J}_{v,Cdiag0\_1\_R\_H}(t) \cdot \frac{\Delta t_{2\_LFFSSP}^4}{4} + \\
& \hat{J}_{v,tpR\_R\_H}(t)^T \cdot \widehat{W}_{LFFSSP\_v,1} \cdot \hat{J}_{v,tpR\_R\_H}(t) \cdot \Delta t_{2\_LFFSSP}^2 + \\
& \bar{\Phi}_{\theta_3}^T \cdot W_{P,\theta_3} \cdot \bar{\Phi}_{\theta_3} \cdot \frac{\Delta t_{3\_LFFSSP}^4}{4} + \bar{\Phi}_{\theta_3}^T \cdot W_{V,\theta_3} \cdot \bar{\Phi}_{\theta_3} \cdot \Delta t_{3\_LFFSSP}^2 \tag{5.44}
\end{aligned}$$

$$\begin{aligned}
\bar{G}_{LFFSSP,2} = & \left[ \begin{array}{c} \bar{P}_{tpR_r}(t + \Delta t_{2\_LFFSSP}) - \bar{P}_{tpR_a}(t) - \hat{J}_{v,tpR_V}(t) \cdot \dot{\bar{q}}_{L_R}(t) \cdot \Delta t_{2\_LFFSSP} \\ - \hat{J}_{v,tpR_V}(t) \cdot \dot{\bar{q}}_{L_R}(t) \cdot \frac{\Delta t_{2\_LFFSSP}^2}{2} \end{array} \right]^T \\
& \cdot \widehat{W}_{LFFSSP\_P,tpR} \cdot \hat{J}_{v,tpR\_R\_H_V}(t) \cdot \frac{\Delta t_{2\_LFFSSP}^2}{2} \\
& - \ddot{\bar{q}}_{L\_Hr_c}(t)^T \cdot \hat{J}_{v,tpR\_L\_Hr_V}(t)^T \cdot \widehat{W}_{LFFSSP\_P,tpR} \cdot \hat{J}_{v,tpR\_R\_H_V}(t) \cdot \frac{\Delta t_{2\_LFFSSP}^4}{4} \\
& + \left[ \begin{array}{c} \bar{v}_{1_r}(t + \Delta t_{2\_LFFSSP}) - \hat{J}_{v,tpR}(t) \cdot \dot{\bar{q}}_{L_R}(t) \\ - \hat{J}_{v,tpR}(t) \cdot \dot{\bar{q}}_{L_R}(t) \cdot \Delta t_{2\_LFFSSP} \end{array} \right]^T \cdot \widehat{W}_{LFFSSP\_v,1} \cdot \hat{J}_{v,tpR\_R\_H}(t) \cdot \Delta t_{2\_LFFSSP} \\
& - \ddot{\bar{q}}_{L\_Hr_c}(t)^T \cdot \hat{J}_{v,tpR\_L\_Hr}(t)^T \cdot \widehat{W}_{LFFSSP\_v,1} \cdot \hat{J}_{v,tpR\_R\_H}(t) \cdot \Delta t_{2\_LFFSSP}^2 \\
& + \left[ \begin{array}{c} \bar{C}_{diag_r}^{(0,1)}(t + \Delta t_{2\_LFFSSP}) - \bar{C}_{diag_a}^{(0,1)}(t) \\ - \hat{J}_{v,Cdiag0\_1}(t) \cdot \dot{\bar{q}}_{L_R}(t) \cdot \Delta t_{2\_LFFSSP} - \hat{J}_{v,Cdiag0\_1}(t) \cdot \dot{\bar{q}}_{L_R}(t) \cdot \frac{\Delta t_{2\_LFFSSP}^2}{2} \end{array} \right]^T \\
& \cdot \widehat{W}_{LFFSSP\_OR,1} \cdot \hat{J}_{v,Cdiag0\_1\_R\_H}(t) \cdot \frac{\Delta t_{2\_LFFSSP}^2}{2} - \\
& \ddot{\bar{q}}_{L\_Hr_c}(t)^T \cdot \hat{J}_{v,Cdiag0\_1\_L\_Hr}(t)^T \cdot \widehat{W}_{LFFSSP\_OR,1} \cdot \hat{J}_{v,Cdiag0\_1\_R\_H}(t) \cdot \frac{\Delta t_{2\_LFFSSP}^4}{4} - \\
& [\bar{q}_{R_H}(t) - \bar{q}_{R_H0}]^T \cdot \widehat{W}_{LFFSSP\_qR\_H} \cdot \frac{\Delta t_{2\_LFFSSP}^2}{2} - \\
& \dot{\bar{q}}_{R_H}(t)^T \cdot \widehat{W}_{LFFSSP\_qR\_H} \cdot \frac{\Delta t_{2\_LFFSSP}^3}{2} - \bar{q}_{R_H}(t)^T \cdot \bar{\Phi}_{\theta_3}^T \cdot W_{P,\theta_3} \cdot \bar{\Phi}_{\theta_3} \cdot \frac{\Delta t_{3\_LFFSSP}^2}{2} - \\
& \dot{\bar{q}}_{R_H}(t)^T \cdot \bar{\Phi}_{\theta_3}^T \cdot W_{P,\theta_3} \cdot \bar{\Phi}_{\theta_3} \cdot \frac{\Delta t_{3\_LFFSSP}^3}{2} - \dot{\bar{q}}_{R_H}(t)^T \cdot \bar{\Phi}_{\theta_3}^T \cdot W_{V,\theta_3} \cdot \bar{\Phi}_{\theta_3} \cdot \Delta t_{3\_LFFSSP} \tag{5.45}
\end{aligned}$$

$\widehat{W}_{LFFSSP\_P,tpR}$ ,  $\widehat{W}_{LFFSSP\_OR,1}$ ,  $\widehat{W}_{LFFSSP\_v,1}$ ,  $\widehat{W}_{LFFSSP\_qR,H}$ ,  $W_{P,\theta_3}$ ,  $W_{V,\theta_3}$  and  $\widehat{W}_{LFFSSP\_qR,Hdd}$  are weighting coefficients or diagonal matrices with weighting coefficients.

With derived expression, optimum command accelerations from Body 17 to Body 1 for LFFSSP can be calculated by equation (5.46):

$$\ddot{q}_{R,H_c}(t) = \left[ \bar{G}_{LFFSSP,2} \cdot \hat{Z}_{LFFSSP,2}^{-1} \right]^T \quad (5.46)$$

### 5.1.1.3. For RFFDSP

Optimum command accelerations for joint space variables from Body 3 to Body 17 and from Body 2 to Body 17 are calculated according to given reference inputs for Body 17 and its mass center by defining 2 separate cost functions. In order to calculate feasible command accelerations, these cost functions are combined and subjected to kinematic constraint equations. Otherwise, physically unrealizable command accelerations produce inappropriate actuator torques from computed torque control block, which enforce bodies to move incompatibly with respect to kinematic constraints formed by closed kinematic chain. Then, inappropriate actuator torques calculated by computed torque control block cause unpredictable joint accelerations during the direct dynamic solution which ensures specified kinematic conditions as a part of the solution. Consequently, unpredictable joint space accelerations practically lead to blind or unconscious control of the biped system.

Optimum command accelerations for dropped joint space variables are taken as zero due to locomotion phase assumptions. Command acceleration  $\ddot{\theta}_{3_c}$  is taken as zero as similar to RFFSSP, since Body 3 is assumed to be rigidly fixed to the ground in RFFDSP too.

#### 5.1.1.3.1. Definition of Variables

$t$  is the present phase time and  $\Delta t_{RFFDSP}$  is the prediction time range used during the calculation of optimum command accelerations in RFFDSP.

$$\overline{\Delta P}_{RFFDSP\_c,17fR\_f} = \bar{P}_{c,17_r}(t + \Delta t_{RFFDSP}) - \bar{P}_{c,17\_fR\_a}(t + \Delta t_{RFFDSP})$$

Then,

$$\begin{aligned} \overline{\Delta P}_{RFFDSP\_c,17fR\_f} = & \\ & \bar{P}_{c,17_r}(t + \Delta t_{RFFDSP}) - \bar{P}_{c,17\_fR\_a}(t) - \hat{J}_{v,17\_fR_V}(t) \cdot \dot{\bar{q}}_{R\_Hr}(t) \cdot \Delta t_{RFFDSP} - \\ & \hat{J}_{v,17\_fR_V}(t) \cdot \dot{\bar{q}}_{R\_Hr}(t) \cdot \frac{\Delta t_{RFFDSP}^2}{2} - \hat{J}_{v,17\_fR_V}(t) \cdot \ddot{\bar{q}}_{R\_Hr}(t) \cdot \frac{\Delta t_{RFFDSP}^2}{2} \end{aligned} \quad (5.47)$$

Similarly:

$$\overline{\Delta P}_{RFFDSP\_c,17fL\_f} = \bar{P}_{c,17_r}(t + \Delta t_{RFFDSP}) - \bar{P}_{c,17\_fL\_a}(t + \Delta t_{RFFDSP})$$

Then,

$$\begin{aligned} \overline{\Delta P}_{RFFDSP\_c,17fL\_f} = & \\ & \bar{P}_{c,17_r}(t + \Delta t_{RFFDSP}) - \bar{P}_{c,17\_fL\_a}(t) - \hat{J}_{v,17\_fL\_all_V}(t) \cdot \dot{\bar{q}}_{L\_H}(t) \cdot \Delta t_{RFFDSP} - \\ & \hat{J}_{v,17\_fL\_all_V}(t) \cdot \dot{\bar{q}}_{L\_H}(t) \cdot \frac{\Delta t_{RFFDSP}^2}{2} - \hat{J}_{v,17\_fL\_all_V}(t) \cdot \ddot{\bar{q}}_{L\_H}(t) \cdot \frac{\Delta t_{RFFDSP}^2}{2} \end{aligned} \quad (5.48)$$

$$\overline{\Delta v}_{RFFDSP\_17fR\_f} = \bar{v}_{17_r}(t + \Delta t_{RFFDSP}) - \bar{v}_{17\_fR\_a}(t + \Delta t_{RFFDSP}), \text{ for}$$

$$\bar{v}_{17}(t + \Delta t_{RFFDSP}) = \begin{bmatrix} \bar{V}_{c,17}(t + \Delta t_{RFFDSP}) \\ \bar{W}_{17}(t + \Delta t_{RFFDSP}) \end{bmatrix}$$

Then,

$$\begin{aligned} \overline{\Delta v}_{RFFDSP\_17fR\_f} = & \\ & \bar{v}_{17_r}(t + \Delta t_{RFFDSP}) - \hat{J}_{v,17\_fR}(t) \cdot \dot{\bar{q}}_{R\_Hr}(t) - \hat{J}_{v,17\_fR}(t) \cdot \dot{\bar{q}}_{R\_Hr}(t) \cdot \Delta t_{RFFDSP} - \\ & \hat{J}_{v,17\_fR}(t) \cdot \ddot{\bar{q}}_{R\_Hr}(t) \cdot \Delta t_{RFFDSP} \end{aligned} \quad (5.49)$$

Similarly:

$$\overline{\Delta v}_{RFFDSP\_17fL\_f} = \bar{v}_{17_r}(t + \Delta t_{RFFDSP}) - \bar{v}_{17\_fL\_a}(t + \Delta t_{RFFDSP})$$

Then,

$$\begin{aligned} \overline{\Delta v}_{RFFDSP_{17fL_f}} = \\ \bar{v}_{17_r}(t + \Delta t_{RFFDSP}) - \hat{J}_{v,17_{fL\_all}}(t) \cdot \dot{\bar{q}}_{L_H}(t) - \hat{J}_{v,17_{fL\_all}}(t) \cdot \dot{\bar{q}}_{L_H}(t) \cdot \Delta t_{RFFDSP} - \\ \hat{J}_{v,17_{fL\_all}}(t) \cdot \ddot{\bar{q}}_{L_H}(t) \cdot \Delta t_{RFFDSP} \end{aligned} \quad (5.50)$$

Considering

$$\overline{\Delta OR}_{RFFDSP_{17fR_f}} = \bar{C}_{diag_r}^{(0,17)}(t + \Delta t_{RFFDSP}) - \bar{C}_{diag_a}^{(0,17_{fR})}(t + \Delta t_{RFFDSP}),$$

it can be expressed that

$$\begin{aligned} \overline{\Delta OR}_{RFFDSP_{17fR_f}} = \bar{C}_{diag_r}^{(0,17)}(t + \Delta t_{RFFDSP}) - \bar{C}_{diag_a}^{(0,17_{fR})}(t) - \\ \hat{J}_{v,cdiag0_{17_{fR}}}(t) \cdot \dot{\bar{q}}_{R_{Hr}}(t) \cdot \Delta t_{RFFDSP} - \hat{J}_{v,cdiag0_{17_{fR}}}(t) \cdot \dot{\bar{q}}_{R_{Hr}}(t) \cdot \frac{\Delta t_{RFFDSP}^2}{2} - \\ \hat{J}_{v,cdiag0_{17_{fR}}}(t) \cdot \ddot{\bar{q}}_{R_{Hr}}(t) \cdot \frac{\Delta t_{RFFDSP}^2}{2} \end{aligned} \quad (5.51)$$

Similarly,

$$\begin{aligned} \overline{\Delta OR}_{RFFDSP_{17fL_f}} = \bar{C}_{diag_r}^{(0,17)}(t + \Delta t_{RFFDSP}) - \bar{C}_{diag_a}^{(0,17_{fL})}(t + \Delta t_{RFFDSP}) \\ \overline{\Delta OR}_{RFFDSP_{17fL_f}} = \bar{C}_{diag_r}^{(0,17)}(t + \Delta t_{RFFDSP}) - \bar{C}_{diag_a}^{(0,17_{fL})}(t) - \\ \hat{J}_{v,cdiag0_{17_{fL\_all}}}(t) \cdot \dot{\bar{q}}_{L_H}(t) \cdot \Delta t_{RFFDSP} - \hat{J}_{v,cdiag0_{17_{fL\_all}}}(t) \cdot \dot{\bar{q}}_{L_H}(t) \cdot \frac{\Delta t_{RFFDSP}^2}{2} - \\ \hat{J}_{v,cdiag0_{17_{fL\_all}}}(t) \cdot \ddot{\bar{q}}_{L_H}(t) \cdot \frac{\Delta t_{RFFDSP}^2}{2} \end{aligned} \quad (5.52)$$

$\overline{\Delta q}_{RFFDSP_{R_{Hr}_f}} = \bar{q}_{R_{Hr}_a}(t + \Delta t_{RFFDSP}) - \bar{q}_{R_{Hr}_0}$ , where  $\bar{q}_{R_{Hr}_0}$  is taken as a vector with zero components only.

Then,

$$\overline{\Delta q}_{RFFDSP_{R_{Hr}_f}} = \bar{q}_{R_{Hr}}(t) + \dot{\bar{q}}_{R_{Hr}}(t) \cdot \Delta t_{RFFDSP} + \ddot{\bar{q}}_{R_{Hr}}(t) \cdot \frac{\Delta t_{RFFDSP}^2}{2} - \bar{q}_{R_{Hr}_0} \quad (5.53)$$

Similarly:

$\overline{\Delta q}_{RFFDSP\_L\_H\_f} = \bar{q}_{L\_H\_a}(t + \Delta t_{RFFDSP}) - \bar{q}_{L\_H\_0}$ , where  $\bar{q}_{L\_H\_0}$  is taken as a vector with zero components only. Then,

$$\overline{\Delta q}_{RFFDSP\_L\_H\_f} = \bar{q}_{L\_H}(t) + \dot{\bar{q}}_{L\_H}(t) \cdot \Delta t_{RFFDSP} + \ddot{\bar{q}}_{L\_H}(t) \cdot \frac{\Delta t_{RFFDSP}^2}{2} - \bar{q}_{L\_H_0} \quad (5.54)$$

As a result, cost functions for optimum command accelerations calculation in RFFDSP are defined as shown below:

$$\begin{aligned} C_{RFFDSP,a} = & \frac{1}{2} \overline{\Delta P}_{RFFDSP\_c,17fR\_f}^T \cdot \widehat{W}_{RFFDSP\_P,17a} \cdot \overline{\Delta P}_{RFFDSP\_c,17fR\_f} + \\ & \frac{1}{2} \overline{\Delta OR}_{RFFDSP\_17fR\_f}^T \cdot \widehat{W}_{RFFDSP\_OR,17a} \cdot \overline{\Delta OR}_{RFFDSP\_17fR\_f} + \\ & \frac{1}{2} \overline{\Delta v}_{RFFDSP\_17fR\_f}^T \cdot \widehat{W}_{RFFDSP\_v,17a} \cdot \overline{\Delta v}_{RFFDSP\_17fR\_f} + \\ & \frac{1}{2} \overline{\Delta q}_{RFFDSP\_R\_Hr\_f}^T \cdot \widehat{W}_{RFFDSP\_qR\_Hr} \cdot \overline{\Delta q}_{RFFDSP\_R\_Hr\_f} + \\ & \frac{1}{2} \ddot{\bar{q}}_{R\_Hr}(t)^T \cdot \widehat{W}_{RFFDSP\_qR\_Hrdd} \cdot \ddot{\bar{q}}_{R\_Hr}(t) \end{aligned} \quad (5.55)$$

$$\begin{aligned} C_{RFFDSP,b} = & \frac{1}{2} \overline{\Delta P}_{RFFDSP\_c,17fL\_f}^T \cdot \widehat{W}_{RFFDSP\_P,17b} \cdot \overline{\Delta P}_{RFFDSP\_c,17fL\_f} + \\ & \frac{1}{2} \overline{\Delta OR}_{RFFDSP\_17fL\_f}^T \cdot \widehat{W}_{RFFDSP\_OR,17b} \cdot \overline{\Delta OR}_{RFFDSP\_17fL\_f} + \\ & \frac{1}{2} \overline{\Delta v}_{RFFDSP\_17fL\_f}^T \cdot \widehat{W}_{RFFDSP\_v,17b} \cdot \overline{\Delta v}_{RFFDSP\_17fL\_f} + \\ & \frac{1}{2} \overline{\Delta q}_{RFFDSP\_L\_H\_f}^T \cdot \widehat{W}_{RFFDSP\_qL\_H} \cdot \overline{\Delta q}_{RFFDSP\_L\_H\_f} + \\ & \frac{1}{2} \ddot{\bar{q}}_{L\_H}(t)^T \cdot \widehat{W}_{RFFDSP\_qL\_Hdd} \cdot \ddot{\bar{q}}_{L\_H}(t) \end{aligned} \quad (5.56)$$

$$C_{RFFDSP} = C_{RFFDSP,a} + C_{RFFDSP,b} \quad (5.57)$$

Construction of kinematic constraint equations is shown below.

For  $\begin{bmatrix} \bar{\alpha}_{c,17fR} \\ \bar{\alpha}_{17fR} \end{bmatrix} = \begin{bmatrix} \bar{\alpha}_{c,17fL} \\ \bar{\alpha}_{17fL} \end{bmatrix}$ , equation (4.85) and (4.86) of the direct dynamic solution of RFFDSP can be used such that:

$$\begin{bmatrix} \hat{A}_{17R}(\bar{q}) \\ \hat{A}_{\alpha 17R}(\bar{q}) \end{bmatrix} \ddot{\bar{q}} + \begin{bmatrix} \bar{B}_{17R}(\bar{q}, \dot{\bar{q}}) \\ \bar{B}_{\alpha 17R}(\bar{q}, \dot{\bar{q}}) \end{bmatrix} = \begin{bmatrix} \hat{A}_{17L}(\bar{q}) \\ \hat{A}_{\alpha 17L}(\bar{q}) \end{bmatrix} \ddot{\bar{q}} + \begin{bmatrix} \bar{B}_{17L}(\bar{q}, \dot{\bar{q}}) \\ \bar{B}_{\alpha 17L}(\bar{q}, \dot{\bar{q}}) \end{bmatrix}$$

Which can be simplified into the form as shown below.

$$[\hat{A}_{T17R}(\bar{q}) \quad \hat{0}] \begin{bmatrix} \bar{q}_{lower} \\ \bar{q}_{upper} \end{bmatrix} + \bar{B}_{T17R}(\bar{q}, \dot{\bar{q}}) = [\hat{A}_{T17L}(\bar{q}) \quad \hat{0}] \begin{bmatrix} \bar{q}_{lower} \\ \bar{q}_{upper} \end{bmatrix} + \bar{B}_{T17L}(\bar{q}, \dot{\bar{q}}) \quad (5.58)$$

For  $\dot{\bar{q}}_{R,L} = \begin{bmatrix} \dot{\bar{q}}_{R,Hr} \\ \dot{\bar{q}}_{L,H} \end{bmatrix}$ , the final form of the equation (5.58) is found as:

$$\widehat{\Delta A}_{T17rec\_RFFDSP}(\bar{q}) \ddot{\bar{q}}_{R,L} = \overline{\Delta B}_{T17\_RFFDSP}(\bar{q}, \dot{\bar{q}}) \quad (5.59)$$

Reconfiguration of equations from equation (5.58) to (5.59) is achieved according to the equations (5.60) and (5.61)

$$[\hat{A}_{T17R} - \hat{A}_{T17L}] \cdot \ddot{\bar{q}}_{lower} = \widehat{\Delta A}_{T17rec\_RFFDSP} \cdot \ddot{\bar{q}}_{R,L} \quad (5.60)$$

$$\overline{\Delta B}_{T17\_RFFDSP} = \bar{B}_{T17L} - \bar{B}_{T17R}. \quad (5.61)$$

### 5.1.1.3.2. Calculation Procedure

In consequence, finding optimum command accelerations for RFFDSP results to an optimization problem such that:

Minimize  $C_{RFFDSP}$ , subject to  $\widehat{\Delta A}_{T17rec\_RFFDSP}(\bar{q}) \cdot \ddot{\bar{q}}_{R,L} = \overline{\Delta B}_{T17\_RFFDSP}(\bar{q}, \dot{\bar{q}})$ .

Using the method of Lagrange Multipliers, optimum command accelerations for RFFDSP are determined.

$$\ddot{\bar{q}}_{R,L_c} = [\bar{G}_{RFFDSP,a} + \bar{G}_{RFFDSP,b} + \beta \cdot \widehat{\Delta A}_{T17rec\_RFFDSP}] \cdot \begin{pmatrix} \hat{\varphi}_{R,Hr}^T \cdot \hat{Z}_{RFFDSP,a} \\ + \hat{\varphi}_{L,H}^T \cdot \hat{Z}_{RFFDSP,b} \end{pmatrix}^{-1} \quad (5.62)$$

Components of equation (5.62) are shown by equation (5.63), (5.64), (5.65), (5.66), (5.67), (5.68), (5.69) and (5.60).

$$\beta = \begin{bmatrix} \overline{\Delta B}_{T17RFFDSP}^T - (\overline{G}_{RFFDSP,a} + \overline{G}_{RFFDSP,b}) \\ \cdot \left( \widehat{\Phi}_{R_{Hr}}^T \cdot \widehat{Z}_{RFFDSP,a} + \widehat{\Phi}_{L_H}^T \cdot \widehat{Z}_{RFFDSP,b} \right)^{-1} \widehat{\Delta A}_{T17recRFFDSP}^T \end{bmatrix} \cdot \begin{bmatrix} \widehat{\Delta A}_{T17rec\_RFFDSP} \cdot \left( \widehat{\Phi}_{R_{Hr}}^T \cdot \widehat{Z}_{RFFDSP,a} + \widehat{\Phi}_{L_H}^T \cdot \widehat{Z}_{RFFDSP,b} \right)^{-1} \cdot \widehat{\Delta A}_{T17rec\_RFFDSP}^T \end{bmatrix}^{-1} \quad (5.63)$$

$\widehat{\Phi}_{R_{Hr}}$  and  $\widehat{\Phi}_{L_H}$  are matrices for extraction, defined by equation (5.64) and (5.65):

$$\widehat{\Phi}_{R_{Hr}} \cdot \ddot{\mathbf{q}}_{R_L} = \ddot{\mathbf{q}}_{R_{Hr}} \quad (5.64)$$

$$\widehat{\Phi}_{L_H} \cdot \ddot{\mathbf{q}}_{R_L} = \ddot{\mathbf{q}}_{L_H}. \quad (5.65)$$

$$\begin{aligned} \widehat{Z}_{RFFDSP,a} = & \widehat{W}_{RFFDSP\_qR\_Hrdd} + \widehat{W}_{RFFDSP\_qR\_Hr} \cdot \widehat{\Phi}_{R_{Hr}} \cdot \frac{\Delta t_{RFFDSP}^4}{4} + \\ & \widehat{J}_{v,17\_fR_v}(t)^T \cdot \widehat{W}_{RFFDSP\_P,17a} \cdot \widehat{J}_{v,17\_fR_v}(t) \cdot \widehat{\Phi}_{R_{Hr}} \cdot \frac{\Delta t_{RFFDSP}^4}{4} + \\ & \widehat{J}_{v,Cdiag0\_17\_fR}(t)^T \cdot \widehat{W}_{RFFDSP\_OR,17a} \cdot \widehat{J}_{v,Cdiag0\_17\_fR}(t) \cdot \widehat{\Phi}_{R_{Hr}} \cdot \frac{\Delta t_{RFFDSP}^4}{4} + \\ & \widehat{J}_{v,17\_fR}(t)^T \cdot \widehat{W}_{RFFDSP\_v,17a} \cdot \widehat{J}_{v,17\_fR}(t) \cdot \widehat{\Phi}_{R_{Hr}} \cdot \Delta t_{RFFDSP}^2 \end{aligned} \quad (5.66)$$

$$\begin{aligned} \widehat{Z}_{RFFDSP,b} = & \widehat{W}_{RFFDSP\_qL\_Hdd} + \widehat{W}_{RFFDSP\_qL\_H} \cdot \widehat{\Phi}_{L_H} \cdot \frac{\Delta t_{RFFDSP}^4}{4} + \\ & \widehat{J}_{v,17\_fL\_all_v}(t)^T \cdot \widehat{W}_{RFFDSP\_P,17b} \cdot \widehat{J}_{v,17\_fL\_all_v}(t) \cdot \widehat{\Phi}_{L_H} \cdot \frac{\Delta t_{RFFDSP}^4}{4} + \\ & \widehat{J}_{v,Cdiag0\_17\_fL\_all}(t)^T \cdot \widehat{W}_{RFFDSP\_OR,17b} \cdot \widehat{J}_{v,Cdiag0\_17\_fL\_all}(t) \cdot \widehat{\Phi}_{L_H} \cdot \frac{\Delta t_{RFFDSP}^4}{4} + \\ & \widehat{J}_{v,17\_fL\_all}(t)^T \cdot \widehat{W}_{RFFDSP\_v,17b} \cdot \widehat{J}_{v,17\_fL\_all}(t) \cdot \widehat{\Phi}_{L_H} \cdot \Delta t_{RFFDSP}^2 \end{aligned} \quad (5.67)$$

$$\begin{aligned}
& \bar{G}_{RFFDSP,a} \\
&= \left[ \begin{array}{c} \bar{P}_{c,17_r}(t + \Delta t_{RFFDSP}) - \bar{P}_{c,17_{fR}_a}(t) - \hat{J}_{v,17_{fR}_V}(t) \cdot \dot{\bar{q}}_{R_{Hr}}(t) \cdot \Delta t_{RFFDSP} \\ -\hat{J}_{v,17_{fR}_V}(t) \cdot \dot{\bar{q}}_{R_{Hr}}(t) \cdot \frac{\Delta t_{RFFDSP}^2}{2} \end{array} \right]^T \\
& \cdot \hat{W}_{RFFDSP_P,17a} \cdot \hat{J}_{v,17_{fR}_V}(t) \cdot \hat{\Phi}_{R_{Hr}} \cdot \frac{\Delta t_{RFFDSP}^2}{2} \\
& + \left[ \begin{array}{c} \bar{v}_{17_r}(t + \Delta t_{RFFDSP}) - \hat{J}_{v,17_{fR}}(t) \cdot \dot{\bar{q}}_{R_{Hr}}(t) \\ -\hat{J}_{v,17_{fR}}(t) \cdot \dot{\bar{q}}_{R_{Hr}}(t) \cdot \Delta t_{RFFDSP} \end{array} \right]^T \cdot \hat{W}_{RFFDSP_{v,17a}} \cdot \hat{J}_{v,17_{fR}}(t) \cdot \hat{\Phi}_{R_{Hr}} \cdot \Delta t_{RFFDSP} \\
& + \left[ \begin{array}{c} \bar{C}_{diag_r}^{(0,17)}(t + \Delta t_{RFFDSP}) - \bar{C}_{diag_a}^{(0,17_{fR})}(t) \\ -\hat{J}_{v,Cdiag0_{17_{fR}}}(t) \cdot \dot{\bar{q}}_{R_{Hr}}(t) \cdot \Delta t_{RFFDSP} - \hat{J}_{v,Cdiag0_{17_{fR}}}(t) \cdot \dot{\bar{q}}_{R_{Hr}}(t) \cdot \frac{\Delta t_{RFFDSP}^2}{2} \end{array} \right]^T \\
& \cdot \hat{W}_{RFFDSP_{OR,17a}} \cdot \hat{J}_{v,Cdiag0_{17_{fR}}}(t) \cdot \hat{\Phi}_{R_{Hr}} \cdot \frac{\Delta t_{RFFDSP}^2}{2} - \\
& [\bar{q}_{R_{Hr}}(t) - \bar{q}_{R_{Hr}0}]^T \cdot \hat{W}_{RFFDSP_{qR_{Hr}}} \cdot \hat{\Phi}_{R_{Hr}} \cdot \frac{\Delta t_{RFFDSP}^2}{2} - \\
& \dot{\bar{q}}_{R_{Hr}}(t)^T \cdot \hat{W}_{RFFDSP_{qR_{Hr}}} \cdot \hat{\Phi}_{R_{Hr}} \cdot \frac{\Delta t_{RFFDSP}^3}{2} \tag{5.68}
\end{aligned}$$

$$\begin{aligned}
& \bar{G}_{RFFDSP,b} \\
&= \left[ \begin{array}{c} \bar{P}_{c,17_r}(t + \Delta t_{RFFDSP}) - \bar{P}_{c,17_{fL}_a}(t) - \hat{J}_{v,17_{fL}_{all}_V}(t) \cdot \dot{\bar{q}}_{L_H}(t) \cdot \Delta t_{RFFDSP} \\ -\hat{J}_{v,17_{fL}_{all}_V}(t) \cdot \dot{\bar{q}}_{L_H}(t) \cdot \frac{\Delta t_{RFFDSP}^2}{2} \end{array} \right]^T \\
& \cdot \hat{W}_{RFFDSP_P,17b} \cdot \hat{J}_{v,17_{fL}_{all}_V}(t) \cdot \hat{\Phi}_{L_H} \cdot \frac{\Delta t_{RFFDSP}^2}{2} \\
& + \left[ \begin{array}{c} \bar{v}_{17_r}(t + \Delta t_{RFFDSP}) - \hat{J}_{v,17_{fL}_{all}}(t) \cdot \dot{\bar{q}}_{L_H}(t) \\ -\hat{J}_{v,17_{fL}_{all}}(t) \cdot \dot{\bar{q}}_{L_H}(t) \cdot \Delta t_{RFFDSP} \end{array} \right]^T \cdot \hat{W}_{RFFDSP_{v,17b}} \cdot \hat{J}_{v,17_{fL}_{all}}(t) \cdot \hat{\Phi}_{L_H} \cdot \Delta t_{RFFDSP} \\
& + \left[ \begin{array}{c} \bar{C}_{diag_r}^{(0,17)}(t + \Delta t_{RFFDSP}) - \bar{C}_{diag_a}^{(0,17_{fL})}(t) \\ -\hat{J}_{v,Cdiag0_{17_{fL}_{all}}}(t) \cdot \dot{\bar{q}}_{L_H}(t) \cdot \Delta t_{RFFDSP} - \hat{J}_{v,Cdiag0_{17_{fL}_{all}}}(t) \cdot \dot{\bar{q}}_{L_H}(t) \cdot \frac{\Delta t_{RFFDSP}^2}{2} \end{array} \right]^T \\
& \cdot \hat{W}_{RFFDSP_{OR,17b}} \cdot \hat{J}_{v,Cdiag0_{17_{fL}_{all}}}(t) \cdot \hat{\Phi}_{L_H} \cdot \frac{\Delta t_{RFFDSP}^2}{2} - \\
& [\bar{q}_{L_H}(t) - \bar{q}_{L_H0}]^T \cdot \hat{W}_{RFFDSP_{qL_H}} \cdot \hat{\Phi}_{L_H} \cdot \frac{\Delta t_{RFFDSP}^2}{2} - \\
& \dot{\bar{q}}_{L_H}(t)^T \cdot \hat{W}_{RFFDSP_{qL_H}} \cdot \hat{\Phi}_{L_H} \cdot \frac{\Delta t_{RFFDSP}^3}{2} \tag{5.69}
\end{aligned}$$

#### 5.1.1.4. For LFFDSP

Optimum command accelerations for joint space variables from Body 4 to Body 17 and from Body 1 to Body 17 are calculated according to given reference inputs for Body 17 and its mass center by defining 2 separate cost functions. These cost functions are combined and subjected to kinematic constraint equations.

Command acceleration  $\ddot{\theta}_{4_c}$  is taken as zero as similar to LFFSSP, since Body 4 is assumed to be rigidly fixed to the ground in LFFDSP too. The procedure similar to the one shown in RFFDSP is applied in LFFDSP.

##### 5.1.1.4.1. Definition of Variables

$t$  is the present phase time and  $\Delta t_{LFFDSP}$  is the prediction time range used during the calculation of optimum command accelerations in LFFDSP.

$$\overline{\Delta P}_{LFFDSP\_c,17fL\_f} = \bar{P}_{c,17_r}(t + \Delta t_{LFFDSP}) - \bar{P}_{c,17\_fL_a}(t + \Delta t_{LFFDSP})$$

Then,

$$\begin{aligned} \overline{\Delta P}_{LFFDSP\_c,17fL\_f} = & \\ & \bar{P}_{c,17_r}(t + \Delta t_{LFFDSP}) - \bar{P}_{c,17\_fL_a}(t) - \hat{J}_{v,17\_fL_v}(t) \cdot \dot{\bar{q}}_{L_Hr}(t) \cdot \Delta t_{LFFDSP} - \\ & \hat{J}_{v,17\_fL_v}(t) \cdot \dot{\bar{q}}_{L_Hr}(t) \cdot \frac{\Delta t_{LFFDSP}^2}{2} - \hat{J}_{v,17\_fL_v}(t) \cdot \ddot{\bar{q}}_{L_Hr}(t) \cdot \frac{\Delta t_{LFFDSP}^2}{2} \end{aligned} \quad (5.70)$$

Similarly:

$$\overline{\Delta P}_{LFFDSP\_c,17fR\_f} = \bar{P}_{c,17_r}(t + \Delta t_{LFFDSP}) - \bar{P}_{c,17\_fR_a}(t + \Delta t_{LFFDSP})$$

Then,

$$\begin{aligned} \overline{\Delta P}_{LFFDSP\_c,17fR\_f} = & \\ & \bar{P}_{c,17_r}(t + \Delta t_{LFFDSP}) - \bar{P}_{c,17\_fR_a}(t) - \hat{J}_{v,17\_fR\_all_v}(t) \cdot \dot{\bar{q}}_{R_H}(t) \cdot \Delta t_{LFFDSP} - \\ & \hat{J}_{v,17\_fR\_all_v}(t) \cdot \dot{\bar{q}}_{R_H}(t) \cdot \frac{\Delta t_{LFFDSP}^2}{2} - \hat{J}_{v,17\_fR\_all_v}(t) \cdot \ddot{\bar{q}}_{R_H}(t) \cdot \frac{\Delta t_{LFFDSP}^2}{2} \end{aligned} \quad (5.71)$$

Defining  $\overline{\Delta v}_{LFFDSP_{17fL_f}} = \bar{v}_{17_r}(t + \Delta t_{LFFDSP}) - \bar{v}_{17_{fL}_a}(t + \Delta t_{LFFDSP})$ , for

$$\bar{v}_{17}(t + \Delta t_{LFFDSP}) = \begin{bmatrix} \bar{V}_{c,17}(t + \Delta t_{LFFDSP}) \\ \bar{w}_{17}(t + \Delta t_{LFFDSP}) \end{bmatrix}:$$

$$\begin{aligned} \overline{\Delta v}_{LFFDSP_{17fL_f}} = & \\ & \bar{v}_{17_r}(t + \Delta t_{LFFDSP}) - \hat{J}_{v,17_{fL}}(t) \cdot \dot{\bar{q}}_{L_{Hr}}(t) - \hat{J}_{v,17_{fL}}(t) \cdot \dot{\bar{q}}_{L_{Hr}}(t) \cdot \Delta t_{LFFDSP} - \\ & \hat{J}_{v,17_{fL}}(t) \cdot \ddot{\bar{q}}_{L_{Hr}}(t) \cdot \Delta t_{LFFDSP} \end{aligned} \quad (5.72)$$

Similarly:

$$\overline{\Delta v}_{LFFDSP_{17fR_f}} = \bar{v}_{17_r}(t + \Delta t_{LFFDSP}) - \bar{v}_{17_{fR}_a}(t + \Delta t_{LFFDSP})$$

Then,

$$\begin{aligned} \overline{\Delta v}_{LFFDSP_{17fR_f}} = & \\ & \bar{v}_{17_r}(t + \Delta t_{LFFDSP}) - \hat{J}_{v,17_{fR_{all}}}(t) \cdot \dot{\bar{q}}_{R_H}(t) - \hat{J}_{v,17_{fR_{all}}}(t) \cdot \dot{\bar{q}}_{R_H}(t) \cdot \Delta t_{LFFDSP} - \\ & \hat{J}_{v,17_{fR_{all}}}(t) \cdot \ddot{\bar{q}}_{R_H}(t) \cdot \Delta t_{LFFDSP} \end{aligned} \quad (5.73)$$

Considering

$$\overline{\Delta OR}_{LFFDSP_{17fL_f}} = \bar{C}_{diag_r}^{(0,17)}(t + \Delta t_{LFFDSP}) - \bar{C}_{diag_a}^{(0,17_{fL})}(t + \Delta t_{LFFDSP}),$$

it can be expressed that:

$$\begin{aligned} \overline{\Delta OR}_{LFFDSP_{17fL_f}} = & \bar{C}_{diag_r}^{(0,17)}(t + \Delta t_{LFFDSP}) - \bar{C}_{diag_a}^{(0,17_{fL})}(t) - \\ & \hat{J}_{v,cdiag0_{17_{fL}}}(t) \cdot \dot{\bar{q}}_{L_{Hr}}(t) \cdot \Delta t_{LFFDSP} - \hat{J}_{v,cdiag0_{17_{fL}}}(t) \cdot \dot{\bar{q}}_{L_{Hr}}(t) \cdot \frac{\Delta t_{LFFDSP}^2}{2} - \\ & \hat{J}_{v,cdiag0_{17_{fL}}}(t) \cdot \ddot{\bar{q}}_{L_{Hr}}(t) \cdot \frac{\Delta t_{LFFDSP}^2}{2} \end{aligned} \quad (5.74)$$

Similarly:

$$\overline{\Delta OR}_{LFFDSP_{17fR_f}} = \bar{C}_{diag_r}^{(0,17)}(t + \Delta t_{LFFDSP}) - \bar{C}_{diag_a}^{(0,17_{fR})}(t + \Delta t_{LFFDSP})$$

Then,

$$\begin{aligned}
\overline{\Delta OR}_{LFFDSP_{17fR_f}} &= \bar{C}_{diag_r}^{(0,17)}(t + \Delta t_{LFFDSP}) - \bar{C}_{diag_a}^{(0,17_fR)}(t) - \\
\hat{J}_{v,Cdiag0_{17_fR\_all}}(t) \cdot \ddot{q}_{R_H}(t) \cdot \Delta t_{LFFDSP} - \hat{J}_{v,Cdiag0_{17_fR\_all}}(t) \cdot \dot{q}_{R_H}(t) \cdot \frac{\Delta t_{LFFDSP}^2}{2} - \\
\hat{J}_{v,Cdiag0_{17_fR\_all}}(t) \cdot \ddot{q}_{R_H}(t) \cdot \frac{\Delta t_{LFFDSP}^2}{2}
\end{aligned} \quad (5.75)$$

$\overline{\Delta q}_{LFFDSP_{L_Hr_f}} = \bar{q}_{L_Hr_a}(t + \Delta t_{LFFDSP}) - \bar{q}_{L_Hr_0}$ , where  $\bar{q}_{L_Hr_0}$  is taken as a vector with zero components only.

Then,

$$\overline{\Delta q}_{LFFDSP_{L_Hr_f}} = \bar{q}_{L_Hr}(t) + \dot{q}_{L_Hr}(t) \cdot \Delta t_{LFFDSP} + \ddot{q}_{L_Hr}(t) \cdot \frac{\Delta t_{LFFDSP}^2}{2} - \bar{q}_{L_Hr_0} \quad (5.76)$$

Similarly:

$\overline{\Delta q}_{LFFDSP_{R_H_f}} = \bar{q}_{R_H_a}(t + \Delta t_{LFFDSP}) - \bar{q}_{R_H_0}$ , where  $\bar{q}_{R_H_0}$  is taken as a vector with zero components only.

$$\text{Then, } \overline{\Delta q}_{LFFDSP_{R_H_f}} = \bar{q}_{R_H}(t) + \dot{q}_{R_H}(t) \cdot \Delta t_{LFFDSP} + \ddot{q}_{R_H}(t) \cdot \frac{\Delta t_{LFFDSP}^2}{2} - \bar{q}_{R_H_0} \quad (5.77)$$

As a result, cost functions for optimum command accelerations calculation in LFFDSP are defined as shown below:

$$\begin{aligned}
C_{LFFDSP,a} &= \\
&\frac{1}{2} \overline{\Delta P}_{LFFDSP_{c,17fL_f}}^T \cdot \widehat{W}_{LFFDSP_{P,17a}} \cdot \overline{\Delta P}_{LFFDSP_{c,17fL_f}} + \\
&\frac{1}{2} \overline{\Delta OR}_{LFFDSP_{17fL_f}}^T \cdot \widehat{W}_{LFFDSP_{OR,17a}} \cdot \overline{\Delta OR}_{LFFDSP_{17fL_f}} + \\
&\frac{1}{2} \overline{\Delta v}_{LFFDSP_{17fL_f}}^T \cdot \widehat{W}_{LFFDSP_{v,17a}} \cdot \overline{\Delta v}_{LFFDSP_{17fL_f}} + \\
&\frac{1}{2} \overline{\Delta q}_{LFFDSP_{L_Hr_f}}^T \cdot \widehat{W}_{LFFDSP_{qL_Hr}} \cdot \overline{\Delta q}_{LFFDSP_{L_Hr_f}} + \\
&\frac{1}{2} \ddot{q}_{L_Hr}(t)^T \cdot \widehat{W}_{LFFDSP_{qL_Hrdd}} \cdot \ddot{q}_{L_Hr}(t)
\end{aligned} \quad (5.78)$$

$$\begin{aligned}
C_{LFFDSP,b} = & \\
& \frac{1}{2} \overline{\Delta P}_{LFFDSP,c,17fR_f}^T \cdot \widehat{W}_{LFFDSP_P,17b} \cdot \overline{\Delta P}_{LFFDSP,c,17fR_f} + \\
& \frac{1}{2} \overline{\Delta OR}_{LFFDSP_17fR_f}^T \cdot \widehat{W}_{LFFDSP_OR,17b} \cdot \overline{\Delta OR}_{LFFDSP_17fR_f} + \\
& \frac{1}{2} \overline{\Delta v}_{LFFDSP_17fR_f}^T \cdot \widehat{W}_{LFFDSP_v,17b} \cdot \overline{\Delta v}_{LFFDSP_17fR_f} + \\
& \frac{1}{2} \overline{\Delta q}_{LFFDSP_R_H_f}^T \cdot \widehat{W}_{LFFDSP_qR_H} \cdot \overline{\Delta q}_{LFFDSP_R_H_f} + \\
& \frac{1}{2} \ddot{\bar{q}}_{R_H}(t)^T \cdot \widehat{W}_{LFFDSP_qR_Hdd} \cdot \ddot{\bar{q}}_{R_H}(t)
\end{aligned} \tag{5.79}$$

$$C_{LFFDSP} = C_{LFFDSP,a} + C_{LFFDSP,b} \tag{5.80}$$

For  $\dot{\bar{q}}_{R_L} = \begin{bmatrix} \dot{\bar{q}}_{R_H} \\ \dot{\bar{q}}_{L_Hr} \end{bmatrix}$ , constraint equations are expressed similar to RFFDSP as shown:

$$\widehat{\Delta A}_{T17rec\_LFFDSP}(\bar{q}) \cdot \ddot{\bar{q}}_{R_L} = \overline{\Delta B}_{T17\_LFFDSP}(\bar{q}, \dot{\bar{q}}) \tag{5.81}$$

#### 5.1.1.4.2. Calculation Procedure

In consequence, finding optimum command accelerations for LFFDSP results to an optimization problem such that:

$$\text{Minimize } C_{LFFDSP}, \text{ subject to } \widehat{\Delta A}_{T17rec\_LFFDSP}(\bar{q}) \cdot \ddot{\bar{q}}_{R_L} = \overline{\Delta B}_{T17\_LFFDSP}(\bar{q}, \dot{\bar{q}}).$$

Using the method of Lagrange Multipliers, optimum command accelerations for LFFDSP are determined.

$$\ddot{\bar{q}}_{R_L} = [\bar{G}_{LFFDSP,a} + \bar{G}_{LFFDSP,b} + \beta \cdot \widehat{\Delta A}_{T17rec\_LFFDSP}] \cdot \begin{pmatrix} \widehat{\Phi}_{L_Hr}^T \cdot \hat{Z}_{LFFDSP,a} \\ + \widehat{\Phi}_{R_H}^T \cdot \hat{Z}_{LFFDSP,b} \end{pmatrix}^{-1} \tag{5.82}$$

Components of equation (5.82) are shown by equation (5.83), (5.84), (5.85), (5.86), (5.87), (5.88), (5.89) and (5.81).

$$\beta = \left[ \begin{array}{c} \overline{\Delta B}_{T17LFFDSP}^T - (\overline{G}_{LFFDSP,a} + \overline{G}_{LFFDSP,b}) \\ \left( \widehat{\Phi}_{L_{Hr}}^T \cdot \hat{Z}_{LFFDSP,a} \right)^{-1} \\ \left( \widehat{\Phi}_{R_H}^T \cdot \hat{Z}_{LFFDSP,b} \right) \end{array} \right] \cdot \widehat{\Delta A}_{T17recLFFDSP}^T \cdot \left[ \widehat{\Delta A}_{T17recLFFDSP} \cdot \left( \widehat{\Phi}_{L_{Hr}}^T \cdot \hat{Z}_{LFFDSP,a} + \widehat{\Phi}_{R_H}^T \cdot \hat{Z}_{LFFDSP,b} \right)^{-1} \cdot \widehat{\Delta A}_{T17recLFFDSP}^T \right]^{-1} \quad (5.83)$$

$\widehat{\Phi}_{L_{Hr}}$  and  $\widehat{\Phi}_{R_H}$  are matrices for extraction, defined by equation (5.84) and (5.85):

$$\widehat{\Phi}_{L_{Hr}} \cdot \ddot{q}_{R_L} = \ddot{q}_{L_{Hr}} \quad (5.84)$$

$$\widehat{\Phi}_{R_H} \cdot \ddot{q}_{R_L} = \ddot{q}_{R_H} \quad (5.85)$$

$$\begin{aligned} \hat{Z}_{LFFDSP,a} = & \\ & \widehat{W}_{LFFDSP_{qL_{Hr}dd}} + \widehat{W}_{LFFDSP_{qL_{Hr}}} \cdot \widehat{\Phi}_{L_{Hr}} \cdot \frac{\Delta t_{LFFDSP}^4}{4} + \\ & \hat{J}_{v,17_{fL_V}}(t)^T \cdot \widehat{W}_{LFFDSP_{P,17a}} \cdot \hat{J}_{v,17_{fL_V}}(t) \cdot \widehat{\Phi}_{L_{Hr}} \cdot \frac{\Delta t_{LFFDSP}^4}{4} + \\ & \hat{J}_{v,Cdiag0_{17_{fL}}}(t)^T \cdot \widehat{W}_{LFFDSP_{OR,17a}} \cdot \hat{J}_{v,Cdiag0_{17_{fL}}}(t) \cdot \widehat{\Phi}_{L_{Hr}} \cdot \frac{\Delta t_{LFFDSP}^4}{4} + \\ & \hat{J}_{v,17_{fL}}(t)^T \cdot \widehat{W}_{LFFDSP_{v,17a}} \cdot \hat{J}_{v,17_{fL}}(t) \cdot \widehat{\Phi}_{L_{Hr}} \cdot \Delta t_{LFFDSP}^2 \end{aligned} \quad (5.86)$$

$$\begin{aligned} \hat{Z}_{LFFDSP,b} = & \\ & \widehat{W}_{LFFDSP_{qR_{H}dd}} + \widehat{W}_{LFFDSP_{qR_H}} \cdot \widehat{\Phi}_{R_H} \cdot \frac{\Delta t_{LFFDSP}^4}{4} + \\ & \hat{J}_{v,17_{fR_{all_V}}}(t)^T \cdot \widehat{W}_{LFFDSP_{P,17b}} \cdot \hat{J}_{v,17_{fR_{all_V}}}(t) \cdot \widehat{\Phi}_{R_H} \cdot \frac{\Delta t_{LFFDSP}^4}{4} + \\ & \hat{J}_{v,Cdiag0_{17_{fR_{all}}}}(t)^T \cdot \widehat{W}_{LFFDSP_{OR,17b}} \cdot \hat{J}_{v,Cdiag0_{17_{fR_{all}}}}(t) \cdot \widehat{\Phi}_{R_H} \cdot \frac{\Delta t_{LFFDSP}^4}{4} + \\ & \hat{J}_{v,17_{fR_{all}}}(t)^T \cdot \widehat{W}_{LFFDSP_{v,17b}} \cdot \hat{J}_{v,17_{fR_{all}}}(t) \cdot \widehat{\Phi}_{R_H} \cdot \Delta t_{LFFDSP}^2 \end{aligned} \quad (5.87)$$

$$\begin{aligned}
& \bar{G}_{LFFDSP,a} \\
&= \left[ \begin{array}{c} \bar{P}_{c,17_r}(t + \Delta t_{LFFDSP}) - \bar{P}_{c,17_{fL}_a}(t) \\ -\hat{J}_{v,17_{fL}_V}(t) \cdot \dot{\bar{q}}_{L_{Hr}}(t) \cdot \Delta t_{LFFDSP} - \hat{J}_{v,17_{fL}_V}(t) \cdot \dot{\bar{q}}_{L_{Hr}}(t) \cdot \frac{\Delta t_{LFFDSP}^2}{2} \end{array} \right]^T \\
& \cdot \hat{W}_{LFFDSP_P,17a} \cdot \hat{J}_{v,17_{fL}_V}(t) \cdot \hat{\Phi}_{L_{Hr}} \cdot \frac{\Delta t_{LFFDSP}^2}{2} \\
& + \left[ \begin{array}{c} \bar{v}_{17_r}(t + \Delta t_{LFFDSP}) - \hat{J}_{v,17_{fL}}(t) \cdot \dot{\bar{q}}_{L_{Hr}}(t) \\ -\hat{J}_{v,17_{fL}}(t) \cdot \dot{\bar{q}}_{L_{Hr}}(t) \cdot \Delta t_{LFFDSP} \end{array} \right]^T \cdot \hat{W}_{LFFDSP_v,17a} \cdot \hat{J}_{v,17_{fL}}(t) \cdot \hat{\Phi}_{L_{Hr}} \cdot \Delta t_{LFFDSP} \\
& + \left[ \begin{array}{c} \bar{C}_{diag_r}^{(0,17)}(t + \Delta t_{LFFDSP}) - \bar{C}_{diag_a}^{(17_{fL})}(t) \\ -\hat{J}_{v,Cdiag0_{17_{fL}}}(t) \cdot \dot{\bar{q}}_{L_{Hr}}(t) \cdot \Delta t_{LFFDSP} - \hat{J}_{v,Cdiag0_{17_{fL}}}(t) \cdot \dot{\bar{q}}_{L_{Hr}}(t) \cdot \frac{\Delta t_{LFFDSP}^2}{2} \end{array} \right]^T \\
& \cdot \hat{W}_{LFFDSP_OR,17a} \cdot \hat{J}_{v,Cdiag0_{17_{fL}}}(t) \cdot \hat{\Phi}_{L_{Hr}} \cdot \frac{\Delta t_{LFFDSP}^2}{2} - \\
& [\bar{q}_{L_{Hr}}(t) - \bar{q}_{L_{Hr}0}]^T \cdot \hat{W}_{LFFDSP_{qL_{Hr}}} \cdot \hat{\Phi}_{L_{Hr}} \cdot \frac{\Delta t_{LFFDSP}^2}{2} - \\
& \dot{\bar{q}}_{L_{Hr}}(t)^T \cdot \hat{W}_{LFFDSP_{qL_{Hr}}} \cdot \hat{\Phi}_{L_{Hr}} \cdot \frac{\Delta t_{LFFDSP}^3}{2} \tag{5.88}
\end{aligned}$$

$$\begin{aligned}
& \bar{G}_{LFFDSP,b} \\
&= \left[ \begin{array}{c} \bar{P}_{c,17_r}(t + \Delta t_{LFFDSP}) - \bar{P}_{c,17_{fR}_a}(t) \\ -\hat{J}_{v,17_{fR}_{all}_V}(t) \cdot \dot{\bar{q}}_{R_H}(t) \cdot \Delta t_{LFFDSP} - \hat{J}_{v,17_{fR}_{all}_V}(t) \cdot \dot{\bar{q}}_{R_H}(t) \cdot \frac{\Delta t_{LFFDSP}^2}{2} \end{array} \right]^T \\
& \cdot \hat{W}_{LFFDSP_P,17b} \cdot \hat{J}_{v,17_{fR}_{all}_V}(t) \cdot \hat{\Phi}_{R_H} \cdot \frac{\Delta t_{LFFDSP}^2}{2} \\
& + \left[ \begin{array}{c} \bar{v}_{17_r}(t + \Delta t_{LFFDSP}) - \hat{J}_{v,17_{fR}_{all}}(t) \cdot \dot{\bar{q}}_{R_H}(t) \\ -\hat{J}_{v,17_{fR}_{all}}(t) \cdot \dot{\bar{q}}_{R_H}(t) \cdot \Delta t_{LFFDSP} \end{array} \right]^T \\
& \cdot \hat{W}_{LFFDSP_v,17b} \cdot \hat{J}_{v,17_{fR}_{all}}(t) \cdot \hat{\Phi}_{R_H} \cdot \Delta t_{LFFDSP} \\
& + \left[ \begin{array}{c} \bar{C}_{diag_r}^{(0,17)}(t + \Delta t_{LFFDSP}) - \bar{C}_{diag_a}^{(17_{fR})}(t) \\ -\hat{J}_{v,Cdiag0_{17_{fR}_{all}}}(t) \cdot \dot{\bar{q}}_{R_H}(t) \cdot \Delta t_{LFFDSP} \\ -\hat{J}_{v,Cdiag0_{17_{fR}_{all}}}(t) \cdot \dot{\bar{q}}_{R_H}(t) \cdot \frac{\Delta t_{LFFDSP}^2}{2} \end{array} \right]^T
\end{aligned}$$

$$\begin{aligned}
& \cdot \widehat{W}_{LFFDSP\_OR,17b} \cdot \widehat{J}_{v,Cdiag0\_17\_fR\_all}(t) \cdot \widehat{\Phi}_{R,H} \cdot \frac{\Delta t_{LFFDSP}^2}{2} - \\
& [\bar{q}_{R,H}(t) - \bar{q}_{R,H_0}]^T \cdot \widehat{W}_{LFFDSP\_qR,H} \cdot \widehat{\Phi}_{R,H} \cdot \frac{\Delta t_{LFFDSP}^2}{2} - \\
& \dot{\bar{q}}_{R,H}(t)^T \cdot \widehat{W}_{LFFDSP\_qR,H} \cdot \widehat{\Phi}_{R,H} \cdot \frac{\Delta t_{LFFDSP}^3}{2} \quad (5.89)
\end{aligned}$$

### 5.1.2. For UpperBodies

Calculation of optimum command accelerations for joint space variables from Body 17 to Body 27 (from  $\theta_{18}$  to  $\theta_{27}$ ) is explained under this heading. Since there are no reference trajectories defined for any upperbodies, all upperbodies are expected to maintain their initial position and orientation with respect to its adjacent bodies. Then, optimum command accelerations for upperbodies are calculated locally to keep related joint space positions and velocities close to their initial values.

For a joint variable  $\theta_k$ , present phase time  $t$  and its prediction time range  $\Delta t_k$  the cost function is defined as

$$C_{\theta_k} = \frac{1}{2} \cdot W_{P,\theta_k} [\theta_k(t + \Delta t_k) - \theta_{k_0}]^2 + \frac{1}{2} \cdot W_{V,\theta_k} [\dot{\theta}_k(t + \Delta t_k) - \dot{\theta}_{k_0}]^2 \quad (5.90)$$

where  $\theta_{k_0}$  and  $\dot{\theta}_{k_0}$  are initial values of  $\theta_k$  and  $\dot{\theta}_k$ .  $\theta_{k_0}$ ,  $\dot{\theta}_{k_0}$  are taken as zero in the simulation and  $W_{P,\theta_k}$ ,  $W_{V,\theta_k}$  are related weighting coefficients.

Using truncated Taylor Series Expansion of  $\theta_k(t + \Delta t_k)$  and  $\dot{\theta}_k(t + \Delta t_k)$ ,  $\frac{dC_{\theta_k}}{d\ddot{\theta}_k} = 0$  for optimum cost value as similar to calculations for lowerbodies;

optimum command acceleration for joint space variable  $\theta_k$  is calculated as:

$$\begin{aligned}
& \ddot{\theta}_{k_c} \\
& = - \frac{W_{P,\theta_k} \cdot [\theta_k(t) - \theta_{k_0}] \cdot \frac{\Delta t_k^2}{2} + W_{P,\theta_k} \cdot \dot{\theta}_k(t) \cdot \frac{\Delta t_k^3}{2} + W_{V,\theta_k} \cdot [\dot{\theta}_k(t) - \dot{\theta}_{k_0}] \cdot \Delta t_k}{W_{P,\theta_k} \cdot \frac{\Delta t_k^4}{4} + W_{V,\theta_k} \cdot \Delta t_k^2}
\end{aligned}$$

Using this procedure, all command accelerations are calculated for upperbodies such that:

$$\ddot{\bar{q}}_{upper_c} = \begin{bmatrix} \ddot{\theta}_{18} \\ \ddot{\theta}_{19} \\ \vdots \\ \ddot{\theta}_{27} \end{bmatrix}$$

## 5.2. Calculation of Actuator Torques

Computed torque control method is applied to calculate actuator torques [64]. Using kinematic equations related with the current locomotion phase, dynamic equations can be expressed in the form presented in direct dynamic solution procedure of chapter 4 as shown below:

$$\bar{Z}(\bar{q}, \dot{\bar{q}}, \ddot{\bar{q}}) = \hat{K}(\bar{q})\bar{F}$$

Using calculated command accelerations  $\ddot{\bar{q}}_c$  and known joint space variables  $\bar{q}, \dot{\bar{q}}$ :

$$\begin{bmatrix} \bar{Z}(\bar{q}, \dot{\bar{q}}, \ddot{\bar{q}}_c) \\ \bar{Z}_c \end{bmatrix} = \begin{bmatrix} \hat{K}(\bar{q}) \\ \hat{K}_c \end{bmatrix} \bar{F} \quad (5.91)$$

$\bar{Z}_c$  and  $\hat{K}_c$  are constructed according to assumptions of the current locomotion phase. Using equation (5.91), necessary forces and moments between bodies in order to achieve supplied command accelerations can be calculated. Required actuator torques are found by extracting relevant components of moments that are needed to be acted upon bodies using the expression  $\bar{T} = \hat{\phi}\bar{F}$  which is explained in the direct dynamic solution procedure of chapter 4.

Actuator torque  $T_1$  is always calculated to be zero during RFFSSP and RFFDSP, as long as  $\bar{M}_{1,3}^{(3)}$  is assumed to be zero. However  $M_{1,3y}^{(3)}$ , which is eventually  $T_1$ , can be assumed different from zero within reasonable limits in order to manually increase or decrease the magnitude of ground reaction forces and moments on Body 1 and Body 3 for various purposes. The similar interpretation can be made for  $T_2$  and the assumption of  $M_{2,4y}^{(4)}$  during LFFSSP and LFFDSP.

### 5.2.1. For RFFSSP

Forces and moments that are assumed to be zero during RFFSSP are as shown below:

$$\begin{bmatrix} \bar{F}_{1,3}^{(3)} \\ \bar{M}_{1,3}^{(3)} \\ \bar{F}_{0,4}^{(4)} \\ \bar{M}_{0,4}^{(4)} \\ \bar{F}_{0,2}^{(2)} \\ \bar{M}_{0,2}^{(2)} \end{bmatrix} = \hat{K}_{c\_RFFSSP} \cdot \bar{F} = \bar{Z}_{c\_RFFSSP} \text{ for } \bar{Z}_{c\_RFFSSP} = \bar{0}.$$

$\bar{F}_{0,4}^{(4)}$ ,  $\bar{M}_{0,4}^{(4)}$ ,  $\bar{F}_{0,2}^{(2)}$ ,  $\bar{M}_{0,2}^{(2)}$  and  $\bar{F}_{1,3}^{(3)}$ ,  $\bar{M}_{1,3}^{(3)}$  are taken as zero; since it is assumed that Body 2, Body 4 do not interact with the ground and interaction between Body 1, Body 3 are negated due to being rigidly fixed to the ground during RFFSSP.

After determining  $\hat{K}_{c\_RFFSSP}$  and  $\bar{Z}_{c\_RFFSSP}$ , required actuator torques can be found by:

$$\bar{T} = \hat{\phi} \cdot \begin{bmatrix} \hat{K}(\bar{q}) \\ \hat{K}_{c\_RFFSSP} \end{bmatrix}^{-1} \cdot \begin{bmatrix} \bar{Z}(\bar{q}, \dot{\bar{q}}, \ddot{\bar{q}}_c) \\ \bar{Z}_{c\_RFFSSP} \end{bmatrix} \quad (5.92)$$

### 5.2.2. For LFFSSP

Forces and moments that are assumed to be zero during LFFSSP are as shown below:

$$\begin{bmatrix} \bar{F}_{2,4}^{(4)} \\ \bar{M}_{2,4}^{(4)} \\ \bar{F}_{0,3}^{(3)} \\ \bar{M}_{0,3}^{(3)} \\ \bar{F}_{0,1}^{(1)} \\ \bar{M}_{0,1}^{(1)} \end{bmatrix} = \hat{K}_{c\_LFFSSP} \cdot \bar{F} = \bar{Z}_{c\_LFFSSP} \text{ for } \bar{Z}_{c\_LFFSSP} = \bar{0}.$$

$\bar{F}_{0,3}^{(3)}$ ,  $\bar{M}_{0,3}^{(3)}$ ,  $\bar{F}_{0,1}^{(1)}$ ,  $\bar{M}_{0,1}^{(1)}$  and  $\bar{F}_{2,4}^{(4)}$ ,  $\bar{M}_{2,4}^{(4)}$  are taken as zero; since it is assumed that Body 1, Body 3 do not interact with the ground and interaction between Body 2, Body 4 are negated due to being rigidly fixed to the ground during LFFSSP.

After determining  $\hat{K}_{c\_LFFSSP}$  and  $\bar{Z}_{c\_LFFSSP}$ , required actuator torques can be found by:

$$\bar{T} = \hat{\phi} \cdot \begin{bmatrix} \hat{K}(\bar{q}) \\ \hat{K}_{c\_LFFSSP} \end{bmatrix}^{-1} \cdot \begin{bmatrix} \bar{Z}(\bar{q}, \dot{\bar{q}}, \ddot{\bar{q}}_c) \\ \bar{Z}_{c\_LFFSSP} \end{bmatrix} \quad (5.93)$$

### 5.2.3. For RFFDSP

Forces and moments that are assumed to be zero during RFFDSP are as shown below:

$$\begin{bmatrix} \bar{F}_{1,3}^{(3)} \\ \bar{M}_{1,3}^{(3)} \\ \bar{F}_{0,4}^{(4)} \\ \bar{M}_{0,4}^{(4)} \end{bmatrix} = \hat{K}_{c\_RFFDSP} \cdot \bar{F} = \bar{Z}_{c\_RFFDSP} \text{ for } \bar{Z}_{c\_RFFDSP} = \bar{0}.$$

$\bar{F}_{0,4}^{(4)}$ ,  $\bar{M}_{0,4}^{(4)}$  and  $\bar{F}_{1,3}^{(3)}$ ,  $\bar{M}_{1,3}^{(3)}$  are taken as zero; since it is assumed that Body 4 does not interact with the ground and interaction between Body 1, Body 3 are negated due to being rigidly fixed to the ground during RFFDSP.

After determining  $\hat{K}_{c\_RFFDSP}$  and  $\bar{Z}_{c\_RFFDSP}$ , required actuator torques cannot be found due to redundancy of unknowns in the system of linear equations shown below:

$$\bar{Z}_{T\_RFFDSP} = \hat{K}_{T\_RFFDSP} \bar{F} \quad (5.95)$$

$$\text{where } \bar{Z}_{T\_RFFDSP} = \begin{bmatrix} \bar{Z}(\bar{q}, \dot{\bar{q}}, \ddot{\bar{q}}_c) \\ \bar{Z}_{c\_RFFDSP} \end{bmatrix} \text{ and } \hat{K}_{T\_RFFDSP} = \begin{bmatrix} \hat{K}(\bar{q}) \\ \hat{K}_{c\_RFFDSP} \end{bmatrix}.$$

In order to cope with the redundancy, an optimization problem based on the minimization of forces and moments included in  $\bar{F}$  is introduced such that:

$$\text{Minimize } C_{CTC\_RFFDSP} = \frac{1}{2} \bar{F}^T \cdot \hat{W}_{act\_RFFDSP} \cdot \bar{F},$$

$$\text{subject to } \hat{K}_{T\_RFFDSP} \cdot \bar{F} = \bar{Z}_{T\_RFFDSP},$$

where  $\hat{W}_{act\_RFFDSP}$  is a diagonal matrix with weighting coefficients.

Since minimization of actuator torques is significantly important, weighting coefficients related with actuator torques are taken considerably big relative to others. Using the method of Lagrange Multipliers, required actuator torques can be expressed as:

$$\bar{T} = \hat{\phi} \cdot \hat{W}_{act\_RFFDSP}^{-1} \cdot \hat{K}_{T\_RFFDSP}^T \cdot \left( \hat{K}_{T\_RFFDSP} \cdot \hat{W}_{act\_RFFDSP}^{-1} \cdot \hat{K}_{T\_RFFDSP}^T \right)^{-1} \cdot \bar{Z}_{T\_RFFDSP} \quad (5.96)$$

#### 5.2.4. For LFFDSP

Forces and moments that are assumed to be zero during LFFDSP are as shown below:

$$\begin{bmatrix} \bar{F}_{2,4}^{(4)} \\ \bar{M}_{2,4}^{(4)} \\ \bar{F}_{0,3}^{(3)} \\ \bar{M}_{0,3}^{(3)} \end{bmatrix} = \hat{K}_{c\_LFFDSP} \cdot \bar{F} = \bar{Z}_{c\_LFFDSP} \text{ for } \bar{Z}_{c\_LFFDSP} = \bar{0}.$$

$\bar{F}_{0,3}^{(3)}$ ,  $\bar{M}_{0,3}^{(3)}$  and  $\bar{F}_{2,4}^{(4)}$ ,  $\bar{M}_{2,4}^{(4)}$  are taken as zero; since it is assumed that Body 3 does not interact with the ground and interaction between Body 2, Body 4 are negated due to being rigidly fixed to the ground during LFFDSP.

Similar to RFFDSP, required actuator torques cannot be found after determining  $\hat{K}_{c\_LFFDSP}$  and  $\bar{Z}_{c\_LFFDSP}$  due to redundancy of unknowns in the system of linear equations shown below:

$$\bar{Z}_{T\_LFFDSP} = \hat{K}_{T\_LFFDSP} \cdot \bar{F} \quad (5.97)$$

$$\text{where } \bar{Z}_{T\_LFFDSP} = \begin{bmatrix} \bar{Z}(\bar{q}, \dot{\bar{q}}, \ddot{\bar{q}}_c) \\ \bar{Z}_{c\_LFFDSP} \end{bmatrix} \text{ and } \hat{K}_{T\_LFFDSP} = \begin{bmatrix} \hat{K}(\bar{q}) \\ \hat{K}_{c\_LFFDSP} \end{bmatrix}.$$

In order to cope with the redundancy, an optimization problem based on the minimization of forces and moments included in  $\bar{F}$  is introduced such that:

$$\text{Minimize } C_{CTC\_LFFDSP} = \frac{1}{2} \bar{F}^T \cdot \hat{W}_{act\_LFFDSP} \cdot \bar{F},$$

$$\text{subject to } \hat{K}_{T\_LFFDSP} \cdot \bar{F} = \bar{Z}_{T\_LFFDSP},$$

where  $\hat{W}_{act\_LFFDSP}$  is a diagonal matrix with weighting coefficients.

Weighting coefficients related with actuator torques are taken significantly bigger relative to others, considering that minimization of actuator torques is more important. Using the method of Lagrange Multipliers, required actuator torques can be expressed as:

$$\bar{T} = \hat{\phi} \cdot \hat{W}_{act\_LFFDSP}^{-1} \cdot \hat{K}_{T\_LFFDSP}^T \cdot \left( \hat{K}_{T\_LFFDSP} \cdot \hat{W}_{act\_LFFDSP}^{-1} \cdot \hat{K}_{T\_LFFDSP}^T \right)^{-1} \cdot \bar{Z}_{T\_LFFDSP} \quad (5.98)$$

## CHAPTER 6

### SIMULATION ENVIRONMENT AND RESULTS

The computer simulation of the biped locomotion is carried out by Simulink which is a tool of MATLAB software for modeling, simulating and analyzing dynamic systems. Since Simulink is fully integrated with MATLAB; in addition to Simulink's own applications, it is possible to implement MATLAB's specialized functions in a Simulink model.

There are various reasons to use Simulink for the simulation of a biped locomotion in 3D space. Function library of Simulink and MATLAB are rich enough to render the need of writing additional functions for various calculations unnecessary. Also, the method which Simulink models are built by enables a modular structure; so that arrangements or changes in the model can be achieved without affecting the general order of the model. Furthermore visualization of the simulation, which is essential to provide a general impression about and visual feedback of the modeled dynamic system to the user, can be done by using Virtual Reality Toolbox of Simulink. Also, SimMechanics Toolbox of Simulink is beneficial for simulating mechanical systems with rigid bodies. SimMechanics Toolbox can analyze a mechanical system in 4 modes which are forward dynamics, inverse dynamics, kinematics and trimming[65].

In the thesis, SimMechanics Toolbox is not used to model the biped robot for various reasons. First of all, all SimMechanics models are adjusted to their "home configurations" at the beginning of simulations. In other words, setting SimMechanics models to their home configurations which are defined by parameters in Body blocks is performed at the beginning of simulation; even if conditional subsystems that these SimMechanics models belong to are not active. For this reason, it is not able model all phases of the locomotion in the same

simulation model by using SimMechanics; because home configuration of the SimMechanics model related with the current phase has to be set at the beginning of each phase, not at the beginning of simulation. Since it is not possible set the home configuration of a SimMechanics model at different than the beginning of simulation, each phase has to be simulated in separate Simulink models. So, the simulation of biped locomotion can be achieved by running a M-file which starts simulation models of each phases orderly, supply simulation outputs recorded to MATLAB workspace by previous simulation models to the current simulation model for home configuration of SimMechanics model at the beginning of related Simulink model. This kind of simulation method is hard to implement, because it requires the transfer of many simulation outputs between simulation models and is problematic to supply simulation results to the user in terms of continuous animation. On top of that, the mathematical model describing the biped robot is not supplied by SimMechanics. However, kinematic and dynamic equations of the biped robot have to be derived in order to implement the control strategy. After considering all possible problems related with using SimMechanics in the simulation, mathematical modeling of the biped robot is achieved by user defined functions in Simulink model.

Numerical values of important variables are stored by Data Store blocks. Using Data Store blocks brings several advantages and disadvantages to the simulation model. The requirement of loading numerical values of variables to MATLAB workspace prior to the simulation is eliminated; so the simulation model includes all necessary information. Also Data Store blocks increase orderliness and flexibility of the simulation model, since numerical values can be read from or written to these blocks at any part of the simulation. However, reading and writing order of Data Store blocks must be checked carefully by using Data Store block diagnostics. For this reason, execution order of subsystems or blocks must be taken into the consideration. Moreover, changes in data store blocks are not reflected during minor time steps of fixed step continuous solvers. Therefore, few blocks related with conditional subsystems are taken as “fixed in minor step” by setting the sample time as “[0,1]”.

The simulation continues as long as the trajectory definition subsystem supplies reference inputs. Therefore, simulation stop time should be adjusted accordingly.

Variable step continuous solvers are not used in the simulation; because of unidentified problems resulting from the selection of step times. The accuracy and the computation time of simulation depend on the solver, its step size and model dynamics. Computational complexity and accuracy of the simulation increase by solver number, such as from ode1(Euler's Method) to ode5(Dormand-Prince Formula) [66]. Firstly the solver number and secondly the step size is increased until no visible differences in simulation results are observed. However, selection of the most efficient solver and step size may differ with respect to the nature of reference input and weighting coefficients of the control strategy too. Therefore, solver ode3 and step size 0.01 seconds are selected for all simulations instead of using trial and error based selection procedure explained previously for each simulation.

For convenience, different names or expressions are used in Simulink model of the simulation. For this reason, there exists an equivalence table shown Appendix A.

All numerical values are transferred in column vectors (expressed with "1D" in the simulation model), so several minor operations are performed for conversions throughout Simulink Model.

Illustrations are limited to exemplary subsystems for simplicity. Therefore whole simulation model is not illustrated by figures.

## **6.1. Simulation Model**

The simulation model consists of 11 major subsystems:

- Phase Selector
- Trajectory Definition
- RFFSSP, LFFSSP, RFFDSP and LFFDSP
- Results of Dynamic Solution
- Integration

- Visualization
- Definition of Physical Parameters
- Reading and Arrangement of Several Variables

Most of Data Store Memory blocks are located in the top-level system in order to ensure reading and writing accessibility from any location in the model. Overview of top level system of the model is shown in Figure 6.1.

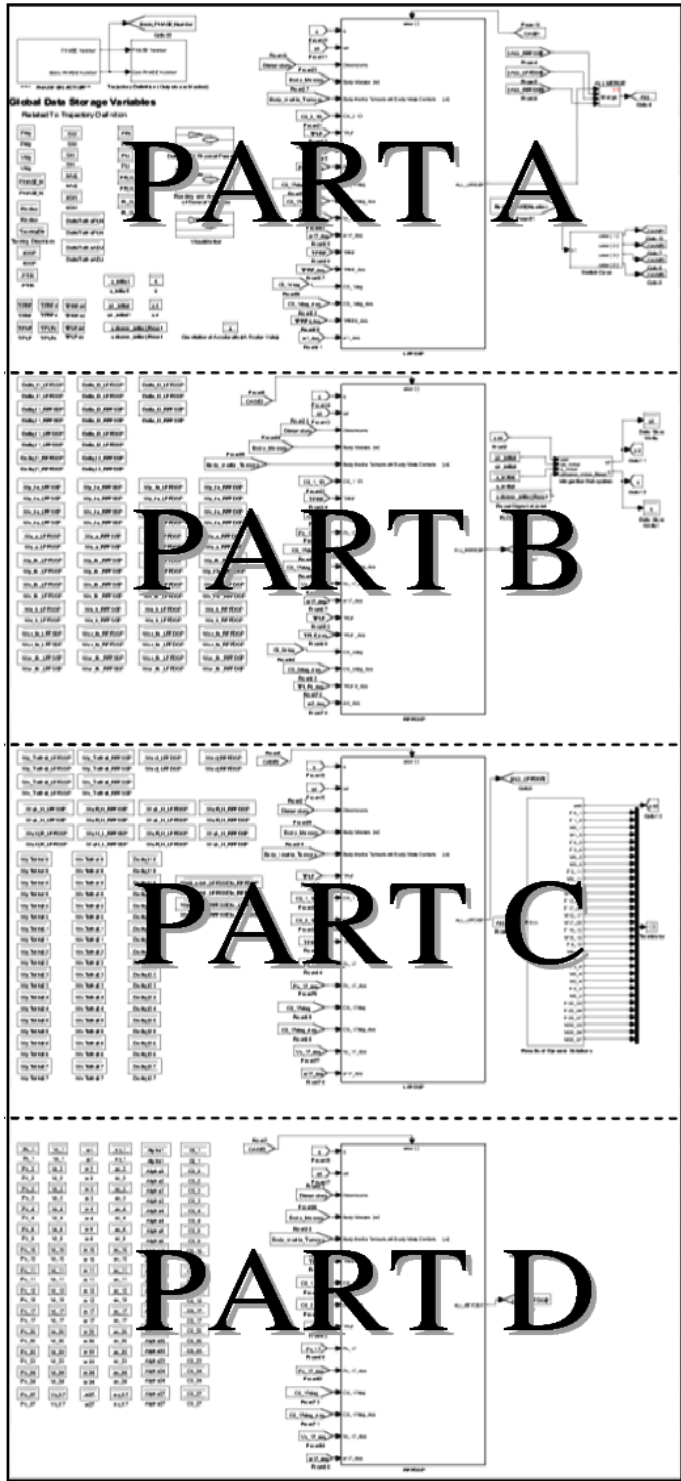


Figure 6.1: Overview of Top Level System

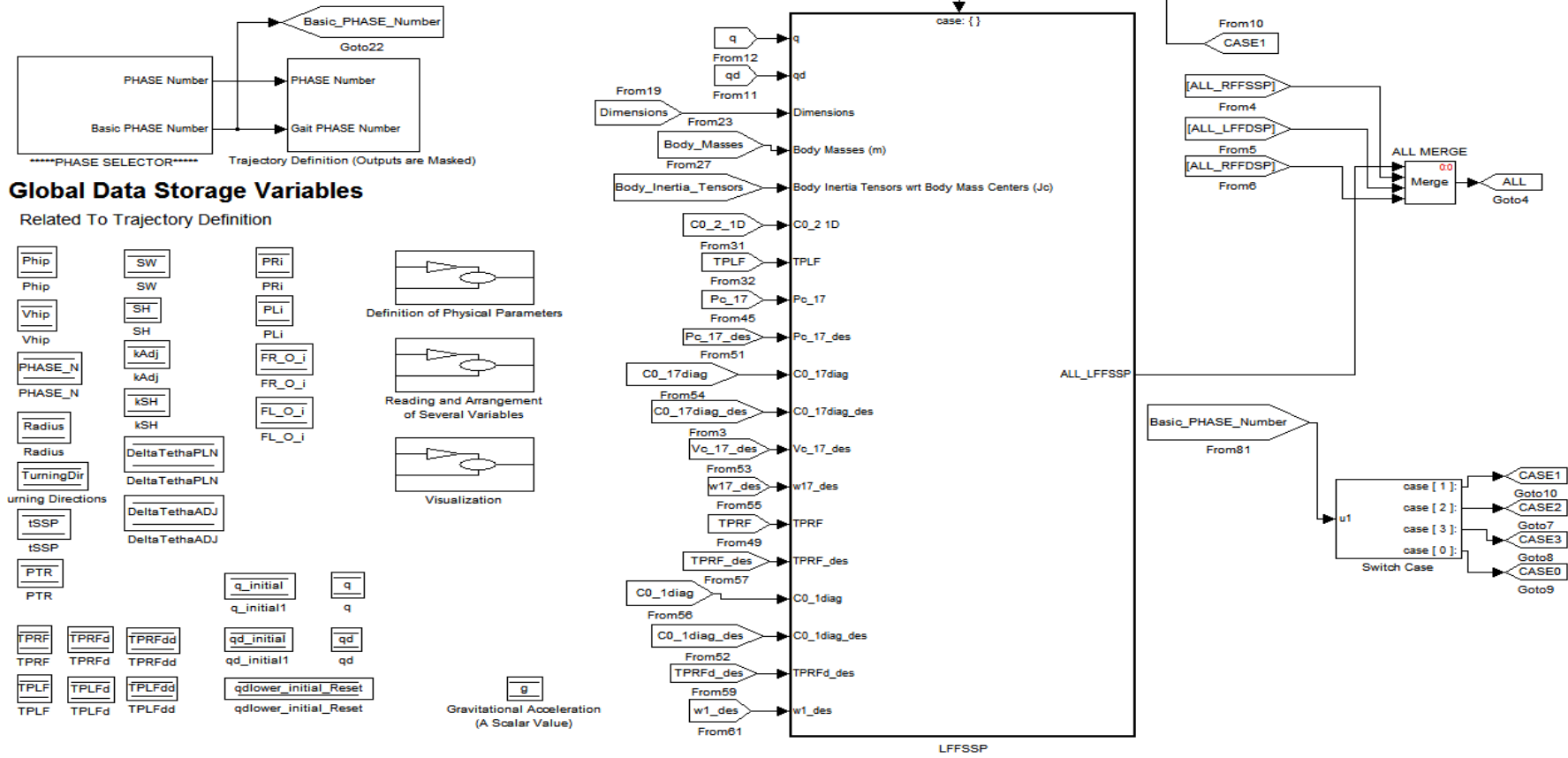


Figure 6.2: Part A of Top Level System

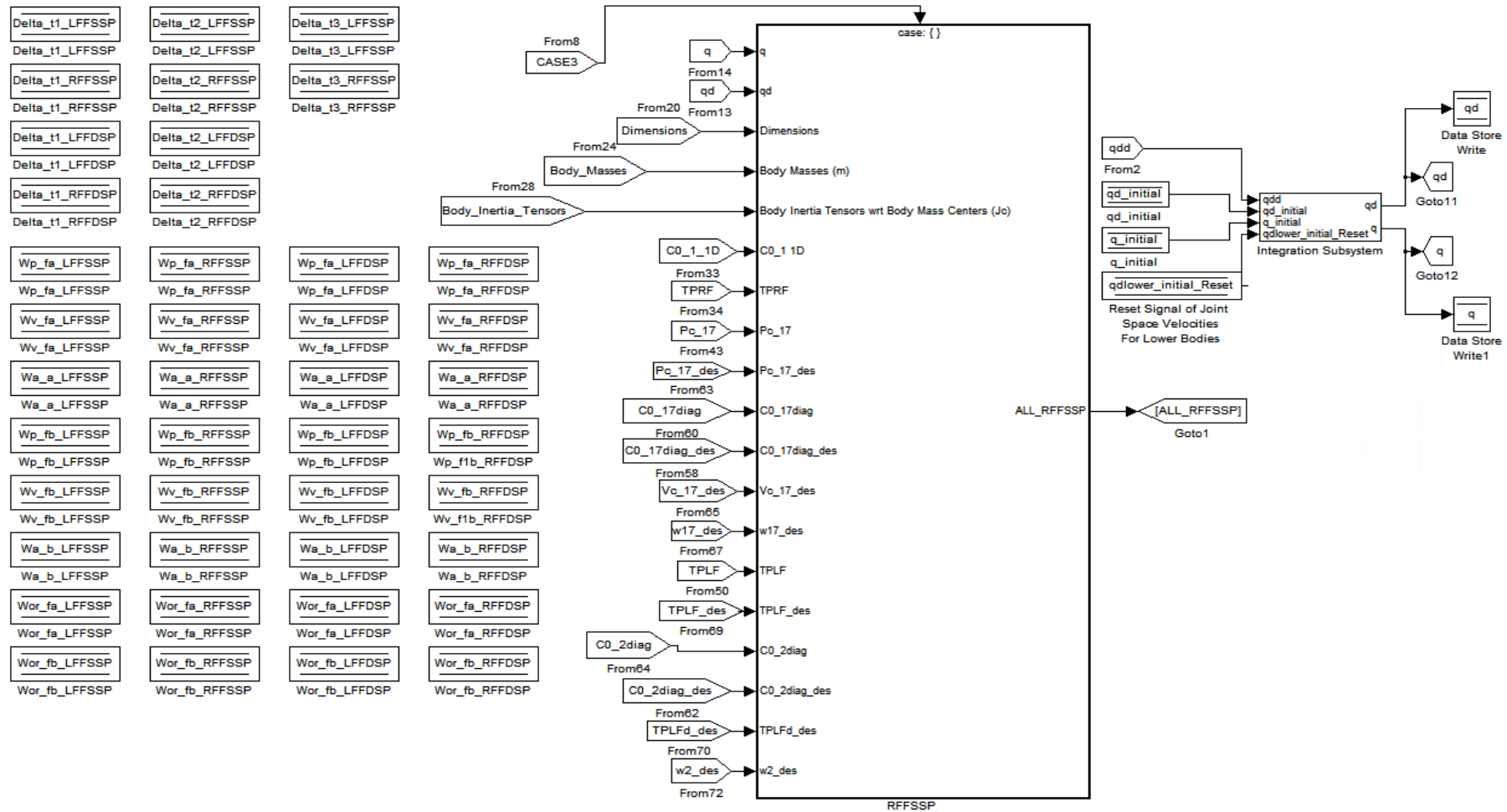


Figure 6.3: Part B of Top Level System

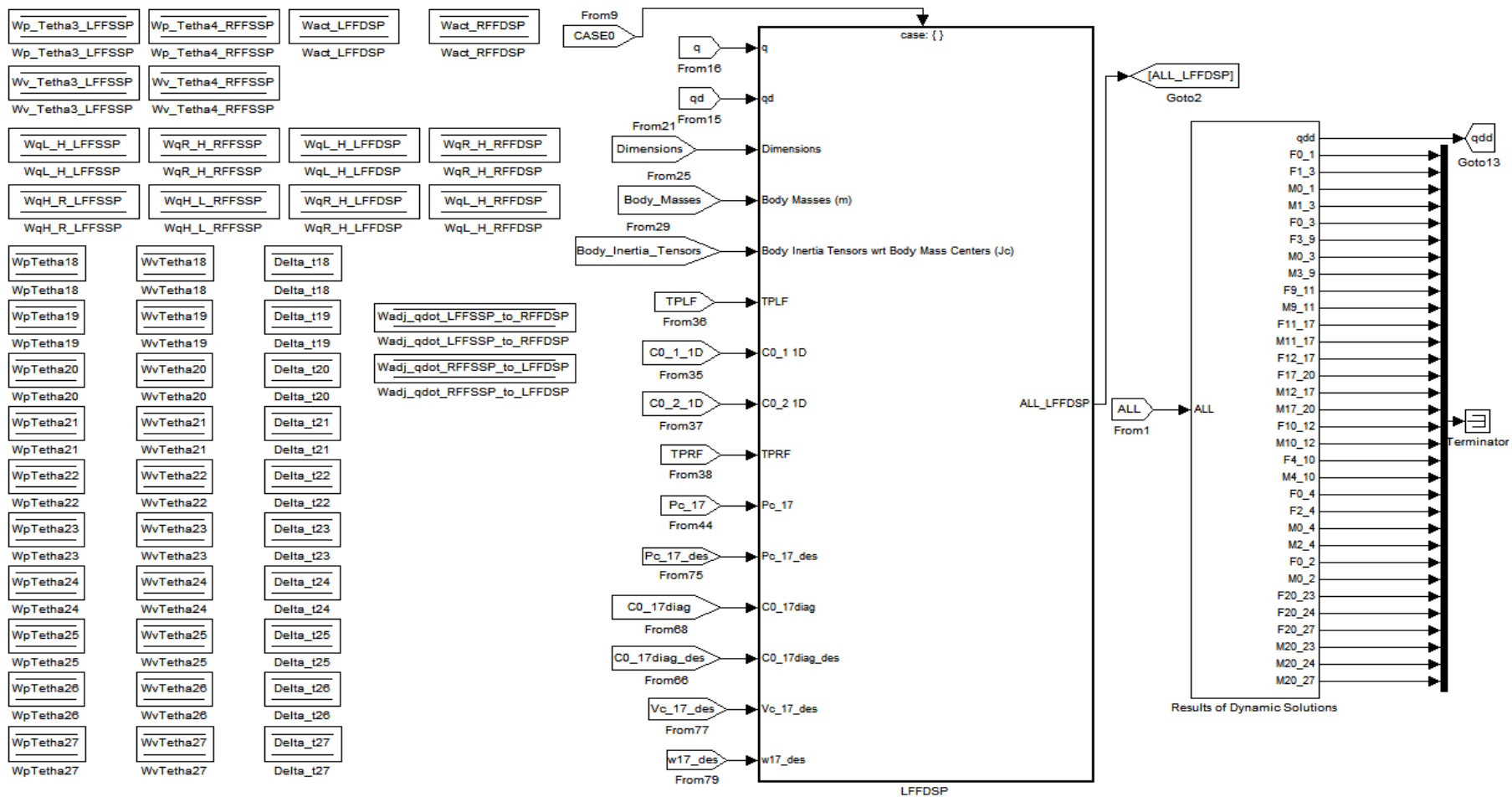


Figure 6.4: Part C of Top Level System

Pc_1	Vc_1	w1	ac_1	Alpha1	C0_1
Pc_1	Vc_1	w1	ac_1	Alpha1	C0_1
Pc_2	Vc_2	w2	ac_2	Alpha2	C0_2
Pc_2	Vc_2	w2	ac_2	Alpha2	C0_2
Pc_3	Vc_3	w3	ac_3	Alpha3	C0_3
Pc_3	Vc_3	w3	ac_3	Alpha3	C0_3
Pc_4	Vc_4	w4	ac_4	Alpha4	C0_4
Pc_4	Vc_4	w4	ac_4	Alpha4	C0_4
Pc_9	Vc_9	w9	ac_9	Alpha9	C0_9
Pc_9	Vc_9	w9	ac_9	Alpha9	C0_9
Pc_10	Vc_10	w10	ac_10	Alpha10	C0_10
Pc_10	Vc_10	w10	ac_10	Alpha10	C0_10
Pc_11	Vc_11	w11	ac_11	Alpha11	C0_11
Pc_11	Vc_11	w11	ac_11	Alpha11	C0_11
Pc_12	Vc_12	w12	ac_12	Alpha12	C0_12
Pc_12	Vc_12	w12	ac_12	Alpha12	C0_12
Pc_17	Vc_17	w17	ac_17	Alpha17	C0_17
Pc_17	Vc_17	w17	ac_17	Alpha17	C0_17
Pc_20	Vc_20	w20	ac_20	Alpha20	C0_20
Pc_20	Vc_20	w20	ac_20	Alpha20	C0_20
Pc_23	Vc_23	w23	ac_23	Alpha23	C0_23
Pc_23	Vc_23	w23	ac_23	Alpha23	C0_23
Pc_24	Vc_24	w24	ac_24	Alpha24	C0_24
Pc_24	Vc_24	w24	ac_24	Alpha24	C0_24
Pc_27	Vc_27	w27	ac_27	Alpha27	C0_27
Pc_27	Vc_27	w27	ac_27	Alpha27	C0_27

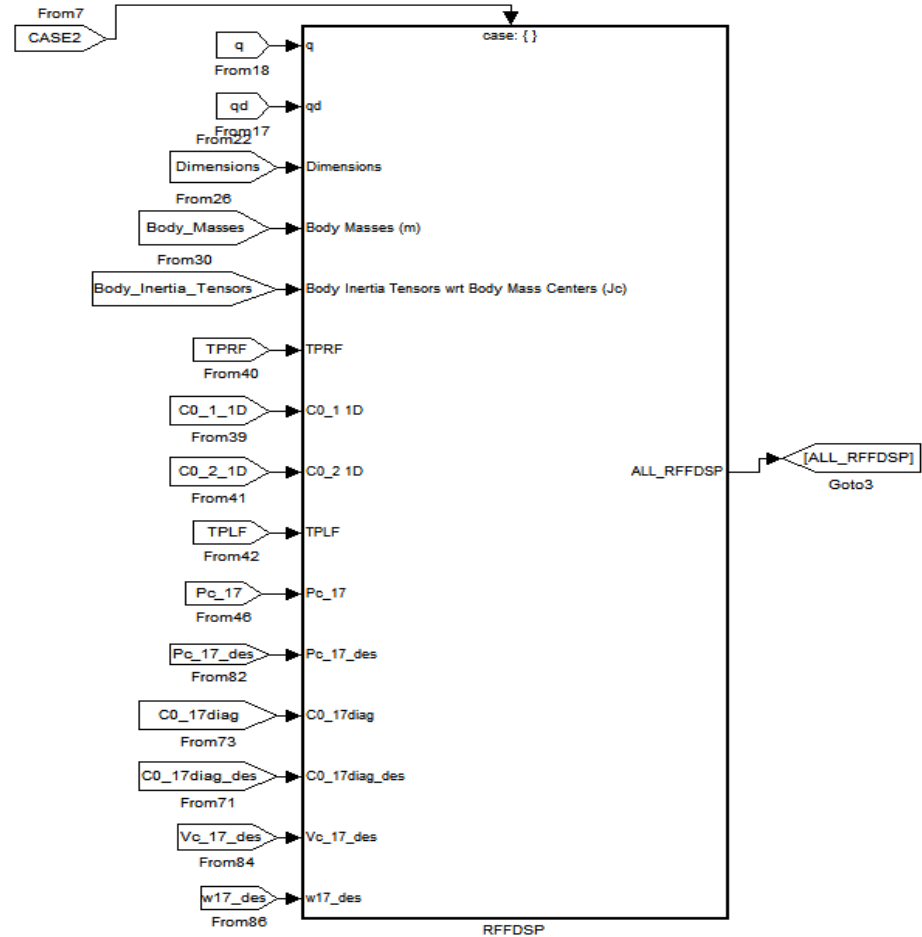
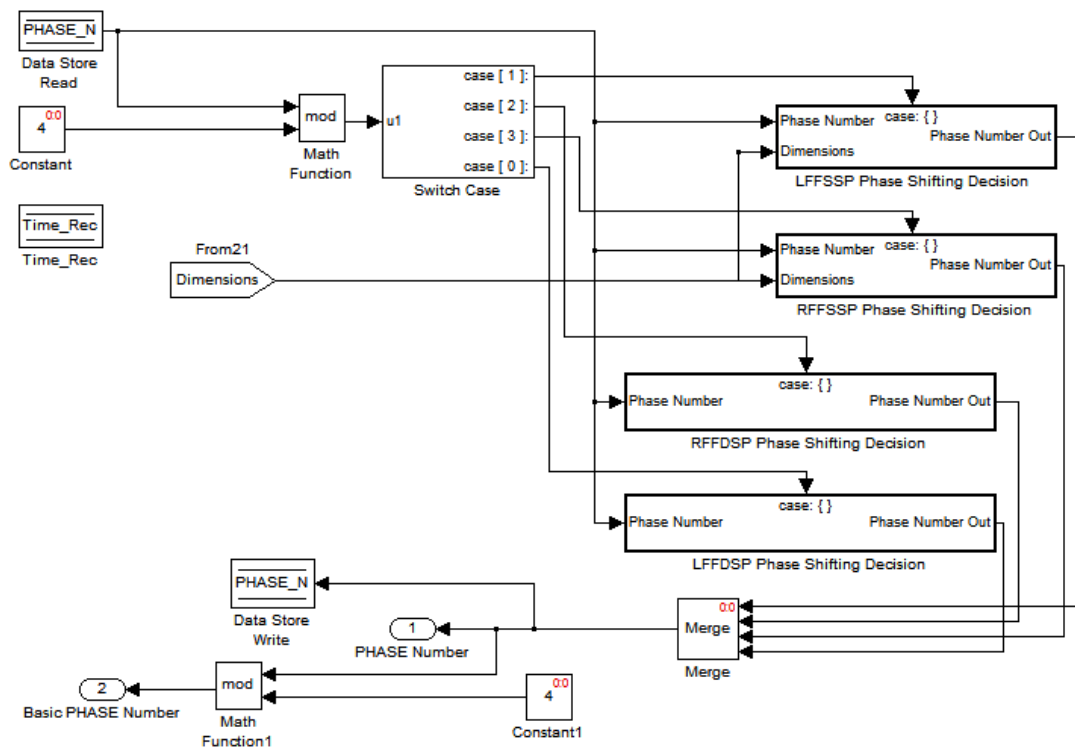


Figure 6.5: Part D of Top Level System

### 6.1.1. Phase Selector

At any step of the simulation, firstly phase selector subsystem runs to determine the current locomotion phase. According to the current phase number of biped locomotion, basic phase number and consequently current locomotion phase is detected. Then, related conditional subsystem which makes the decision if phase change is required or not is activated by a switch case block. Outputs of phase selector subsystem are supplied to trajectory definition subsystem and activate the conditional subsystem of the current locomotion phase which is located in the top level system (like RFFSSP).



**Figure 6.6: Phase Selector**

The procedure behind phase shifting decision subsystems are explained for single and double support phases separately.

### 6.1.1.1. Phase Shifting Decision for Single Support Phases

According to supplied phase number and parameters which are used for the definition of reference trajectories, expected positions for the toe point of swinging foot (for example, the toe point on Body 1 for LFFSSP) and mass center of Body 17 at the end of current phase are calculated in the subsystem labeled as “Expected Resultant Hip and Toe Point Locomotions for the Current Phase”. 2 conditions are specified in order to make a decision about ending the current phase. Both conditions have to be satisfied for phase change.

$$\text{For } \bar{P}_{tpR} = \begin{bmatrix} P_{tpR_x} \\ P_{tpR_y} \\ P_{tpR_z} \end{bmatrix} \text{ and } \bar{P}_{tpL} = \begin{bmatrix} P_{tpL_x} \\ P_{tpL_y} \\ P_{tpL_z} \end{bmatrix},$$

- $(P_{tpR_z} \text{ or } P_{tpL_z}) - 0.015 < 0.001 \text{ m}$
- $\left\{ \left[ \begin{array}{c} (P_{tpR_x} \text{ or } P_{tpL_x}) \\ - (P_{tpR,i_x} \text{ or } P_{tpL,i_x}) \end{array} \right]^2 + \left[ \begin{array}{c} (P_{tpR_y} \text{ or } P_{tpL_y}) \\ - (P_{tpR,i_y} \text{ or } P_{tpL,i_y}) \end{array} \right]^2 \right\}^{0.5} > 0.3 \times$   
 $\left( \left[ \begin{array}{c} (P_{tpR,f_x} \text{ or } P_{tpL,f_x}) \\ - (P_{tpR,i_x} \text{ or } P_{tpL,i_x}) \end{array} \right]^2 + \left[ \begin{array}{c} (P_{tpR,f_y} \text{ or } P_{tpL,f_y}) \\ - (P_{tpR,i_y} \text{ or } P_{tpL,i_y}) \end{array} \right]^2 \right)^{0.5}$

$\bar{P}_{tpR,i}$  or  $\bar{P}_{tpL,i}$  is the toe point position at the beginning of current phase.  $\bar{P}_{tpR,f}$  or  $\bar{P}_{tpL,f}$  is the expected toe point position at the end of current phase.

$P_{tpL_x}$ ,  $P_{tpL_y}$  and  $P_{tpL_z}$  are used for RFFSSP. Similarly  $P_{tpR_x}$ ,  $P_{tpR_y}$  and  $P_{tpR_z}$  are used for LFFSSP. In the first condition, the toe part of foot is assumed to be in contact with the ground when  $\vec{u}_3^{(0)}$  component of toe point position is less than 0.015 m which is a dimension of the modeled body within a tolerance of 0.001 m. The second condition is imposed to avoid phase shifting at the beginning of locomotion phase; because the first condition is satisfied since the swinging foot is almost flatly in contact with the ground at the beginning of SSPs. According to the second condition, the toe point of swinging foot must move more than at least 0.3 times of total expected displacement in the plane defined by  $\vec{u}_1^{(0)}$  and  $\vec{u}_2^{(0)}$ .

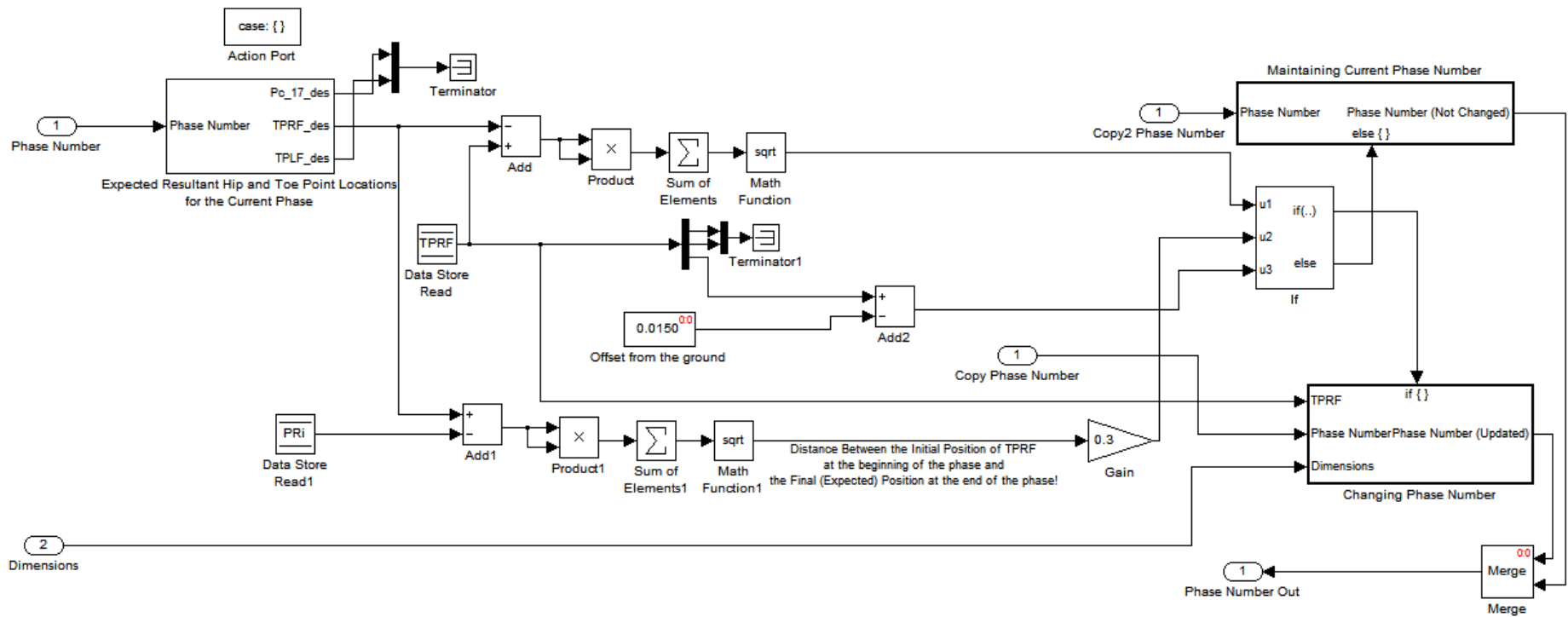


Figure 6.7: LFSSP Phase Shifting Decision

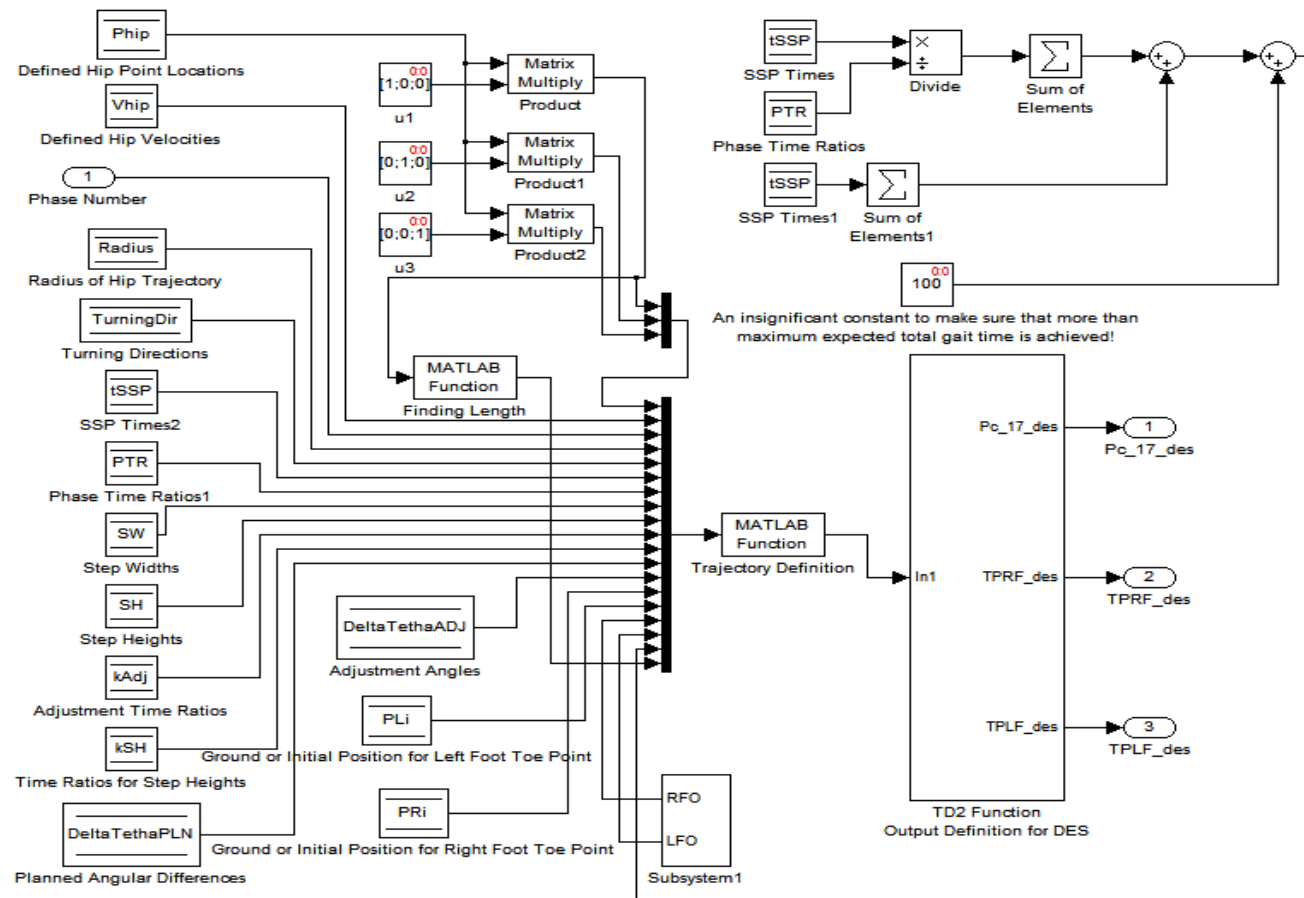


Figure 6.8: Expected Resultant Hip and Toe Point Locations for the Current Phase

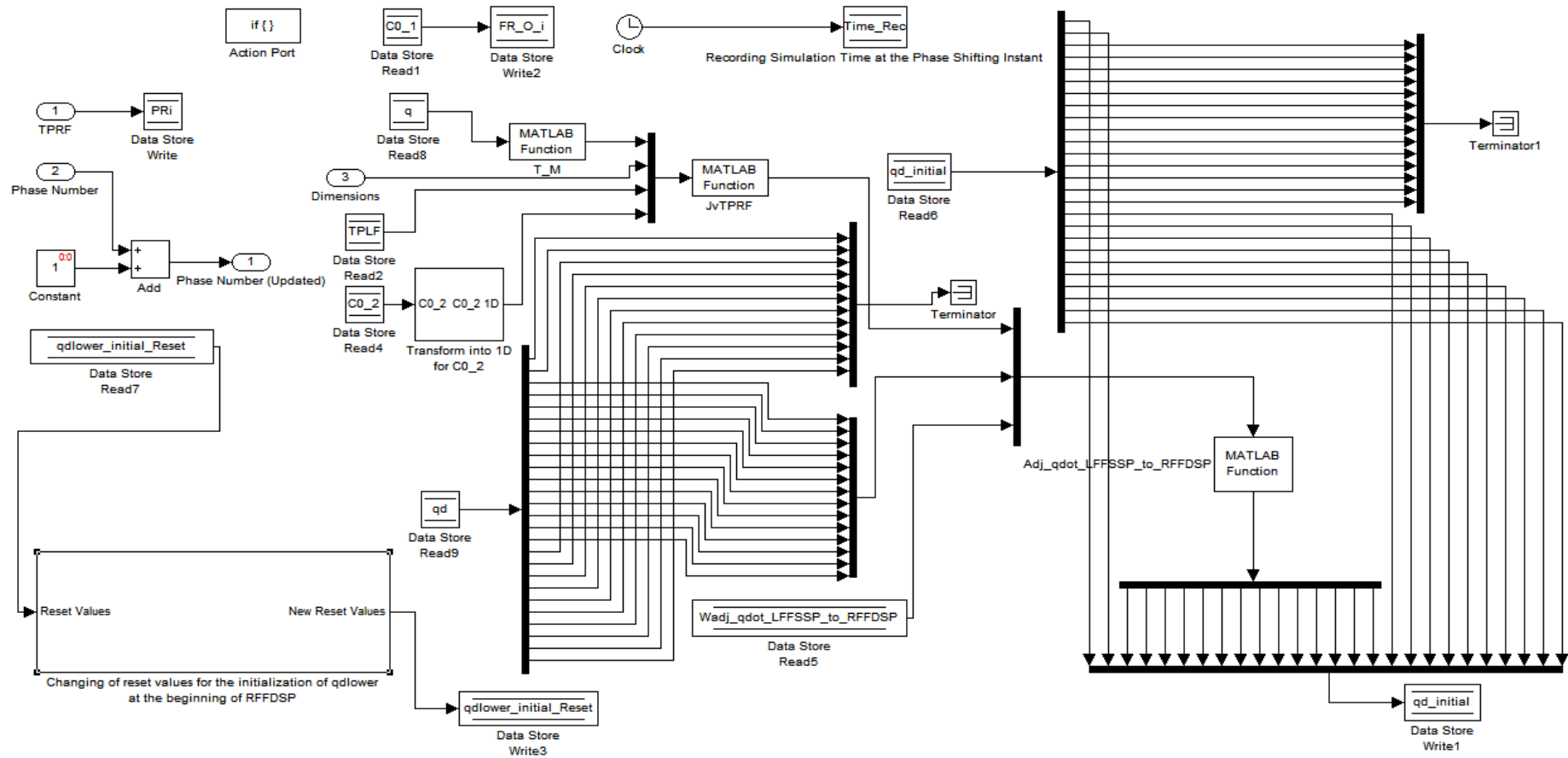
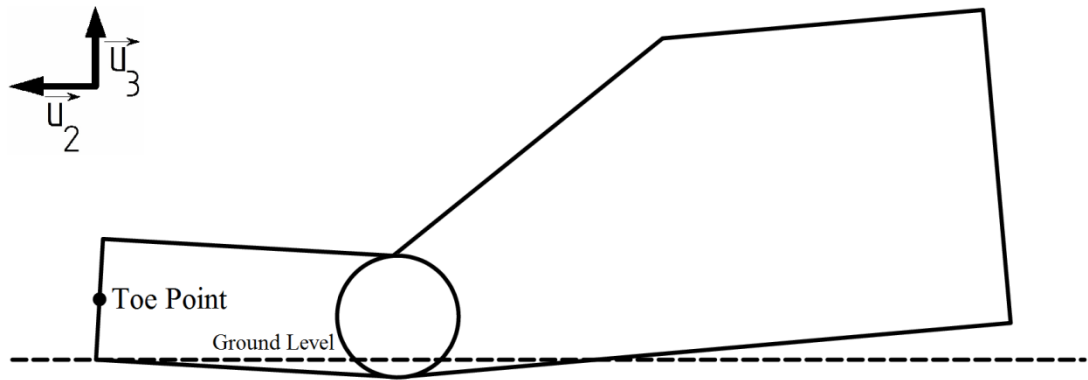
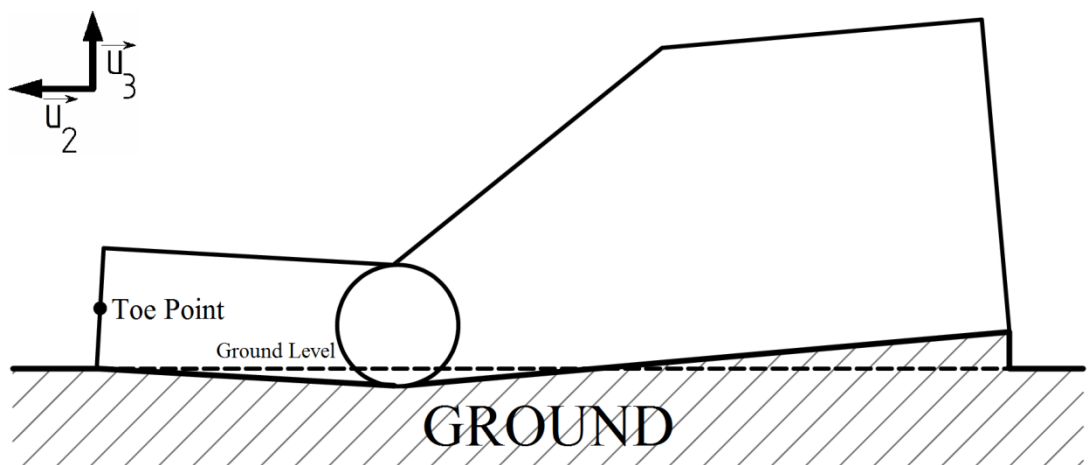


Figure 6.9: Changing Phase Number in LFFSSP

To summarize, only the position of toe point is considered for phase shifting decision. Moreover, the orientation of contacting bodies is ignored. When these phase shifting conditions are met, kinematic condition as specified in chapter 4 are applied for bodies assumed to be in contact, neglecting if contacting bodies are flat or not relative to the ground as illustrated in Figure 6.10 and Figure 6.11. Therefore, it is left to the user's responsibility that the orientation of contacting bodies should be eventually parallel to the ground at the end of single support phases.



**Figure 6.10: Contacting Bodies Before Phase Change**



**Figure 6.11: Contacting Bodies After Phase Change**

In the subsystem where expected positions are calculated as shown in Figure 6.8, a numerical value bigger than expected total simulation time is supplied to ensure that the trajectory definition function calculates its output for the end of the current phase. The trajectory definition function calculates its output for the beginning of the current phase if the simulation time is smaller than the specified time for the beginning of current phase. Similarly, the trajectory definition function calculates its output for the end of current phase, if the simulation time exceeds specified time for the end of current phase. For example, assume that the specified time for the end of phase which is numbered as 5 is 6 seconds which can be calculated by using numerical values included in  $t_{SSP}$  and  $PTR$ . At the instant where the current phase number is 5 and simulation time is 6.4 seconds, the trajectory definition function will calculate its outputs for the end of phase number 5 until the phase number is changed. So by supplying numerical values big enough to exceed specified end time for the current phase, it is ensured that the trajectory definition function will supply expected positions at the end of current phase.

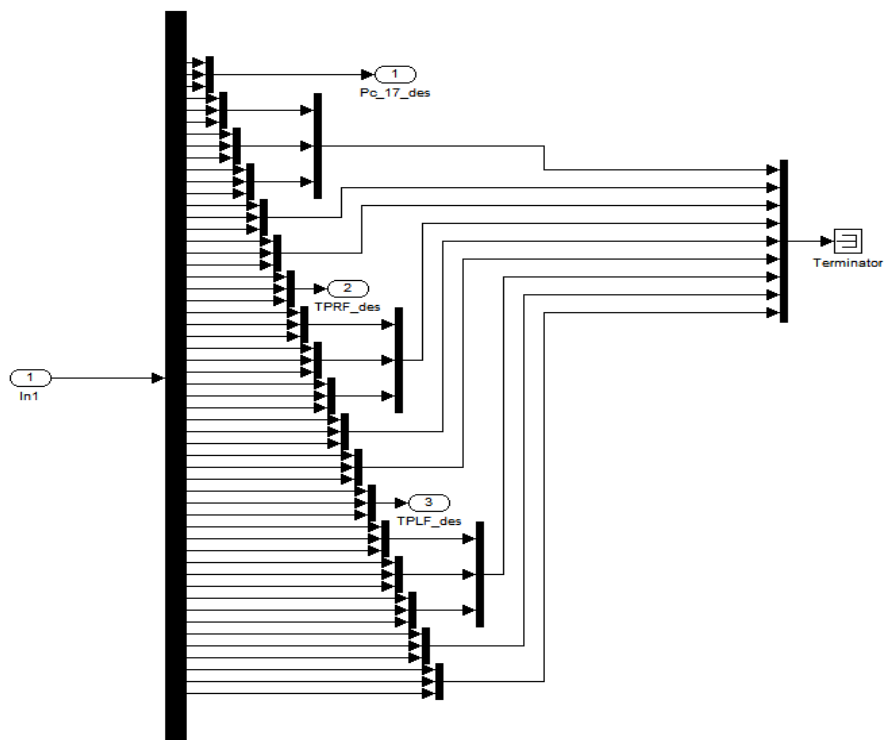


**Figure 6.12: TD2 Function Output Definition for DES**

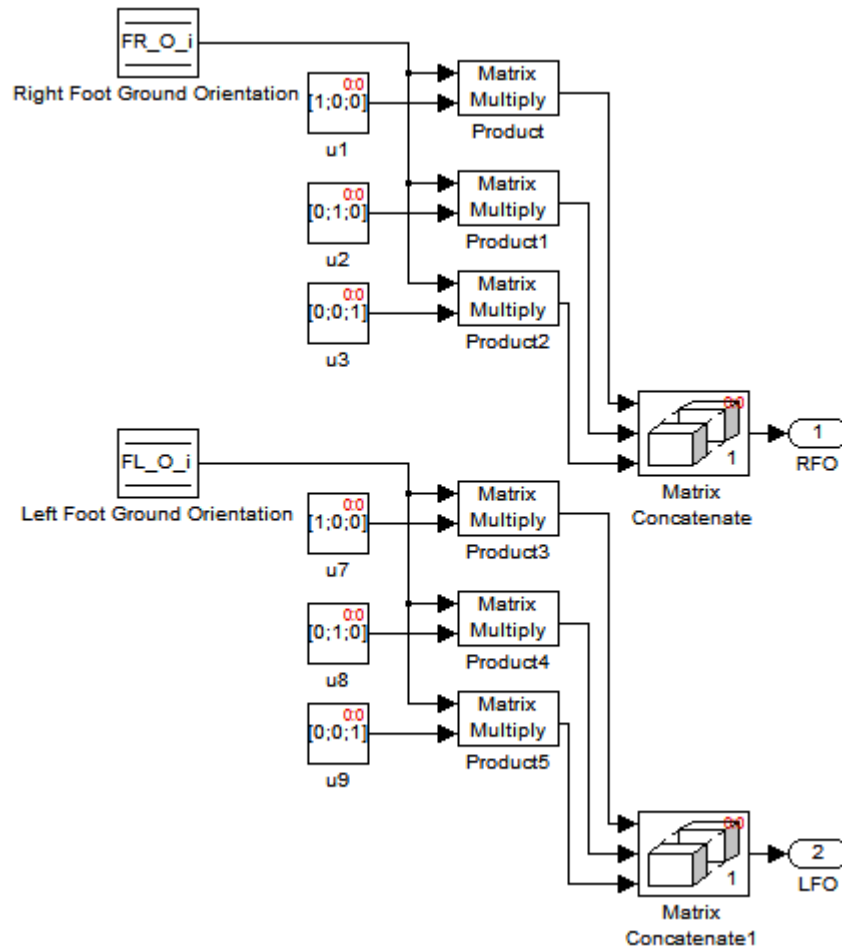


**Figure 6.13: Subsystem1**

Required outputs, which are positions, are extracted in the subsystem shown in Figure 6.12 and arrangement of some inputs into the column vector format is done in the subsystem shown in Figure 6.13 labeled as “Subsystem1”, where these subsystems are included in the subsystem shown in Figure 6.8.

If the phase change is decided; in addition to increasing phase number by one, the related subsystem shown in Figure 6.9 is run to perform operations for the transition from single support to double support phases explained in Chapter 4; otherwise phase number is supplied back without being changed by the subsystem labeled as “Maintaining Current Phase Number” . Calculations are carried out by user defined function `Adj_qdot_LFFSSP_to_RFFDSP` or `Adj_qdot_RFFSSP_to_LFFDSP`.

Computed values are written into the data store block “qd\_initial” to be used as the initial condition source for integration blocks in the integration subsystem. Also the simulation time at the instant of phase change is recorded in the data store block “Time\_Rec” to assist determining elapsed time in double support phases for phase changing decision subsystems of double support phases. Moreover, position and orientation of toe point and its related body at the end of phase are stored to be supplied to the trajectory definition function in following phases. External reset values of integration blocks used in the integration subsystem are changed by the subsystem shown in Figure 6.14.

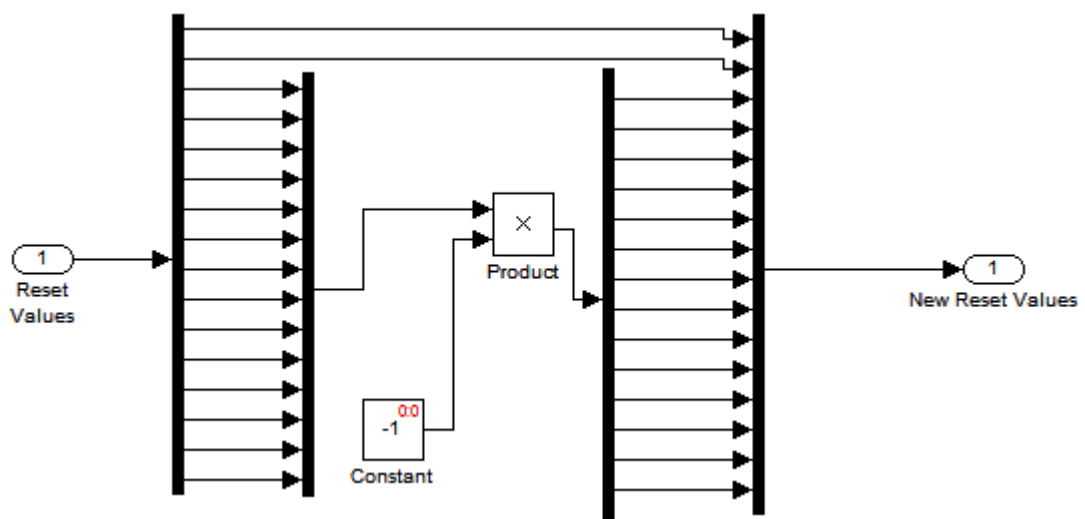


**Figure 6.14: Changing of Reset Values for the Initialization of  $\bar{q}_{lower}$  at the Beginning of RFFDSP**

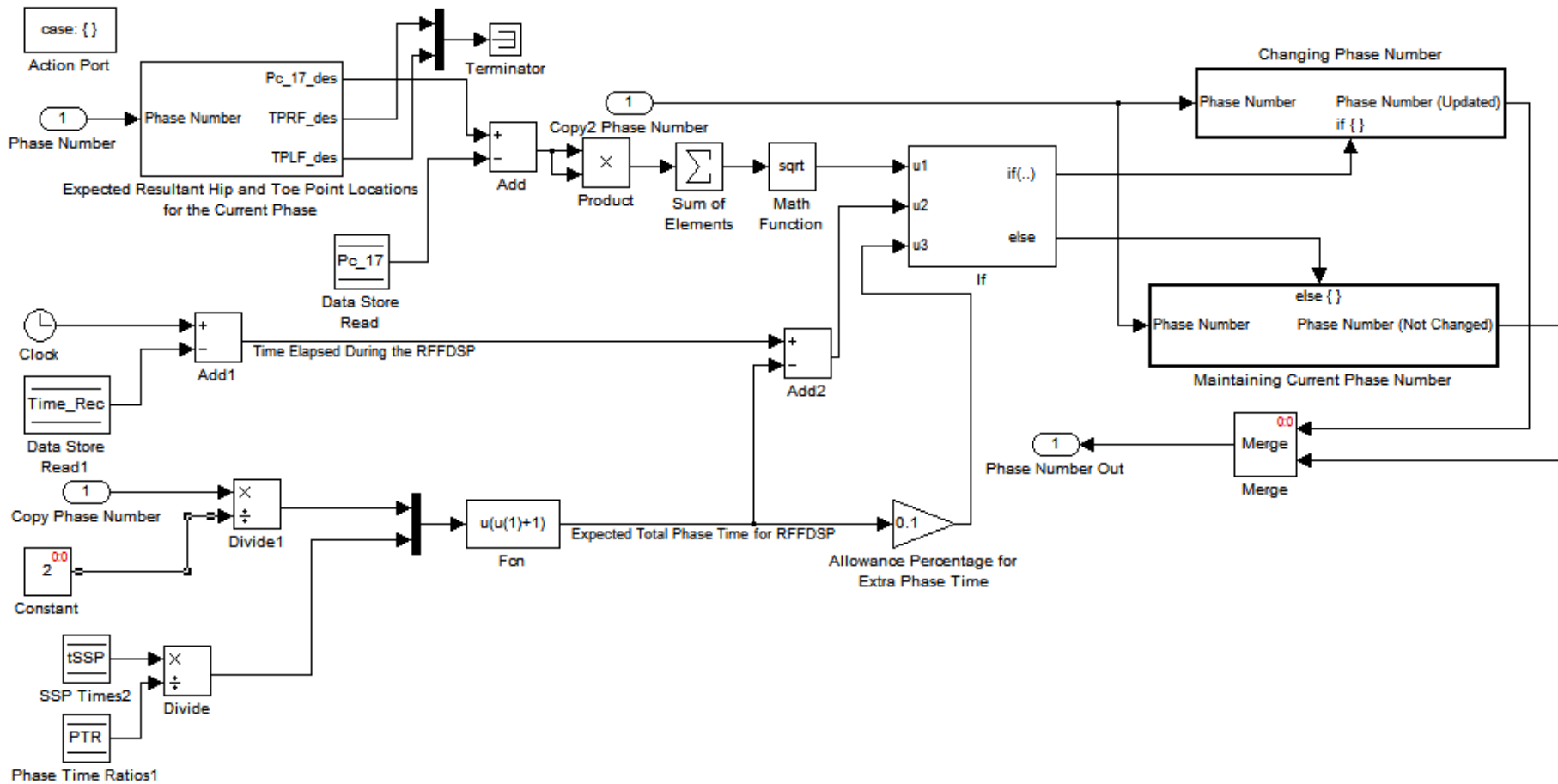
### 6.1.1.2. Phase Shifting Decision for Double Support Phases

Expected position of the mass center of Body 17 at the end of the current phase is calculated in the subsystem labeled as “Expected Resultant Hip and Toe Point Locomotions for the Current Phase” which is exactly the same subsystem used in single support phases. 2 conditions are specified.

At least one of these conditions has to be satisfied for phase change:

- $\sqrt{\left(P_{c,17_x} - P_{c,17,f_x}\right)^2 + \left(P_{c,17_y} - P_{c,17,f_y}\right)^2 + \left(P_{c,17_z} - P_{c,17,f_z}\right)^2} < 0.05 \text{ m}$
- $(t - t_{DSP,k}) > 0.1 \times t_{DSP,k}$

The first condition implies that the double support phase ends if the distance between expected position of the mass center of Body 17 at the end of current phase and current position of the mass center of Body 17 is less than 0.05 m. Due to the second condition, the double support phase ends if the current phase lasts ten percent longer than given duration time  $t_{DSP,k}$  for the related double support phase. If the phase change is decided; phase number is increased by one in the subsystem “Changing Phase Number”. Otherwise, the same phase number is supplied back by “Maintaining Current Phase Number” subsystem. The subsystem “Expected Resultant Hip and Toe Point Locations for the Current Phase” is the same subsystem used in single support phases as shown in Figure 6.8



184

Figure 6.15: RFFDSP Phase Shifting Decision

## 6.1.2. Trajectory Definition

Once the trajectory definition subsystem is supplied with basic phase number and phase number, 2 sets of reference input are calculated. Reference inputs for 2 different times are calculated due to the usage of 2 different prediction times in single support phases.

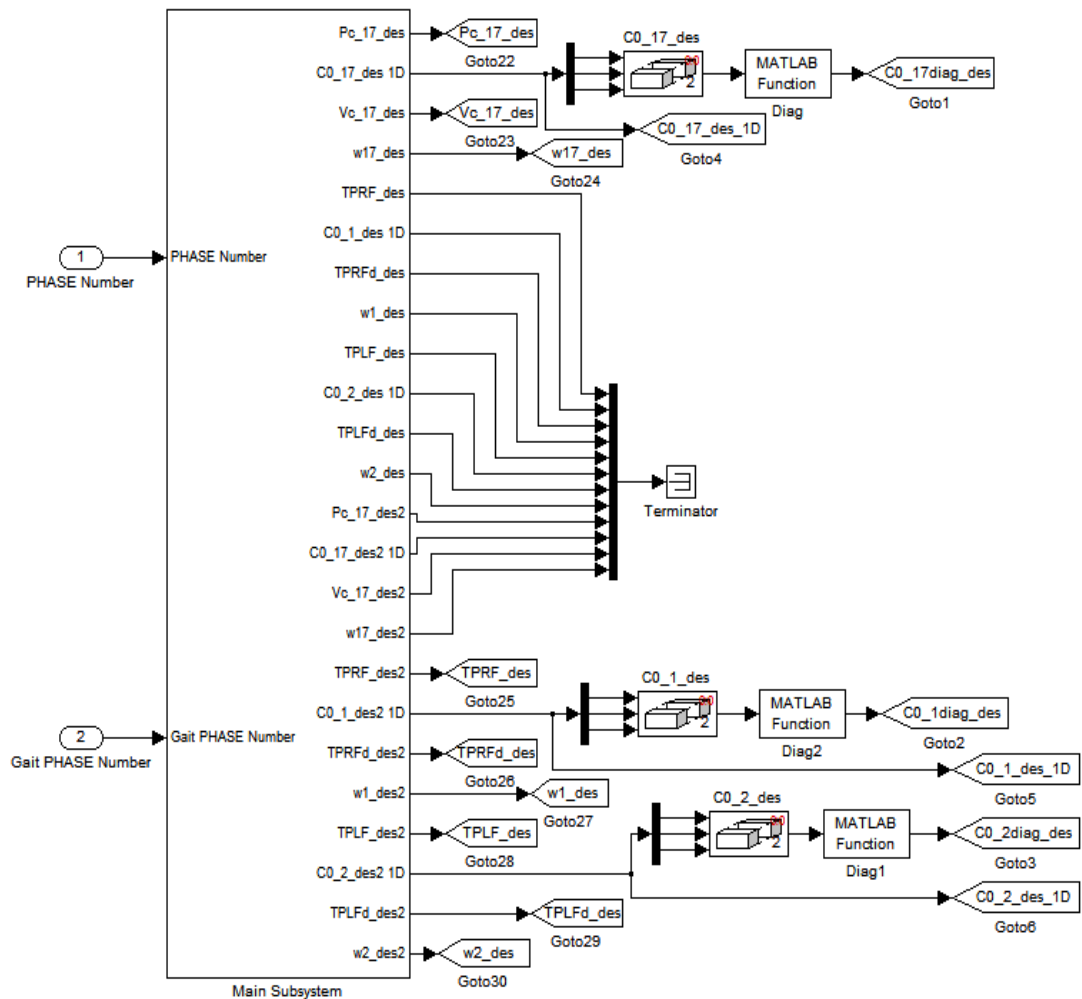


Figure 6.16: Overall View of Trajectory Definition

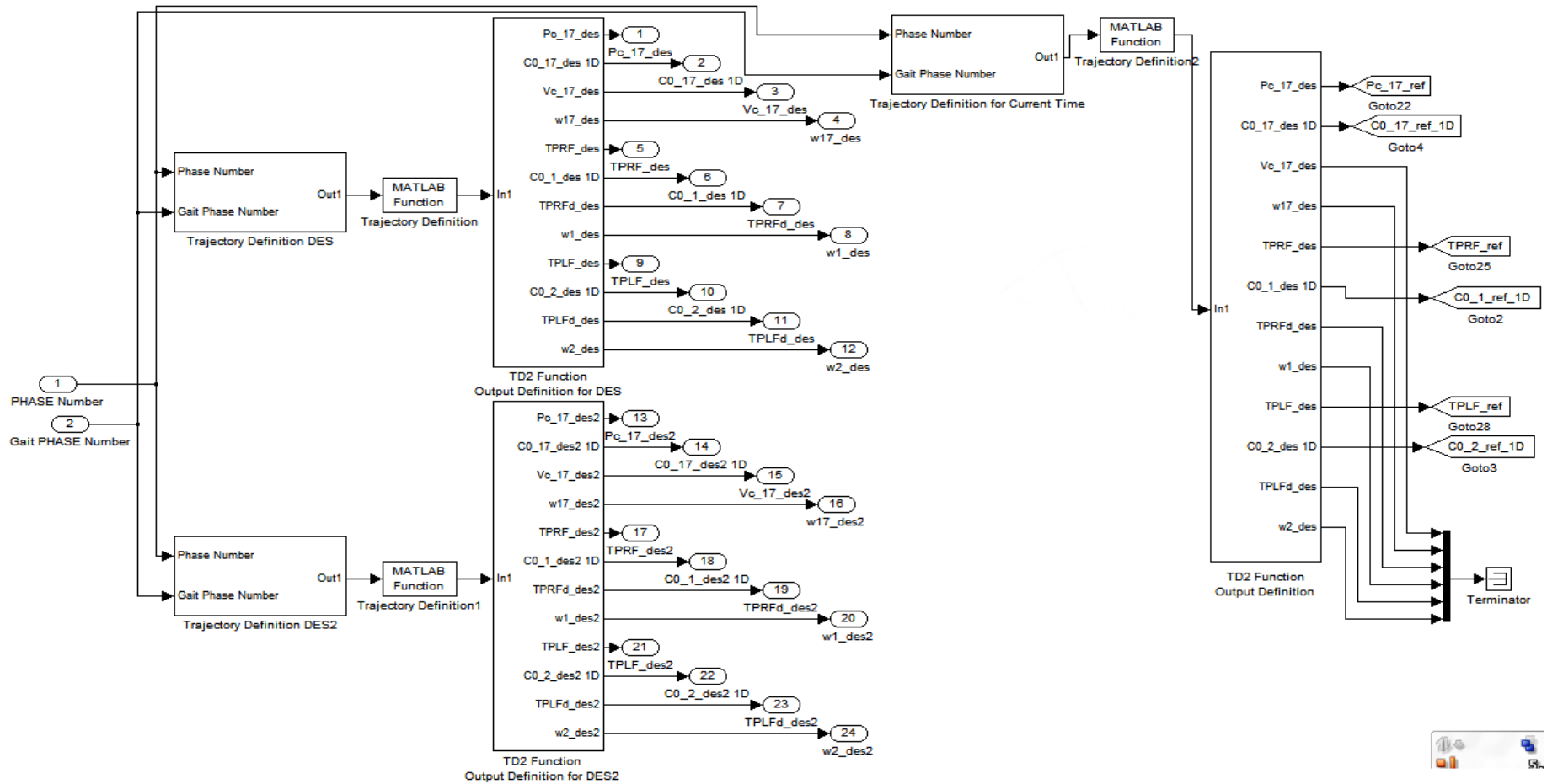


Figure 6.17: Main Subsystem of Trajectory Definition

Inputs to trajectory definition functions are prepared in 2 subsystems named as “Trajectory Definition DES” and “Trajectory Definition DES2”. The only difference between “Trajectory Definition DES” and “Trajectory Definition DES2” is the time information to be supplied to trajectory definition functions. In single support phases during optimum command acceleration calculations, the prediction time for Body 17 and its mass center is used in “Trajectory Definition DES” subsystem; also the prediction time for the toe point and its related body is used in “Trajectory Definition DES2” subsystem. In double support phases, the same prediction time is used for both subsystems since only one prediction time is employed during optimum command accelerations calculation. Also, there exists an additional subsystem labeled as “Trajectory Definition for Current Time” which supplies reference input for the current simulation time to be used in the virtual environment for animating the reference input.

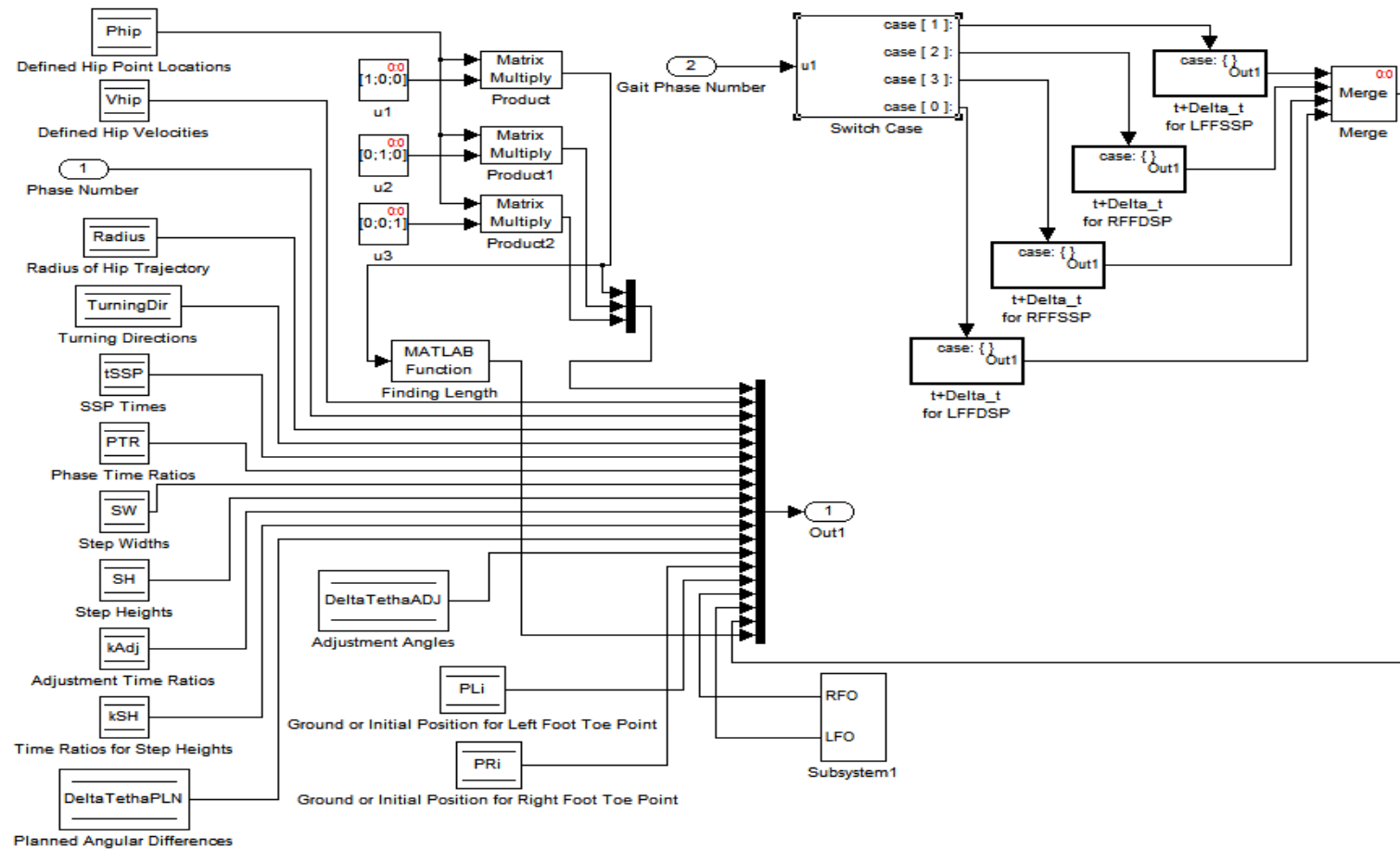
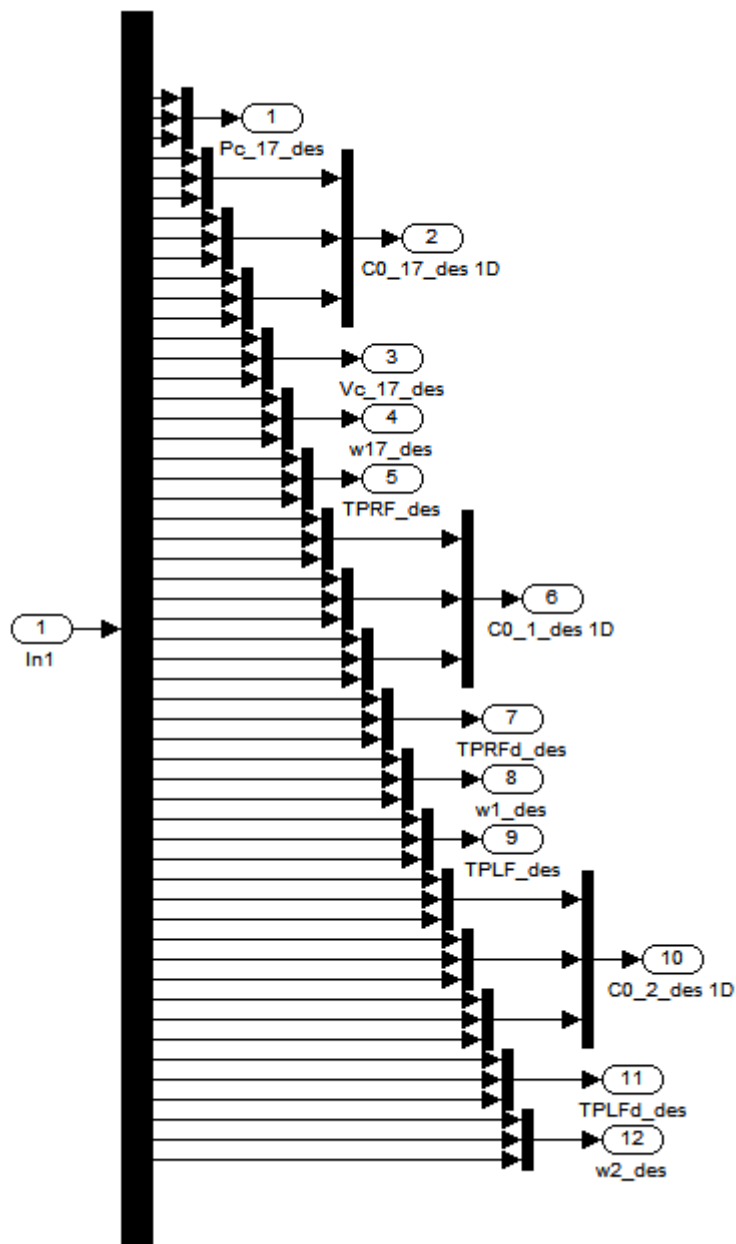


Figure 6.18: Trajectory Definition DES or DES2

Arrangement of some inputs into the column vector format is done in the subsystem shown in Figure 6.13 labeled as “Subsystem1” which is a part of the subsystem shown in Figure 6.18.

Outputs of trajectory definition functions are extracted in subsystems labeled as “TD2 Function Output Definition for DES”, “TD2 Function Output Definition for DES2” and “TD2 Function Output Definition” which have the same structure other than output label names.



**Figure 6.19: TD2 Function Output Definition for DES**

### 6.1.3. Models Related with Locomotion Phases (RFFSSP, LFFSSP, RFFDSP, LFFDSP)

Application of mathematical models regarding locomotion phases are achieved in these subsystems. These subsystems are divided into 4 basic subsystems which are calculations related with kinematics, optimum command accelerations, computed torque control and direct dynamic solution. The overall view of the subsystem “LFFSSP” is shown in Figure 6.20, Figure 6.21 and Figure 6.22

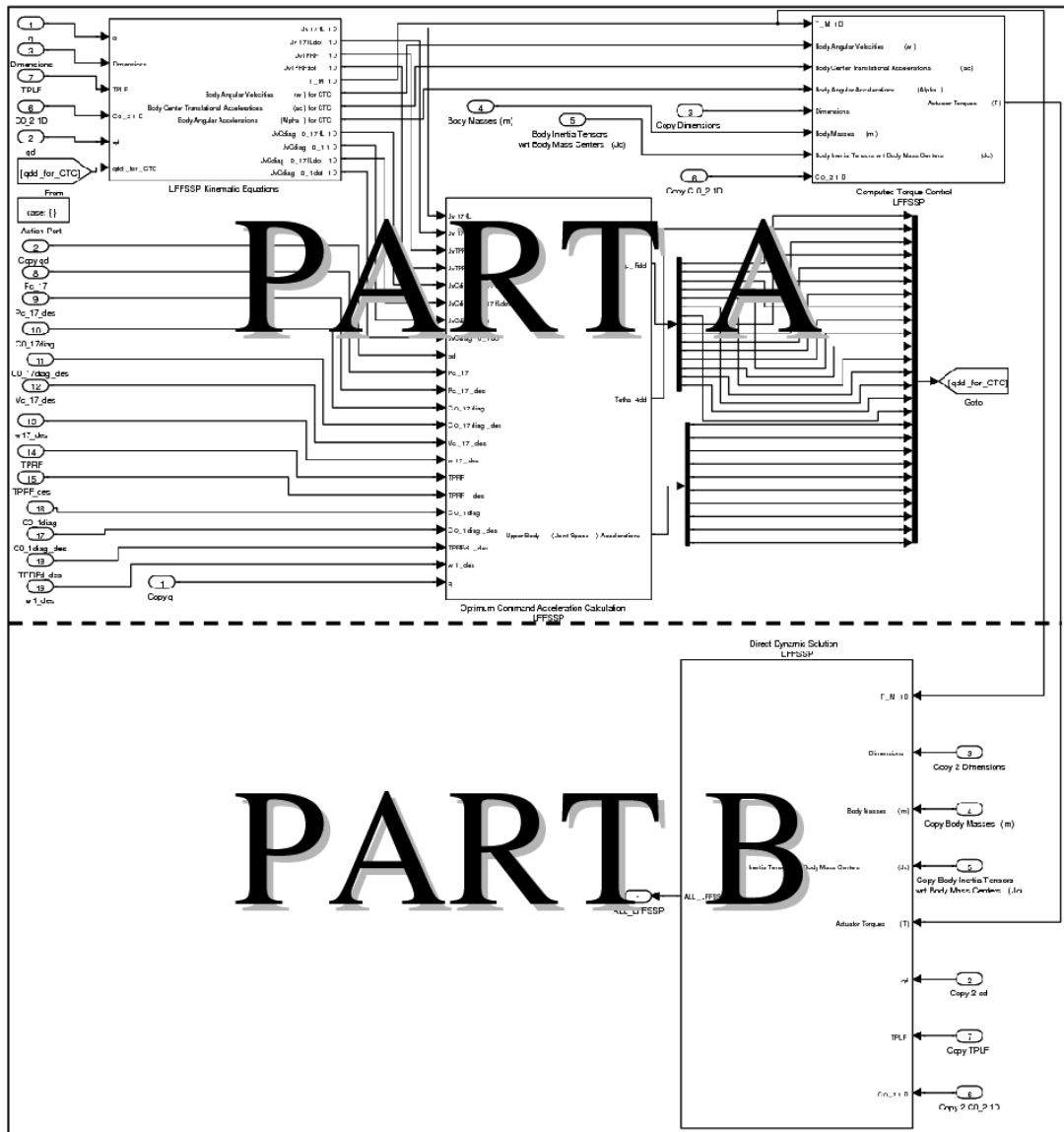


Figure 6.20: Overall View of LFFSSP

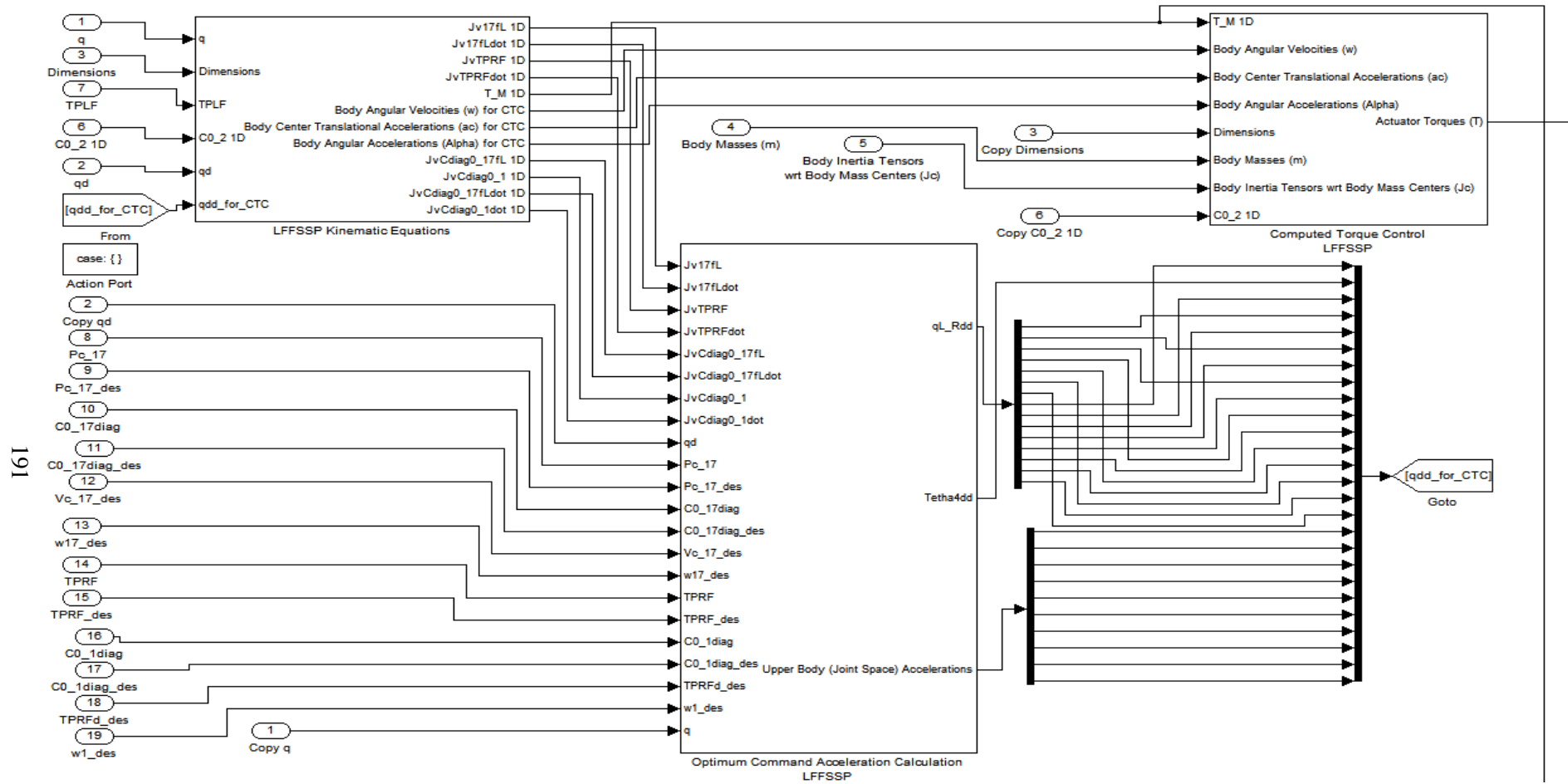
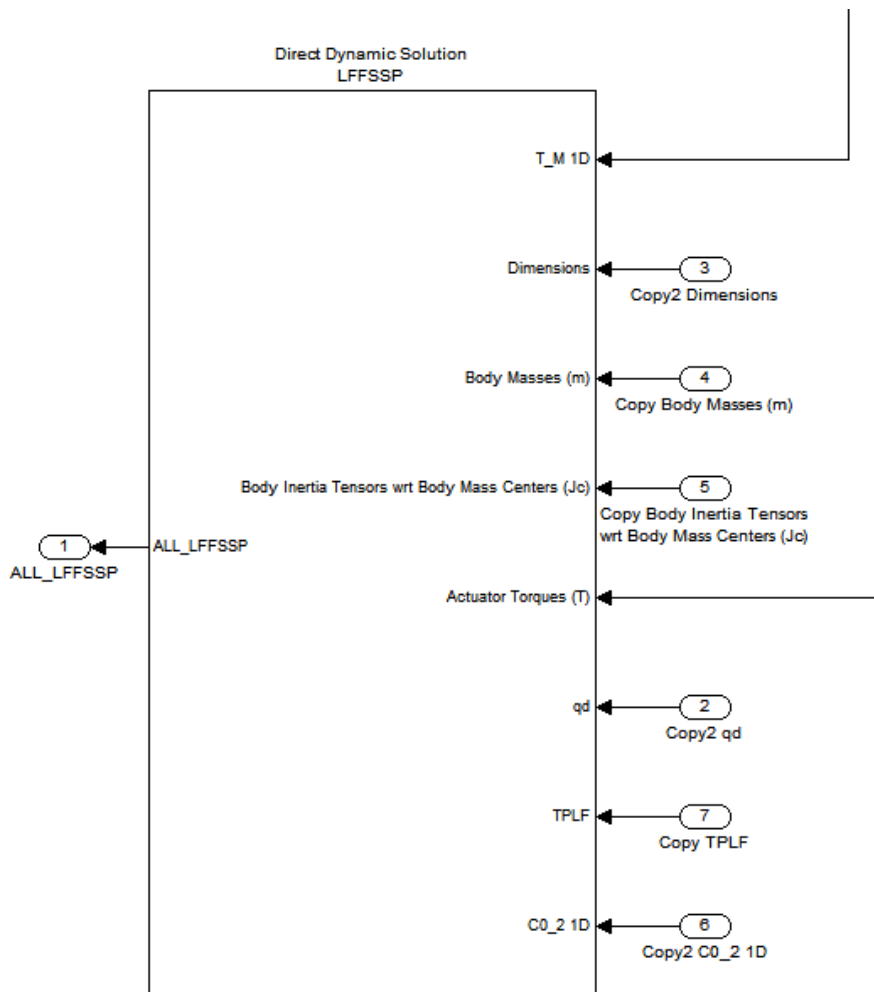


Figure 6.21: Part A of LFSSP



**Figure 6.21: Part B of LFFSSP**

Calculations of jacobian matrices and kinematic values which are supplied to the computed torque control subsystem are done in the subsystem regarding kinematics. Also, matrices and vectors used for the construction of kinematic constraint equations in optimum command accelerations calculation of double support phases are calculated in this subsystem too. Moreover, kinematic equations are called internally in various user defined matlab functions, which can not be observed on the Simulink model.



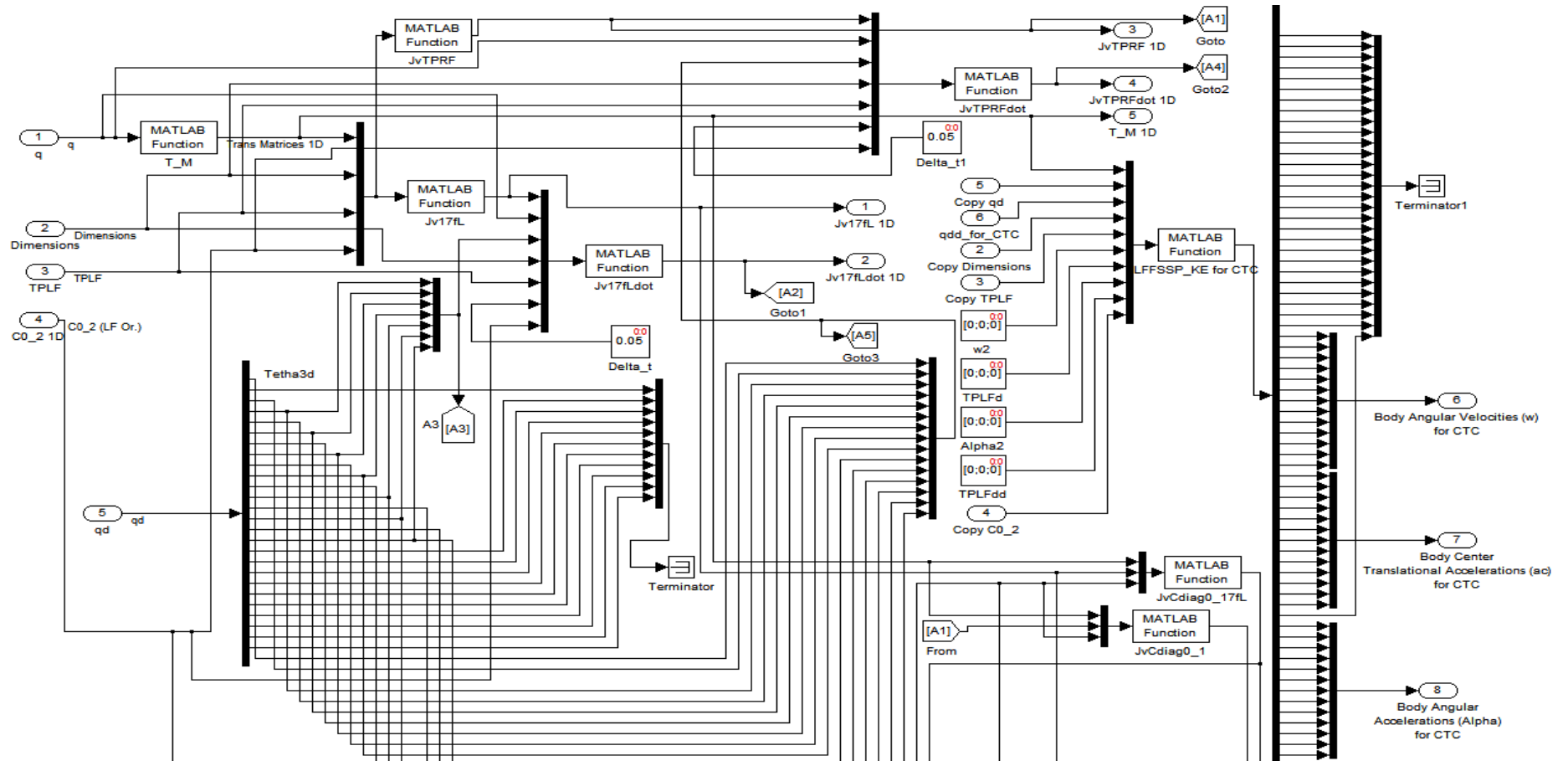


Figure 6.23: Part A of LFSSP Kinematic Equations

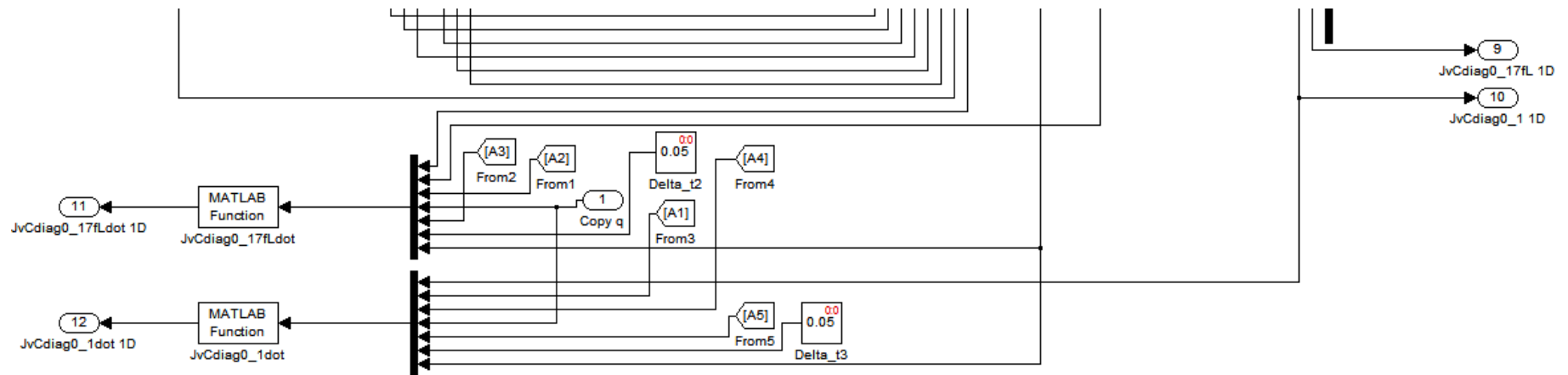


Figure 6.23: Part B of LFSSP Kinematic Equations



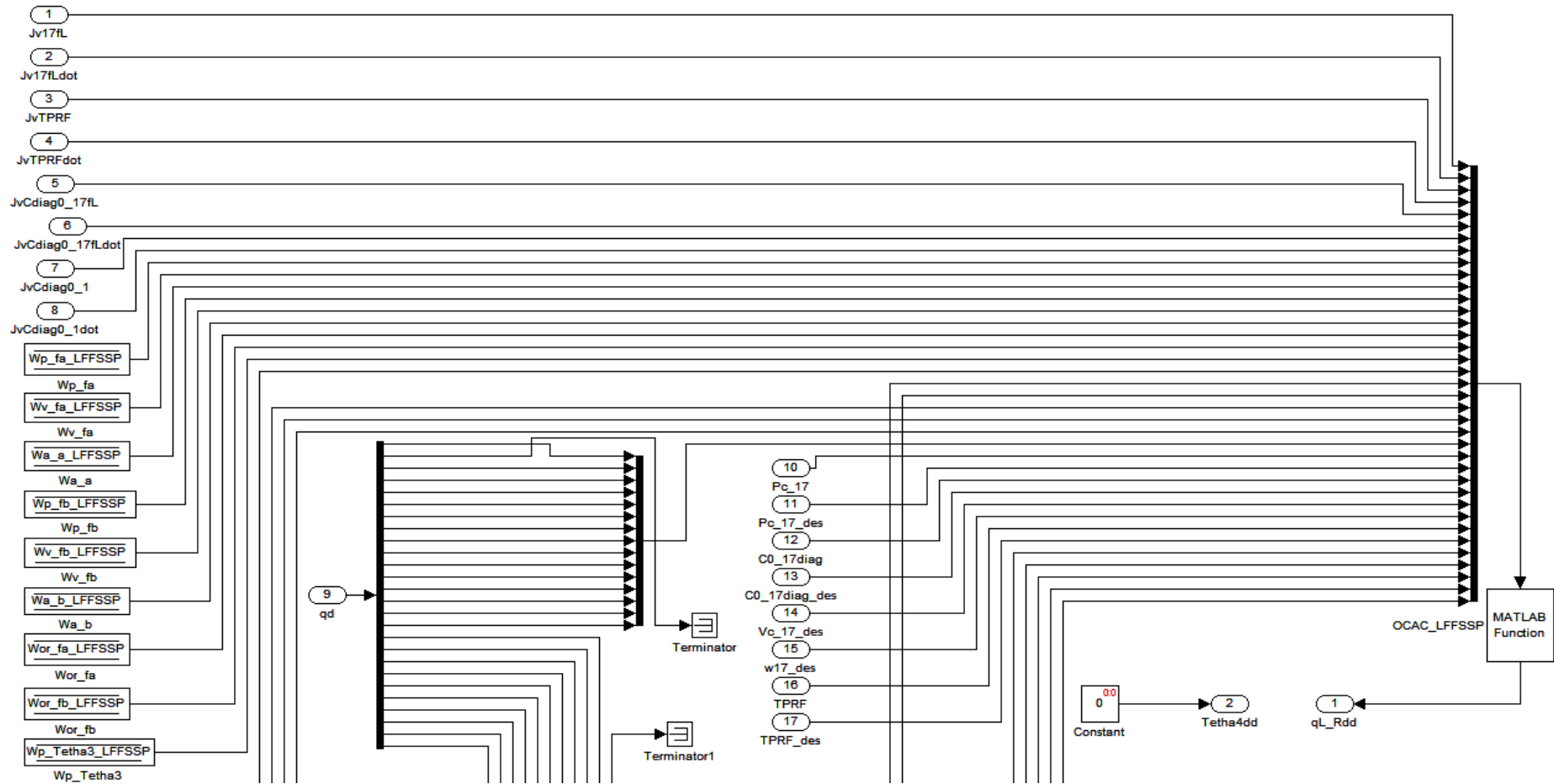


Figure 6.25: Part A of Optimum Command Accelerations Calculation LFFSSP

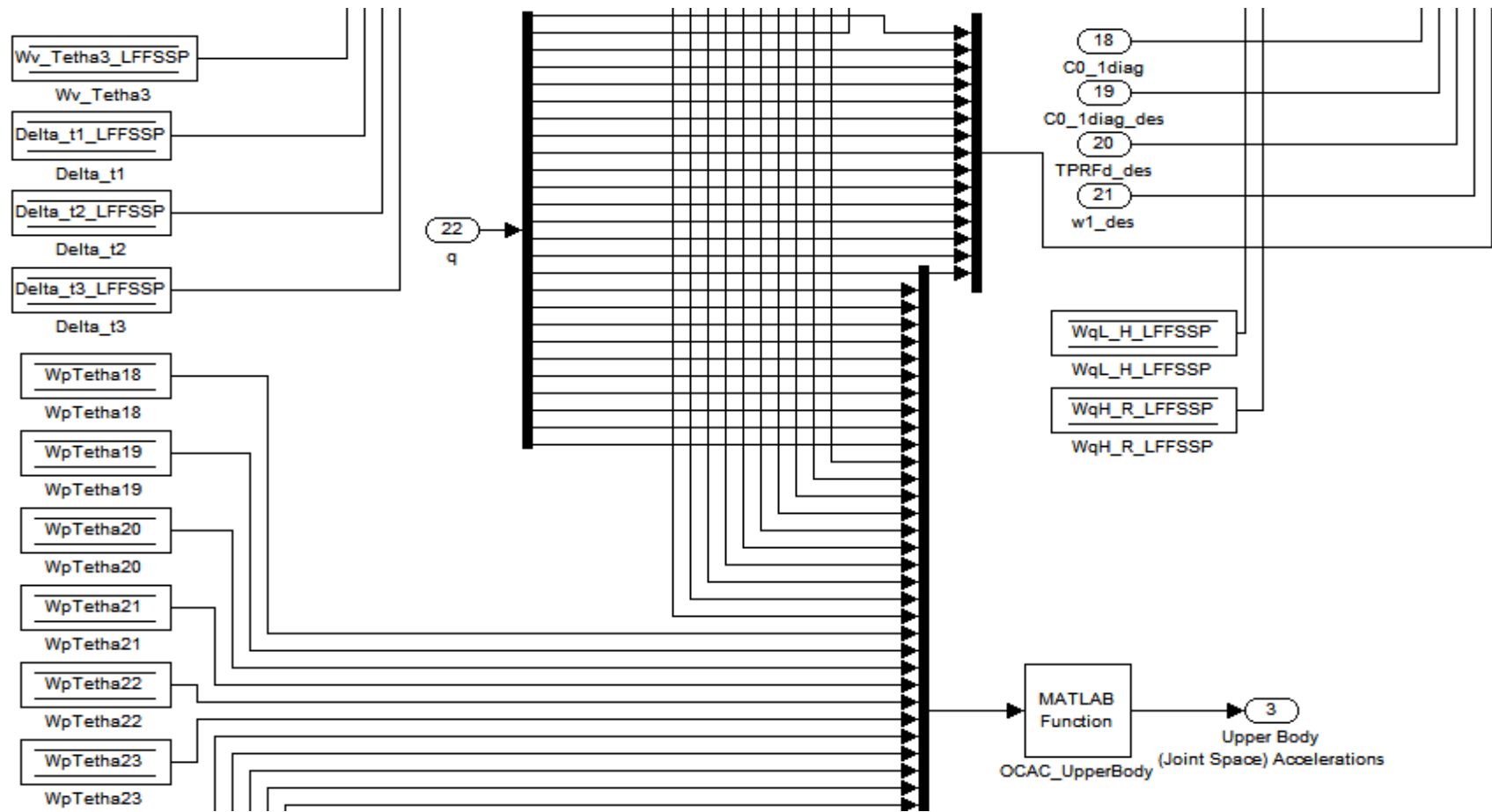
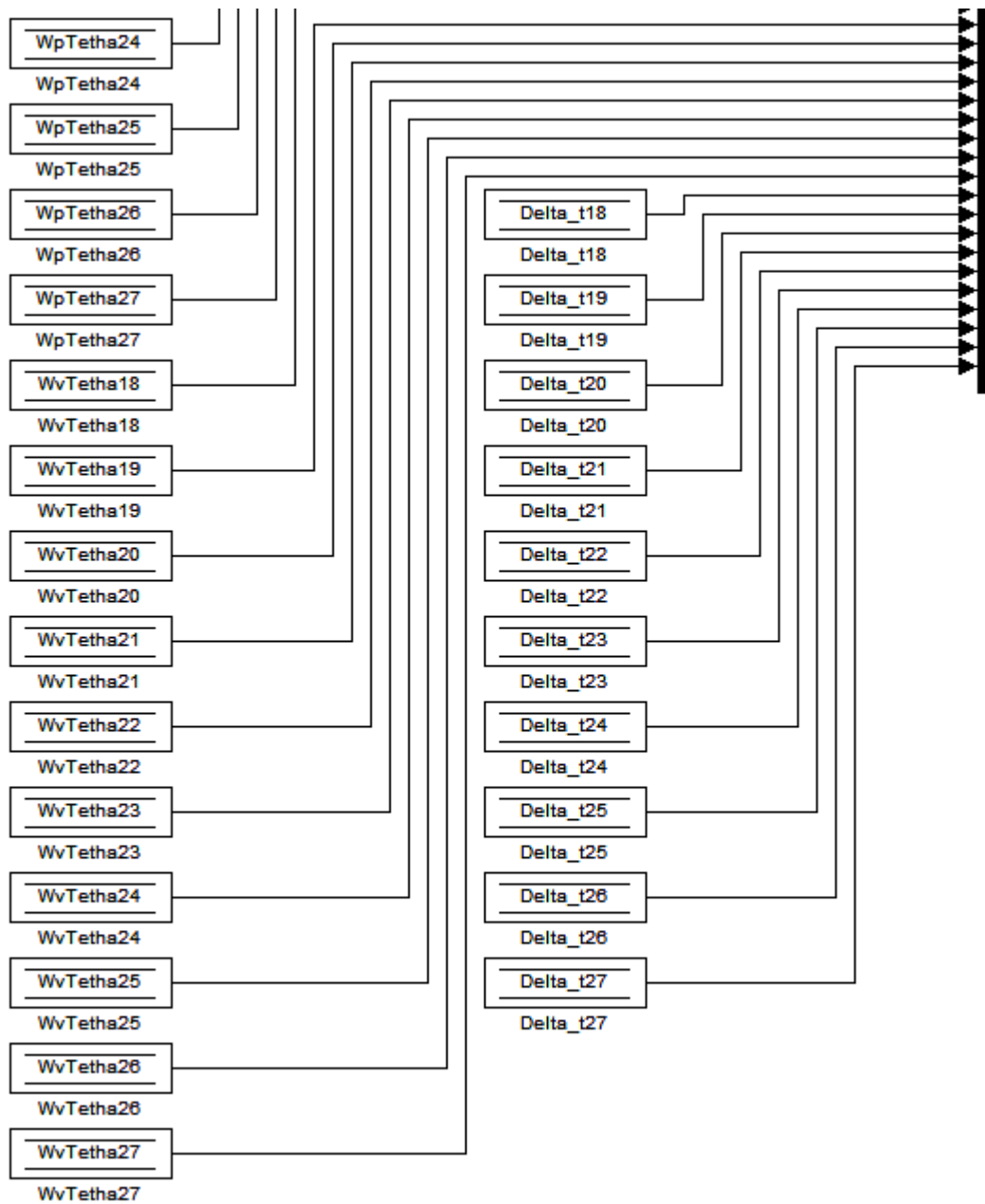


Figure 6.26: Part B of Optimum Command Accelerations Calculation LFFSSP



**Figure 6.27: Part B of Optimum Command Accelerations Calculation LFFSSP**

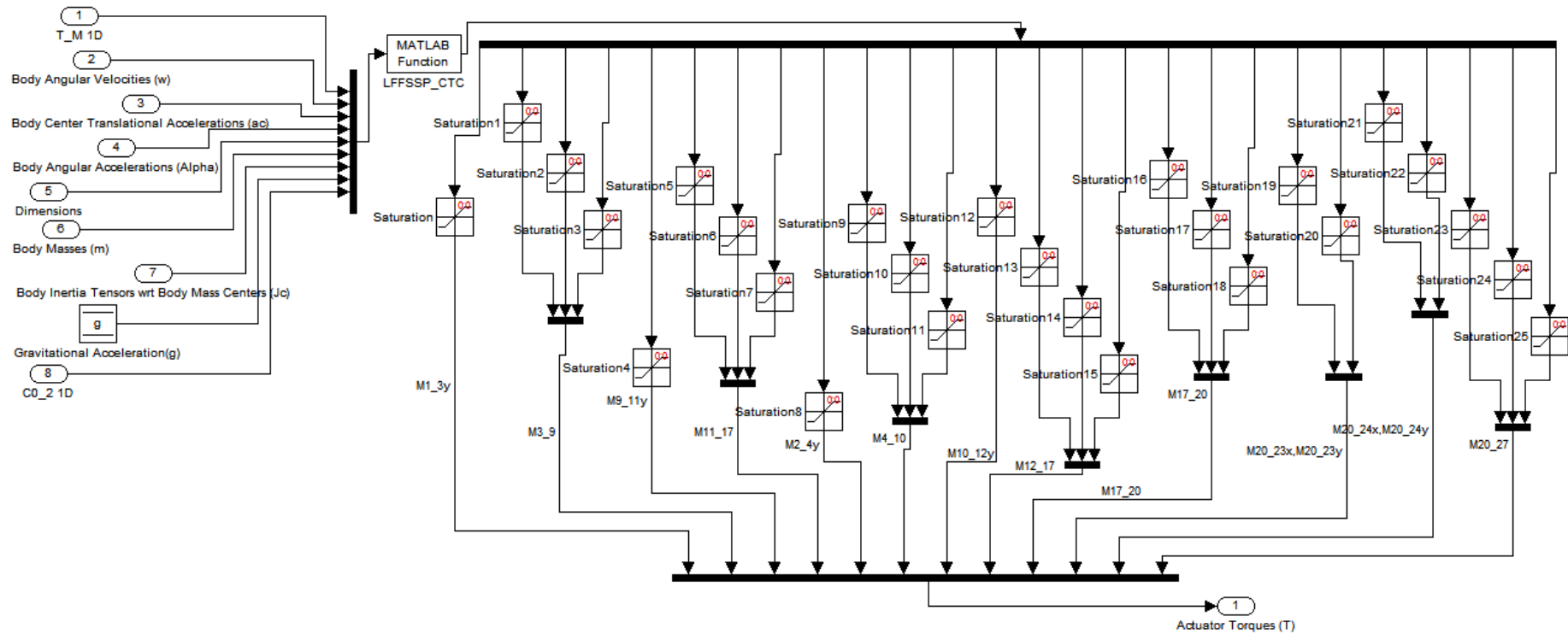
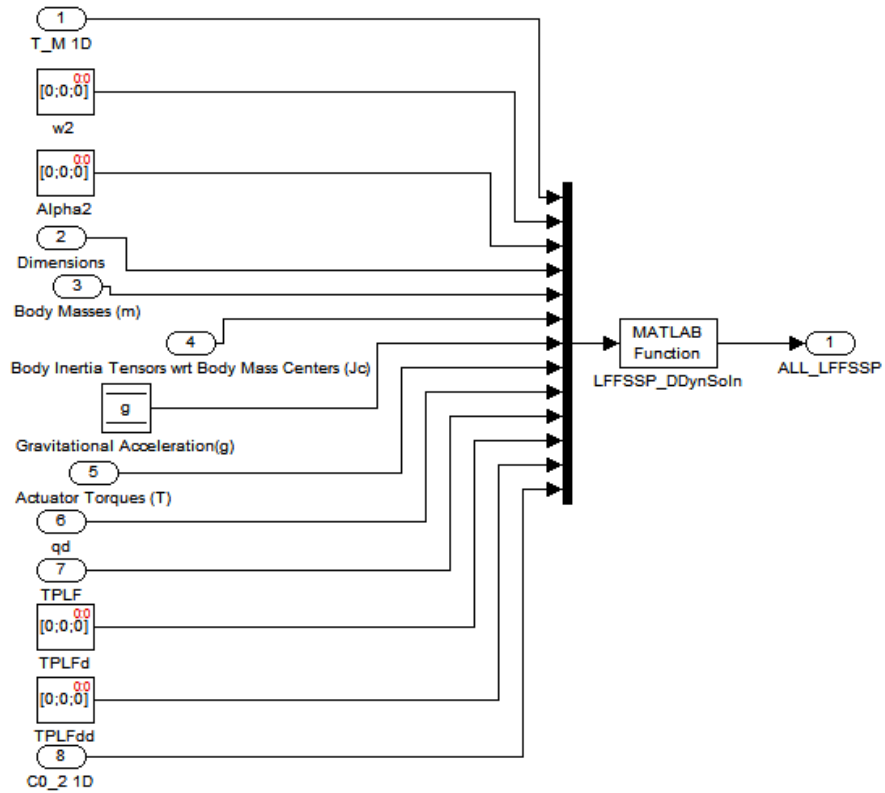


Figure 6.28: Computed Torque Control LFFSSP



**Figure 6.29: Direct Dynamic Solution LFFSSP**

#### 6.1.4. Results of Dynamic Solutions

Joint space accelerations, reaction forces and moments are extracted from the output vector of direct dynamic solutions in this subsystem. Extracted joint space accelerations are sent to the integration subsystem.

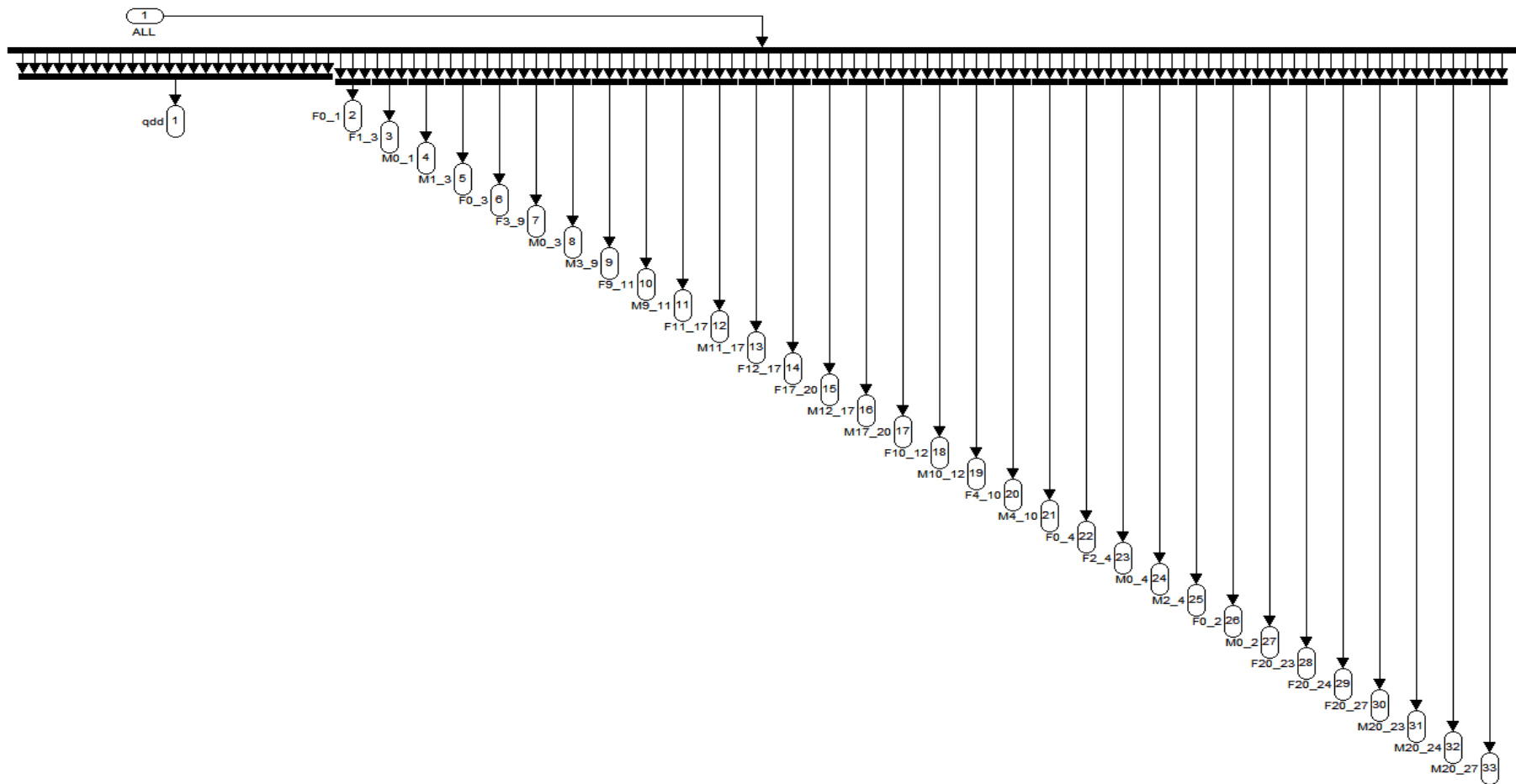


Figure 6.30: Results of Dynamic Solutions

### 6.1.5. Integration

Using continuous time integration blocks, joint space velocities and joint space positions are found from joint space accelerations. Readjustment of several joint space velocities during the transition from single to double support phases is achieved by changing external reset values and supplying modified initial joint space velocities to the integrator block. So as the external reset value of the integrator block changes according to specified criteria, the output of the integrator block is initialized to the initial condition value which is externally supplied. Modification of external reset and initial condition values is done in phase shifting decision subsystems of the phase selector.

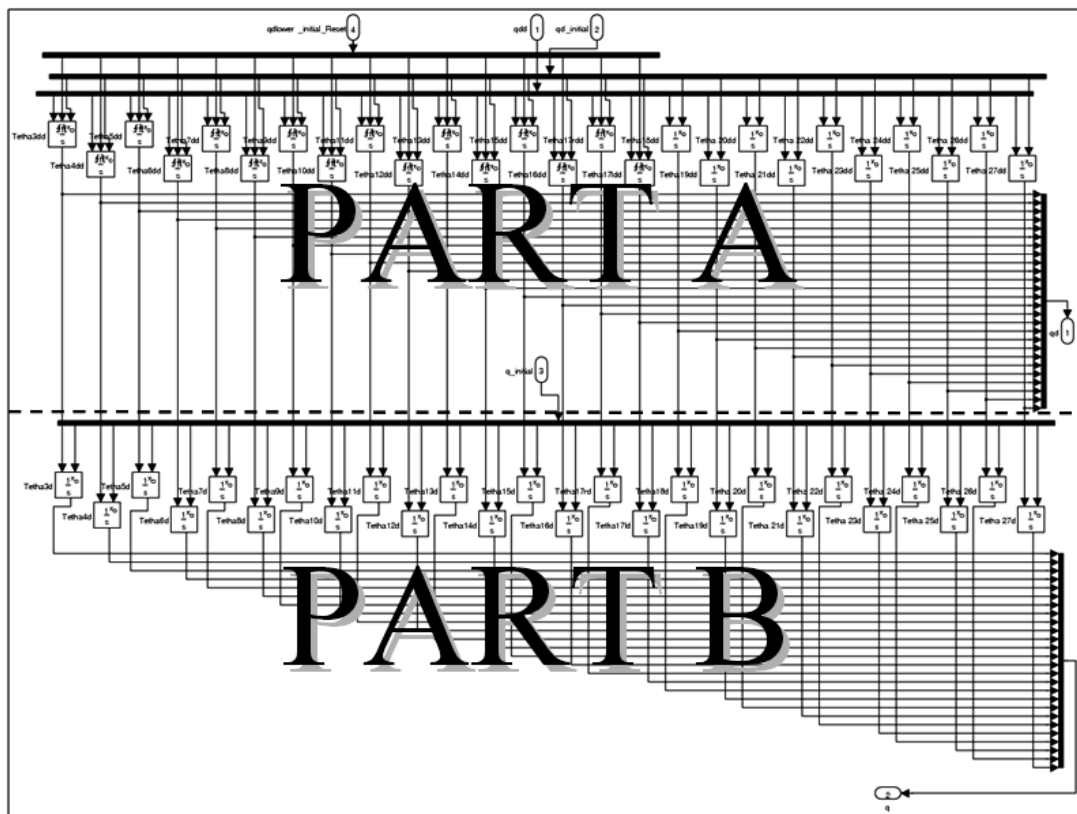


Figure 6.31: Overall View of Integration Subsystem

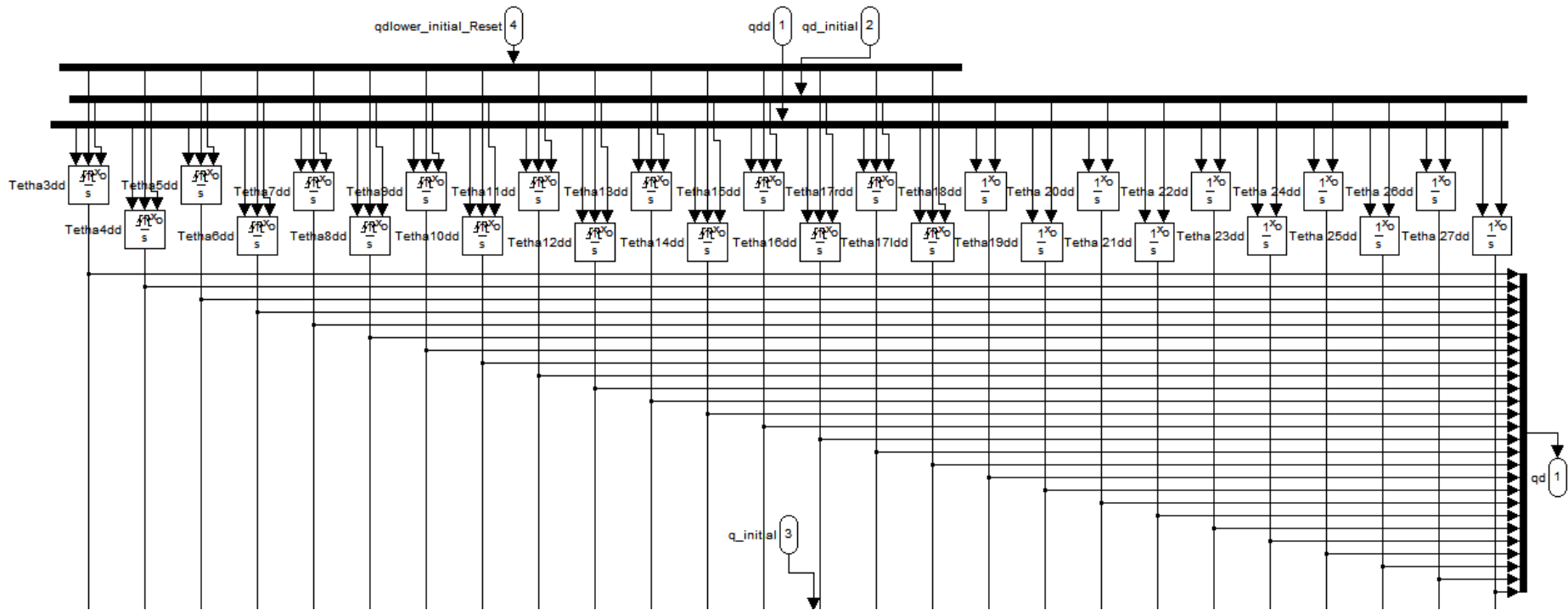


Figure 6.32: Part A of Integration Subsystem

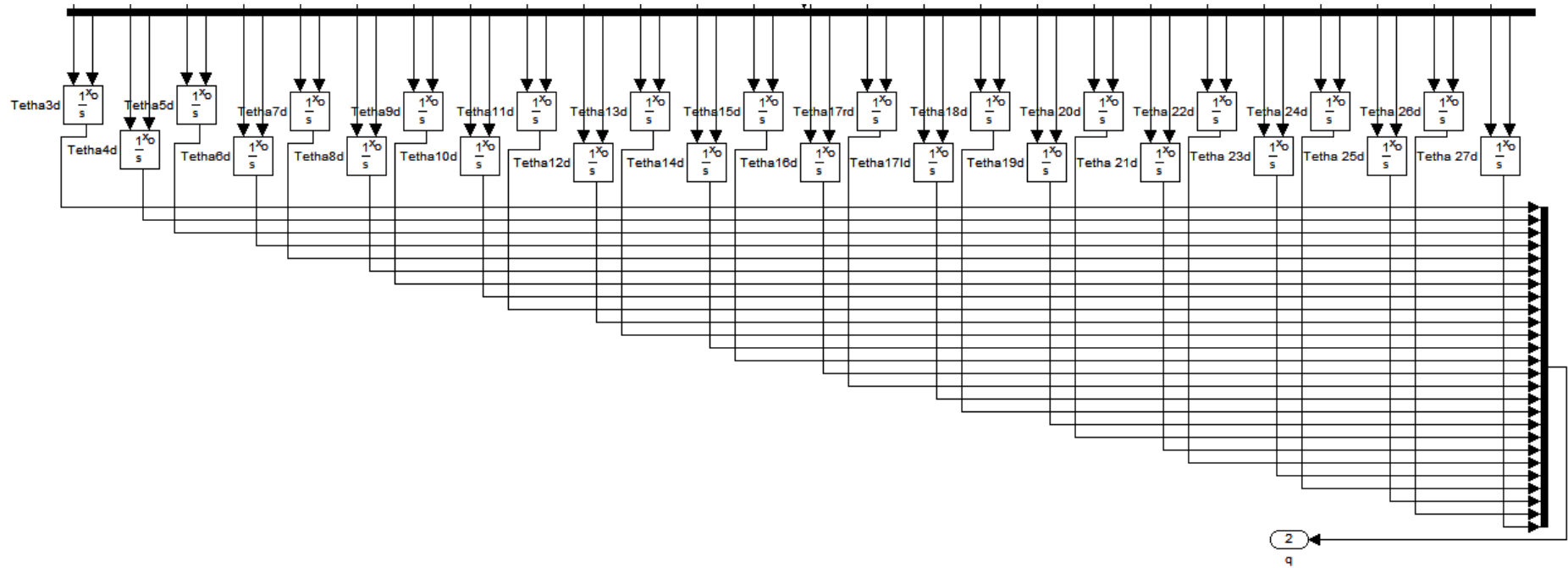
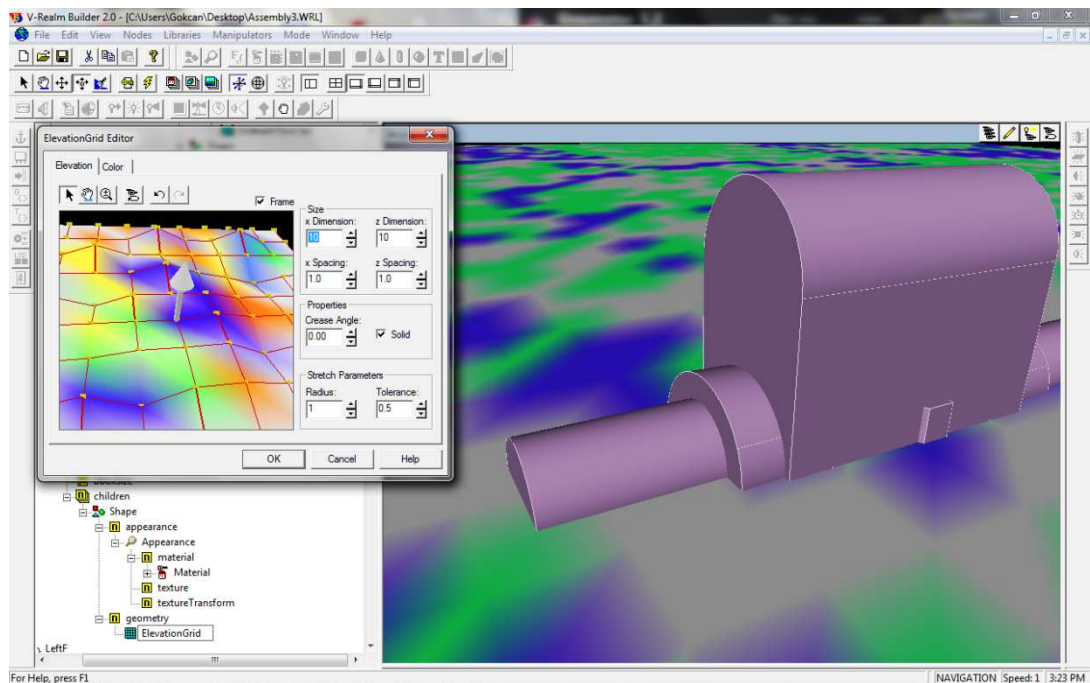


Figure 6.33: Part B of Integration Subsystem

### 6.1.6. Visualization

According to the current locomotion phase, the related subsystem runs to calculate task space positions, velocities and accelerations which are stored by Data Store Write blocks by using outputs of integration subsystem and direct dynamic solutions which are joint space positions, velocities and accelerations. Computed task space positions are used for animation in “Virtual Reality Interface” subsystem by using components of Virtual Reality Toolbox.

Virtual environment is constructed by using V-Realm Builder 2.0 as shown in Figure 6.34



**Figure 6.34: V-Realm Builder**

The orientation of model coordinate system in the CATIA model with respect to the body is the same as the orientation of its body coordinate system with respect to the body shown in chapter 2 and the origin of model coordinate system is also the mass center, where these details are essential in order to adjust position and orientation of bodies easily before manipulating in the virtual environment. CATIA models of bodies are converted into wrl file format. Then, virtual reality model of these bodies

are added to the object library of V-Realm Builder. From the object library, virtual reality models of bodies are inserted to virtual reality model of the simulation. Mass centers of all bodies are located at the origin of coordinate system of the virtual reality model. As the simulation starts and necessary parameters are initialized, bodies are moved to their proper positions and orientations. Mass center positions of bodies and body orientations with respect virtual reality coordinate system are supplied to “VR Sink” block for animation. Since the inertial and virtual reality coordinate systems are different from each other, necessary transformation of results to virtual reality coordinate system is made. Additionally the motion of Body 1, Body 2 and Body 17 according to given reference positions and orientations is attached to the animation. Therefore, tracking performance can be observed by comparing resultant and reference motion of bodies.

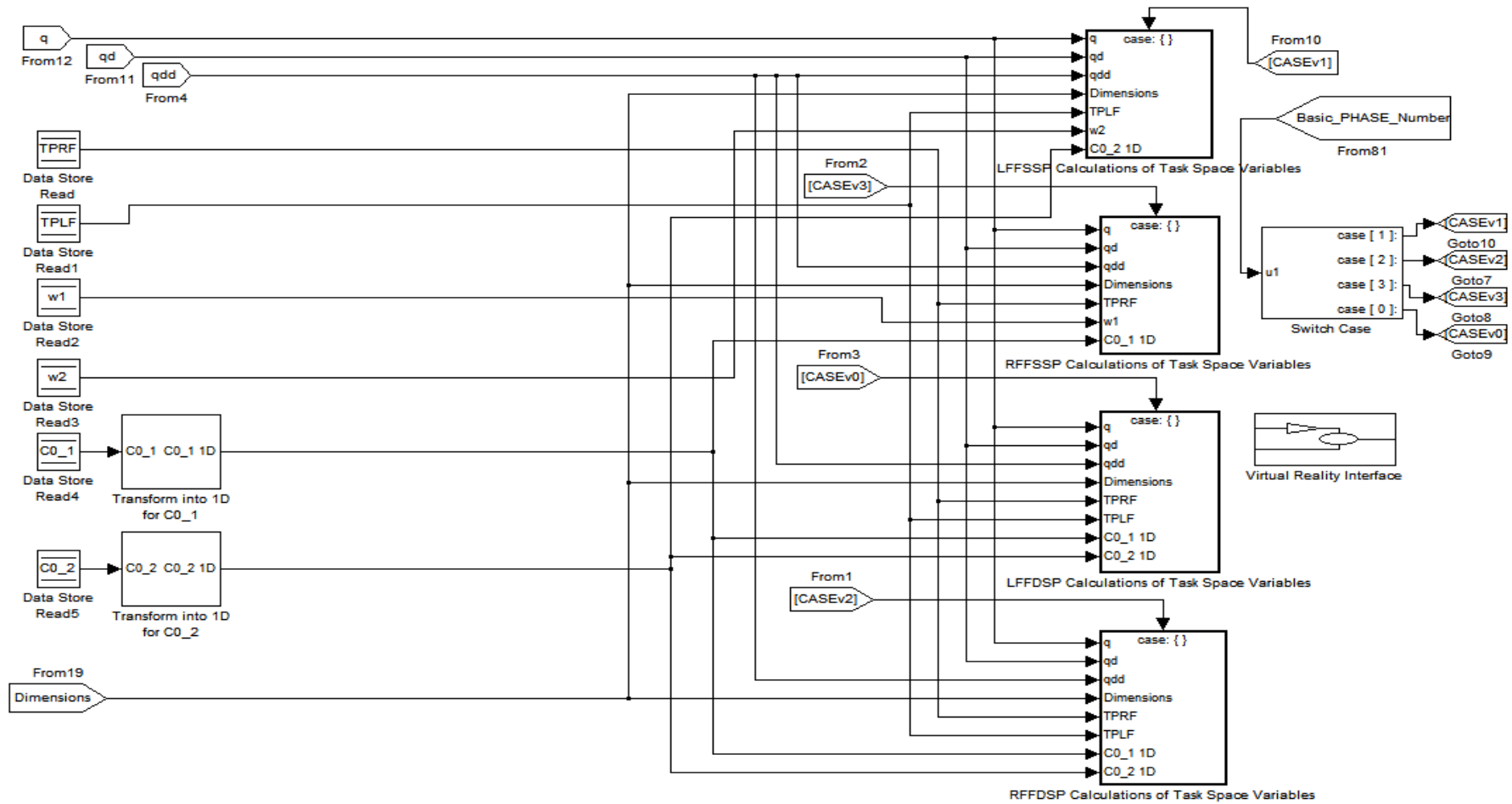


Figure 6.35: Overall View of Visualization Subsystem

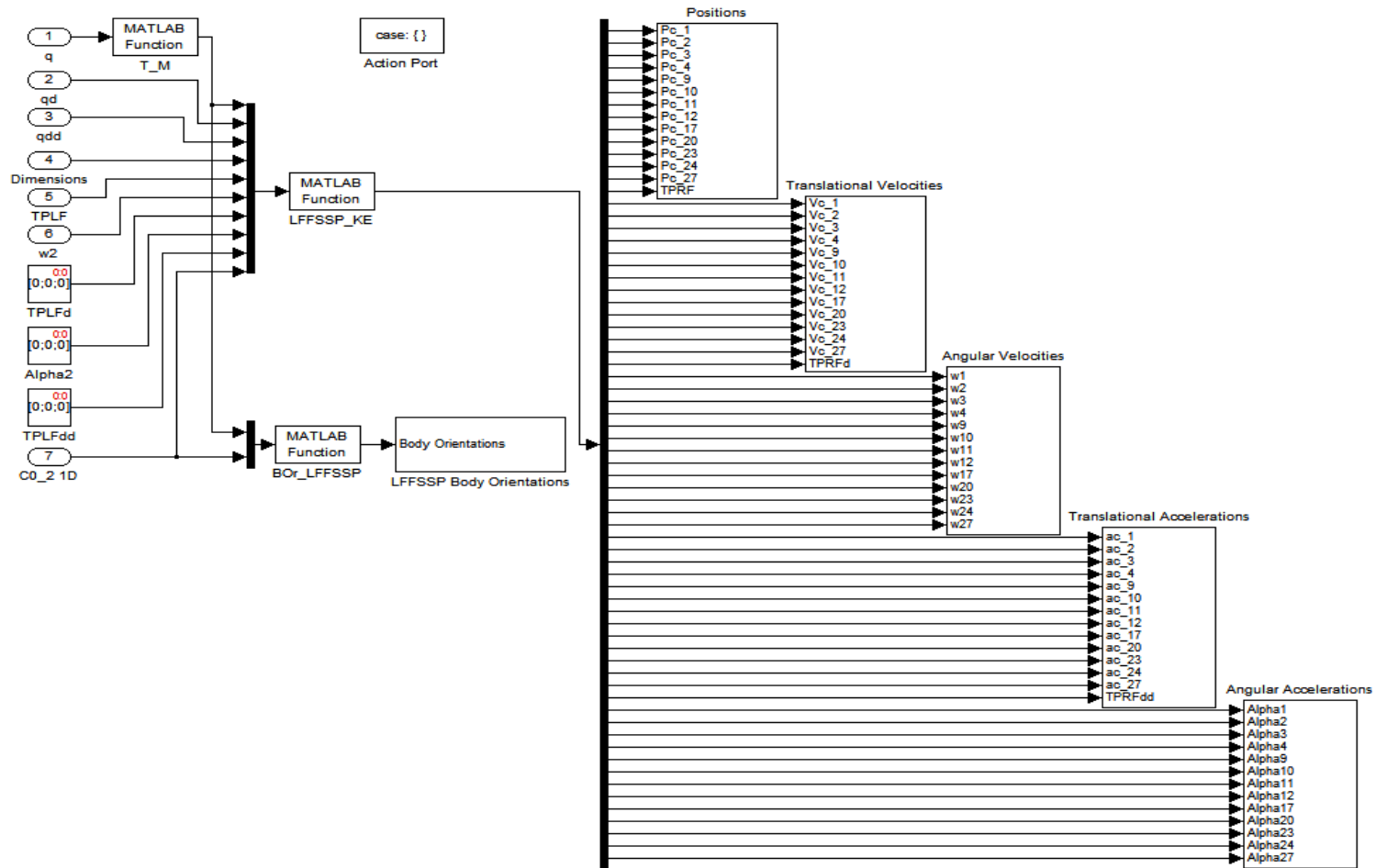


Figure 6.36: LFFSSP Calculation of Task Space Variables

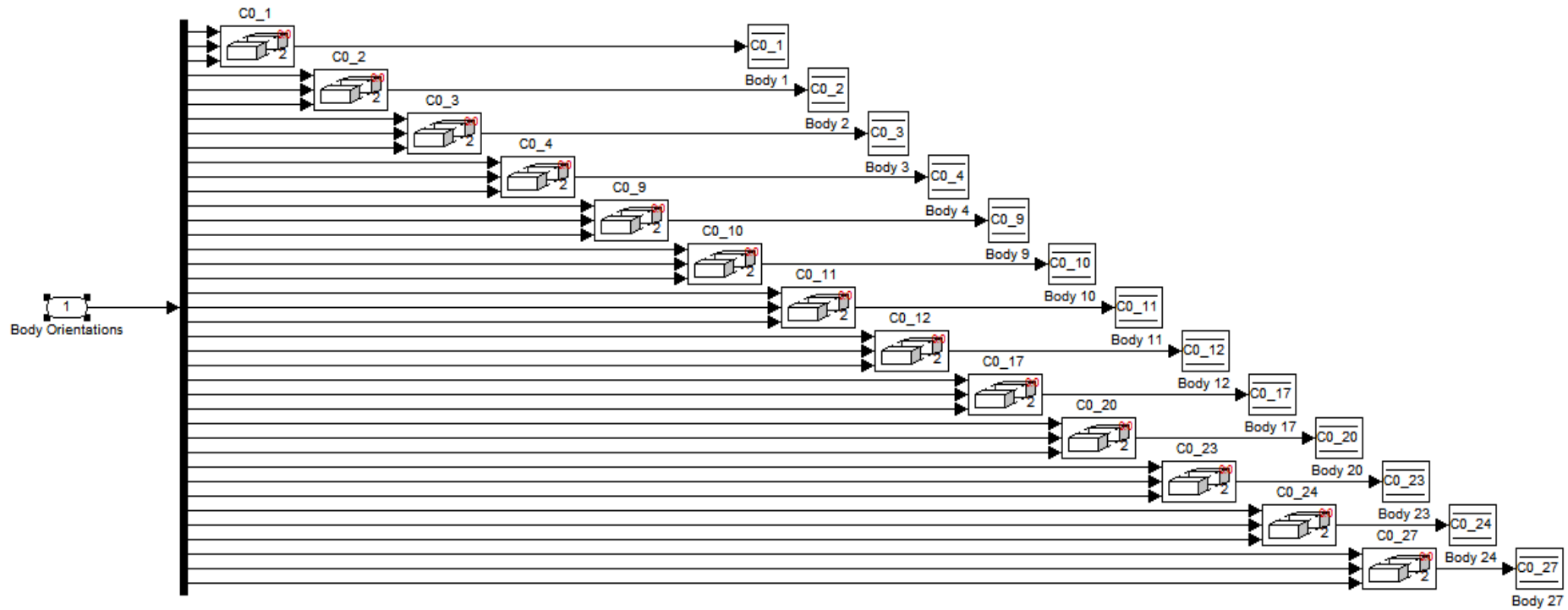
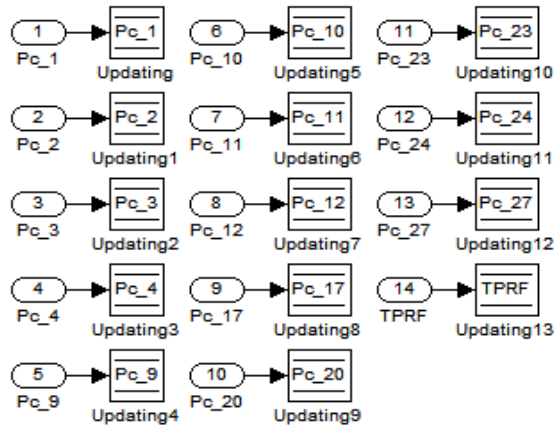
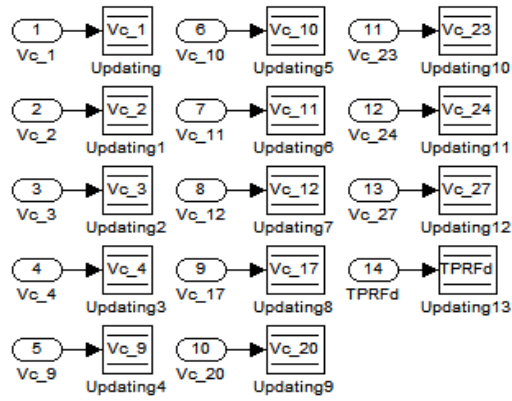


Figure 6.37: LFFSSP Body Orientations



**Figure 6.38: Positions**



**Figure 6.39: Translational Velocities**

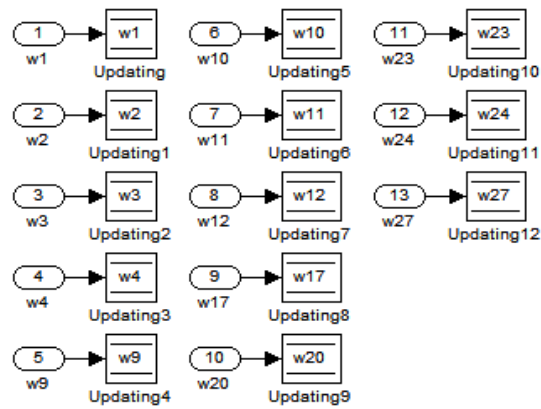


**Figure 6.40: Angular Velocities**

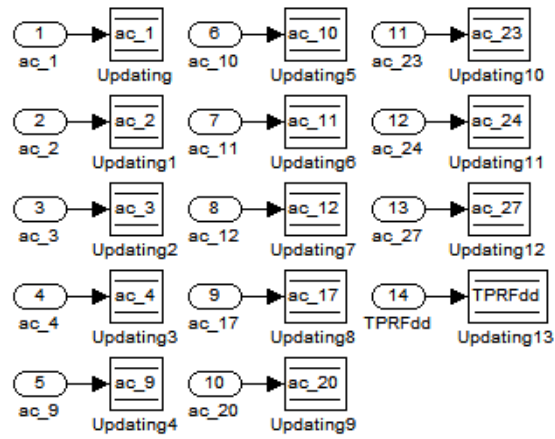


**Figure 6.41: Translational Accelerations**

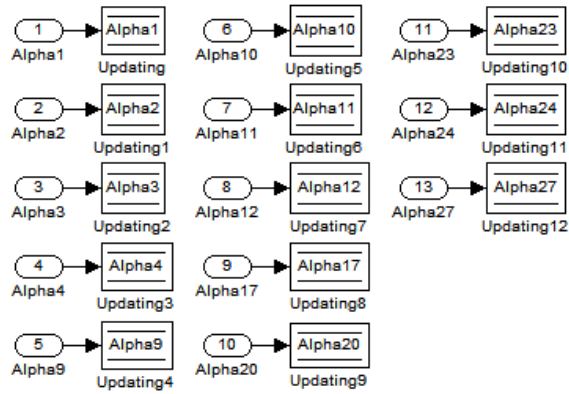


**Figure 6.42: Angular Accelerations**

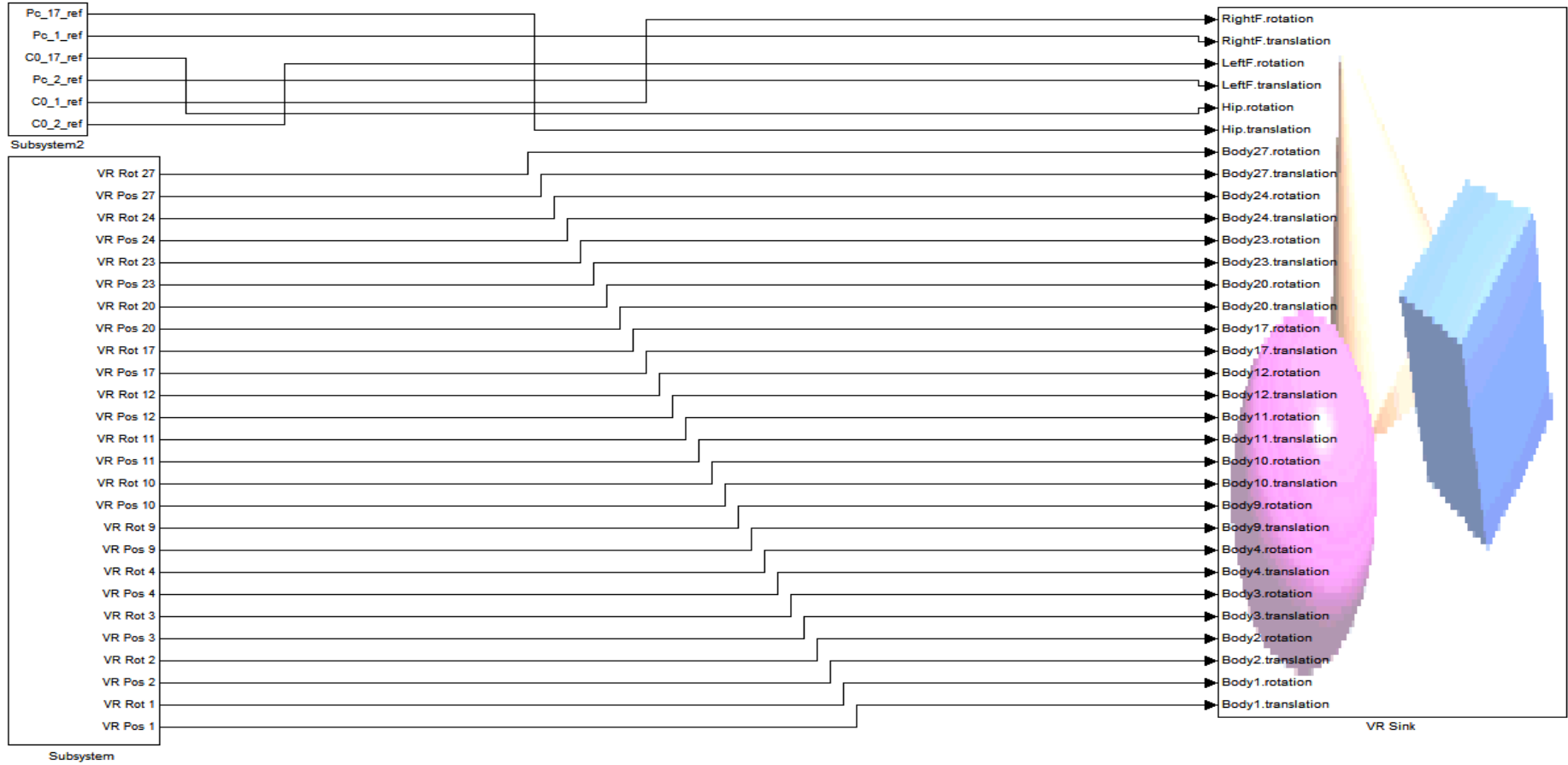


Figure 6.43: Virtual Reality Interface

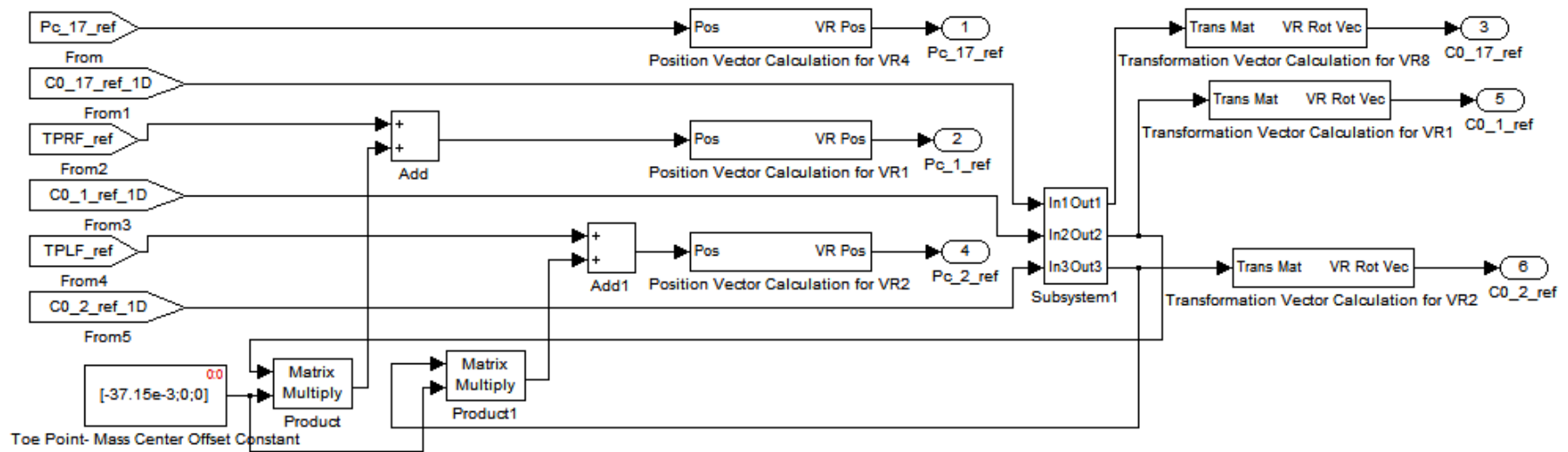


Figure 6.44: Subsystem2 in Virtual Reality Interface



Figure 6.45: Subsystem in Virtual Reality Interface

### 6.1.7. Definition of Physical Parameters

Necessary dimensions, mass and inertia tensor properties of bodies are defined in and supplied from this subsystem.

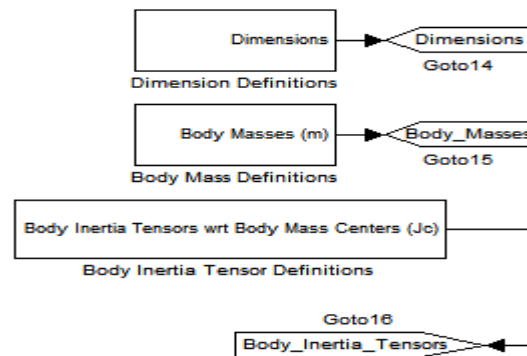


Figure 6.46: Definition of Physical Parameters

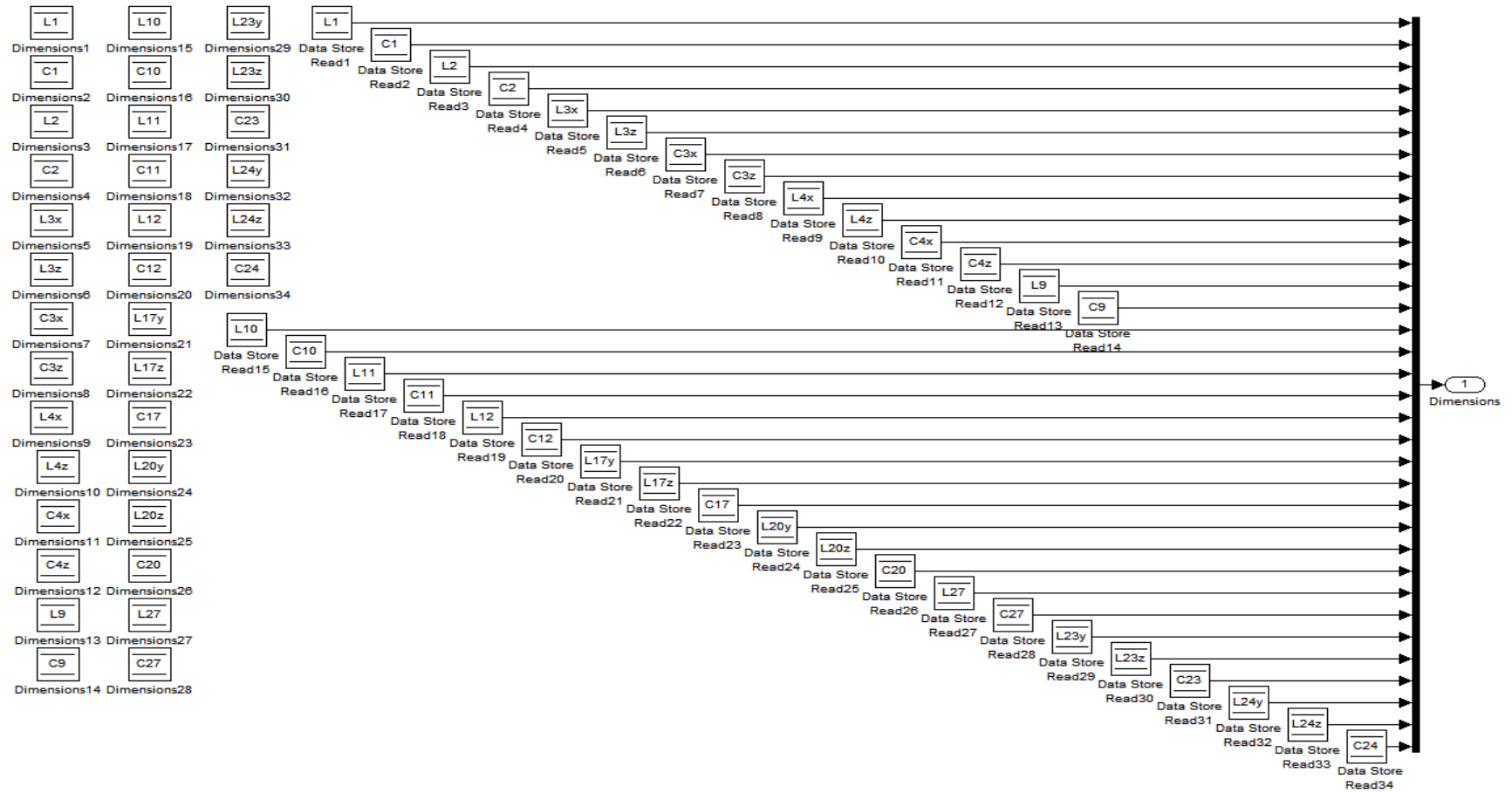
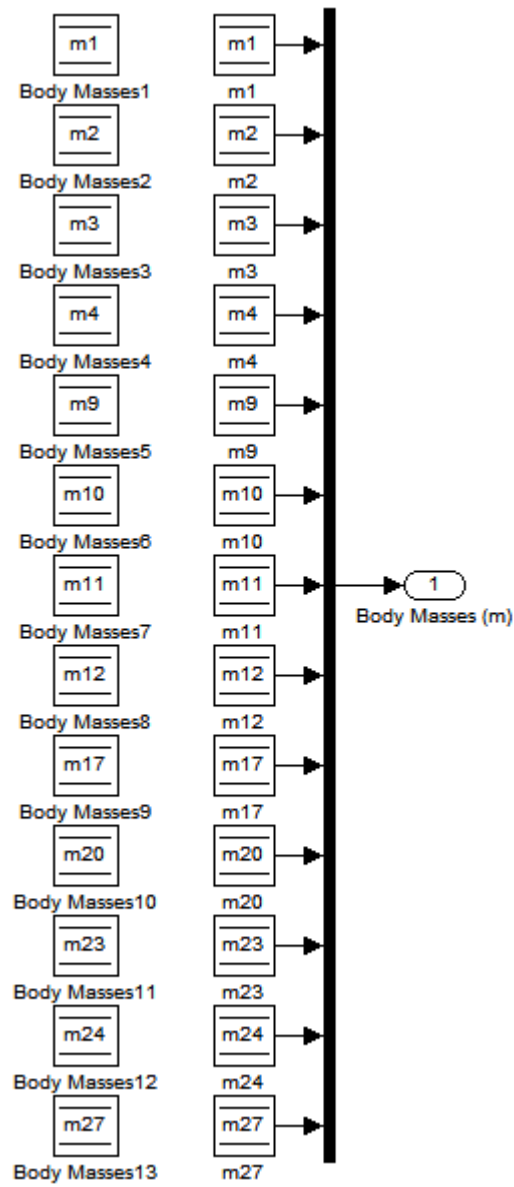
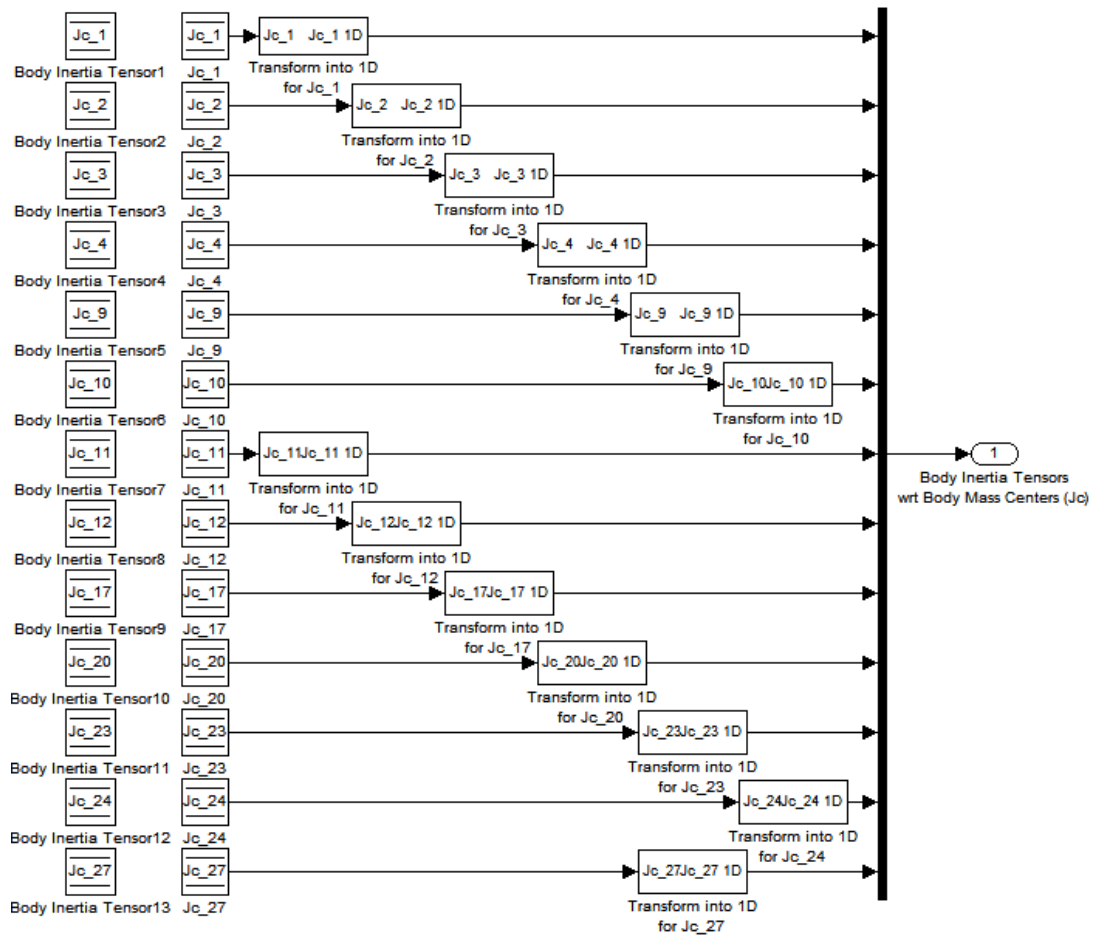


Figure 6.47: Dimensions Definitions



**Figure 6.48: Body Mass Definitions**



**Figure 6.49: Body Inertia Tensor Definitions**

### 6.1.8. Reading and Arrangement of Several Variables

Some minor operations in the top level system are gathered into this subsystem.

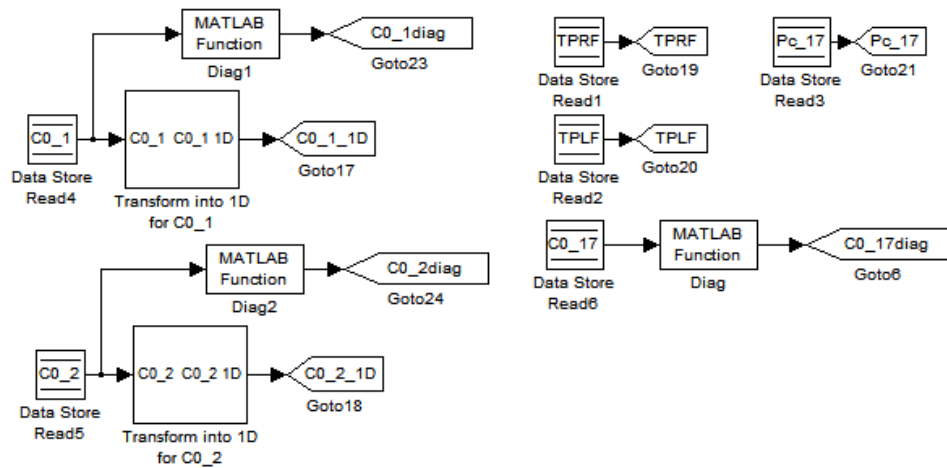


**Figure 6.50: Reading and Arrangement of Several Values**

## 6.2. Simulation Results

Simulation results for 3 parameter sets are given. 3 different types of reference input are given for demonstration. For Simulation Number 1, a reference input with no general order is given. A reference input to track a circular path is given in Simulation Number 2. In Simulation Number 3, a linear path which does not require turning of the robot body is defined. Detailed results are given for Simulation Number 1. For the rest, reference input and the tracking performance are shown.

### 6.2.1. Simulation Number 1

Simulation results for parameter set 1 which is shown in Appendix B.1 are illustrated under this heading.

#### 6.2.1.1. Reference Input

According to numerical values of parameters which define the nature of locomotion, the trajectory generation algorithm creates reference input information for the simulation model. Reference trajectories for parameter set 1 can be illustrated by Figure 6.51, Figure 6.52 and Figure 6.53. Green and black colored curves represent the reference trajectory for  $P_{tpR}$  and  $P_{tpL}$ . Red, blue, magenta and cyan colored curves

represent the reference trajectory for the mass center of Body 17 during LFFSSP, RFFDSP, RFFSSP and LFFDSP respectively.

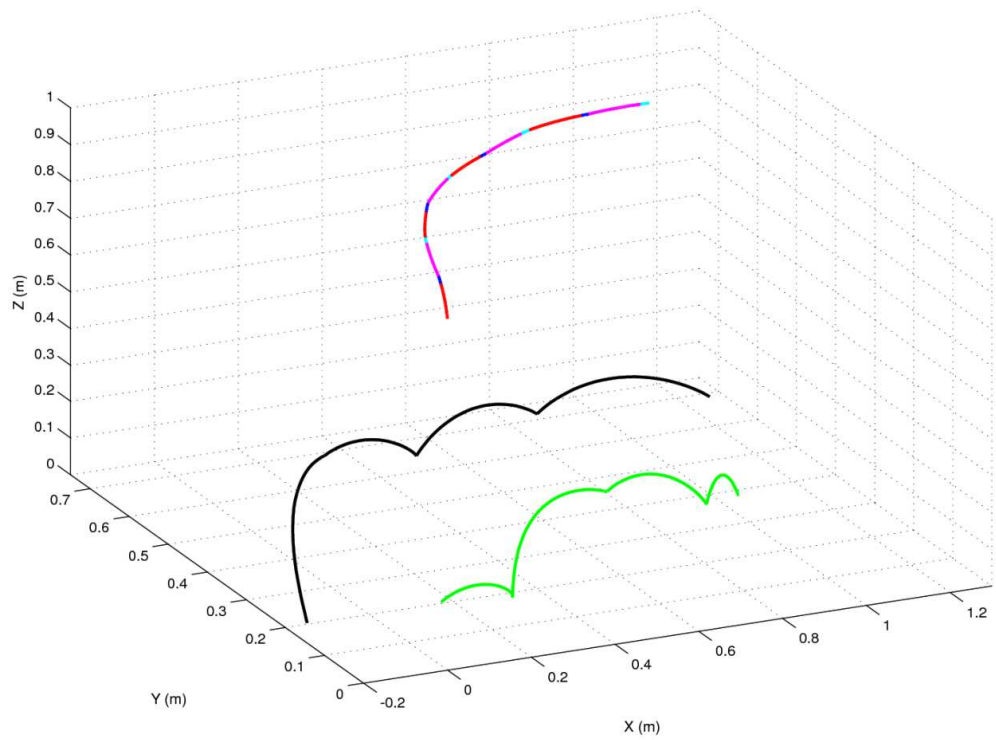


**Figure 6.51: Isometric View of Reference Trajectories for Parameter Set 1**

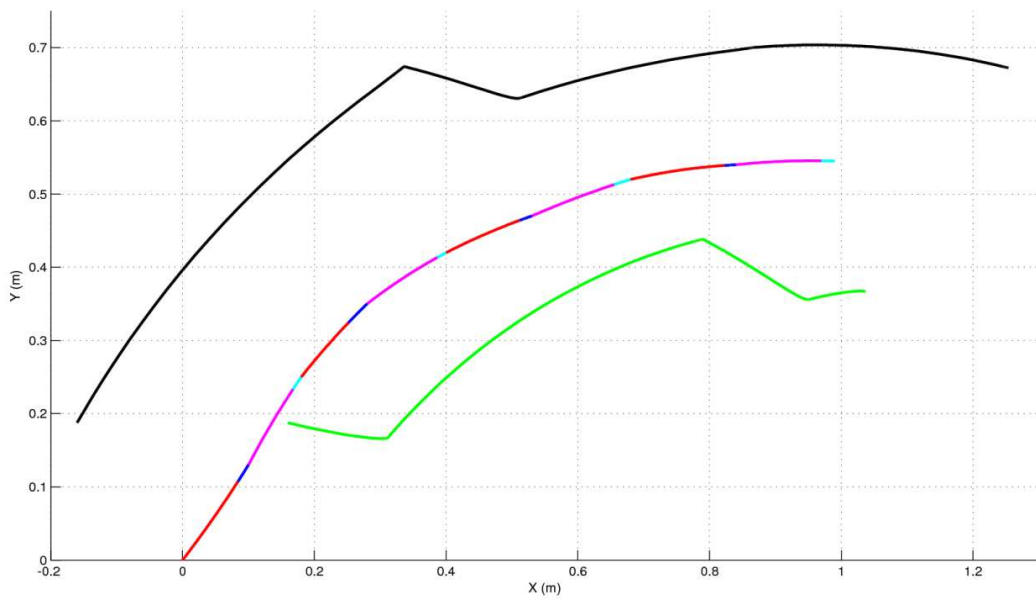


**Figure 6.52: Reference Trajectories on X-Y Plane for Parameter Set 1**

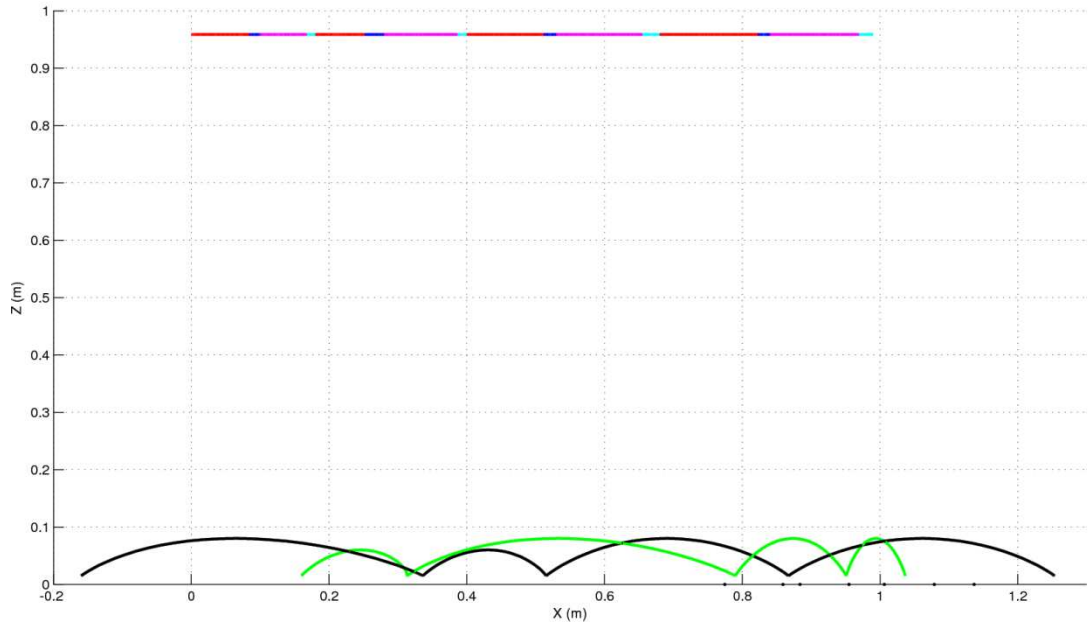


**Figure 6.53: Reference Trajectories on X-Z Plane for Parameter Set 1**

### 6.2.1.2. Joint Space Positions

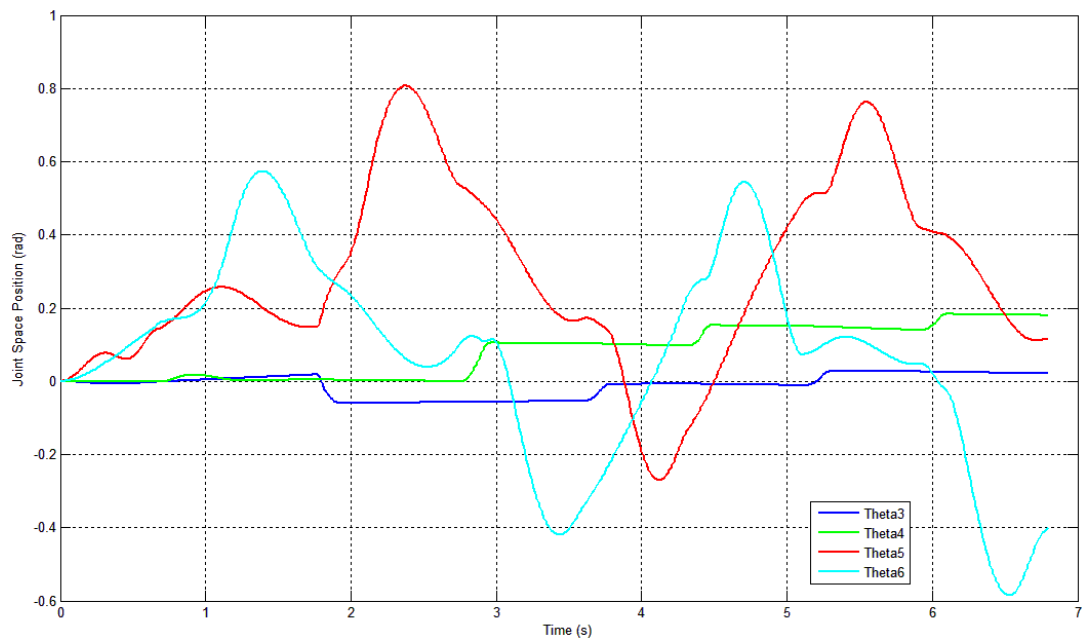


**Figure 6.54: Joint Space Positions from  $\theta_3$  to  $\theta_6$**

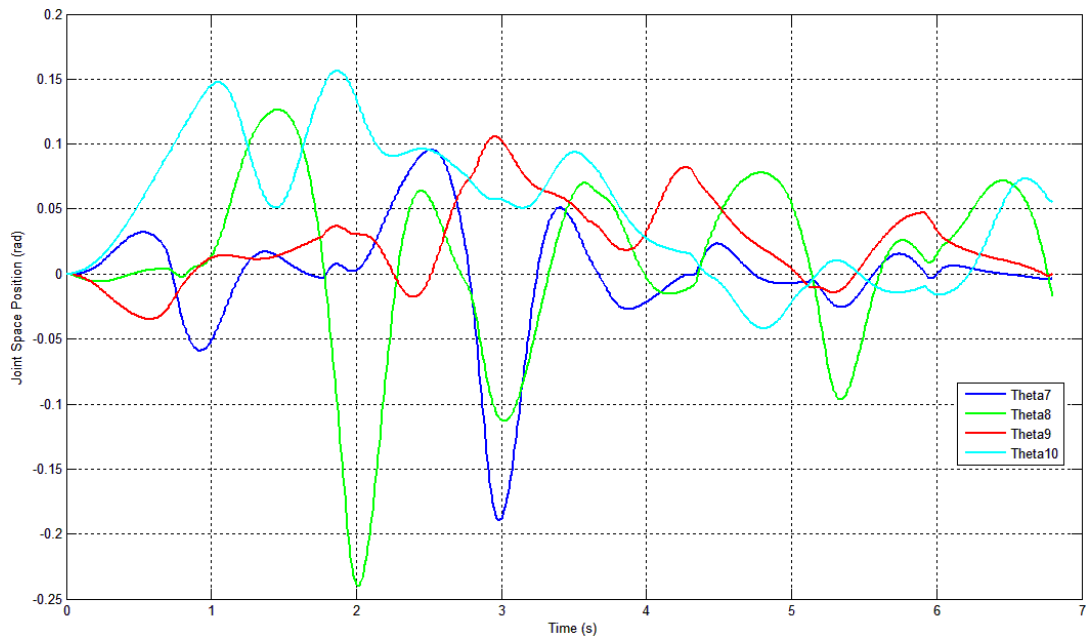


**Figure 6.55: Joint Space Positions from  $\theta_7$  to  $\theta_{10}$**

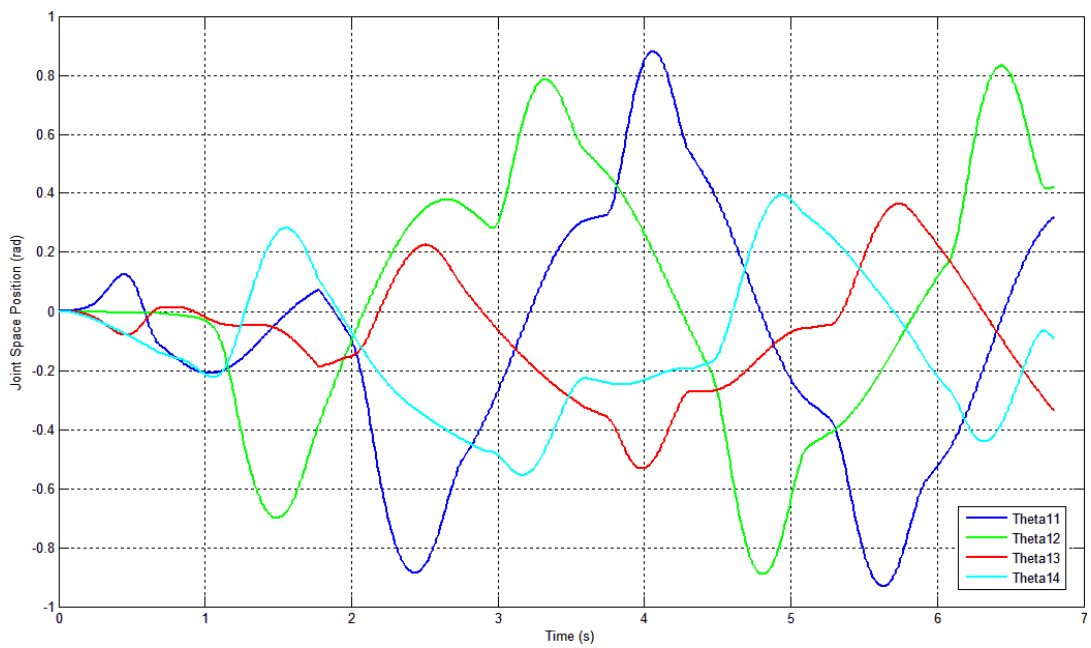


**Figure 6.56: Joint Space Positions from  $\theta_{11}$  to  $\theta_{14}$**

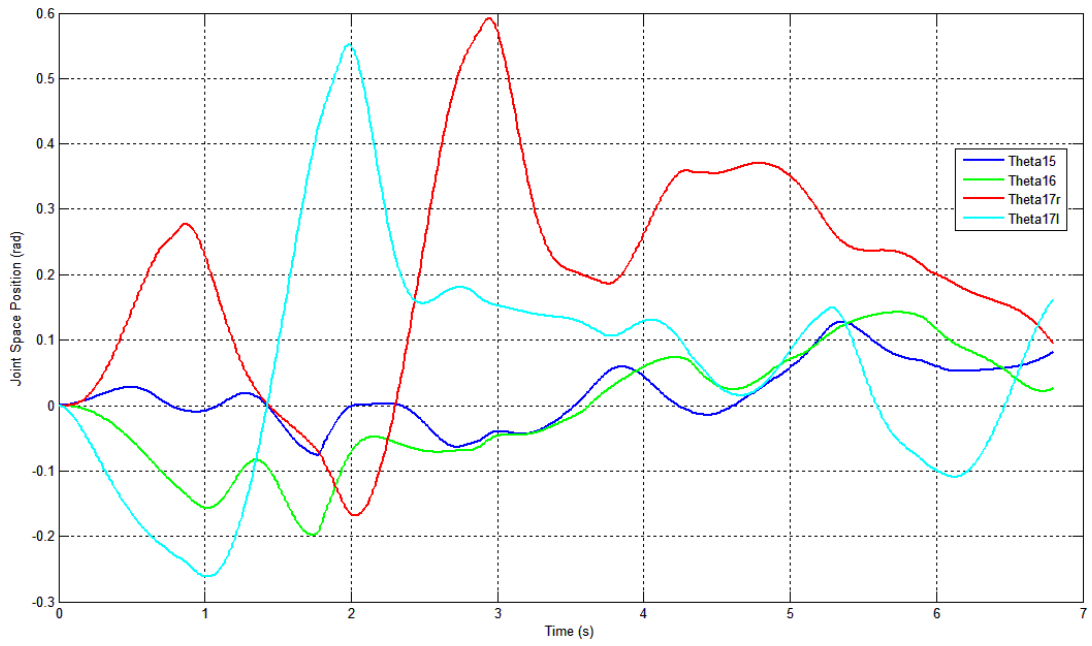


**Figure 6.57: Joint Space Positions from  $\theta_{15}$  to  $\theta_{17l}$**

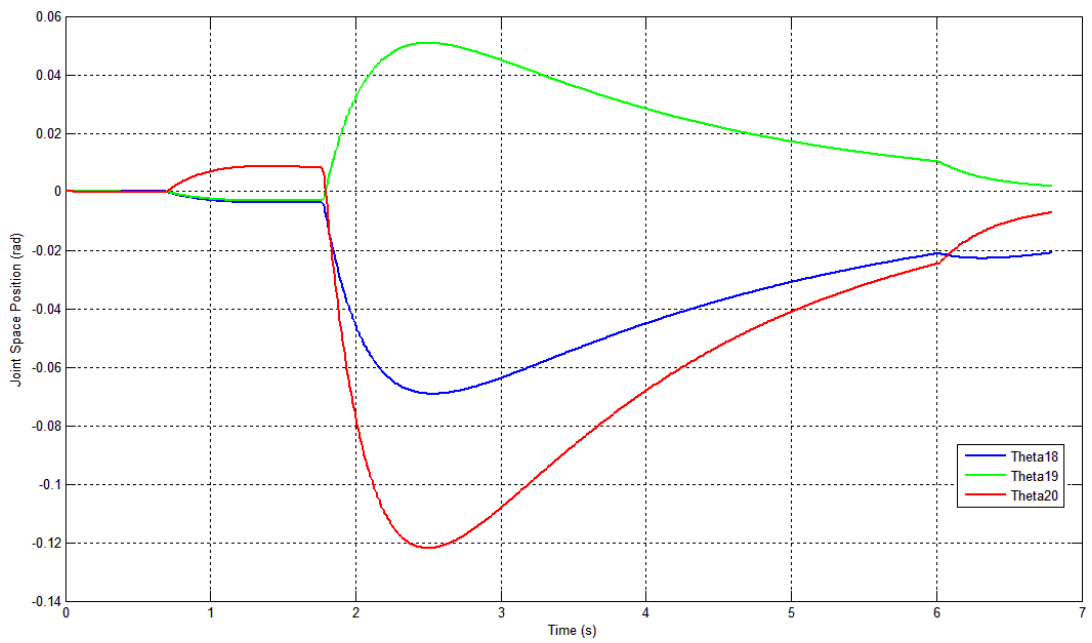


**Figure 6.58: Joint Space Positions from  $\theta_{18}$  to  $\theta_{20}$**

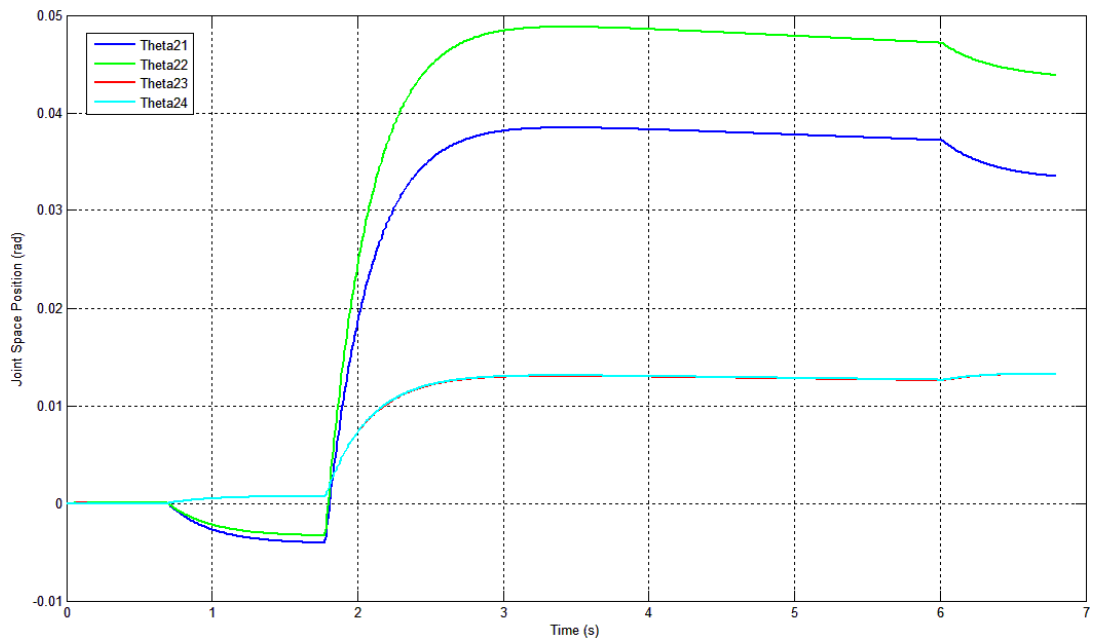


**Figure 6.59: Joint Space Positions from  $\theta_{21}$  to  $\theta_{24}$**

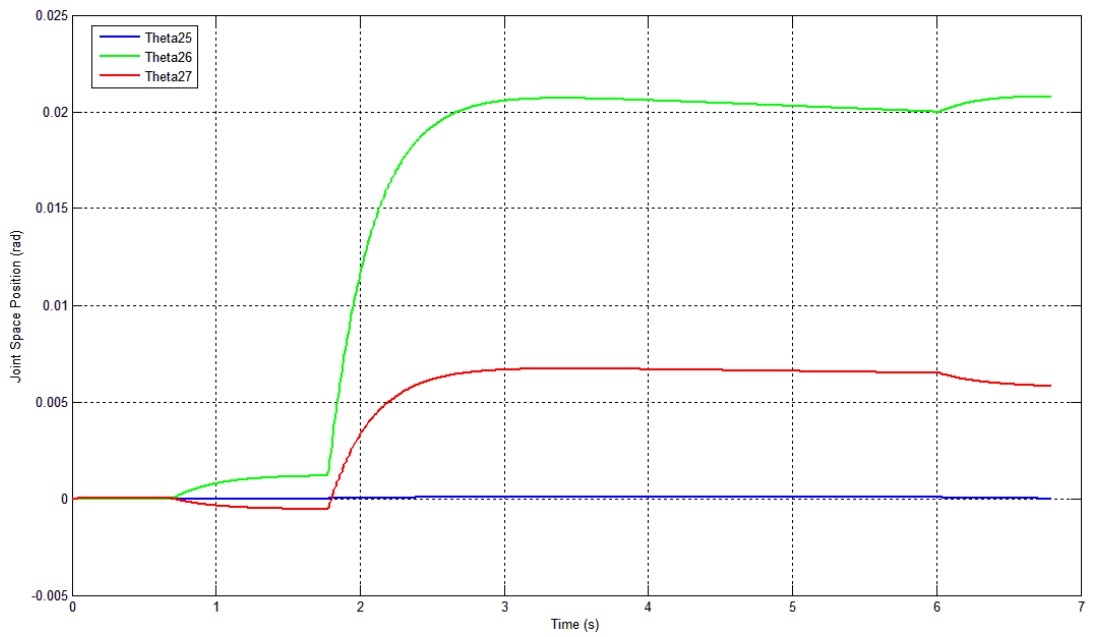


**Figure 6.60: Joint Space Positions from  $\theta_{25}$  to  $\theta_{27}$**

### 6.2.1.3. Task Space Positions

Simulation results with their reference inputs are shown by Figure 6.61, Figure 6.62 and Figure 6.63. All components are resolved in the inertial frame.

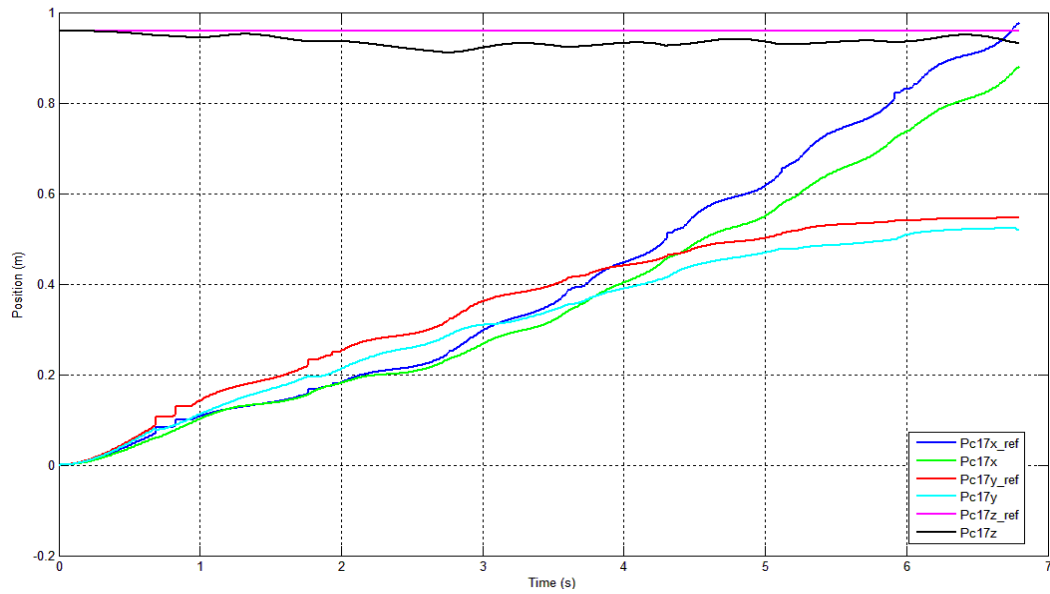


**Figure 6.61: Position of Mass Center of Body 17 with Its Reference Input**

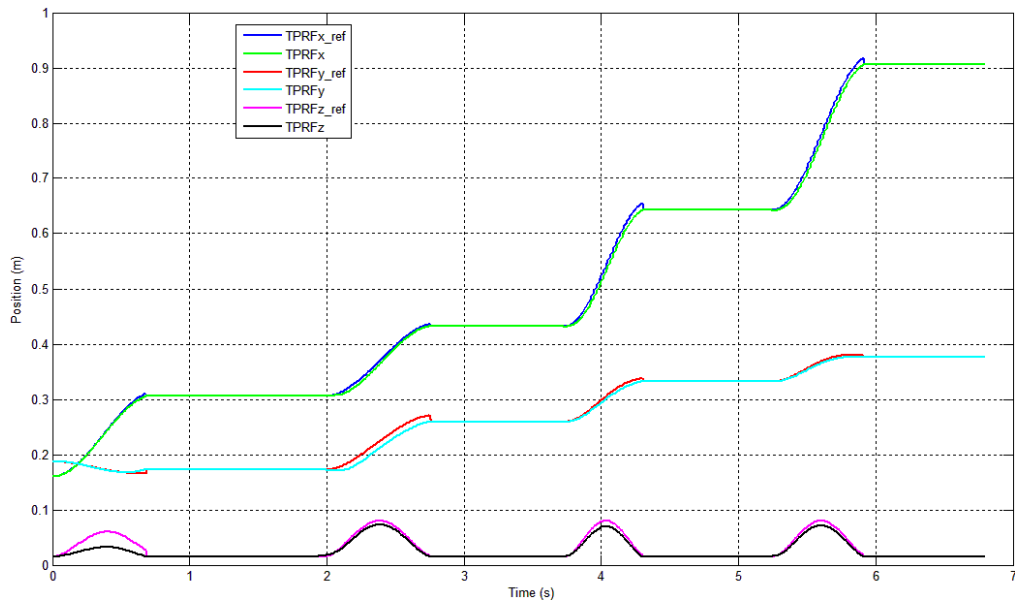


**Figure 6.62: Position of Toe Point on Right Foot (Body 1) with Its Reference Input**

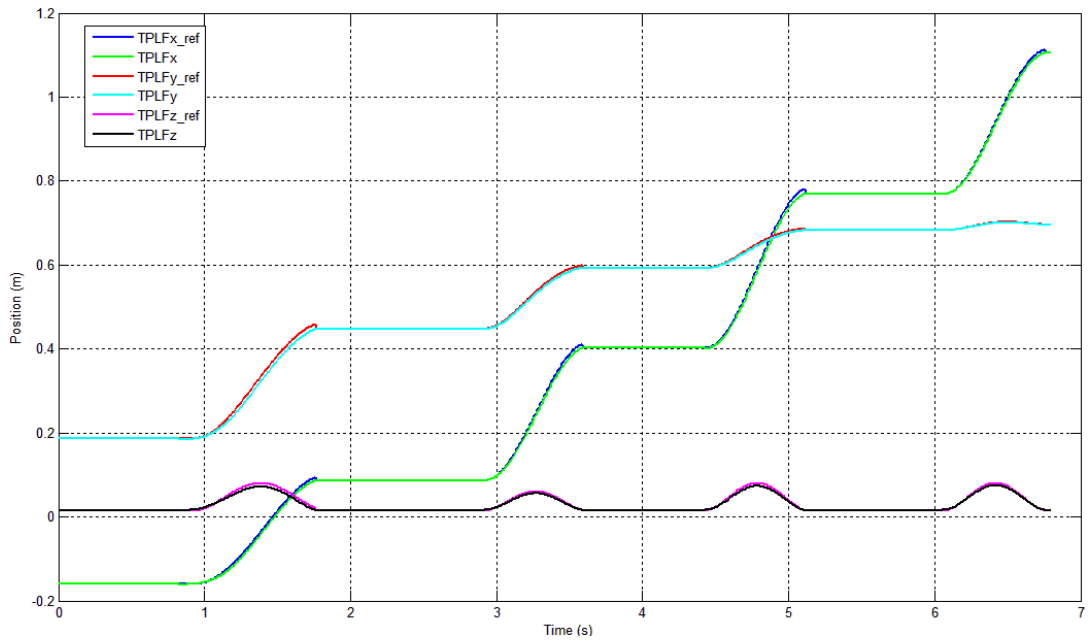


**Figure 6.63: Position of Toe Point on Left Foot (Body 2) with Its Reference Input**

#### 6.2.1.4. Actuator Torques

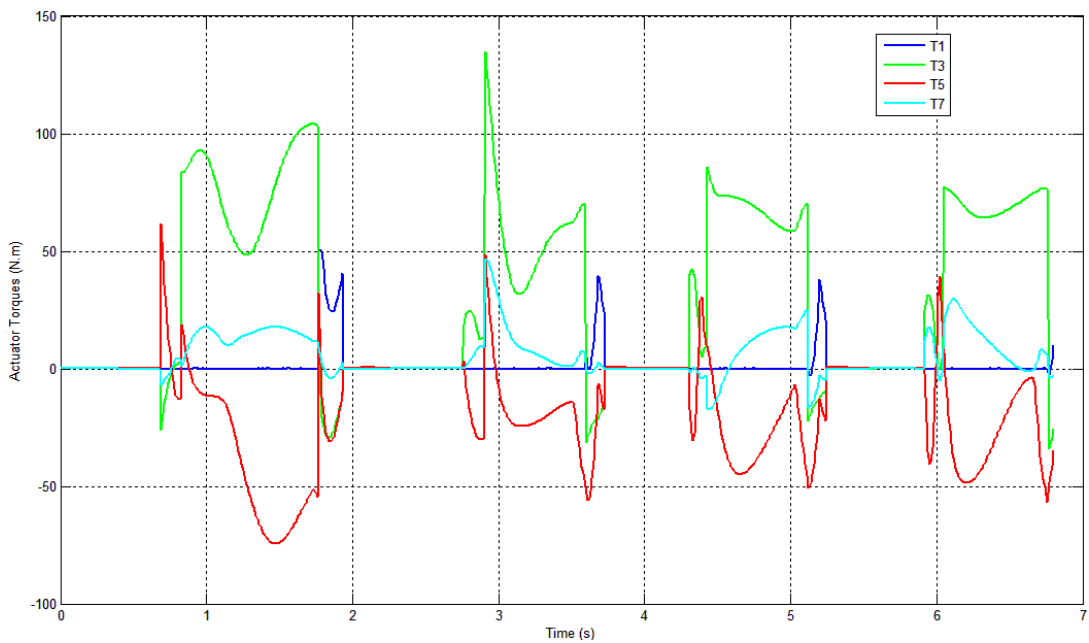


**Figure 6.64: Actuator Torques from  $T_1$  to  $T_7$  in the Right Leg**

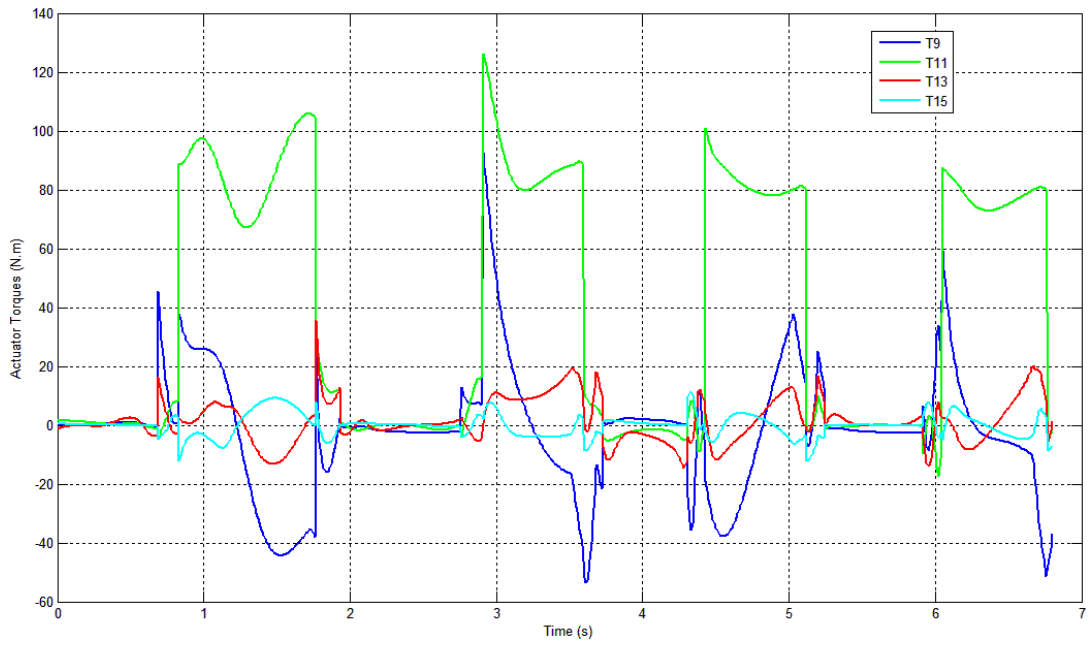


**Figure 6.65: Actuator Torques  $T_9$  to  $T_{15}$  in the Right Leg**

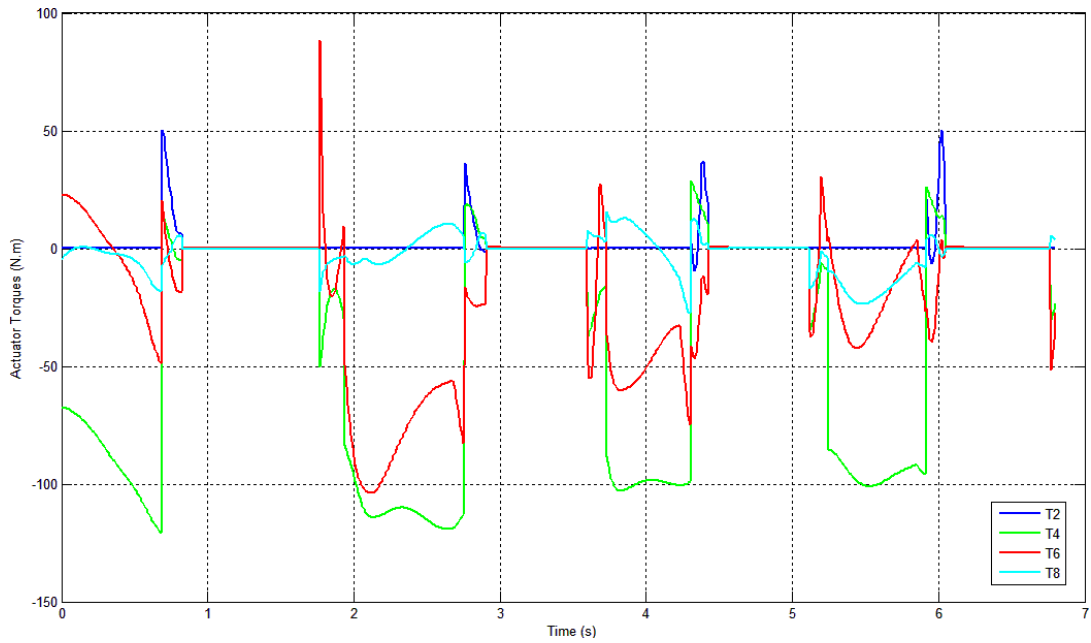


**Figure 6.66: Actuator Torques from  $T_2$  to  $T_8$  in the Left Leg**

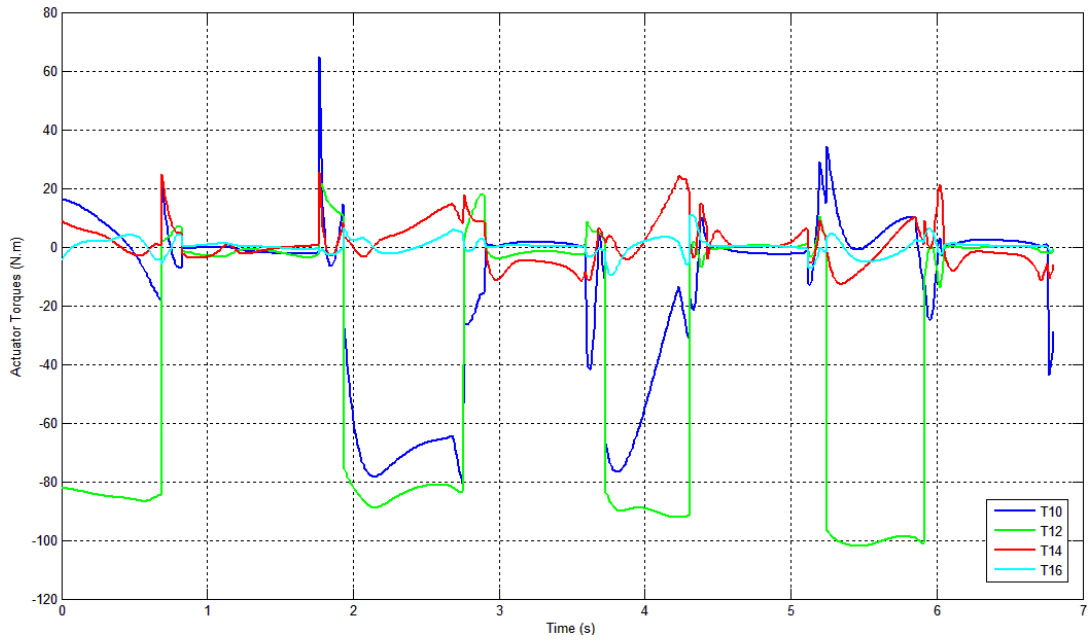


**Figure 6.67: Actuator Torques from T<sub>10</sub> to T<sub>16</sub> in the Left Leg**

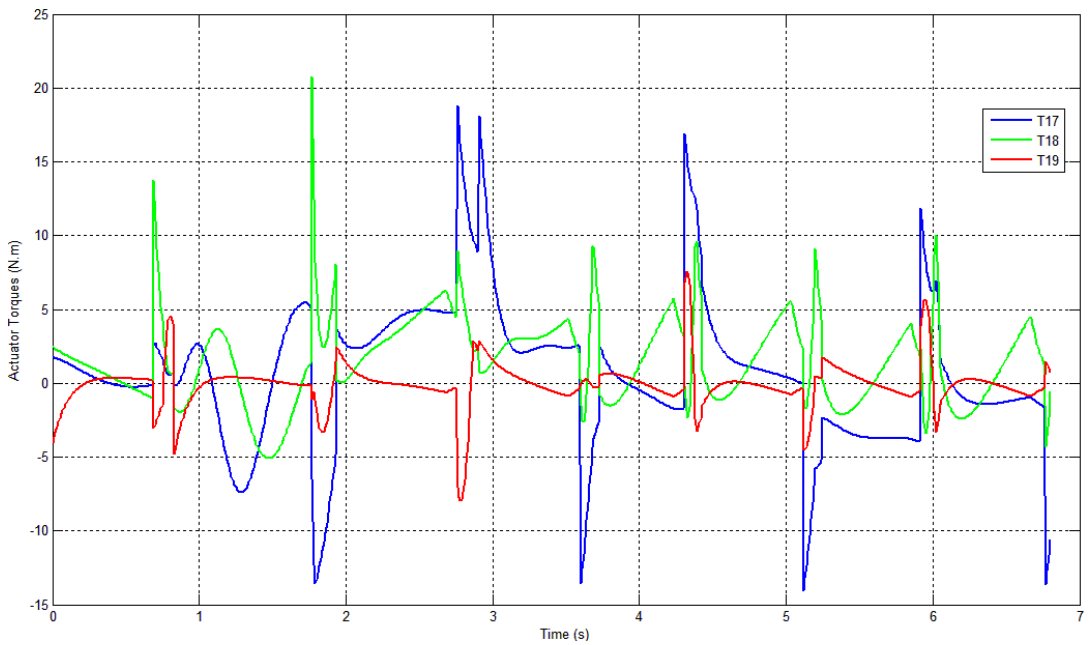


**Figure 6.68: Actuator Torques from T<sub>17</sub> to T<sub>19</sub>**

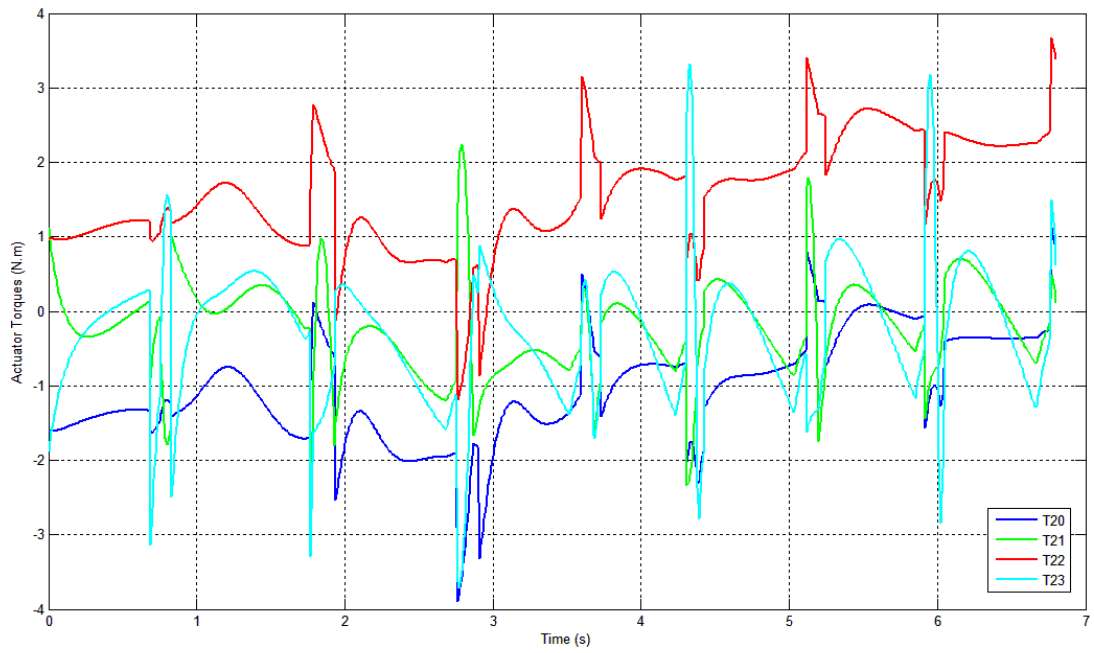


**Figure 6.69: Actuator Torques from T<sub>20</sub> to T<sub>23</sub>**

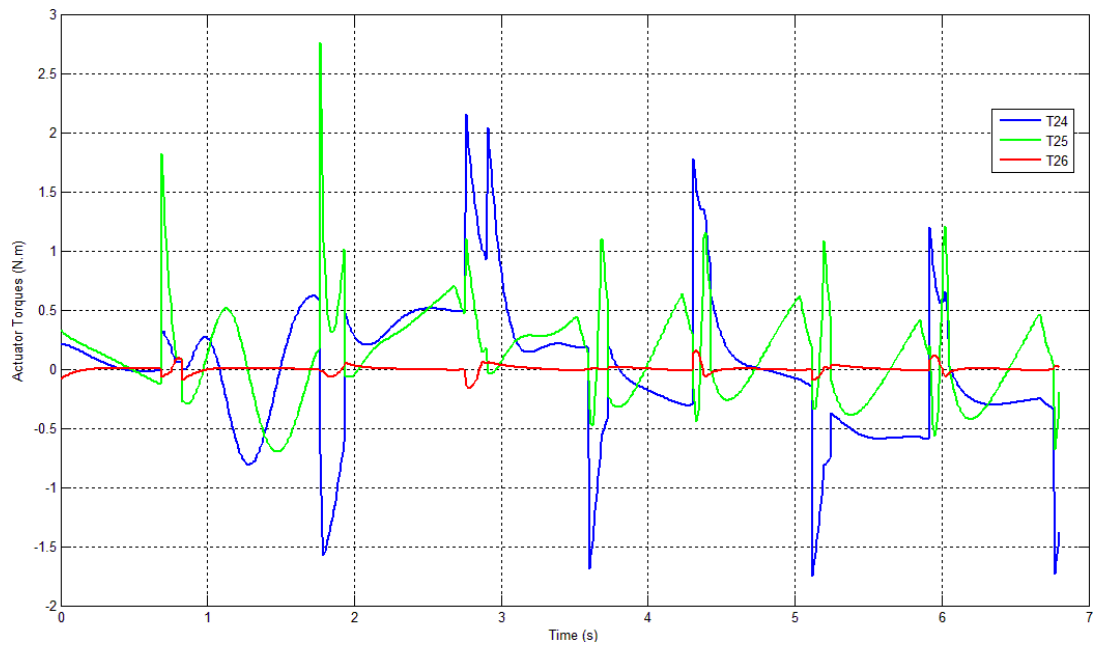


**Figure 6.70: Actuator Torques from T<sub>24</sub> to T<sub>26</sub>**

### 6.2.1.5. Ground Reaction Forces and Moments

Components of ground reaction forces and moments are resolved in body coordinate systems by regarding the convention for forces and moments in Newton-Euler equations in chapter 4.

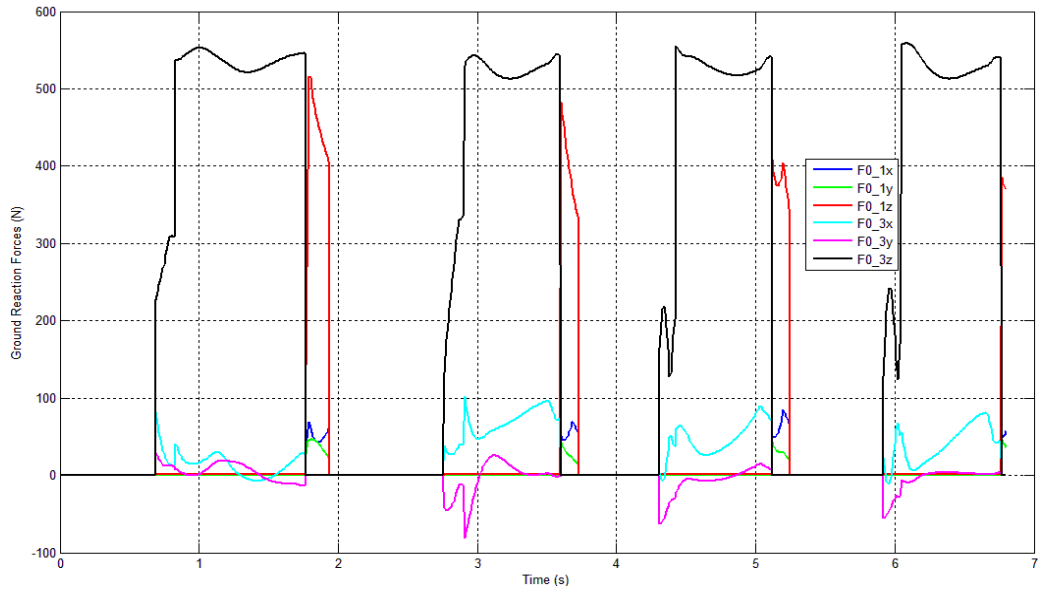


**Figure 6.71: Ground Reaction Forces for Body 1 and Body 3**

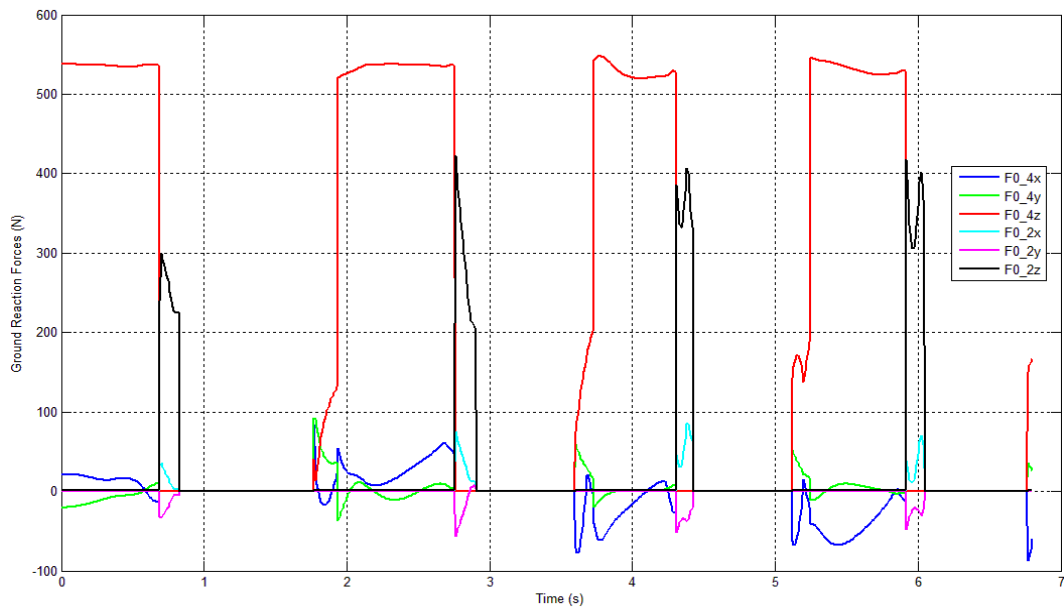


**Figure 6.72: Ground Reaction Forces for Body 2 and Body 4**

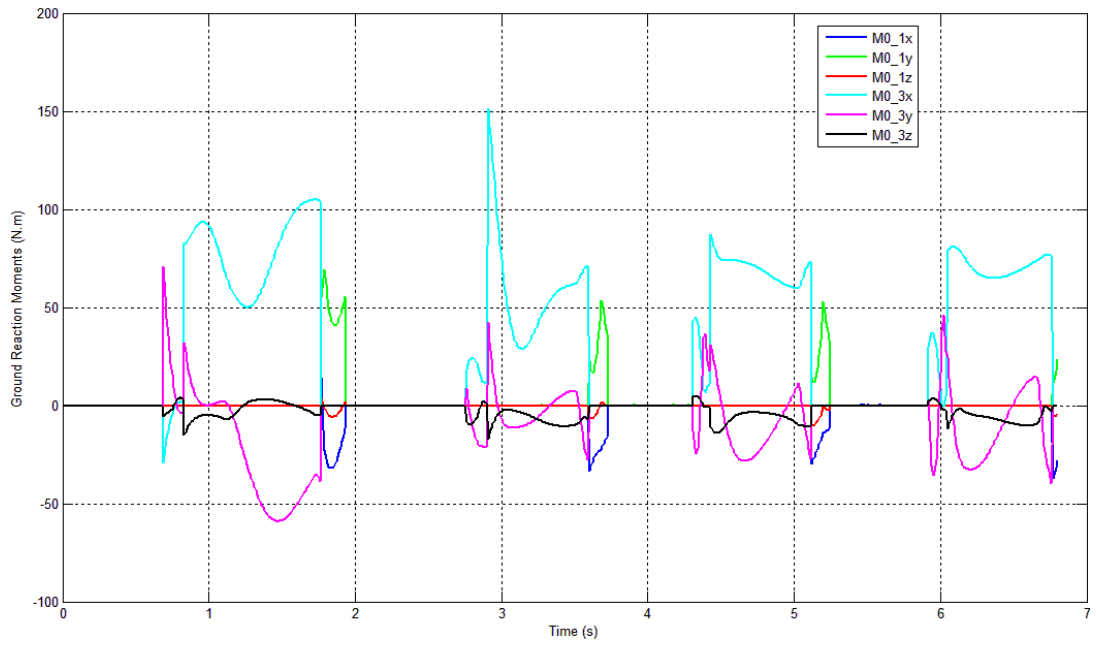


**Figure 6.73: Ground Reaction Moments**

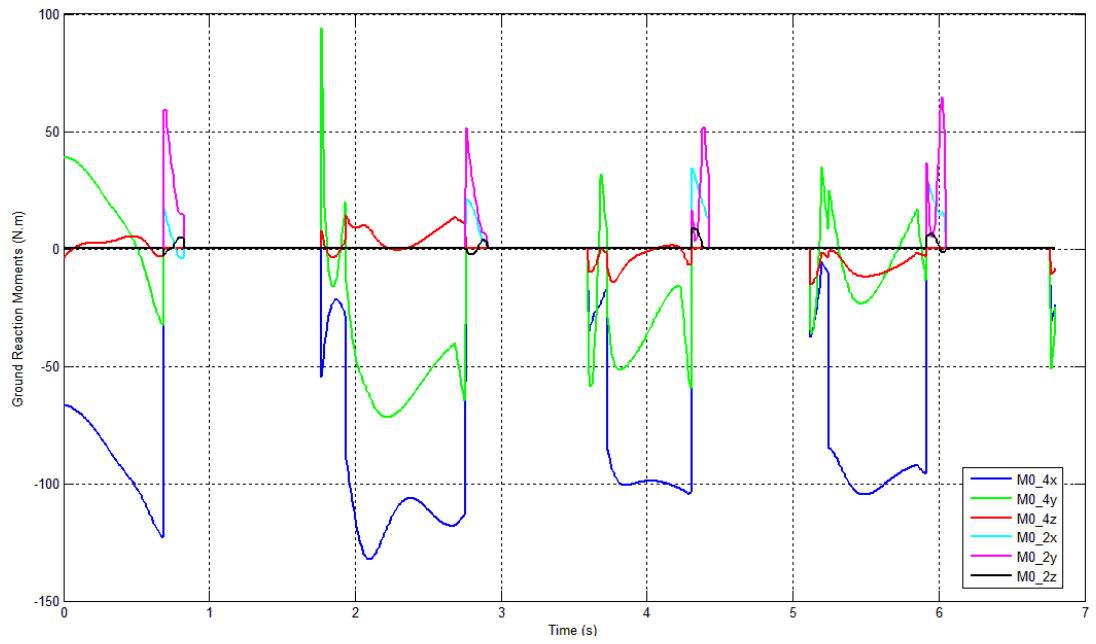


**Figure 6.74: Ground Reaction Moments**

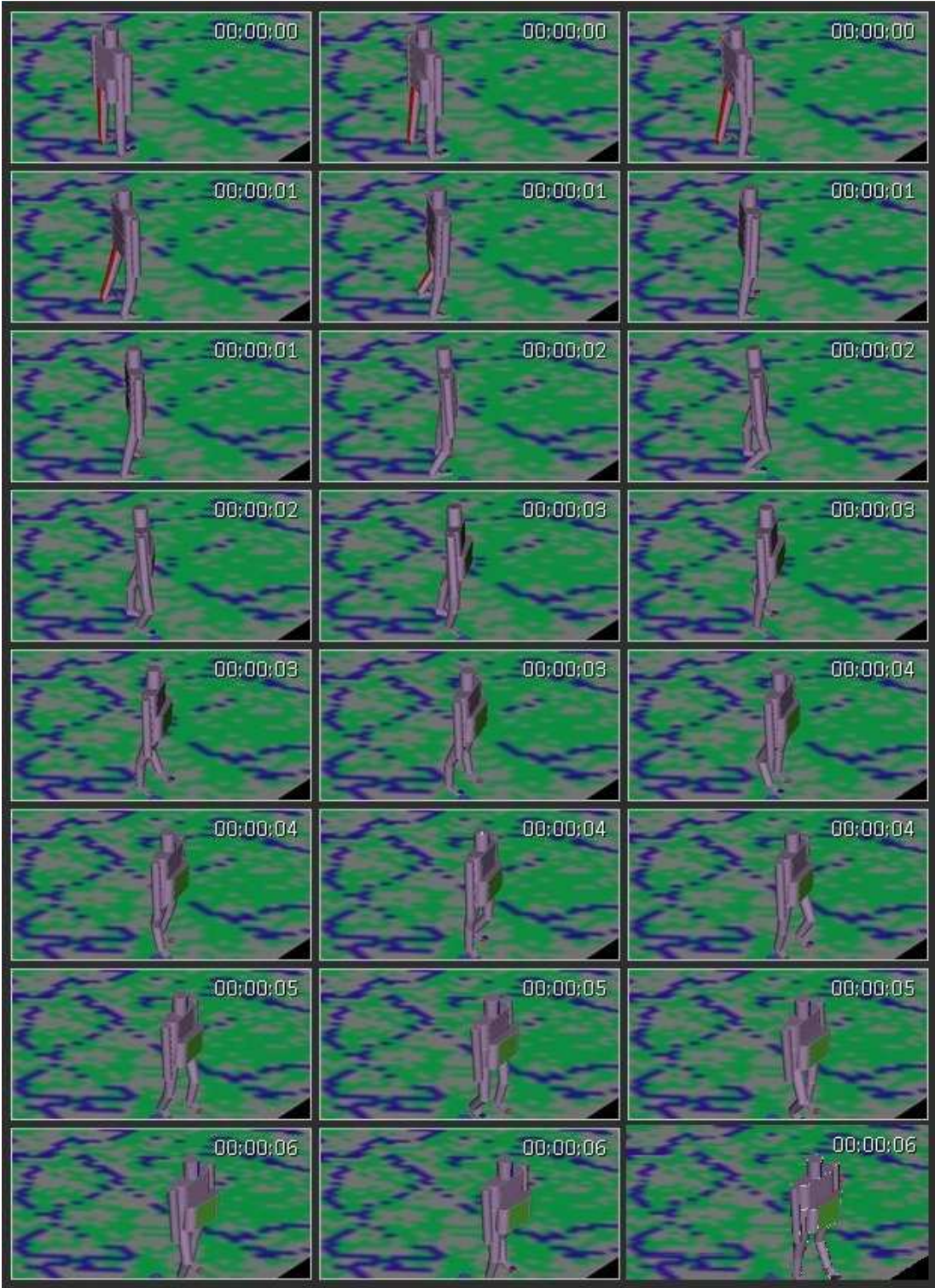


**Figure 6.75: Simulation Output for Simulation Number 1 in Virtual Reality Environment**

## 6.2.2. Simulation Number 2

Simulation results for parameter set 2 which is shown in Appendix B.2 are illustrated under this heading.

### 6.2.2.1. Reference Input

Reference trajectories for parameter set 2 can be illustrated by Figure 6.76, Figure 6.77 and Figure 6.78. Green and black colored curves represent the reference trajectory for  $P_{tpR}$  and  $P_{tpL}$ . Red, blue, magenta and cyan colored curves represent the reference trajectory for the mass center of Body 17 during LFFSSP, RFFDSP, RFFSSP and LFFDSP respectively.

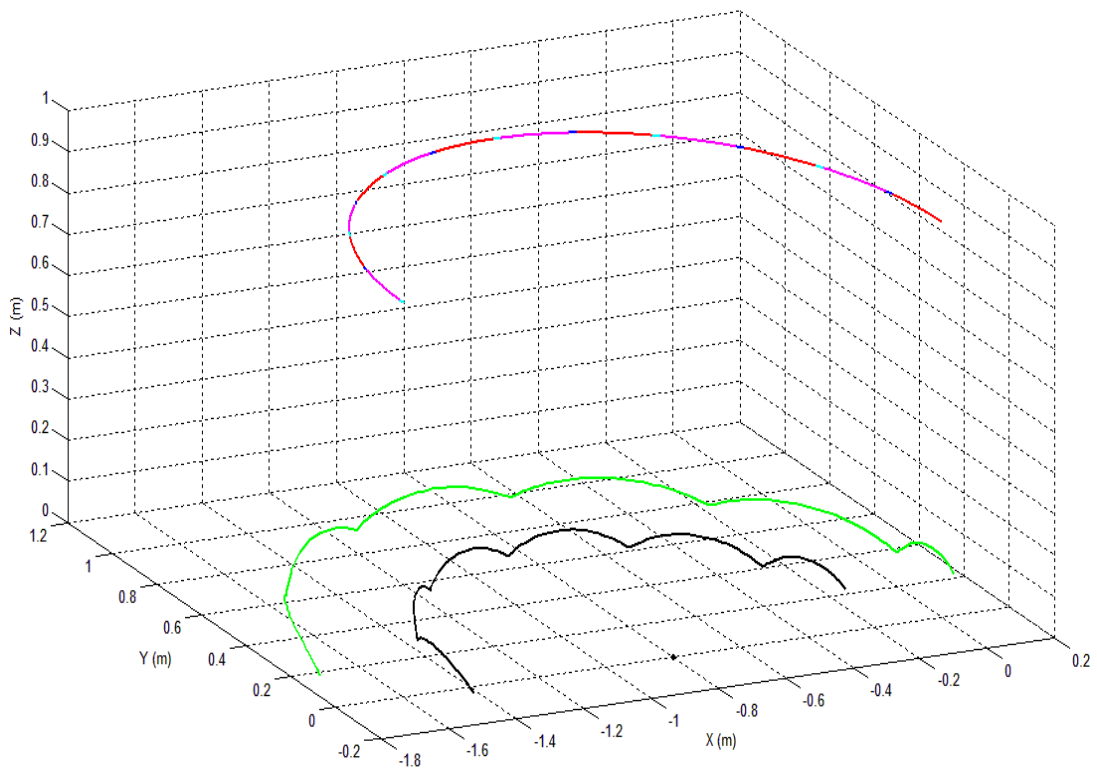


**Figure 6.76: Isometric View of Reference Trajectories for Parameter Set 2**

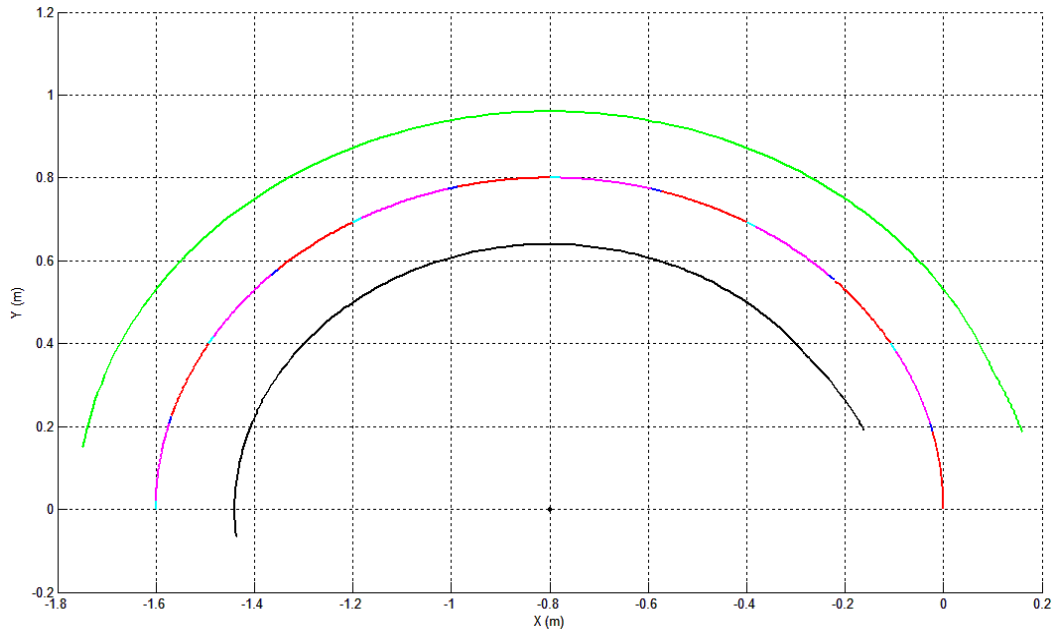


**Figure 6.77: Reference Trajectories on X-Y Plane for Parameter Set 2**

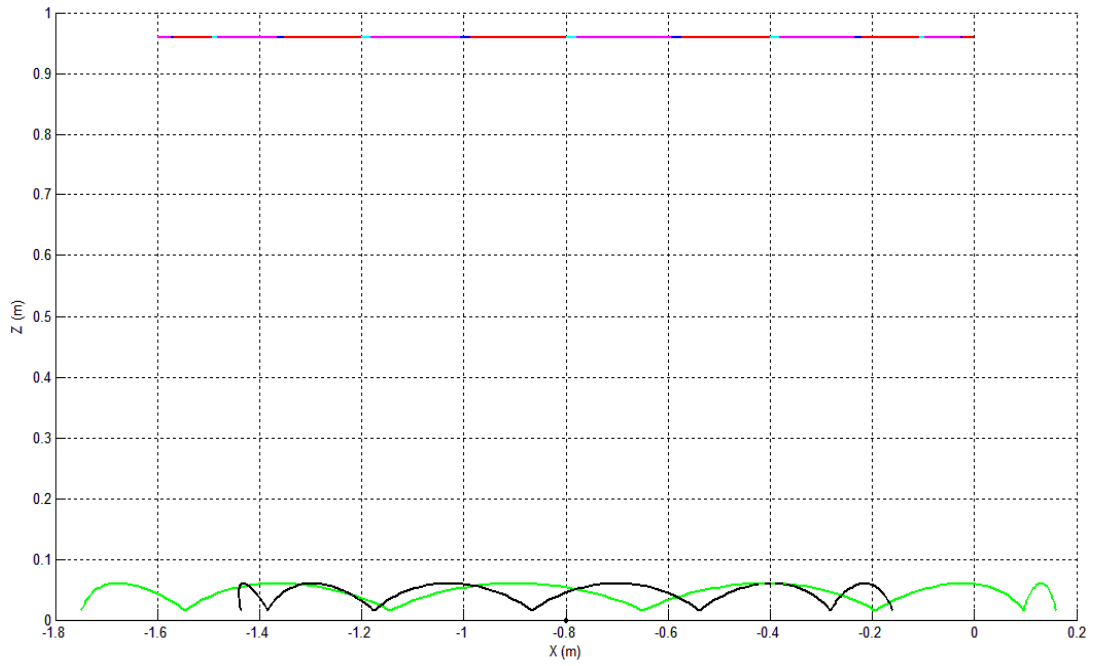


**Figure 6.78: Reference Trajectories on X-Z Plane for Parameter Set 2**

### 6.2.2.2. Task Space Positions

Simulation results with their reference inputs are shown by Figure 6.79, Figure 6.80 and Figure 6.81. All components are resolved in the inertial frame.

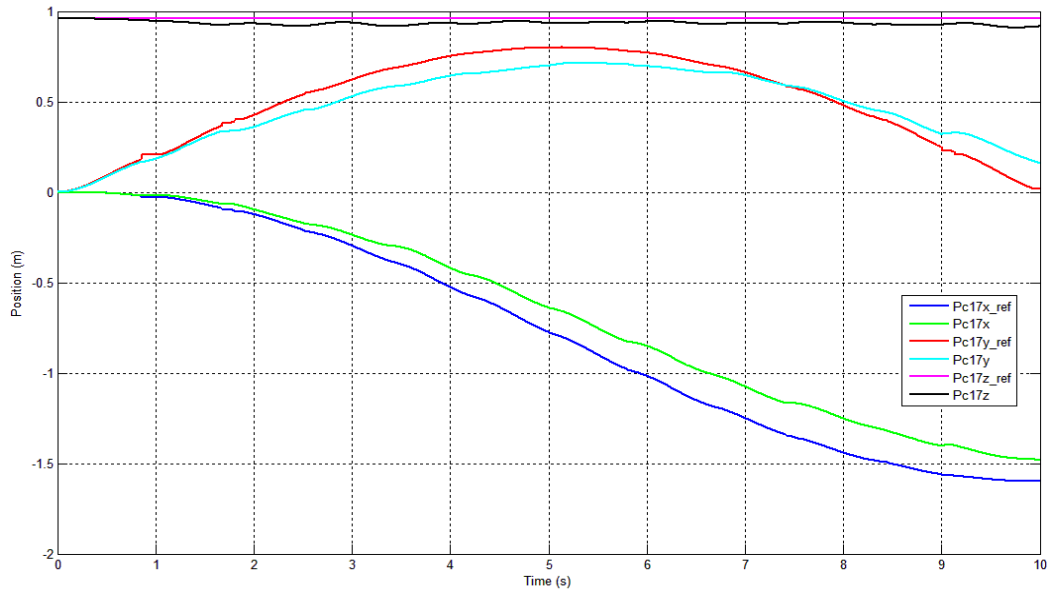


**Figure 6.79: Position of Mass Center of Body 17 with Its Reference Input**

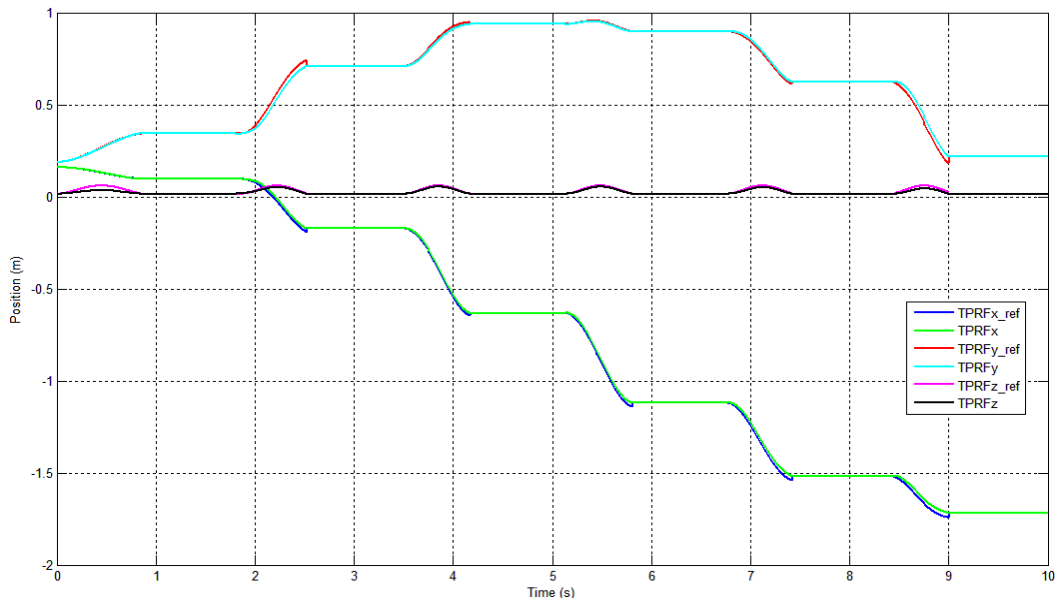


**Figure 6.80: Position of Toe Point on Right Foot (Body 1) with Its Reference Input**

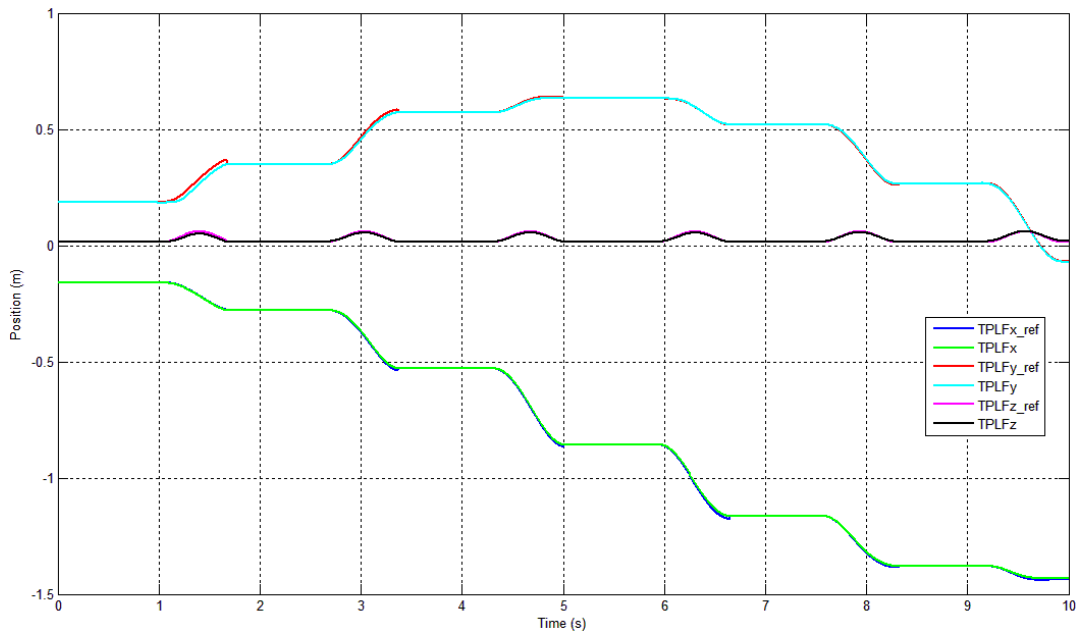


**Figure 6.81 Position of Toe Point on Left Foot (Body 2) with Its Reference Input**

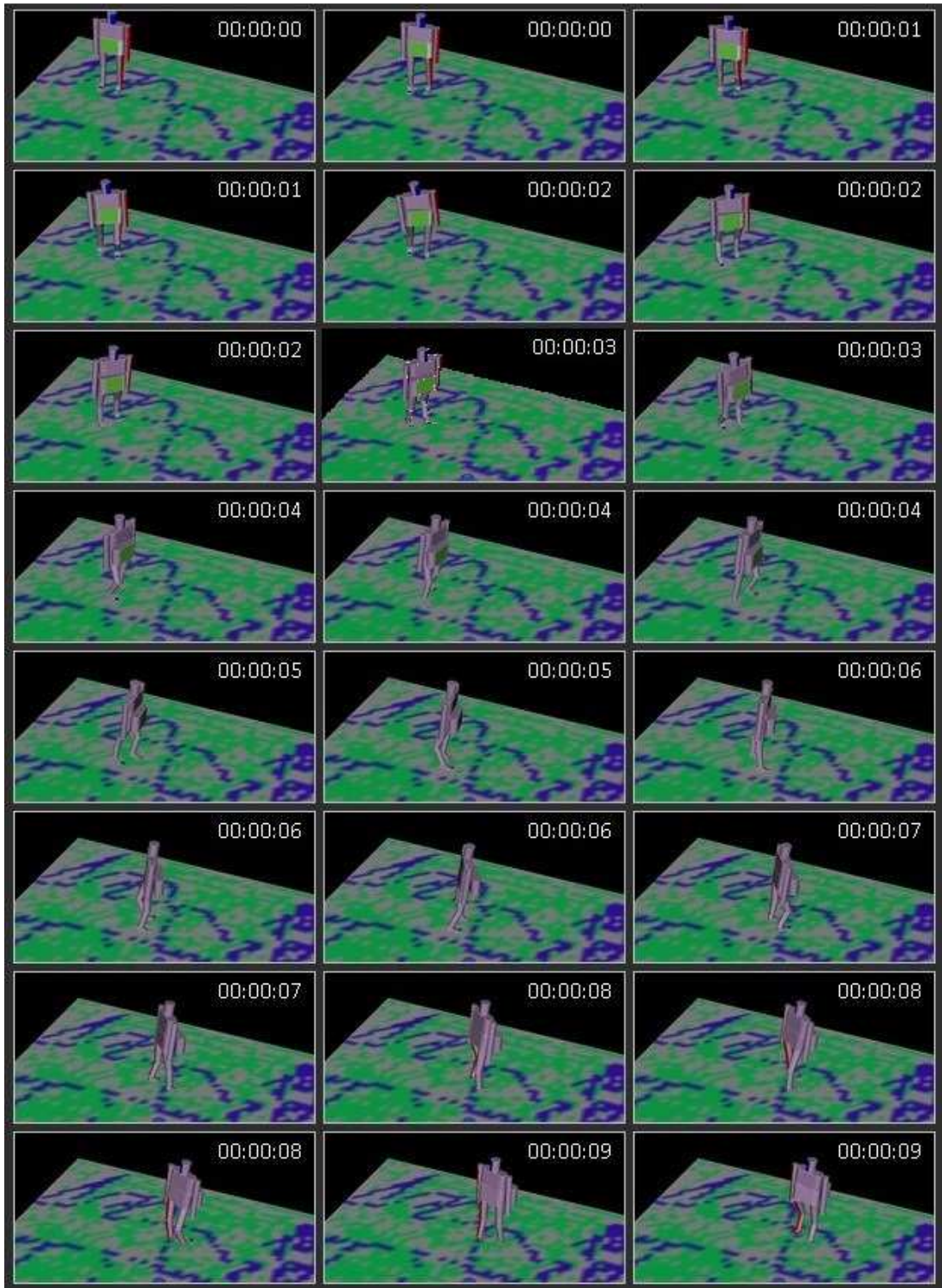


**Figure 6.82: Simulation Output for Simulation Number 2 in Virtual Reality Environment**

### 6.2.3. Simulation Number 3

Simulation results for parameter set 3 which is shown in Appendix B.3 are illustrated under this heading.

#### 6.2.3.1. Reference Input

Reference trajectories for parameter set 3 can be illustrated by Figure 6.83 and Figure 6.84. Green and black colored curves represent the reference trajectory for  $P_{ipR}$  and  $P_{ipL}$ . Red, blue, magenta and cyan colored curves represent the reference trajectory for the mass center of Body 17 during LFFSSP, RFFDSP, RFFSSP and LFFDSP respectively.

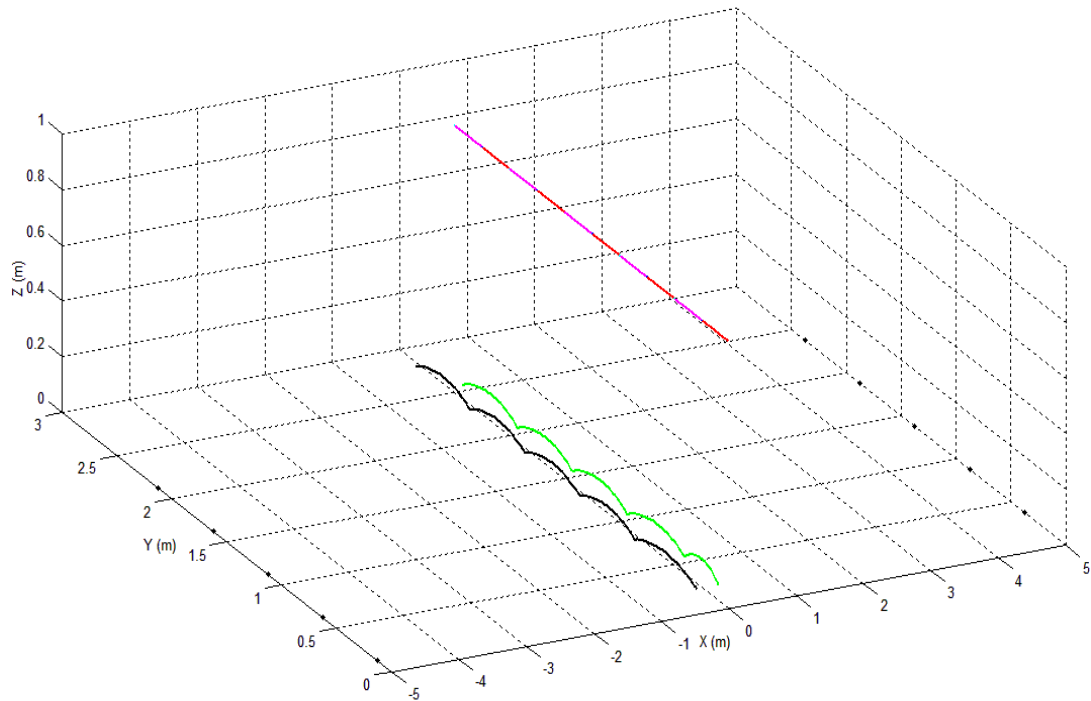


**Figure 6.83: Isometric View of Reference Trajectories for Parameter Set 3**

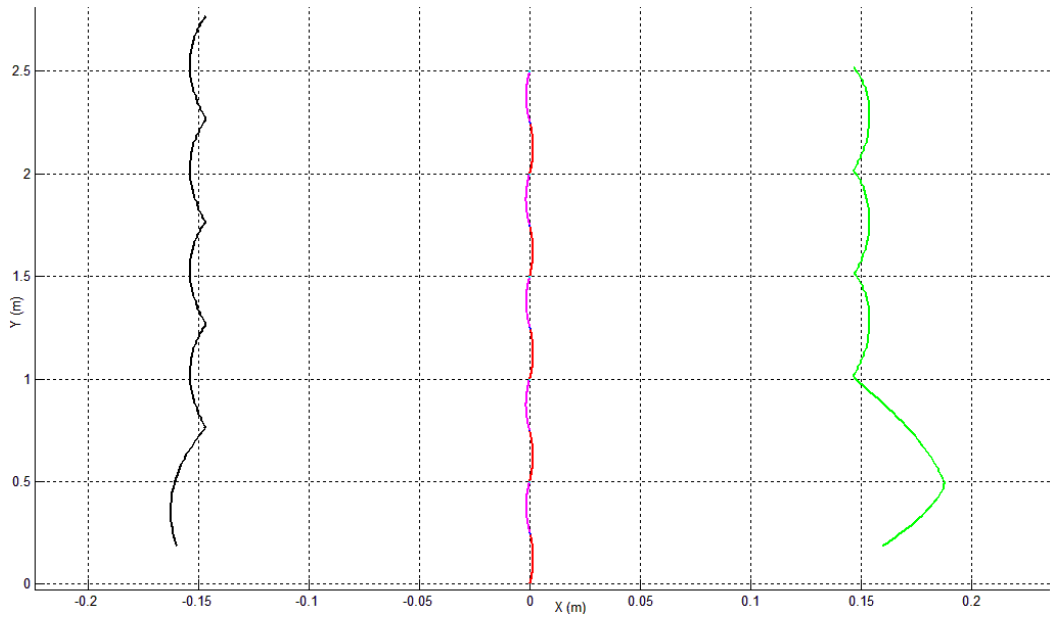


**Figure 6.84: Reference Trajectories on X-Y Plane for Parameter Set 3**

### 6.2.3.2. Task Space Positions

Simulation results with their reference inputs are shown by Figure 6.79, Figure 6.80 and Figure 6.81. All components are resolved in the inertial frame.

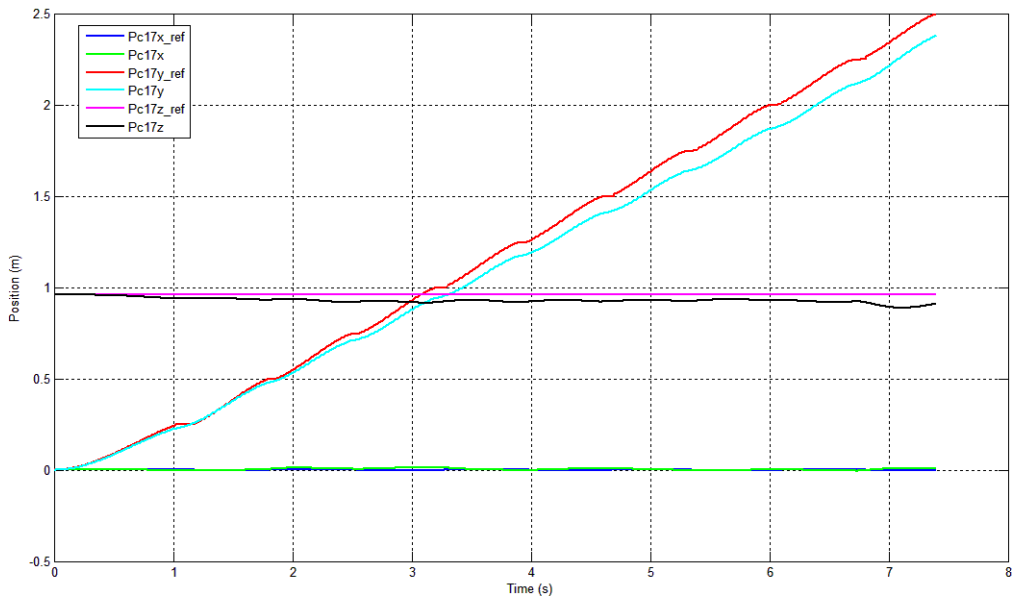


**Figure 6.85: Position of Mass Center of Body 17 with Its Reference Input**

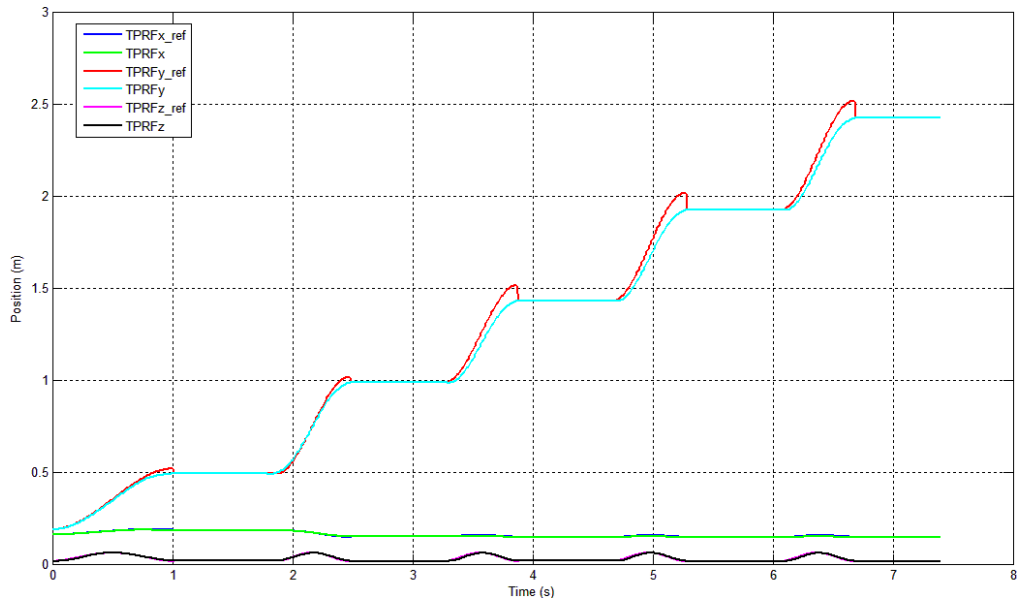


**Figure 6.86: Position of Toe Point on Right Foot (Body 1) with Its Reference Input**

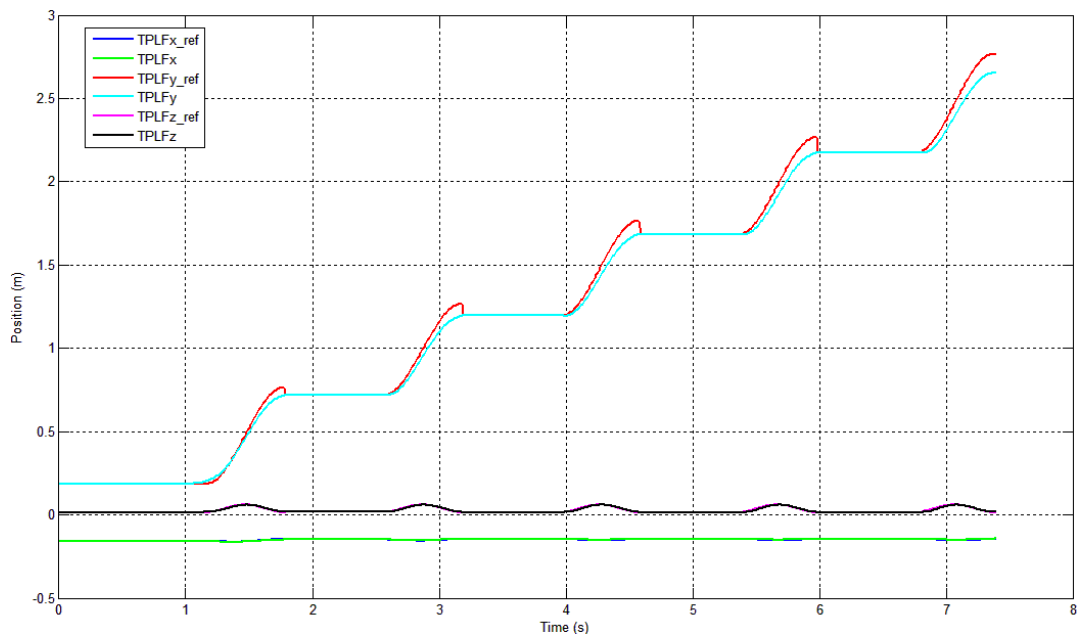


**Figure 6.87 Position of Toe Point on Left Foot (Body 2) with Its Reference Input**

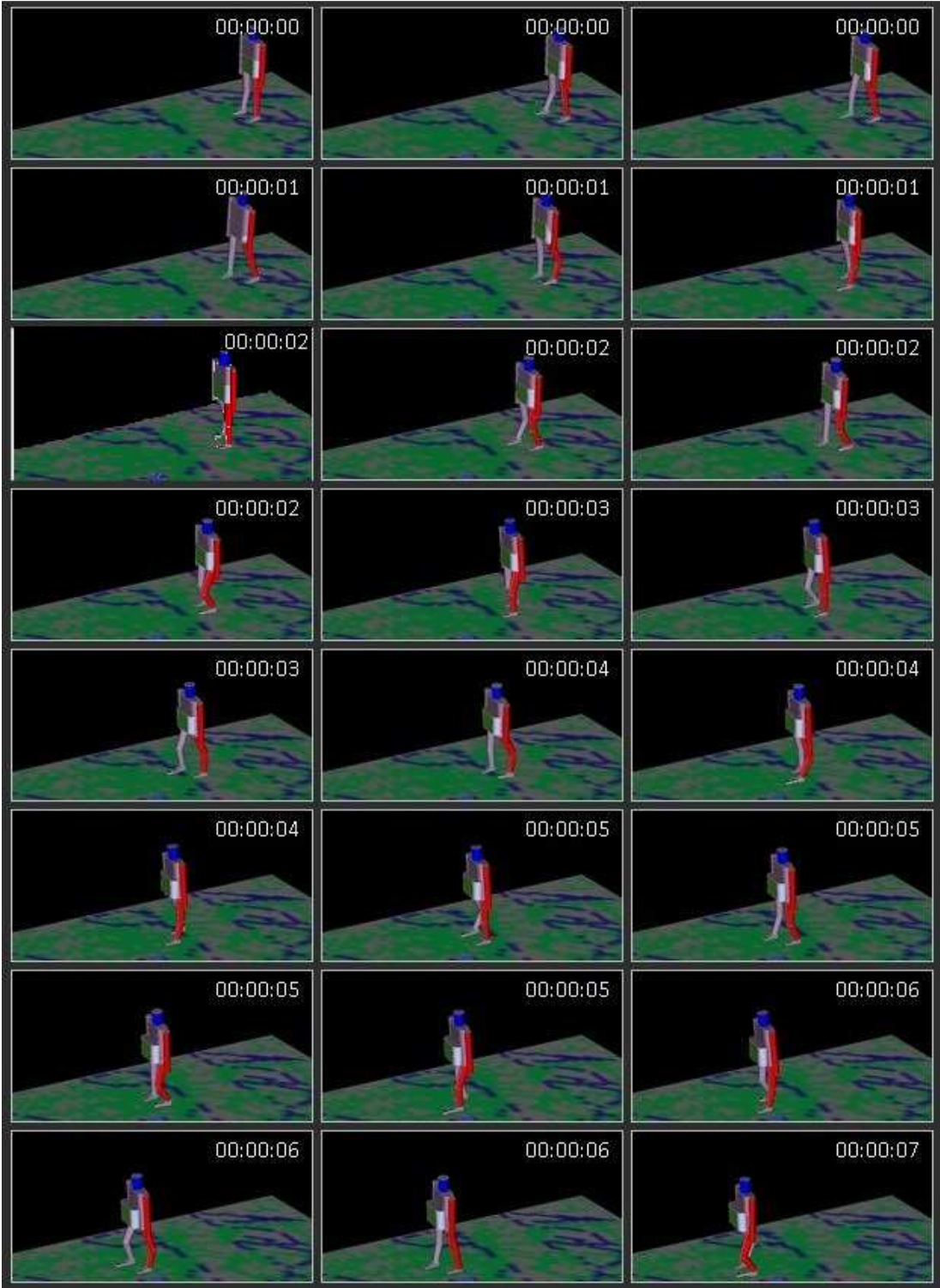


**Figure 6.88: Simulation Output for Simulation Number 3 in Virtual Reality Environment**

## CHAPTER 7

### DISCUSSION AND CONCLUSION

In this chapter, the thesis work is evaluated in a general manner. Deficiencies of the simulation model and the related future work are discussed.

Firstly, a decision is made for the physical model of the humanoid robot where other steps of the thesis study are based. In order to avoid limitations, provide flexibility for a variety of locomotion tasks and imitate human gait more realistically, each leg includes a kinematic configuration enabling 8 DOF with respect to the hip (Body 17). This kinematic configuration of legs, which have redundant DOF with respect to the hip, brings both advantages and disadvantages to the locomotion problem. Ground friction conditions, ground elevation and inclination, avoiding internal collision between bodies and exterior collision with obstacles, being exposed to external forces and moments and various other unexpected circumstances impose restrictions on possible biped locomotion patterns. That is why the realization of biped locomotion in 3D space requires flexibility in motions, which is an advantage of having legs with redundant DOF. However, the unavailability of simple conversion of task space variables into joint space variables results to additional computational burden which is not a preferable situation for online applications. In addition to bodies directly related with the biped locomotion which are from Body 1 to Body 17, upper bodies are included in the physical model, too. Therefore, dynamic effects of upper bodies to the biped locomotion are modeled instead of a lumped body modeling all upper body characteristics; which is one more step closer to the realistic simulation. After deciding the kinematic configuration, physical parameters of the humanoid robot is found.

During the derivation of mathematical models especially for dynamic equations, differences sourced from different locomotion phases are modeled by additional

equations which are included in direct dynamic solution procedures as much as possible to keep equations general for all locomotion phases. Using Newton-Euler equations enable the computation of dynamic equations numerically without going through analytical derivation procedure which is unpractical for a complex system with 26 DOF and to calculate reaction forces and moments between bodies which might be beneficial for the preliminary stage of mechanical design.

Time derivatives of jacobian matrices which are employed in the calculation of optimum command accelerations are obtained numerically by simple approximations. However, application of advanced numerical methods can be implemented for more accurate calculations especially for movements with high accelerations; where significant computation errors may lead to unpractical command accelerations during the procedure of optimum command accelerations calculation.

For a given reference input, 490 numerical values in total are supplied to the simulation model; where most of them are weighting coefficients used in the control strategy and remaining ones are for modeling and computational purposes. Therefore, it requires a lengthy trial and error procedure for finding appropriate numerical values for a given set of input supplied to the reference trajectory generation algorithm. Both generated reference trajectories and supplied weighting coefficients must be proper so that a sustainable biped locomotion is achieved for a given reference input. However, it is observed that a single set of weighting coefficients may not be able to sustain biped locomotion for an infinitely long time. In order to achieve that, a high level controller which can modify reference trajectories and weighting coefficients online to more feasible ones for adapting to changing conditions during the locomotion is required. In this thesis, such kind of a high level controller does not exist. Therefore, the control strategy eventually begins to show poor tracking performance or fails by using weighting coefficients that are constant throughout the simulation, especially for reference trajectories defining a motion including significantly different characteristics.

In this study, reference trajectories are defined for toe points and their related bodies, Body 17 and its mass center. However, motions of upper bodies like Body 20, Body

23, Body 24 and Body 27 play active role during the biped locomotion too. Since the assessment of upper bodies' contribution to the biped locomotion is directly related with an in depth reference trajectory generation study which is not in the scope of this thesis, reference joint space positions of related upper bodies which are from  $\theta_{18}$  to  $\theta_{27}$  are defined as 0. In other words, it is desired that upper bodies maintain their initial positions with respect to each other throughout the simulation. At first, zeros as command space accelerations for joints related with these upper bodies are supplied to the computed torque control method in order to keep upper bodies in their initial positions. However, it is observed that the deviation from initial positions for upper bodies due to cumulative errors becomes significant enough to affect the control of biped locomotion. As a result, (similar but simpler to the one used for lower bodies) an optimization problem about predicted joint space position and velocity error is used to define command space accelerations for each joint space variable concerning upper bodies.

Since generated reference trajectories are constructed by polynomials, selection of parameters which are supplied to the trajectory definition algorithm must be handled carefully. Unrealistic definitions like high duration times for small distances and high velocities can result to oscillatory solutions for the considered time interval.

It is expected that dynamic effects and weight of bodies are compensated by ground reaction forces and moments which are spread on all bodies contacting the ground. However, spreading of these ground reaction forces and moments do not include toe part of the flat foot like Body 1 during RFFDSP and RFFSSP or Body 2 during LFFSSP and LFFDSP. In other words, ground reaction forces and moments on Body 1 and Body 2 compensate forces and moments only related with their own weights regardless of other bodies. The reason for this phenomenon is due to the assumption that reaction forces and moments between Body 1 and Body 3 during RFFSSP and RFFDSP, Body 2 and Body 4 during LFFSSP and LFFDSP are zero. Calculation of reaction forces and moments between these bodies require an additional modeling effort which is not accomplished in this thesis. Moreover, it is possible to obtain unrealistic ground reaction forces and moments due to the assumption that contacting bodies are rigidly fixed to the ground. For example, a ground reaction force with negative  $\vec{u}_3$  component of related body coordinate system can be obtained; which

actually means the contacting body is to part from the ground but unable to do it due to the kinematic constraints imposed on the body. Similarly, it is possible to obtain a ground reaction moment where its resultant moment of  $\vec{u}_1$  and  $\vec{u}_2$  components can not be achieved with  $\vec{u}_3$  component of calculated ground reaction force within the contact area of the related body for related body coordinate system; which actually means that the contacting body is to roll but unable to do it due to the kinematic constraints imposed on the body. Also, ground reaction forces in the plane formed by  $\vec{u}_1$  and  $\vec{u}_2$  of the related body coordinate system are assumed to be supplied without any limitations imposed by the friction between contacting body and the ground. In this thesis, considerations for unrealistic ground reaction forces and moments are left to user's responsibility in the thesis. As a future study, a detailed model to find forces and moments which simulate the interaction between ground and contacting bodies can be devised for a more realistic simulation.

The most critical part of the simulation is the influence of the impact of swinging foot to joint space velocities during the transition from single to double support phases. Therefore, proper modeling of the impact is essential for a realistic simulation; which is a modeling problem that must be investigated in a detailed fashion. In this thesis, joint space velocities are modified manually based on a simple optimization problem where weighting coefficients determine aftereffect of the impact.

Depending on the selection of actuators during the mechanical design, actuator dynamics can be included in the simulation as a future work. In this study, actuator dynamics is neglected and actuator torques are bounded between certain values by saturation blocks in the simulation.

Each second is equivalent to 100 seconds in the simulation with a "Intel Core 2 Duo P8400 2.27 GHz" central processor unit. The simulation time is fairly high due to many calculation loops for numerical computations in user defined MATLAB functions. Also, most user defined MATLAB functions are written to work independently in calculation-wise. Therefore these user defined MATLAB functions recall other MATLAB functions as subroutines. Simulation time can be decreased by reducing the independency of user defined MATLAB functions and converting

shared calculations into common user defined functions. However, this kind of a simulation structure requires major editing effort for even small computational modifications and much effort to track operations. To summarize, computational burden for the simulation can be more than necessary due to the existence of repeated calculations in different user defined MATLAB functions; because the arrangement of user defined functions are task oriented instead of calculation oriented.

All in all, a simulation environment is constructed for the biped locomotion in 3D space of humanoid robots with a proposed control strategy. In this thesis, the devised simulation environment covers an important portion for a comprehensive simulation tool for humanoid robots. Since the integration of detailed models which are not covered in this thesis study into the simulation environment is possible, a complete simulation tool for various studies related with humanoid robots can be formed. Also, by the help of task oriented user defined MATLAB functions different control strategies can be tested by necessary rearrangements for a more general simulation structure.

## REFERENCES

- [1]Robots and people working together to build vehicles, last visited on March 26, 2010, [http://www.gm.com/experience/education/5-8/making\\_vehicles/robots.jsp](http://www.gm.com/experience/education/5-8/making_vehicles/robots.jsp)
- [2]Xie, M., *Fundamentals of Robotics: Linking Perception to Action*, World Scientific Publishing Company, Incorporated, 2003, p. 8,
- [3]Sano, A., Furusho, J., *Realization of natural dynamic walking using the angular momentum information*. Proceedings of the IEEE International Conference on Robotics and Automation, Vol. 3; 1990. p. 1476–1481
- [4]Tan, L. W., Chew, K. C. and Meng, C., *Evolutionary Robotics: From Algorithms to Implementations*, Vol. 28, World Scientific Series in Robotics and Intelligent Systems, World Scientific, 2006, p. 8-9
- [5]Skelly, M. M. and Chizeck, H. J., *Simulation of Bipedal Walking*, UWEE Technical Report, Number 2001-0001.: Department of Electrical Engineering, University of Washington, Washington D.C., USA, 3 October 2001
- [6]Gilchrist, L. A. and Winter, D. A., *A Multisegment Computer Simulation of Normal Human Gait*, IEEE Transactions on Rehabilitation Engineering, Vol. 5, No. 4, December 1997, p. 290-299
- [7]Wojtyra, M., *Dynamical Analysis of Human Walking*, 15th European ADAMS Users' Conference Technical Papers, Rome, Italy, 2000
- [8]Zhang, R., Vadakkepat, P. and Chew C. M., *Development And Walking Control of A Biped Robot*, IEEE Transactions on Mechatronics, 2003,
- [9]Mu, X. And Wu, Q., *Development of a complete dynamic model of Development And Walking Control of A Biped Robot a planar five-link biped and sliding mode control of its locomotion during the double support phase*, International Journal of Control, Vol. 77, Issue 8, 20 May 2004, p.789-799

- [10]Liu,Z., Li, C. and Xu, W., *Hybrid control of biped robots in the double-support phase via  $H_\infty$  approach and fuzzy neural networks*, IEE Proceedings Control Theory Appl., Vol. 150, No.4, July 2003, p. 347-354
- [11]Takahashi, T. and Kawamura, A., *Position and Altitude Tracking Control for Toe Support Phase of Biped Walking*, Electrical Engineering in Japan, Vol. 157, No. 1, October 2006, p. 72-79
- [12]Tlalolini, D., Chevallereau, C. and Aoustin, Y., *Comparison of different gaits with rotation of the feet for a planar biped*, Robotics and Autonomous Systems, Vol. 57, Issue 4, 30 April 2009, p. 371-383
- [13]Peasgood, M., Kubica, E. and McPhee, J., *Stabilization and energy optimization of a dynamic walking gait simulation*,. ASME J Comp Nonl Dyn 2:65–72, 2007
- [14]Anderson, F. C. and Pandy M. G., *Dynamic Optimization of Human Walking*, Journal of Biomechanical Engineering, Vol. 123, October 2001, p. 381-390
- [15]Shih, C. L. and Gruver, W. A., *Control of a Biped Robot in the Double Support Phase*, IEEE Transaction on Systems, Man and Cybernetics, Vol 22, No. 4, July-August 1992, p. 729-735
- [16]Hase, K., *Computer Simulation of Human Gait for Rehabilitation Applications*, AIST Today, Vol. 2, No. 3, 2002, p.13
- [17]Nakanishi, J, Moritomo, J, Endo, G, Cheng, G., Schaal, S. and Kawato, M., *Learning from demonstration and adaptation of biped locomotion*, Robotics and Autonomous Systems, Vol. 47, Issues 2-3, 30 June 2004, p. 79-91
- [18]Yamaguchi, T. and Shibata, M., *Walking Planning Based on Artificial Vector Field with Prediction Simulation for Biped Robot*, Electrical Engineering in Japan, Vol.159, No. 4 ,2007, p. 54-61
- [19]Wieber, P. B. and Chevallereau, C., *Online adaptation of reference trajectories for the control of walking systems*, Robotics and Autonomous Systems, Vol. 54, Issue 7, 31 July 2006, p. 559–566

- [20]Huang, Q, Yokoi, K., Kajita, S., Kaneko, K., Arai, H., Koyachi, N. and Tanie, K., *Planning Walking Patterns for a Biped Robot*, IEEE Transactions on Robotics and Automation, Vol. 17, No. 3, June 2001, p. 280-289
- [21]Denk, J. and Schmidt, G., *Synthesis of a Walking Primitive Database for a Humanoid Robot using Optimal Control Techniques*, Proceedings of IEEE-RAS International Conference on Humanoid Robots (HUMANOIDS2001), November 2001, p. 319–326
- [22]Hu, L., Zhou, C. and Sun, Z., *Estimating Biped Gait Using Spline-Based Probability Distribution Function With Q-Learning*, IEEE Transactions on Industrial Electronics, Vol. 55, No.3, March 2008
- [23]Vukobratović, M. and Borovac, B., *Zero-Moment Point Thirty Five Years of Its Life*, International Journal of Humanoid Robotics, Vol. 1, No. 1, 2004, p. 157–173
- [24]Goswami, A., *Foot-rotation indicator (FRI) point: A new gait planning tool to evaluate postural stability of biped robots*, Proc. IEEE ICRA, Detroit, 1999, pp. 47–52.
- [25]Sardain, P. and Bessonnet, G., *Forces Acting on a Biped Robot. Center of Pressure-Zero Moment Point*, IEEE Transactions on Systems, Man and Cybernetics-Part A: Systems and Humans, Vol. 34, NO. 5, September 2004, p. 630-637
- [26]Zheng, Y. F. and Shen, J., *Gait Synthesis for the SD-2 Biped Robot to Climb Sloping Surface*, IEEE Transactions on Robotics and Automation, Vol. 6, No. 1, February 1990
- [27] Cuevas, E., Zaldivar, D. and Rojas, R., *Walking trajectory control of a biped robot*, Technical report B-04-18, Freie Universität Berlin, Institut für Informatik Takusstr, Berlin, Germany and Universidad de Guadalajara, Jal, México, 16 November 2004
- [28]Kajita, S., Kanehiro, F., Kaneko, K., Fujiwara, K., Yokoi, K. and Hirukawa, H., *Biped walking pattern generation by a simple three-dimensional inverted pendulum model*, Advanced Robotics, Vol. 17, No. 2, 2003, p. 131–147
- [29]Vanderborght, B., Verrelst, B., Ham, R. V., Damme, M. V. and Lefeber, D., *Objective locomotion parameters based inverted pendulum trajectory generator*, Robotics and Autonomous Systems, Vol. 56, 2008, p. 738–750

- [30]Kitamura, S., Kurematsu, Y. and Iwata, M., *Motion Generation of a Biped Locomotive Robot Using an Inverted Pendulum Model and Neural Networks*, Proceedings of the 29th Conference on Decision and Control, December 1990, p. 3308-3312
- [31]Kajita, S., Kanehiro, F., Kaneko, K., Fujiwara, K., Harada, K., Yokoi, K. and Hirukawa, H., *Biped Walking Pattern Generation by using Preview Control of Zero-Moment Point*, Proceedings of the 2003 IEEE International Conference on Robotics and Automation, September 14-19 2003, p.1620-1626
- [32]Shih, C. L. and Chiou, C. J., *The Motion Control of a Statically Stable Biped Robot on an Uneven Floor*, IEEE Transactions on Systems, Man and Cybernetics-Part B: Cybernetics, Vol. 28, No. 2, April 1998, p. 244-249
- [33]Ha, T. and Choi, C. H., *An effective trajectory generation method for bipedal walking*, Robotics and Autonomous Systems, Vol.55, 2007, p. 795–810
- [34]Nakamura, Y., Mori, T., Sato, M. and Ishii, S., *Reinforcement learning for a biped robot based on a CPG-actor-critic method*, Neural Networks, Vol. 20, 2007, p. 723-735
- [35]Matsubara, T., Morimoto, J., Nakanishi, J., Sato, M. and Doya, K., *Learning CPG-based biped locomotion with a policy gradient method*, Robotics and Autonomous Systems, Vol. 54, 2006, p. 911–920
- [36]Ogihara, N. and Yamazaki, N., *Generation of human bipedal locomotion by a bio-mimetic neuro-musculo-skeletal model*, Biological Cybernetics Vol. 84, No. 1, January 2001, p. 1-11
- [37]Hirai, K., Hirose, M., Haikawa, Y. and Takenaka, T., *The Development of Honda Humanoid Robot*, Proceedings of the 1998 IEEE International Conference on Robotics and Automation, May 1998, p. 1321- 1326
- [38]Jalics, L., Hemami, H. and Clymer, B., *A Control Strategy for Adaptive Bipedal Locomotion*, Proceedings of the 1996 IEEE International Conference on Robotics and Automation, Vol. 1, April 1996, p. 563-569

[39]Wollherr, D., Buss, M., Hardt, M. and Stryk, O. V., *Research and Development Towards an Autonomous Biped Walking Robot*, Proceedings of the IEEE/ASME International Conference on Advanced Intelligent Mechatronics (AIM2003), 2003, p. 968-973

[40]Sano, A. and Furusho, J., *Control of Torque Distribution for the BLR-G2 Biped Robot*, Advanced Robotics, 1991. 'Robots in Unstructured Environments', 91 ICAR., Fifth International Conference on, Vol. 1, 1991, p. 729-734

[41]Deman, L., Wenlu, W., Fu, L. Z. and Chaowan, Y., *Adaptive Control of the Heel-Off to Toe-Off Motion of a Dynamic Biped Gait*, Proceedings of the 32nd Conference on Decision and Control, Vol. 3, December 1993, p. 2662-2663

[42]Honda Technology, last visited on April 29, 2010, <http://world.honda.com/ASIMO/technology/>

[43]National Institute of Advanced Industrial Science and Technology, Japan, last visited on April 29, 2010, [http://www.aist.go.jp/aist\\_e/latest\\_research/2009/20090513/20090513.html](http://www.aist.go.jp/aist_e/latest_research/2009/20090513/20090513.html)

[44]Pal Technology Robotics, last visited on April 29, 2010, <http://www.pal-robotics.com/specifications.html>

[45]Nishiwaki, K., Kuffner, J., Kagami, S., Inaba, M. and Inoue, H., *The experimental humanoid robot H7: a research platform for autonomous behaviour*, Philosophical Transactions of Royal Society A, Vol. 365, No. 1850, 2007, p. 79–107

[46]Park, I. W., Kim, J. Y., Lee J. and Oh, J. H., *Mechanical design of the humanoid robot platform, HUBO*, Advanced Robotics, Vol. 21, No. 11, 2007, p. 1305–1322

[47]Development of Humanoid Robot HUBO2, last visited on April 29, 2010, [http://hubolab.kaist.ac.kr/hubo\(khr-4\)\\_Specification.php](http://hubolab.kaist.ac.kr/hubo(khr-4)_Specification.php)

[48]WABIAN-2R, last visited on April 29, 2010, <http://www.takanishi.mech.waseda.ac.jp/top/research/wabian/index.htm#mechanism>

[49]Ogura, Y., Aikawa, H., Shimomura, K., Kondo, H., Morishima, A., Lim, H. O. and Takanishi, A., *Development of a New Humanoid Robot WABIAN-2*, Proceedings of the 2006 IEEE International Conference on Robotics and Automation, May 2006, p. 76-81

[50]Unimate, last visited on March 26, 2010, [http://www.maschinenbau.fh-wiesbaden.de/eLearning/module/module/robotik/22\\_unimate\\_1954\\_1961.html](http://www.maschinenbau.fh-wiesbaden.de/eLearning/module/module/robotik/22_unimate_1954_1961.html)

[51]Viking 1 Lander Model, last visited on March 29, 2010, <http://nssdc.gsfc.nasa.gov/nmc/masterCatalog.do?sc=1975-075C>

[52]The Descriptive Stages of Gait Cycle, last visited on March 30, 2010, <http://orthoteers.blogspot.com/2007/10/gait.html>

[53]ASIMO History, last visited on April 28, 2010, <http://world.honda.com/ASIMO/history/>

[54]National Institute of Advanced Science and Technology, last visited on April 29, 2010, [http://www.aist.go.jp/aist\\_e/latest\\_research/2009/20090513/20090513.html](http://www.aist.go.jp/aist_e/latest_research/2009/20090513/20090513.html)

[55]Pal Technology Robotics, last visited on April 29, 2010, <http://www.pal-robotics.com/media.html>

[56]Perception-Action Integrated Humanoid Robot: H6 & H7, last visited on April 29, 2010, <http://www.jsk.t.u-tokyo.ac.jp/research/h6>

[57]HUBO2 by Yonhap News Agency, last visited on April 29, 2010, <http://www.yonhapnews.co.kr/bulletin/2009/12/05/0200000000AKR20091205067400017.HTML>

[58]Biped Humanoid Robot Group WABIAN-2, last visited on April 29, 2010, [http://www.takanishi.mech.waseda.ac.jp/top/research/wabian/wabian2\\_2LL/wabian2\\_2LL.htm#top](http://www.takanishi.mech.waseda.ac.jp/top/research/wabian/wabian2_2LL/wabian2_2LL.htm#top)

[59]Jones, F. W., *Annals of the Royal College of Surgeons of England*, Vol. 5, No. 1, 1949, p. 32-33

[60]Denavit, J.and Hartenberg R.S., *A kinematic notation for lower-pair mechanisms based on matrices*, ASME Journal of Applied Mechanics ,1955, p. 215-221

[61]MATLAB Documentation – Function Reference Vol.1: A-E, version 7, downloaded on June 28, 2010, published at [http://www.mathworks.com/access/helpdesk/help/techdoc/matlab\\_product\\_page2.html](http://www.mathworks.com/access/helpdesk/help/techdoc/matlab_product_page2.html), p.179-180

[62]Rodrigues, O., *Des lois geometrique qui regissent les deplacements d'un systeme solide dans l'espace*, Journal de Mathematique Pures et Appliquees de Liouville, vol. 5, 1840, p. 380–440.

[63]Lang, S., *Calculus of Several Variables*, Reading, MA: Addison-Wesley, 1973, , p. 140

[64]Lewis, F. L., Dawson, D. M. and Abdallah, C. T., *Robot Manipulator Control:Theory and Practice*, 2nd Ed., Marcel Dekker Inc., 2004, p. 169-252

[65]MATLAB Simulink Documentation – SimMechanics Version 3.2 User Guide, downloaded on June 28, 2010, published at <http://www.mathworks.com/access/helpdesk/help/toolbox/physmod/mech/index.html>

[66]MATLAB Simulink Documentation – Simulink Version 7.5 User Guide , downloaded on June 28, 2010, published at <http://www.mathworks.com/access/helpdesk/help/toolbox/simulink/index.html>

[67]Özgören, M. K., *Topological analysis of six-joint serial manipulators and their inverse kinematic solutions*, Journal of Mechanism and Machine Theory, Vol. 37, 2002, p. 511-547

[68]Özyurt , G., *3-D Humanoid Gait Simulation Using An Optimal Predictive Control*, Master of Science Thesis, Middle East Technical University, 2005

[69]Yüksel, B., *Towards the enhancement of biped locomotion and control techniques*, Doctoral Thesis, Middle East Technical University, 2008

## APPENDIX A

### EQUIVALANCE TABLE FOR DATA STORE BLOCK AND USER DEFINED MATLAB FUNCTION LABELS IN THE SIMULATION MODEL

**Table A.1: Equivalence Table**

In the Thesis	In the Simulation Model
$P_{hip}$	Phip
$V_{hip}$	Vhip
R	Radius
$T_{dir}$	TurningDir
$t_{SSP}$	tSSP
PTR	PTR
SW	SW
SH	SH
$k_{Adj}$	kAdj
$k_{SH}$	kSH
$\Delta\theta_{PLN}$	DeltaTethaPLN
$\Delta\theta_{ADJ}$	DeltaTethaADJ
$P_{TPR,i}$	PRi
$P_{TPL,i}$	PLi
$\hat{C}^{(0,1)}_{initial}$	FRO_i
$\hat{C}^{(0,2)}_{initial}$	FLO_i
$\bar{q}_{initial}$	q_initial
$\dot{\bar{q}}_{initial}$	qd_initial
$\bar{q}$	q
$\dot{\bar{q}}$	qd
$\bar{\bar{P}}_{tpR}$	TPRF
$\bar{\bar{P}}_{tpL}$	TPLF
$\bar{\bar{V}}_{tpR}$	TPRFd
$\bar{\bar{V}}_{tpL}$	TPLFd
$\bar{\bar{a}}_{tpR}$	TPRFdd
$\bar{\bar{a}}_{tpL}$	TPLFdd
g	g
$\Delta t_{1\_LFFSSP}$	Delta_t1_LFFSSP
$\Delta t_{2\_LFFSSP}$	Delta_t2_LFFSSP
$\Delta t_{3\_LFFSSP}$	Delta_t3_LFFSSP

**Table A.1: Equivalence Table (Continued)**

$\Delta t_{1\_RFFSSP}$	Delta_t1_RFFSSP
$\Delta t_{2\_RFFSSP}$	Delta_t2_RFFSSP
$\Delta t_{3\_RFFSSP}$	Delta_t3_RFFSSP
$\Delta t_{1\_LFFDSP}$	Delta_t1_LFFDSP
$\Delta t_{2\_LFFDSP}$	Delta_t2_LFFDSP
$\Delta t_{1\_RFFDSP}$	Delta_t1_RFFDSP
$\Delta t_{2\_RFFDSP}$	Delta_t2_RFFDSP
$\widehat{W}_{LFFSSP\_P,17}$	Wp_fa_LFFSSP
$\widehat{W}_{RFFSSP\_P,17}$	Wp_fa_RFFSSP
$\widehat{W}_{LFFDSP\_P,17a}$	Wp_fa_LFFDSP
$\widehat{W}_{RFFDSP\_P,17a}$	Wp_fa_RFFDSP
$\widehat{W}_{LFFSSP\_v,17}$	Wv_fa_LFFSSP
$\widehat{W}_{RFFSSP\_v,17}$	Wv_fa_RFFSSP
$\widehat{W}_{LFFDSP\_v,17a}$	Wv_fa_LFFDSP
$\widehat{W}_{RFFDSP\_v,17a}$	Wv_fa_RFFDSP
$\widehat{W}_{LFFSSP\_qL\_Hrdd}$	Wa_a_LFFSSP
$\widehat{W}_{RFFSSP\_qR\_Hrdd}$	Wa_a_RFFSSP
$\widehat{W}_{LFFDSP\_qL\_Hrdd}$	Wa_a_LFFDSP
$\widehat{W}_{RFFDSP\_qR\_Hrdd}$	Wa_a_RFFDSP
$\widehat{W}_{LFFSSP\_P,tpR}$	Wp_fb_LFFSSP
$\widehat{W}_{RFFSSP\_P,tpL}$	Wp_fb_RFFSSP
$\widehat{W}_{LFFDSP\_P,17b}$	Wp_fb_LFFDSP
$\widehat{W}_{RFFDSP\_P,17b}$	Wp_fb_RFFDSP
$\widehat{W}_{LFFSSP\_v,1}$	Wv_fb_LFFSSP
$\widehat{W}_{RFFSSP\_v,2}$	Wv_fb_RFFSSP
$\widehat{W}_{LFFDSP\_v,17b}$	Wv_fb_LFFDSP
$\widehat{W}_{RFFDSP\_v,17b}$	Wv_fb_RFFDSP
$\widehat{W}_{LFFSSP\_qR\_Hdd}$	Wa_b_LFFSSP
$\widehat{W}_{RFFSSP\_qL\_Hdd}$	Wa_b_RFFSSP
$\widehat{W}_{LFFDSP\_qR\_Hdd}$	Wa_b_LFFDSP
$\widehat{W}_{RFFDSP\_qL\_Hdd}$	Wa_b_RFFDSP
$\widehat{W}_{LFFSSP\_OR,17}$	Wor_fa_LFFSSP
$\widehat{W}_{RFFSSP\_OR,17}$	Wor_fa_RFFSSP
$\widehat{W}_{LFFDSP\_OR,17a}$	Wor_fa_LFFDSP
$\widehat{W}_{RFFDSP\_OR,17a}$	Wor_fa_RFFDSP
$\widehat{W}_{LFFSSP\_OR,1}$	Wor_fb_LFFSSP
$\widehat{W}_{RFFSSP\_OR,2}$	Wor_fb_RFFSSP
$\widehat{W}_{LFFDSP\_OR,17b}$	Wor_fb_LFFDSP
$\widehat{W}_{RFFDSP\_OR,17b}$	Wor_fb_RFFDSP
$W_{P,\theta_3}$	Wp_Tetha3_LFFSSP
$W_{V,\theta_3}$	Wv_Tetha3_LFFSSP
$W_{P,\theta_4}$	Wp_Tetha4_RFFSSP
$W_{V,\theta_4}$	Wv_Tetha4_RFFSSP

**Table A.1: Equivalence Table (Continued)**

$\widehat{W}_{act\_LFFDSP}$	Wact_LFFDSP
$\widehat{W}_{act\_RFFDSP}$	Wact_RFFDSP
$\widehat{W}_{LFFSSP\_qL\_Hr}$	WqL_H_LFFSSP
$\widehat{W}_{LFFSSP\_qR\_H}$	WqH_R_LFFSSP
$\widehat{W}_{RFFSSP\_qR\_Hr}$	WqR_H_RFFSSP
$\widehat{W}_{RFFSSP\_qL\_H}$	WqH_L_RFFSSP
$\widehat{W}_{LFFDSP\_qL\_Hr}$	WqL_H_LFFDSP
$\widehat{W}_{LFFDSP\_qR\_H}$	WqR_H_LFFDSP
$\widehat{W}_{RFFDSP\_qR\_Hr}$	WqR_H_RFFDSP
$\widehat{W}_{RFFDSP\_qL\_H}$	WqL_H_RFFDSP
$W_{P,\theta_{18}}$	WpTetha18
$W_{P,\theta_{19}}$	WpTetha19
$W_{P,\theta_{20}}$	WpTetha20
$W_{P,\theta_{21}}$	WpTetha21
$W_{P,\theta_{22}}$	WpTetha22
$W_{P,\theta_{23}}$	WpTetha23
$W_{P,\theta_{24}}$	WpTetha24
$W_{P,\theta_{25}}$	WpTetha25
$W_{P,\theta_{26}}$	WpTetha26
$W_{P,\theta_{27}}$	WpTetha27
$W_{V,\theta_{18}}$	WvTetha18
$W_{V,\theta_{19}}$	WvTetha19
$W_{V,\theta_{20}}$	WvTetha20
$W_{V,\theta_{21}}$	WvTetha21
$W_{V,\theta_{22}}$	WvTetha22
$W_{V,\theta_{23}}$	WvTetha23
$W_{V,\theta_{24}}$	WvTetha24
$W_{V,\theta_{25}}$	WvTetha25
$W_{V,\theta_{26}}$	WvTetha26
$W_{V,\theta_{27}}$	WvTetha27
$\Delta t_{18}$	Delta_t18
$\Delta t_{19}$	Delta_t19
$\Delta t_{20}$	Delta_t20
$\Delta t_{21}$	Delta_t21
$\Delta t_{22}$	Delta_t22
$\Delta t_{23}$	Delta_t23
$\Delta t_{24}$	Delta_t24
$\Delta t_{25}$	Delta_t25
$\Delta t_{26}$	Delta_t26
$\Delta t_{27}$	Delta_t27
$\widehat{W}_{adj,LFFSSP\_RFFDSP}$	Wadj_qdot_LFFSSP_to_RFFDSP
$\widehat{W}_{adj,RFFSSP\_LFFDSP}$	Wadj_qdot_RFFSSP_to_LFFDSP

**Table A.1: Equivalence Table (Continued)**

$\bar{P}_{c,1}$	Pc_1
$\bar{P}_{c,2}$	Pc_2
$\bar{P}_{c,3}$	Pc_3
$\bar{P}_{c,4}$	Pc_4
$\bar{P}_{c,9}$	Pc_9
$\bar{P}_{c,10}$	Pc_10
$\bar{P}_{c,11}$	Pc_11
$\bar{P}_{c,12}$	Pc_12
$\bar{P}_{c,17}$	Pc_17
$\bar{P}_{c,20}$	Pc_20
$\bar{P}_{c,23}$	Pc_23
$\bar{P}_{c,24}$	Pc_24
$\bar{P}_{c,27}$	Pc_27
$\bar{V}_{c,1}$	Vc_1
$\bar{V}_{c,2}$	Vc_2
$\bar{V}_{c,3}$	Vc_3
$\bar{V}_{c,4}$	Vc_4
$\bar{V}_{c,9}$	Vc_9
$\bar{V}_{c,10}$	Vc_10
$\bar{V}_{c,11}$	Vc_11
$\bar{V}_{c,12}$	Vc_12
$\bar{V}_{c,17}$	Vc_17
$\bar{V}_{c,20}$	Vc_20
$\bar{V}_{c,23}$	Vc_23
$\bar{V}_{c,24}$	Vc_24
$\bar{V}_{c,27}$	Vc_27
$\bar{w}_1$	w1
$\bar{w}_2$	w2
$\bar{w}_3$	w3
$\bar{w}_4$	w4
$\bar{w}_9$	w9
$\bar{w}_{10}$	w10
$\bar{w}_{11}$	w11
$\bar{w}_{12}$	w12
$\bar{w}_{17}$	w17
$\bar{w}_{20}$	w20
$\bar{w}_{23}$	w23
$\bar{w}_{24}$	w24
$\bar{w}_{27}$	w27
$\bar{a}_{c,1}$	ac_1
$\bar{a}_{c,2}$	ac_2
$\bar{a}_{c,3}$	ac_3
$\bar{a}_{c,4}$	ac_4
$\bar{a}_{c,9}$	ac_9

**Table A.1: Equivalence Table (Continued)**

$\bar{a}_{c,10}$	ac_10
$\bar{a}_{c,11}$	ac_11
$\bar{a}_{c,12}$	ac_12
$\bar{a}_{c,17}$	ac_17
$\bar{a}_{c,20}$	ac_20
$\bar{a}_{c,23}$	ac_23
$\bar{a}_{c,24}$	ac_24
$\bar{a}_{c,27}$	ac_27
$\bar{\alpha}_1$	Alpha1
$\bar{\alpha}_2$	Alpha2
$\bar{\alpha}_3$	Alpha3
$\bar{\alpha}_4$	Alpha4
$\bar{\alpha}_9$	Alpha9
$\bar{\alpha}_{10}$	Alpha10
$\bar{\alpha}_{11}$	Alpha11
$\bar{\alpha}_{12}$	Alpha12
$\bar{\alpha}_{17}$	Alpha17
$\bar{\alpha}_{20}$	Alpha20
$\bar{\alpha}_{23}$	Alpha23
$\bar{\alpha}_{24}$	Alpha24
$\bar{\alpha}_{27}$	Alpha27
$\hat{C}^{(0,1)}$	C0_1
$\hat{C}^{(0,2)}$	C0_2
$\hat{C}^{(0,3)}$	C0_3
$\hat{C}^{(0,4)}$	C0_4
$\hat{C}^{(0,9)}$	C0_9
$\hat{C}^{(0,10)}$	C0_10
$\hat{C}^{(0,11)}$	C0_11
$\hat{C}^{(0,12)}$	C0_12
$\hat{C}^{(0,17)}$	C0_17
$\hat{C}^{(0,20)}$	C0_20
$\hat{C}^{(0,23)}$	C0_23
$\hat{C}^{(0,24)}$	C0_24
$\hat{C}^{(0,27)}$	C0_27
$\hat{J}_{v,tpR}$	JvTPRF
$\dot{\hat{J}}_{v,tpR}$	JvTPRFdot
$\hat{J}_{v,17_fL}$	Jv17fL
$\dot{\hat{J}}_{v,17_fL}$	Jv17fLdot
$\hat{J}_{v,cdiag0_17_fL}$	JvCdiag0_17fL
$\dot{\hat{J}}_{v,cdiag0_17_fL}$	JvCdiag0_17fLdot
$\hat{J}_{v,cdiag0_1}$	JvCdiag0_1
$\dot{\hat{J}}_{v,cdiag0_1}$	JvCdiag0_1dot
$\hat{J}_{v,tpL}$	JvTPLF
$\dot{\hat{J}}_{v,tpL}$	JvTPLFdot

**Table A.1: Equivalence Table (Continued)**

$\hat{J}_{v,17\_fR}$	Jv17fR
$\dot{\hat{J}}_{v,17\_fR}$	Jv17fRdot
$\hat{J}_{v,Cdiag0\_17\_fR}$	JvCdiag0_17fR
$\dot{\hat{J}}_{v,Cdiag0\_17\_fR}$	JvCdiag0_17fRdot
$\hat{J}_{v,Cdiag0\_2}$	JvCdiag0_2
$\dot{\hat{J}}_{v,Cdiag0\_2}$	JvCdiag0_2dot
$\hat{J}_{v,17\_fR\_all}$	Jv17fR_all
$\dot{\hat{J}}_{v,17\_fR\_all}$	Jv17fR_alldot
$\hat{J}_{v,Cdiag0\_17\_fR\_all}$	JvCdiag0_17fR_all
$\dot{\hat{J}}_{v,Cdiag0\_17\_fR\_all}$	JvCdiag0_17fR_alldot
$\hat{J}_{v,17\_fL\_all}$	Jv17fL_all
$\dot{\hat{J}}_{v,17\_fL\_all}$	Jv17fL_alldot
$\hat{J}_{v,Cdiag0\_17\_fL\_all}$	JvCdiag0_17fL_all
$\dot{\hat{J}}_{v,Cdiag0\_17\_fL\_all}$	JvCdiag0_17fL_alldot
$\bar{F}_{0,1}^{(1)}$	F0_1
$\bar{F}_{1,3}^{(3)}$	F1_3
$\bar{M}_{0,1}^{(1)}$	M0_1
$\bar{M}_{1,3}^{(3)}$	M1_3
$\bar{F}_{0,3}^{(3)}$	F0_3
$\bar{F}_{3,9}^{(9)}$	F3_9
$\bar{M}_{0,3}^{(3)}$	M0_3
$\bar{M}_{3,9}^{(9)}$	M3_9
$\bar{F}_{9,11}^{(11)}$	F9_11
$\bar{M}_{9,11}^{(11)}$	M9_11
$\bar{F}_{11,17}^{(17)}$	F11_17
$\bar{M}_{11,17}^{(17)}$	M11_17
$\bar{F}_{12,17}^{(17)}$	F12_17
$\bar{F}_{17,20}^{(20)}$	F17_20
$\bar{M}_{12,17}^{(17)}$	M12_17
$M_{17,20}^{(20)}$	M17_20
$\bar{F}_{10,12}^{(12)}$	F10_12
$\bar{M}_{10,12}^{(12)}$	M10_12
$\bar{F}_{4,10}^{(10)}$	F4_10
$\bar{M}_{4,10}^{(10)}$	M4_10
$\bar{F}_{0,4}^{(4)}$	F0_4
$\bar{F}_{2,4}^{(4)}$	F2_4
$\bar{M}_{0,4}^{(4)}$	M0_4
$\bar{M}_{2,4}^{(4)}$	M2_4

**Table A.1: Equivalence Table (Continued)**

$\bar{F}_{0,2}^{(2)}$	F0_2
$\bar{M}_{0,2}^{(2)}$	M0_2
$\bar{F}_{20,23}^{(23)}$	F20_23
$\bar{F}_{20,24}^{(24)}$	F20_24
$\bar{F}_{20,27}^{(27)}$	F20_27
$\bar{M}_{20,23}^{(23)}$	M20_23
$\bar{M}_{20,24}^{(24)}$	M20_24
$\bar{M}_{20,27}^{(27)}$	M20_27

## APPENDIX B

### SIMULATION PARAMATERS

#### B.1. Simulation Number 1

$$\begin{matrix}
 & \begin{bmatrix} 0.0000 & 0.0000 & 0.9588 \\ 0.1000 & 0.1300 & 0.9588 \\ 0.1800 & 0.2500 & 0.9588 \\ 0.2800 & 0.3500 & 0.9588 \\ 0.4000 & 0.4200 & 0.9588 \\ 0.5300 & 0.4700 & 0.9588 \\ 0.6800 & 0.5200 & 0.9588 \\ 0.8400 & 0.5400 & 0.9588 \\ 0.9900 & 0.5450 & 0.9588 \end{bmatrix} & \text{(m)}, & \begin{matrix} V_{hip} = \begin{bmatrix} 0.00 \\ 0.20 \\ 0.25 \\ 0.25 \\ 0.25 \\ 0.30 \\ 0.30 \\ 0.35 \\ 0.35 \\ 0.40 \\ 0.40 \\ 0.40 \\ 0.40 \\ 0.40 \\ 0.40 \\ 0.40 \\ 0.40 \\ 0.40 \end{bmatrix} & \text{(m/s), PHASE\_N=1}
 \end{matrix}
 \end{matrix}$$

$$Radius = [1.600 \quad 1.200 \quad 1.100 \quad 0.865 \quad 1.100 \quad 1.500 \quad 1.100 \quad 1.200]^T \text{ (m)}$$

$$TurningDir = [+1 \quad -1 \quad -1 \quad -1 \quad -1 \quad -1 \quad -1 \quad -1]^T$$

$$tSSP = [0.8 \quad 0.9 \quad 0.8 \quad 0.7 \quad 0.6 \quad 0.7 \quad 0.7 \quad 0.7]^T \text{ (s)}$$

$$PTR = [6 \quad 6 \quad 6 \quad 6 \quad 6 \quad 6 \quad 6 \quad 6]^T$$

$$SW = [0.32 \quad 0.40 \quad 0.32 \quad 0.32 \quad 0.32 \quad 0.28 \quad 0.32 \quad 0.32]^T \text{ (m)}$$

$$SH = [0.06 \quad 0.08 \quad 0.08 \quad 0.06 \quad 0.08 \quad 0.08 \quad 0.08 \quad 0.08]^T \text{ (m)}$$

$$kAdj = [1.1 \quad 1.1 \quad 1.1 \quad 1.1 \quad 1.1 \quad 1.1 \quad 1.1 \quad 1.1]^T$$

$$kSH = [0.5 \quad 0.5 \quad 0.5 \quad 0.5 \quad 0.5 \quad 0.5 \quad 0.5 \quad 0.5]^T$$



$$Wv\_fa\_LFFDSP = \begin{bmatrix} 100 \\ 100 \\ 100 \\ 100 \\ 100 \\ 100 \end{bmatrix}, Wv\_fa\_RFFDSP = \begin{bmatrix} 100 \\ 100 \\ 100 \\ 100 \\ 100 \\ 100 \end{bmatrix}$$

$$Wa\_a\_LFFSSP = \begin{bmatrix} 0.1 \\ 1.2 \\ 0.9 \\ 0.7 \\ 0.3 \\ 0.4 \\ 0.5 \end{bmatrix}, Wa\_a\_RFFSSP = \begin{bmatrix} 0.1 \\ 0.8 \\ 0.9 \\ 0.5 \\ 0.3 \\ 0.4 \\ 0.8 \end{bmatrix}$$

$$Wa\_a\_LFFDSP = \begin{bmatrix} 0.1 \\ 0.3 \\ 0.3 \\ 0.5 \\ 0.4 \\ 0.4 \\ 0.8 \end{bmatrix}, Wa\_a\_RFFDSP = \begin{bmatrix} 0.1 \\ 0.3 \\ 0.3 \\ 0.5 \\ 0.4 \\ 0.4 \\ 0.8 \end{bmatrix}$$

$$Wp\_fb\_LFFSSP = \begin{bmatrix} 2000 \\ 2000 \\ 100000 \end{bmatrix}, Wp\_fb\_RFFSSP = \begin{bmatrix} 10000 \\ 10000 \\ 1000000 \end{bmatrix}$$

$$Wp\_fb\_LFFDSP = \begin{bmatrix} 1000 \\ 1000 \\ 30000 \end{bmatrix}, Wp\_fb\_RFFDSP = \begin{bmatrix} 100 \\ 100 \\ 10000 \end{bmatrix}$$

$$Wv\_fb\_LFFSSP = \begin{bmatrix} 10000 \\ 10000 \\ 100000 \\ 5000 \\ 5000 \\ 5000 \end{bmatrix}, Wv\_fb\_RFFSSP = \begin{bmatrix} 40000 \\ 40000 \\ 200000 \\ 5000 \\ 5000 \\ 5000 \end{bmatrix}$$

$$Wv\_fb\_LFFDSP = \begin{bmatrix} 100 \\ 100 \\ 100 \\ 100 \\ 100 \\ 100 \end{bmatrix}, Wv\_fb\_RFFDSP = \begin{bmatrix} 100 \\ 100 \\ 100 \\ 100 \\ 100 \\ 100 \end{bmatrix}$$

$$Wa\_b\_LFFSSP = \begin{bmatrix} 1 \\ 0.1 \\ 1.2 \\ 0.9 \\ 0.3 \\ 0.4 \\ 0.5 \\ 0.5 \end{bmatrix}, Wa\_b\_RFFSSP = \begin{bmatrix} 1 \\ 0.1 \\ 0.8 \\ 0.9 \\ 0.3 \\ 0.4 \\ 0.5 \\ 0.9 \end{bmatrix}$$

$$Wa\_b\_LFFDSP = \begin{bmatrix} 0.05 \\ 0.1 \\ 0.3 \\ 0.3 \\ 0.8 \\ 0.6 \\ 0.6 \\ 1 \end{bmatrix}, Wa\_b\_RFFDSP = \begin{bmatrix} 0.01 \\ 0.1 \\ 0.3 \\ 0.3 \\ 0.8 \\ 0.6 \\ 0.6 \\ 1 \end{bmatrix}$$

$$Wor\_fa\_LFFSSP = \begin{bmatrix} 10000 \\ 10000 \\ 10000 \end{bmatrix}, Wor\_fa\_RFFSSP = \begin{bmatrix} 200000 \\ 200000 \\ 200000 \end{bmatrix}$$

$$Wor\_fa\_LFFDSP = \begin{bmatrix} 1000 \\ 1000 \\ 1000 \end{bmatrix}, Wor\_fa\_RFFDSP = \begin{bmatrix} 5000 \\ 5000 \\ 5000 \end{bmatrix}$$

$$Wor\_fb\_LFFSSP = \begin{bmatrix} 8000 \\ 8000 \\ 8000 \end{bmatrix}, Wor\_fb\_RFFSSP = \begin{bmatrix} 100000 \\ 100000 \\ 100000 \end{bmatrix}$$

$$Wor\_fb\_LFFDSP = \begin{bmatrix} 1000 \\ 1000 \\ 1000 \end{bmatrix}, Wor\_fb\_RFFDSP = \begin{bmatrix} 3000 \\ 3000 \\ 3000 \end{bmatrix}$$

$$Wp\_Tetha3\_LFFSSP = 1000000, Wp\_Tetha4\_RFFSSP = 100000$$

$$Wv\_Tetha3\_LFFSSP = 100000, Wv\_Tetha4\_RFFSSP = 40000$$

$$Wact\_LFFDSP = Wact\_RFFDSP = [1 \ 1 \ 1 \ 1 \ 1 \ 1 \ 1 \ 1 \ 1 \ 1 \ 1000 \ 1 \ 1 \ 1 \ 1 \ 1 \ 1 \ 1 \ 1 \ 1 \ 1 \ 1 \ 1000 \ 1000 \ 1000 \ 1 \ 1 \ 1 \ 1 \ 1000 \ 1000 \ 1000 \ 1000 \ 1 \ 1 \ 1 \ 1 \ 1 \ 1 \ 1000 \ 1000 \ 1000 \ 1 \ 1 \ 1 \ 1 \ 1 \ 1 \ 1 \ 1 \ 1 \ 1 \ 1000 \ 1 \ 1 \ 1 \ 1 \ 1 \ 1 \ 1 \ 1 \ 1 \ 1 \ 1000 \ 1000 \ 1 \ 1000 \ 1000 \ 1 \ 1000 \ 1000 \ 1000]^T$$

$$\begin{aligned}
WqL\_H\_LFFSSP &= \begin{bmatrix} 0.1 \\ 30000 \\ 1 \\ 1000 \\ 0.2 \\ 0.4 \\ 0.6 \end{bmatrix}, WqR\_H\_RFFSSP = \begin{bmatrix} 0.1 \\ 30000 \\ 1 \\ 1000 \\ 0.2 \\ 0.4 \\ 0.6 \end{bmatrix} \\
WqL\_H\_LFFDSP &= \begin{bmatrix} 0.2 \\ 0.8 \\ 1 \\ 0.3 \\ 0.4 \\ 0.5 \\ 1 \end{bmatrix}, WqR\_H\_RFFDSP = \begin{bmatrix} 0.2 \\ 0.8 \\ 1 \\ 0.3 \\ 0.4 \\ 0.5 \\ 1 \end{bmatrix} \\
WqH\_R\_LFFSSP &= \begin{bmatrix} 0.05 \\ 0.1 \\ 25000 \\ 1 \\ 1000 \\ 0.2 \\ 0.4 \\ 0.8 \end{bmatrix}, WqH\_L\_RFFSSP = \begin{bmatrix} 0.05 \\ 0.1 \\ 25000 \\ 1 \\ 1000 \\ 0.2 \\ 0.4 \\ 0.8 \end{bmatrix} \\
WqR\_H\_LFFDSP &= \begin{bmatrix} 8000 \\ 0.4 \\ 0.8 \\ 1 \\ 0.5 \\ 0.3 \\ 0.5 \\ 0.8 \end{bmatrix}, WqL\_H\_RFFDSP = \begin{bmatrix} 100 \\ 0.4 \\ 0.8 \\ 1 \\ 0.5 \\ 0.3 \\ 0.5 \\ 0.8 \end{bmatrix}
\end{aligned}$$

$$WpTetha18 = 300, WvTetha18 = 120, Delta\_t18 = 0.3 \text{ (s)}$$

$$WpTetha19 = 200, WvTetha19 = 60, Delta\_t19 = 0.3 \text{ (s)}$$

$$WpTetha20 = 200, WvTetha20 = 60, Delta\_t20 = 0.3 \text{ (s)}$$

$$WpTetha21 = 10, WvTetha21 = 100, Delta\_t21 = 0.3 \text{ (s)}$$

$$WpTetha22 = 10, WvTetha22 = 100, Delta\_t22 = 0.3 \text{ (s)}$$

$$WpTetha23 = 10, WvTetha23 = 100, Delta\_t23 = 0.3 \text{ (s)}$$

$$WpTetha24 = 10, WvTetha24 = 100, Delta\_t24 = 0.3 \text{ (s)}$$

$$WpTetha25 = 10, WvTetha25 = 100, Delta\_t25 = 0.3 \text{ (s)}$$

$$WpTetha26 = 10, WvTetha26 = 100, Delta\_t26 = 0.3 \text{ (s)}$$

$$WpTetha27 = 10, WvTetha27 = 100, Delta\_t27 = 0.3 \text{ (s)}$$

$$Wadj\_qdot\_LFFSSP\_to\_RFFDSP$$

$$= [1 \ 1 \ 1 \ 3 \ 1.8 \ 1.8 \ 1.8 \ 1 \ 1 \ 1 \ 3 \ 1.8 \ 1.8 \ 1.8]^T$$

$$Wadj\_qdot\_LFFSSP\_to\_RFFDSP =$$

$$[1 \ 1 \ 1 \ 3 \ 1.8 \ 1.8 \ 1.8 \ 1 \ 1 \ 1 \ 3 \ 1.8 \ 1.8 \ 1.8]^T$$

$$Saturation = [-30,30](N.m), Saturation1 = [-150,150](N.m)$$

$$Saturation2 = [-150,150](N.m), Saturation3 = [-150,150](N.m)$$

$$Saturation4 = [-150,150](N.m), Saturation5 = [-150,150](N.m)$$

$$Saturation6 = [-150,150](N.m), Saturation7 = [-150,150](N.m)$$

*Saturation8* = [-30,30](*N.m*), *Saturation9* = [-150,150](*N.m*)  
*Saturation10* = [-150,150](*N.m*), *Saturation11* = [-150,150](*N.m*)  
*Saturation12* = [-150,150](*N.m*), *Saturation13* = [-150,150](*N.m*)  
*Saturation14* = [-150,150](*N.m*), *Saturation15* = [-150,150](*N.m*)  
*Saturation16* = [-180,180](*N.m*), *Saturation17* = [-180,180](*N.m*)  
*Saturation18* = [-180,180](*N.m*), *Saturation19* = [-100,100](*N.m*)  
*Saturation20* = [-100,100](*N.m*), *Saturation21* = [-100,100](*N.m*)  
*Saturation22* = [-100,100](*N.m*), *Saturation23* = [-100,100](*N.m*)  
*Saturation24* = [-100,100](*N.m*), *Saturation25* = [-100,100](*N.m*)

$$Pc\_1 = \begin{bmatrix} 0.1600 \\ 0.1505 \\ 0.0150 \end{bmatrix} \text{ (m), } Vc\_1 = w1 = ac\_1 = Alpha1 = \bar{0}_{3 \times 1} \text{ (m/s, rad/s, m/s}^2\text{, rad/s}^2\text{)}$$

$$Pc\_2 = \begin{bmatrix} -0.160 \\ 0.1505 \\ 0.0150 \end{bmatrix} \text{ (m), } Vc\_2 = w2 = ac\_2 = Alpha2 = \bar{0}_{3 \times 1} \text{ (m/s, rad/s, m/s}^2\text{, rad/s}^2\text{)}$$

$$Pc\_3 = \begin{bmatrix} 0.1600 \\ 0.0286 \\ 0.0351 \end{bmatrix} \text{ (m), } Vc\_3 = w3 = ac\_3 = Alpha3 = \bar{0}_{3 \times 1} \text{ (m/s, rad/s, m/s}^2\text{, rad/s}^2\text{)}$$

$$Pc\_4 = \begin{bmatrix} -0.1600 \\ 0.0286 \\ 0.0351 \end{bmatrix} \text{ (m), } Vc\_4 = w4 = ac\_4 = Alpha4 = \bar{0}_{3 \times 1} \text{ (m/s, rad/s, m/s}^2\text{, rad/s}^2\text{)}$$

$$Pc\_9 = \begin{bmatrix} 0.1600 \\ 0.0000 \\ 0.2487 \end{bmatrix} \text{ (m), } Vc\_9 = w9 = ac\_9 = Alpha9 = \bar{0}_{3 \times 1} \text{ (m/s, rad/s, m/s}^2\text{, rad/s}^2\text{)}$$

$$Pc\_10 = \begin{bmatrix} -0.1600 \\ 0.0000 \\ 0.2487 \end{bmatrix} \text{ (m), } Vc\_10 = w10 = ac\_10 = Alpha10 = \bar{0}_{3 \times 1} \text{ (m/s, rad/s, m/s}^2\text{, rad/s}^2\text{)}$$

$$Pc\_11 = \begin{bmatrix} 0.1600 \\ 0.0000 \\ 0.6212 \end{bmatrix} \text{ (m), } Vc\_11 = w11 = ac\_11 = Alpha1 = \bar{0}_{3 \times 1} \text{ (m/s, rad/s, m/s}^2\text{, rad/s}^2\text{)}$$

$$Pc\_12 = \begin{bmatrix} -0.1600 \\ 0.0000 \\ 0.6212 \end{bmatrix} \text{ (m), } Vc\_12 = w12 = ac\_12 = Alpha12 = \bar{0}_{3 \times 1} \text{ (m/s, rad/s, m/s}^2\text{, rad/s}^2\text{)}$$

$$Pc\_17 = \begin{bmatrix} 0.0000 \\ 0.0000 \\ 0.9588 \end{bmatrix} \text{ (m), } Vc\_17 = w17 = ac\_17 = Alpha17 = \bar{0}_{3 \times 1} \text{ (m/s, rad/s, m/s}^2\text{, rad/s}^2\text{)}$$

$$Pc\_20 = \begin{bmatrix} 0.0000 \\ 0.0000 \\ 1.2524 \end{bmatrix} \text{ (m), } Vc\_20 = w20 = ac\_20 = Alpha20 = \bar{0}_{3 \times 1} \text{ (m/s, rad/s, m/s}^2\text{, rad/s}^2\text{)}$$

$$Pc_{23} = \begin{bmatrix} 0.2900 \\ 0.0000 \\ 1.0452 \end{bmatrix} \text{ (m), } Vc_{23} = w_{23} = ac_{23} = Alpha_{23} = \bar{0}_{3 \times 1} \text{ (m/s, rad/s, m/s}^2, \text{ rad/s}^2)$$

$$Pc_{24} = \begin{bmatrix} -0.2900 \\ 0.0000 \\ 1.0452 \end{bmatrix} \text{ (m), } Vc_{24} = w_{24} = ac_{24} = Alpha_{24} = \bar{0}_{3 \times 1} \text{ (m/s, rad/s, m/s}^2, \text{ rad/s}^2)$$

$$Pc_{27} = \begin{bmatrix} 0.0000 \\ 0.0000 \\ 1.4997 \end{bmatrix} \text{ (m), } Vc_{27} = w_{27} = ac_{27} = Alpha_{27} = \bar{0}_{3 \times 1} \text{ (m/s, rad/s, m/s}^2, \text{ rad/s}^2)$$

$$C0_{1} = C0_{2} = \dots = C0_{27} = \begin{bmatrix} 0 & -1 & 0 \\ 1 & 0 & 0 \\ 0 & 0 & 1 \end{bmatrix}$$

$$L1 = L2 = 0.0743 \text{ (m), } C1 = C2 = 0.0372 \text{ (m), } L3x = L4x = 0.1133 \text{ (m)}$$

$$L3z = L4z = 0.0630 \text{ (m), } C3x = C4x = 0.2860 \text{ (m), } C3z = C4z = 0.4290 \text{ (m)}$$

$$L9 = L10 = 0.3220 \text{ (m), } C9 = C10 = 0.1513 \text{ (m), } L11 = L12 = 0.4120 \text{ (m)}$$

$$C11 = C12 = 0.1908 \text{ (m), } L17y = 0.1600 \text{ (m), } L17z = 0.2936 \text{ (m)}$$

$$C17 = 0.1468 \text{ (m), } L20y = 0.2400 \text{ (m), } L20z = 0.2936 \text{ (m), } C20 = 0.1468 \text{ (m)}$$

$$L27 = 0.2010 \text{ (m), } C27 = 0.1005 \text{ (m), } L23y = L24y = 0.050 \text{ (m)}$$

$$L23z = L24z = 0.7080 \text{ (m), } C23 = C24 = 0.3540 \text{ (m)}$$

$$m1 = m2 = 0.130 \text{ (kg), } m3 = m4 = 0.521 \text{ (kg), } m9 = m10 = 1.979 \text{ (kg)}$$

$$m11 = m12 = 5.213 \text{ (kg), } m17 = m20 = 14.674 \text{ (kg), } m23 = m24 = 2.651 \text{ (kg)}$$

$$m27 = 4.708 \text{ (kg)}$$

$$Jc_{1} = Jc_{2} = \begin{bmatrix} 0.00007 & 0.00000 & 0.00000 \\ 0.00000 & 0.00007 & 0.00000 \\ 0.00000 & 0.00000 & 0.00012 \end{bmatrix} \text{ (kg.m}^2)$$

$$Jc_{3} = Jc_{4} = \begin{bmatrix} 0.00048 & 0.00000 & 0.00012 \\ 0.00000 & 0.00100 & 0.00000 \\ 0.00012 & 0.00000 & 0.00100 \end{bmatrix} \text{ (kg.m}^2)$$

$$Jc_{9} = Jc_{10} = \begin{bmatrix} 0.01800 & 0.00000 & 0.00000 \\ 0.00000 & 0.01800 & 0.00000 \\ 0.00000 & 0.00000 & 0.00300 \end{bmatrix} \text{ (kg.m}^2)$$

$$Jc_{11} = Jc_{12} = \begin{bmatrix} 0.07900 & 0.00000 & 0.00000 \\ 0.00000 & 0.07900 & 0.00000 \\ 0.00000 & 0.00000 & 0.01200 \end{bmatrix} \text{ (kg.m}^2)$$

$$Jc_{17} = Jc_{20} = \begin{bmatrix} 0.35300 & 0.00000 & 0.00000 \\ 0.00000 & 0.13500 & 0.00000 \\ 0.00000 & 0.00000 & 0.27700 \end{bmatrix} \text{ (kg.m}^2)$$

$$Jc_{23} = Jc_{24} = \begin{bmatrix} 0.11200 & 0.00000 & 0.00000 \\ 0.00000 & 0.11200 & 0.00000 \\ 0.00000 & 0.00000 & 0.00300 \end{bmatrix} \text{ (kg.m}^2)$$

$$Jc_{27} = \begin{bmatrix} 0.02300 & 0.00000 & 0.00000 \\ 0.00000 & 0.02300 & 0.00000 \\ 0.00000 & 0.00000 & 0.01500 \end{bmatrix} \text{ (kg.m}^2)$$



$$kSH = [0.5 \ 0.5 \ 0.5 \ 0.5 \ 0.5 \ 0.5 \ 0.5 \ 0.5 \ 0.5 \ 0.5 \ 0.5 \ 0.5]^T$$

$$DeltaTethaPLN =$$

$$\left[ \frac{7.5 \times \pi}{180} \ \frac{7.5 \times \pi}{180} \ \frac{7.5 \times \pi}{180} \ \frac{7.5 \times \pi}{180} \ \frac{7.5 \times \pi}{180} \ \frac{7.5 \times \pi}{180} \ \frac{7.5 \times \pi}{180} \ \frac{7.5 \times \pi}{180} \ \frac{7.5 \times \pi}{180} \ \frac{7.5 \times \pi}{180} \ \frac{7.5 \times \pi}{180} \ \frac{7.5 \times \pi}{180} \right]^T$$

(rad)

$$DeltaTethaADJ =$$

$$\left[ -\frac{6 \times \pi}{180} \ -\frac{6 \times \pi}{180} \ -\frac{6 \times \pi}{180} \ -\frac{6 \times \pi}{180} \ -\frac{6 \times \pi}{180} \ -\frac{6 \times \pi}{180} \ -\frac{6 \times \pi}{180} \ -\frac{6 \times \pi}{180} \ -\frac{6 \times \pi}{180} \ -\frac{6 \times \pi}{180} \ -\frac{6 \times \pi}{180} \ -\frac{6 \times \pi}{180} \right]^T$$

(rad)

$$PRi = TPRF = [0.1600 \ 0.1876 \ 0.0150] \text{ (m)}, TPRFd = TPRFdd = \bar{0}_{3 \times 1} \text{ (m)}$$

$$PLi = TPLF = [-0.1600 \ 0.1876 \ 0.0150] \text{ (m)}, TPLFd = TPLFdd = \bar{0}_{3 \times 1} \text{ (m)}$$

$$FR_{O_i} = \begin{bmatrix} 0 & -1 & 0 \\ 1 & 0 & 0 \\ 0 & 0 & 1 \end{bmatrix}, FL_{O_i} = \begin{bmatrix} 0 & -1 & 0 \\ 1 & 0 & 0 \\ 0 & 0 & 1 \end{bmatrix}$$

$$q = q_{initial} = qd = qd_{initial} = \bar{0}_{26 \times 1} \text{ (rad)}, g = 9.81 \text{ (m/s}^2\text{)}$$

$$qdlower_{initial\_Reset}$$

$$= [1 \ 1 \ 1 \ 1 \ 1 \ 1 \ 1 \ 1 \ 1 \ 1 \ 1 \ 1 \ 1 \ 1 \ 1 \ 1 \ 1]^T$$

$$Delta\_t1\_LFFSSP = Delta\_t1\_RFFSSP = 0.1 \text{ (s)}$$

$$Delta\_t2\_LFFSSP = Delta\_t2\_RFFSSP = Delta\_t1\_LFFDSP =$$

$$Delta\_t2\_LFFDSP = Delta\_t1\_RFFDSP = Delta\_t2\_RFFDSP = 0.05 \text{ (s)}$$

$$Delta\_t3\_LFFSSP = Delta\_t3\_RFFSSP = 0.02 \text{ (s)}$$

$$Wp\_fa\_LFFSSP = \begin{bmatrix} 1000 \\ 1000 \\ 70000 \end{bmatrix}, Wp\_fa\_RFFSSP = \begin{bmatrix} 1000 \\ 1000 \\ 70000 \end{bmatrix},$$

$$Wp\_fa\_LFFDSP = \begin{bmatrix} 10000 \\ 10000 \\ 90000 \end{bmatrix}, Wp\_fa\_RFFDSP = \begin{bmatrix} 10000 \\ 10000 \\ 90000 \end{bmatrix}$$

$$Wv\_fa\_LFFSSP = \begin{bmatrix} 600 \\ 600 \\ 1000 \\ 100 \\ 100 \\ 1000 \end{bmatrix}, Wv\_fa\_RFFSSP = \begin{bmatrix} 600 \\ 600 \\ 1000 \\ 100 \\ 100 \\ 1000 \end{bmatrix}$$

$$Wv\_fa\_LFFDSP = \begin{bmatrix} 100 \\ 100 \\ 100 \\ 100 \\ 100 \\ 100 \end{bmatrix}, Wv\_fa\_RFFDSP = \begin{bmatrix} 100 \\ 100 \\ 100 \\ 100 \\ 100 \\ 100 \end{bmatrix}$$

$$Wa\_a\_LFFSSP = \begin{bmatrix} 0.1 \\ 1.2 \\ 0.9 \\ 0.7 \\ 0.3 \\ 0.4 \\ 0.5 \end{bmatrix}, Wa\_a\_RFFSSP = \begin{bmatrix} 0.1 \\ 1.2 \\ 0.9 \\ 0.7 \\ 0.3 \\ 0.4 \\ 0.5 \end{bmatrix}$$

$$Wa\_a\_LFFDSP = \begin{bmatrix} 0.1 \\ 0.3 \\ 0.3 \\ 0.5 \\ 0.4 \\ 0.4 \\ 0.8 \end{bmatrix}, Wa\_a\_RFFDSP = \begin{bmatrix} 0.1 \\ 0.3 \\ 0.3 \\ 0.5 \\ 0.4 \\ 0.4 \\ 0.8 \end{bmatrix}$$

$$Wp\_fb\_LFFSSP = \begin{bmatrix} 2000 \\ 2000 \\ 800000 \end{bmatrix}, Wp\_fb\_RFFSSP = \begin{bmatrix} 2000 \\ 2000 \\ 800000 \end{bmatrix}$$

$$Wp\_fb\_LFFDSP = \begin{bmatrix} 1000 \\ 1000 \\ 30000 \end{bmatrix}, Wp\_fb\_RFFDSP = \begin{bmatrix} 1000 \\ 1000 \\ 30000 \end{bmatrix}$$

$$Wv\_fb\_LFFSSP = \begin{bmatrix} 10000 \\ 10000 \\ 100000 \\ 5000 \\ 5000 \\ 5000 \end{bmatrix}, Wv\_fb\_RFFSSP = \begin{bmatrix} 10000 \\ 10000 \\ 100000 \\ 5000 \\ 5000 \\ 5000 \end{bmatrix}$$

$$Wv\_fb\_LFFDSP = \begin{bmatrix} 100 \\ 100 \\ 100 \\ 100 \\ 100 \\ 100 \end{bmatrix}, Wv\_fb\_RFFDSP = \begin{bmatrix} 100 \\ 100 \\ 100 \\ 100 \\ 100 \\ 100 \end{bmatrix}$$

$$Wa\_b\_LFFSSP = \begin{bmatrix} 1 \\ 0.1 \\ 1.2 \\ 0.9 \\ 0.3 \\ 0.4 \\ 0.5 \\ 0.5 \end{bmatrix}, Wa\_b\_RFFSSP = \begin{bmatrix} 1 \\ 0.1 \\ 1.2 \\ 0.9 \\ 0.3 \\ 0.4 \\ 0.5 \\ 0.5 \end{bmatrix}$$

$$Wa\_b\_LFFDSP = \begin{bmatrix} 0.05 \\ 0.1 \\ 0.3 \\ 0.3 \\ 0.8 \\ 0.6 \\ 0.6 \\ 1 \end{bmatrix}, Wa\_b\_RFFDSP = \begin{bmatrix} 0.05 \\ 0.1 \\ 0.3 \\ 0.3 \\ 0.8 \\ 0.6 \\ 0.6 \\ 1 \end{bmatrix}$$

$$Wor\_fa\_LFFSSP = \begin{bmatrix} 10000 \\ 10000 \\ 10000 \end{bmatrix}, Wor\_fa\_RFFSSP = \begin{bmatrix} 10000 \\ 10000 \\ 10000 \end{bmatrix}$$

$$Wor\_fa\_LFFDSP = \begin{bmatrix} 5000 \\ 5000 \\ 5000 \end{bmatrix}, Wor\_fa\_RFFDSP = \begin{bmatrix} 5000 \\ 5000 \\ 5000 \end{bmatrix}$$

$$Wor\_fb\_LFFSSP = \begin{bmatrix} 8000 \\ 8000 \\ 8000 \end{bmatrix}, Wor\_fb\_RFFSSP = \begin{bmatrix} 8000 \\ 8000 \\ 8000 \end{bmatrix}$$

$$Wor\_fb\_LFFDSP = \begin{bmatrix} 1000 \\ 1000 \\ 1000 \end{bmatrix}, Wor\_fb\_RFFDSP = \begin{bmatrix} 1000 \\ 1000 \\ 1000 \end{bmatrix}$$

$$Wp\_Tetha3\_LFFSSP = 100000, Wp\_Tetha4\_RFFSSP = 100000$$

$$Wv\_Tetha3\_LFFSSP = 40000, Wv\_Tetha4\_RFFSSP = 40000$$



*Saturation* = [-30,30](N.m), *Saturation1* = [-150,150](N.m)  
*Saturation2* = [-150,150](N.m), *Saturation3* = [-150,150](N.m)  
*Saturation4* = [-150,150](N.m), *Saturation5* = [-150,150](N.m)  
*Saturation6* = [-150,150](N.m), *Saturation7* = [-150,150](N.m)  
*Saturation8* = [-30,30](N.m), *Saturation9* = [-150,150](N.m)  
*Saturation10* = [-150,150](N.m), *Saturation11* = [-150,150](N.m)  
*Saturation12* = [-150,150](N.m), *Saturation13* = [-150,150](N.m)  
*Saturation14* = [-150,150](N.m), *Saturation15* = [-150,150](N.m)  
*Saturation16* = [-180,180](N.m), *Saturation17* = [-180,180](N.m)  
*Saturation18* = [-180,180](N.m), *Saturation19* = [-100,100](N.m)  
*Saturation20* = [-100,100](N.m), *Saturation21* = [-100,100](N.m)  
*Saturation22* = [-100,100](N.m), *Saturation23* = [-100,100](N.m)  
*Saturation24* = [-100,100](N.m), *Saturation25* = [-100,100](N.m)

$$Pc\_1 = \begin{bmatrix} 0.1600 \\ 0.1505 \\ 0.0150 \end{bmatrix} \text{ (m), } Vc\_1 = w1 = ac\_1 = Alpha1 = \bar{0}_{3 \times 1} \text{ (m/s, rad/s, m/s}^2\text{, rad/s}^2\text{)}$$

$$Pc\_2 = \begin{bmatrix} -0.160 \\ 0.1505 \\ 0.0150 \end{bmatrix} \text{ (m), } Vc\_2 = w2 = ac\_2 = Alpha2 = \bar{0}_{3 \times 1} \text{ (m/s, rad/s, m/s}^2\text{, rad/s}^2\text{)}$$

$$Pc\_3 = \begin{bmatrix} 0.1600 \\ 0.0286 \\ 0.0351 \end{bmatrix} \text{ (m), } Vc\_3 = w3 = ac\_3 = Alpha3 = \bar{0}_{3 \times 1} \text{ (m/s, rad/s, m/s}^2\text{, rad/s}^2\text{)}$$

$$Pc\_4 = \begin{bmatrix} -0.1600 \\ 0.0286 \\ 0.0351 \end{bmatrix} \text{ (m), } Vc\_4 = w4 = ac\_4 = Alpha4 = \bar{0}_{3 \times 1} \text{ (m/s, rad/s, m/s}^2\text{, rad/s}^2\text{)}$$

$$Pc\_9 = \begin{bmatrix} 0.1600 \\ 0.0000 \\ 0.2487 \end{bmatrix} \text{ (m), } Vc\_9 = w9 = ac\_9 = Alpha9 = \bar{0}_{3 \times 1} \text{ (m/s, rad/s, m/s}^2\text{, rad/s}^2\text{)}$$

$$Pc\_10 = \begin{bmatrix} -0.1600 \\ 0.0000 \\ 0.2487 \end{bmatrix} \text{ (m), } Vc\_10 = w10 = ac\_10 = Alpha10 = \bar{0}_{3 \times 1} \text{ (m/s, rad/s, m/s}^2\text{, rad/s}^2\text{)}$$

$$Pc\_11 = \begin{bmatrix} 0.1600 \\ 0.0000 \\ 0.6212 \end{bmatrix} \text{ (m), } Vc\_11 = w11 = ac\_11 = Alpha1 = \bar{0}_{3 \times 1} \text{ (m/s, rad/s, m/s}^2\text{, rad/s}^2\text{)}$$

$$Pc\_12 = \begin{bmatrix} -0.1600 \\ 0.0000 \\ 0.6212 \end{bmatrix} \text{ (m), } Vc\_12 = w12 = ac\_12 = Alpha12 = \bar{0}_{3 \times 1} \text{ (m/s, rad/s, m/s}^2\text{, rad/s}^2\text{)}$$

$$Pc\_17 = \begin{bmatrix} 0.0000 \\ 0.0000 \\ 0.9588 \end{bmatrix} \text{ (m), } Vc\_17 = w17 = ac\_17 = Alpha17 = \bar{0}_{3 \times 1} \text{ (m/s, rad/s, m/s}^2\text{, rad/s}^2\text{)}$$

$$Pc_{20} = \begin{bmatrix} 0.0000 \\ 0.0000 \\ 1.2524 \end{bmatrix} \text{ (m), } Vc_{20} = w20 = ac_{20} = Alpha20 = \bar{0}_{3 \times 1} \text{ (m/s, rad/s, m/s}^2, \text{ rad/s}^2)$$

$$Pc_{23} = \begin{bmatrix} 0.2900 \\ 0.0000 \\ 1.0452 \end{bmatrix} \text{ (m), } Vc_{23} = w23 = ac_{23} = Alpha23 = \bar{0}_{3 \times 1} \text{ (m/s, rad/s, m/s}^2, \text{ rad/s}^2)$$

$$Pc_{24} = \begin{bmatrix} -0.2900 \\ 0.0000 \\ 1.0452 \end{bmatrix} \text{ (m), } Vc_{24} = w24 = ac_{24} = Alpha24 = \bar{0}_{3 \times 1} \text{ (m/s, rad/s, m/s}^2, \text{ rad/s}^2)$$

$$Pc_{27} = \begin{bmatrix} 0.0000 \\ 0.0000 \\ 1.4997 \end{bmatrix} \text{ (m), } Vc_{27} = w27 = ac_{27} = Alpha27 = \bar{0}_{3 \times 1} \text{ (m/s, rad/s, m/s}^2, \text{ rad/s}^2)$$

$$C0_1 = C0_2 = \dots = C0_{27} = \begin{bmatrix} 0 & -1 & 0 \\ 1 & 0 & 0 \\ 0 & 0 & 1 \end{bmatrix}$$

$$L1 = L2 = 0.0743 \text{ (m), } C1 = C2 = 0.0372 \text{ (m), } L3x = L4x = 0.1133 \text{ (m)}$$

$$L3z = L4z = 0.0630 \text{ (m), } C3x = C4x = 0.2860 \text{ (m), } C3z = C4z = 0.4290 \text{ (m)}$$

$$L9 = L10 = 0.3220 \text{ (m), } C9 = C10 = 0.1513 \text{ (m), } L11 = L12 = 0.4120 \text{ (m)}$$

$$C11 = C12 = 0.1908 \text{ (m), } L17y = 0.1600 \text{ (m), } L17z = 0.2936 \text{ (m)}$$

$$C17 = 0.1468 \text{ (m), } L20y = 0.2400 \text{ (m), } L20z = 0.2936 \text{ (m), } C20 = 0.1468 \text{ (m)}$$

$$L27 = 0.2010 \text{ (m), } C27 = 0.1005 \text{ (m), } L23y = L24y = 0.050 \text{ (m)}$$

$$L23z = L24z = 0.7080 \text{ (m), } C23 = C24 = 0.3540 \text{ (m)}$$

$$m1 = m2 = 0.130 \text{ (kg), } m3 = m4 = 0.521 \text{ (kg), } m9 = m10 = 1.979 \text{ (kg)}$$

$$m11 = m12 = 5.213 \text{ (kg), } m17 = m20 = 14.674 \text{ (kg), } m23 = m24 = 2.651 \text{ (kg)}$$

$$m27 = 4.708 \text{ (kg)}$$

$$Jc_1 = Jc_2 = \begin{bmatrix} 0.00007 & 0.00000 & 0.00000 \\ 0.00000 & 0.00007 & 0.00000 \\ 0.00000 & 0.00000 & 0.0012 \end{bmatrix} \text{ (kg.m}^2)$$

$$Jc_3 = Jc_4 = \begin{bmatrix} 0.00048 & 0.00000 & 0.00012 \\ 0.00000 & 0.00100 & 0.00000 \\ 0.00012 & 0.00000 & 0.00100 \end{bmatrix} \text{ (kg.m}^2)$$

$$Jc_9 = Jc_{10} = \begin{bmatrix} 0.01800 & 0.00000 & 0.00000 \\ 0.00000 & 0.01800 & 0.00000 \\ 0.00000 & 0.00000 & 0.00300 \end{bmatrix} \text{ (kg.m}^2)$$

$$Jc_{11} = Jc_{12} = \begin{bmatrix} 0.07900 & 0.00000 & 0.00000 \\ 0.00000 & 0.07900 & 0.00000 \\ 0.00000 & 0.00000 & 0.01200 \end{bmatrix} \text{ (kg.m}^2)$$

$$Jc_{17} = Jc_{20} = \begin{bmatrix} 0.35300 & 0.00000 & 0.00000 \\ 0.00000 & 0.13500 & 0.00000 \\ 0.00000 & 0.00000 & 0.27700 \end{bmatrix} \text{ (kg.m}^2)$$

$$Jc_{23} = Jc_{24} = \begin{bmatrix} 0.11200 & 0.00000 & 0.00000 \\ 0.00000 & 0.11200 & 0.00000 \\ 0.00000 & 0.00000 & 0.00300 \end{bmatrix} \text{ (kg.m}^2)$$

$$Jc_{27} = \begin{bmatrix} 0.02300 & 0.00000 & 0.00000 \\ 0.00000 & 0.02300 & 0.00000 \\ 0.00000 & 0.00000 & 0.01500 \end{bmatrix} \text{ (kg.m}^2)$$





$$Wv\_fa\_LFFDSP = \begin{bmatrix} 100 \\ 100 \\ 100 \\ 100 \\ 100 \\ 100 \end{bmatrix}, Wv\_fa\_RFFDSP = \begin{bmatrix} 100 \\ 100 \\ 100 \\ 100 \\ 100 \\ 100 \end{bmatrix}$$

$$Wa\_a\_LFFSSP = \begin{bmatrix} 0.1 \\ 1.2 \\ 0.9 \\ 0.7 \\ 0.3 \\ 0.4 \\ 0.5 \end{bmatrix}, Wa\_a\_RFFSSP = \begin{bmatrix} 0.1 \\ 1.2 \\ 0.9 \\ 0.7 \\ 0.3 \\ 0.4 \\ 0.5 \end{bmatrix}$$

$$Wa\_a\_LFFDSP = \begin{bmatrix} 0.1 \\ 0.3 \\ 0.3 \\ 0.5 \\ 0.4 \\ 0.4 \\ 0.8 \end{bmatrix}, Wa\_a\_RFFDSP = \begin{bmatrix} 0.1 \\ 0.3 \\ 0.3 \\ 0.5 \\ 0.4 \\ 0.4 \\ 0.8 \end{bmatrix}$$

$$Wp\_fb\_LFFSSP = \begin{bmatrix} 60000 \\ 60000 \\ 80000000 \end{bmatrix}, Wp\_fb\_RFFSSP = \begin{bmatrix} 60000 \\ 60000 \\ 80000000 \end{bmatrix}$$

$$Wp\_fb\_LFFDSP = \begin{bmatrix} 1000 \\ 1000 \\ 30000 \end{bmatrix}, Wp\_fb\_RFFDSP = \begin{bmatrix} 1000 \\ 1000 \\ 30000 \end{bmatrix}$$

$$Wv\_fb\_LFFSSP = \begin{bmatrix} 18000 \\ 18000 \\ 8000 \\ 5000 \\ 5000 \\ 5000 \end{bmatrix}, Wv\_fb\_RFFSSP = \begin{bmatrix} 18000 \\ 18000 \\ 8000 \\ 5000 \\ 5000 \\ 5000 \end{bmatrix}$$

$$Wv\_fb\_LFFDSP = \begin{bmatrix} 100 \\ 100 \\ 100 \\ 100 \\ 100 \\ 100 \end{bmatrix}, Wv\_fb\_RFFDSP = \begin{bmatrix} 100 \\ 100 \\ 100 \\ 100 \\ 100 \\ 100 \end{bmatrix}$$

$$Wa\_b\_LFFSSP = \begin{bmatrix} 1 \\ 0.1 \\ 1.2 \\ 0.9 \\ 0.3 \\ 0.4 \\ 0.5 \\ 0.5 \end{bmatrix}, Wa\_b\_RFFSSP = \begin{bmatrix} 1 \\ 0.1 \\ 1.2 \\ 0.9 \\ 0.3 \\ 0.4 \\ 0.5 \\ 0.5 \end{bmatrix}$$

$$Wa\_b\_LFFDSP = \begin{bmatrix} 0.05 \\ 0.1 \\ 0.3 \\ 0.3 \\ 0.8 \\ 0.6 \\ 0.6 \\ 1 \end{bmatrix}, Wa\_b\_RFFDSP = \begin{bmatrix} 0.05 \\ 0.1 \\ 0.3 \\ 0.3 \\ 0.8 \\ 0.6 \\ 0.6 \\ 1 \end{bmatrix}$$

$$Wor\_fa\_LFFSSP = \begin{bmatrix} 2000 \\ 2000 \\ 2000 \end{bmatrix}, Wor\_fa\_RFFSSP = \begin{bmatrix} 2000 \\ 2000 \\ 2000 \end{bmatrix}$$

$$Wor\_fa\_LFFDSP = \begin{bmatrix} 5000 \\ 5000 \\ 5000 \end{bmatrix}, Wor\_fa\_RFFDSP = \begin{bmatrix} 5000 \\ 5000 \\ 5000 \end{bmatrix}$$

$$Wor\_fb\_LFFSSP = \begin{bmatrix} 8000 \\ 8000 \\ 8000 \end{bmatrix}, Wor\_fb\_RFFSSP = \begin{bmatrix} 8000 \\ 8000 \\ 8000 \end{bmatrix}$$

$$Wor\_fb\_LFFDSP = \begin{bmatrix} 1000 \\ 1000 \\ 1000 \end{bmatrix}, Wor\_fb\_RFFDSP = \begin{bmatrix} 1000 \\ 1000 \\ 1000 \end{bmatrix}$$

$$Wp\_Tetha3\_LFFSSP = 100000, Wp\_Tetha4\_RFFSSP = 100000$$

$$Wv\_Tetha3\_LFFSSP = 40000, Wv\_Tetha4\_RFFSSP = 40000$$

$$Wact\_LFFDSP = Wact\_RFFDSP = [1 \ 1 \ 1 \ 1 \ 1 \ 1 \ 1 \ 1 \ 1 \ 1 \ 1000 \ 1 \ 1 \ 1 \ 1 \ 1 \ 1 \ 1 \ 1 \ 1 \ 1 \ 1000 \ 1000 \ 1000 \ 1 \ 1 \ 1 \ 1 \ 1000 \ 1 \ 1 \ 1 \ 1 \ 1000 \ 1000 \ 1000 \ 1 \ 1 \ 1 \ 1 \ 1 \ 1 \ 1000 \ 1000 \ 1000 \ 1 \ 1 \ 1 \ 1 \ 1 \ 1 \ 1 \ 1 \ 1 \ 1 \ 1000 \ 1 \ 1 \ 1 \ 1 \ 1 \ 1 \ 1 \ 1 \ 1 \ 1 \ 1000 \ 1000 \ 1 \ 1000 \ 1000 \ 1 \ 1000 \ 1000 \ 1000]^\top$$

$$\begin{aligned}
WqL\_H\_LFFSSP &= \begin{bmatrix} 0.1 \\ 30000 \\ 1 \\ 1000 \\ 0.2 \\ 0.4 \\ 0.6 \end{bmatrix}, WqR\_H\_RFFSSP = \begin{bmatrix} 0.1 \\ 30000 \\ 1 \\ 1000 \\ 0.2 \\ 0.4 \\ 0.6 \end{bmatrix} \\
WqL\_H\_LFFDSP &= \begin{bmatrix} 0.2 \\ 0.8 \\ 1 \\ 0.3 \\ 0.4 \\ 0.5 \\ 1 \end{bmatrix}, WqR\_H\_RFFDSP = \begin{bmatrix} 0.2 \\ 0.8 \\ 1 \\ 0.3 \\ 0.4 \\ 0.5 \\ 1 \end{bmatrix} \\
WqH\_R\_LFFSSP &= \begin{bmatrix} 0 \\ 0.1 \\ 25000 \\ 1 \\ 1000 \\ 0.2 \\ 0.4 \\ 0.8 \end{bmatrix}, WqH\_L\_RFFSSP = \begin{bmatrix} 0 \\ 0.1 \\ 25000 \\ 1 \\ 1000 \\ 0.2 \\ 0.4 \\ 0.8 \end{bmatrix} \\
WqR\_H\_LFFDSP &= \begin{bmatrix} 8000 \\ 0.4 \\ 0.8 \\ 1 \\ 0.5 \\ 0.3 \\ 0.5 \\ 0.8 \end{bmatrix}, WqL\_H\_RFFDSP = \begin{bmatrix} 8000 \\ 0.4 \\ 0.8 \\ 1 \\ 0.5 \\ 0.3 \\ 0.5 \\ 0.8 \end{bmatrix}
\end{aligned}$$

$$WpTetha18 = 300, WvTetha18 = 120, Delta\_t18 = 0.3 \text{ (s)}$$

$$WpTetha19 = 200, WvTetha19 = 60, Delta\_t19 = 0.3 \text{ (s)}$$

$$WpTetha20 = 200, WvTetha20 = 60, Delta\_t20 = 0.3 \text{ (s)}$$

$$WpTetha21 = 10, WvTetha21 = 100, Delta\_t21 = 0.3 \text{ (s)}$$

$$WpTetha22 = 10, WvTetha22 = 100, Delta\_t22 = 0.3 \text{ (s)}$$

$$WpTetha23 = 10, WvTetha23 = 100, Delta\_t23 = 0.3 \text{ (s)}$$

$$WpTetha24 = 10, WvTetha24 = 100, Delta\_t24 = 0.3 \text{ (s)}$$

$$WpTetha25 = 10, WvTetha25 = 100, Delta\_t25 = 0.3 \text{ (s)}$$

$$WpTetha26 = 10, WvTetha26 = 100, Delta\_t26 = 0.3 \text{ (s)}$$

$$WpTetha27 = 10, WvTetha27 = 100, Delta\_t27 = 0.3 \text{ (s)}$$

$$Wadj\_qdot\_LFFSSP\_to\_RFFDSP$$

$$= [1 \ 1 \ 1 \ 3 \ 1.8 \ 1.8 \ 1.8 \ 1 \ 1 \ 1 \ 3 \ 1.8 \ 1.8 \ 1.8]^T$$

$$Wadj\_qdot\_LFFSSP\_to\_RFFDSP =$$

$$[1 \ 1 \ 1 \ 3 \ 1.8 \ 1.8 \ 1.8 \ 1 \ 1 \ 1 \ 3 \ 1.8 \ 1.8 \ 1.8]^T$$

$$Saturation = [-30,30](N.m), Saturation1 = [-150,150](N.m)$$

$$Saturation2 = [-150,150](N.m), Saturation3 = [-150,150](N.m)$$

$$Saturation4 = [-150,150](N.m), Saturation5 = [-150,150](N.m)$$

$$Saturation6 = [-150,150](N.m), Saturation7 = [-150,150](N.m)$$

*Saturation8* = [-30,30](*N.m*), *Saturation9* = [-150,150](*N.m*)  
*Saturation10* = [-150,150](*N.m*), *Saturation11* = [-150,150](*N.m*)  
*Saturation12* = [-150,150](*N.m*), *Saturation13* = [-150,150](*N.m*)  
*Saturation14* = [-150,150](*N.m*), *Saturation15* = [-150,150](*N.m*)  
*Saturation16* = [-180,180](*N.m*), *Saturation17* = [-180,180](*N.m*)  
*Saturation18* = [-180,180](*N.m*), *Saturation19* = [-100,100](*N.m*)  
*Saturation20* = [-100,100](*N.m*), *Saturation21* = [-100,100](*N.m*)  
*Saturation22* = [-100,100](*N.m*), *Saturation23* = [-100,100](*N.m*)  
*Saturation24* = [-100,100](*N.m*), *Saturation25* = [-100,100](*N.m*)

$$Pc\_1 = \begin{bmatrix} 0.1600 \\ 0.1505 \\ 0.0150 \end{bmatrix} \text{ (m), } Vc\_1 = w1 = ac\_1 = Alpha1 = \bar{0}_{3 \times 1} \text{ (m/s, rad/s, m/s}^2\text{, rad/s}^2\text{)}$$

$$Pc\_2 = \begin{bmatrix} -0.160 \\ 0.1505 \\ 0.0150 \end{bmatrix} \text{ (m), } Vc\_2 = w2 = ac\_2 = Alpha2 = \bar{0}_{3 \times 1} \text{ (m/s, rad/s, m/s}^2\text{, rad/s}^2\text{)}$$

$$Pc\_3 = \begin{bmatrix} 0.1600 \\ 0.0286 \\ 0.0351 \end{bmatrix} \text{ (m), } Vc\_3 = w3 = ac\_3 = Alpha3 = \bar{0}_{3 \times 1} \text{ (m/s, rad/s, m/s}^2\text{, rad/s}^2\text{)}$$

$$Pc\_4 = \begin{bmatrix} -0.1600 \\ 0.0286 \\ 0.0351 \end{bmatrix} \text{ (m), } Vc\_4 = w4 = ac\_4 = Alpha4 = \bar{0}_{3 \times 1} \text{ (m/s, rad/s, m/s}^2\text{, rad/s}^2\text{)}$$

$$Pc\_9 = \begin{bmatrix} 0.1600 \\ 0.0000 \\ 0.2487 \end{bmatrix} \text{ (m), } Vc\_9 = w9 = ac\_9 = Alpha9 = \bar{0}_{3 \times 1} \text{ (m/s, rad/s, m/s}^2\text{, rad/s}^2\text{)}$$

$$Pc\_10 = \begin{bmatrix} -0.1600 \\ 0.0000 \\ 0.2487 \end{bmatrix} \text{ (m), } Vc\_10 = w10 = ac\_10 = Alpha10 = \bar{0}_{3 \times 1} \text{ (m/s, rad/s, m/s}^2\text{, rad/s}^2\text{)}$$

$$Pc\_11 = \begin{bmatrix} 0.1600 \\ 0.0000 \\ 0.6212 \end{bmatrix} \text{ (m), } Vc\_11 = w11 = ac\_11 = Alpha1 = \bar{0}_{3 \times 1} \text{ (m/s, rad/s, m/s}^2\text{, rad/s}^2\text{)}$$

$$Pc\_12 = \begin{bmatrix} -0.1600 \\ 0.0000 \\ 0.6212 \end{bmatrix} \text{ (m), } Vc\_12 = w12 = ac\_12 = Alpha12 = \bar{0}_{3 \times 1} \text{ (m/s, rad/s, m/s}^2\text{, rad/s}^2\text{)}$$

$$Pc\_17 = \begin{bmatrix} 0.0000 \\ 0.0000 \\ 0.9588 \end{bmatrix} \text{ (m), } Vc\_17 = w17 = ac\_17 = Alpha17 = \bar{0}_{3 \times 1} \text{ (m/s, rad/s, m/s}^2\text{, rad/s}^2\text{)}$$

$$Pc\_20 = \begin{bmatrix} 0.0000 \\ 0.0000 \\ 1.2524 \end{bmatrix} \text{ (m), } Vc\_20 = w20 = ac\_20 = Alpha20 = \bar{0}_{3 \times 1} \text{ (m/s, rad/s, m/s}^2\text{, rad/s}^2\text{)}$$

$$Pc_{23} = \begin{bmatrix} 0.2900 \\ 0.0000 \\ 1.0452 \end{bmatrix} \text{ (m), } Vc_{23} = w_{23} = ac_{23} = Alpha_{23} = \bar{0}_{3 \times 1} \text{ (m/s, rad/s, m/s}^2, \text{ rad/s}^2)$$

$$Pc_{24} = \begin{bmatrix} -0.2900 \\ 0.0000 \\ 1.0452 \end{bmatrix} \text{ (m), } Vc_{24} = w_{24} = ac_{24} = Alpha_{24} = \bar{0}_{3 \times 1} \text{ (m/s, rad/s, m/s}^2, \text{ rad/s}^2)$$

$$Pc_{27} = \begin{bmatrix} 0.0000 \\ 0.0000 \\ 1.4997 \end{bmatrix} \text{ (m), } Vc_{27} = w_{27} = ac_{27} = Alpha_{27} = \bar{0}_{3 \times 1} \text{ (m/s, rad/s, m/s}^2, \text{ rad/s}^2)$$

$$C0_{1} = C0_{2} = \dots = C0_{27} = \begin{bmatrix} 0 & -1 & 0 \\ 1 & 0 & 0 \\ 0 & 0 & 1 \end{bmatrix}$$

$$L1 = L2 = 0.0743 \text{ (m), } C1 = C2 = 0.0372 \text{ (m), } L3x = L4x = 0.1133 \text{ (m)}$$

$$L3z = L4z = 0.0630 \text{ (m), } C3x = C4x = 0.2860 \text{ (m), } C3z = C4z = 0.4290 \text{ (m)}$$

$$L9 = L10 = 0.3220 \text{ (m), } C9 = C10 = 0.1513 \text{ (m), } L11 = L12 = 0.4120 \text{ (m)}$$

$$C11 = C12 = 0.1908 \text{ (m), } L17y = 0.1600 \text{ (m), } L17z = 0.2936 \text{ (m)}$$

$$C17 = 0.1468 \text{ (m), } L20y = 0.2400 \text{ (m), } L20z = 0.2936 \text{ (m), } C20 = 0.1468 \text{ (m)}$$

$$L27 = 0.2010 \text{ (m), } C27 = 0.1005 \text{ (m), } L23y = L24y = 0.050 \text{ (m)}$$

$$L23z = L24z = 0.7080 \text{ (m), } C23 = C24 = 0.3540 \text{ (m)}$$

$$m1 = m2 = 0.130 \text{ (kg), } m3 = m4 = 0.521 \text{ (kg), } m9 = m10 = 1.979 \text{ (kg)}$$

$$m11 = m12 = 5.213 \text{ (kg), } m17 = m20 = 14.674 \text{ (kg), } m23 = m24 = 2.651 \text{ (kg)}$$

$$m27 = 4.708 \text{ (kg)}$$

$$Jc_{1} = Jc_{2} = \begin{bmatrix} 0.00007 & 0.00000 & 0.00000 \\ 0.00000 & 0.00007 & 0.00000 \\ 0.00000 & 0.00000 & 0.00012 \end{bmatrix} \text{ (kg.m}^2)$$

$$Jc_{3} = Jc_{4} = \begin{bmatrix} 0.00048 & 0.00000 & 0.00012 \\ 0.00000 & 0.00100 & 0.00000 \\ 0.00012 & 0.00000 & 0.00100 \end{bmatrix} \text{ (kg.m}^2)$$

$$Jc_{9} = Jc_{10} = \begin{bmatrix} 0.01800 & 0.00000 & 0.00000 \\ 0.00000 & 0.01800 & 0.00000 \\ 0.00000 & 0.00000 & 0.00300 \end{bmatrix} \text{ (kg.m}^2)$$

$$Jc_{11} = Jc_{12} = \begin{bmatrix} 0.07900 & 0.00000 & 0.00000 \\ 0.00000 & 0.07900 & 0.00000 \\ 0.00000 & 0.00000 & 0.01200 \end{bmatrix} \text{ (kg.m}^2)$$

$$Jc_{17} = Jc_{20} = \begin{bmatrix} 0.35300 & 0.00000 & 0.00000 \\ 0.00000 & 0.13500 & 0.00000 \\ 0.00000 & 0.00000 & 0.27700 \end{bmatrix} \text{ (kg.m}^2)$$

$$Jc_{23} = Jc_{24} = \begin{bmatrix} 0.11200 & 0.00000 & 0.00000 \\ 0.00000 & 0.11200 & 0.00000 \\ 0.00000 & 0.00000 & 0.00300 \end{bmatrix} \text{ (kg.m}^2)$$

$$Jc_{27} = \begin{bmatrix} 0.02300 & 0.00000 & 0.00000 \\ 0.00000 & 0.02300 & 0.00000 \\ 0.00000 & 0.00000 & 0.01500 \end{bmatrix} \text{ (kg.m}^2)$$